



HAL
open science

Identification of novel factors involved in the exacerbation of HIV-1 infection and spread among macrophages in the tuberculosis context

Maeva Dupont

► **To cite this version:**

Maeva Dupont. Identification of novel factors involved in the exacerbation of HIV-1 infection and spread among macrophages in the tuberculosis context. Immunology. Université Paul Sabatier - Toulouse III, 2019. English. NNT : 2019TOU30211 . tel-02942740

HAL Id: tel-02942740

<https://theses.hal.science/tel-02942740>

Submitted on 18 Sep 2020

HAL is a multi-disciplinary open access archive for the deposit and dissemination of scientific research documents, whether they are published or not. The documents may come from teaching and research institutions in France or abroad, or from public or private research centers.

L'archive ouverte pluridisciplinaire **HAL**, est destinée au dépôt et à la diffusion de documents scientifiques de niveau recherche, publiés ou non, émanant des établissements d'enseignement et de recherche français ou étrangers, des laboratoires publics ou privés.



Université
de Toulouse

THÈSE

En vue de l'obtention du

DOCTORAT DE L'UNIVERSITÉ DE TOULOUSE

Délivré par : *l'Université Toulouse 3 Paul Sabatier (UT3 Paul Sabatier)*

Présentée et soutenue le *6th of December 2019* par :

Maeva DUPONT

Identification of novel factors involved in the exacerbation of HIV-1 infection and spread among macrophages in the tuberculosis context

JURY

MRS. CHRISTEL MOOG-LUTZ	University Professor	President
M. PAUL CROCKER	University Professor	Reviewer Expert
MRS. CAROLINE GOUJON	Principal Investigator	Reviewer Expert
M. MAXIMILIANO GUTIERREZ	Research Director	Reviewer Expert
M. OLIVIER NEYROLLES	Research Director	Examiner
M. GEANNCARLO LUGO-VILLARINO	Principal Investigator	PhD Director
MRS. CHRISTEL VEROLLET	Principal Investigator	PhD Co-director

École doctorale et spécialité :

BSB : Immunologie

Unité de Recherche :

IPBS - Institute of Pharmacology and Structural Biology (UMR 5089)

Directeur(s) de Thèse :

Dr. Geanncarlo LUGO-VILLARINO et Dr. Christel VEROLLET

Rapporteurs :

Pr. Paul CROCKER, Dr. Caroline GOUJON et Dr. Maximiliano GUTIERREZ

“Nothing in life is to be feared, it is only to be understood. Now is the time to understand more, so that we may fear less.”— Marie Curie

“The art and science of asking questions is the source of all knowledge.” – Thomas Berger

“Scientists have become the bearers of the torch of discovery in our quest for knowledge.” – Stephen Hawking

“Success is a science; if you have the conditions, you get the result.” – Oscar Wilde

Abstract

Mycobacterium tuberculosis (Mtb), the bacteria causing tuberculosis (TB), and the human immunodeficiency virus type 1 (HIV-1), the etiological agent of acquired immunodeficiency syndrome (AIDS), act in synergy to exacerbate the progression of each other in co-infected patients. While clinical evidence reveals a frequent increase of the viral load at co-infected anatomical sites, the mechanisms explaining how Mtb favours HIV-1 progression remain insufficiently understood.

Macrophages are the main target for Mtb. Their infection by the bacilli likely shapes the microenvironment that favours HIV-1 infection and replication at sites of co-infection. To address this issue, I took advantage of an *in vitro* model mimicking the TB-associated microenvironment (cmMTB, “conditioned media of Mtb-infected macrophages”) previously established in the laboratory; a model that renders macrophages susceptible to intracellular pathogens like Mtb. Upon joining the team, I participated in the study on how Mtb exacerbates HIV-1 replication in macrophages, using this model. We found that cmMTB-treated macrophages (M(cmMTB)) have an enhanced ability to form intercellular membrane bridges called tunneling nanotubes (TNT), which increase the capacity of the virus to transfer from one macrophage to another, leading to the exacerbation of HIV-1 production and spread.

The principal objective of my PhD thesis was to identify novel factors that are involved in the exacerbation of HIV-1 replication in macrophages in the context of tuberculosis. To this end, a transcriptomic analysis of M(cmMTB) was conducted, and revealed two key factors: the Siglec-1 receptor and type I interferon (IFN-I)/STAT1 signaling.

The first part of my PhD thesis dealt with the characterization of Siglec-1 as a novel factor involved in the synergy between Mtb and HIV-1 in macrophages. First, I demonstrated that its increased expression in M(cmMTB) was dependent on IFN-I. Second, in Mtb and simian immunodeficiency virus co-infected non-human primates, I established a positive correlation between the abundance of Siglec-1⁺ alveolar macrophages and the pathology, associated with the activation of the IFN-I/STAT-1 pathway. Third, I revealed that Siglec-1 is localized on a specific subset of thick TNT. These thick Siglec-1⁺ TNT were longer and contained high HIV-1 cargos compared to Siglec-1⁻ TNT, suggesting that the virus might preferentially use these TNT. Finally, I showed that Siglec-1 was responsible for the enhanced HIV-1 replication by increasing viral capture and cell-to-cell transfer, at least in part through TNT. These findings argue that Siglec-1 has a physiological significance to macrophage and TNT biology. It may also be a potential target for designing new therapies aimed at reducing viral dissemination in a co-infection context.

In the second part of my PhD project, I determined that TB dysregulates the IFN-I/STAT-1 signaling pathway to diminish the antiviral response. Indeed, upon exogenous IFN-I stimulation, I noticed a reduced STAT1 activation and lower expression of the interferon-stimulated genes (ISG) in M(cmMTB) compared to control cells, indicating a potential desensitization to the IFN-I/STAT-1 pathway. By blocking IFNAR2 or inhibiting STAT-1 gene expression during cmMTB-treatment, I prevented this desensitization to exogenous IFN-I and restored control of HIV-1 infection in macrophages. Altogether, these results point to a deleterious role of IFN-I in the co-infection setting.

My thesis work unveils the capacity of Mtb to dysregulate host-antiviral responses against HIV-1. Modulation of the macrophage response by TB-induced IFN-I, including upregulation of Siglec-1 expression, explains how these cells become vessels for viral spread that contributes to co-infection severity. In addition, the identified factors in this project may be used as new diagnostic tools or therapeutic targets to ameliorate the diagnosis and treatment of co-infected individuals.

Résumé

Mycobacterium tuberculosis (Mtb), la bactérie responsable de la tuberculose (TB), et le virus de l'immunodéficience humaine (VIH-1), l'agent du syndrome de l'immunodéficience acquise (SIDA), accélèrent leurs progressions mutuelles chez les patients co-infectés. Alors que de nombreuses données cliniques rapportent une augmentation de la charge virale dans les sites anatomiques co-infectés, les mécanismes qui en sont responsables restent insuffisamment décrits.

Mtb cible principalement les macrophages. Nous émettons l'hypothèse que l'infection des macrophages par Mtb crée un microenvironnement propice à la réplication du VIH-1 au niveau des sites co-infectés. Pour le montrer, j'ai utilisé un modèle *in vitro* précédemment établi par mes équipes (le cmMTB – pour « conditioned media of Mtb-infected macrophages »). Celui-ci permet de mimer un environnement tuberculeux, par la différenciation et l'activation des macrophages vers un profil « M(cmMTB) », largement retrouvé dans les poumons lors d'une tuberculose active. En rejoignant le laboratoire, j'ai participé à l'étude des mécanismes responsables de l'augmentation de la réplication virale dans le contexte de co-infection, en utilisant ce modèle. Nous avons trouvé que les M(cmMTB) forment de nombreux nanotubes (ponts intercellulaires), leur permettant de transférer plus de virus d'un macrophage à l'autre, et conduit à une forte augmentation de la production virale.

L'objectif principal de ma thèse a donc été d'identifier, dans un contexte tuberculeux, de nouveaux facteurs impliqués dans l'augmentation de la réplication du VIH-1 dans les macrophages. Pour cela, une analyse transcriptomique des M(cmMTB) a été réalisée, révélant deux facteurs essentiels : le récepteur Siglec-1 et les interférons de type I (IFN-I) *via* STAT1.

Dans un premier temps, j'ai étudié le rôle de Siglec-1 dans la synergie entre Mtb et le VIH-1 dans les macrophages. D'abord, j'ai montré que son expression de surface était augmentée par le cmMTB, de façon dépendante des IFN-I. Ensuite, j'ai établi que l'abondance des macrophages alvéolaires exprimant Siglec-1 chez les primates non-humains co-infectés avec Mtb et le virus de l'immunodéficience simienne corrélait avec la sévérité de la pathologie, et était associée à la signalisation des IFN-I, *via* l'activation de STAT1. De plus, j'ai identifié une nouvelle localisation de Siglec-1 le long d'un sous-type de nanotubes. Ceux-ci, plus larges et plus longs, contenaient plus de VIH-1 que les autres, suggérant que le virus puisse les emprunter en majorité. Enfin, j'ai montré que Siglec-1 était responsable de l'augmentation de la réplication du VIH-1, grâce à une meilleure capture du virus et de son transfert intercellulaire, potentiellement grâce aux nanotubes. Ces résultats permettent de proposer que Siglec-1 a un rôle physiologique dans la biologie des nanotubes et des macrophages.

Dans un second temps, j'ai déterminé que la TB dérégule la signalisation IFN-I/STAT1 dans les macrophages et diminue leur réponse antivirale. Après stimulation des M(cmMTB) par de l'IFN-I exogène, j'ai démontré une diminution de l'activation de STAT1 et de l'expression des gènes de réponse à l'IFN, indiquant une potentielle désensibilisation de ces cellules à l'IFN-I. Ces observations, ainsi que la perte de contrôle de la réplication du VIH-1, ont été reversées par l'inhibition du récepteur aux IFN-I (IFNAR2) ou du facteur de transcription STAT1. Ensemble, ces résultats indiquent que les IFN-I ont un rôle délétère pour l'hôte dans le contexte de la co-infection.

Mon projet de thèse a permis de révéler la capacité de Mtb à déréguler les réponses antivirales de l'hôte contre le VIH-1, participant ainsi à la gravité de la co-infection. Les facteurs identifiés au cours de ma thèse pourraient à plus long terme être utilisés à des fins diagnostiques ou thérapeutiques, dans le but d'améliorer la prise en charge des patients co-infectés.

Acknowledgements

Many thanks to the jury

I first would like to thank the members of my thesis jury, Pr. Paul Crocker, Dr. Caroline Goujon, Dr. Maximiliano Gutierrez and Pr. Christel Moog-Lutz. I am honoured by the interest you showed to examine my research and thankful you accepted to evaluate it. Thank you for the nice discussion we had and for your patience with all the last minute changes we had to face, I hope I will get the chance to meet you in person soon.

I would also like to thank the members of my thesis committee, Pr. Pierre Delobel and Dr. Olivier Schwartz, for their constructive comments and their support all along my PhD. Our discussions, along with your advices, were truly helpful for me to move on and evolve with the project. I would also like to thank here Olivier and Isabelle for welcoming me in their teams, and for trusting us with the co-infection project. It means a lot to all of us!

Thanks to my supervisors

Then, I would like to thank my mentors, starting with Dr. Luciana Balboa. Thank you for taking care of my travels and your help with the Argentinian life. I really appreciated the time we spent together, our scientific discussions, and also how you shared your experience with me about being a researcher and more. I really hope you will continue to provide the scientific community with the good research you perform, but more importantly, that you will keep guiding young researchers to find their paths, as you did for me. Also, give my best regards to Pablo, Fer, and Manuel, to whom I sing with you "Susanita tien un raton, un raton chiquitin ...". I wish you all the best for the future!

I would also like to thank particularly my PhD director Dr. Geanncarlo Lugo-Villarino. Thank you for choosing me to continue the co-infection project and for trusting me with it. As you mentioned at the beginning of this adventure, this project became "my baby", I saw it grow, evolve, and I am proud to have achieved this by your side. Despite a tough beginning, I am glad and proud of our achievement, both on the professional and personal level. I am happy we get to know each other better. Thank you for all the lessons you taught me and for helping me to become a researcher, which involves much more than bench work. Thank you for showing me how to read and criticize papers, how to review them, and how to write them. Thank you for making me a good speaker, an asset that will be useful for my entire carrier. Finally, thank you for your support, especially in difficult times and for helping me to feed my white wolf. I really appreciated it and have no words to express my gratitude for the humanity, patience and kindness you showed me. I hope we will stay in touch, and I wish you all the best and good luck you deserve for the new chapter of your life (fingers crossed!) in the USA.

Je vais maintenant passer au français pour remercier ma co-directrice de thèse, le Dr. Christel Vérolet. Chris, j'ai beaucoup aimé travailler avec toi depuis mon M2, ton soutien et la détermination que tu as montrée, avec Bibi, pour me faire passer en M2R IMI directement et ne pas repasser par la case M1 ! Je suis heureuse d'avoir pu faire ma thèse ici, à Toulouse, sous ta direction et celle de GC,

avec qui vous vous complétez en tant qu'encadrants. Merci pour la confiance que tu as placée en moi et dans le travail que j'ai réalisé, merci de m'avoir soutenue et aidée avec les manips, les IF, les infections, et les quantifs ! On forme une belle équipe, efficace, et j'espère pouvoir trouver à l'avenir un binôme aussi agréable et positif que toi ! Bien sûr, je te remercie surtout pour m'avoir appris ce qu'est une chercheuse et pour m'avoir fait grandir, aussi bien scientifiquement que personnellement. J'admire sincèrement ton énergie positive et tes capacités de travail qui paraissent sans limite, et j'espère un jour développer ces mêmes qualités ! Tu es une super chercheuse et je te souhaite toute la réussite du monde pour ton avenir en tant que DR.

Merci aux ParNeys

Je remercie sincèrement chacun des membres des équipes Neyrolles et Parini. Même s'il n'a pas toujours été facile de naviguer entre les deux équipes, j'ai fini par me sentir aussi bien dans l'une que dans l'autre, et cela a été très enrichissant : deux fois plus de science, deux fois plus de conseils, mais surtout, deux fois plus d'humanité, de soutien, et de rigolade, pour que chaque moment passé au labo soit agréable !

Merci Nono, pour ton éternelle bonne humeur (ou presque ;p), mon petit rayon de soleil au quotidien va me manquer, mais je compte bien sur toi pour m'envoyer ton sourire régulièrement ! Et merci aussi pour ce super cours de kung-fu, j'ai eu si mal que je m'en souviendrai toute ma vie !

Merci Bibi, pour tant de choses que les mots me manquent. J'ai appris la rigueur scientifique grâce à toi, à répondre aux questions, à discuter d'un projet et tellement plus encore ! Merci d'être venue me soutenir pour le grand jour et d'avoir été la première à me faire grandir ! Prends bien soin de toi !

Merci Yoann, pour tous tes conseils sur Siglec-1, pour toutes nos conversations philosophiques sur cette « nouvelle génération de glandeur », ou du moins, celle qui peut attendre jusqu'à demain pour regarder les résultats de ses ELISA :) L'arsouille que tu es va me manquer aussi en Angleterre, après tout, avec qui vais-je me battre là-bas ? Ah et je t'envoierai une robopette pour tes filles, comme ça, tu ne m'oublieras pas ! ;p

Merci Claude, pour avoir partagé ton bureau avec moi tout au long de ma première année de thèse, et pour les conseils que tu m'as donnés, qui m'ont aidé aussi à prendre en main mon projet. Merci aussi pour ta gentillesse et ta compassion dans les moments difficiles.

Merci Denis, pour l'exemple que tu donnes, le dévouement que tu as à l'égard de l'enseignement et de tes élèves (si seulement il y en avait plus comme toi !), et pour m'avoir impliquée dans ce beau projet qu'est l'escape game immuno ! J'espère avoir l'occasion de venir y jouer moi aussi !

Merci aussi à Myriam, pour nos discussions au labo, pour ton aide avec la quantif des histos et avec les buffy ! Continue de positiver, et n'oublie pas de me donner des nouvelles ! Prends bien soin de toi et de Julien, et profite à fond de chaque moment :)

Merci à Véro, Renaud, Fred, Yannick et Flo, pour tous ces bons moments passés ensemble au court des 3 dernières années, je suis contente d'avoir eu la chance de travailler à vos côtés. Fred, je compte sur toi pour produire cette Siglec-1 – RFP !

Merci aux personnes de l'IPBS

Merci à Céline, Etienne, Arnaud pour votre aide sur mon projet, que ce soit en histo, en signalisation interféron ou en prise d'image de dernière minute pour avoir la plus belle présentation possible. Je suis ravie de ces années passées à vos côtés et je vous souhaite une belle continuation dans notre belle ville rose.

Merci aux copains

Lucie, mon chat, merci pour toutes ces aventures et ces 7 superbes années ! Que cela va faire drôle de ne plus te voir tous les jours, de ne pas te voir faire des bêtises, de ne plus avoir de bleus après nos entraînements (tout du moins des bleus causés par toi :p) ! Tu vas incroyablement me manquer, et tu as intérêt à me tenir au courant ! Après tout, tu es ma demoiselle d'honneur ! Merci mon chat, pour m'avoir soutenu tout ce temps, pour avoir essuyé mes larmes et supporté toutes mes râleries. Tu as une place toute particulière dans mon cœur, sache-le, et tu pourras toujours compter sur moi ! <3

Natacha, tu es une incroyablement belle personne. Même si le début de notre relation n'a pas été des plus aisées, je suis sincèrement ravie de te connaître et de te compter parmi mes amies proches. Tu as énormément de qualités, j'espère que nos chemins continueront de se croiser régulièrement. Après tout, on a une ferme pédagogique à mettre en place, ainsi que notre entreprise de guide touristique en montagne !

Karine, ma petite Karinette. Merci pour tout ! Tu as été mon roc pendant la période la plus difficile de ma thèse et je ne suis pas certaine que j'aurais pu continuer si tu ne m'avais pas secouée quand il le fallait ! Ça a été difficile de te voir partir du labo, surtout quand toi seule pouvait comprendre la difficulté d'être entre deux équipes. Sache que je ne suis pas que de passage dans ta vie, et que tu as intérêt à me donner des nouvelles et à venir me voir en Angleterre, sinon, ma vengeance sera terrible ! Reste comme tu es, tu es une parfaite petite licorne, et je suis très fière de te compter parmi mes amies.

Rémi, j'ai toute confiance que tu t'en sortiras très bien, et que ton projet va évoluer et que tu feras de super trucs avec ! J'ai hâte de voir ce que ce petit transfert que j'ai initié va devenir, et je suis très contente que tu en aies pris la suite ; tout comme je suis contente de te connaître. Tes petits sarcasmes vont me manquer, je ne suis pas sûre de me faire à l'humour anglais... Alors n'oublie pas de m'envoyer des blagues régulièrement ! Ne te décourage surtout pas, tu y arriveras très bien, et je serai toujours là si besoin, alors n'hésite pas et appelle-moi !

Tamara, ma petite Tam Tam ! Je suis super contente d'avoir appris à te connaître, de toutes les discussions qu'on a pu avoir concernant le labo, la vie, les mecs ! Je suis heureuse pour toi pour ton appartement, tu vas voir c'est une belle aventure. Profite aussi à fond de cette superbe occasion que tu as de travailler avec Ben, et surtout (rien à voir), je t'attends de pied ferme à Oxford !

Thibaut, merci avant tout pour ton aide des plus précieuses la semaine avant la soutenance. Je crois bien que sans toi, je n'aurais jamais soutenu à la date prévue ! Au-delà de cette semaine particulièrement importante, merci pour ton amitié et tous ces moments de partage, Je s'appelle Groot !

Giulia, petite Giugiu, je suis désolée, même après 4 ans je n'ai toujours pas acquis les bases pour comprendre le rôle de DCIR dans le cancer du côlon... Mais j'ai une idée plus précise et c'est grâce à toi quand même ! I also wanted to tell you that I am going to miss you so much, you with whom we built an entire new world where PhD students are not drawn into work and don't lack so much sleeping hours! All our conversations helped me to go through, especially when I really felt I was going to give up, so thank you Giugiu, for your support, for sharing my ideal and for being true, without ever judging. Vieni a trovarmi a Oxford, tesoro, perché già mi manchi, y ti amo ! (if only my Italian wasn't so bad...)

BYM, merci pour ta gentillesse, ton amitié, et pour mon petit stage spécial « vraie science » ! Tu as été un super encadrant pendant ces 2 semaines, même si malgré tous nos efforts, nous n'avons pas réussi à produire de plasmide Siglec-1-RFP. Courage pour l'année qu'il te reste, et surtout, n'oublie pas de lever le coude !

Alexia, je suis contente d'avoir appris à te connaître. Merci pour les cours d'escalade, les soirées d'anniversaire chez toi et pour avoir aimé mon petit zozo à qui tu manques beaucoup ! Merci aussi pour ta gentillesse et ton soutien lors de la rédaction et la préparation de mon oral, cela m'a été très précieux. Je ne doute pas que l'on va se retrouver sur une des aires d'autoroute de la vie, et j'attends impatiemment qu'on s'y arrête ensemble, pour savourer ces précieux moments d'amitié.

Aurélien, le petit piou-piou-shifu du labo, fétichiste des oreilles et blagueur de première ! Tes petites blagues vont beaucoup me manquer (oui même si j'ai beaucoup râlé quand j'ai dû ranger mon bureau... en vrai c'était marrant !). Je ne serai plus là pour te rendre la pareille, mais compte sur moi pour pourrir ta boîte mail et continuer de t'embêter à distance. Et qui sait, si tu passes à Oxford, t'auras ptet droit à un gâteau au chocolat ;))

Shanti, merci à toi aussi, car si tu n'avais pas été là, je n'aurais probablement pas fait ma thèse ici à l'IPBS. Tu as commencé un super projet, même si difficile, il est quand même incroyablement enrichissant et fascinant ! Plus qu'un projet ou un travail, merci d'avoir partagé avec moi ton expérience et ta gentillesse. Mais aussi, merci pour Derby, de m'avoir aidée à en prendre soin, même si on n'était pas toujours d'accord, je sais qu'il a reçu beaucoup d'amour, et de carottes de ta part ☺, et cela me reconforte chaque fois que j'y pense. Je te souhaite plein de bonnes choses pour la suite, et j'attends ta crémaillère avec impatience !

Javier, muchas gracias por tu consejos. Fue muy agradable de conocerte ! Ademas, gracias por la propuesta de hacer mis WB pero como sabes, 20 o 50€ (no me recuerdo), era muy caro !

Ben, thank you, and Emma, for helping with my PhD corrections. I am really glad I met you, even though it was for such a short time. I really hope you will fully appreciate your stay in France and make the most out of it, both on the personal and professional level. If we are lucky enough, our paths will cross again, and I look forward to it.

Margot, je ne t'aurais pas connu pour très longtemps comparé à d'autres, mais merci pour tes précieux conseils à l'approche de la soutenance, pour la rédaction aussi, mais surtout pour le fait de profiter pleinement du bonheur et de la fierté que l'on retire de nos soutenances. Grâce à toi, ce moment est gravé dans ma mémoire comme un des plus importants et des plus positifs de mes études.

Marion, tu nous as rejoint il n'y a pas si longtemps et m'a piqué ma paillasse... Mais je ne t'en veux pas du tout ;) merci pour les petites sucreries et les conseils chats, j'espère que ta petite boule de poils fera moins de bêtises en grandissant.

Dan, merci pour tes conseils et toutes les publis et techniques auxquelles tu as pensé pour que je puisse améliorer mes readouts. Je regrette de ne pas avoir pu les intégrer, ou de n'avoir pas réussi à les faire marcher. Merci aussi pour les soirées jeux et les raclettes, c'était bien sympa et ces soirées vont me manquer ! Bon courage pour la fin, j'ai hâte de voir jusqu'où vous irez avec Denis pour ce beau projet.

Alison, je suis heureuse d'avoir pu te retrouver au labo après le M2, j'ai ainsi pu apprendre à mieux te connaître. Tu es quelqu'un d'adorable, à qui il arrive toujours quelque chose d'extraordinaire, et tu m'as beaucoup fait rire depuis que tu nous as rejoint. Je n'ai qu'un regret, ne pas avoir pu assister à un de tes spectacles d'impro, mais à charge de revanche !

Merci Camille, mon chat, ma chérie comme tu dis si souvent, pour tes conseils et toutes ces discussions dans les rues de Leiden. Ce voyage a été le moment où l'on s'est le plus rapprochées et où l'on a développé une grande complicité, ce qui fait que tu me manques beaucoup depuis que tu es partie loin, loin là-bas, aux USA !

Merci aussi à Jacques, tu as toujours su me prêter une oreille attentive et merci de m'avoir initiée à l'escalade toi aussi ! J'espère que tout se passe bien pour toi aux USA.

Merci aussi à mes copains du sport, Camille, Elora, Alexandre, Zeba, Francois, Julien, Léa pour votre soutien et votre aide à la préparation de la ceinture. Ces années passées avec vous ont ravivé mon affection pour notre sport, et je suis fière d'avoir obtenu ce diplôme à vos côtés.

Merci aussi aux copains de l'ENSTBB, Antoine, Mounir, Joëlle, Johanna, Adrien, Flo, et les autres, c'était super de continuer à vous voir, à partager de bons moments ensemble et pour ceux qui étaient à Toulouse, c'était génial pour faire la transition dans la vie après l'école, d'autant qu'étant tous dans le même bateau, on a pu se soutenir les uns les autres.

Merci à ma famille

Merci à tous mes oncles et mes tantes, ainsi qu'à mes cousins et à mes grands-parents pour votre soutien et la fierté que vous portez à mon égard. Toujours unis, nous partagerons ensemble encore beaucoup de merveilleux moments.

Merci à Pierre et Evelyne, mes beaux-parents, pour m'avoir accueilli dans votre famille comme une des vôtres. Je me suis toujours sentie bienvenue parmi vous, et vous remercie sincèrement pour tous les bons moments que nous avons partagés, les repas du samedi soir faits maison, les restos, les cinés et les promenades en montagnes. Tout cela va me manquer en partant, mais nous ouvrons maintenant de nouveaux horizons pour découvrir de nouveaux paysages, et partager de nouvelles aventures. Merci aussi à Romain, pour tes taquineries qui m'ont souvent permis de décompresser.

Merci à Arnaud, mon amoureux comme je dis toujours, pour ton soutien, ton amour, et ta force. Merci de toujours prendre mon parti face à l'adversité. Merci d'avoir géré et de t'être occupé de nos vacances aux Baléares et en Ecosse, pour tous ces moments de bonheur et de réconfort. On aura tenu le coup pendant ces 3 années, et nous voilà partis pour une nouvelle vie, sans la manche et l'hexagone qui nous séparent !

Enfin, merci à papa et maman, pour tout. Sans vous, je ne serais jamais arrivée jusqu'ici. Vous m'avez toujours laissé choisir mon chemin, et avez toujours été là pour me relever quand je tombais. Vous m'avez guidé tout en respectant mes choix, et je vous suis indéfiniment reconnaissante de toujours croire en moi, même quand je pense que je n'en suis pas capable, que je ne peux pas le faire, vous m'avez toujours soutenu le contraire, et au final, vous avez toujours raison. Alors merci encore, pour être de si bons parents, car cette réussite n'est pas seulement la mienne, c'est aussi la vôtre. En attendant que j'ai le prix Nobel, célébrons cette étape, et en route pour de nouvelles aventures !

Scientific contributions

The work presented in this manuscript aims at understanding the mechanisms by which *Mycobacterium tuberculosis* (Mtb) infection exacerbates the replication of the human immunodeficiency virus (HIV-1) in macrophages, in the context of co-infection. More precisely, my PhD project involved the identification of novel factors involved in this phenomenon, which in the future could be used as a diagnostic tool or therapeutic target to improve the diagnosis of co-infected patients, as well as monitoring disease progression. The studies performed during my time at IPBS in the laboratories of Drs O. Neyrolles and I. Maridonneau-Parini, under the supervision of Drs G. Lugo-Villarino and C. Vérollet led to articles that have been published in various peer-review international scientific journals while others remain in the preparation process.

The first paper presented in the current manuscript, in the introduction section is:

1. Tunneling Nanotubes: Intimate Communication between Myeloid Cells. **Dupont M**, Souriant S, Lugo-Villarino G, Maridonneau-Parini I, Vérollet C. *Front Immunol.* 2018 Jan 25;9:43. doi: 10.3389/fimmu.2018.00043. eCollection 2018. Review. **PMID:** 29422895

I participated to the bibliographical research and to the writing of the review, in collaboration with Drs C. Vérollet and G. Lugo-Villarino. Dr. S. Souriant was responsible for the figure presented in the review and, together with Dr. I. Maridonneau-Parini, she helped with the manuscript corrections.

The second article presented in this document is an original research article:

2. Tuberculosis Exacerbates HIV-1 Infection through IL-10/STAT3-Dependent Tunneling Nanotube Formation in Macrophages. Souriant S, Balboa L, **Dupont M**, Pingris K, Kviatcovsky D, Cougoule C, Lastrucci C, Bah A, Gasser R, Poincloux R, Raynaud-Messina B, Al Saati T, Inwentarz S, Poggi S, Moraña EJ, González-Montaner P, Corti M, Lagane B, Vergne I, Allers C, Kaushal D, Kuroda MJ, Sasiain MDC, Neyrolles O, Maridonneau-Parini I, Lugo-Villarino G*, Vérollet C*. *Cell Rep.* 2019 Mar 26;26(13):3586-3599.e7. doi: 10.1016/j.celrep.2019.02.091. **PMID:** 30917314

* : *equivalent contribution of the authors to the work*

Upon arrival to the laboratory, I reproduced the phenotype obtained after monocyte exposure to a tuberculous-associated microenvironment, *i.e.* the upregulation of the following markers: CD16, CD163 and MerTK. I also reproduced the exacerbation of HIV-1 replication in macrophages in the co-infection context. I also performed, analyzed and interpreted the experiments requested during the revision process of the manuscript (detailed further in the Result Section – chapter I) and helped with the manuscript corrections.

The third paper presented here has been submitted to Cell Reports journal:

3. Tuberculosis-associated IFN-I induces Siglec-1 on microtubule-containing tunneling nanotubes and favours HIV-1 spread in macrophages. **Dupont M**, Souriant S*, Balboa L*, Vu Manh TP, Pingris K, Rousset S, Cougoule C, Rombouts Y, Poincloux P, Ben Neji M, Allers C, Kaushal D, Kuroda MJ, Benet S, Martinez-Picado J, Izquierdo-Useros N, Sasiain MC, Maridonneau-Parini I#, Neyrolles O#, Vérollet C#¶ and Lugo-Villarino G#¶

* and # : equivalent contribution of the junior (*) and senior (#) authors to the work

¶: corresponding authors

In this article, I performed the majority of the experiments, except those involving macaques' infection, follow-up and sacrifice, along with the histological staining that were performed by our collaborators (Drs. MJ Kuroda and D. Kaushal) and the histology platform of Toulouse-Purpan. However, I quantified all histological staining of the alveolar macrophages. I also analysed (except the raw transcriptomic data which were processed by TP Vu Manh), quantified and interpreted all data obtained in this study and constructed the majority of the figures, including movies. Finally, I participated in the writing and correction of the manuscript.

The last paper presented in this document is a paper manuscript under preparation concerning the second objective of my PhD thesis:

4. Unpublished data: Dysregulation of the type-I Interferon signaling pathway by Mycobacterium tuberculosis leads to HIV-1 exacerbation in human macrophages

For this part, I performed the vast majority of the experiments, analyzed all the data, and I created the figures. I received help from my master student, Stella Rousset, who I trained for her master degree to do flow cytometry, qPCR and western blots, but also from our team engineer, Karine Pingris, for WB and qPCR experimentations, which allowed us to confirm the upregulation of several ISG at both mRNA and protein levels in cmMTB-treated cells.

Before my thesis, I had the chance to do my master internship at IPBS, under the supervision of Drs. C. Vérollet and B. Raynaud-Messina in the team of Dr I. Maridonneau-Parini. During my 6-month internship, I spend a month in the laboratory of Dr S. Bénichou, Institut Cochin, Paris, where I learned how to work in a BSL-3 facility and to efficiently perform HIV-1 transfer experiments. This expertise was used to produce data for our research project on the mechanisms of infection of osteoclasts and how their functions are modified upon infection. The results I obtained were part of an original research article that was published in PNAS in 2018:

5. Bone degradation machinery of osteoclasts: An HIV-1 target that contributes to bone loss. Raynaud-Messina B, Bracq L*, **Dupont M***, Souriant S, Usmani SM, Proag A, Pingris K, Soldan V, Thibault C, Capilla F, Al Saati T, Gennero I, Jurdic P, Jolicoeur P, Davignon JL, Mempel TR, Benichou S, Maridonneau-Parini I, Vérollet C.

Proc Natl Acad Sci U S A. 2018 Mar 13;115(11):E2556-E2565. doi: 10.1073/pnas.1713370115. Epub 2018 Feb 20.

PMID: 29463701

* : *equivalent contribution of the authors to the work*

My contributions for this paper were mainly experimental, as I acquired the viral cell-to-cell transfer system used by our collaborators in Paris. I performed, analysed and quantified all data presented in Figure 3 and participated in manuscript corrections.

Finally, during my thesis, I also participated in a study conducted by our Argentinian collaborators on the mechanisms involved in the formation of foamy macrophages upon *Mycobacterium tuberculosis* infection of macrophages:

6. Formation of Foamy Macrophages by Tuberculous Pleural Effusions Is Triggered by the Interleukin-10/Signal Transducer and Activator of Transcription 3 Axis through ACAT Upregulation. Genoula M, Marín Franco JL*, **Dupont M***, Kviatcovsky D, Milillo A, Schierloh P, Moraña EJ, Poggi S, Palmero D, Mata-Espinosa D, González-Domínguez E, León Contreras JC, Barrionuevo P, Rearte B, Córdoba Moreno MO, Fontanals A, Crotta Asis A, Gago G, Cougoule C, Neyrolles O, Maridonneau-Parini I, Sánchez-Torres C, Hernández-Pando R, Vérollet C, Lugo-Villarino G, Sasiain MDC, Balboa L.

Front Immunol. 2018 Mar 9;9:459. doi: 10.3389/fimmu.2018.00459. eCollection 2018.

PMID: 29593722

* : *equivalent contribution of the authors to the work*

For this work, I was involved in the experimental procedures and analysis (Figure 6 and 7) as well as the training of the first author of the paper when she came for several internships at IPBS to learn new techniques. I also participated in the revision process and the manuscript corrections.

Table of content

Abstract	1
Résumé.....	2
Acknowledgements	3
Scientific contributions.....	9
Table of content	12
Abbreviations	17
Table index	21
Figures index.....	22
Preamble	24
I. Monocytes-macrophages at a glance.....	26
A. Monocytes.....	26
B. Macrophages	28
II. Type I interferon responses in macrophages.....	30
Part 1: Introduction to the co-infection between <i>Mycobacterium tuberculosis</i> and HIV-1	33
Chapter I: <i>Mycobacterium tuberculosis</i> infection and the macrophage response	34
I. <i>Mycobacterium tuberculosis</i> : the etiological agent of tuberculosis	34
A. Koch's tubercle bacillus	34
a. Historical perspective	34
b. Epidemiology	36
c. Pulmonary and extra-pulmonary disease	37
d. Mycobacteria taxonomy and characteristics	37
e. The mycobacterial cell envelope.....	38
B. Therapeutic tools to detect and treat tuberculosis	40
a. Prevention	40
b. Diagnostic.....	42
c. Treatment.....	44
II. Macrophages at the heart of host-pathogen interactions with <i>Mycobacterium tuberculosis</i>	46
A. Physiopathology of the <i>Mycobacterium tuberculosis</i> infection.....	46
a. Establishment of the cellular response	46
b. Importance of cytokines in the immune response.....	50

B.	Macrophages and <i>Mycobacterium tuberculosis</i> : an ongoing evolutionary arms-race	53
a.	Mtb recognition through PRR and initiation of the host response	53
i.	Toll Like Receptors (TLR)	53
ii.	C-type lectin receptors (CLR)	54
	(1) MRC1 (CD206)	54
	(2) DC-SIGN (CD209)	54
iii.	Other receptors	55
b.	Macrophages and Mtb immunity: a complex interplay between bacterial control and escape mechanisms	56
i.	The Mtb phagosome	56
ii.	Oxidative and hypoxic stresses in response to Mtb internalization	58
iii.	Nutrients deprivation	59
iv.	Bacterial intoxication with metals	60
c.	Role of specific macrophages subsets induced by Mtb infection	61
i.	Macrophages polarization in Mtb-infection	61
ii.	Multinucleated Giant Langhans Cells	62
iii.	Foamy macrophages: an energy reservoir for the bacteria	62
C.	Induction of the innate immune type I interferon response	65
a.	Role of IFN-I in bacterial infection	65
b.	Accentuated IFN-I responses during active tuberculosis	66
c.	Balance between IL-1 β and IFN-I in TB-disease	68
D.	Establishment of a chronic inflammation to promote <i>Mycobacterium tuberculosis</i> transmission.	70
a.	Obligate pathogen	70
b.	Effect on the monocyte/macrophage compartment	71
i.	Impact on monocytes	71
ii.	Impact on macrophages	72
	Chapter II: Aspects of the immune response to HIV-1 infection	74
I.	HIV-1 infection: an overview	74
A.	History of AIDS and epidemiology	74
a.	History and origins of HIV	74
b.	Epidemiology	76
B.	Therapeutic tools to fight the epidemic	78
a.	Transmission and prevention	78

b.	Diagnosis and treatment	79
i.	Diagnosis.....	79
ii.	Treatment.....	79
II.	Physiopathology of HIV infection and immune defenses	80
A.	What is HIV-1?	80
a.	Generalities about the virus	80
i.	Taxonomy	80
ii.	Structure and genome.....	82
iii.	Viral tropism	84
b.	General course of the infection and critical features.....	86
B.	HIV-1-induced immune activation is a critical feature of HIV-1 chronic phase establishment 87	
a.	Alteration of the gut barrier and impact on immune system activation	87
b.	Systemic immune cell activation induces the recruitment of target cells to the site of infection, along with premature immune senescence.....	88
C.	The host IFN-I responses in HIV-1 infection	89
a.	Potentials of IFN-I as therapeutic tools in humans	89
b.	IFN-I responses in HIV-1 pathogenesis: what we have learned from animal models... 91	
i.	Expected antiviral effect in the early phase of the infection	91
ii.	Deleterious consequences during chronic infection	92
c.	Specific cellular responses to HIV-1 induced IFN-I: a zoom into macrophages	94
i.	PRR-mediated recognition of HIV-1 leads to antiviral gene expression	94
ii.	HIV-1 is able to avoid IFN-I induction in macrophages	96
iii.	Restriction factors and how HIV-1 circumvents them in macrophages.....	96
III.	Intimate relationship between HIV-1 and the host: a focus on macrophages	99
A.	Contribution of macrophages to AIDS in human and animal models.....	100
a.	Mouse model.....	100
b.	NHP	100
c.	Humans.....	101
d.	Evidence of macrophages as a main reservoir for HIV.....	101
B.	Viral replication cycle in macrophages and its consequences	103
a.	Entry	103
b.	Nuclear import	104
c.	Transcription.....	106

d.	Assembly and release	106
e.	Consequences on macrophage functions	109
C.	Macrophages in HIV-1 latency and communication with other cell types	110
a.	Induction of latency in macrophages	110
b.	Role of macrophage the establishment of CD4 ⁺ T cells reservoir	111
c.	Interplay with other cell-types: importance of exosomes	112
D.	HIV-1 cell-to-cell transfer: a master in disguise	113
a.	Role of lectins in HIV-1 capture and trans-infection	113
i.	C-type lectins: recognition of the viral protein gp120	113
ii.	Sialic acid-binding immunoglobulin-type lectin: Siglec-1	114
b.	The virological synapse.....	117
c.	Phagocytosis of infected T-cells by macrophages.....	118
d.	HIV-1-induced cell fusion mechanisms	118
e.	Tunneling nanotubes: bridges for HIV-1 spread	119
	Chapter III: <i>Mycobacterium tuberculosis</i> -HIV-1 co-infection - the deadly duo.....	128
I.	Clinical considerations of the co-infection	128
A.	Historical overview	128
B.	Synergy between HIV-1 and Mtb	130
C.	Clinical challenges raised by the co-infection	131
a.	Difficulty to diagnosis	131
b.	Drug interactions and TB IRIS.....	131
II.	HIV-1 exacerbates Mtb growth	132
A.	Depletion of Mtb-specific effector T cells	132
B.	Functional changes in Mtb-reactive T cells	133
C.	Alteration of the macrophage response	134
a.	Alteration of cytokines responses and cell death	134
b.	Inhibition of phagocytosis and autophagy	136
III.	Mtb exacerbates HIV-1 replication.....	136
A.	Mtb triggers viral transcription in infected cells	138
B.	Mtb accelerates the progression to AIDS by increasing HIV-1 strains diversity	140
C.	Mtb renders cells permissive to HIV-1 infection and favours viral cell-to-cell transmission	140
	Thesis objectives.....	142
	Part 2: Results	144

Chapter IV: Tuberculosis exacerbates HIV-1 infection through IL-10/STAT3-dependent tunneling nanotube formation in macrophages.	145
I. Paper summary	145
II. Results	147
III. Scientific contribution to the paper	185
Chapter V: Tuberculosis-associated IFN-I induces Siglec-1 on microtubule-containing tunneling nanotubes and favours HIV-1 spread in macrophages.	188
I. Paper summary	188
II. Results	190
III. Discussion	235
Chapter VI: Dysregulation of the type-I Interferon signaling pathway by <i>Mycobacterium tuberculosis</i> leads to HIV-1 exacerbation in human macrophages	240
I. Introduction.....	240
I. Results	241
II. Discussion	256
Part 3: Discussion and perspectives	240
References.....	269
Annex.....	314
I. Formation of Foamy Macrophages by Tuberculous Pleural Effusions Is Triggered by the Interleukin-10/Signal Transducer and Activator of Transcription 3 Axis through ACAT Upregulation.....	314
II. Tuberculosis is associated with expansion of a motile, permissive and immunomodulatory CD16(+) monocyte population via the IL-10/STAT3 axis.....	314
III. Bone degradation machinery of osteoclasts: An HIV-1 target that contributes to bone loss.	314

Abbreviations

AIDS	acquired immuno-deficiency syndrom	CPZ	chimpanzees
2D	two dimension	CSF-3	colony-stimulating factor 3
3D	three dimension	CTL	cytotoxic T cell
ACAT	acetyl-CoA acetyltransferase	CXCR4	C-X-C chemokine receptor 4
ADAM9	disintegrin and metalloproteinase domain-containing protein 9	CYPA	cyclophilin A
Ag85	antigen 85	DAI	DNA-dependent activator of IFN
AGM	african green monkeys	DAPI	4',6-diamidino-2-phénylindole
AMP	adenosine monophosphate	DC	dendritic cell
AnsA	asparaginase A	DCIR	dendritic cell immunoreceptor
Ansp1	asparagine transporter	DC-SIGN	dendritic cell-specific intercellular adhesion molecule-3-grabbing non-integrin
AP-1	adaptor protein 1	DC-STAMP	dendritic cell-specific transmembrane protein
Arg1	arginase 1	DIM	phitiocerol dimycocerosate
ASK1	Apoptosis signal-regulating kinase 1	DNA	deoxyribonucleic acid
ATP	adenosine triphosphate	dNTP	deoxyribonucleotide triphosphate
ATPase	adenosine triphosphatase	EEA1	early endosomal antigen 1
AZT	azidothymidine	ELISA	enzyme-linked immunosorbent assay
B.C.	Before Christ	Env	envelop
BAL	broncho-alveolar lavage	ESAT-6	6kDa early secretory antigenic target
BCG	Bacillus Calmette-Guerin	ESX-1	early secretory antigenic target 6 system-1
BLT mouse	Bone, Liver, Thymus humanized mouse	FcγRIII	Fc gamma receptor type III
BST-2	bone marrow stromal antigen 2	FDA	food and drug administration
C/EBPβ	CCAAT/enhancer-binding protein beta	GBP	guanylate-binding protein
(c)ART	(combined) antiretroviral therapy	GFP	green fluorescent protein
CCL	C-C motif chemokine ligand	GI	gastro-intestinal
CCR5/7, ...	C-C chemokine receptor 5/7, ...	GM3	monosialodihexosylganglioside
CD4/8, ...	cluster of differentiation 4/8, ...	GM-CSF	granulocyte macrophage colony-stimulating factor
CFP-10	cell filtrate protein 10	GMP	guanosine monophosphate
CFU	colony forming unit	gp41/120, ...	glycoprotein 41/120, ...
cGAMP	Cyclic guanosine monophosphate–adenosine monophosphate	GPI	glycosylphosphatidylinositol
cGAS	cyclic GMP-AMP Synthase	GTP	guanosine triphosphate
CLR	C-type lectin receptor	GTPase	guanosine triphosphatase
cmCTR	conditioned media from control cells	Hck	hematopoietic cell kinase
cmMTB	conditioned media from Mtb-infected cells	HIV-1	human immunodeficiency virus type 1
CPSF6	polyadenylation specific factor 6	HLA-DR	human leukocyte antigen-DR

HRP	horse radish peroxidase	LTR	long terminal repeat
HSC	hematopoietic stem cell	LXA4	lipoxin A 4
ICAM	intercellular adhesion molecule	ManLAM	mannose-capped lipoarabinomannan
IDO	indoleamine 2,3-dioxygenase	MAPK	mitogen-activated protein kinase
IFI16	interferon-inducible myeloid differentiation transcriptional activator	MarP	mycobacterium acid resistance protease
IFIT	interferon-induced protein with tetratricopeptide repeats	MCP-1	monocyte chemoattractant protein-1
IFN	interferon	M-CSF	macrophage-colony stimulating factor
IFNAR	Interferon α/β receptor	MDA5	melanoma Differentiation-Associated protein 5
IFNγR	interferon gamma receptor	MDM	monocyte-derived macrophages
IFN-I	type I interferon	MDR	multi-drug resistant
IgG	Immunoglobulin G	MerTK	myeloid-epithelial-reproductive tyrosine kinase
IGRA	interferon-gamma release assay	MGC	multi-nucleated giant cells
IKKϵ	I κ B kinase ϵ	MGLC	Multi-nucleated giant langhans cells
IL-1/12, ...	interleukin 1/12, ...	MHC-I/II	major histocompatibility complex type I/II
ILI	intracytosolic lipid inclusion	MMP	matrix metallo-proteinase
iNOS	induced nitric oxide synthase	MOI	multiplicity of infection
INSTI	integrase strand transfer inhibitors	MoM	myeloid-only mouse
IRF3/7, ...	interferon regulator factor 3/7, ...	MRC1	mannose receptor
IRIS	immune reconstitution inflammatory syndrome	MSM	men having sex with men
ISG	interferon stimulated gene	Mtb	<i>Mycobacterium tuberculosis</i>
ISGF3	ISG factor 3	MTBC	<i>Mycobacterium tuberculosis</i> complex
ISRE	interferon stimulated response element	MX1/2	myxovirus resistance 1/2
JAK	janus kinase	MyD88	myeloid differentiation primary response 88
KatG	catalase-peroxidase	NADPH	nicotinamide adenine dinucleotide phosphate
kb	kilo base	Nef	negative regulatory factor
kDa	kilo Dalton	NFATc	nuclear factor of activated T-cells
KIF3A	kinesin-like protein F3A	NFκB	nuclear factor kappa B
KO	knock-out	NHP	non-human primate
LAM	lipoarabinomannan	NK	natural killer
LAMP-2	lysosomal-associated membrane protein	NKT	natural killer T cell
LEF-1	lymphoid enhancer-binding factor-1	NLR	NOD-like receptor
LFA-I	lymphocyte function-associated antigen 1	NLRP	NOD-like receptor family, pyrin domain containing 3
LM	lipomannan	NNRTI	non-nucleoside reverse transcriptase inhibitors
LPS	lipopolysaccharide	NO	nitric oxide
LRRK2	Leucine-rich repeat kinase 2	NOD	nucleotide-binding oligomerization domain-containing protein
		NOS	nitric oxide synthase

NOX2	nicotinamide adenine dinucleotide phosphate oxidase 2	Siglec	Sialic acid-binding immunoglobulin-type lectins
Nramp1	natural resistance-associated macrophage protein 1	siRNA	Small interfering RNA
NRTI	nucleotide reverse transcriptase inhibitors	SIV	simian immunodeficiency virus
NS	Nitric oxide species	sMerTK	soluble MerTK
NTM	non-tuberculous mycobacteria	SOCS	Suppressor of cytokine signaling
OAS1	2'-5'-Oligoadenylate Synthetase 1	STAT	Signal transducer and activator of transcription
OASL	2'-5'-oligoadenylate synthetase-like protein	STI	successive treatment interruption
PAMP	pathogen-associated molecular pattern	STING	stimulator of interferon genes
PBMC	peripheral blood mononuclear cell	TAG	triacylglycerol
PD-1	programmed death 1	TANK	TRAF family member-associated NF-kappa-B activator
pDC	plasmacytoid dendritic cell	TB	tuberculosis
PD-L1	programmed death ligand 1	TBK1	TANK-binding kinase 1
PEG-IFNα	pegylated-interferon alpha	TCR	T cell receptor
PEP	post-exposition prophylaxy	TDM	trehalose dimycolate
PE-TB	pleural effusion from tuberculous patient	TDR	totally drug resistant
PET-SCAN	positron-emission tomography scanner	TGFβ	transforming growth factor beta
PGE2	prostaglandin E2	Th	T helper
PI	phosphatidyl-myo-inositol	TIM4	T-cell immunoglobulin mucin protein 4
PI3K	phosphoinositide 3-kinase	TLR	Toll-like receptor
PI3P	phosphatidylinositol 3-phosphate	TNFα	tumor necrosis factor alpha
PIC	pre-integration complex	TNT	tunelling nanotube
PIM	phosphatidyl- <i>myo</i> -inositol mannosides	TNTi	tunelling nanotube inhibitor
PPARγ	peroxisome proliferator-activated receptor gamma	TREX	repair exonuclease 1
PrEP	pre-exposition prophylaxy	TRIM5a	tripartite motif-containing protein 5
PRR	pattern recognition receptor	TST	tuberculin-skin test
pSTAT	phosphorylated-STAT	TYK2	tyrosine kinase 2
RalA	Ras-related protein A	USP18	ubiquitin specific peptidase 18
RD1	region of difference 1	VCC	virus-containing compartment
RIG-I	retinoic acid-inducible gene I	Vif	viral infectivity factor
RNA	Ribonucleic acid	VLP	virus-like particles
ROS	reactive oxygen species	Vpr	viral protein R
RTC	reverse transcription complex	Vpu	viral protein U
RT-qPCR	reverse transcription-quantitative polymerase chain reaction	VSVG	vesicular stomatitis virus glycoprotein
SAMHD1	sterile α motif domain and histidine aspartic acid (HD) domain 1	WHO	world health organization
sCD163	soluble CD163	WT	wild type
SCID	severe combined immunodeficiency	XDR	extremely drug resistant
SHP2	Src homology region 2 domain-containing phosphatase-2		

Table index

Table 1: Monocytes subsets and their functions (from [5]).....	25
Table 2: Macrophages activation profiles and nomenclature (adapted from [6]).....	25
Table 3: Summary of the global HIV epidemic (from [262])	75
Table 4: Gene transcriptomic signature and expression in cmMTB-treated cells compared to control.	246

Figures index

Figure 1: Distribution and functions of tissular macrophages (adapted from [14])	27
Figure 2: Type I interferon induction and signaling pathway (adapted from [18], [19])	29
Figure 3: Immuno-suppression induced by IFN-I (from [18]).....	31
Figure 4: New Mtb infections worldwide in 2017 (from [1]).....	35
Figure 5: Structure of the mycobacterial cell wall (adapted from [54]).....	39
Figure 6: BCG vaccination efficiency.	41
Figure 7: Spectrum of tuberculosis disease and associated diagnosis (adapted from [35]).....	43
Figure 8: Epithelial secretion of MMP9 and innate cells recruitment to the site of infection (from [86])	45 47
Figure 9 : Macrophages activation profile during Mtb infection (adapted from [95])	47
Figure 10: The cellular response to Mtb infection (from [71]).....	49
Figure 11: The mature tuberculous granuloma structure (from [86])	51
Figure 12: Lipid bodies structure (adapted from [198]).....	63
Figure 13: Dichotomy of IFN-I responses during Mtb infection (adapted from [233]).....	67
Figure 14: Necrosis of Mtb-infected macrophages (from [86])	69
Figure 15: Increased risk incidence of acquiring HIV among key populations, global (from [262]).....	77
Figure 16: Number of HIV new infections from 1990 to 2018 with 2020 milestone, global (from [262])	77
Figure 17: HIV-1 virion structure observed by electron microscopy (from [309]).....	81
Figure 18: HIV-1 virion structure	81
Figure 19: HIV-1 genome.....	81
Figure 20: HIV-1 entry into target cell (from [310]).	83
Figure 21: General course of HIV-1 progression (adapted from [331]).	85
Figure 22: HIV-1 replication cycle and restriction factors (from [406]).	93
Figure 23: Sensing of HIV-1 (from [406]).....	95
Figure 24: Virus-containing compartments are not late endosomes (from [516]).....	105
Figure 25: Virus-containing compartments ultrastructural reconstitution (from [528])	107
Figure 26: Siglec-1 captures, internalizes particles in virus-containing compartments, and transfers HIV-1 from myeloid cell to T cells (adapted from [630]).....	115
Figure 27: Historical timeline showing advances in the co-infection fight ([263])	127

Figure 28: HIV-1 and Mtb synergy increases the risk of progression of both pathologies (from [675]).	129
Figure 29: Nef impairs the macrophage phagosome maturation and alters the Mtb control (from [675]).	137
Figure 30: <i>In vivo</i> evidence of co-infected macrophages (from [753])	139
Figure 31: Mtb infection and TB-associated environment induce C-type lectin receptor expression on macrophages.	139
Figure 32: Quantification of tunneling nanotube (TNT) formation in several conditions.	186
Figure 33: Siglec-1 and GM3 are localized on thick TNTs.....	236
Figure 34: Structure and stability of TNT.	236
Figure 35: The cmMTB-treated macrophages are characterized by an IFN-I signature, which is also found in TB patient monocytes and whole blood.	246
Figure 36: The interferon-stimulated gene signature obtained in the transcriptome and cell phenotype depend on the timing of cmMTB conditioning.	248
Figure 37: The interferon-stimulated gene signature of cmMTB cells is deleterious for the control of HIV-1 replication.....	250
Figure 38: IFN-I exposure upon cmMTB treatment renders cells hypo-responsive to additional stimulation with IFN β	252
Figure 39: The IFN-I inducible USP18 regulatory factor seems responsible for the exacerbation of HIV- 1 replication in cmMTB cells.	254
Figure 40: cmMTB-treatment induces the expression of the IFN-I receptor IFNAR.	255
Figure 41: cmMTB upregulates OASL and IRF7 gene expression, but not IRF7 protein level.....	255
Figure 42: OASL inhibits type I interferon signaling by degrading IRF7 mRNA (inspired from [804]).	259
Figure 43: IFN-I negative regulators are enhanced by cmMTB during the course of HIV-1 infection, while restriction factors are downregulated.	261
Figure 44: The number of Siglec-1 ⁺ blood monocytes is increased in TB and TB-HIV-1 patients.	265

Preamble

The presented work has been conducted under the direction and collaboration of two teams at the Institute of Pharmacology and Structural Biology (IPBS) in Toulouse: the team of Dr O. Neyrolles, specialized in host-pathogen interactions in the context of tuberculosis (TB); and the team of Dr I. Maridonneau-Parini, specialized in phagocyte differentiation and functions under physiological and pathological conditions, including infection with the human immunodeficiency virus type 1 (HIV-1). A strong participation of Argentinian collaborators from the IMEX-CONICET Institute in Buenos Aires allowed us to get access to samples from TB patients, and sometimes from TB-HIV co-infected patients. Moreover, the laboratory of Dr M.C. Sasiain and Dr L. Balboa has a strong expertise in TB research, especially in the development of drug resistant TB. The long collaboration arrangement between these three laboratories has been granted the status of “Laboratoire International Associé” (LIA #1167), by the government scientific agencies in France (CNRS) and Argentina (Conicet), which also funded my PhD scholarship from the University of Toulouse.

The research program of the LIA is centered on the understanding of how *Mycobacterium tuberculosis* (Mtb), the etiological agent of TB, exacerbates HIV-1 infection and replication in macrophages. Indeed, TB-HIV-1 co-infection is a serious clinical issue at a global scale for several reasons. There are about 14 million co-infected individuals around the world, among which about 300 000 die every year [1]). A major problem in co-infection is that its diagnosis is quite complicated and difficult to detect since there are no biomarkers available to follow the progression of the disease. Moreover, co-infection diagnosis requires a large amount of resources that are not readily available everywhere, especially in low-income countries where co-infection prevalence is high. In addition, treatment of co-infected patients is challenging due to drug interactions. On top of that, it is well known that Mtb and HIV-1 act in synergy to potentiate one another within the host, notably by accelerating the deterioration of the immune system through mechanisms that are not fully understood yet. While it is widely accepted that HIV-1 induces susceptibility to TB due to CD4⁺ T cell depletion (important cell for the control of TB) [2], the mechanisms by which Mtb favours HIV-1 replication remain insufficiently understood. In the context of the LIA project and my PhD project, we focused on the role of macrophages in TB-HIV-1 co-infection, as these cells are the main target of Mtb and important target for HIV-1, as they mediate viral dissemination throughout the host and act as viral reservoirs (for more details, see introduction, chapter II section III.A.d.) [3], [4]. Two main tasks have been determined for our collaborative project: (i) mapping and characterizing the pathways established in macrophages during Mtb-driven exacerbation of HIV-1 infection, and (ii) identification of the changes in factors involved in macrophage activation and metabolic processes during Mtb-driven exacerbation of HIV-1 infection. During my PhD, I focused on the identification of novel factors induced by Mtb-associated environment that could participate to the exacerbation of HIV-1 replication in macrophages, by using a genome-wide transcriptomic analysis, and I identified the lectin receptor Siglec-1 and IFN-I/STAT1 signaling as important factors.

For all reasons stated above, I will focus my introduction on the macrophage responses in both Mtb and HIV-1 infection, with a specific emphasis on type I interferon (IFN-I) responses involved in both pathologies. The reason for this is that we found that IFN-I signaling pathway is the main pathway

Monocyte subset	Marker	Chemokine Receptor	Main functions
Classical	CD14 ^{high} CD16 ⁻	CCR2 ^{high} CX3CR1 ^{low}	Immune responses, phagocytosis
Intermediate	CD14 ^{high} CD16 ⁺	CCR2 ^{low} CX3CR1 ^{high}	Pro-inflammatory response, tissue repair
Non-classical	CD14 ^{low} CD16 ^{high}	CCR2 ^{low} CX3CR1 ^{high}	Patrolling, fibrosis

Table 1: Monocytes subsets and their functions (from [5])

	Pro-inflammatory macrophages			Anti-inflammatory macrophages		
NOMENCLATURE	M1	M1	M2a	M2b	M2c	M2d
	M(IFN γ)	M(LPS)	M(IL-4)	M(Immune complex)	M(IL-10)	M(IL-6)
INDUCTION	IFN γ	LPS	IL-4	Immune complex	IL-10	IL-6
DISTINCTIVE GENES	pSTAT1, IRF5, iNOS, Ido1, KYNU	IRF5	IRF4, SOCS1, GATA3, Arg1	-	SOCS3	VEGF
RECEPTORS	CD68, CD80, CD86, MHC-II	CD68, CD80, CD86, MHC-II	MHC-II, Dectin-1, MRC1, STAB1, MARCO, CD163	CD36, CD86, MHC-II, DC-SIGN	CD16, MerTK, CD163, MRC1	CD68, CD163, CD204, MHC-II, MRC1
MATRIX	-	MMP9	FN, TGFB1, MMP1, MMP12, TG	-	-	-
CYTOKINES	IL-12, IL-23, TNF α	TNF α , IL-6, IL-1 β	IL-10, TGF β , IL-1ra	IL-1, IL-6, IL-10, TNF α	IL-10, TGF β	IL-10, IL-12, TNF α , TGF β
CHEMOKINES	CCL18	CXCL10, IL-8	CCL4, CCL13, CCL17, CCL18	-	-	-
OTHER PRODUCTS	NOS, ROS	NOS, ROS	-	-	-	-
FUNCTIONS	Th1 response induction Intracellular pathogen killing Anti-tumoral growth	Th1 response induction Intracellular pathogen killing Anti-tumoral growth	Th2 response induction Parasite clearance	Th2 response induction Anti-tumoral growth Antigen presentation	Immuno-regulation Tissue remodelling Apoptotic bodies clearance	Angiogenesis Tumor-associated macrophages

Table 2: Macrophages activation profiles and nomenclature (adapted from [6])

modified in the TB context, and we thought it might have a role in the exacerbation of HIV-1 infection of macrophages (see Results, chapter III).

I. Monocytes-macrophages at a glance

Both monocytes and macrophages belong to the mononuclear phagocyte system and are involved in tissue homeostasis, host defense mechanisms against pathogens, auto-immune disease, and tissue repair [7]. These cells have an important role in the immune response, as they sequentially participate to danger signal recognition, leukocyte recruitment and migration to the site of inflammation, elimination of the inflammatory element and finally to the resolution of inflammation, which comprises tissue damage repair and subsequent return to homeostasis. When these mechanisms fail to clear the inflammatory element (*e.g.* bacteria, viruses), a constant danger signal persists in the host and leads to chronic inflammatory diseases [8]. Here, I will briefly discuss the origin, phenotype and function of monocytes and macrophages, as my PhD work is centered on the role of macrophages in Mtb and HIV-1 co-infection settings.

A. Monocytes

Monocytes are derived from the bone marrow, and more precisely from hematopoietic stem cells (HSC). They represent about 10% of blood circulating leukocytes in humans. Monocytes are categorized into three different subsets, according to their expression of two specific markers: CD14, the receptor for lipopolysaccharide (LPS), and CD16, a receptor belonging to the FcγRIII family [9]. The so-called “classical” monocytes are characterized by the high expression of CD14 and the absence of CD16 (CD14^{high}CD16⁻) and represent about 85-90% of the monocyte population under physiological conditions. The “intermediate” CD14^{high}CD16⁺ monocytes are less abundant and display pro-inflammatory properties. Upon inflammation, this population of monocytes expands [10], and is often correlated with disease severity, as in Mtb infection [251] (see Introduction, chapter I section II.D.b.i.), HIV-1 infection [11] (see Introduction, chapter II section II.A.a.iii.) or sepsis [12]. Finally, CD14^{low}CD16^{high} constitute the last subset of monocytes, also known as “non-classical” monocytes [13](see Table 1 for a summary of the different subset functions).

Functionally, monocytes establish the link between the induction of inflammatory responses by the innate immune system and the establishment of the adaptive immune response. As circulating innate immune cells, they can migrate from the blood into tissues, they are capable of phagocytosis, antigen presentation to T cells, cytokine production and present a strong phenotypical plasticity [9]. Indeed, the destiny of monocyte is to differentiate into innate immune cells, specialized in specific functions depending on the tissue where they migrate, their microenvironment and the physiological or pathogenic context. Depending on the signals they receive, monocytes differentiate into dendritic cells (DC) or macrophages, which then adopt the appropriate phenotype to fulfil the specific functions associated to tissue specificity.

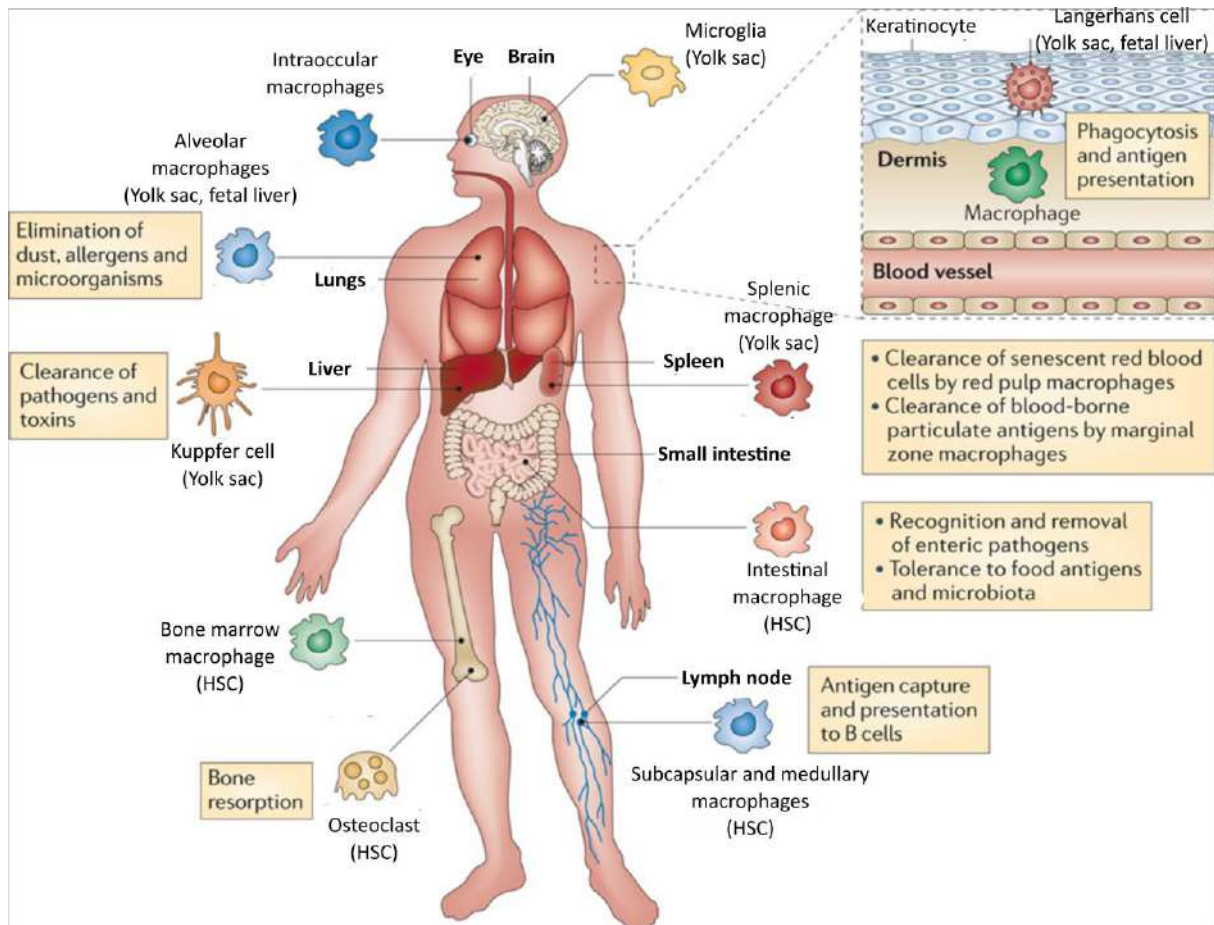


Figure 1: Distribution and functions of tissue macrophages (adapted from [14])

Mononuclear phagocytes can be generated from the yolk sac during embryogenesis, from fetal liver, or from committed haematopoietic stem cells (HSC) located in the bone marrow. Macrophage precursors of hematopoietic origin are released into the blood circulation as monocytes. They quickly migrate into any tissues of the body, where they differentiate into mature macrophages to replenish the tissue macrophage pool. Certain tissue macrophages, which originate from the yolk sac, are capable of self-renewal and are particularly long-lived. Various populations of mature tissue macrophages are strategically located throughout the body and perform important immune surveillance activities, including phagocytosis (e.g. alveolar macrophages, splenic macrophages), antigen presentation (e.g. Kupffer cells, subcapsular macrophages) and immune suppression (e.g. intestinal macrophages).

B. Macrophages

Like monocytes, macrophages are involved in tissue homeostasis, defense against invaders and tissue repair. In addition, macrophages are important for embryogenic development [9]. Several types of macrophages have been described, according to their origin, functions and the developmental stage of the organism. Primitive macrophages originate from the yolk sac and appear during the first stages of embryonic development. They are long-lived tissue resident macrophages (*e.g.* microglia in the brain, Kupffer cells in the liver or macrophages in the pancreas) and are capable of *in situ* self-renewal during adult life. Fetal liver macrophages are closer to macrophages found in adults. They are present in the majority of organs (*e.g.* splenic macrophages, Langerhans cells in the derma), and are renewed, at least in part, by macrophages deriving from HSC of the bone marrow (*e.g.* macrophages in the heart or the gastro-intestinal (GI) tract) [15]. In certain tissues, macrophages display mixed origins and fulfil different functions (Figure 1). For example in the lung, alveolar macrophages come from embryogenic origins (*i.e.* from the yolk sac and replenish independently of blood monocyte differentiation), while interstitial macrophages derive from hematopoietic origin and are renewed by circulating monocytes [15].

Macrophages are highly plastic cells, able to adapt their phenotype and function to their microenvironment. In the bone for instance, the main myeloid cells are osteoclasts, cell specialized in bone degradation while in the GI tract, monocyte-derived macrophages are specialized in phagocytosis [14]. According to their environment, and particularly during inflammation, macrophages acquire an activation or polarization program. By definition, macrophage activation/polarization (both terms are used interchangeably in this manuscript) correspond to the cell perturbation in response to an exogenous agent (*e.g.* cytokines, growth factors, pathogens), which results in a distinct pattern of gene and protein expression within and at the surface of macrophages [6]. Historically, macrophage activation was separated into two categories: classical “M1” pro-inflammatory macrophages and non-classical “M2” anti-inflammatory macrophages, based on the type-1 and type-2 (Th1 and Th2) immunity possessed by T cells [16]. However, this nomenclature poorly reflects the spectrum of macrophage polarization profiles. Therefore, a scientific consensus was implemented and proposed that the nomenclature to the specific signals induced upon macrophage activation, also taking into account the factors expressed by these macrophages (refer to table 2)[6]. Typically, “M1” macrophages are polarized in response to IFN γ , TNF α , and LPS (M(IFN γ), M(TNF α), and M(LPS) respectively). Generally, the “M1” macrophage family is highly microbicidal and anti-tumoral, produce pro-inflammatory cytokines and are resistant to intracellular pathogens. Their antimicrobial function mainly derives from their capacity to produce reactive oxygen (ROS) and nitrogen species by inducing NADPH oxidase (nicotinamide adenine dinucleotide phosphate oxidase) and inducible nitric oxide synthase (iNOS). Conversely, “M2” macrophages are mainly anti-inflammatory and immunoregulatory. They usually balance the host response to avoid tissue damage. The “M2” category comprises several types of macrophages, including:

- M(IL-4) or M(IL-13), responsible for tissue repair and control of allergy and parasite infection [17];
- M(Immune complex), strong antigen presenting cells, particularly important in anti-tumoral responses;

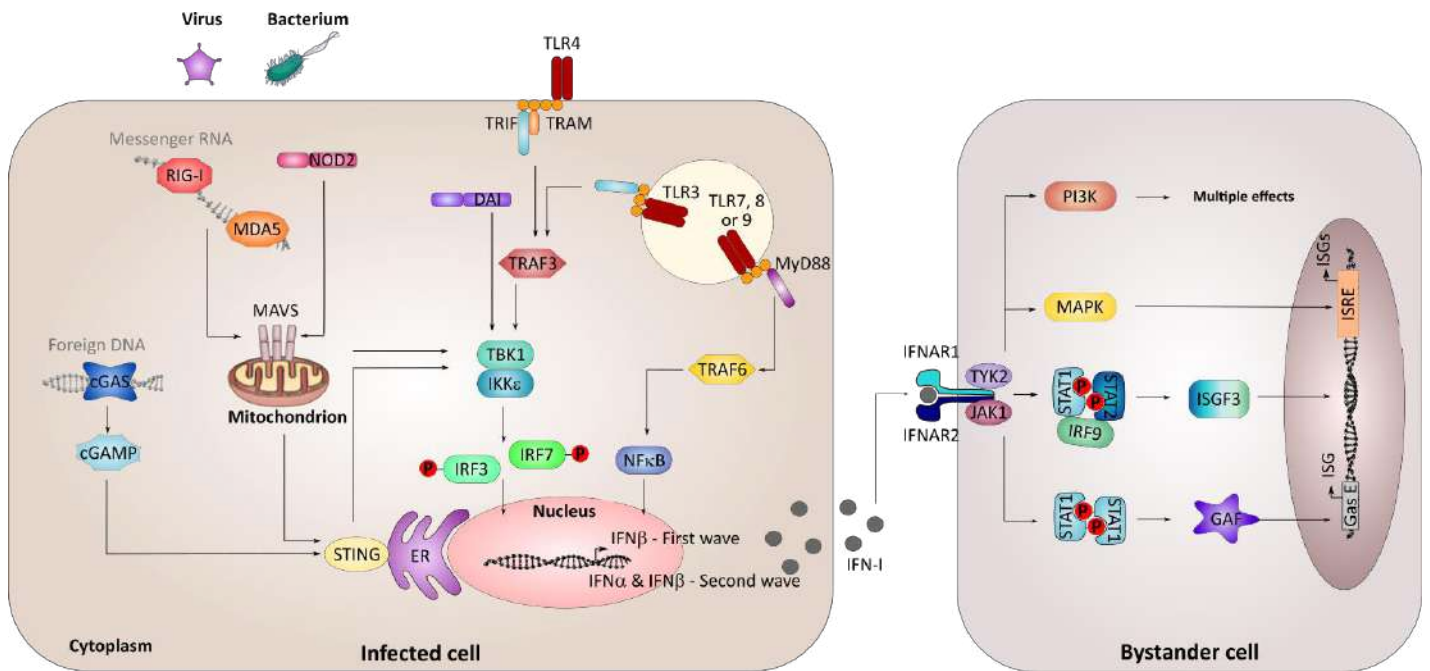


Figure 2: Type I interferon induction and signaling pathway (adapted from [18], [19])

Upon pathogen attack, microbial products are recognized through different cell-surface and intracellular pattern recognition receptors (PRR), including Toll-like receptors (TLR), RNA and DNA sensors and NOD-like receptor (NLR), which engage different signaling pathway to lead to the induction of a first wave of IFN β . This is followed by a second wave of IFN-I production, including all subtypes. IFN-I will activate the infected cell and bystander cells by binding to its receptor, IFNAR. Consequently, multiple downstream signaling pathways can be induced, leading to a diverse range of biological effects, the main consequence being the induction of IFN-inducible gene (ISG) induction. Both MAPK and ISGF3 complex, composed of STAT1-STAT2 heterodimers and IRF9, activate the IFN-stimulated response elements (ISRE) in gene promoters, leading to induction of a large number of ISG. IFN-I can also signal through STAT1 homodimers, which are more commonly associated with the IFN γ -mediated signalling pathway. Other signaling pathways like PI3K activate a response to IFN-I, leading to diverse effects on the cell.

cGAS: cytosolic GAMP synthase; cGAMP: cyclic di-GMP-AMP; DAI: DNA-dependent activator of IRF; ER: endoplasmic reticulum; GAS E: cGAS-activated sequence; IKK ϵ : I κ B kinase- ϵ ; MAVS: mitochondrial antiviral signalling protein; MDA5: melanoma differentiation-associated gene 5; MyD88: myeloid differentiation primary response protein 88; NF κ B: nuclear factor- κ B; NOD2: NOD-containing protein 2; STING: stimulator of IFN genes; TBK1: TANK-binding kinase 1; TRAF: TNF receptor-associated factor; TRAM: TLR adaptor molecule; TRIF: TIR domain-containing adaptor protein inducing IFN β ; TYK2: tyrosine kinase 2; JAK1: Janus kinase 1; IRF: interferon regulatory factor.

- M(IL-6), which are more pro-inflammatory than the others and associated with a poor prognosis in patients with cancer [20]; and
- M(IL-10), involved in the clearance of apoptotic bodies and inhibition of Th1 responses, while they induce tolerance in the tissue by activating regulatory T cells [21].

During the course of inflammation, a dynamic modification of macrophage polarization occurs, resulting in either beneficial or detrimental outcomes for the host, according to the nature and stage of the inflammation. For example, as discussed in the rest of this manuscript, the transition from “M1” polarization towards an “M2” (general term used here to include the different pro-inflammatory – M(IFN γ), M(TNF α) - and anti-inflammatory macrophages – M(IL-4), M(IL-10), respectively) profile during a pathological infection, with either Mtb or HIV-1, is associated with the establishment of disease chronicity and aggravation.

II. Type I interferon responses in macrophages

Among the different weapons the immune system can wage against pathogen invasion, interferons (IFN) are key. They are able to trigger many different signaling pathways and genes that play an important role in the host defense against both viruses and bacteria. There are three families of IFN. In this manuscript, I will particularly focus on the multi-gene type I IFN (IFN-I) family, and how they are modulated by Mtb and HIV-1. Several subtypes are encoded by IFN-I, including 13 homologous IFN α in humans, 1 IFN β and several other single genes, which have been poorly studied so far: IFN ϵ , IFN τ , IFN κ , IFN ω , IFN δ and IFN ξ [18], [19]. Here, only IFN α and IFN β will be discussed, as they have been studied in more depth than the other subtypes.

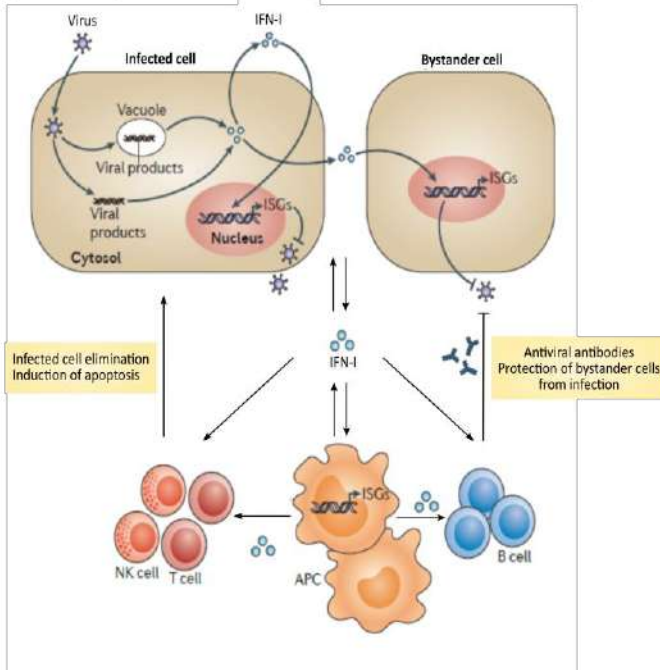
In the body, almost all cells are able to produce and respond to IFN-I, usually after the stimulation of pathogen recognition receptors (PRR) by microbial products. Microbial nucleic acids count for one of the best IFN-I inducers. For example, foreign messenger RNA is recognized by RIG-I¹, MDA5² [22], or even cytosolic molecular sensors NOD1³ and NOD2, the latter being involved in cytosolic Mtb recognition [23]. These different sensors rely on the adaptor mitochondrial antiviral signaling protein MAVS to activate the TANK-binding kinase 1 (TBK1). Phosphorylated TBK1 then recruits and activates the IFN regulatory factor 3 (IRF3) [19], which subsequently translocates to the nucleus, binds to the IFN-I promoter sequence and induces the expression of IFN α 4 and IFN β subtypes. After this first wave of IFN-I synthesis, secreted IFN-I act both in an autocrine and paracrine manner to trigger IRF7 transcription, which then mediates a positive feedback loop, leading to the transcription of all IFN-I gene subtypes [24]–[26]. Besides foreign RNA, exogenous DNA can also provoke IFN-I production. In the cytosol, DNA motifs can be recognized by DNA-dependent activator of IFN (DAI)

¹ **RIG-I**: retinoic acid-inducible gene I is an RNA helicase. It is a PRR involved in viral sensing that recognizes short double or single stranded uncapped RNA molecules.

² **MDA5**: melanoma differentiation-associated gene 5 belongs to RIG-I PRR family and recognizes shorter RNA molecules, including viral RNA.

³ **NOD**: Nucleotide-binding oligomerization domain-containing protein is involved in bacterial molecule and immune reaction.

A. Host protection against invaders involves cells from the innate and adaptive immunity



B. Sustained IFN-I production induces immunosuppression pathways

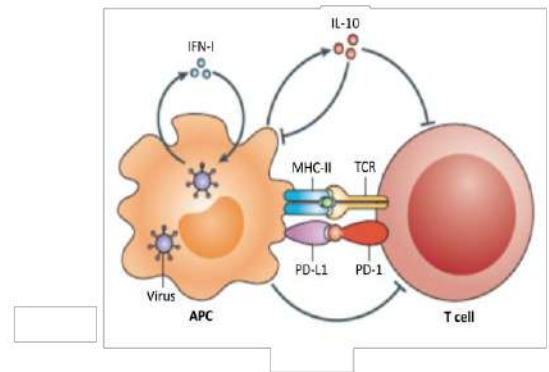


Figure 3: Immuno-suppression induced by IFN-I (from [18])

A | Virus-infected cells produce type I interferons (IFN-I) in response to the infection. The released IFN-I then act in an autocrine and paracrine manner to protect the bystander cells from becoming infected and to block the viral replication cycle in the infected cells. Interferon stimulated genes (ISG) are responsible for these functions. IFN-I also act on innate immune cells, including professional antigen-presenting cells (APC), natural killer (NK) cells, T cells and B cells to enhance their immune functions.

B | During chronic viral infection, IFN-I are produced for a longer period of time, compared to acute infection. Consequently, to avoid immuno-pathology, sustained IFN-I expression induce the secretion of immunoregulatory cytokines such as interleukin-10 (IL-10), and the expression of immunosuppressive ligands (such as programmed cell death 1 ligand 1 (PD-L1)) for T cell-inhibitory receptors (such as PD1, the PD-L1 receptor). These factors lead to the suppression of T cell function and, often, failure to clear infection.

regulatory factors, by DEAD and DEAH boxes and by cGAS⁴. Recognition of foreign DNA leads to the activation of I κ B kinase ϵ (IKK ϵ), which then recruits and activates IRF7, whose subsequent nuclear translocation induces further IFN-I synthesis [18]. Notably, recognition of foreign DNA molecules by cGAS leads to the production of the second messenger cGAMP⁵ that recruits and activates the stimulator of IFN genes, STING, which then signals through the TBK1/IRF3 pathway to induce IFN-I transcription [18], [27]. Other PRR, such as TLR, are also able to mediate IFN-I synthesis and involve signal transduction through the MyD88/NF κ B axis, as recapitulated in figure 2 [18].

Secreted IFN-I bind and signal through their receptor IFNAR, composed of two subunits, IFNAR1 and IFNAR2. Globally, ligand-receptor binding activates the receptor-associated kinases JAK1 and TYK2, which phosphorylate both the signal transducer and activator of transcription 1 (STAT1) and STAT2. Upon activation, STAT1 and STAT2 heterodimerize and recruit IRF9 to form the ISG factor 3 (ISGF3) complex. Subsequently, ISGF3 translocates into the nucleus and binds to IFN-stimulated response element (ISRE) in the interferon stimulated genes (ISG) promoter [18], [19]. Consequently, ISG are expressed and mediate the adequate response to control the pathogen invader. IFN-I can also induce signaling through homodimerization of STAT1, more commonly associated to IFN γ -signaling, and through other STAT (STAT3, 4 and 5) despite their typical role in other cytokine signaling (see Figure 2) [18]. Altogether, this diversity in possible signaling pathways engaged by IFN-I could explain, in part, the broad effects of IFN-I signaling and different outcomes observed in several infectious settings.

ISG are expressed constitutively in response to the low levels of IFN-I present in the microenvironment. More commonly, ISG are induced at higher levels in response to IFN-I production occurring in response to viral infection. Most of these genes display antiviral properties, which act both in the infected cells to restrict the viral replication cycle and in bystander cells to prevent the spread of infection [18], [28]. Moreover, IFN-I are able to activate immune cells to enhance the immune response to the infection, for example by recruiting T cells and NK cells to kill the infected cells, often through the induction of apoptosis. It also stimulates B cell humoral responses. When prolonged, IFN-I can also induce immunosuppression, in order to halt inflammation and T cell mediated-killing (Figure 3).

Now that macrophages and IFN-I responses in immune cells have been briefly described, I will introduce and discuss the current literature on HIV-1 and TB pathologies. For the entire manuscript, a particular focus will be brought on IFN-I responses and on the role of macrophages in the control or the exacerbation of each disease, but also in the co-infection context.

⁴ **cGAS**: Cyclic GMP-AMP synthase is a cytosolic DNA sensor that activates IFN-I responses by binding to self and microbial DNA present in cell cytoplasm, and is responsible for cGAMP synthesis.

⁵ **cGAMP**: Cyclic guanosine monophosphate–adenosine monophosphate is synthesized from ATP and GTP (adenosine or guanosine triphosphate) by cGAS and function as second messenger in IFN-I induction.

Part 1: Introduction to the co-infection
between *Mycobacterium tuberculosis* and
HIV-1

Chapter I: *Mycobacterium tuberculosis* infection and the macrophage response

Although the main cause of morbidity and mortality in developed countries have progressively shifted towards non-transmissible pathologies grouped under the designation “chronic diseases” (e.g., cancers, cardio-vascular diseases, obesity, diabetes), infectious diseases remain the principal cause of death in children and young adults worldwide, and in adulthood in developing countries [1]. In 2016, lower respiratory infections including tuberculosis, killed 3 million people, reaching the 4th ranked leading cause of death worldwide. Nowadays, and despite a reduction in the epidemic burden, tuberculosis remains the deadliest disease caused by a single infectious agent on the world scale [1].

I. *Mycobacterium tuberculosis*: the etiological agent of tuberculosis

A. Koch's tubercle bacillus

a. *Historical perspective*

Tuberculosis (TB) is an old and highly contagious disease, infecting humans for thousands of years [29]. The oldest record of the disease dates back to 1550-1080 B.C. [30], and phylogenetic studies reported that the *Mycobacterium tuberculosis* complex (MTBC), composed of *Mycobacterium tuberculosis* and other closely related species (*africanum*, *canettii* and *bovis*), had a common African ancestor about 35 000 to 15 000 years ago [30]. It appears that ancient Egyptian society already suffered from TB 5 000 years ago, as typical skeletal abnormalities of TB, including Pott's deformities⁶, were found in Egyptian mummies [31]. Throughout history, the disease was referred to under several names (*schachepheh* in the Old Testament, *phthisis* by Hippocrates in the Greek literature, *cunsumptio* in Roman era or *consumption* in occidental countries during the XIXth century). However, it was only in 1834 that J. L. Schönlein unified the nosology and proposed the name “tuberculosis” due to the presence of tubercles in all forms of the disease [32]. The contagious nature of TB was first suggested by Benjamin Marten, but it was the French military surgeon J-A. Villemin who convincingly proved the contagious nature of the disease in 1865, by inoculating a rabbit with “a small amount of purulent liquid from a tuberculous cavity” obtained from the autopsy of a TB patient [30].

The history of TB changed dramatically when its etiological agent, *Mycobacterium tuberculosis* (Mtb) or Koch bacillus, was identified for the first time in 1882 by the German Dr. R. Koch; a discovery that was awarded the Nobel Prize in 1905. Following this crucial finding, tuberculin, an extract of Mtb proteins, was first used as a therapy, which failed, and then in animals and humans to identify TB infection by intra-dermal skin testing [32]. Between 1908 and 1921, A. Calmette and C. Guérin sub-

⁶ **Pott deformity:** clinical manifestation of spine infection attributed to Mtb. One of the most common forms of extra-pulmonary TB, characterized by back pain, tenderness, paraplegia or paraparesis, and kyphotic or scoliotic deformities.

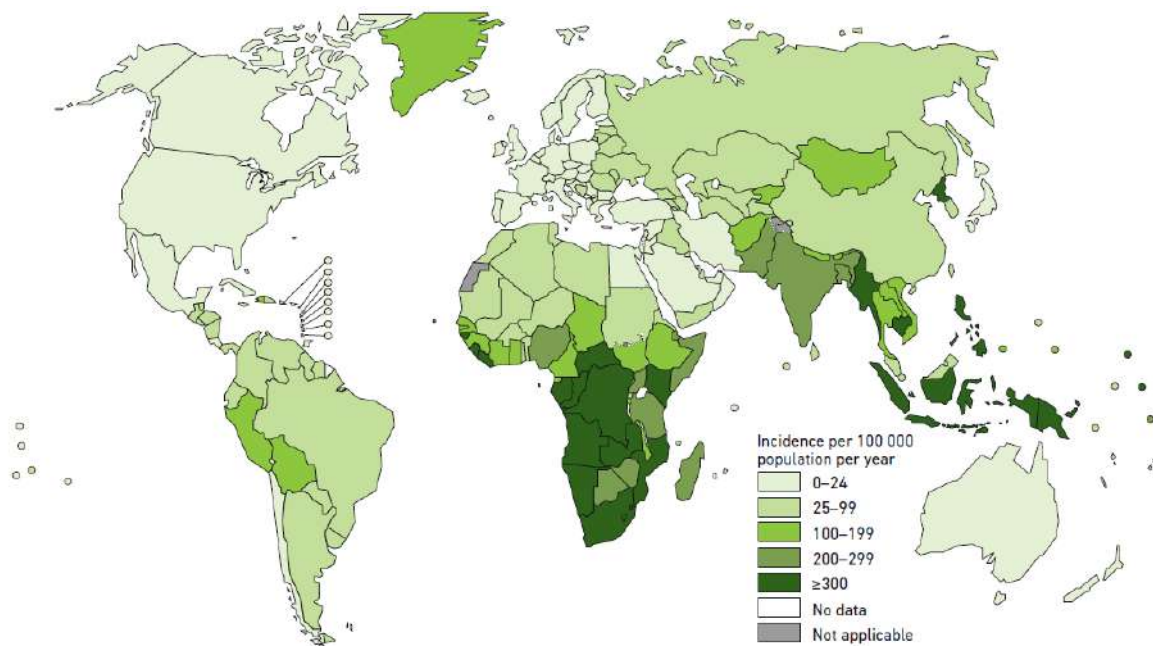


Figure 4: New Mtb infections worldwide in 2017 (from [1])

The severity of national TB epidemics in terms of the annual number of new TB cases relative to population size (the incidence rate) varied widely among countries in 2017. There were less than 10 incident cases per 100 000 persons in most high-income countries (North America, Western Europe, Oceania), 150–400 in most of the 30 highest TB burden countries (e.g. India, Mongolia), and above 500 in a few countries including the Democratic People’s Republic of Korea, Lesotho, Mozambique, the Philippines and South Africa (WHO TB report, 2018).

cultured the close Mtb relative *Mycobacterium bovis* more than 200 times, and showed that the resulting bacterium had lost its virulence in a large number of animal models. This final bacterial strain, today referred to as BCG (for Bacillus Calmette-Guérin) was used as a vaccine to prevent TB, and proved to be efficient at protecting infants from TB meningitis and other infectious diseases in infants (described later in this chapter – section I.A.c.).

In the late 1880s, TB prevalence was equated to about 500 cases per 100 000 inhabitants in Europe and one of the leading causes of death, according to the National Vital Registration system. At the turn of the 20th century, the improvement of incomes, hygiene and nutrition, as well as the socio-economic development, brought about a slow decline in the number of TB cases and deaths in Western Europe and Northern America [33], [34]. From the 1940s, the discovery, development and use of effective antibiotherapy (*i.e.* discovery of streptomycin in 1943 by A. Schatz [30], [32]) accelerated this trend, reducing the disease incidence nowadays to less than 10 cases per 100 000 inhabitants and less than 1 death per 100 000 inhabitants per year in European and North American countries [1].

This progression in the control of the epidemic in developed countries has given the false impression that TB is now a disease of the past. However, for many countries, the “end” of the TB pandemic is still a distant reality, despite the possibility to be cured with timely diagnosis and proper treatment. Even with the call to consider TB as a global health emergency by the World Health Organization (WHO) in 1993, the progress made to fight the epidemic remains insufficient, calling for more efforts to step up the political commitments that have intensified in 2017 and 2018 [1].

b. Epidemiology

Since 1997, the WHO publishes a yearly report to follow the evolution of the epidemic. Worldwide, TB remains the leading cause of death due to a single infectious agent, with millions of people becoming sick with the disease each year and 10 million newly infected people in 2017. The same year, TB caused 1.3 million deaths among the HIV negative population. Today, we estimate that one quarter of the global population is latently infected with Mtb, meaning that these infected people do not present any symptoms of the disease [1]. Despite a continuous decline in TB prevalence, the importance to continue the fight against TB resides in the fact that multi-drug resistant (MDR) and extensively drug resistant (XDR) Mtb strains, which cannot be eradicated by conventional antibiotherapy, are flourishing every year, representing almost a half of new TB cases in low-income countries (India, China and the Russian Federation in particular). For example, in India, TB incidence was of 204/100 000 in 2017, among which 92% of Mtb infections were MDR [1].

Several factors are involved in TB susceptibility. First, TB is officially considered as a disease of the poor and is tightly linked with the social and economic stability of the country. Other important factors related to TB susceptibility are hygiene, overcrowding and malnutrition, which all related to poverty status. In 2017, two-third of the cases were reported to occur in 8 countries (see Figure 4): India (27%), China (9%), Indonesia (8%), the Philippines (6%), Pakistan (5%), Nigeria (4%), Bangladesh (4%) and South Africa (3%). It was estimated that among the 10 million new infections annually, 1.9 million are due to malnutrition. Other factors that increase susceptibility to TB are: alcoholism, smoking, diabetes and co-infection with HIV-1 (described in Chapter III of the present manuscript) [1].

In addition, intrinsic factors also have an impact on TB incidence repartition worldwide. Indeed, age, sex and genetic factors also play a role in the disease development. The WHO reported that in the new cases identified in 2017, 90% were adults over 15 years old, among which 64% were males, indicating an incidence of about 2 males infected for 1 female [1].

c. Pulmonary and extra-pulmonary disease

Mtb is a facultative slow growing (generation time around 20h) intracellular pathogen whose reservoir is exclusively human, and that is particularly well-adapted to its main cell target: the macrophage. In conditions where the immune system is unable to control the bacterial growth (between 5 to 10% of the time [35], [36]), the disease symptoms (*e.g.* fever, cough, weight loss) appear. This form of TB is referred to as “active TB” and results in patients transmitting the infection to new hosts by aerosol release. In the absence of treatment or in drug inefficiency settings, 50% of patients die of TB due to destruction of the lungs caused by exacerbated inflammation [35], [37]. Fortunately, in 90% of the cases, the immune system is able to contain the infection in an asymptomatic latent stage, during which Mtb is dormant and does not proliferate [36]. This form of the disease, which is non-transmittable, is the most common form of TB worldwide.

In certain cases, active TB can develop into an extra-pulmonary manifestation of the disease. These manifestations involve bacterial dissemination through the bloodstream to reach several organs, including the pleural cavity, lymph node, spleen, liver, bone, urogenital and peritoneal tracts, and brain (for review, see [38]). The prevalence of extra-pulmonary TB varies with geographical location and is more frequent in low-income countries. The most common form of extra-pulmonary TB is the pleural manifestation of the disease. It is characterized by the abnormal presence of fluids in the pleural cavity surrounding the lungs. This fluid contains leukocytes, of which 50% are lymphocytes. This type of extra-pulmonary TB is highly prevalent in African countries like Burundi, where more than 25% of TB patients have pleural effusions [39]. The incidence of this type of TB manifestation is strongly increased in immuno-compromised patients, such as those co-infected with HIV-1 [40]. The deadliest form of TB is TB meningitis, for which more than 100 000 new cases are estimated to occur each year, a majority of which affect children. This form of TB is difficult to diagnose due to the long time needed to culture the bacteria. Moreover, it is likely that antibiotherapy is poorly effective against this form of the disease since drug access to the brain is quite limited [41].

d. Mycobacteria taxonomy and characteristics

Mtb is an acid-fast resistant Gram-positive bacterium that belongs to the *Mycobacteriaceae* family. The genus *Mycobacterium* comprises more than 170 species, most of which are environmental organisms [42]. Generally, pathogenic or opportunistic Mycobacteria can be divided into three major groups for the purpose of diagnosis and treatment: first, the MTBC which causes TB and includes Mtb, *M. bovis*, *M. africanum*, *M. microti*, *M. canetti* and other species; second, *M. leprae* that causes leprosy; and third, the non-tuberculous mycobacteria or NTMs (*M. avium*, *M. kansasii*, *M. abscessus*, *M. chelonae*, *M. fortuitum*, *M. pregrinum* and *M. marinum*) that can cause pathology in immuno-compromised individuals. The MTBC group is unique as it is an obligate human pathogen, with no

known animal or environmental reservoir. Moreover, its virulence is also unique as it mainly relies on its transmission between individuals [42]. From now on, I will particularly focus on Mtb, which is responsible for the human pandemic of TB.

Under optimal conditions, Mtb grows at 37°C with a generation time of about 18 to 24h. It can also be cultured on solid culture media, where colonies appear within two to three weeks [43]. However, the host environment is not optimal for bacterial growth. To circumvent this issue, Mtb is able to enter a dormant, non-replicative state that is characterized by low metabolic activity and phenotypic drug resistance [43]. The genome of Mtb H37Rv strain, the most commonly used in laboratory research, was sequenced in 1998 by Cole and colleagues [44]. The genome is 4 million base pairs, encoding for almost 4 000 genes, among which many are highly conserved in the *Mycobacteriaceae* family, and more specifically genes involved in lipid metabolism [45]. Another conserved region of the Mtb genome, the RD1⁷ locus, is involved in Mtb virulence and encodes a secretory apparatus, the ESX-1⁸ secretion system responsible for exporting virulence factors such as cell filtrate protein 10 (CFP-10) and early secretory antigen 6 (ESAT-6); both of which play a key role in Mtb pathogenesis (for more detail, refer to section II.) [46].

e. The mycobacterial cell envelope

The *Mycobacteriaceae* family is characterized by the peculiar structure of its cell wall that comprises complex lipids and sugars, and contains high levels of glycosylation, which allow it to be recognized by the host immune system [47], [48]. The mycobacterial cell wall (Figure 5) is divided into two sections: the inner and the outer layers. The inner layer is composed of (i) peptidoglycan, (ii) arabinogalactan and (iii) mycolic acids [48]–[50]. These three components form an insoluble core that is essential for viability of mycobacteria, and it is the main target for drug development to combat Mtb [51]. The outer layer, called capsule, has only minor amounts of lipids and consist of a loosely-bound structure of polysaccharides, proteins and non-covalently linked glycoconjugates, such as phosphatidyl-*myo*-inositol (PI) mannosides (PIMs), lipomannan (LM) and lipoarabinomannan (LAM). These mannosylated molecules are thought to play important roles in the integrity of the cell wall and pathogenesis of Mtb [52].

The nature and quantity of the different cell envelope layer components vary between Mtb isolates and impact their interaction with the host cells. Such is the case with the lipid composition of the cell wall, which represents 60% of this structure and is responsible for Mtb resistance to antibiotics. Mtb dedicates 6% of its genome to lipid metabolism [53], a phenomenon that favours the lipid repertoire expressed at the bacterial cell wall. The genomes of different Mtb clinical isolates are well conserved and show no sign of exogenous genetic material acquisition despite the high variability in the mycomembrane components [45]. Therefore, the resistance of the bacteria to antibiotics targeting Mtb lipids is conferred by punctual mutations in the Mtb genome.

⁷ **RD1**: region of difference 1 expressed by all virulent strains of Mtb, encodes 9 genes involved in Mtb virulence, including CFP-10 and ESAT-6.

⁸ **ESX-1**: early secretory antigenic target 6 system-1 is required for Mtb virulence and secretion of the bacterial protein CFP-10 and ESAT-6.

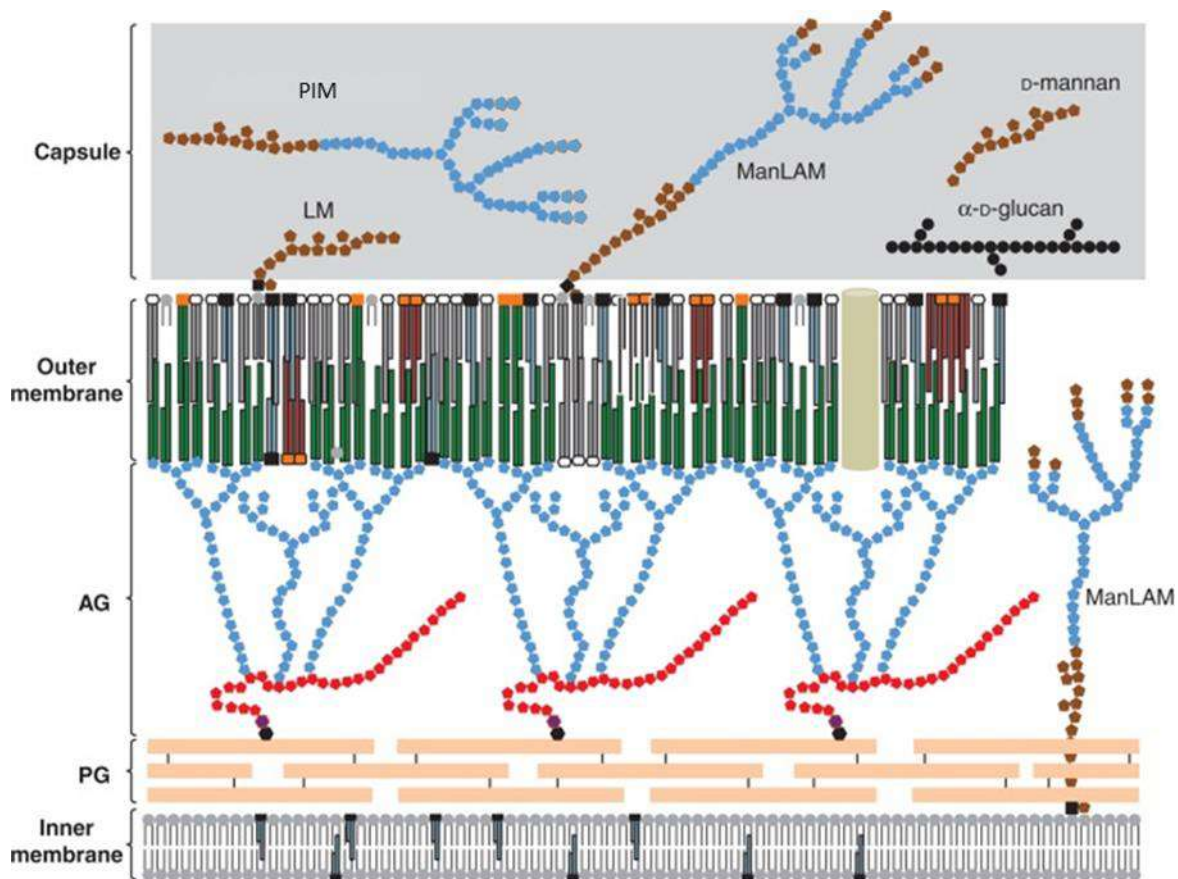


Figure 5: Structure of the mycobacterial cell wall (adapted from [54])

Mtb cell envelope is composed of a plasma membrane containing glycolipids, lipoglycans and lipoproteins. The peptidoglycane (PG) is covalently linked to arabinogalactane (AG) and form a complex that is bound to mycolic acid (shown in dark green). Those are covered with lipids, and together form the mycomembrane, on which the capsule, containing proteins and polysaccharides (lipomannan [LM], phosphatidyl-myo-inositol mannosides [PIM] and lipoarabinomannan [ManLAM]), is lying.

Blue symbols: arabinose residues; red symbols: galactose residues; brown symbols: mannose residues; black circles: glucose residues.

Its genome encodes for many factors responsible for its virulence (*e.g.* RD1 region encodes for ESAT-6, one of the most important virulence factors of Mtb) and for its resistance to antibiotics. In the following section, I will discuss the methods of prevention, diagnosis and treatment for Mtb infections.

B. Therapeutic tools to detect and treat tuberculosis

a. Prevention

To date, the only available vaccine to prevent Mtb infection and the development of TB is the BCG vaccine, based on the living BCG attenuated strain. In 1902, the first isolate of BCG was obtained from TB-infected cattle, and since then, cultured for decades, reducing this strain virulence by inducing a loss of the RD1 region in its genome [55]. It was used for human vaccination for the first time in 1921, and since then, a number of laboratories continue to culture BCG, which explains the high diversity of genetic variance used for vaccination.

Over time, history and clinical data revealed that the BCG vaccine efficiency is quite variable. Indeed, it effectively protects children (90%) against pulmonary TB, but also against extra-pulmonary forms of the disease such as TB meningitis (see section I.A.c.) [55], [56]. However, BCG vaccine protection in adults is only relatively efficient (50% of the cases [1], [35], [57]) and depends on the (i) patient age at the moment of vaccination, (ii) contact with environmental mycobacteria, (iii) host genetics, (iv) strain of BCG used for the vaccine formulation and (v) Mtb strain virulence [58]. Consequently, new strategies to prevent Mtb infection are crucial to halt the pandemics, especially with regards to co-infections settings like HIV-1, since HIV-infected people present higher risk of developing TB and MDR-TB (up to 24% more MDR-TB occur in HIV-1⁺ patients [59]) [60].

Several strategies have been developed to create new vaccines to protect the population against TB infection (Figure 6). Indeed, the vaccine strategy seems appropriate considering that our immune system is able, in the majority of the cases, to control the bacteria and to maintain it in a dormant status. However, vaccine development is more difficult than expected since the immune memory induced by a primary Mtb infection is not entirely efficient: patients who have been infected once with Mtb are still highly susceptible to be re-infected [61], even though a recent study in macaques reported an efficient protection against secondary infection with different Mtb strains after primary Mtb infection [62]. Therefore, new strategies will aim at preventing new infections (pre-exposition vaccines), but also at targeting both replicative and dormant bacteria to aid in its eradication (post-exposition vaccines) [63]–[65]. Any strategy should take into consideration (i) the improvement of immune memory induction by a rapid stimulation and recruitment of Mtb-specific T cells, (ii) the prevention of Mtb transmission and (iii) to protect lung tissue against Mtb-mediated inflammation [66]–[68]. As of today, there are two main strategies being carried out to develop new vaccine candidates [69]. The first strategy aims at replacing BCG with safer, more immunogenic vaccine that induces long-lasting protection against highly virulent clinical isolates (*e.g.*, Mtb Beijing strains, MDR strains). This includes the improvement of BCG by introducing immunodominant Mtb antigens (*e.g.*, ESAT-6), overexpressing mycobacterial antigens (*e.g.*, Ag85), or genetically engineering new strains for superior immune efficacy. Alternatively, this first strategy also includes the manipulation of Mtb

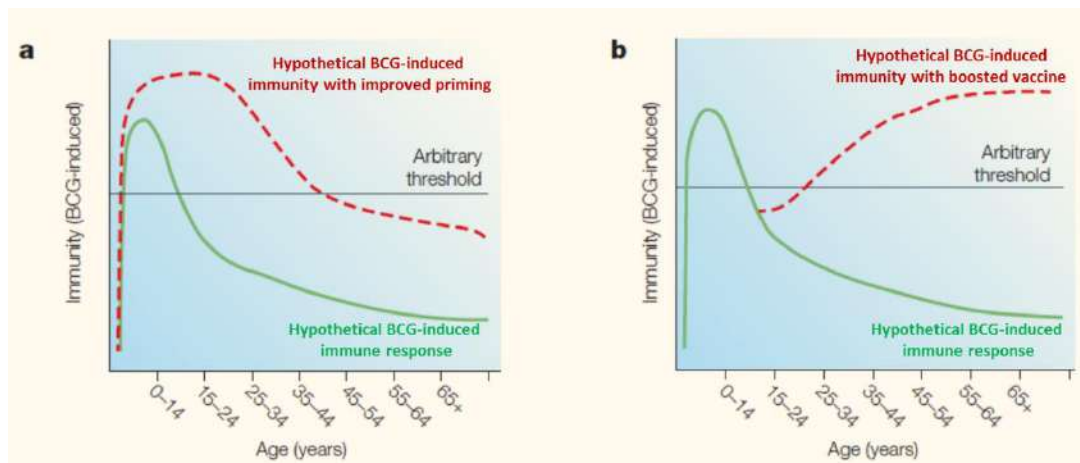


Figure 6: BCG vaccination efficiency.

Hypothetical curve showing the immune response to vaccination with BCG vaccine (solid green line) and the proposed action of improved priming (a) and boosting (b) vaccines (red dashed line). When immunity drops under an arbitrary threshold (black line), the vaccine no longer protects the individual to become latently infected with Mtb. Improved priming vaccines aim to keep the immune response above this threshold for longer, whereas intervention in the form of a booster vaccine (more immunogenic Mtb component, stronger adjuvant) is hypothesized to induce a long-lasting protective immunity to levels remaining above the threshold

attenuated strains by deleting of essential metabolic (*e.g.*, panCD) or virulence (*e.g.*, phoP) genes [69]. The second strategy aims to boost BCG with sub-unit vaccines either in the form of protein-lipid mycobacterial antigens (*e.g.*, ESAT-6, Ag85) with different adjuvants (*e.g.*, liposome/TLR4 agonist), or recombinant viral vectors (*e.g.*, modified vaccinia Ankara virus) [69].

Collectively, despite its limitations, the BCG vaccine is not easily replaced because it is safe and offers multiple advantages. Its improvement remains the best alternative for the rational design of a tuberculosis vaccine. Major efforts should be rallied towards the identification of new mycobacterial epitopes and antigens, and for the improvement of the immune stimulatory capacity, to make a multi-valent BCG vaccine.

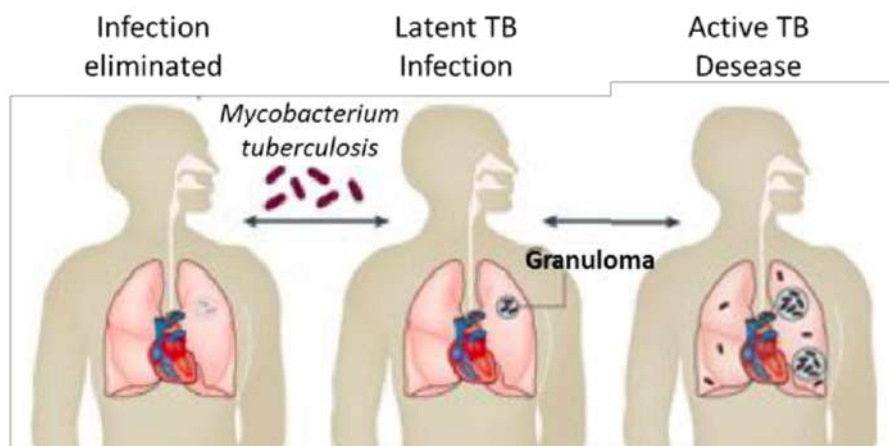
b. Diagnostic

TB is a highly contagious airborne infection. In the respiratory tract, Mtb can be eliminated before the establishment of a successful infection by mucocilliary clearance, or it can be efficiently controlled and eradicated by the immune system. Sometimes, the bacillus succeeds to establish a niche in the lung where it either stays latent or replicates to progress towards the disease (Figure 7) [70]. To avoid this progression and the transmission of the infection, an early and accurate diagnosis is necessary [71].

Tuberculin Skin Test (TST) is usually used to detect asymptomatic latent TB [72], [73]. A commercial extract of mycobacteria antigens (common antigens between several mycobacteria species, including Mtb and BCG species) is injected under the patient skin. After 3 days, the induration (local inflammation) is measured to determine if the patient is infected. A limiting factor of that method is that it is not specific for Mtb and the quantification of the inflammation is not precise. Therefore, false positives occur, frequently due to a reaction to BCG vaccination [72], [74]. This TST can be complemented by a blood test, measuring interferon gamma (IFN γ) (IFN γ Release Assay – IGRA) [72]. This test measures *ex vivo* T-cell release of IFN γ after stimulation with Mtb-specific antigens, and allows physicians to discriminate TST false-positive results [72], [74].

Diagnosis of active TB is more time-consuming and expensive since it requires the detection of the pathogen from a patient sputum or lung tissue. These samples are then observed by microscopy to detect Mtb, a method which is poorly sensitive [75]. In addition, a bacterial culture from these samples is conducted (Figure 7), as well as bacterial DNA amplification, in order to identify the pathogen. The limit of this culture method is the Mtb generation time, which delays the results [75], [76]. Finally, lung X-ray, and more recently, PET-SCAN exams, allow physicians to visualize characteristic structures of the disease in infected patients and the bacterial activity and load [77].

Despite TB diagnostic tools improvement these last five years, specifically with the implementation of the Xpert MTB/RIF molecular test that simultaneously detects Mtb resistance to rifampicin, strong efforts still remain to be done to improve TB infection identification, especially in patients also infected with HIV-1. Indeed, TB diagnosis is particularly difficult in HIV-1 co-infected individuals who often display atypical, non-specific clinical presentation and smear-negative disease (from 21 to 61% of cases) with less cavitory lesions, along with increased propensity to develop extra-pulmonary TB [59]. In addition, and particularly in low-income countries, greater advancements are



TST	Positive	Positive	Positive
IGRA	Positive	Positive	Positive
Culture	Negative	Negative	Positive
Infectious	No	No	Yes
Symptoms	None	None	Mild to severe

Figure 7: Spectrum of tuberculosis disease and associated diagnosis (adapted from [35]).

Upon inhalation of Mtb-aerosol, the bacteria will be eliminated in the upper airways either by mechanisms independent of the immune system (mucociliary clearance), or by an efficient intervention of immune cells (infection clearance). If the pathogen is not cleared, the immune system will establish a cellular response to contain the bacteria. When successful, this response maintains the bacteria in a dormant, non-replicative stage. The disease is then latent and asymptomatic, and can remain so for decades. Under certain conditions, *e.g.* an immune-deficiency, Mtb can re-enter a replicative state and escape immune surveillance, leading to the disease reactivation. This form of the disease is called active TB and allows the transmission of the bacilli to other individuals. Both tuberculin skin test (TST) and interferon gamma release assay (IGRA) are used to diagnose latent TB, while active TB can be detected by bacterial culture from the patient sputum or broncho-alveolar lavages.

needed to improve TB diagnostic in children, which is challenging, notably because of the low sensitivity of traditional diagnostic tools. Clinical diagnosis lacks standardized methods and there is lack of laboratory and clinical centers able to process samples from TB patient for Mtb growth in low-income countries [78], [79].

c. Treatment

Upon active TB diagnosis, the patient receives a standard first line treatment: an oral antibiotherapy combining four different antibiotics for two months (isoniazid, rifampicin, pyrazinamide and ethambutol). This step is then followed by four months of oral ingestion of isoniazid and rifampicin [80]. This treatment is both long and constraining due to the daily basis of drug ingestion. However, if taken seriously and accurately supported by a physician, this antibiotherapy has a curative efficiency of 95% [81]. A limitation of this treatment is the absence of a rapid method to verify its efficiency. Indeed, two months are necessary to validate Mtb elimination from the patient sputum using the *in vitro* bacterial culture method. Moreover, Mtb clearance efficiency relies on the patient strict compliance to the treatment, which is not always respected. This leads to the development of drug-resistant bacteria (MDR, XDR and TDR: total drug resistant), which decreases the treatment effectiveness and renders control of the pandemic difficult [82].

Emergence of antibiotic resistance (especially to rifampicin and isoniazid) required the establishment of a second-line of treatment: an antibiotherapy combining oral and injectable antibiotics (fluoroquinolones, acid para-amino-salicylic, aminoglycoside, ethionamid and cycloserine). The use of this line of drugs extends the treatment duration up to two years, induces severe secondary effects and reduces Mtb clearance efficiency to 50% [35], [82], [83]. Unfortunately, the number of MDR cases is increasing every year [1] and allows the emergence of highly resistant strains called XDR and TDR [84], [85], which are not sensitive to any line of antibiotics. For example, in an MDR-TB patient cohort in 2015, treatment success of MDR-TB was lower than 50% in China and India. In fact, India, the Russian federation and Ukraine accounted for 75% of XDR-TB cohort recruited by the WHO, and mortality rates reached 42% in the Indian study [1]. In addition, known cohorts of MDR and XDR-TB infected patients (2015, WHO) treated with second-line of treatment controlled the infection in only 20% of cases [1]. Early in 2019, the FDA approved the use of a novel antibiotic, Pretomanid, in combination with two other antibiotics for six months, to treat XDR-TB and intolerant or non-responsive MDR-TB.

TB remains a burden at the world scale, with the possibility of a rebound of epidemic within the coming years, even in countries where it is not highly prevalent (Northern and Western Europe, North America) due to the increasing population and wealth inequalities. On top of that, there is the rapid emergence of MDR, XDR and TDR-Mtb strains, of which diagnosis is not always obvious, especially in co-infection settings with other pathogens such as HIV-1. All things considered, finding new treatments and preventive alternatives to eradicate Mtb infection remains an urgent global health priority.

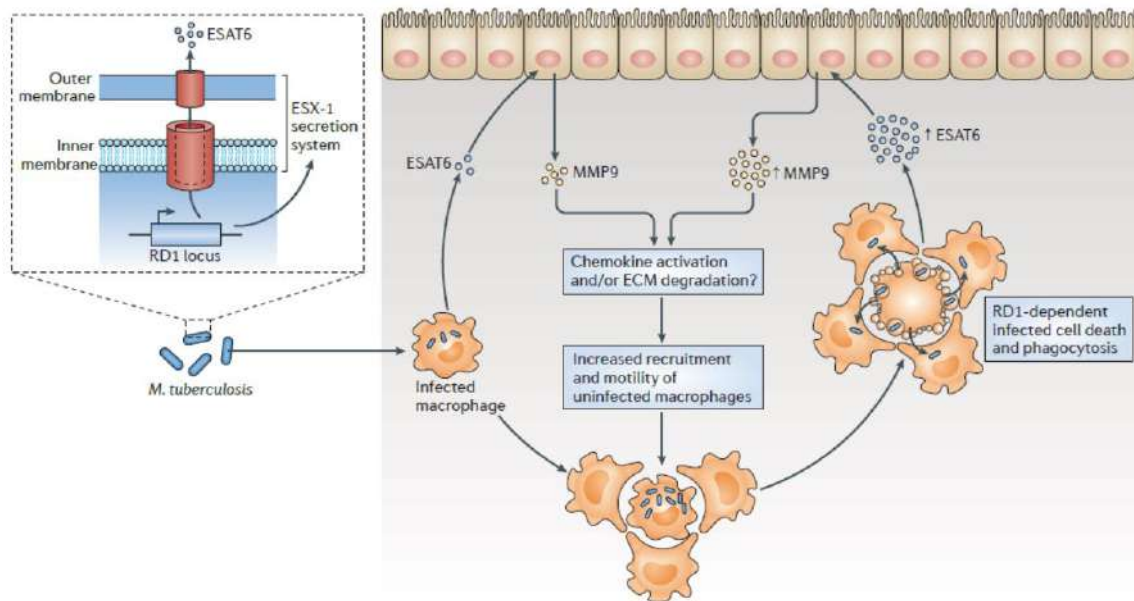


Figure 8: Epithelial secretion of MMP9 and innate cells recruitment to the site of infection (from [86])

Mtb takes advantage of macrophage infection to secrete virulence factors (e.g. ESAT-6) through its ESX-1 secretion system encoded by the RD1 locus. The release of ESAT-6 through secretion or macrophage apoptosis caused by the infection alarms surrounding cells, in particular epithelial cells that will produce and secrete MMP-9. As a result, uninfected macrophages are recruited to the site of infection and accumulate there, forming a mass: the immature granuloma.

II. Macrophages at the heart of host-pathogen interactions with *Mycobacterium tuberculosis*

A. Physiopathology of the *Mycobacterium tuberculosis* infection

a. Establishment of the cellular response

The host defense against Mtb requires the intervention of both the innate and adaptive immune system. When an infected individual with active tuberculosis sneezes or coughs, he/she exhales Mtb-rich droplets that can be inhaled by uninfected surrounding individuals. After inhalation, the droplets can either get stuck in the upper airways, or reach the lower lung, depending on their size (from 0.65 to < 0.7 μm [87], [88]). In the former case, airway epithelial cells detect Mtb through PAMP recognition by Pathogen Recognition Receptors (PRR), and present Mtb antigens to MAIT T cells that rapidly produce $\text{IFN}\gamma$ and $\text{TNF}\alpha$, and activate innate macrophages towards a microbicidal profile that then perform an efficient bacterial clearance [88], [89]. However, in the latter case, small droplets (\approx 0.65 μm [87]) can reach the lower airways, where Mtb is able to efficiently invade the host [88], [90], [91].

Once in the alveoli, inhaled Mtb bacilli are recognized through several PRR such as TLR and C-type lectin receptors (CLR), among others (see section II.B.a of this chapter), and are subsequently ingested by alveolar macrophages. Engagement of these PRR drive the macrophages to secrete several cytokines, including $\text{TNF}\alpha$, $\text{IL-1}\alpha/\beta$, IL-12 and IL-6 [71], [92]. By using a mouse model of Mtb infection, Cohen and colleagues found *in vivo* that early Mtb productive infection occurs exclusively in the airway resident alveolar macrophages, which are leukocytes derived from embryonic origin [93]. Following their infection, alveolar macrophages translocate to the lung interstitium through the epithelial barrier, involving mechanisms dependent on Mtb ESX-1 secretion system and MyD88/IL-1R⁹ inflammasome signaling [93]. Mtb also takes advantage of macrophages infection by secreting virulence factors encoded by the RD1 genomic region *via* its ESX-1 secretion system. Among these factors, ESAT-6 alarms surrounding epithelial cells, which start to secrete metalloproteinase 9 (MMP-9) (Figure 8). Consequently, new innate immune cells including neutrophils, DC and monocytes/macrophages are actively recruited to the site of infection, at a high rate and speed [90], [86], and eventually participate in Mtb uptake. Of note, recruited monocytes undergo differentiation into macrophages with different activation profiles (see preamble and figure 9). According to the signals received upon recruitment, monocytes may become “M1” macrophages, which are pro-inflammatory effector cells, like interstitial macrophages deriving from a hematopoietic lineage, and are responsible for Mtb clearance. Likewise, monocytes also polarize into “M2” macrophages, which regulate inflammation to protect the host against immunopathology. However, these “M2” macrophages are permissive to Mtb infection and display characteristics of alveolar macrophages. Indeed, the group of D.G. Russell reported that the alveolar macrophages lineage exhibits higher bacterial burden than interstitial macrophages lineage, due to different metabolic state; alveolar macrophages are committed to fatty acid oxidation, whereas interstitial macrophages are glycolytically active, allowing for control of bacterial growth [94]. Infected alveolar macrophages also contribute to

⁹ **MyD88**: Myeloid differentiation primary response 88; **IL-1R**: interleukin-1 receptor

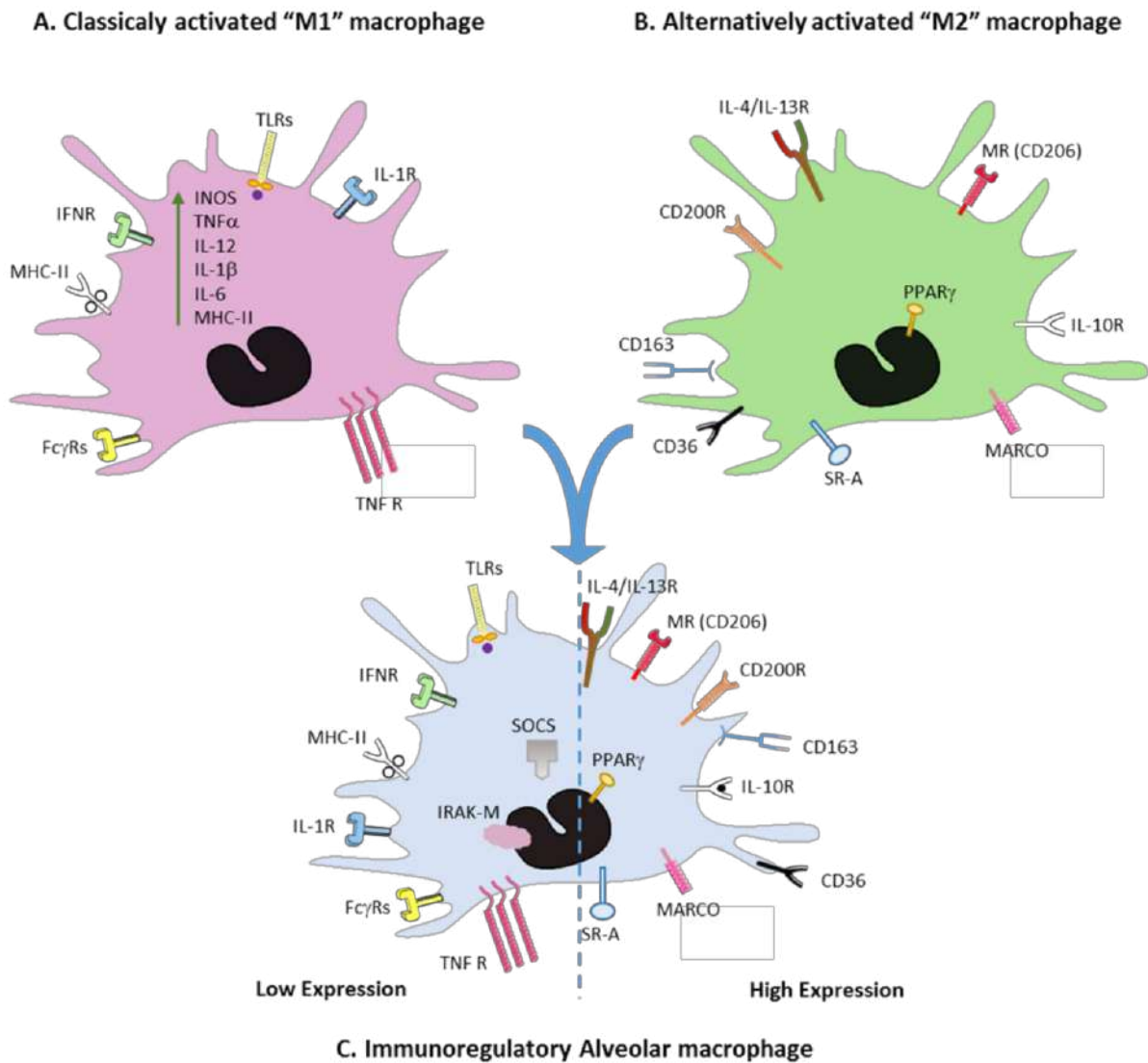


Figure 9 : Macrophages activation profile during Mtb infection (adapted from [95])

A | Classically activated "M1" macrophages are differentiated by IFN γ , LPS and TNF α . They are characterized by the expression of pro-inflammatory cytokines (e.g. TNF α , IL-1 β , IL-12 and IL-6), and receptors (e.g. MHC-II, TLR, and Fc γ R).

B | Alternatively activated "M2" macrophages are differentiated by IL-4, IL-13, IL-10, immune complexes, etc. Mostly, "M2" macrophages display an anti-inflammatory signature with increased expression of the MRC1, PPAR γ , IL-10, CD200R, CD163, CD36, and MARCO.

C | Alveolar macrophages are unique immunoregulatory cells which express both M1 and M2 markers. Their activation is tightly regulated by molecules such as PPAR γ , IRAK-M, IL-10 and SOCS proteins. Alveolar macrophages are susceptible to Mtb, however, they are able to contain the bacteria to certain extent. Usually, Mtb is killed by interstitial macrophages, which display "M1" activation profile and are highly microbicidal.

the recruitment of natural killer (NK) cells and NKT cells to the infected tissue. These cells produce IFN γ in response to Mtb and favour monocytes differentiation towards an “M1” phenotype, restraining Mtb growth. However, this control is temporary and lasts for about 14 to 21 days. The secretion of exosomes enriched in Mtb lipids by infected macrophages is a mechanism by which the bacillus manipulates the immune system. Mtb exosomes increase pro-inflammatory signals and cytokines production (*e.g.* TNF α , IL-1 α , IL-10, CCL2, CXCL10) that in turn, accelerate the recruitment of neutrophils, DC and macrophages to the site of infection, therefore providing the pathogen with new target cells. In addition, exosomes containing Mtb lipids not only trigger macrophage activation, but also prevent IFN γ secretion by activated T cells [96]. The agglomeration of all these innate cells around the translocated infected macrophages represent the first step of granuloma formation: an amorphous mass exists initially as a preliminary form of the classical tuberculous granuloma, which is a much more complex, highly organized and stratified structure [86], [97]. During the recruitment of new cells to the site of infection, a proportion of newly infected macrophages leave the primary granuloma and migrate through the tissue to establish a secondary granuloma [71], [98].

In parallel, tissue-recruited monocytes also differentiate towards DC, which mature upon Mtb exposure and/or infection. Within 10 to 14 day post-infection, infected DC migrate to the draining lymph node while secreting interleukin 12 (IL-12), CCL19¹⁰ and CCL21¹¹ (Figure 10). This is a major characteristic of Mtb infection which is heavily investigated; indeed, two weeks is quite a long time to observe DC recruitment to the draining lymph node as compared to other pulmonary infections that require a few hours to maximum 3 days ([86], [99]–[102]). Once in the lymph node, DC present Mtb antigens to naive T cells. They are able to cross-prime CD4⁺ T cells through MHC-II¹² molecules, and CD8⁺ T cells through MHC-I. CD4⁺ T cells acquire a T-helper 1 (Th1) profile, and quickly migrate to the lungs and aggregate around the amorphous granuloma (Figure 10) [90]. Th1 cells are the main producer of a key cytokine that helps to contain the infection: IFN γ , which triggers the macrophage microbicidal functions and is secreted by NK and NKT cells at the site of infection, prior to Th1 cell recruitment.

Finally, B cells and fibroblasts are recruited to close the granuloma that finally harbors the distinctive mature TB granuloma phenotype (Figure 11). Classically, mature granulomas are structured around a necrotic center, surrounded by an inner ring composed of epithelioid “M1”-like macrophages, multi-nucleated giant macrophages and foamy macrophages, which are mainly microbicidal. A second ring surrounds the inner ring with IFN γ ⁺-TNF α ⁺ T cells and “M2” macrophages that prevent lung inflammation and damages, while also replenishing the pool of Mtb-killer macrophages in the inner ring. Finally, close to the granuloma, lymphoid structures composed of antibody-secreting B cells form to provide the host with humoral responses to Mtb [86], [97]. The formation and maintenance of this structure deeply relies on the macrophage production of TNF α , but is also mediated by Mtb virulence factors. Indeed, Volkman and colleagues showed that Mtb virulence plays a role in granuloma formation in the zebrafish model. Using a Δ RD1 mutant strain of *M. marinum*, the authors found that despite its capacity to grow in macrophages, Δ RD1 bacteria failed to elicit

¹⁰ **CCL19**: chemokine C-C motif ligand 19, also known as macrophage inflammatory protein 3b (MIP-3b), is involved in lymphocytes recirculation and homing, through ligation to C-C chemokine receptor 7 (CCR7).

¹¹ **CCL21**: chemokine C-C motif ligand 21 is a chemoattractant to CCR7-expressing cells.

¹² **MHC**: major histocompatibility complex, receptor found on antigen presenting cells (MHC-II) or ubiquitous (MHC-I) involved in antigen presentation to T cells that initiate adaptive immune responses.

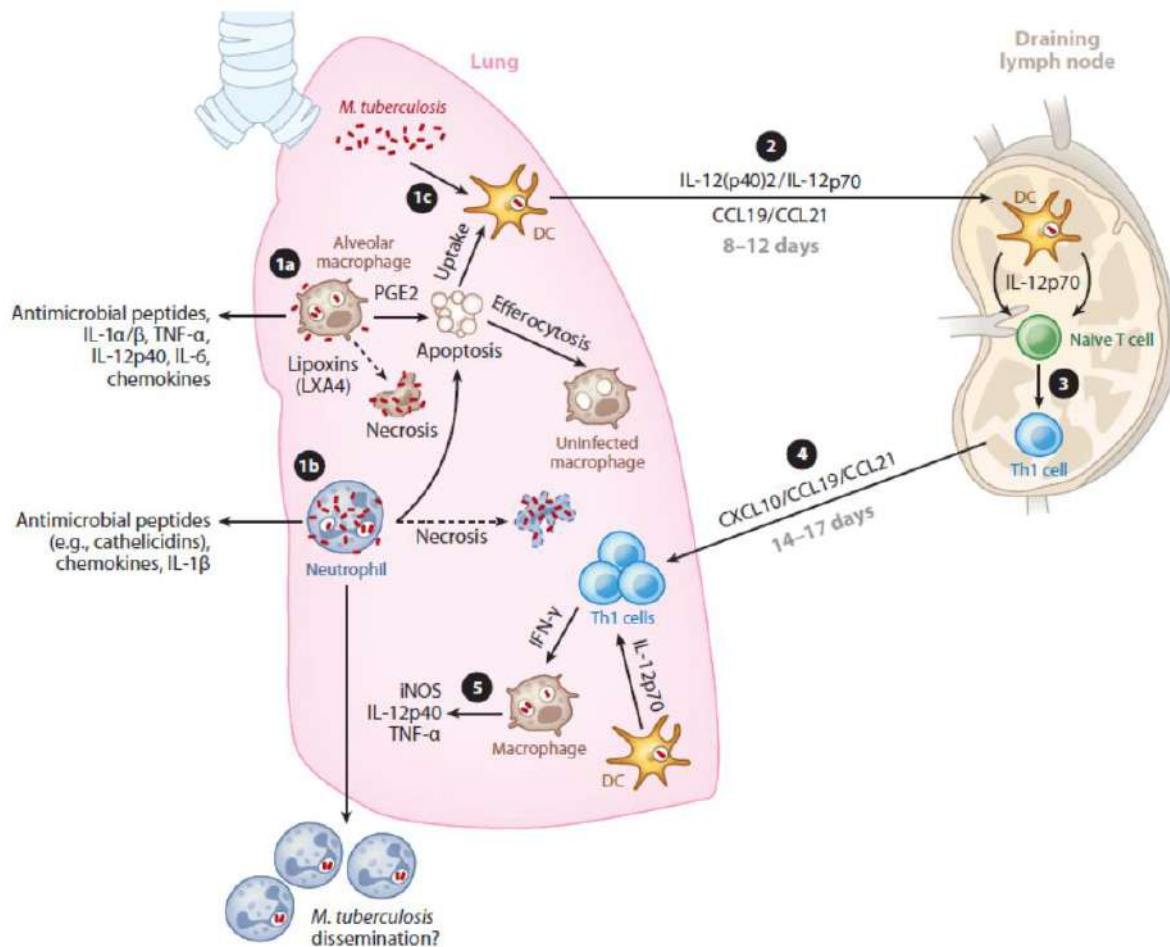


Figure 10: The cellular response to Mtb infection (from [71])

Following aerosol infection of the lower lungs with Mtb, resident lung alveolar macrophages (1a), and neutrophils (1b) can be infected, leading to the subsequent production and secretion of host defense molecules (e.g. antimicrobial peptides, cytokines, and chemokines). Depending on the balance between prostaglandin E2 (PGE2) and lipoxin A4 (LXA4), infected macrophages will undergo either apoptosis or necrosis, leading to the recruitment of new cells. Lung DCs (1c) close to the infection site can then phagocytize Mtb antigens and apoptotic debris. Subsequently, and with a strong delay in the case of Mtb infection (8-12 days instead of 72h in influenza infection for example), DCs secrete IL-12 (2) and migrate into the draining lymph node to activate naïve CD4⁺ T cell towards a Th1 activation program (3). Protective antigen-specific Th1 cells migrate back to the lungs in a chemokine-dependent manner 14–17 days after the point of initial infection/exposure (4) and produce IFN γ , leading to macrophage activation, cytokine production, the induction of microbicidal factors including iNOS (5). This usually contains efficiently the bacteria, but in some cases, Mtb escapes this response and spreads within the host, potentially by manipulating neutrophils.

granuloma formation, leading to a reduced bacterial burden compared to wild type (WT) *Mycobacteria* [103]. In the adult zebrafish model, the same observation was made, showing that it was a default in the macrophage mobility that decreased granuloma formation and that limited *M. marinum* growth in infected animals [104]. These studies contribute to the growing evidence for how Mtb virulence modulates granuloma formation to establish a proliferative niche for infection by manipulating macrophages functioning.

Once formed, the granuloma is encapsulated in a fibrous capsule and remains well vascularized. The center of the structure slowly becomes hypoxic, leading to Mtb containment. While Mtb growth during granuloma formation is exponential, once hypoxic environment is established in the necrotic caseous center, Mtb metabolism switches to a non-replicative persistent state [71], [90], [86]. Progressive granulomas develop with time, and several granulomas at different stages of development are present in a single individual. Upon reactivation of the disease in immunocompromised situations (e.g. HIV-1 co-infection, diabetes, malnutrition), the natural evolution of the granuloma moves towards caseation liquefaction, finally leading to the disruption of the structure. As a consequence, thousands of viable infectious bacteria are released in the lung, upgrading the disease to a transmissible status [97].

b. Importance of cytokines in the immune response

Cytokines are key players of the immune system, and their involvement in Mtb immune responses tightly intertwine innate and adaptive immunity. Some of them, like TNF α and IL-12/IFN γ cannot be circumvented. Several studies reported a critical role in Mtb burden control by TNF α . Indeed, patients receiving anti-TNF therapy to treat rheumatoid arthritis or Crohn's disease showed a more than 5-fold increase in their susceptibility to TB reactivation [105]. These patients exhibited disseminated bacteria and extra-pulmonary disease, despite the presence of normal granuloma [106], [107]. The same observations were made in non-human primate (NHP) animal models receiving anti-TNF α treatment [108], as well as the mouse model [109], [110]. Strikingly, TNF α ^{-/-} mice showed an increased susceptibility to Mtb infection, and a delayed granuloma formation [111], [112], supporting the key role of TNF α in the formation and maintenance of this structure. In the mouse model of TB reactivation using anti-TNF α antibodies, treated infected mice showed an increased bacterial load, increased necrosis in granuloma and in all cases, a lethal reactivation of the disease [110], [113]. Further supporting the key role of both macrophages and TNF α in the formation of granuloma, Egen and colleagues found that efficient recruitment of T cells and myeloid cells to mature granuloma in mice was highly dependent on TNF α signals [114]. In addition, anti-TNF treatment led to a decrease in granuloma size, due to few numbers of recruited macrophages [114]. Altogether, these studies show the importance of TNF α , which is mainly secreted by macrophages, in the control of the pathology, by boosting the intracellular killing of Mtb, as reported by other publications [115].

The IL-12/IFN γ axis is crucial to fight against Mtb, as it activates macrophages microbicidal function, allowing for the control and elimination of the bacteria by "M1" macrophages. As previously discussed, IFN γ is secreted by CD4⁺ T cells, NKT, CD8⁺ T cells and NK cells, in response to IL-12 signaling. When migrating to the draining lymph node, Mtb-activated DC secrete IL-12 that primes naive T cells and engages their Th1 activation program [99], [116]. In IFN γ ^{-/-} mice [117], as well as in IL-12^{-/-} mice,

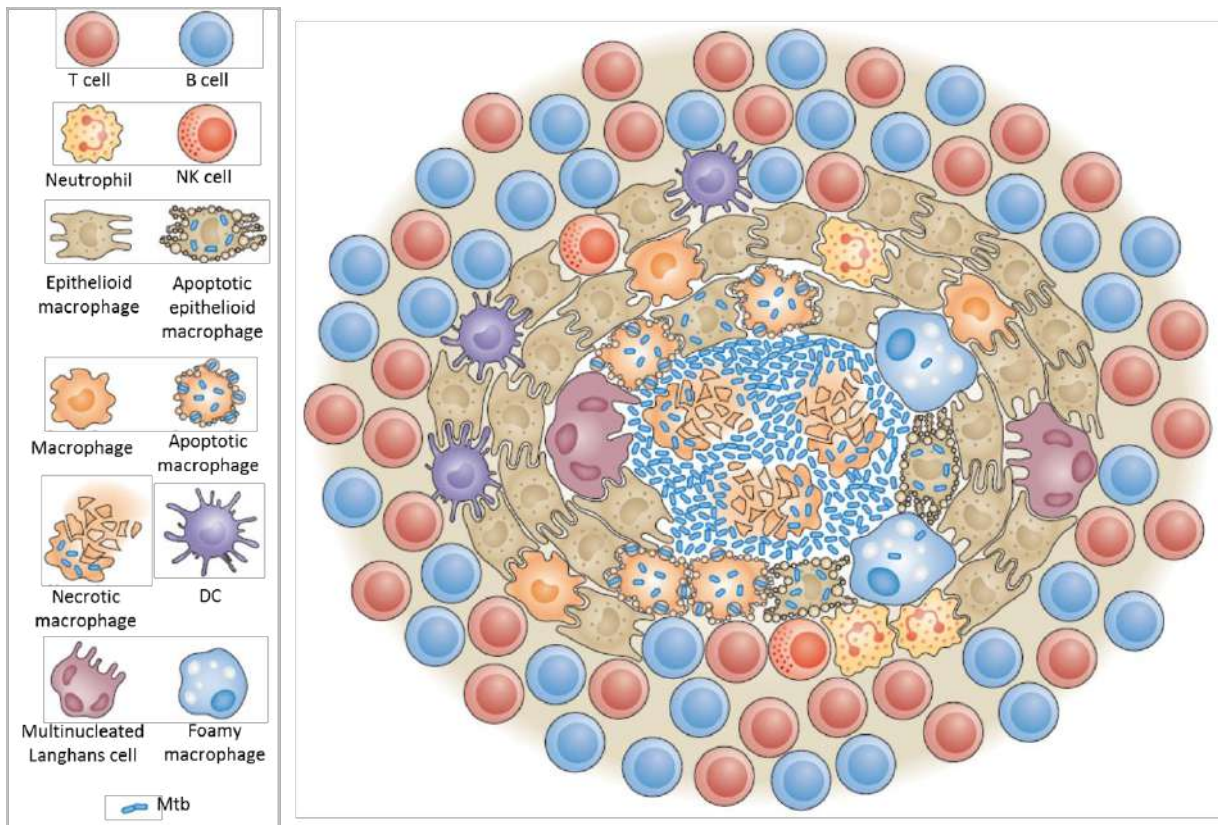


Figure 11: The mature tuberculous granuloma structure (from [86])

The tuberculous granuloma is composed of a macrophage necrotic center and free bacilli, surrounded by an inner ring with innate cells (neutrophils, macrophages infected or not, foamy cells, multinucleated Langhans giant cells and epithelioid macrophages that cannot become infected). The second ring is composed of DC, neutrophils and uninfected macrophages displaying either an “M1” activation program, to replenish the inner ring with bactericidal macrophages, or a “M2” polarization that protects the surrounding tissue of immune damages. Finally, T cells and B cells surrounds the structure to maintain an adaptive immune response to the infection: T cells produce $IFN\gamma$, a crucial cytokine to polarize macrophages towards a microbicidal profile, and to maintain $TNF\alpha$ secretion, which is necessary for granuloma formation and maintenance.

researchers reported a lack of reactive oxygen and nitrogen species (ROS, NS) in macrophages, a progressive destruction of the lung integrity and, importantly, a lack of control of bacterial growth [99], [116], [118]. IL-12 mutations in human, especially in children from consanguineous marriages, predispose these individuals to severe TB infections [119]. In NHP models of co-infection with the simian immunodeficiency virus (SIV), latently TB-infected macaques presented with an increased frequency of Mtb-specific IFN γ ⁺IL-2⁺ T cell responses between 2-5 weeks post-SIV infection. After this spike, the IFN γ ⁺ T cells decreased to low levels, corresponding to a fall in CD4⁺ T cell counts. This led to rapid reactivation of TB in certain animals, who showed greater bacteria burden and high pathology scores at the necrotic granuloma. Therefore, in co-infection settings, increased proportion of IFN γ ⁺IL-2⁺ CD4⁺ T cells specific for Mtb during acute SIV infection suggests an increased level of Mtb antigen, leading to TB-reactivation [120]. These results were corroborated with the observation that in TB-HIV-1 co-infected patients, the level of IFN γ ⁺IL-2⁺ CD4⁺ T cells was inversely proportional to viral load [121].

Considering all these studies, an efficient establishment of IFN γ along with other cytokine responses is essential to control the bacterial growth and to create an environment in which Mtb can be contained and consequently eliminated.

B. Macrophages and *Mycobacterium tuberculosis*: an ongoing evolutionary arms-race

a. Mtb recognition through PRR and initiation of the host response

As previously mentioned, macrophages are the main effector cell against Mtb. To fulfill this function, these cells must first come in contact with Mtb, internalize and destroy it, and engage in an appropriate immune response to activate both the innate and adaptive arms of the immune system. To accomplish this, several PRR have been involved in Mtb recognition by the host, including TLR, CLR, nucleotide-binding oligomerization domain-like receptors, or NOD-Like Receptors (NLR), scavenger receptors and complement and Fc- γ receptors. The engagement of the different PRR drives macrophage activation through different signaling pathways, leading to combinatory signals that result in the establishment of the host innate immune response. However, macrophages play a dual role in tuberculosis because they are also the primary host cell reservoir for Mtb. In fact, the bacillus has evolved different strategies to hijack the function of PRR. Here, I will give some examples that illustrate these principles.

i. Toll Like Receptors (TLR)

TLR belong to a highly-conserved family of transmembrane receptors of which the extracellular domain recognizes PAMP, while their intracytoplasmic domain induces a signaling cascade in the cell upon ligand recognition [122]. They are expressed by almost all immune cells, including alveolar macrophages, neutrophils, lymphocytes and DC. Upon ligand binding, most of the signaling cascades involve the activation of MyD88 and NF κ B¹³, which translocate to the cell nucleus and stimulate inflammatory responses, including the up-regulation of their various negative regulators. Once the pro-inflammatory response is initiated, microbicidal functions of the activated innate cell become effective and control the growth of the bacteria. The innate immune cells then engage a long-lasting adaptive immune response led by Th1 immunity [122]. As TLR are numerous and activate many different signaling pathways, they can also lead to alternate signaling cascades, resulting in anti-inflammatory responses [71], [95]. Mtb is recognized through the plasma membrane TLR2 and 4, and by the phagosomal TLR9. Of note, TLR2 expression is lower in alveolar macrophages compared to other cell types, whereas TLR4 and TLR9 are expressed at similar or higher levels, respectively [95].

TLR are important PRR in Mtb pathogenesis. Indeed, several studies reported that individuals with genetic variants of TLR2, which binds to Mtb lipomannan (LM) and phosphatidylinositol-mannosides (PIMs) [95], are more susceptible to Mtb infection [123]. Moreover, TLR2 can form heterodimers with TLR1 and TLR6. These heterodimers have been implicated in the recognition of mycobacterial cell wall components, such as LAM, LM, and PIM and mediate a Th1-driven immune response to Mtb [122]. In addition, MyD88-deficient mice lose resistance to Mtb infection and display an impaired production of Th1 cytokines (*e.g.* IL-12, and TNF α) and of inducible nitric oxide synthase

¹³ **NF κ B**: nuclear factor kappa-light-chain-enhancer of activated B cells is a protein complex expressed by almost all cell types that controls transcription of DNA, cytokine production and cell survival upon stimulation.

(iNOS)¹⁴ [124]. Moreover, TLR are responsible for the activation of the IFN-I responses in the cell, a subject that will be discussed in this chapter, section C.

ii. *C-type lectin receptors (CLR)*

Many CLR have been described to bind glycosylated molecules expressed by host cells and/or pathogens. Most of them contain a carbohydrate recognition domain that acts in a calcium-dependent manner. Here, I will particularly focus on two CLR described in both Mtb and HIV-1 pathogenesis: the mannose receptor (MRC1) and dendritic cell-specific intercellular adhesion molecule-3-grabbing non-integrin (DC-SIGN).

(1) MRC1 (CD206)

This is a predominant CLR expressed by non-activated macrophages, including alveolar macrophages. It contains a carbohydrate recognition domain that binds with high affinity to mannans present on host cells, but also on several pathogens, and maintains host homeostasis [95], [125]. Pathogens like Mtb and HIV-1 express mannosylated structures in their wall/envelope. MRC1 specifically recognizes glycosylated ligands in the Mtb envelope, including LAM, ManLAM and PIMs (see chapter I section I.A.e.) [126]. Importantly, MRC1 is involved in the modulation of the immune responses against Mtb, and is usually associated with an anti-inflammatory program in macrophages that is protective against immunopathology [127].

It is thought that the development of these highly mannosylated PAMP play a role as molecular mimics, by which Mtb evades the immune system through cloaking itself in molecules similar to those from the host [128]. Upon Mtb recognition through MRC1, the bacteria are internalized into phagosomes, which are deficient for fusion abilities with the lysosomal compartment. In addition, infected cells display anti-inflammatory cytokines secretion that inhibit IL-12 [129] and ROS secretion [130]. These immunosuppressive properties are regulated by the peroxisome proliferator-activated receptor γ (PPAR γ), which inhibits NF κ B activation, and in an indirect manner, IFN γ production. Indeed, this molecule is key in Mtb evasion mechanisms since its deletion in mice leads to growth reduction of virulent Mtb and lower granuloma infiltration, along with enhanced pro-inflammatory cytokines secretion [131]. By contrast, MRC1-deficient mice did not show any particular phenotypic changes after Mtb infection, suggesting that its expression is not essential in Mtb pathology, probably due to the functional redundancy of PRR [126].

(2) DC-SIGN (CD209)

DC-SIGN is expressed by a small proportion of macrophages, including alveolar macrophages as well as DC, and recognizes mannosylated glycol-conjugates such as N-linked high mannose structures [126]. Initially, DC-SIGN was highlighted for its capacity to bind HIV-1 particles through

¹⁴ iNOS: one of the three isoforms of the nitric oxide synthase that produces azote monoxide and that is synthesized by phagocytes as a microbicidal molecule. Other forms of NOS are constitutively expressed in neuronal and epithelial cells and are controlled by intracellular calcium concentrations.

recognition of the viral glycoprotein gp120, and to mediate trans-infection of CD4⁺ T cells (see chapter II section III.D.a.i) [132], [133]. Since then, it was shown that this lectin is able to recognize several other pathogens, including viruses, bacteria and parasites [134]. Along with others, my group, led by O. Neyrolles, has published important breakthroughs on the role of DC-SIGN in Mtb pathology, and was one of the first to show that DC-SIGN binds to Mtb [135], [136]. Human DC-SIGN assembles in tetramers for optimal ligand binding and recognizes the same molecules as MRC1 (*i.e.*, PIM and ManLAM) that are expressed by Mtb, leading to clathrin-dependent endocytosis of the complex [126]. Interestingly, while DC-SIGN is not usually expressed in non-activated macrophages, Mtb has the capacity to up-regulate its expression on these cells. Indeed, my group found that in TB patients, up to 70% of alveolar macrophages from broncho-alveolar lavages (BAL) express DC-SIGN (against 1.7% in healthy individuals), and the bacilli are concentrated in DC-SIGN enriched pulmonary regions [137]. *Ex vivo*, Tailleux and colleagues showed that this Mtb-induced expression of the lectin is dependent on TLR4, IL-4 and IL-13 signaling. My group also showed that DC-SIGN⁺ alveolar macrophages constitute a preferential target for Mtb since blocking of DC-SIGN lead to decreased bacterial uptake [137].

Additional studies performed in the lab showed an increased expression of DC-SIGN both in CD68⁺ lung macrophages from Mtb-infected NHP and in pleural effusion cells from TB patients. *In vitro*, DC-SIGN expression is particularly high on IL-4 induced monocyte-derived macrophages (MDM). After DC-SIGN depletion in these cells, a genome-wide transcriptomic analysis revealed the up-regulation of pro-inflammatory signals in response to Mtb challenge and a reduced permissiveness to infection despite equivalent levels of bacterial uptake. Altogether, these results indicate that DC-SIGN plays a dual role in Mtb infection, by inducing anti-inflammatory responses that protect the host from immunopathology, resulting in reduced inflammatory responses against Mtb, therefore promoting bacterial proliferation [138].

Other C-type lectins are also involved in Mtb binding. For example, the transmembrane PRR Dectin-1 binds to Mtb β -glucan and induces phagocytosis of the bacteria, initiating signaling cascades that interact with TLR activated pathways, leading to macrophage activation and IL-12 production in DC. The C-type lectin Mincle is mainly expressed by myeloid cells after exposure to various inflammatory stimuli, such as cytokines and TLR activation, and can recognize Mtb trehalose dimycolate (TDM), but is not essential in Mtb control in mice despite its involvement in the regulation of anti-mycobacterial immune responses [126].

iii. Other receptors

Other receptors families have been shown to recognize Mtb antigens. Among them, we can find scavenger receptors, NLR, integrins, FC- γ and complement receptors. Among scavenger receptors, which participate in homeostatic functions and bind to oxidized low density lipoproteins, MARCO has been well described [95]. Indeed, MARCO binds to Mtb TDM and acts in combination with TLR2 signaling to induce pro-inflammatory responses [139], therefore participating in the establishment of anti-Mtb responses in the host.

Complement Receptor 3 (CR3 or integrin $\alpha\beta 2$) is a heterodimeric receptor that belongs to the integrin family expressed on neutrophils, monocytes, natural killer cells and macrophages. CR3 recognizes C3b opsonized Mtb *in vitro*, however, it is unlikely that this interaction happens *in vivo* due to low concentrations of complement molecules in the lung [126].

Finally, the intracellular NLR family comprises molecules such as NOD1 and NOD2, able to detect gram-positive and gram-negative bacterial peptidoglycans. Their expression is abundant in human macrophages. Upon ligation to its target, NOD2 activates MAPK, the mitogen-activated protein kinase, that indirectly allows NF κ B activation [126]. NOD2 is also able to directly bind and activate caspase-1 and interacts with the inflammasome [140]. This particular NLR is therefore important for Mtb-induced immune responses since it induces IL-1 β , IL-6 and TNF α secretion, allowing for the establishment of a strong pro-inflammatory response against Mtb. In addition, NOD2 deficiency in mice and in human macrophages leads to enhanced Mtb growth [141], further supporting the role of NLR in the activation of microbicidal pathways in innate immune cells.

Macrophages express numerous PRR able to recognize different components of the bacteria, including cell wall components, proteins, lipids, and nucleic acid. Binding of these different ligands lead to macrophage activation by stimulation of relevant pathways, leading to bacterial internalization and engagement of bactericidal functions. However, some of these PRR are involved in maintaining the balance between pro- and anti-inflammatory cytokine responses, and protect the host from immunopathology (*e.g.* MRC1). As PRR are numerous and can have different consequences for the host immune response, particularly in an Mtb infection context, a better understanding of the PRR homeostatic and inflammatory roles is key to develop host-targeted therapies to cure TB, based on the modulation of PRR activity.

b. Macrophages and Mtb immunity: a complex interplay between bacterial control and escape mechanisms

i. The Mtb phagosome

Now that we have seen how Mtb is recognized by PRR, I will focus on how the bacterium is processed by macrophages. These cells specialize in the ingestion of cell debris and microbes; they are professional cleaners of the body. As such, macrophages exhibit different processes, including phagocytosis. During normal phagocytosis, actin-mediated movements of the phagocyte cell membrane engulf cell debris or microbes into a specific intracellular compartment: the phagosome [87]. Once inside the macrophage, a sequence of events leads to phagosome maturation. First, Rab GTPases¹⁵ are recruited to the phagosomal membrane, which then attract the vacuolar v-ATPases to acidify the phagosome content. At this stage, the pH decreases from 6.5 to 6. Finally, the phagosome fuses with a pre-formed lysosome to merge their contents, including lysosomal acid hydrolases. This

¹⁵ **Rab GTPases:** member of the Ras superfamily of small G-proteins possessing a GTPase fold. They regulate many steps of membrane trafficking, including vesicle formation, transport and endo/exocytosis. Of note, these proteins switch between inactive conformation, linked to guanosine diphosphate and active conformation that is linked to guanosine triphosphate.

process is known as phagosome maturation. After degradation, microbial debris is either recycled or destroyed. In TB, this process is impaired through many mechanisms. Actually, Mtb is able to inhibit phagosome maturation and fusion with lysosomes. Often, the bacilli are contained in phagosomes with an abnormally high pH of ≈ 6.2 [142]. This is best exemplified by the study of Mwandumba and colleagues where large non-acidified vacuoles, containing a large number of bacilli, are observed in alveolar macrophages isolated from active TB patients due to inhibition of phagosome-lysosome fusion [143].

Mtb possesses many mechanisms to stop phagosome maturation, most of which involve cell wall lipids and virulence factors. First, maturation is arrested by the alteration of the Rab GTPases, which in physiological conditions, regulate the intracellular trafficking of organelles [144], [145]. Previous studies have shown that this blockage occurred between the maturation stage controlled by Rab5, an early endosomal marker that is accumulated normally to the phagosomal membrane, and Rab7, whose recruitment to the phagosome was inhibited (late lysosomal marker) [146]. Tightly intertwined with this mechanism, the implication of the Rab5 effector EEA1 (early endosomal autoantigen 1) has also been reported. Mtb ManLAM was shown to interfere with EEA1 recruitment to the phagosome, therefore preventing the complexation of EEA1 with Rab5 and leading to inhibition of phago-lysosome membrane fusion [144], [145]. ManLAM also inhibits the formation of PI3K-calmodulin complex, inducing PI3P exclusion from the phagosomal membrane. This blocks phagosome maturation since PI3P is a critical lipid for the attraction of v-GTPases and v-ATPases¹⁶ to this cellular compartment, preventing its acidification [146]–[148]. Finally, Hartlova and colleagues reported the implication of the negative regulator of phagosomal maturation LRRK2 in the recruitment of PI3K and its negative regulation of phagosomes in human macrophages, leading to uncontrolled bacterial growth [149]. In addition, Mtb is able to resist phagosome acidification, which is the last step of phagosome maturation. Indeed, the mycobacterial envelope is poorly permissive to proton entry and thus acidification, and additionally possesses proteases like MarP¹⁷ and RipA¹⁸ that allows for the secretion of basic component such as ammoniac, leading to phagolysosome pH neutralization [150], [151].

One way for the host to circumvent Mtb escape from these organelles is to induce spacious phagosomes. This event was observed thanks to electron microscopy studies, notably in monocytes from active TB patients [152]. These structures were induced in an IFN γ -dependent manner, up-regulating the endosomal protein Rab20 machinery. Indeed, the overexpression of Rab20 in a macrophage cell line induced the formation of large phagosomes, which contained several bacilli that showed decreased growth capacities compared to controls, and displayed late endosomal markers such as LAMP-2, demonstrating their maturation. By contrast, Rab20^{-/-} bone marrow-derived murine macrophages were unable to form spacious organelles and were unable to maintain membrane integrity, leading to subsequent bacterial growth enhancement. Finally, the capacity of macrophages to form spacious phagosomes was dependent on Mtb virulence factors, especially those encoded in the RD1 genome region [153]. However, Mtb is also a “Houdini” master at escaping phagosomes by disrupting their membrane integrity through ESAT-6, leading to subsequent colonization of the

¹⁶ **v-ATPase or v-GTPase:** vacuolar ATPase or GTPase

¹⁷ **MarP:** Mycobacterium acid resistance protease

¹⁸ **RipA:** peptidoglycan endopeptidase that cleaves the bond between D-glutamate and meso-diaminopimelate, binds and degrades high-molecular weight peptidoglycan expressed by bacteria.

macrophage cytosol [89], [154]. In particular, the Mtb lipid phthiocerol dimycocerosates (DIM) was shown to facilitate Mtb colonization of the host cytoplasm [155].

Upon damage induced by Mtb, permeable phagosomes are rapidly recognized by the autophagosome machinery. Autophagy is a process similar to phagocytosis, except that instead of ingesting extracellular components, macrophages either recycle or degrade internal components, including organelles into a structure called the autophagosome [87]. As for phagosomes, Mtb is able to inhibit autophagosome fusion with lysosomes through the ESX-1 system [156]. Autophagy is initiated through Mtb ubiquitination, but also induced by IFN γ activation. In addition, the active form of vitamin D3 induces autophagy in human macrophages in a cathelicidin-dependent manner. Of note, cathelicidin is an anti-microbial peptide involved in the transcription of autophagy-related genes. In fact, vitamin D deficiency is linked with an increased risk of developing active TB [157]. Historically, sunlight exposure and vitamin D administration were used to treat TB; however, subsequent clinical trials reported only a moderate efficacy of this treatment [158].

ii. Oxidative and hypoxic stresses in response to Mtb internalization

Phagosome maturation works in tandem with the activities of toxic components such as reactive oxygen and nitrogen species (ROS and NS respectively), which kill ingested bacteria. ROS and NS are toxic derivatives of oxygen and nitrogen metabolism within macrophages, and notably include nitric oxide (NO), hydrogen peroxide (H₂O₂) and peroxide ion (O₂⁻). Their production is mediated by iNOS and NOX2¹⁹ proteins, which act synergistically to provide macrophage phagosomes with high bactericidal potential, particularly by triggering bacterial lipid, nucleic acid and protein oxidation [159]. In addition to killing the bacteria, these two pathways are also involved in the regulation of the inflammation caused by Mtb. Indeed, high inflammation, often caused by exacerbated cell death as a consequence of Mtb infection, is detrimental to the host. This cell death is usually driven by high inflammasome activation, which was reported to induce high inflammation, responsible for the more severe forms of tuberculosis, such as TB-IRIS and TB meningitis (see section I.A.c of the present chapter) [160]. In macrophages' NO pathway, NOS2, a nitric oxide synthase involved in (i) neurotransmission, (ii) anti-tumoral and (iii) antimicrobial activities, takes part in the regulation of Mtb-driven inflammation by inhibiting the activation of the NLRP3²⁰/Caspase 1 inflammasome in macrophages, reducing IL-1 secretion, and therefore, cell death. A molecule of the ROS pathway, Phox, is also involved in the inhibition of inflammasome activation [160].

As for other killing strategies, Mtb possesses several enzymes allowing it to escape these oxidative stresses. For example, the superoxide dismutase (SodAC) and the peroxidase KatG secreted by Mtb act sequentially to transform O₂⁻ ions into H₂O₂, and then water. The bacillus can also prevent

¹⁹ **NOX2**: nicotinamide adenine dinucleotide phosphate oxidase 2 is a cofactor involved in anabolic reactions and requires NADPH as a reducing agent.

²⁰ **NLRP3 inflammasome**: nucleotide-binding and oligomerization domain-like receptors 3 inflammasome is primarily found in immune and inflammatory cells following activation by inflammatory stimuli. NLRP3 activates caspase 1 cascade, leading to the production of pro-inflammatory cytokines (*i.e.* IL-1 β and IL-18), and induces cell pyroptosis, a form of programmed cell death.

iNOS fixation to the phagosome membrane to avoid NO importation into this compartment [161], thereby promoting a more favourable environment for survival.

In the TB granuloma, the necrotic center becomes hypoxic. Because of a reduction in oxygen availability, nitrite and nitrate pathways are of even higher importance for both Mtb control by the host and Mtb survival. In hypoxic environments, Mtb enters a dormant state, where its replication is almost arrested [162]. Despite the low oxygen concentration, Mtb is still able to survive, due to nitrate reductases that transform nitrates into oxygen [163]. In a study conducted in my team, the horizontal acquisition of *moaA1-D1* genes by Mtb allowed the bacteria to better use nitrate respiration. *In vitro*, under hypoxia, *moaA1-D1* genes were upregulated and allowed the bacteria to survive, while Mtb *moaA1-D1*-null mutants were unable to survive oxygen depletion *via* nitrate respiration. *In vivo*, the mutant strain presented an impaired survival in hypoxic granulomas of C3HeB/FeJ mice [164], further supporting the role of *moaA1-D1* genes in nitrate respiration and Mtb survival in hypoxic environments such as the granuloma.

iii. Nutrients deprivation

Although Mtb has multiple mechanisms to avoid phagosome maturation, macrophages employ other means to kill the bacteria, including nutrients deprivation in the Mtb phagosome [165]. An example of nutrient access restriction set by the host is iron deprivation. Like human cells, Mtb needs iron to survive, grow and spread. The host keeps key nutrients, like iron and manganese, away from the bacteria by complexing them into proteins such as transferrin and ferritin, or by pumping them out of the phagosome using cation transporters [166]. In the case of iron, the expression of Nramp1²¹ at the phagosome membrane allows iron exportation out of the vacuole, thereby limiting its access to the bacteria [165]. Unfortunately for the host, Mtb has also evolved to capture host-sequestered iron cations through siderophores and heme utilization [167], [168]. For example, the carboxymycobactins siderophores are specialized in iron removal from transferrin and ferritin [169]. This mechanism is an important tool for Mtb, since increased loads of iron within the host have been shown to be an exacerbating factor for TB disease [170].

Lipids are also important nutrients for Mtb metabolism and represent the main source of carbon available during the infection, and more specifically cholesterol and triacylglycerol (TAG). Mtb infection of macrophages leads to the accumulation of TAG droplets in the cell, which in turn can become foamy macrophages. The bacteria are able to import the fatty acid that derives from TAG processing, a process that indicates that the bacteria is entering a dormant state [171], [172]. In addition, Mtb strains depleted of the *mce4* operon coding for cholesterol transporters display attenuated growth in infected mice, indicating that cholesterol is required in the later phases of Mtb infection [173].

As a last example, my team has identified aspartate and asparagine as the major source of nitrogen for the bacteria. Access to aspartate is possible within the phagosome, through its import by the bacterial nitrogen transporter protein Ansp1. Indeed, Mtb Ansp1 null mutants have a reduced

²¹ **Nramp1**: Natural resistance-associated macrophage protein 1, involved in iron metabolism and resistance to certain pathogens

capacity to proliferate in mice [174]. The other nitrogen source for Mtb is asparagine, the favoured source of nitrogen for the bacteria *in vitro*. In fact, my team showed that Mtb employs the asparagine transporter AnsP2 and the secreted asparaginase AnsA to assimilate nitrogen in phagosomes. It also uses these proteins to resist acid stress by hydrolyzing asparagine and releasing it in the cell cytosol [175].

iv. Bacterial intoxication with metals

In addition to nutrient deprivation, limited oxygen access, and acidic and oxidative environments, Mtb must face the risk of metal intoxication inside the phagosome. For example, copper is an essential redox-active metal used as an enzyme cofactor at steady state. Under pathological conditions, copper intoxication represents an efficient way to intoxicate the microbe. In fact, copper deficiency in animal models proved to be detrimental for the ability of macrophages and neutrophils to induce the respiratory burst, leading to impaired elimination of the phagocytosed bacilli [176], [177]. In the lungs of Mtb-infected guinea pigs, primary granuloma exhibited elevated copper levels compared to unaffected tissue [178]. In the Mtb phagosome, copper ions imported in this compartment after macrophage activation encounter hydrogen peroxide and react to generate superoxide radical anions. This process exposes the surrounding bacteria to an oxidative stress that inflicts damage to its lipids and cell wall. This attack may not kill the bacteria; however, it could prime it for subsequent destruction mediated by other phagosomal functions such as acidification [179], [180].

Metal intoxication is also mediated by zinc flux inside macrophages. Indeed, zinosomes (vacuoles containing free zinc) span the entire endocytic pathway, including within Rab5 early endosome where Mtb is often sequestered [181], [182]. Zinc toxicity occurs due to the replacement of other cations in essential enzymes, consequently inhibiting their activity [182]. Copper and zinc both accumulate in Mtb phagosomes in order to kill the bacteria. However, as for many other host-defense mechanisms, Mtb has evolved to circumvent both copper and zinc intoxication by expressing efflux pumps such as CtpV [183] and CtpC [184], respectively. Indeed, Mtb is particularly sensitive to copper since concentrations lower than that found in the phagosome of macrophages are able to kill the bacteria *in vitro* [178]. For this reason, copper resistance, conferred by CtpV, is essential for Mtb virulence. The same is true for Mtb resistance to zinc poisoning. My team previously showed that in *in vitro* Mtb-infected macrophages, the zinc efflux pump CtpC is upregulated while free zinc concentration in the cytosol of macrophages was increased within few hours post-infection [184].

To conclude, Mtb has evolved for millenia with its natural host, and has acquired numerous escape mechanisms to counteract the immune response, more specifically to elude the microbicidal functions of macrophages. The major focal point of this hide-and-seek game between the host and the pathogen seem to be the phagosome, whose functions have been met equally by Mtb throughout evolution.

c. Role of specific macrophages subsets induced by Mtb infection

Primary Mtb infection occurs in lung alveolar macrophages and triggers the recruitment of innate immune cells to the site of infection. Consequently, and with the establishment of the adaptive immune response, a granuloma forms around Mtb-infected cells, mainly macrophages, to contain the bacilli. The infection of macrophages leads to their differentiation into particular subtypes, including epithelioid macrophages, multinucleated giant macrophages (MGC, also called Langhans cells) and foamy macrophages. The implication and specific functions of these different subtypes are poorly described to date, especially for epithelioid macrophages, which were mainly used as a marker of granulomatous lesions within TB infected lung biopsies, allowing for disease identification. However, few studies have investigated the function of MGC and foamy macrophages during TB disease and are hereafter discussed.

i. Macrophages polarization in Mtb-infection

As mentioned in the preamble, macrophage polarization is mainly driven by type-1 and type-2 inflammatory signals. In TB, defense against the pathogen strongly requires type-1 immunity, since expression of inflammatory cytokines of this type are associated with efficient anti-Mtb immune responses [185]. During infection, T cells produce large amount of IFN γ , which drive macrophage differentiation within the granuloma towards an M1 or M(IFN γ) profile. These cells are professional killers of Mtb and are the first to intervene in the early phase of infection [186]. However, the bacillus has evolved and developed strategies to circumvent “M1” polarization by shifting macrophages towards “M2” anti-inflammatory programs, which are immunomodulatory and poorly microbicidal [187]. It is frequently observed that during pathogen infection, a shift from M1 to M2 program of macrophage polarization occurs at the sites of inflammation. This shift is associated with the adaptive immune transition from acute to chronic phases, and is probably necessary for the resolution of inflammation and for tissue repair [188].

To induce the shift towards an M2 profile in macrophages, Mtb express virulence factors, such as ManLAM or ESAT-6 that prevent IFN γ -mediated differentiation of macrophages, by inhibiting the activation of NF κ B and IFN γ regulatory factors [186]. In addition to IFN γ signaling inactivation, Mtb can also influence TLR signaling by targeting DC-SIGN and MRC1 to induce IL-10 production. M(IL-10) macrophages counteract pro-inflammatory responses and protect the host from immunopathology and as such, they are poorly microbicidal and highly permissive to intracellular pathogens like Mtb [189]. The bacterium also modifies the metabolism of macrophages to control their polarization. Indeed, in mice models of Mtb infection, NO production is reduced, while iron availability is increased, therefore providing the mycobacteria with a permissive intracellular environment to grow [190]. In another study, it was shown that Mtb infection induces the expression of arginase 1 through the MyD88 pathway, resulting in the inhibition of NO production [191], thus rendering cells permissive to the infection. In addition to iNOS metabolism, Mtb is also able to trigger the accumulation of lipids as carbon sources in infected macrophages, leading to their differentiation into foamy cells (described later in section II.B.c.iii.).

ii. *Multinucleated Giant Langhans Cells*

Macrophage fusion is a hallmark of several inflammatory pathologies, such as HIV-1 [192] and Mtb infection [86], [98], [191]. Multinucleated giant Langhans cells (MGLC) are usually present in granulomas, and are considered as a host defense mechanism. When caused by a pathogen infection, MGLC formation can be induced to phagocytize large and indigestible microorganisms. Few studies have reported the specific role of MGLC during Mtb infection. However, few studies suggest a role for MRC1 in the fusion process between macrophages during TB [95]. Despite a possible role of MRC1 in fusion induction, fully differentiated MGLC did not express CD11b or MRC1 [193]. Another molecule related to fusion processes in monocytes, called dendritic cell-specific transmembrane protein (DC-STAMP), was shown to be upregulated during the formation of MGLC. Indeed, when DC-STAMP was inhibited by small RNA interference (siRNA), MGLC formation was dampened by 2-fold. The authors showed that entry receptor expression was induced by IFN γ secreted by T cells. In fact, in this study, T cell-macrophages interactions through CD40/CD40L interactions proved to be essential for Langhans cells formation [194]. Another study conducted at IPBS reported the involvement of TLR2/ADAM9²²/ β 1 integrin axis in MGLC formation. This cascade of events starts with the recognition of bacterial lipomannans by macrophages. Fusion into MGLC required the β 1-integrin/ADAM9 cell fusion machinery. Indeed, in an *in vitro* model where granuloma-like structures are induced using virulent Mtb glycolipids-coated beads, anti- β 1 integrin or anti-ADAM9 utilization prevented MGLC formation [195].

Despite these breakthroughs in possible macrophage fusion mechanisms, these studies did not report any specific functions for MGLC in TB disease. In fact, the only reported function of MGLC was to present Mtb antigen, when other macrophage bactericidal functions like phagocytosis were lost [196].

iii. *Foamy macrophages: an energy reservoir for the bacteria*

Foamy macrophages are characterized by the abundance of lipid bodies, rich in TAG and neutral lipids that accumulate within lipid droplets in the cytosol. They play a central role in several inflammatory diseases such as atherosclerosis or chronic infectious diseases, including co-infection between HIV-1 and *M. avium* [197], [198]. In the context of Mtb infection, foamy macrophages mainly localize at the interface between the immune cells ring and the necrotic center of the granuloma [172]. The presence of foamy macrophages within granulomas has been described both in infected animals

²² **ADAM9**: Disintegrin and metalloproteinase domain-containing protein 9 is a membrane-anchored protein involved in cell-cell and cell-matrix interactions

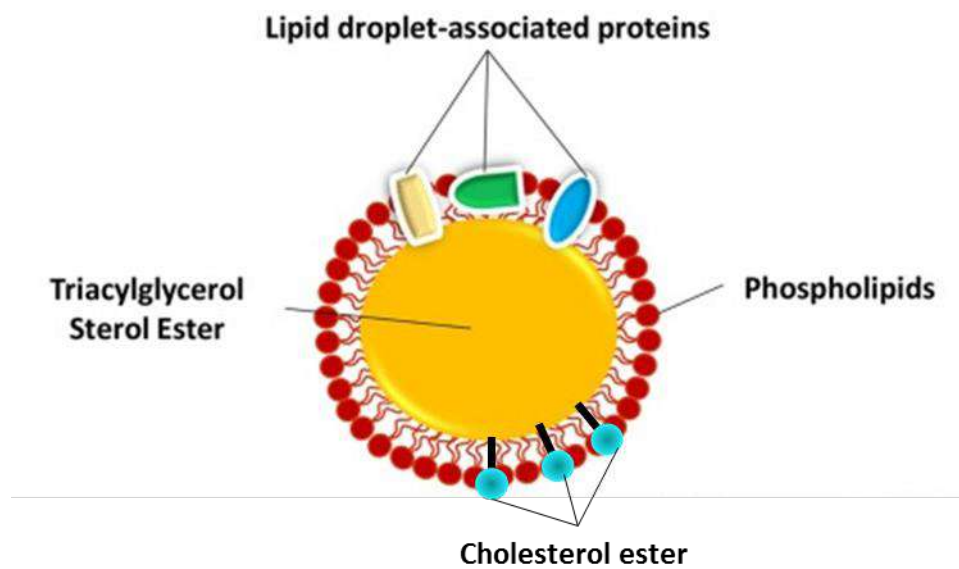


Figure 12: Lipid bodies structure (adapted from [198])

Lipid bodies are composed of a core of triacylglycerol (TAG) and sterol esters surrounded by a phospholipid monolayer. Several proteins are inserted in the monolayer, along with cholesterol molecules and associated proteins.

and patients [199], [200]. Because of the many changes occurring upon progression to TB, Mtb has to adapt to the host in order to survive. Among these adaptations, the accumulation of neutral lipids within the bacterial cytosol in compartments called ILI (intracytosolic lipid inclusions), serve as carbon and energy reservoirs and are thus of main importance to bacterial survival [201]. ILI induction in Mtb was proposed to be a hallmark of persistent and non-dividing bacteria, especially when considering the abundance of Mtb genes encoding for proteins involved in lipid metabolism [44].

Lipid bodies in most eukaryote and prokaryote cells display a similar structure (Figure 12). They are composed of a core of neutral lipids, mainly sterol esters and TAG, surrounded by a monolayer of phospholipids in which cholesterol esters and proteins are inserted. In eukaryotes, these lipid bodies are thought to originate from the endoplasmic reticulum, where fatty acids are used to re-synthesize TAG and sterol esters [198]. The high cell density and hypoxic environment within the TB granuloma are the basis for foamy macrophage formation [202]. In addition, the close proximity of foamy macrophages to the necrotic center of the granuloma may provide these cells with neutral lipids and phospholipids from dying cells [203]. However, the question remains to unveil the factors triggering foamy macrophage formation and to understand how Mtb gains access to host lipids and transports them into their own cytosol. Previous work showed that Mtb cell wall mycolic acid is a key component for foamy macrophage induction, as peritoneal injection of these lipids in mice leads to the foamy phenotype in the peritoneal cavity and airways [204]. However, work conducted at IPBS showed that only virulent Mtb were able to induce foam cell formation through mycolic acid [172]. In this study, Peyron and colleagues showed that Mtb present in foamy macrophages were internalized prior to foamy differentiation. At the functional level, in addition to their inability to phagocytize new bacilli, foamy macrophage cells displayed a decreased microbicidal activity and capacity to induce a respiratory burst. Finally, upon the differentiation of foamy macrophages, Mtb entered a dormant state by up-regulating dormant genes [172]. More recently, in a study published by the Argentinian laboratory, where I had the opportunity to perform part of my PhD research, led by Drs. Saisian and Balboa, they showed that foamy macrophage formation was induced by Mtb lipids and whole bacteria, as well as with monocytes treated with acellular fractions of TB patient pleural effusion. These cells contained high levels of TAG and cholesterol, along with an increased expression of IL-10 and CD36, a receptor involved in free lipid capture, and a decreased secretion of TNF α . This phenotype was acquired in an IL-10/STAT3-dependent manner, through activation of the enzyme acyl CoA:cholesterol acyl transferase (ACAT). Functionally, foamy macrophages were able to activate CD4⁺ T cells. Yet, the number of IFN γ producing clones was lower compared to control macrophages (Annex 1 [205]). Finally, a genome-wide analysis of TB granulomas performed by Kim and colleagues allowed the identification of genes involved in lipid sequestration and metabolism. They found an enrichment of cells expressing adipophilin, acyl-coA-synthase and saposin C around the necrotic center and identified the lipid species that were overexpressed in the caseum, namely cholesterol, cholesterol esters, TAG and lactosylceramide [203]. These findings suggest a similar structure for eukaryotic lipid droplets and bacterial ILI. In Mtb, ILI are not only carbon and energy sources, but also help the bacilli fight against oxidative and metabolic stresses [198].

To conclude, foamy macrophages induced by Mtb mycolic acid form a secure reservoir of carbon and energy for dormant Mtb, allowing it to persist in the host, hidden from immune responses.

C. Induction of the innate immune type I interferon response

IFN α and IFN β are well known for their ability to induce antiviral responses upon viral infection, both in infected and bystander cells, mainly by interfering with different stages of the viral replication pathway [19], [18], [24], [27]. Nonetheless, both cytokines have numerous other functions that influence the immune response to not only viruses, but other microbes, including parasites, fungi and bacteria. With the increasing number of studies deciphering the role of IFN-I in different pathological settings, it has become obvious that the outcome of the IFN-I response upon infection is highly dependent on the context. In fact, IFN-I modulated responses can be either beneficial or detrimental to the host, all depending on when, where and how abundant IFN-I are.

a. Role of IFN-I in bacterial infection

During bacterial infections, IFN-I can either be detrimental or protective to the host, depending on the bacterial challenge [18]. On the one hand, intracellular pathogens usually induce a type-1 immunity (characterized by Th1 cells), including the activation of M1 microbicidal macrophages. On the other hand, extracellular bacteria require a combination of antibody-mediated responses, activation of phagocytes (neutrophils and macrophages), and Th17-dependent immune responses [18]. To coordinate the responses to either intra- or extracellular pathogens, many cytokines, chemokines and antibacterial effector molecules, usually IFN inducible (mainly through IFN γ signaling) are necessary. However, under various conditions, host antibacterial effector molecules together with pro-inflammatory cytokines can be inhibited by IFN-I [18], [206]. Yet, the mechanisms by which IFN-I promote host protection or susceptibility to bacterial infection are far from fully understood [18].

In *Chlamydia trachomatis* infection, IFN-I are beneficial for the host since mice treated with exogenous IFN-I are protected against the pathogen. The mechanism underlying this protection involves the IDO²³-mediated depletion of L-tryptophan, an essential amino acid for several cellular functions. The reduction of L-tryptophan levels reduces its availability to the intracellular pathogen, which leads to a lethal outcome [207], [208]. Protection against *Chlamydia pneumoniae* infection, through a cooperation between IFN-I and IFN γ that induces antibacterial effectors, was also reported and shown to be mainly dependent on IFN γ -induced responses [209]. Finally, IFN-I receptor IFNAR knocked-out (IFNAR^{-/-}) macrophages are more sensitive to *Legionella pneumophila* infection compared to their WT counterpart, an effect mediated by macrophage polarization towards pro-inflammatory activation and iNOS expression [210].

While IFN-I can help the host against bacterial assault, it is also true that some bacteria are able to use it to their advantage. The best examples are bacterial pathogens such as *Listeria monocytogenes*, *Tropheryma whipplei* and Mtb (see the following section for IFN-I responses to Mtb). Indeed, IFNAR^{-/-} mice are resistant to *L. monocytogenes* infection, a phenotype characterized by a longer survival and by lower spleen and liver bacterial load compared to their wild type littermates [211]–[213]. This reduced susceptibility to the infection in IFNAR^{-/-} mice is due to lower levels of IFN-

²³ IDO: Indoleamine-pyrrole 2,3-dioxygenase is a heme-containing enzyme that catalyzes the O₂-dependent oxidation of L-tryptophan.

inducible apoptosis associated genes, leading to reduced cell death by apoptosis [213]. IFN-I are also detrimental in *Tropheryma whipplei* infection, by the diversion of macrophage polarization towards an alternate activation profile, which are more permissive to infection and with higher apoptosis rates [214]. Finally, IFN-I has been studied in Mtb infection context by several groups, whose observations are discussed further here-after.

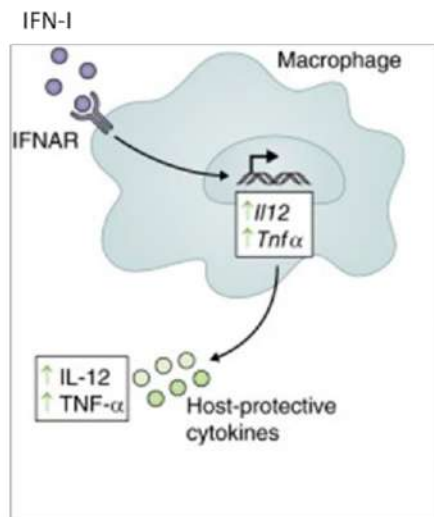
b. Accentuated IFN-I responses during active tuberculosis

Multiple studies conducted both in patients and mouse models collectively point towards a detrimental role of IFN-I in TB, as evidenced by a decrease in bacterial load and/or improved survival of the host either in the absence of IFN-I signaling through different approaches [214]–[217], including IFNAR^{-/-} deficient mice [27], [218]–[220]. Whole blood transcriptional profiling of patients with active TB were dominated by IFN-I inducible gene signatures, particularly overexpressed in neutrophils and monocytes, correlating with the disease severity assessed by X-ray scans. This signature diminished along with successful treatment [221]. Overexpression of several ISG, such as STAT1, Myxovirus resistance 1 (MX1), Interferon-induced protein with tetratricopeptide repeats (IFITs), oligoadenylate synthetase (OAS1), guanylate-binding protein (GBPs) and IRF1, among others, was detected early on in the blood of individuals who were in contact with TB patients and who progressed towards active disease [222], [223], further suggesting that peripheral blood activation of IFN-I signaling precedes the evolution and apparition of clinical manifestations of active TB.

Other evidence supporting the notion that IFN-I activation is deleterious for the host in the context of TB infection come from different clinical and experimental settings. For instance, there is a well-documented reactivation of TB disease in patients receiving IFN α based therapy for chronic hepatitis C infection [224], [225]. In addition, IFN-I production during the chronic phase of Mtb infection leads towards the establishment of immunosuppressive effects; for example, the induction of IL-10 production in macrophages [226] and in CD4⁺ T cells [227] limits immune-mediated tissue destruction, but also favours bacterial persistence [27], [228]. Likewise, treatment of human macrophages with exogenous IFN-I impaired their antimicrobial activity [229] and favoured the establishment of type-2 immunity (characterized by Th2 cell activation and humoral responses), thereby facilitating bacterial growth and reducing host survival [230]. Corroborating these observations, experiments using hypervirulent strains of Mtb showed that increased levels of IFN-I correlated with increased Mtb virulence [215]–[217], [230]. Moreover, exogenous IFN-I instillation in the mouse model of TB infection induced pulmonary injuries to the host, further supporting the detrimental role of IFN-I in the TB setting [230]. Finally, IFN-I have been shown to promote early cell death of alveolar macrophages and to boost the local accumulation of permissive myeloid cells, further contributing to the spread of the infection and pulmonary inflammation [219], [231].

The above evidence is in line with studies using knock-out mice for various IFN-related molecules, which are used to evaluate the role of IFN-I during the course of the disease. One of them, for example, is a mouse model carrying a loss-of-function mutation within the ISG, ubiquitin-specific peptidase 18 (USP18), one of the negative regulator of IFN-I signaling. These mice showed that such deficiency led to hyperactivation of IFN-I signaling during bacterial infection, resulting in a higher susceptibility to Mtb infection, increased bacterial burden and a decreased survival [27], [232].

A | Early and/or low level of IFN-I signaling



B | Late and/or high level of IFN-I signaling

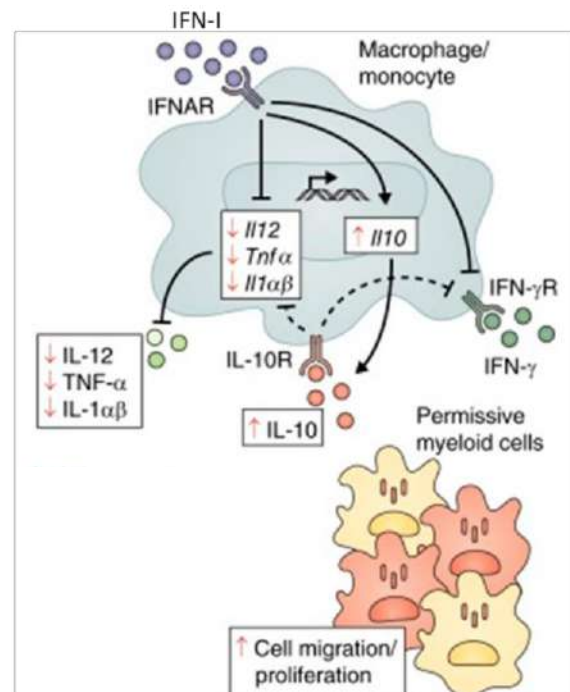


Figure 13: Dichotomy of IFN-I responses during Mtb infection (adapted from [233])

In Mtb infection, type I IFN (IFN-I) have been reported to display both detrimental and beneficial functions to the host.

A | Initial secretion of type I IFN (IFN-I), which acts both in autocrine and paracrine manner, induces the expression of protective cytokines, such as IL-12 and TNF α .

B | However, later in the infection stage, high and sustained levels of IFN-I promote the production of immunoregulatory factors like IL-10, and inhibit the production of protective cytokines (e.g. IL-12, TNF α , IL-1 α , and IL-1 β). Downstream of IFN-I, IL-10 exerts a negative feedback loop on IFN-I signaling, further decreasing the production of IL-12 and TNF α . Sustained IFN-I secretion also inhibits myeloid cell responsiveness to IFN γ , stripping the host of its protection. In addition, IFN-I can promote alveolar macrophage cell death and recruitment of permissive myeloid cells at the site of infection.

IFNAR: IFN-I receptor; IFN γ R: IFN γ receptor; IL-10R: IL-10 receptor.

Other studies have focused on the different ways that Mtb sustains IFN-I responses that would benefit its survival and spread. These studies point to bacterial genes like ESAT-6 and CFP-10 that induce IFN-I mainly through the TBK1/IRF3 axis. Indeed, IRF3^{-/-} mice are resistant to Mtb and *Listeria monocytogenes* infections, even more than IFNAR^{-/-} mice [24], [216]. There are also mycobacterial components that contribute to the activation of IFN-I in the host. For example, our team has shown that the sensing of Mtb lipids such as TDM (in this particular study, a synthetic mimic was used) by CLR (in this case, Mincle) in macrophages can induce IFN-I responses in B cells [234]. Other groups demonstrated that recognition of Mtb peptidoglycans in the infected macrophage cytosol by NOD2 activates TBK1 that recruits IRF5, leading to the production of IFN-I [27]. Mtb-mediated activation of TLR is also a way for the bacilli to increase target cell susceptibility to the infection. For instance, deletion of MAPK8, a negative regulator of IFN-I downstream of TLR signaling, leads to increased levels of IFN-I and bacterial burden [235]. These two effects were abrogated in MAPK8^{-/-}IFNAR^{-/-}, translating in better bacterial control, which correlated with decreased levels of IL-10 and increased concentrations of IL-12 in the mouse sera. Collectively, these studies indicate that Mtb possesses a wide range of effectors able to trigger IFN-I responses in the host, that act in favour of bacterial proliferation and to the detriment of the host.

Despite the large amount of evidence pointing at the deleterious role of IFN-I to the host in TB, this cytokine can also have a protective effect to a certain extent and under specific conditions, described in figure 13. Several clinical studies reported improved clinical symptoms and decreased bacterial burden after a co-administration of IFN α and anti-mycobacterial chemotherapy to patients with active TB who did not respond to conventional antibiotherapy [236], [237]. Other evidence of a possible beneficial effect of IFN-I in TB was reported in the specific context of knock-out mice models. The IFNAR and I Φ NI Γ R (the receptor for IFN γ) double knock-out mouse model exhibits higher mortality rates after Mtb infection than in the single I Φ NI Γ R^{-/-} knock-out mice, arguing that IFN-I could protect the host in the absence of IFN γ [238], [239].

c. Balance between IL-1 β and IFN-I in TB-disease

IFN-I has been reported to inhibit the production of the key inflammatory cytokines IL-1 α and IL-1 β , crucial for host defense against Mtb [18], [240]. Their production is inhibited by IFN-I both in mice and human leukocytes. One of the mechanisms involves the inhibition of NOD sensors and consequent activation of both NOD-like receptor family, pyrin domain containing 1 and 3 (NLRP1 and NLRP3) inflammasomes. Nonetheless, NLRP3 inflammasome is necessary for IL-1 β maturation and secretion [27], [241]. Other mechanisms are dependent on host lipids mediators such as eicosanoids, which are critical determinants of the death modality in alveolar macrophages [24], [27]. Among eicosanoids, prostaglandin E2 (PGE2) has been shown to be a critical mediator of IL-1-dependent host resistance to Mtb infection. As for IL-1 production, IFN-I can also limit PGE2 levels both in human and mouse cells [242]. During TB disease, PGE2 has been described to prevent macrophages necrosis upon Mtb infection by promoting apoptosis [27]. Moreover, PGE2 is known to be a critical determinant of alveolar macrophage death modality. This specific function is mediated by the balance of modulation between the levels of PGE2 and the lipoxin LXA4, a non-classic eicosanoid, in the cells. This balance is what determines whether alveolar macrophages undergo apoptosis or necrosis, which can be beneficial for the host or pathogen, thus influencing the infection outcome [24], [243]–[245]. Indeed, virulent Mtb strains induce LXA4 production in alveolar macrophages, causing PGE2 synthesis to shut

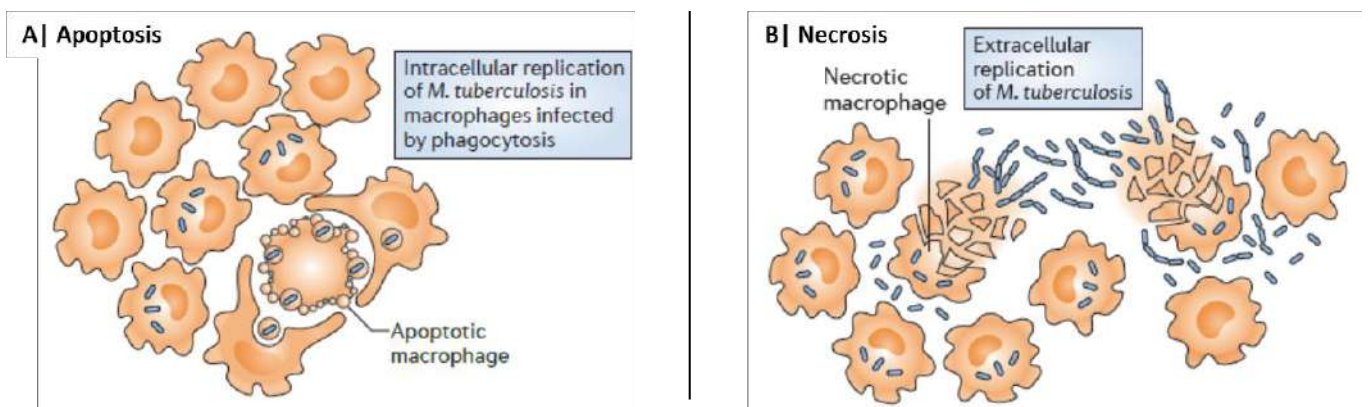


Figure 14: Necrosis of Mtb-infected macrophages (from [86])

A | When Mtb-infected macrophages undergo apoptosis, the cellular debris, which can still contain bacteria, are phagocytized by surrounding uninfected macrophages, resulting in the repartition of the bacilli between multiple cells.

B | Necrotic infected macrophages lose their membrane integrity, leading to bacterial release in the extracellular milieu, which is highly permissive for mycobacterial growth. When the number of bacteria in the extracellular milieu reaches exuberant levels, the necrotic center of the granuloma liquefies and cause the structure disruption, together with the liberation of thousands of infectious bacilli into the lungs.

down and pushing cell death towards necrosis, ultimately helping Mtb to evade the immune system. [24].

Reciprocally, IL-1 β signaling is involved in the negative regulation of STING-dependent IFN-I production in macrophages and DC through inhibition of TBK1-STING association [246], consequently suppressing the advantages given for mycobacteria survival in the host [18]. In these settings, shifting the balance from LXA4 towards higher PGE2 levels proved to be responsible for IFN-I synthesis inhibition, which resulted in a decrease in the production of IL-10 and IL-1 receptor antagonist, resulting in an increase of IL-1 production and enhanced protection against Mtb in macrophages [24], [242], [247].

Collectively, elevated levels of IFN-I are associated with Mtb virulence and increased host susceptibility to bacterial growth, underlying the pathological role of this cytokine in TB. Several mechanisms, including down-regulation of the IL-12/IFN γ and IL-1/PGE2 host-protective pathways, are responsible for this phenomenon. Yet, IFN-I can also play a protective role against the bacilli under certain conditions, including time of exposure and cytokine abundance, highlighting the complex role of IFN-I in TB. Of note, IFN-I cytokines are involved in the disease chronicity, a feature discussed in the following section.

D. Establishment of a chronic inflammation to promote *Mycobacterium tuberculosis* transmission.

a. Obligate pathogen

We have seen that the immune response to Mtb infection is complex and involves many different factors. The formation of the granuloma, in 90 to 95% of cases allows the host to control the bacterial burden and to induce dormancy of the bacteria. Latency is not an inert state, neither to the host, nor to the pathogen. Indeed, the Mtb dormancy state needs continuous local immunity to support bacterial growth control. The constant recruitment of CD4⁺ T cells is necessary to maintain the integrity of the granuloma. Any impairment in these dynamics can lead to TB reactivation, due to several factors, including environmental factors, malnutrition, co-infections with HIV-1 (this setting will be discussed in chapter III) and immunocompromised patients. For example, patients who receive anti-TNF α for rheumatoid polyarthritis or Crohn's disease have a higher risk of developing active TB [107], [248].

Macrophage necrosis in the granuloma center is also a factor influencing the granuloma fate. When necrosis takes over apoptosis, the granuloma undergoes a caseation process and liquefies, causing the granuloma explosion and liberation of thousands of viable infectious bacteria into the lungs [86]. Data obtained from human lung biopsies of TB patients showed a correlation between enhanced bacterial growth and caseum presence, particularly in regions rich in macrophages and in bacterial exudate harboring cellular debris, evidence of cell necrosis [86] (Figure 14). Necrosis is not induced similarly in differentially activated macrophages. Lerner and colleagues reported that despite equivalent susceptibility to Mtb intracellular growth, GM-CSF- and M-CSF-activated macrophages are not equally susceptible to necrotic cell death. Propidium Iodine-positive cells were enriched in M-CSF

macrophage populations, indicating higher levels of macrophages undergoing necrosis. Consequently, Mtb growth rate was increased in these cells, even after IFN γ stimulation [249].

The constant immune system renewal during latent TB in order to keep disease reactivation in check categorizes TB within the family of chronic inflammatory diseases. In the next section, I will discuss how this chronicity impacts the monocyte/macrophage compartment.

b. Effect on the monocyte/macrophage compartment

i. Impact on monocytes

In mammals, CD14⁺ monocytes subsets are distinguished by the expression of the Fc γ RIII – CD16 receptor. In healthy individuals, CD14⁺CD16⁺ are in the minority and only represent 5 to 10% of the total monocyte population (see preamble) [13]. In inflammatory conditions like lupus, rheumatoid arthritis, cancer or HIV-1 infection, the proportion of CD16⁺ monocytes is significantly increased [12]. Similarly, circulating CD14^{high}CD16⁺ monocytes are enriched in TB patients and express relatively low levels of phagocyte maturation, differentiation and function [250]. Moreover, these sub-population can be infected by Mtb, and produce more TNF α and less IL-10 after 6h of infection than CD16⁻ subsets. Mtb-infected CD16⁺ monocytes are also more susceptible to apoptosis during their differentiation towards macrophages [250]. In addition to their increased levels in the bloodstream in Mtb infection context, CD16⁺ monocytes can represent 80% of pleural effusion cells and up to 50% of all circulating monocytes. Additionally, their abundance correlates with both TNF α levels in the blood and the disease severity, as assessed by chest X-rays in TB infected patients [251]. In the same study, our Argentinian collaborators showed that TB-induced CD16⁺ populations displayed a phenotype different from that of healthy donors. In TB patients, monocytes up-regulated CD14, CD16, CD11b, TLR2, TLR4 and the chemokines receptors CCR1, CCR2 and CCR5, indicating that these cells could be efficiently recruited to the site of infection. Using *in vitro* and *in vivo* models, the same team showed that CD16⁺ subsets are more permissive to Mtb infection and have reduced migratory capacities. In fact, in the lungs and BAL of SCID mice adoptively transferred with either CD16⁻ or CD16⁺ monocytes from Mtb-infected WT mice, CD16⁻ cells had higher inflammatory responses than CD16⁺ monocytes, along with decreased necrotic cell death [252].

Monocytes physiologically differentiate towards the macrophage (including osteoclasts) or DC fate, according to the homeostatic and inflammatory signals encountered in the blood and in tissues [9]. In their study, Balboa and colleagues studied the capacity of both monocyte subsets to differentiate into DC in the context of TB. As expected, healthy human monocytes differentiated normally into DC (under GM-CSF/IL-4 treatment), characterized by a cell-surface CD16⁻CD1a⁺CD86^{high}DC-SIGN^{high} phenotype, ability to trigger high activation and proliferation of T cells (upon irradiated Mtb stimulation) and to secrete significant levels of IL-12 and IL-1 β [253]. By contrast, monocytes isolated from active TB patients yielded a CD16⁺CD1a⁻CD86^{high}DC-SIGN⁺ phenotype that poorly activated T cells due to intrinsically high levels of activated p38 MAP kinase [253], which is known to affect monocyte differentiation towards DC [254]. Altogether, this study showed that CD16⁺ monocytes from TB patients are deficient in the induction of DC differentiation.

ii. Impact on macrophages

The presently described studies have shown the importance of CD16⁺ monocyte subpopulations in TB disease. However, only their ability to differentiate in DC has been studied. In this section, I will focus on how TB chronicity impacts the macrophage population.

Macrophages polarization is an important feature in the immune response to Mtb infection. A range of macrophages activation profiles, modulated by the bacilli, are involved during the evolution of the disease. Actually, early stage of TB seems to be marked by the enrichment of M1 pro-inflammatory macrophages (please refer to preamble and chapter I section II.B.c.i.), in favour of pathogen clearance through high microbicidal mechanisms. Later stages of the infection are characterized by an inversion in the balance between pro and anti-inflammatory cells; where M2 macrophages are enriched and serve to reduce inflammation and protect the host from tissue damages [187], [255].

Early after infection, Mtb-infected macrophages display an activation profile close to IFN γ -activated M1 phenotype [256], [257]. Six days post Mtb infection, macrophages collected from mice BAL are polarized in a “M1” programs and are highly microbicidal, especially efficient at producing NS and IFN γ . Later during the infection, between day 21 and 60, an extended presence of “M2” polarized macrophages is detected in lung biopsies in mice [258]. Importantly, TB severity is positively correlated with the abundance of the anti-inflammatory cytokines IL-4, IL-13 and IL-10 [259], suggesting that the shift in macrophages population towards inflammation resolution activities is beneficial for the pathogen. In fact, this phenomenon is largely triggered by Mtb. The bacterial virulence factor ESAT-6 is able to interfere with the “M1” activation profile, by inhibiting MyD88-dependent activation of NF κ B [260]. Using an *in vitro* model mimicking the Mtb-associated microenvironment, my team previously identified a mechanism that triggers the transition of macrophages towards an “M2” profile. This model consists of the utilization of bacteria-free supernatants from Mtb-infected human macrophages (conditioned media MTB, or cmMTB) to differentiate primary human monocytes. Monocyte treatment with cmMTB induced the up-regulation of CD16, CD163 and MerTK at the cell surface. The acquisition of this “M2” profile was due to the high concentration of the anti-inflammatory cytokine IL-10, which activated the STAT3 signaling pathway. These cells showed high motility and 3D migration capacities in dense matrices, immunosuppressive properties, illustrated by a poor capacity to secrete inflammatory cytokines and to activate T cells, and a decreased control of bacterial intracellular growth. Presence of these CD16⁺CD163⁺ macrophages was also observed in lung biopsies of Mtb-infected macaques and correlated with high bacterial burden. Finally, thanks to our close collaboration with the Argentinian group, my team found that TB patient monocytes expressing CD16 were enriched in the blood. While CD163 and MerTK expression was not detected at the cell-surface in CD16^{pos} cells, the plasma of active TB patients was enriched with their soluble forms. Indeed, sMerTK and sCD163 abundance correlated with the disease severity in these patients. Altogether, this study showed that the TB-associated microenvironment induces an “M2” activation profile in macrophages through the IL-10/STAT3 axis, which is more sensitive to Mtb-infection than other polarizations (Annex 2) [261].

In conclusion, the immune response to Mtb infection is quite complex and involves many cellular and molecular factors of both the innate and adaptive immune system to contain the bacteria. The main characteristics of a controlled infection is the formation of granulomas, which encapsulate

Mtb and prevent it from disseminating systematically in the host. Macrophages are the center of this response, and they play a dual role in Mtb infection as the main effector and target cell. As an ancient human pathogen, Mtb has evolved with its host for centuries and has developed ways to circumvent aggressive host responses. This pathogen is highly adapted to macrophages, as it is able to survive many imposed stresses, such as low pH, oxidation, nutrient deprivation, and heavy metal poisoning. To do so, Mtb is able to orient macrophages towards more permissive profiles, allowing the bacilli to survive and maintain its cellular niche for years.

Chapter II: Aspects of the immune response to HIV-1 infection

Acquired ImmunoDeficiency Syndrome (AIDS) is caused by the infection by Human Immunodeficiency Virus (HIV). In 2000, HIV-1/AIDS used to be the 7th highest cause of death worldwide, but as of 2016 has declined to 770 000 - 1 000 000 deaths per year. However, despite the global progress made to prevent the spread of the infection and to reduce AIDS-related co-morbidities, we are still far from controlling and eliminating the HIV pandemic [262], [263].

I. HIV-1 infection: an overview

A. History of AIDS and epidemiology

a. History and origins of HIV

AIDS was first recognized as a new sexually transmissible disease in 1981, when increasing numbers of young homosexual men were found to die from unusual opportunistic infections like *Pneumocystis carinii* pneumonia and rare malignancies such as Kaposi's sarcoma in the USA [264]. In 1983, the French researcher Dr. F. Barré-Sinoussi and colleagues were the first to identify the causative agent of AIDS, a retrovirus belonging to the lentivirus genus [265], which specifically targets CD4⁺ T cells [266]. This discovery was awarded the Nobel Prize in medicine in 2008, shared between herself and Dr. L. Montagnier. One year later, the teams of Drs. R. Gallo and L.S. Oshiro both described the virus using different names than the one coined by the French team [267], [268], and unveiled a more widespread epidemic than originally thought. It was only in 1985 that the virus responsible for AIDS was officially designated HIV-1. The same year, the first clinical test to detect the virus was approved by the FDA [269]. Additionally, Ratner *et al.*, Sanchez-Pescador *et al.*, and Wain-Hobson *et al.*, described the first complete viral DNA sequence, revealing the complexity of the viral genome and providing insights into the replication modalities of the virus [270]–[272]. The first antiviral drug, azidothymidine (AZT), was approved in 1987 [273]. The discovery of HIV-1 proteins, in particular the protease and reverse transcriptase in 1989 [274], aided in the development of both antiretroviral drugs and therapy (ART) and vaccine design. In fact, the first HIV-1 vaccine using the viral envelope glycoprotein gp120 was shown to protect chimpanzees from infection [275]. During the following years, many discoveries helped to better understand HIV-1 pathogenesis (*e.g.* continuous viral replication even in the chronic phase of infection [276]; role for CD8⁺ T cells in controlling the viral load [277]; identification of entry receptors and co-receptors [278], [279]; establishment of viral reservoirs [280]) and the development of additional drugs to fight infection, along with clues for vaccine design.

Ever since HIV-1 was discovered, intensive research was conducted to understand its origin, how it emerged and the reasons behind its unique pathogenicity. The first clue arose in 1986 when a






	People living with HIV in 2018	People newly infected with HIV in 2018	HIV-related deaths 2018
 Total	37.9 million [32.7 million – 44.0 million]	1.7 million [1.4 million – 2.3 million]	770 000 [570 000 – 1.1 million]
 Adults	36.2 million [31.3 million – 42.0 million]	1.6 million [1.2 million – 2.1 million]	670 000 [500 000 – 920 000]
 Women	18.8 million [16.4 million – 21.7 million]	–	–
 Men	17.4 million [14.8 million – 20.5 million]	–	–
 Children (<15 years)	1.7 million [1.3 million – 2.2 million]	160 000 [110 000 – 260 000]	100 000 [64 000 – 160 000]

Table 3: Summary of the global HIV epidemic (from [262])

morphologically similar but antigenically distinct retrovirus was found to cause AIDS in patients in Western Africa [281]. Interestingly, this new virus, called HIV-2, was only distantly related to HIV-1 but quite similar to simian immunodeficiency virus (SIV) that infects macaques [282]. Soon after this discovery, several other SIV viruses were reported in different monkey species, such as African Green Monkeys (AGM), Sooty Mangabeys, Mandrills, and Chimpanzees (CPZ). Strikingly, these viruses were inoffensive in their natural host, but infection in non-natural hosts was highly pathogenic [282]. In addition, close SIV relatives of HIV-1 and HIV-2 were found to infect Chimpanzees and Sooty Mangabeys, respectively [283], [284]. Together, these results led to the hypothesis that HIV viruses infecting humans resulted from multiple cross-species transmission of the parental SIV naturally infecting AGM (SIV_{AGM}) [285], which led to the effective infection of Humans, due to the HIV-1 high mutation rate (1 million time faster than mammalian DNA).

SIV infection has only been found in AGM and Apes, suggesting that primate lentiviruses originated in Africa [282]. Moreover, studies undertaken to date the age of SIV infection in geographically isolated subspecies of monkeys, indicate that this virus has existed for at least 30 000 years [286]. These findings support the idea that Africa was the birthplace of HIV-1 emergence. Several reports confirmed this idea, and more particularly identified Leopold city (actual Kinshasa in Congo) as the cradle of the HIV-1 epidemic. Most probably, human contamination by SIV occurred from the traditional hunting of monkeys amongst the African population, where hunters were in direct contact with the animals blood and mucus. Consumption of raw meat from infected animals could also aid the contamination process [287]. If human acquisition of SIV_{AGM} mostly resulted in limited spread in human, contamination with SIV_{CPZ}, originally in Cameroon, gave birth to HIV-1, responsible for today's pandemic [282]. Phylogenetic and statistical analyses indicated that after the first emergence of HIV-1 epidemic in West Central Africa between 1910 and 1930, the virus spread for some 50 to 70 years before being recognized as a pandemic infection [288].

To summarize, HIV-1/AIDS is quite a young infectious disease that was born in Africa from the cross-species transmission of a primate lentivirus. HIV-1 was able to adapt quickly from its original host to a new one, as well as being quite efficient at spreading among individuals "silently" for the past 70 years before it was considered a top priority in health research. From now on, I will focus on HIV-1, since HIV-2 infection does not lead to AIDS, except in very rare cases [282].

b. Epidemiology

Since the beginning of the pandemic, HIV-1 infection has claimed more than 35 million lives. Currently, it is estimated that approximately 37.9 million people live with HIV-1. In 2018, 1.7 million people became newly infected with the virus while it caused the death of 770 000 individuals (summary of the global epidemic is presented in Table 3) [262], [263]. HIV-1, like TB, can be considered a disease of poverty. Indeed, its repartition on the globe is quite unequal. Africa is the most affected region and represent 54% of the world population living with HIV-1, representing 25.7 million people in 2018 and 61% of AIDS-related deaths. Moreover, even if access to treatment has increased, only 64% of HIV-1 infected people in Africa receive ART [262], [263].

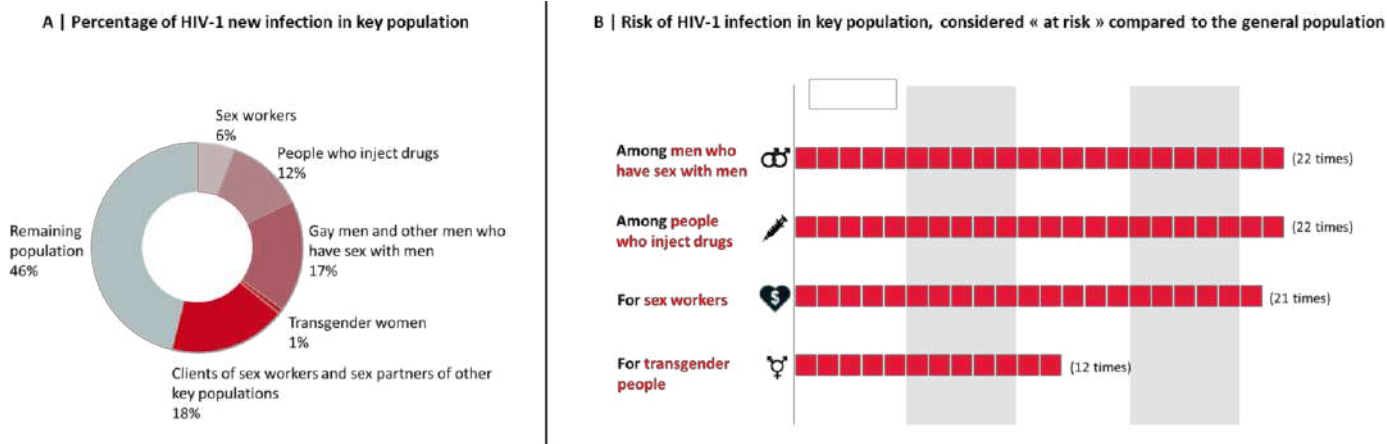


Figure 15: Increased risk incidence of acquiring HIV among key populations, global (from [262])

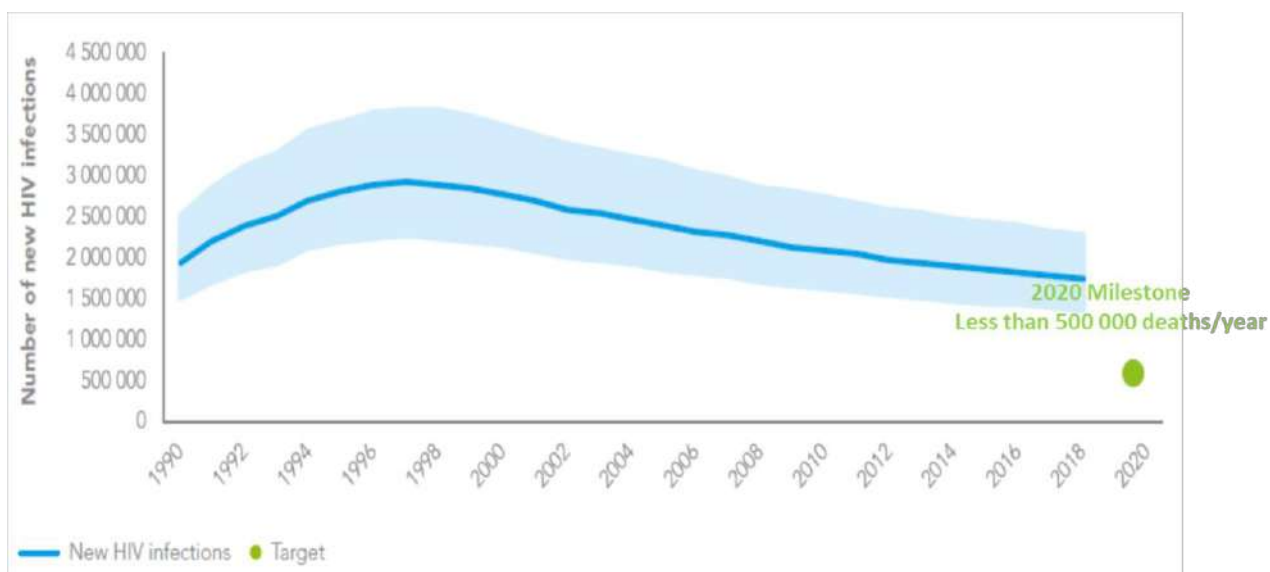


Figure 16: Number of HIV new infections from 1990 to 2018 with 2020 milestone, global (from [262])

Certain populations, considered as “at risk” populations, are more susceptible to the infection. These populations include homosexual men and men having sex with men (MSM), transgender people, sex workers and people injecting drugs (see Figure 15). In fact, MSM and people injecting drugs have a 22 times higher chance of becoming infected with the virus compared to the general population (Figure 15), thus increasing the risk of developing AIDS [262]. An important issue when dealing with the pandemic is to consider all population and to ignore prejudices. Many efforts are being conducted in order to reach the point where all populations will get access to adequate diagnosis and treatment. These efforts have already led to improvements, notably by slowly decreasing the number of new infections per year, as well as in drug distribution (*e.g.* people receiving ART in Africa represented 24% of HIV-1 infected people in this region in 2010, against 64% today) [262]. Since 2010, AIDS-related mortality has declined by 33%, with this mainly occurring in Eastern and Southern Africa. However, this is not sufficient to stop the epidemic by 2030, an objective set by the WHO. Indeed, at the global scale, reaching the 2020 milestone of fewer than 500 000 deaths will require further declines of about 135 000 per year (Figure 16), a goal which is unattainable today [260].

In conclusion, many efforts remain to be made to stop the pandemic and to increase the population with access to ART. To reach the 2030 milestone, more funding and government initiatives in the fight will be needed, if we want to, one day, succeed in the eradication of HIV-1 infection.

B. Therapeutic tools to fight the epidemic

a. Transmission and prevention

The main axis for HIV-1 to pass from one individual to another is horizontal transmission, occurring through contaminated body fluids. These fluids include blood, mucosal fluids such as sperm, vaginal and rectal mucus, and can be exchanged *via* needle exchange between drug users, blood transfusion or transplantation (which happened before 1991) and sexual relations. In addition, vertical transmission occurs when the virus is able to pass from a mother to her baby either during pregnancy through the placental barrier, labor and delivery, or breast-feeding *via* contaminated milk. Globally, 80% of adults infected with the virus were contaminated after exposure to contaminated mucus while the remaining 20% were infected through intravenous inoculation [289]. To prevent infection, several solutions exist: use of condoms, use of sterile needle, voluntary medical male circumcision, which reduces the risk of heterosexually acquired HIV-1 by 60%, and proper education concerning HIV-1 infection and how it is transmitted. While this can prevent horizontal transmission, it is not an effective mean to prevent vertical transmission.

ART can also be used to avoid HIV-1 transmission between partners or from mother to child during pregnancy. Indeed, multiple clinical trials have reported ART regimens as efficient ways to avoid HIV-1 transmission when followed with good compliance, and reduced the risk of acquiring HIV-1 to uninfected partner by 96%. Moreover, antiretrovirals can be used daily as pre-exposure prophylaxis (PrEP) treatment by HIV-1 negative partners to prevent viral infection. More than 10 randomized studies have demonstrated PrEP efficiency in different populations, including MSM, transgender, and heterosexual couples [290]. In addition, antiretroviral drugs can also be taken as a post-exposure prophylaxis (PEP) for HIV-1, for 28 day post-exposure, and were shown to protect the exposed

individual from becoming infected if started within 72h post-HIV-1 exposure. Finally, ART is also very efficient to avoid mother-to-child viral transmission.

b. Diagnosis and treatment

i. Diagnosis

HIV-1 infection does not cause any uniquely specific symptoms, and typically includes fever, headache, rash or sore throat, and can vary during the course of the infection. As the infection slowly progresses, symptoms evolve into swollen lymph nodes, weight loss, and lymphopenia. It is during the first few months that infected people are the most contagious, and one of the major issues with HIV-1 is that a large part of the human reservoir is constituted with people who ignore their infection, and therefore contribute to feeding the pandemic. That is why early diagnosis is key if we are to control the infection both at an individual and a global scale. Several diagnostic tools are available to diagnose HIV-1. The most common is the serological blood test, which assesses if the individual has developed a humoral response to the virus by measuring the anti-HIV-1 antibody titers in the patient plasma. This test is often confirmed by western blot on blood samples, where the viral proteins (p24, Gag) are tested for. The limit of this technique is that the humoral response takes several weeks to occur, delaying the diagnosis. Using the same samples, the viral protein p24 can also be quantified by ELISA. A more precise and sensitive method of detection is possible by measuring the viral DNA and RNA levels in the patient blood cells, a technique mostly used in babies born from infected mothers. These tests must be accomplished in health care centers, which unfortunately are not always accessible to all populations. That is why automated tests that work on the basis of an ELISA, have been developed [262], [263], [291].

ii. Treatment

Improvements in diagnosis have led to an increase in the global coverage of people receiving ART, which reached 62% in 2018. However, more efforts are needed to scale up treatment, particularly for children and adolescents, as only 54% were reported to receive ART at the end of 2018 [259]. Since the discovery of the epidemic, the development of ART has helped transform HIV-1 infection from a fatal disease to a chronic inflammatory disease, with hope of a cure still not on the horizon. Indeed, a rapid decrease in HIV-1-related morbidities and mortality was observed upon ART in the USA in the 1990s [292]. Nonetheless, the virus rapidly evolved and developed resistance to certain antiretroviral drugs like AZT [293]. To avoid this, ART are now used in combination (cART) to target different steps of the viral replication cycle (see section II.C.b). There are seven classes of drugs that can be used in combination: non-nucleoside reverse transcriptase inhibitors (NNRTI), nucleotide reverse transcriptase inhibitors (NRTI), proteases inhibitors, fusion inhibitors, CCR5 antagonists (which compete with the entry co-receptor CCR5), integrase strand transfer inhibitors (INSTI) and post-attachment inhibitors [263]. Within these classes, a combination of three drugs is proposed to HIV-1 infected patients, according to their infection susceptibility to the drugs, but also on the side-effects and to possible drug interactions. The main effect of cART is to control the viral replication and plasma

viral load in infected patients. Yet, the treatment is unable to eliminate latent viral cellular reservoirs that become established during the early stages of infection, and these reservoirs can be reactivated upon treatment cessation. Even though these therapies enable patients to live a long and almost “normal” life, cART is a life-long treatment that needs to be taken daily, carries a number of side effects and is costly. In addition, increased life expectancy revealed that HIV-1-infected patients have higher chances of developing other pathologies, including neuropathologies whose prevalence are increasing despite cART, and bone disorders, with up to a 6.4-fold increased risk of developing osteoporosis [294].

Since its discovery in 1983, huge efforts have been made to control and eliminate HIV-1 infection, responsible for an important epidemic at the global scale. However, the capacity of HIV-1 to establish persistent reservoirs within its host makes treatment mandatory for a lifetime but prevents complete elimination of the pathogen. In addition to that, HIV-1 diagnosis, even if improved, remains an issue since a large proportion of infected people ignore their infection, and feed the invisible epidemic. As the infection continues to spread and cannot be cured, more efforts are still necessary to develop effective prevention measures, as well as to find a curative treatment. Within the last few years, several programs and world consortium have intensively focused their research on creating a vaccine against the virus, yet, designing an efficient vaccine against HIV-1 is more difficult than expected (for review, see [295]–[297]). Most of the vaccine approaches are based on the utilization of soluble Env soluble trimers (HIV-1 receptors that allow the virus to infect a target cell), with the ultimate goal to create immune memory against the HIV-1 entry receptor by inducing broadly neutralizing antibodies. However, Env trimers are relatively stable in solution and harbor different conformations, including some that are irrelevant to induce efficient neutralizing antibody production. A second issue with these trimers is that they expose unwanted immuno-dominant surfaces (*i.e.* glycan) that can distract the immune system from the conserved neutralization-relevant surfaces on the trimer. Indeed, Env loop V1, V2 and V3, are the primary target of antibodies, but as they are hypervariable regions they do not provide a protective role against all HIV-1 strains present in the host. In addition to the few number of Env conserved regions, their accessibility to antibodies is restricted by the high glycosylation levels of the protein. Finally, the number of Env spike at the surface of the virus is suboptimal for cross-linking to B cell receptors, thus rendering it difficult to establish an effective humoral memory [297], [298].

II. Physiopathology of HIV infection and immune defenses

A. What is HIV-1?

a. Generalities about the virus

i. Taxonomy

HIV-1 is a virus belonging to the *Retroviridae* family, *Otrhoretrovirinae* sub-family, *lentivirus* genus. Its genome is composed of two copies of single stranded RNA molecules, which are reverse transcribed prior to integration within the host DNA. Diverse groups of HIV-1 exist, due to the fast evolution of the viral genome. Indeed, the short generation time (about 17h in CD4⁺ T cells, and up to

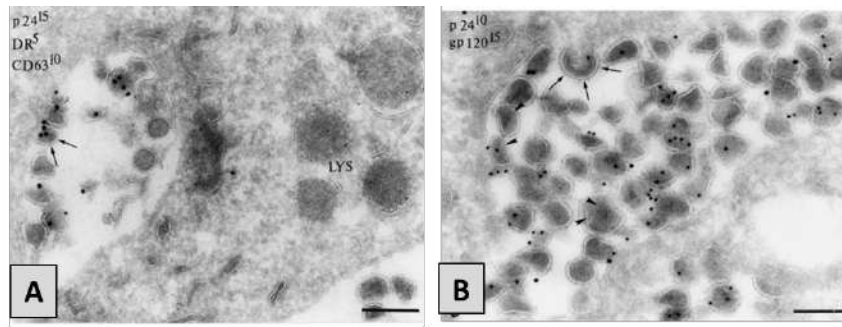


Figure 17: HIV-1 virion structure observed by electron microscopy (from [309])

A | Ultra-thin cryosection of macrophage infected with HIV-1 for 14 days. Electron microscopy image showing immunogold labelled p24, HLA-DR and CD63, as indicated. Lysosomal compartment (Lys) do not contain p24-positive particles. B | As in A, but double-immunogold labeled for p24 and gp120.

Arrow: budding of the p24-positive particles at the limiting membrane; Arrowhead: p24 label; Scale bars: 200 nm

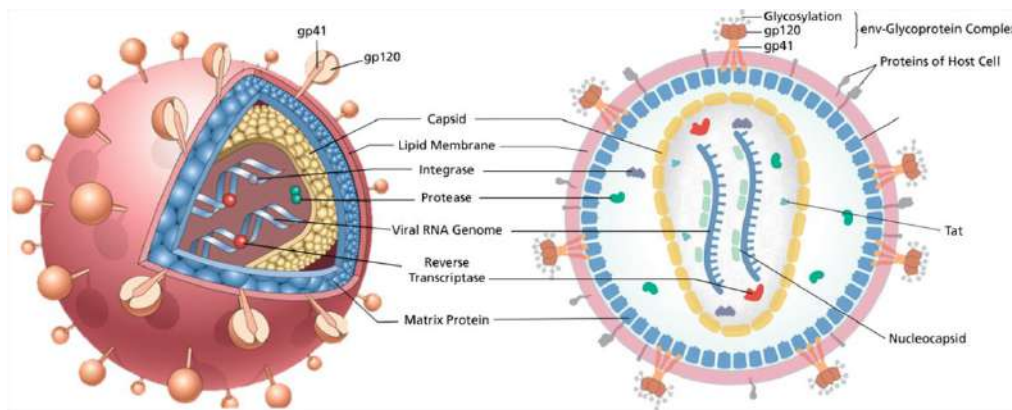


Figure 18: HIV-1 virion structure

HIV-1 genome and proteinase (*i.e.* reverse transcriptase, protease and integrase) are encapsulated in a capsid, surrounded by a matrix protein core that also contains accessory proteins. This structure is enveloped with a lipid-membrane bearing the viral envelope protein gp41 and gp120, along with host-cell membrane protein that were embedded in the viral envelope during viral budding.

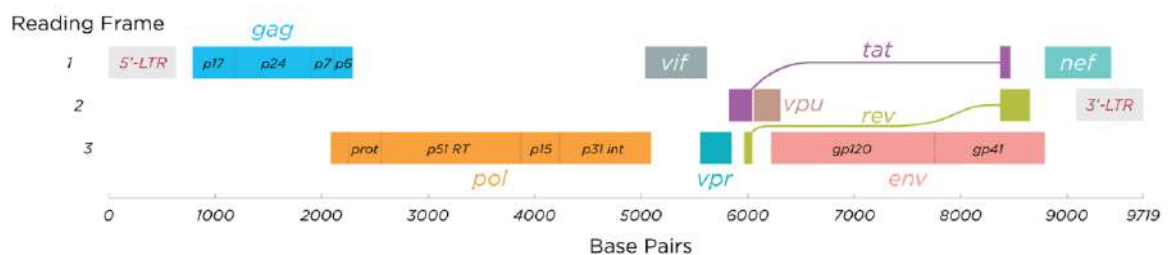


Figure 19: HIV-1 genome.

HIV-1 genome is about 10 kb and encodes for *gag*, *pol* and *env* polyproteins, that are cleaved after translation. It also encodes accessory proteins (*i.e.* *Nef*, *Vif*, *Vpr*, *Vpu*, *Tat*, and *Rev*) that allow the virus to replicate efficiently in its host and to escape viral clearance mechanisms induced in the infected cells. At both extremities, the HIV-1 is flanked by long terminal repeat sequences (LTR), which upon activation enhance the viral genome transcription.

48h in macrophages) and high propensity of the viral reverse transcriptase to make mistakes (1 error every 10^4 to 10^5 nucleotides) when transcribing RNA to DNA favour HIV-1 mutations [299]. Phylogenetic studies have classified four subgroups of HIV-1 [300]. The main one, group M, comprises 99.6% of HIV-1 strains and is responsible for the global HIV-1 epidemic. Strains discovered in the 1990s in Africa form the outlier group O and infect about 1% of the global population. Group N strains were identified in 1998 and are even less prevalent than group O strains, with 13 cases reported, all localized in Cameroon. Finally, a fourth group was created in 2009, group P, with a strain that does not present any recombination with strains from other groups [301] and that have been reported to infect 2 women in Cameroon [282].

ii. Structure and genome

HIV-1 is a spherical enveloped virus, with an average diameter of 100 nm, a size that depends on the maturation state of the virus (Figure 17: virus observed by EM). Its envelope is composed of a lipid bilayer derived from the host cell and into which viral glycoproteins, including gp120 and the transmembrane gp41 (both derived from the cleavage of the gp160 precursor), are inserted [302]. Once a cell is infected, these proteins are present at the surface of the host-infected cell as a complex, a trimer of gp120 and gp41 incorporated in the lipid bilayer through the transmembrane region of gp41 [303]. A budding virion usually incorporates 7 to 14 trimers in a single viral particle [304]. The inner leaflet of the viral envelope is lined up with the matrix protein p17, which surrounds a conical capsid, a p24 protein-rich structure that contains the viral genome – two copies of single-stranded RNA – of about 10 kb. The viral RNA is encapsulated with all the needed material for its replication and integration, including the nucleoprotein p7, the p10 protease, the p32 integrase and the p66/p51 reverse transcriptase (see figure 18: HIV-1 viral structure). The HIV-1 genome encodes for three major genes common between all viruses: *gag*, *pol* and *env*, encoding respectively for structural proteins of the viral core and matrix, enzymes (protease, integrase and reverse transcriptase) and for envelope glycoproteins (gp120 and gp41). These different proteins are first synthesized as polyproteins that are then cleaved to form their final and active form. The genome also encodes the regulatory proteins Tat and Rev, along with accessory proteins: Vif, Vpr, Vpu and Nef. Finally, the genome is edged by long terminal repeat non-coding sequences (LTR), involved in viral replication regulation, particularly during (reverse) transcription, splicing and encapsulation steps (see genome structure in figure 19).

Each protein plays its own role during the viral replication cycle, which will be described in details in the specific case of macrophage infection in section III.B of the current chapter. Briefly, the envelope glycoproteins gp120 and gp41 are responsible for attachment to the main HIV-1 receptor CD4 and co-receptor CCR5 or CXCR4, and then fusion between the viral and host cell membranes, respectively [305]. Upon entry into the cell, the viral RNA is reverse transcribed into double-stranded DNA by the viral reverse transcriptase p66/p51. This DNA then enters the nuclei where the viral integrase p32 integrates the viral genome into transcriptionally active regions of the host's genome [306]. The viral genome is then expressed by the host, resulting in the synthesis of viral RNA and proteins, Tat and Rev, which are required for the viral replication cycle. Meanwhile, accessory proteins facilitate the viral escape from immune recognition [307], ensuring viral persistence, assembly and dissemination [308].

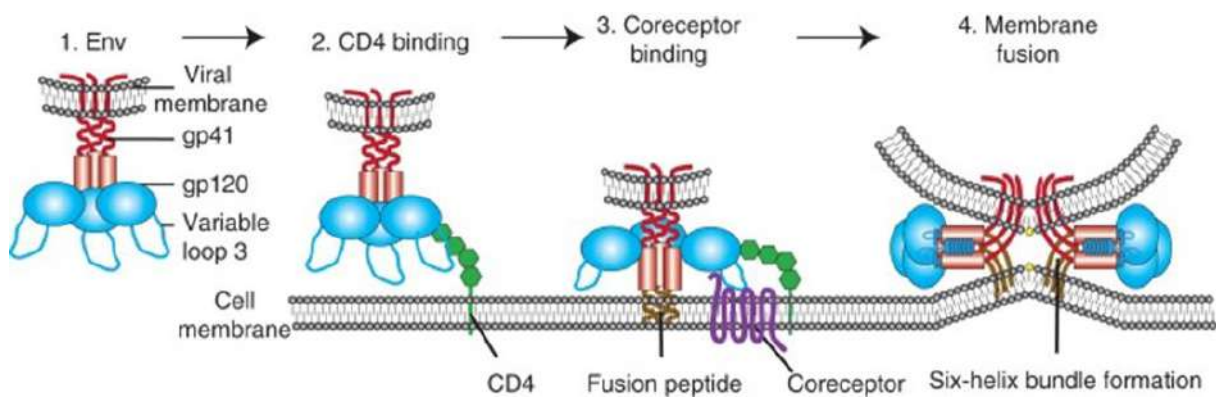


Figure 20: HIV-1 entry into target cell (from [310]).

Upon recognition of the entry receptor CD4, the viral protein gp120, organized in trimers, undergoes a conformational change, liberating the binding site of gp41. Binding of gp41 to the cell co-receptor induces a second conformational change and the injection of HIV-1 fusion peptide into the cell membrane, ultimately leading to viral and cell membranes fusion, prior viral entry into the cell.

In the team of Dr. I. Maridonneau-Parini, one of my supervisors studied the accessory protein Nef, a small protein (27 kDa) that is rapidly and abundantly expressed in the host cell. A significant proportion of HIV-1 pathogenesis has been assigned to Nef, including the improvement of viral production and infectivity [311]–[313]. One of the main function of Nef is to disrupt intracellular trafficking and signaling pathways, especially those related to endosomal protein trafficking. Indeed, Nef is responsible for the internalization and sequestration of cell surface proteins such as CD4 (to avoid infection with other HIV-1 virion after primo-infection and favours efficient viral replication), CD28, and MHC-I and II complexes [314]. In addition, Nef is a master regulator of the cytoskeleton in infected host cells [315], [316]. My PhD mentor, Dr. C. V  rollet focused her research on Nef-mediated perturbation of the F-actin cytoskeleton in macrophages [317]–[319]. I will detail her work as well as that of others, on Nef and the alteration of macrophage function in section III.B.e.

Altogether, the virus is well equipped to efficiently infect and replicate in its target cells. The HIV-1 genome (relatively small) encodes for proteins allowing its replication and integration into the host genome, while simultaneously providing accessory proteins to protect it from immune system detection.

iii. Viral tropism

To infect a target cell, viruses need to bind to their cell surface receptor and fuse with the cell to finally use its machinery to replicate. The main and mandatory receptor of HIV-1 is the cell surface receptor CD4 that is mainly expressed by CD4⁺ T cells, the main target of the virus, as well as by cells of the myeloid lineage, including DC, CD16⁺ subset of monocytes [11], macrophages and osteoclasts [320]–[323]. In fact, the principal characteristic of HIV-1 infection in humans is the depletion of effector CD4⁺ T cells, in which the infection and viral replication are highly efficient compared to resting CD4⁺ T cells. High affinity binding of gp120 to CD4 [324], [325] induces a conformational change of gp120, exposing gp120 binding sites to the co-receptor (see Figure 20) [310]. Viral tropism is defined by the affinity of gp120 for its co-receptor. Thus, R5 tropic viruses use the co-receptor CCR5 to enter the cells, while X4 tropic viruses use CXCR4. Some strains, called R5X4 strains, are able to use either CCR5 or CXCR4. These chemokine receptors belong to the G-protein family, involved in different signaling pathways, and more specifically in cell migration [326]. In fact, there are three classes of HIV-1: (i) R5 T cell tropic, (ii) X4 T cell tropic and (iii) M-tropic (for macrophage-tropic). Real M-tropic viruses are noticeably more infectious for macrophages than R5-tropic viruses, although all R5-tropic viruses can enter macrophages at least to some extent. In addition, M-tropic strains are very efficient at infecting cells with low CD4 density, which is not the case for R5-tropic viruses [327]. Whatever the virus strain, binding of gp120 to its co-receptor further changes the protein conformation, leading to exposure and trimerization of gp41, which injects its fusion peptide into the membrane, leading to cell and viral membrane fusion.

In addition to CD4, the presence of co-receptors is essential for efficient HIV-1 infection of the target cell. Indeed, when using co-receptor inhibitors [328], [329], or when downregulating co-receptor expression using gene constructs [330], the viral infectivity is reduced. Another argument supporting this statement is the existence of two patients who were cured of HIV-1 infection. These two patients who were infected with the virus also had a leukemia. The first patient Timothy Ray

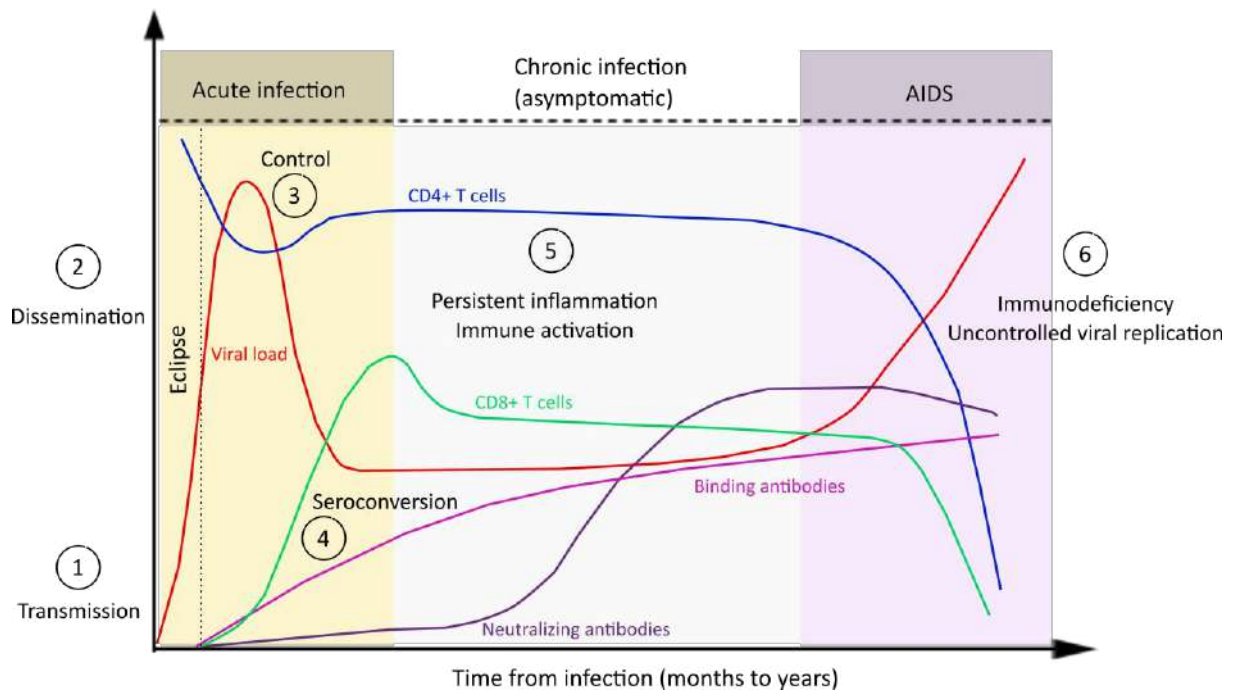


Figure 21: General course of HIV-1 progression (adapted from [331]).

After transmission (1), the virus replicates and start to disseminate (2) from mucosal site to the lymph node (eclipse phase). However, it remains undetectable for any diagnostic test. During the first weeks following HIV-1 transmission, considered as the acute phase of the infection, the virus multiplies actively (red line) while the number of CD4⁺ T cells drops (blue line) (3). Six weeks post-infection, the humoral immune response occurs and the first HIV-1-binding antibodies can be detected in patient plasma (pink line) (4). This is accompanied by an increase in CD8⁺ cytotoxic T cells in the blood (green line). The chronic phase (5), which can last for several years, is characterized by a balance between the viral replication and the viral restriction imposed by the host. The number of CD4⁺ and CD8⁺ T cells stabilizes, along with the viral load, while the levels of neutralizing antibodies (purple line) increase until reaching a plateau. Finally, the disease progresses towards AIDS (6), the last phase of the infection, which is defined by a drastic drop of CD4⁺ T cell count, CD8⁺ T cell exhaustion and death, and uncontrolled viral replication.

Brown, known as the “Berlin patient”, was the first to receive, in 2007, a stem cell transplant that eliminated the virus from his system. Ten years later, he was followed by the “London patient”, who was also free of the virus after receiving a bone marrow transplant. These two men received their new stem cells from healthy donors carrying the $\Delta 32$ mutation in the CCR5 gene, which proved to be protective against the virus since both patients were the only one described to be able to stop their antiretroviral therapy without experiencing viral rebound, with undetectable viral loads since their remission [332]. These successes have inspired scientists to look for gene therapy-mediated mutations of the co-receptor gene in order to reduce HIV-1 spread. Research progress on this topic are reviewed in [333]. Particular attention was focused on CCR5, which is thought to be the main co-receptor used at the viral entry site in newly-infected hosts. When the virus enters the host mucosa at the transmission stage, it is commonly thought that the primary cells to be infected are DC and macrophages (expressing higher levels of CCR5 than CXCR4), which upon activation, recruit CD4⁺ T cells [334]. This is important because most R5 tropic viral strains are myeloid cell tropic, although some R5 strains are T cell tropic as well. Yet, it is thought that transmitted viruses are mostly R5-tropic strains that rapidly infect the first cells they encounter in mucosa, mainly the myeloid cells. Also, during progression of the infection, the main tropism switches from R5 to X4 or R5X4 [335].

Finally, if CCR5 and CXCR4 are the main co-receptors for HIV-1 entry, alternate receptors expressed by myeloid cells, in particular lectins and C-type lectins, were also shown to be involved in HIV-1 capture and transfer to T cells and will be discussed later in this chapter, section III.D.a.

b. General course of the infection and critical features

Specific markers, testifying uniformly of the evolution towards AIDS, are used to characterize HIV-1 infection (*e.g.* plasma viral load and, CD4⁺ T cells counts). Disease progression is assessed according to CD4⁺ T cell count in the patients blood along with plasma viral load [336], and follow four defined phases, represented in figure 21.

The eclipse phase, first to occur, happens when the virus succeeds in infecting a new host, and establishes the infection in the exposed local tissue. During this phase, which is believed to last for 10 days, HIV-1 dissemination in the systemic circulation has not yet occurred [337]. In the majority of the cases, HIV-1 enters the host through mucosal routes and crosses the mucosal barrier to reach the target cells. To do so, the virus has three options: first, it can cross the barrier *via* transcytosis through the inter-epithelial layer by binding to exposed DC dendrites. Second, the virus is small enough to pass through intercellular spaces between epithelial cells and to reach cells present in the lamina propria [338], [339]. Last, it has been suggested that HIV-1 gp120 is able to alter the mucosal membrane by initiating the secretion of inflammatory cytokines, which in terms leads to increased barrier permeability [340]. Once in the lamina propria, HIV-1 encounters DC, macrophages and CD4⁺ T cells that become infected. It is also in this time frame that ART can prevent the virus from establishing infection.

The eclipse phase is followed by the primo-infection or acute infection stage. This step can be asymptomatic or carry flu-like symptoms (*e.g.* headaches, nausea, and muscle pain) [341]. It is this stage during which the patient is most contagious, due to a high viral replication rate and increasing

viral levels in the blood. It usually lasts for two to four weeks after HIV-1 transmission. Indeed, at this step, HIV-1 has already spread to lymphoid tissues and into the blood, and its replication increases rapidly to a peak level, with a doubling viral population rate of 20h [337]. During ramp up viremia, only the viral RNA can be detected from blood. After seven days, p24 antigen (capsid protein, see Chapter II – II.A.a.ii) detection is possible, even before the apparition of HIV-1 neutralizing antibodies [336]. Acute phase is characterized by high viremia and a strong immune system activation where the CD4⁺ T cell count transiently drops [342]. After the viremia peak, the viral load dramatically decreases while CD4⁺ T cell count goes back up to normal levels.

Once normal T cell counts are reached, the infection enters the phase of latency, or chronic phase, an asymptomatic period that can last from a few months to years in untreated people, and can be largely prolonged in patients receiving cART [343]. During this phase, the virus continues to replicate at a slower rate while the number of CD4⁺ T cells slowly decreases, both because of infection, but mainly because of the constant activation leading to apoptosis [344], [345]. The immune system is constantly activated, leading to eventual exhaustion.

Finally, the AIDS phase is declared when the CD4⁺ T cell count drops under 200 cells/mm³ of blood. The antibody titers and CD8⁺ T cell count drop while viral replication peaks again, no longer “controlled” by the immune system [331]. Because of the induced immunodeficiency, AIDS patients are highly contagious and highly susceptible to opportunistic infections, disease reactivation (*e.g.* tuberculosis) and to cancers. Without treatment, AIDS patients usually die within 3 years after their status has been declared [346].

B. HIV-1-induced immune activation is a critical feature of HIV-1 chronic phase establishment

a. Alteration of the gut barrier and impact on immune system activation

The gastrointestinal tract (GI) represent a structural and immunological barrier against microorganism invasion of the host. It is the system containing the highest proportion of T lymphocytes in the entire organism [347]. Alteration of this barrier is a main feature of HIV-1 infection and is partly responsible for the establishment of the virus-mediated chronic inflammation that characterizes the disease. In 1984, Kotler and colleagues reported the observation of histological abnormalities in GI samples collected from jejunal and rectal biopsies in AIDS symptomatic patients. The patients presented with D-xylose malabsorption, steatorrhea, partial villus atrophy with crypt hyperplasia, increased number of intraepithelial lymphocytes, mast cells infiltration in the lamina propria and focal cell degeneration near the crypt base [348]. These enteropathies are also detected in pathogenic SIV infection in rhesus macaques and are mainly characterized by inflammatory infiltrates of lymphocytes and damage to the epithelial barrier (*e.g.* atrophy, hyperplasia) [349]. More recent studies found that the majority of CD4⁺ T cells of the GI tract were depleted during the acute phase of both HIV-1 and SIV infection [350]–[354]. Depletion of CD4⁺ T cells of the GI tract continues for the entire course of the disease and is poorly reflected by the CD4⁺ T cell count in the peripheral blood: gut T cell loss is much higher than what is observed in the blood circulation, especially after cART, mainly because the treatment fails to replenish the gut CD4⁺ T cell pool. This T cell subset is not the only one to be depleted

during the infection. Th17 cells, a specific subset of helper T cells abundant in the gut and essential for the host's protection against fungi and bacteria, are also lost subsequent to HIV-1 infection [355]. In addition, the gene expression landscape in the GI tract biopsies of HIV-1-infected non-progressors revealed a downregulation of genes involved in the cell cycle regulation, lipid metabolism and digestive functions [356]. The epithelial barrier alteration during the course of HIV-1 comes with translocation of the gut commensal microorganisms into the bloodstream. This can be followed by an increasing level of LPS detectable in patients' plasma, particularly high in the chronic stage of the infection [357], which correlates with systemic immune activation; that is high number of activated memory CD8⁺ T cells – immune cells keep encountering microbial antigens and thus remain constantly activated and recruit more immune cells to clear the infection – and elevated levels of soluble CD14 and IFN α in the blood [347].

b. Systemic immune cell activation induces the recruitment of target cells to the site of infection, along with premature immune senescence

Translocation of commensals bacteria into the bloodstream leads to constant danger signal detection by immune cells. Recognition of the circulating PAMP by patrolling monocytes, DC and macrophages induces the production of pro-inflammatory signals like TNF α , IL-1 β , IL-6, CCL5 (also known as RANTES) and of IFN-I [358], which favours surrounding cell activation, and lead to systemic inflammation. Consequently, patients progress faster to the disease and display accelerated decline of overall immune competence. HIV-associated immune activation is mainly characterized by dysfunctional T regulatory cells and display an ageing immune phenotype, similar to that seen in the elderly, including high expression of IFN-I, which causes thymic dysfunction and impairs the generation of new T cells [358], [359]. This immune senescence is defined by a decreased production of naïve T cells, decreased proliferative capacity in response to antigen stimulation and a reduced T cell longevity [360], [361]. This drop in the lifespan of T cells is notably due to inflammation-mediated cell turnover that imposes a strain on their homeostatic mechanisms [347]. Inflammation-mediated changes in cytokine release increase cell susceptibility to activation of induced-cell death ([360], [362], consequently leading to both CD4⁺ and CD8⁺ T cell apoptosis, further feeding inflammation. As a result, the T cell compartment undergoes exhaustion and immune senescence [358], [363]. Lastly, sustained IFN-I secretion by plasmacytoid DC (pDC) and activated macrophages leads to the synthesis and recruitment of more HIV-1 target cells. Infected macrophages are able to activate the recruited resting CD4⁺ T cells to render them permissive to HIV-1 infection. In addition, they also attract CD8⁺ T cells and mediate their death by apoptosis, leading to immunosuppression [364], [365].

Despite clear evidence that CD8⁺ T cells are involved in the partial control of viral replication [366], [367], they also present intrinsic functional defects. In addition to decreased proliferation, CD8⁺ T cells also have reduced capabilities to produce cytokines such as IL-2 and lack poly-functionality, a characteristic that correlates with a better clinical outcome in HIV-1 pathology [368], [369]. This prevents CD8⁺ T cells from acquiring full effector functions, in part explaining their failure to clear the infection. Chronic inflammation leads to expression of both activation and negative regulatory receptors on T cells, driving their effector activity or their immunosuppression. Programmed death-1 (PD-1) is a crucial negative regulator of T cell function and was reported as an essential marker of

chronic activation. Indeed, PD-1 is highly expressed on HIV-1-specific cytotoxic CD8⁺ T cells (CTL_{HIV-1}) [370], [371] and on CD4⁺ T cells, and this expression is correlated with viral load [370]. Supporting this correlation, lower levels of PD-1 on CTL_{HIV-1} in HIV-1 non-progressors were reported in long term disease compared to HIV-1 progressors [372]. *In vitro* studies also reported an improvement of CTL_{HIV-1} proliferation when PD-1 interactions with its ligand were blocked, further arguing for PD-1 mediated-immunoregulation. One of the direct effects of PD-1 expression by both CD4 and CD8⁺ T cells is the induction of T cells apoptosis [373], which is part of the immune senescence observed in HIV-1 infected people [373]. The expression of PD-1 determines T cells sensitivity to apoptosis and is induced by chronic antigen stimulation. The fact that this expression is lowered upon ART-mediated viral suppression [370], [371] further indicates that PD-1 is a major component of the compensatory immune-downregulation induced during chronic inflammation, which could be targeted to improve the anti-HIV-1 functions of T cells.

Systemic immune activation observed in HIV-1 infected patient is a hallmark of the establishment of chronic disease. Consequently, immunoregulatory functions of regulatory T cells are impaired, the effector T cell pool is depleted mainly by apoptosis of bystander cells, and cytotoxic CD8⁺ T cells become exhausted (high expression of inhibitory receptors like PD-1 and Tim-3 [374]). All these features participate to early immune senescence. Altogether, these changes predispose HIV-1 infected individuals to the development of comorbidities like lung immune dysfunction [375], [376] or cancers [377], but also to age-related comorbidities, such as osteoporosis [378], arthritis [379], cardiovascular [380] and cognitive diseases [381]. As cART increases the lifespan of patients, future drug development should aim at reducing this chronic inflammation in order to slow the fasten aging of infected patients.

C. The host IFN-I responses in HIV-1 infection

HIV-1 infection, as many other viral infections, triggers the establishment of a host IFN-I mediated response. Historically, IFN-I therapy proved to be efficient in the case of several viral infections, such as hepatitis C virus and influenza. Therefore, IFN-I therapy strategies were rapidly applied to treat HIV-1 infection after discovery of the virus, even before understanding the IFN-I response mechanisms to HIV-1 at the cellular level, which remain, even today, poorly described (see paragraph c of the current section). This strategy was partially efficient on a case-by-case basis in HIV-1 pathology, indicating that IFN-I responses in HIV-1-infected host are more complicated than originally thought. Here, I will describe the results of several clinical studies, which set the starting point of our understanding of the role of IFN-I in HIV-1 pathogenesis.

a. Potentials of IFN-I as therapeutic tools in humans

Historically, few molecules, including recombinant IFN α were shown to display efficient inhibition of HIV-1 replication in infected individuals, even before the first cART was available in 1996. The first studies evaluated the impact of IFN α therapy in AIDS-patients with Kaposi sarcoma. One of them reported a decrease in plasma p24 antigen levels in one quarter of the patients [382]. The same year, the group of Salzman obtained similar results, reporting a tightly higher efficiency of IFN α 2a

therapy [383]. These studies were further confirmed by a randomized double blind trial two years later, where the effect of IFN α 2a therapy *versus* placebo was assessed. Patients showed a global tolerance towards the treatment, despite reported flu-like symptoms and neutropenia, which occurred in a treatment dose-dependent manner [384]. In the IFN α 2a group, 41% of the patients became HIV culture negative against only 13% in the placebo group. CD4⁺ T cell counts were maintained and no progression to AIDS was observed in the IFN α 2a group [384]. Several other studies reported similar results, and highlighted the limited potential of using IFN-I as HIV-1 therapy because of the limited number of responders to the treatment and significant side effects observed. Indeed, in the majority of clinical trials, IFN α responders were patients with preserved immune functions (CD4 count > 500/ml) [385]. Overall, IFN-I monotherapy had a moderate impact and its effect were transient, controlling HIV-1 plasma levels for a couple of months at maximum [385].

In order to decrease IFN α 2a-induced side effects, new trials were conducted using PEGylated IFN α 2a, a molecule that displayed more favourable pharmacokinetics and safety profiles than the previously used IFN α formulation. In ART naïve patients with chronic HIV-1 infection and normal CD4⁺ T cell count, PEG-IFN α injection led to a decrease in viral loads and correlated with the induction of ISG in the patient peripheral blood. However, these positive effects of IFN-I therapy were only observed in patients with low basal levels of ISG, contrary to individuals with high IFN-I signatures who proved to be non-responsive to PEG-IFN α treatment [386]. Altogether, these studies highlight the importance of the patient immune system activation status, a criterion that can drive the treatment outcome, along with the time and dosage of IFN α used to control viral replication.

These different trials, along with the promising results of cART on the control of viral load and increased longevity of infected individuals, opened the field for combined treatments utilizing cART and PEG-IFN α therapy. In the INTERVAC-ANRS 105 trial published in 2011, which recruited 168 chronically HIV-1 infected patients, PEG-IFN α administration during cART successive treatment interruptions (STI) was evaluated. After randomization, 84 patients received cART for 12 weeks, followed by 4 weeks of either PEG-IFN α therapy or placebo. This cycle was repeated 3 times. Follow-ups were set at week 48 and 72, and no significant differences in HIV-1 viral load and reservoir size were observed between the two groups. Nonetheless, patients with a low CD4⁺ T cell count and high baseline HIV-DNA showed increased risks of resuming treatment in the IFN-I group, supporting the detrimental role of IFN-I during the chronic phase of HIV-1 infection [387]. Similar results were obtained in the INTERPRIM-ANRS 112 trial, where patients were either treated with: (i) cART for 72 weeks, (ii) cART for 36 weeks followed by STI, or (iii) cART combined with PEG-IFN α during 36 weeks, followed by STI with PEG-IFN α administration [388]. Together, these studies suggest that combined therapy using cART and IFN-I did not significantly improve the decrease in viral load, CD4/CD8 T cell ratio and global CD4⁺ T cell counts compared to cART alone, nor did it prevent the viral rebound after treatment cessation. On the contrary, Azzoni and colleagues performed a proof-of concept clinical trial and found that IFN-I could be used against HIV-1 reservoirs when employed in combination with cART. In this study, patients received combined cART with PEG-IFN α 2a for 5 weeks, followed by 12 to 24 weeks of PEG-IFN α 2a only. This treatment led to viral suppression as soon as 12 weeks in the IFN-I group, and more importantly, subjects with sustained viral loads had decreased levels of integrated HIV-1 DNA despite residual viral loads [389]. This study provides hope that finding effective drug combinations will eventually eliminate HIV-1 reservoirs within the host.

Altogether, the different clinical trials presented here show the potential of IFN-I-mediated therapies. Yet, investigation is still needed to understand the host responses to IFN-I *in vivo*. To continue the development of innovative treatment strategies, research efforts should focus in optimizing the balance between the enhancement of the immune response against the virus while avoiding the deleterious induction of excessive inflammation. Currently, it is thought that the efficiency of IFN-I therapy could be mediated by several strategies. First, the use of other IFN-I subtypes from IFN α 2a should be considered. Indeed, it was shown that IFN- α 8, IFN α 14 and IFN β are more potent at blocking HIV-1 infection [390], [391] and display higher affinity for their receptor than IFN α 2a [391], [392]. In particular, IFN α 8 and IFN α 14 induce higher expression of antiviral genes (*e.g.* Myxovirus resistance 2 (MX2), Tetherin, apolipoprotein B mRNA editing enzyme, catalytic polypeptide-like 3 (APOBEC3)) [391], [392]. In addition, gene therapy where IFN β or IFN α 14 were used conferred a long-term suppression of HIV-1 replication in a humanized mouse model [393]. Second, host viral sensors could be modulated with agonists in order to induce endogenous IFN-I expression [394], [395]. Finally, the IFN-I signaling pathway could be modulated by affecting molecules involved in this pathway [396], [397].

b. IFN-I responses in HIV-1 pathogenesis: what we have learned from animal models

The variability of results obtained in human clinical trials that tested IFN-I administration as a therapy in HIV-1-infected patients shed light on the complexity of IFN-I responses in the host. To better understand the dichotomy of IFN-I, animal studies have been performed. Such studies have pioneered the current understanding of the different cellular response to IFN-I in the context of co-infection, starting by questioning the dogma according to which IFN-I are antiviral cytokines. In fact, it appears that IFN-I retain their antiviral properties under certain conditions, involving acute inflammation, but become deleterious to the host if sustained for too long or if induced too strongly. Here, I will focus on the main results obtained in the context of HIV-1 and SIV infection, which show that IFN-I can mediate an efficient antiviral effect, depending on when it is used.

i. Expected antiviral effect in the early phase of the infection

In this part, I will focus on rhesus macaque models used to test the efficiency of IFN-I or blocking IFNAR, the IFN-I receptor as treatment during SIV infection. The challenge of female animals with SIV results in viral replication at the mucosal infection site. In this model, during the following 10 days, the virus replicates in the tissue and corresponding lymphoid organs, before systemic infection can be observed, as described in HIV-1 infection (see Chapter II-II.A.b)[398]. During these 10 days following infection, cytokine responses are initiated, including the strong and early production of IFN-I at the mucosa [399]. In a study published in 2016, Veazey and colleagues showed that pre-application of IFN β in the vagina of rhesus macaques before SHIV (human and simian immunodeficiency virus chimera) challenge protected the animals from being infected by changing the phenotype of local immune cells. IFN β pre-exposure resulted in increased immune activation in the vagina, together with the up-regulation of restriction factor (for more details on HIV-1 restriction factors, see section II.C.c.iii of this chapter) [400].

Using two complementary methods, Sandler and colleagues dissected the dichotomy of IFN-I in a rhesus macaque model of SIV infection. First, they found that by blocking IFNAR daily for 4 weeks after SIV intrarectal challenge, the antiviral gene expression decreased. This was accompanied by a decrease in CD4⁺ T cell count while the SIV reservoir size was enhanced. Despite reduced T-cell activation, these animals showed signs of progression to AIDS, arguing for a role of IFN-I in animal protection when produced at the beginning of the infection [401]. In the same study, the authors showed that IFN α 2a administration, starting for 1-week prior to SIV infection and lasting for 4 weeks after challenge, upregulated antiviral genes, increasing the number of challenges necessary to lead to efficient infection and prevented systemic inflammation. However, continued IFN α 2a treatment led to IFN-I desensitization with decreased ISG expression, and consequently, to increased viral reservoirs together with an accelerated CD4⁺ T cell loss [401]. Altogether, these results indicate the importance of timing when the host initiates its IFN-I mediated viral response.

ii. *Deleterious consequences during chronic infection*

We just saw that when induced at early stage of the infection, IFN-I exert a protective effect against the virus, which prevents infection. However, when IFN-I are used too late or for too long, the continued exposure to this cytokine renders the cell insensitive to its signal, and antiviral genes are no longer expressed to restrict the infection. Evidence of this detrimental role of IFN-I were first observed when comparing SIV infection in its natural host, the Sooty Mangabey *versus* its non-natural host, the Rhesus Macaque. While both species display IFN-I mediated immune activation during the acute phase of infection, the IFN-I response is rapidly shut down in the natural host, along with decreased inflammation. On the contrary, non-natural host sustained high IFN-I responses during the chronic phase of the disease, which correlated with immune hyperactivation and CD4⁺ T cell loss [402], [403]. Similar observations were made in HIV-1 infected people who presented various susceptibilities towards AIDS progression: rapid progressors, who quickly lose T cells and present with high viral load, display stronger IFN-I blood signatures than viremic non-progressors [18], [404].

Other evidence of the detrimental role of IFN-I has been reported recently in another *in vivo* model. In a BLT (bone marrow, liver and thymus) humanized mouse model of chronic HIV-1 infection, exhaustion and activation markers of CD8⁺ T cells (high level of inhibitory receptor expression such as PD-1, CD38 and TIM-3²⁴) were increased. IFN-I signaling was also chronically elevated during the course of HIV-1, as supported by the constant elevated levels of MX1 gene (antiviral ISG) from 5.5 to 13 weeks post-infection [405]. In this study, Zhen and colleagues showed that blocking IFNAR 13 weeks post-infection lowered ISG expression in the peripheral blood and decreased T cell activation and exhaustion markers, and with time, decreased viral loads. They finally showed that, used in combination with cART, IFN-I treatment accelerated viral suppression and reduced the viral reservoir [405].

Taken together, these data demonstrate how subtle the IFN-I response is when induced by viral infection. Nonetheless, the promising results obtained with IFN-I administration or blocking in

²⁴ **TIM-3:** T-cell immunoglobulin and mucin-domain containing-3 is an inhibitory receptor of CD4 and CD8⁺ T cells that can also regulate macrophages activation.

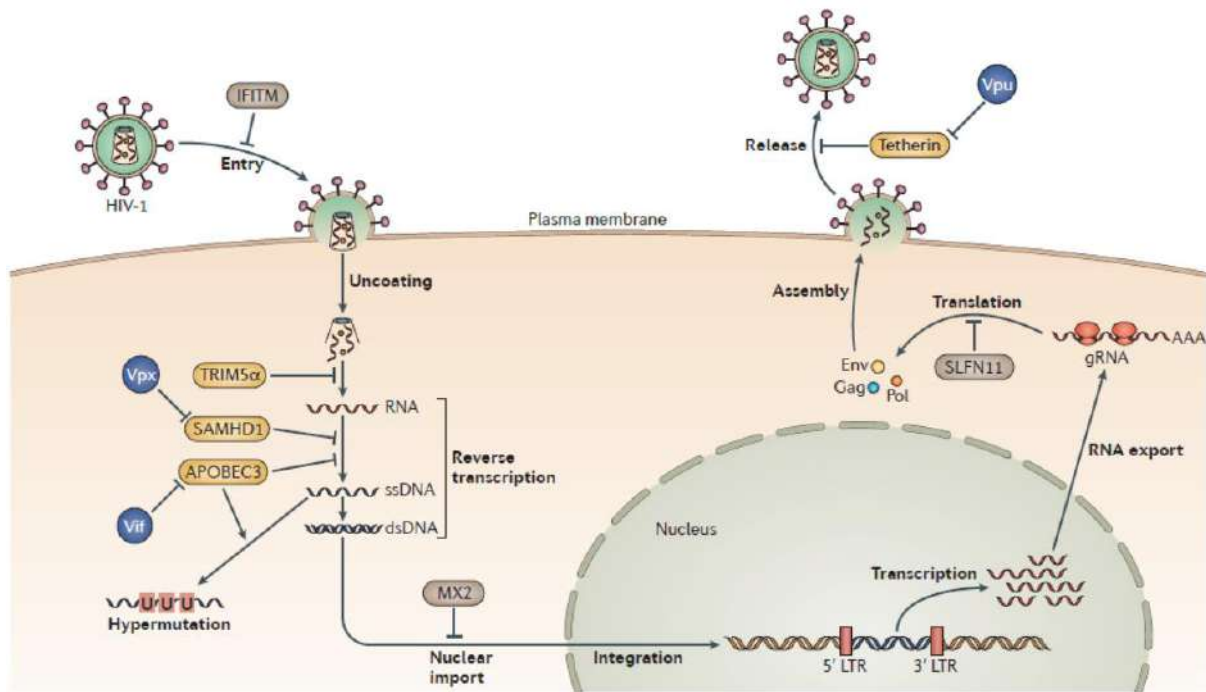


Figure 22: HIV-1 replication cycle and restriction factors (from [406]).

The different steps of the viral replication cycle can be counteracted by specific restriction factors (yellow) expressed by the host cell in response to the infection. Most of these factors are induced by IFN-I. For example, TRIM5a, SAMHD1 and APOBEC3, act to block HIV-1 reverse transcription by inhibiting cDNA synthesis, depleting the dNTP pool necessary for DNA synthesis or by favouring hypermutation of the viral DNA during reverse transcription, respectively. Tetherin prevents the release of budding virion. However, the virus expresses accessory proteins (blue) that are able to counteract the action of these restriction factors, allowing an efficient viral replication. The cell also express resistance factors (brown), such as IFITM, MX2 or SLFN11, which are not counteracted by viral protein. Nevertheless, the virus can escape the cell resistance, for example, by mutating the viral capsid, resulting in the failure of host MX2-resistance.

dsDNA, double-stranded DNA; *gRNA*, viral genomic RNA; *LTR*, long terminal repeat; *ssDNA*, single-stranded DNA

animal models of HIV-1/SIV infection, fuel the hope of using IFN-I as an efficient treatment to prevent viral dissemination in HIV-1 infected individuals.

c. Specific cellular responses to HIV-1 induced IFN-I: a zoom into macrophages

As described in the preamble, IFN-I is expressed in response to pathogen recognition through different PRR (Figure 2 in preamble). IFN-I then acts in an autocrine and paracrine manners to (i) control the viral replication in infected cells, and (ii) prevent bystander cells from getting infected [18], [28], by inducing the expression of IFN-I stimulated genes (ISG) with antiviral properties, usually called restriction or resistance factors (Figure 22) [407]. *In vivo*, it is thought that pDC are the main producers of IFN α , however, there is evidence that there are other leukocytes that also produce IFN-I. Indeed, in the lung, it has been shown that alveolar macrophages are the ones that produce IFN-I during infection with RNA viruses [408]. Here, I will discuss what is currently known of IFN-I responses at the cellular level in the context of HIV-1 infection, with a particular focus on macrophages.

i. PRR-mediated recognition of HIV-1 leads to antiviral gene expression

As mentioned in the preamble, host cells, and more specifically immune cells, possess an entire set of receptors able to detect exogenous material that leads to their activation and, usually, to the induction of IFN-I responses after PRR engagement (including TLR and RIG-I) [406]. In the case of HIV-1, the virus detection and sensing inducing IFN-I production can happen both before and after the viral entry into the target cell, and its sensing differs from one cell type to another, depending on the different PRR expression [406]. When the virus reverse transcribes its RNA into DNA, cytosolic factors such as IFN γ inducible protein 16 (IFI16), which is expressed in cells of the hematopoietic lineage including T cells and myeloid cells (DC, monocytes, macrophages), recognize the viral genome [409], [410]. In CD4⁺ T cells, IFI16 senses incomplete HIV-1 DNA intermediates and, in addition to IFN-I production, IFI16 is also responsible for the induction of caspase 1 activation, leading to cell death by pyroptosis. Importantly, there is evidence indicating that 95% of CD4⁺ T cells deaths occur in quiescent cells, and it points to IFI16-mediated pyroptosis²⁵ as a major contributing mechanism to the decline of CD4⁺ T cells during the course of HIV-1 infection [409], [411].

Another sensor, cGAS, whose expression is restricted to myeloid cells, is also able to bind to HIV-1 DNA [412], [413]. Consequently, cGAS catalyzes cGAMP, a second messenger that activates STING and TBK1, leading to IRF3 phosphorylation and its translocation into the nucleus, which results in IFN-I production. As part of the PRR family, TLR also play an important role in HIV-1 sensing, particularly in pDC. In particular, TLR7 is able to recognize HIV-1 RNA in endosomes and triggers the

²⁵ **Pyroptosis:** highly inflammatory form of programmed cell death requiring caspase 1 activity and that frequently occurs upon intracellular pathogen infections.

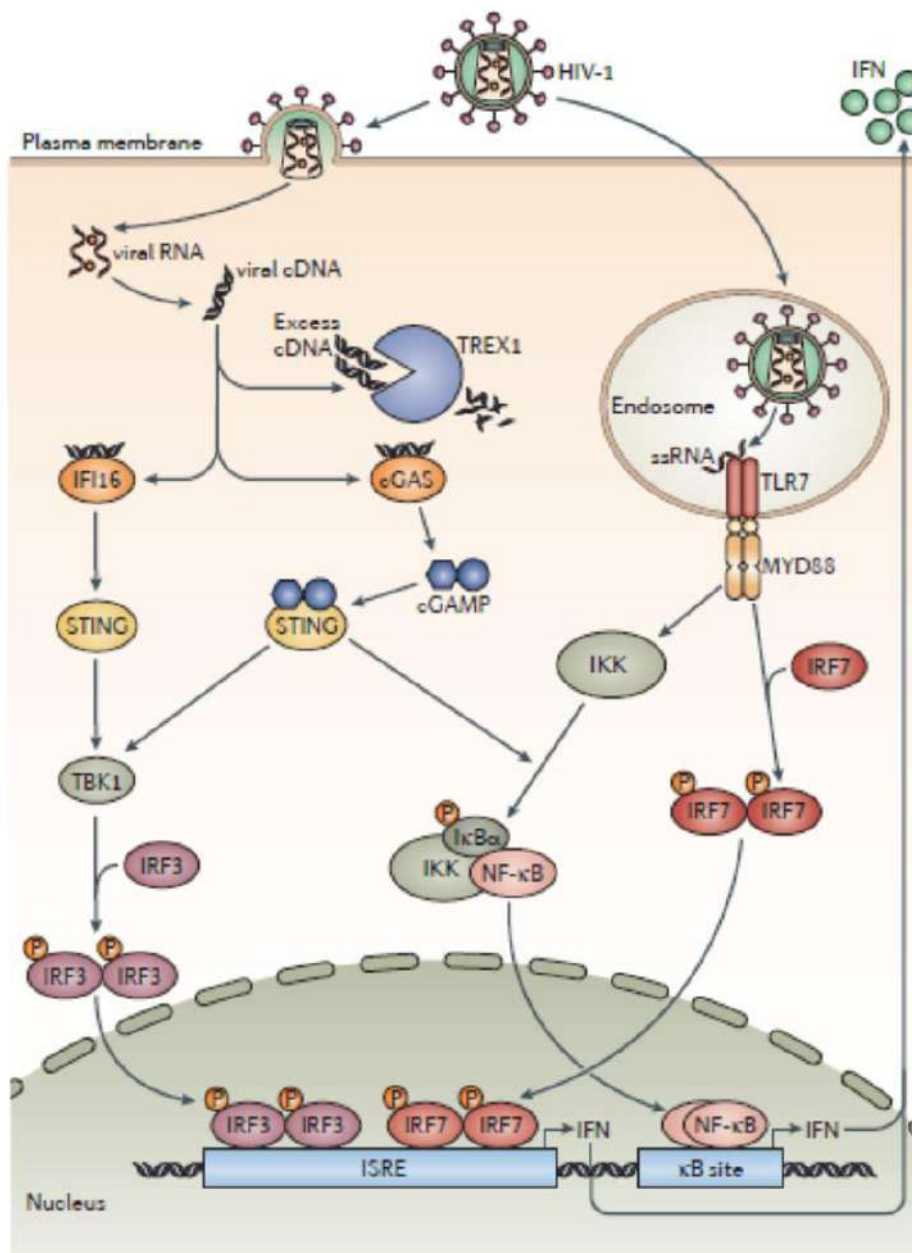


Figure 23: Sensing of HIV-1 (from [406]).

Upon HIV-1 entry into the target cell, the viral RNA is reverse transcribed into cDNA. This molecule is detected by the cytoplasmic receptors IFI16 and cGAS, which induce cGAMP. Consequently, both cGAMP and IFI16 activate STING, which recruits successively TBK1 and IRF3 to activate IFN-I promoter sequence ISRE and lead to IFN-I production. In the cGAS/cGAMP pathway, STING can also activate NF-κB, leading to activation of the κB site promoter and to IFN-I secretion. To avoid this response, HIV-1 uses the cellular protein TREX1, which helps the virus to evade cytosolic sensing by degrading viral cDNA in the cytoplasm. In addition to viral cDNA sensing, viral single stranded (ss) RNA can be detected by TLR, notably in endosomes. TLR7 activation by ssRNA results in the activation of MYD88, which then recruits IRF7 to activate the ISRE promoter and finally leads to IFN-I synthesis.

activation of the MyD88/NF κ B pathway, leading to IFN-I and other cytokines production. Exhaustion or death of pDC was responsible for the natural reversal of IFN-I production in SIV-infected cynomolgus macaques [414]. Moreover, blocking of TLR7 during acute infection of SIV-infected macaques resulted in a diminished IFN-I production, further highlighting the importance of TLR activation in HIV-1 detection [415]. Following these different sensing pathways, seen in figure 23, IFN-I are produced and subsequently activate the JAK/STAT1 signaling pathway (in an autocrine and paracrine manner) to generate ISG expression [18], among which several display antiviral properties.

ii. HIV-1 is able to avoid IFN-I induction in macrophages

In contrast to the IFN-I response induced in pDC, HIV-1 seems to avoid this response in many other cells types [416], [417], by preventing IFN-I production. In this regard, the host repair exonuclease 1 (TREX1) plays a central role as it degrades excess of HIV-1 cDNA produced during reverse transcription and therefore, avoiding viral recognition by IFI16 and cGAS. In human monocyte-derived macrophages, depletion of TREX1 allowed the accumulation of HIV-1 DNA in the cell cytoplasm, resulting in the induction of IFN-I expression *via* the STING/TBK1/IRF3 pathway (Figure 23), thereby preventing HIV-1 replication and spread [418]. HIV-1 is also capable of altering IFN-I signaling pathways either by triggering the induction of IRF2 and IRF8, which downregulates IFN-I signaling [419], or by targeting IRF3 to proteasomal degradation by macrophages [420]. This inhibition of IFN-I signaling activation in macrophages can also be due to the induction of suppressor of cytokine signaling 3 (SOCS3) by HIV-1. Akhtar and colleagues showed that SOCS3 expression attenuated macrophage responses to IFN β , resulting in lower antiviral gene expression and increased viral replication [421]. Another advantage for HIV-1 to prevent IFN-I responses is to avoid the increasing ways through which it can be sensed. Indeed, certain ISG, like tetherin and tripartite motif-containing protein 5 (TRIM5 α) are capable to detect the virus assembly and to restrict it while initiating NF κ B-dependent intracellular signaling pathways [422], [423]. Next, HIV-1 restriction factors will now be discussed.

iii. Restriction factors and how HIV-1 circumvents them in macrophages

Even if HIV-1 is able to prevent IFN-I induction in macrophages, the inhibition of IFN-I production is not absolute. Therefore, macrophages are able to respond to IFN-I produced by other cell types and upregulate ISG in response to this activation, including genes displaying inhibitory activities against HIV-1 [406], [424]. Much of the associated research focuses on the identification of these ISG, termed restriction factors or resistance factors, and their mechanisms of action and regulation, which can occur at different steps of the viral replication cycle [28]. In the next section, I will describe a few and non-exhaustive examples of well-known HIV-1 restriction factors expressed by myeloid cells, including macrophages, that participate in HIV-1 replication control. I will also discuss the mechanisms by which HIV-1 is able to counteract them.

Restriction factors are intrinsic cellular proteins that potently restrict or suppress HIV-1 and SIV replication. To be categorized as such, these proteins must possess the following characteristics [406]:

- they are invariant within an individual and cannot be altered by gene mutation processes;
- they display the hallmark of Darwinian positive selection;
- they are induced by IFN-I;
- they are sufficient to suppress viral replication at a single cell level;
- they are inactive against WT viruses that infect their natural host, (*i.e.* they are counteracted by the virus);
- they protect the host from infection with viruses from other species;
- their activities and downregulation are mediated by degradation, mainly in a ubiquitin-proteasome dependent system.

Of note, viral resistance factors display many properties of restriction factors, but they are not counteracted by the virus.

To date, several restriction factors have been described, including sterile α motif domain and histidine aspartic acid (HD) domain 1 (SAMHD1), TRIM5 α , APOBEC3, IFITM protein family, tetherin, MX2 and others (see Figure 22 and for a detailed review, see [425], [426]). Here, I will discuss three important restriction factors expressed notably by macrophages (*i.e.* SAMHD1, MX2, and Tetherin) that either specifically control HIV-1 replication in myeloid cells or have particular effects in macrophages.

In macrophages, IFN-I appears to interrupt early stages of the HIV replication cycle, as opposed to T cells, in which it acts on terminal stages of the viral cycle. One of the first restriction factors to intervene in HIV-1 replication is SAMHD1, a cytosolic enzyme expressed notably by DC, macrophages and CD4⁺ T cells (but at lower levels than myeloid cells). Its implication in HIV-1 restriction was initially discovered in DC, a viral inhibition that is specific of the myeloid cell lineage [427]. Indeed, SAMHD1 has a phospho-hydrolase activity that induces the degradation of dNTP²⁶ in non-dividing cells. Yet, effector CD4⁺ T cells are highly dividing cells requiring high levels of dNTP in order to expand and control the infection. This is why SAMHD1 is unable to control HIV-1 replication in activated CD4⁺ T cells. In fact, SAMHD1 is post-transcriptionally inactivated in dividing cells, including CD4⁺ T cells [428]. However, Benkirane's team and others showed that SAMHD1-mediated restriction of HIV-1 in quiescent CD4⁺ T cells is maintained [429], [430]. It is through its hydrolase activity that SAMHD1 was shown to inhibit HIV-1 reverse transcription in DC and macrophages, since its depletion markedly increased these cells susceptibility to infection [427], [431]. As a restriction factor, SAMHD1 is counteracted by the viral protein Vpx. The latter is an accessory protein of HIV-2 and SIV, but is absent from the HIV-1 genome. To show how Vpx counteracts SAMHD1, researchers transfected target cells with Vpx plasmids or Vpx-bearing virus-like particles (VLP) and evaluated its capacity to promote HIV-1 infection. It was shown that Vpx targets SAMHD1 for degradation by the proteasome through ubiquitination, subsequently allowing efficient infection of target DC and macrophages [406], [821]. The majority of the studies cited above used molecular tools to study the role of SAMHD1 during

²⁶ **dNTP**: mix of the four nucleotide triphosphate that compose the DNA molecule (adenine, thymine, guanine, and cytosine).

natural HIV-1 infection. The absence of Vpx in HIV-1 and the ability of HIV-1 to replicate in macrophages expressing the restriction factor in its antiviral state, suggests that SAMHD1 could be irrelevant in the control of the virus reverse transcription [407]. Indeed, the low level of dNTP is an obstacle to HIV-2 replication but not for HIV-1, which only needs a low concentration of dNTP to efficiently synthesize its DNA [432]. Yet, SAMHD1 renders DC and macrophages less permissive to HIV-1; as mentioned before, depletion of SAMHD1 increases cell permissiveness to the infection. This effect is more likely due to the nuclease activity of SAMHD1. By degrading HIV-1 RNA, the restriction factor protects the cell from being efficiently infected [433]. This has a dual effect. Despite single cell protection against the infection, SAMHD1 also allows the escape of HIV-1 from immune detection. Schwartz's team reported that during cell-to-cell communication between infected T cell and DC, SAMHD1 prevents viral RNA/DNA sensing in DC [434]. Reduced sensing of the virus also led to decrease antigen presentation capacities of DC [435]. Altogether, these results suggest that increased myeloid cells infection by inhibition of SAMHD1 may shift the balance of antigen presentation and favour specific immune responses to the infection, allowing for reduced immune activation and CD4⁺ T cell turnover. This would result in a natural control of HIV-1 infection, as observed with SIV and HIV-2.

The following restriction factor, MX, is involved at the next step of the HIV-1 replication cycle: nuclear importation of the viral DNA and integration into the host's genome. There are two IFN-inducible MX dynamin-like guanosine triphosphate hydrolases (GTPases) encoded in the human genome: MX1 and MX2 (also known as MXA and MXB, respectively) [436]. MX1 was reported to block a wide range of viruses, except HIV-1, who is specifically blocked by MX2 and more efficiently in non-dividing cells [437], [438]. MX2 is localized at the nuclear envelope, in nuclear pore complexes, but it can also be found in the cytoplasm [439], [440]. It seems to act at the level of nuclear entry and viral DNA integration into the target cell genome, since the abundance of 2'-LTR circular forms of HIV-1 DNA and of integrated viral DNA are reduced in monocytic cell lines overexpressing this protein [438], [439]. The exact mechanisms by which MX2 inhibits HIV-1 remain unknown to date. Yet, some evidence show that the GTPase activity of MX2 is not required for blocking HIV-1 [439]. However, its nuclear location is essential for HIV-1 control. Using engineered chimeric MX1/2 proteins, Goujon and colleagues found that the amino-terminal domain is responsible for MX2 anti-HIV-1 function. By transferring this sequence to the amino terminus of MX1, the engineered protein located to the nucleus and acquired anti-HIV-1 activities [438], [441]. Other studies suggested that MX2 antiviral function depends on the protein interaction with the viral capsid. During the replication cycle, after successful entry, the viral capsid interacts with host's proteins such as cyclophilin A (CYPA), nucleosporin 358 and polyadenylation specific factor 6 (CPSF6). The recruitment of these proteins to the reverse transcription complexes are thought to shield the viral cDNA from sensing by cGAS, and possibly other PRR and ISG, including MX2 [442], [443]. Depletion of CYPA in a 293T cell line abrogated MX2-mediated restriction of HIV-1 [444]. In addition, mutations in the viral capsid proteins rendered HIV-1 resistant to MX2 restriction [439]. Taken together, these results suggest that MX2 associates with the viral capsid-host protein complexes, allowing it to restrict HIV-1 nuclear importation and integration, although the exact mechanisms involved in this function remain to be discovered.

Tetherin, the last restriction factor I will now discuss, acts in the last stage of the HIV-1 replication cycle: the viral assembly and budding from the host cell. Tetherin, also known as bone marrow stromal antigen 2 (BST-2), was discovered in 2008 by Neil et al. and Van Damme et al. [445], [446]. It is a lipid raft-associated protein, because of the glycosylphosphatidylinositol (GPI)

modification in its C-terminal extracellular domain [447]. It is associated particularly with cholesterol-rich lipids rafts where newly synthesized HIV-1 particles bud from [448]. Tetherin retains the newly synthesized HIV-1 particles at the plasma membrane of virus producing cells. When the virus assembles and buds from the infected cell, its envelope contains host-membrane lipid-rafts and proteins, including tetherin, usually as a homodimer. Tetherin integration into the viral envelope and host plasma membrane allows the retention of viral particles, and subsequently leads to the internalization and degradation of the virus in the lysosomes [448], [449]. Several studies have highlighted the importance of the viral accessory protein Vpu for cell type-dependent HIV-1 particle release from virus producing cells [407], [426]. Indeed, the use of Vpu deleted strains of HIV-1 caused a 5- to 10-fold decrease in CD4⁺ T cell viral release [450]. Additionally, this defect was found to be dependent on the cell type: in T cells, viral particles accumulated at the plasma membrane, while in macrophages, tetherin-bound virions were stored in intracellular plasma membrane-connected structures called a virus-containing compartment (VCC, see Chapter II, section III.B.d.) [451], [452]. Tetherin knock-down in macrophages induced a redistribution of VCC, promoting HIV-1 release and cell-to-cell transmission, indicating again how important this ISG is for HIV-1 restriction. The evidence above indicates that Vpu is responsible for counteracting tetherin's antiviral functions. Several studies have shown that Vpu inhibits tetherin function by inducing its sequestration to the endosomal compartment [453]–[455], and it can translocate it to the lysosome by interacting with the small GTPase Rab7a [456]. In macrophages, Vpu restrains tetherin accumulation in VCC and stimulates viral release by reducing the size of VCC [452]. Last, but not least, Vpu is also able to recruit E3 ubiquitin ligase to induce tetherin ubiquitination, targeting it for proteasomal degradation [407], [426]. In light of these data, targeting Vpu or tetherin to either block or enhance their function (respectively) appears to be a promising strategy to help the host to control viral synthesis and dissemination. Yet, such a strategy still needs to be combined with others to fully inhibit HIV-1 replication, since tetherin can only reduce the rate of newly infected cells.

Besides the expression of restriction factors and their role, little is known about the specific IFN-I-mediated responses of macrophages upon HIV-1 infection. In the majority of studies, the impact of IFN-I was described in DC and T cell compartments, a subject reviewed extensively [457]–[459] and that will not be developed here. I will now focus on the role of macrophages within HIV pathology.

III. Intimate relationship between HIV-1 and the host: a focus on macrophages

For about 30 years now, HIV-1 physiopathology has been studied using a variety of *in vitro* and *in vivo* models. Nonetheless, the cellular and tissue tropism in infected humans remains not completely understood and is still open to debate. One particular subject of discrepancy relates to the *in vivo* relevance of the monocyte/macrophage compartment during the course of HIV-1 infection. CD4⁺ T cells have long been described as the major targets for the virus; however, macrophages are also infected and participate in infection-associated pathologies. Importantly, macrophages are present in the brain of infected patients and significantly contribute to HIV-1 dementia [460]. Today, evidence for the presence and implication of infected macrophages in many, if not all, tissues are available. Here, I will discuss about the importance of macrophages in HIV-1 disease.

A. Contribution of macrophages to AIDS in human and animal models

a. Mouse model

Many important aspects of HIV-1 infection cannot be fully evaluated using *in vitro* models or unmodified animal models, in particular with mice who are fully resistant to HIV-1 infection [461]. To circumvent this issue, humanized animals have been developed by transplantation of human cells and/or tissues [462], along with transgenic mice that have been used to study more specifically the role of a given viral protein in a whole-body system. One of the most used models is the Nef-transgenic mouse, which allowed the unveiling of the multifactorial effects of Nef during infection. Indeed, Nef expression in CD4⁺ cells in mice is sufficient to cause an AIDS-like syndrome [463]. Moreover, Nef was shown to be responsible for enhanced migration of macrophages towards the kidney, liver, and gut tissues [317], and for the downregulation of CD4 expression in T cells. Additionally, Nef-expressing macrophages migrate faster and mediate lymphocyte chemotaxis and activation, showing the importance of macrophages infection in the progression of the disease [317], [464].

Humanized mouse models have much evolved (for review see [462], [465]), and the transplantation of severely combined immunodeficiency (SCID) mice with human bone-marrow, liver and thymus (BLT) represents today the best model to study HIV-1 pathogenesis. This is because it possesses an entirely humanized immune system, however the kinetic of HIV-1 pathogenesis differs from that of humans [465]. Using this model, along with the humanized myeloid-only mice (MoM) who are depleted of the T cell compartment, the group of J. Victor Garcia revealed the importance of macrophages during HIV-1 infection. They found these leukocytes, in particular tissue macrophages, are able to sustain HIV-1 replication in the absence of T cells. These macrophages are located in various tissues, including the brain, liver, spleen, bone marrow, and lungs [466]. The same group demonstrated that ART, as reflected by a quick drop in the plasma viral load, rapidly suppresses HIV-1 replication in tissue macrophages and decreases cell-associated viral DNA and RNA. However, a delayed viral rebound occurred in about 33% of infected mice after treatment interruption, indicating that HIV-1 infection is persistent in macrophages, who are part of the viral reservoir [467] (for further details on macrophage reservoirs, see Chapter II section III. A.d.).

b. NHP

The question of HIV-1 infected macrophages serving as a main reservoir has become a significant issue for finding a cure to the infection. Important data on the course of the disease has emerged from NHP infection models. It is widely accepted that the loss of CD4⁺ T cell is a marker of disease progression and the main cause for its terminal endpoint [468]. However, evidence from SIV-infected NHP points to monocyte turnover as a more relevant tool to predict the infection outcome [469]. Supporting this, several studies have reported that under physiological conditions, monocyte turnover in NHP blood is about 5%, however in SIV infection, this is increased up to 50% prior to terminal AIDS progression. Increased turnover of the monocyte population was shown to be predictive of severe HIV-1-associated morbidities, including aggravated lung tissue pathology, cardiovascular disorders and encephalitis [469]–[471]. These morbidities were associated with an increased

macrophages population in the corresponding tissue. In fact, monocyte turnover kinetics was associated with a loss of tissue macrophages, notably in the lymph node, leading to enhanced recruitment of monocytes to replace them [472], [473]. Despite this, the absolute count of peripheral blood monocytes was not impacted, testifying to the high renewal rate of circulating monocytes during the disease course.

The appearance of cardiovascular, neurodegenerative and lung pathology as a result of an increased macrophage population supports the fact that these cells play a critical role in disease progression. Recently, Avalos and colleagues found that brain macrophages harbored replication competent SIV strains in virally suppressed cART-treated macaques. These macrophages were found two years after ART initiation, unveiling macrophages as a long-lived viral reservoir in the brain [474]. Additional studies indicated that macrophages could be part of the viral reservoirs. Indeed, in light of these studies, the lung appeared to be one of the most HIV-1/SIV affected organs under cART, an effect thought to be due to the role of macrophages in chronic immune activation within this organ [473], [475]. In the lung, both interstitial and alveolar macrophages have been shown to be infected by SIV, as they contain viral RNA, but it did not alter the two cell populations equally [468]. SIV infection of interstitial macrophages induced their rapid death by apoptosis, causing a continuous transport of circulating monocytes to the lung in order to maintain organ homeostasis. By contrast, alveolar macrophages showed a low turnover despite their infection, suggesting that this subpopulation of lung macrophages could be part of the long-lived viral reservoir [473], [476].

c. Humans

As observed in the NHP models, macrophages are also targeted by HIV-1 in humans during the acute phase of the infection. Indeed, viral nucleic acids have been detected in macrophages isolated from multiple infected patient organs, including Kupffer cells in the liver [477], microglial cells in the brain [478], macrophages in the GI tract [479] and in alveolar macrophages in the lung [480]. Importantly, similar observations were made in patients under cART in all afore-mentioned organs [479], [481], [482], supporting the idea that macrophage are part of the viral reservoir.

In addition to the evidence that macrophages are the main reservoir for HIV-1, there are also reports on their possible role in predicting the progression of the disease. In children infected with HIV-1, there is a higher monocyte turnover, correlating to a more rapid progression of the disease, and like in adults, could be a more relevant marker to follow this. Indeed, acute plasma viremia in young patients is generally increased 10-fold higher than levels seen in adults [483], suggesting that CD4⁺ T-cell depletion and the degree of immune activation does not consistently correlate with the progression to AIDS [484].

d. Evidence of macrophages as a main reservoir for HIV

HIV-1 is able to induce the formation of a viral reservoir, a characteristic shared by many retroviruses. By definition, a viral reservoir is a cell type, or anatomical site whereby a replication-competent form of HIV-1, either active or latent, can accumulate and persist stably, either as a provirus

or in infected cells [4]. Additionally, reservoirs can be reactivated upon stimulation (*e.g.* immune reactivation, opportunistic infections) and allow the virus to recolonize the host upon treatment cessation.

Macrophages and other cells from the monocytic lineage are more resistant than CD4⁺ T cells to the cytopathic effect of HIV-1 infection. Thus, as they are long-lived, in particular a certain subset of tissue macrophages, like alveolar macrophages that derive from embryonic origin, can harbour the virus for longer periods of time [485], strongly suggesting that they are part of the long-lived viral reservoir installed by HIV-1. Despite several studies in favour of this statement, the extent and relevance of macrophage reservoirs in humans has been a strong subject of debate. Indeed, cART-mediated reduction in the reservoir size, the limited access to relevant tissue samples (*e.g.* brain, lungs), and the inherent weaknesses of the detection techniques have failed to provide convincing data reporting the presence of replication-competent macrophage reservoirs in patients with suppressed viremia [486]. Yet, such data exists in infected-patients, who had detectable HIV-1 DNA in their myeloid cells. Moreover, macrophages persistence and implication in comorbidities (*e.g.* neurological disorders leading to dementia) argues of their importance, if not central role in the constitution of viral reservoir.

The majority of infected macrophages *in vivo* are tissular (*e.g.* microglia, alveolar macrophages, Kupffer cells). For example, evidence of HIV-1 infected macrophages in the brain have been observed since the 1980s. In the organ, it is mainly perivascular macrophages and the microglia that are infected with HIV-1 [487]. Infiltration of the central nervous system by the virus or infected cells occurs as early as eight days after transmission [488], and, structural changes in the brain are readily observable within only a year [489]. In cART naïve patients, brain infection causes an increased activation of glial cells, which induces detectable neuronal injury [490]. Brain infection, as in other organs, results in a lifetime infection and constitutes an important reservoir for HIV-1. Indeed, viral DNA can be detected in the cerebrospinal fluid in cART patient while it is not found in their plasma [491].

Lung macrophages, and particularly alveolar macrophages, as mentioned previously in this section, are also important targeted cells during HIV-1 infection. In SIV infection of macaque, alveolar macrophages were found to be infected within 10 day post-infection, as assessed by the detection of SIV RNA [492]. This study demonstrated that HIV-1 spreads quite early and rapidly to the lungs, where the major cell type infected were alveolar macrophages. In humans, alveolar macrophages isolated from broncho-alveolar lavages (BAL) were also positive for HIV-1 RNA and associated to local tissue damages, corroborating the results obtain in the SIV infection model [493]. Moreover, Jambo and colleagues found HIV-1 material in alveolar macrophages of cART naïve chronically-infected patients. They reported that HIV-1⁺ macrophages displayed impaired phagocytic activity [480]. In cART-treated patients whose plasma viral loads were under the detection levels, alveolar macrophages contained detectable proviral DNA in about 70% of the cases, and half of them also displayed detectable RNA in this cellular compartments [482]. In addition to the brain and lungs, a recent study conducted by Ganor and colleagues reported that urethral macrophages are also part of the macrophage reservoir. They isolated urethral macrophages from the penis of HIV-1-infected men under cART, and they were able to detect HIV-1 DNA, RNA, proteins and even identified the VCC, which will be described in the following section). By contrast, viral component were undetectable in the urethral T cells. When activated by LPS *ex vivo*, urethral macrophages started to replicate the virus and to release it into the

cell supernatant, indicating that a viral rebound had occurred and therefore showing that these cells are part of the HIV-1 reservoir [494].

Collectively, the different animal models and human data point to the important role of macrophages, specifically in tissues, during HIV-1 pathogenesis. Indeed, macrophages are both infected and able to sustain HIV-1 replication *in vivo*, and evidence points to their contribution to the establishment of a viral reservoir in patients under cART, while the monocyte turnover in those patients is predictive of their progression with the disease.

B. Viral replication cycle in macrophages and its consequences

Gartner and colleagues were one of the first to report that macrophages could be infected with HIV-1 by using 5 different isolates of the virus. They found that *in vitro*, infected macrophages from the healthy donor blood, bone marrow, and cord blood produced large amounts of the virus, a production that persisted for at least 40 days, independent of cell proliferation. They also reported that some HIV-1 isolates were more prone to infect macrophages than T cells, and vice-versa, suggesting for the first time that specific HIV-1 variants could have preferential cell tropism, indicating that macrophages are the primary target of these strains of HIV-1 [495]. Since this report, it has been shown that the HIV-1 replication cycle in macrophages differs from that in CD4⁺ T cells in different phases. In this section, I will describe the HIV-1 replication cycle in macrophages and point out the differences observed in the CD4⁺ T cell viral cycle.

a. Entry

In addition to entry through the interaction between gp120 and the main HIV-1 receptor CD4, the most efficient mode, viral entry into macrophages can happen through other mechanisms, including viral particle macropinocytosis, resulting in the degradation of the majority of virions [496], and endocytosis [497]. Upon binding to CD4, gp120 undergoes a conformational change that liberates gp41, allowing it to interact with either CCR5 or CXCR4. These interactions lead to the fusion of the cell and viral membranes, resulting in the entry of the virus into the target macrophage [498]. It is widely accepted that macrophages are mainly infected with R5-tropic viruses, since CCR5 is highly expressed by myeloid cells, and that those are responsible for horizontal transmission of the virus. Recently, infected individuals predominantly harboring R5 isolates [499] and individuals with the $\Delta 32$ mutation in the CCR5 gene (see the Berlin patient in chapter II section II.A.a.iii) have been found to be resistant to HIV-1 infection [500]. As opposed to CCR5-mediated viral entry, discrepancies have been reported in the literature concerning the use of CXCR4 as the co-receptor in myeloid cells. Despite CXCR4 being expressed at low levels both by monocytes and macrophages, it is unclear whether X4 viruses can productively infect macrophages. Most of studies evaluating the ability of X4 viruses to infect macrophages found a very low rate of infection, if any, and it was usually blocked at a post-entry level, concluding that macrophages are refractory to X4 strains [501], [502]. By the contrast, some other groups have reported efficient and productive infection of macrophages when using X4 primary isolates [503]–[505]. These opposing results may be explained by the differences in experimental

conditions, such as macrophage isolation and culture, or assays used to determine HIV-1 replication. Moreover, CXCR4 conformation could also be involved in the differences of X4-infectivity in macrophages, reported by several groups. Indeed, CXCR4 is expressed as a monomer on monocytes and T cells, but it seems to form receptor multimers, of higher molecular weight in macrophages compared to T cells [506]. Additionally, co-immunoprecipitation assay showed that CD4, which associates with its co-receptor upon gp120 binding, precipitates only with the monomer form of CXCR4, providing an explanation as to why there is poor infectivity of X4 strains observed in macrophages [506].

HIV-1 gp120 can also be recognized by alternate receptors present on the cell surface of DC and macrophages, which do not necessarily lead to their infection, but have a role in cell-to-cell infection. Among these receptors, CLR DC-SIGN and MRC1 bind the virus and efficiently transfer it to CD4⁺ T cells, as discussed in section III.D.a.i. This binding is important, since it has been shown that 60% of the initial association of HIV-1 with macrophages is mediated by MRC1 [507].

b. Nuclear import

After viral and cellular membrane fusion, the HIV-1 capsid is released into the cell cytoplasm. At this stage, the viral RNA is reverse transcribed into double stranded DNA by the viral reverse transcriptase. During transcription, LTR sequences are generated at both extremities of the viral DNA, necessary for viral genome integration and regulation of its expression [508]. This process of viral DNA synthesis happens in the so-called reverse transcription complexes (RTC) and as opposed to taking a few hours in T cells, it takes about 36 to 48h in macrophages, for unknown reasons [509]. A hypothesis that explains this difference is the fact that T cells are actively dividing cells, while macrophages are quiescent cells and therefore, the machinery for genome replication is not accessible in the same way in both cell types.

In macrophages, viral DNA and proteins necessary for integration (both from the virus and the host) are part of a nucleoprotein complex called the pre-integration complex (PIC). This complex must pass through the nuclear pores in order to deliver the viral DNA to the host nucleus [510], and this occurs through an active, energy-dependent, mechanism [511]. In macrophages, this process can be blocked, notably by restriction factors such as MX2 as previously discussed (see chapter II part II.C.c.iii.), but also by their activation status. For example, LPS-stimulated macrophages inhibit HIV-1 nuclear import due to the activation of p38 kinase, which can be reversed upon p38 signaling blockage [512]. PIC importation to the nucleus is mediated, notably by the virus central DNA flap, which is a stretch of triple-stranded DNA formed due to the presence of two initiation sites for the positive DNA strand in the virus. These two sites overlap during the positive strand synthesis and enhance nuclear import of the PIC [513]. Viral proteins such as integrase, matrix proteins, and Vpr also promote PIC import into the nucleus due to nuclear localization signals for importin- α/β [514], [515] and by counteracting restriction factors for Vpr. After successful import of the PIC into the nucleus, the viral DNA is integrated in the transcriptionally active region of the genome (*i.e.* euchromatin).

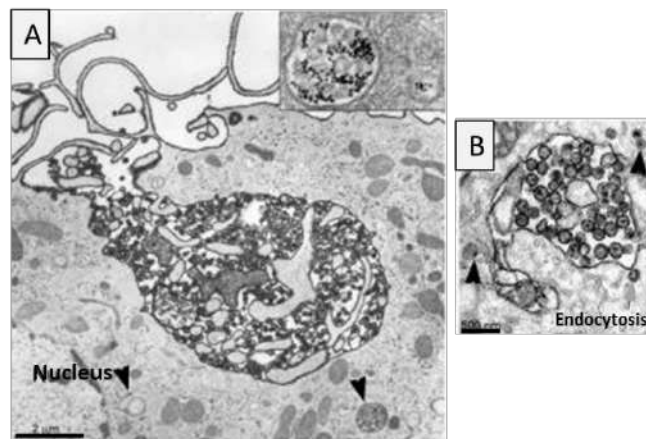


Figure 24: Virus-containing compartments are not late endosomes (from [516]).

Monocyte from healthy donor where differentiated into macrophages for 7 days, and then infected with HIV-1_{BAL}. 10 days post-infection, infected cells were fixed and prepared for electron microscopy analysis in order to visualize the virus-containing compartments (VCC).

A | Large cell-surface invaginations are directly connected to the extra-cellular milieu (as shown by the RR staining in black: RR is a membrane permeant dye that is not internalized in intracellular compartment) and contains numerous RR-stained virions. The inset shows a multivesicular BSA-gold-filled endosome inside the same cell. *Scale bar: 2 μ m.*

B | RR-stained vacuole-like structures containing viral particles. The arrowheads indicate gold-filled endosomes that are not RR-stained and significantly smaller than the virus-filled structures. *Scale bar: 500 nm.*

c. Transcription

Following integration, the HIV-1 genome needs to be transcribed; an event differentially regulated in macrophages and T cells. In T cells, early transcription of HIV-1 mainly depends on transcription factors such as GATA-3, ETS-1, LEF-1 and NFATc [517], [518]. However, in macrophages, HIV-1 transcription depends on the isoforms of the transcription factor C/EBP β ²⁷, which are generated by alternative translational initiation. When present under the small form (16-23 kDa), which is the dominant isoform and is IFN-I inducible (*e.g.* induced by Mtb infection in an IFN β -dependent manner [519]), C/EBP β inhibits HIV-1 replication [520]. By contrast, the larger isoform (30-37 kDa) is the activating form required for HIV-1 replication in macrophages [521]. This transcription factor controls the early transcription of the HIV-1 genome, and results in the production of the viral proteins Tat, Rev, and Nef. The late transcription phase is controlled by the viral protein Tat, which enhances viral RNA elongation [522]. Once the viral genome is expressed under the form of messenger RNA (mRNA), both viral RNA and mRNA encoding viral proteins are exported out of the nucleus. Consequently, mRNA is translated into proteins and the viral assembly to form new viral particles starts within the cell cytoplasm.

d. Assembly and release

New virions are generated after the assembly and budding of viral particles from the infected cell. This process is regulated by the gag polyprotein. In T cells, this process occurs close to the plasma membrane [523]. In macrophages, the virus assembles and buds from the intracellular compartments, late endosomes/multivesicular bodies [524]. Indeed, Welsch and colleagues found 45% of assembling virions on tubular-vesicular endosomal membranes rather than on endosomes themselves. Additionally, 10% of the particles were localized in multivesicular bodies with very few at the plasma membrane. In fact, it has long been known that HIV-1 particles accumulate in intracellular vacuoles in macrophages [525]. At the beginning of the millennium, Raposo and colleagues identified these compartments as the “MHC-II late endocytic compartments” [309]. Moreover, these compartments were shown to fail to acidify due to a lack of recruitment of the v-ATPase, thus providing the virus with an environment where it can survive for long periods of time [526]. Further studies of these HIV-1 containing compartments, later termed as VCC, showed that they were characterized by the expression of multivesicular bodies proteins such as tetraspanin CD9, CD81, CD53, CD63 and CD82 [527]. However, the study conducted by Welsch and colleagues revolutionized the identity of the VCC when they found that new viral particles budded at the plasma membrane of macrophages. Indeed, using ultrastructural approaches, they found that budding virions were mostly localized to the plasma membrane (see figure 24), while secreted virions displayed mainly plasma-membrane-derived proteins [516]. Since then, VCC have been well characterized (for review see [528], [529]). VCC are unlikely to be specific to HIV-1 infection since similar structures do exist in uninfected macrophages [516], however, they are enlarged in HIV-1 infection [530]. 3D-studies of their structure have shown that not all VCC are homologous and form a complex tubulovesicular membranous web that extends into the

²⁷ C/EBP β : CCAAT/enhancer binding protein beta is a transcription factor involved in immune and inflammatory responses

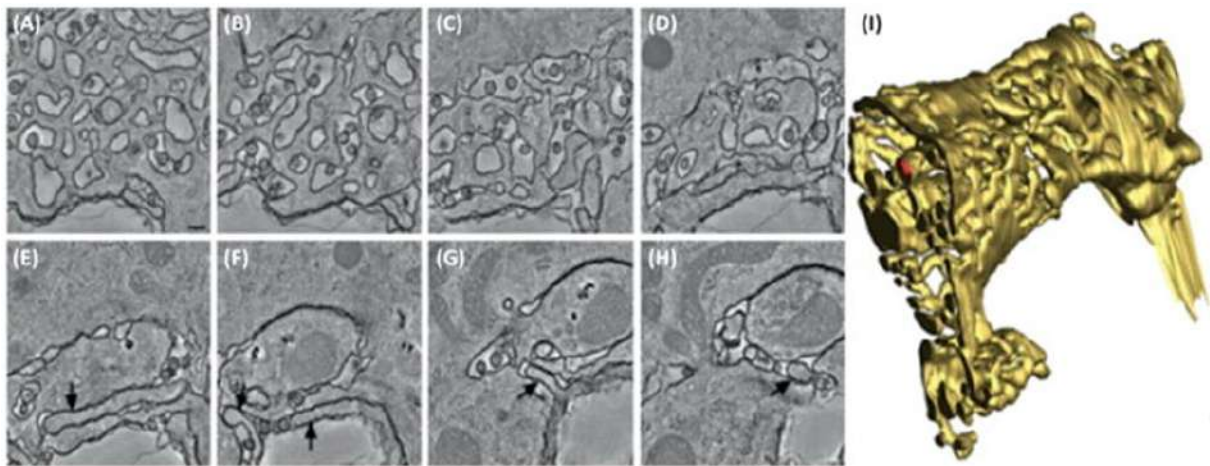


Figure 25: Virus-containing compartments ultrastructural reconstitution (from [528]) .

A–H | Digital slices (from electron tomography) through a region of a HIV-1-infected macrophage depicting the morphological complexity and variability of the virus-containing compartments (VCC). The arrows point to membranous protrusions that were initially thought to be a separated form of VCC, but were later shown to be part of the overall three-dimensional VCC structure.

I | Three-dimensional reconstruction of a VCC containing a virus particle (red). *Scale bars, 200 nm.*

Extracted from [528].

macrophages (see figure 25 from [525]). They do not derive from endosomal origin as shown by BSA-gold labelled endosomes in macrophages which resulted in low numbers of gold particles in VCC, and are positive for the plasma membrane marker CD44, suggesting that they originate from the cell surface [516]. In infected macrophages, VCC represent the main site of HIV-1 assembly and budding [527] although membrane assembly and budding are not excluded [516], [531], and could serve to rapid release of virions for cell free infection of surrounding cells, as opposed to VCC that promote long-term storage of the virus. These structures are proposed to participate in the reservoir function of macrophages and are highly dynamic. Indeed, time-course experiments demonstrated that VCC migrate into the infected macrophage towards the contact zone with T cells, and result in the infection of T cell [532]. In addition, other groups have observed HIV-1 Gag vesicles trafficking through inter-macrophages cytoplasmic bridges [533], [534], further indicating that VCC are dynamic structures enabling HIV-1 trafficking throughout the macrophage and can be used to facilitate the infection of neighboring cells. This trafficking of HIV-1 containing VCC is mediated by the kinesin KIF3A²⁸, a molecular motor that propels cargos along microtubules, and in this case VCC are driven to the plasma membrane for viral release. Indeed, upon silencing of KIF3A, HIV-1 particle release was reduced whereas VCC volume increased, showing that this kinesin is responsible for the movements of VCC within the infected cell [535].

Tetherin is one of the restriction factors that inhibits HIV-1 particle release from the infected cell (see chapter II section II.C.c.iii) by anchoring the virus onto the plasma membrane. In infected macrophages, tetherin is not only present at the cell surface but is also in VCC. In fact, it is an essential element needed for VCC formation, since its knock-down by siRNA decreases VCC volume and size, accompanied by a redistribution of VCC throughout the cell [451]. Furthermore, in HIV-1 infected cells, tetherin inhibition leads to an increase of both viral release and cell-to-cell transmission efficiency. Therefore, tetherin retains HIV-1 virions in the VCC while maintaining the compartment structure. Strikingly, HIV-1 infection induces tetherin expression through the action of Nef, most likely because it provides the virus with a long-term storage compartment [451]. In addition to tetherin, another molecule, the Siglec-1 lectin receptor (described in section III.D.a.ii.), is able to induce VCC formation, independently of macrophage infection. Hammonds and colleagues found that the binding of HIV-1 and virus like particles (VLPs) was directed into pre-existing VCC in infected macrophages, a process that proved to be necessary for subsequent particle transfer and infection of autologous T cells. Depletion of Siglec-1 prevented VLPs and virus uptake, and subsequently resulted in a decreased VCC volume [536].

As main storage centers of HIV-1 particles in infected macrophages, VCC participate in the establishment of the viral reservoir that imposes life-long treatment of HIV-1 infected individuals. VCC protect the virus against neutralizing antibodies and anti-viral drugs [537], [538], while also conferring a long-term storage compartments, allowing the virus to survive within its host for long periods of time. Despite several clues, the mechanisms behind VCC formation are still unclear and need further investigation. Identifying these mechanisms is key to developing directed therapies to ensure the elimination of the viral reservoir.

²⁸ KIF3A: kinesin-like protein is one subunit of the heterotrimeric motor protein, kinesin-2, that transports protein complexes, nucleic acids and organelles towards the "plus" ends of microtubule tracks within cells.

e. Consequences on macrophage functions

HIV-1 infection of macrophages has long been described in infected individuals, and results in the dysregulation of their main functions, including antigen presentation, intracellular pathogen killing, cytokine production, and phagocytosis (reviewed in [539]).

Upon infection with HIV-1, macrophages produce a wide range of pro-inflammatory cytokines and chemokines, such as $\text{TNF}\alpha$, $\text{IL-1}\beta$, IL-6 , $\text{MIP1}\alpha$, $\text{MIP1}\beta$, and CCL5 (RANTES) [540], [541]. These cytokines participate in both the pathogenesis and the chronic activation of the immune system, while also influencing the response of surrounding cells to the infection. Indeed, cytokine release in the extracellular milieu causes the polarization of macrophages towards more or less permissive phenotypes to HIV-1 infection (for review see [187], [542]). Cassol and colleagues found that the “classical M1” polarization of macrophages (see preamble II.B.) are refractory to HIV-1 infection due to a decreased expression of CD4 and an increased inhibition of the viral cycle at the early pre-integration step [543]. By contrast, “M2a anti-inflammatory macrophages” inhibited the HIV-1 cycle at a post-integration level, and for a longer time than M1. All effects observed in the differentially polarized macrophages were reversed 7 days after the removal of the polarization stimuli, suggesting that macrophage polarization could be a mechanism that allows HIV-1 to switch between an active and latent status [543]. In addition to modulating macrophage sensitivity to HIV-1 infection, cytokine production also directly impacts infected cells. For example, $\text{IL-1}\beta$ and IL-6 , as well as IL-6 and $\text{TNF}\alpha$, were shown to act in synergy to stimulate viral replication [544], [545]. In addition, several of the above-mentioned cytokines participate in the inhibition of CD4 and CCR5 expression at the cell surface, together with the viral protein Nef, a beneficial mechanism for HIV-1 replication [546]. During the chronic stage of HIV-1 infection, IFN-I secretion leads to the production of IL-10 , an anti-inflammatory cytokine that inhibits IL-6 and $\text{TNF}\alpha$ production in infected macrophages [547]. However, despite an historical anti-viral role of IL-10 [548], [549], this cytokine has been shown to promote HIV-1 infection and replication in M(IL-10) macrophages [550]–[553].

In addition to the modification of the cytokine production, HIV-1 infection modulates macrophage phagocytosis. The latter is mediated by several receptors, including complement receptor and receptors for the Fc portion of immunoglobulins (FcR), both mediating phagocytosis of the opsonized pathogen. FcR-mediated phagocytosis in HIV-1 infected macrophages is altered by the inhibition of the phosphorylation of Src kinases and other proteins (including Hck, Syk and Paxillin) [554]. The group of Niedergang showed that receptor-mediated phagocytosis is inhibited in HIV-1 infected macrophages in a Nef-dependent manner. In fact, Nef inhibited the recruitment of adaptor protein-1 (AP-1^{29}) to endosomes, thereby preventing optimal phagosome formation [555]. HIV-1 is also able to use phagocytosis to its advantage. Indeed, it was reported that phagocytosis of apoptotic cells by HIV-1 infected macrophages enhanced the virus replication in these cells, in a $\text{TGF}\beta$ -dependent manner [556].

An important function of macrophages as patrolling cells in the maintenance of tissue homeostasis, is their capacity to migrate. In our team, my PhD supervisor showed that HIV-1 infection of macrophages altered their migratory function. 2D and amoeboid 3D migration modes of

²⁹ **AP-1**: proteins that mediate the formation of vesicles for intracellular trafficking and secretion.

macrophages were inhibited by HIV-1, while mesenchymal 3D migration mode, dependent on matrix degradation by matrix proteases, was enhanced in a Nef-dependent manner [318]. Nef expression was necessary and sufficient to induce these effects on macrophages migration, as proven by a Nef-transgenic mice model in which tissue infiltration of Nef-expressing macrophages was enhanced both at steady state and in tumor masses [318]. This mechanism could be a way for the virus to disseminate throughout the host.

Nef can also intervene in macrophages fusion. In fact, my team has shown that the formation of multinucleated giant cells (MGC) are a hallmark of HIV-1 infection in macrophages. The viral protein Nef was sufficient to induce MGC in RAW264.7 macrophages and depended upon its interaction with the host protein p61-Hck isoform, as well as lysosomal proteins (*e.g.* vacuolar adenosine triphosphatase and proteases) [319]. Finally, I participated as a co-author to the study that shows that osteoclasts, bone macrophage-like cells specialized in bone degradation, are targets for HIV-1. Osteoclast infection leads to increased adhesion and osteolytic activities, through modulation of the sealing zone size, which is a particular organization pattern of proteins of the cytoskeleton (*e.g.* actin, vinculin, talin). These effects on bone degradation were found to be mediated by the interaction between Nef and Src protein [323].

HIV-1 infection leads to a modified activation of macrophages and consequently, alters their function. We saw here that HIV-1 induces the production of cytokines that favour its replication in the infected cells while polarizing surrounding cells to a permissive state for viral infection, and that the virus alters mainly the phagocytosis process either to prevent its degradation or enhance its replication. Finally, through the viral protein Nef, HIV-1 alters the macrophage cytoskeleton not only to control intracellular compartments, but also the migration of macrophages through tissues.

C. Macrophages in HIV-1 latency and communication with other cell types

a. Induction of latency in macrophages

To persist in the host, even under cART, HIV-1 is able to become undetectable by entering a state of viral latency, one of the several mechanisms utilized by the virus to survive in its host [557], [558]. This latency is defined by an infection during which infected cells do not produce infectious viral particles, however, this state can be reversed upon stimulation [559]. Usually, latency can be classified into two types: pre-integration latency and post-integration latency. Pre-integration latency is characterized by a poor reverse transcription efficiency and the inhibition of the viral DNA importation into the nucleus and is a common mechanism *in vivo* [560]. Indeed, in brain tissue of HIV-1 infected patients, unintegrated viral DNA quantities were at least 10 times higher than integrated DNA numbers, indicating an essential role for pre-integration latency in this organ [561]. On the contrary, post-integration latency occurs after viral DNA integration into the host genome, and is defined by the silencing of the HIV-1 genome expression [558], [562]. Several mechanisms have been described to explain the induction and maintenance of latency in target cells, including epigenetic gene silencing, which regulates the different regions of the genome that are expressed [558], as well as transcription gene silencing and post-transcriptional gene silencing [563]. Notably in macrophages, HIV-1

preferentially integrates into the transcriptionally active regions of the host chromatin, a process that can be regulated by epigenetic regulation [564]. Overall, restriction factors expressed by the target cells like MX2, SAMHD1, APOBEC3, and others, participate in the latency mechanism (see chapter II.C.c.iii).

Importantly, viral latency is thought to be a rare event. Indeed, an estimated one cell out of 10^6 – 10^7 cells is latently infected [565]. On top of that, *in vivo* study of HIV-1 latency in macrophages is quite difficult to perform due to the small population that can be isolated. To remedy this issue, Brown and colleagues developed an *in vitro* model of a long-term culture of human macrophages derived from blood monocytes and infected with HIV-1-GFP [566]. Interestingly, they found that latency can be established in these macrophages and can be reversed by a co-infection with herpes virus 8, supporting opportunistic infection as a mechanism of HIV-1 reactivation in macrophages [567].

b. Role of macrophage the establishment of CD4⁺ T cells reservoir

In infected macrophages, HIV-1 assembles, buds, and is stored in VCC (see chapter III.B.d) [568], [569]. These VCC provide a safe environment for the virus to survive since they are not accessible by antiretroviral drugs and neutralizing antibodies [570]. Therefore, VCC are a perfect niche for HIV-1 to establish a stable latent infection in macrophages. Studies reported by Benaroch and colleagues indicate that HIV-1 utilizes pre-existing CD36 compartments for its assembly and budding, further arguing that VCC are a way for HIV-1 to establish a viral latent reservoir. Moreover, they found that CD36 is an important molecule in HIV-1 release since its blockage resulted in the inhibition of virus release from infected cells [571].

Upon infection, macrophages secrete a pool of cytokines and chemokines, such as MIP-1 α , MIP-1 β , MCP-1 and CCL5, which attract CD4⁺ T target cells and create an ideal situation for viral dissemination and memory T cell reservoir establishment [572]. After being recruited, macrophages are able to transmit the virus to uninfected T cells, including CD4⁺ memory cells, mostly through the establishment of a virological synapse-like structure, and thereby extend the viral reservoir [573]–[575]. In addition, HIV-1 infected macrophages can induce anti-apoptotic resistance in CD4⁺ T cells they just infected while promoting the killing of bystander cells [576], [577], and therefore facilitate the establishment of a stable infection in these cells in a Nef/TNF α -dependent manner [578]. Through these mechanisms, macrophages allow the establishment of a long-lived T cell reservoir, which is mainly composed of CD4⁺ memory T cells.

Altogether, latent infection of macrophages is part of a mechanism that allows HIV-1 to survive in the host, protected from immune system effectors and cART in specific cellular compartments. Furthermore, latently infected macrophages are able to recruit uninfected target T cells and transfer the virus to them, thereby extending the infection, and possibly the viral reservoir when specific memory CD4⁺ T cells are recruited to the site of infection.

c. Interplay with other cell-types: importance of exosomes

As mentioned previously, HIV-1 infection of macrophages induces a change in their gene expression profile, together with the cytokines and chemokines produced. These changes also modify the interactions between macrophages and the adaptive immune cells, such as CD4⁺ and CD8⁺ T cells, usually resulting in the activation or death by apoptosis of these cells [579]. Clayton and colleagues evaluated the interaction between CD8⁺ T cells and HIV-1 infected macrophages, using autologous cells isolated from the blood of HIV-1⁺ patients. They found that the killing of macrophages by CD8⁺ CTL was impaired when compared to that of CD4⁺ T cells, resulting in inefficient suppression of HIV-1 in culture. In addition, impaired killing of macrophages, which requires caspase 3 and granzyme B, prolonged the contact time between the effector and target cells, as well as IFN γ production by CTL. This subsequently led to production of pro-inflammatory cytokines by macrophages that recruited both monocytes and T cells, contributing to viral persistence and establishment of the chronic inflammation associated with HIV-1 infection [580].

One important way for macrophages to communicate with other cell types, including DC and T cells, is through exosome release. In macrophages, specialized MHC-II⁺ compartments, derived from late endosomes or from multivesicular bodies, can traffic to the cell surface and fuse with the plasma membrane to be released eventually in the extracellular environment as exosomes [581]. By definition, exosomes are small extracellular vesicles (30 to 200 nm in diameter), which contain and traffic nucleic acids (RNA, microRNA, and DNA), proteins, and lipids from the donor cell. Most cell types are able to secrete these nanoparticles into the extracellular milieu, allowing them to carry messages to neighboring cells and to mediate adaptive immune responses against pathogens [581]–[583]. In addition to host materials, exosomes that commonly express the tetraspanins CD9 and CD81 can contain viral proteins [579], [584]–[587]. In HIV-1 pathogenesis, the role of exosomes is complex and controversial. Indeed, some studies reported that exosomes can block HIV-1 infection, notably by transferring to target cells some restriction factors like APOBEC3 [588]. Other studies have reported enhanced infection through HIV-1 entry receptor transfer by exosome release [589]. The exosome pathway was also thought as a Trojan horse by which the immature virus would not only escape lysosomal degradation, but also evade recognition by the host immune system (*e.g.* by not expressing Env at the surface [590]) and anti-viral drugs. In this model, immature HIV-1 particles, present at the cytoplasmic face of late endosomes or the membrane of multivesicular bodies, are internalized into intraluminal vesicles after membrane invagination and fission. These HIV-1-containing vesicles are then transported to the cell plasma membrane where they fuse and are finally released into the extracellular milieu [590], displaying membrane characteristics of exosome, rendering them invisible to the immune system and favouring new infection events [591].

Taken together, the studies performed on HIV-1 particle release through exosome pathway indicate a potential important role of these nanoparticles in the dissemination of the virus and the progression of the disease. As they hide the virus from the immune system as well as target drug therapies, while also mediating entry of the virus into target cells independently of the viral receptor, exosomes-like viruses represent an potentially efficient mechanism of infection, and could even lead to infection of cells that do not express the viral receptors. Consequently, this would cause an increase in the viral spread throughout the organism, even in organs that are normally protected by physical barriers.

D. HIV-1 cell-to-cell transfer: a master in disguise

Most of the studies described above were performed in free-viral particle models of infection. However, cell-to-cell transfer is 100 to 1000 times more efficient than free-viral particle infection and may represent at least half of the new infections *in vivo* [323], [592]–[594]. In the present section, I will discuss the different mechanisms of cell-to-cell transfer that have been described to date.

a. Role of lectins in HIV-1 capture and trans-infection

i. C-type lectins: recognition of the viral protein gp120

Despite CD4, CCR5 and CXCR4 being the main receptors for HIV-1 entry into target cells, the virus also interacts with a wide range of other cell surface molecules, a capacity the virus acquired upon different cellular encounters and evolution of its flexible glycoprotein gp120. The CLR family is one of the groups of receptors able to interact with HIV-1 and are suspected to support efficient viral transfer to CD4⁺ T cells [595]. Well described CLR expressed by both DC and macrophages found to bind HIV-1 are, most notably, DC-SIGN, Langerin and MRC1 [596]. Their primary function is to bind carbohydrate domains present on both pathogens and host tissues. Upon binding to host sugar motifs, CLR promote cell-to-cell communication, particularly between T cells and antigen presenting cells. Alternatively, binding to pathogen sugar motifs can and usually leads to internalization, degradation and antigen loading onto MHC molecules for T cell activation [597]. However, certain pathogens like HIV-1 have hijacked these molecules for its own benefit. Here, I will focus on DC-SIGN and MRC1, which both bind to HIV-1 gp120 [598], [599].

The role of DC-SIGN in HIV-1 binding has been extensively studied, particularly in DC. Indeed, DC-SIGN-expressing cells are particularly numerous at mucosal sites, in particular in the female endo- and ectocervix, both considered sites of HIV-1 sexual transmission [600], [601], as well as in the rectum, where they efficiently bind and transport the virus [602]. DC-SIGN⁺ maternal and fetal macrophages in the placenta were found to play an important role in materno-fetal transmission of the virus [603]. Altogether, the presence of DC-SIGN⁺ cells in anatomically relevant sites of HIV-1 infection suggest an important role for this lectin in the initial viral detection, capture, transport, and transfer to target cells. Moreover, several reports have implicated CLR polymorphism (in particular DC-SIGN) as increased risks of viral transmission, especially from mother to child, since CLR are expressed by placental cells [604]. In spite of the poor permissiveness of DC for HIV-1, interactions between DC-SIGN and gp120 have been shown to be involved in enhanced DC infection [605], [606]. In addition, DC-SIGN has been suggested to be a way out for neutralizing antibodies, whereby, DC-SIGN-expressing myeloid cells have been described for their capacity to bind and efficiently transfer either HIV-1 or SIV to T cells [607]–[611], while protecting it from antibody neutralization [612]. This was shown to be mediated by a rapid internalization of intact viruses into low pH non-lysosomal compartments [613]. DC-SIGN is also highly expressed by macrophages, even more than DC, in the lymph nodes and blood, suggesting that macrophages could play an important role in DC-SIGN-mediated HIV-1 transfer *in vivo*. Of note, both human DC and macrophages display DC-SIGN-independent HIV-1 transmission, possibly involving other alternative receptors, like MRC1 [614], [615].

Like DC-SIGN, MRC1 is expressed by DC, macrophages, spermatozoa, and epithelial cells, particularly at mucosal sites, including the vagina and in semen, and has the potential to capture the virus during the first step of infection [616]. Upon binding to MRC1, HIV-1 has two possible fates: it will either be efficiently transferred to T cells through a virological synapse-like structure [507], or it will be degraded for antigen presentation [617]. Using mass spectrometry, Cunningham and colleagues reported that MRC1 can form homodimers in primary human macrophages and that it is the dimer that recognizes and binds HIV-1 gp120 [618]. Interestingly, Sukegawa and colleagues reported that MRC1 can also display anti-viral protection in ways similar to tetherin. Indeed, the authors found that infected macrophages produced full infectious viral particles, but they accumulated in clusters at the cell surface in the presence of MRC1. HIV-1 could counteract this action by transcriptionally silencing MRC1 mRNA [619]. Moreover, Vigerust and colleagues showed that MRC1 surface expression was reduced by 50% in the presence of the viral protein Nef [620], corroborating previous work that had shown reduced expression and functioning of MRC1 in alveolar macrophages of HIV-1 infected patients.

Altogether, the different studies elucidating the implication of CLR in HIV-1 pathology seem to reveal a role for these receptors in the capture and transmission of the virus to uninfected target cells. However, their role *in vivo* and the modulation between CLR-mediated host protection or diversion remain to be clearly established.

ii. *Sialic acid-binding immunoglobulin-type lectin: Siglec-1*

Siglec-1 (also known as sialoadhesin or CD169) is a transmembrane lectin receptor whose expression is IFN-I-dependent and restricted to myeloid cells. It belongs to the Siglec family of sialic acid-binding immunoglobulin-like lectins that represents a subset of immunoglobulin (Ig) superfamily molecules. Siglecs exploit the huge diversity of glycans structure to fulfill their functions, which is mediated by their amino-terminal V-set immunoglobulin domain that binds to sialic acids present at the surface of most mammalian cells [822]. Generally, Siglecs molecules display a low affinity for sialic acid N-acetylneuraminic acids bound in α 2-3 and α 2-6 linkage to galactose, and different Siglecs have overlapping specificity for such sialosides. However, each Siglec presents a given specificity profile to different sialic acid structures. In the case of Siglec-1, the preferred ligands are 5-N acetylated-neuraminic acids linked in α 2-3 to preceding carbohydrates [823]. Considering that the local concentrations of sialic acid are high on immune cell surface, Siglecs interactions with their preferred ligands can be masked by low affinity liaisons to conceal sialic acid in *cis* interactions, which usually dominate over *trans* interaction [822]. Yet, high-affinity ligand for a given Siglec can outcompete these interactions, resulting in a dynamic equilibrium of *cis* and *trans* interactions where the receptor and its ligand can be redistributed and concentrated at the site of interaction [824]. Siglec-1 might be the exception to this observation due to its specific structure. Indeed, its large extracellular domain, composed of 17 Ig-like domains, renders it taller than the cell glycocalyx (layer of glycolipids and proteins expressed at the cell membrane), and allows it to bind to its ligand both in *cis* and *trans* [621], [622]. In addition to its unique extracellular domain length, Siglec-1 displays a short cytoplasmic tail, poorly conserved compared to other Siglecs in most species, except the pig. Moreover, the C-terminal domain of the lectin has no identified signaling motif or phosphorylation site, suggesting that the primary function of the molecule could

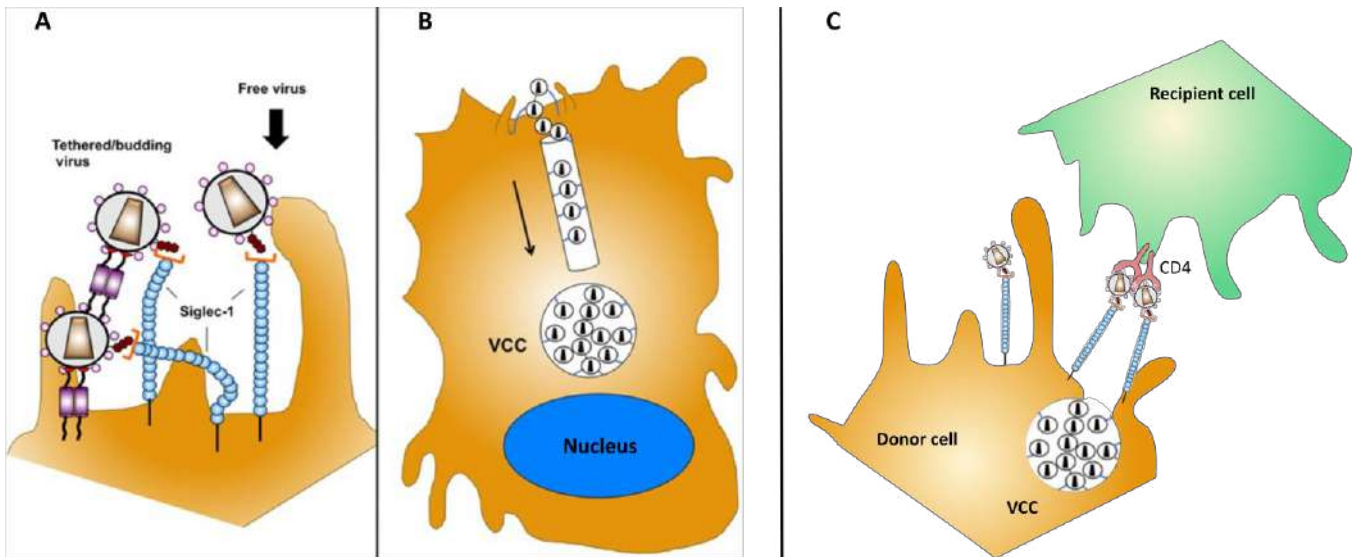


Figure 26: Siglec-1 captures, internalizes particles in virus-containing compartments, and transfers HIV-1 from myeloid cell to T cells (adapted from [630]).

A | Siglec-1, composed of 17 Ig-like domains as an extra-cellular part, a neutral intramembrane domain and a short cytoplasmic tail lacking any signalling motive or phosphorylation site, binds to GM3 gangliosides present at the viral envelope. Tetherin retains budding virion to the cell membrane. Tethered virions, just like cell-free virion, can bind to Siglec-1 molecules.

B | Following capture by Siglec-1, HIV-1 virions are internalized and co-transported with Siglec-1 to the VCC. They will be retained and protected in this compartment.

C | When the HIV-1-containing cell meets another target cell, the viral particles contained in the VCC and bound to Siglec-1 are transported back to the cell surface, where they become accessible to uninfected cell. Siglec-1-bound viruses can be concentrated to the contact zone, therefore Siglec-1 enhances viral cell-to-cell transfer.

be more related to cell-cell and cell-extracellular matrix interactions, rather than in cell signaling, however, it could still have a signaling function through recruitment of co-receptors [825].

Originally, Siglec-1 was reported in mice as a marker of a subpopulation of macrophages able to bind to red blood cells found in the lymph node, liver, and spleen [623]. In primates, Siglec-1⁺ macrophages were found between the red pulp and the marginal zone of the spleen, close to the blood circulation [823]. To date, the function of Siglec-1⁺ macrophages remains under investigation, but their role in regulating the immune system and maintenance of immune tolerance has been reported [624], [625]. For example, some evidence indicates that the close proximity of splenic Siglec-1⁺ macrophages with the circulation is necessary for Siglec-1 physiological functions. This specific location allows the capture of circulating microbial antigens, along with antigen loaded-exosomes [627] in the blood stream and favors the activation of the appropriate immune response through antigen presentation. In fact, Siglec-1⁺ macrophages appeared to be able to cross-present MHC-I and MHC-II loaded with antigenic peptides to CD4⁺ and CD8⁺ T cells, a function normally restricted to DC, and allowing for the establishment of adaptive immune responses [823]. The development of the Siglec-1^{-/-} mouse model has proved to be extremely useful to study Siglec-1 functions *in vivo*. Indeed, Siglec-1^{-/-} mice exhibit decreased levels of soluble IgM, along with B cells and CD8⁺ T cells subtle alterations, supporting the importance of Siglec-1 in priming adaptive immune responses, and likely in vaccine responses [826]. Yet, in autoimmune disease models of experimental allergic encephalitis, or in uveoretinitis, mice knocked-out for Siglec-1 had a reduced disease, characterized by a higher number of regulatory T cells in the CNS or the eye, along with a reduced proliferation of CD4⁺ inflammatory T cells [827], [828], providing the first evidence that Siglec-1 directly modulates T cell behavior *in vivo*. It is also likely that the function of Siglec-1⁺ cells is dependent upon their anatomic localization [626]. In addition to antigen presentation and induction of the appropriate inflammatory responses, it is thought that Siglec-1 may be a phagocytic receptor to clear sialylated pathogens. Moreover, the phagocytic function of Siglec-1⁺ macrophages could be responsible for the induction of tolerance through phagocytosis of debris in the marginal zone [826].

Several studies have reported the ability of Siglec-1 to bind pathogens, and more particularly viruses such as vaccinia, ebola [628] and vesicular stomatitis virus [626]. In fact, above 20 pathogens are known to have evolved to synthesize and/or capture sialic acids from their host and to incorporate them into their own glycoconjugates. This evolution appears to be key in microbial survival in their mammalian host, as they could be seen as molecular mimics of the host cell surface, preventing pathogen clearance mediated by immune responses [829]. For example, Sewald and colleagues pursued an *in vivo* study in mice to evaluate the ability of Siglec-1 to capture retroviruses and transfer them to their target cells. They were able to demonstrate that murine leukemia virus is captured by sinus Siglec-1⁺ macrophages in secondary lymphoid organs, and transferred to B-1 cells, thus enabling viral spread. Using BLT-humanized mice, they also found that HIV-1 was captured in the spleen, indicating a potential role of Siglec-1 in HIV-1 pathology [629]. In fact, Siglec-1 is upregulated in monocytes of HIV-1 infected patients, but its expression is reversed to basal level after successful cART [631]. *In vitro* experiments have shown that HIV-1 binds to Siglec-1 expressing macrophages with high affinity, resulting in the majority of macrophages being infected by the virus [632]. In mature DC, enhanced Siglec-1 expression allows HIV-1 particle capture, independently of the viral envelope, and has been shown to be responsible for *trans*-infection of CD4⁺ T cells [633]. Indeed, Siglec-1 binds the ganglioside, GM3, expressed in abundance on HIV-1 particles, and acquired when budding from the infected cell. Akiyama

and colleagues found that upon capture Siglec-1-bound HIV-1 particles are stored and protected from degradation in Siglec-1-induced VCC. These virions were then able to *trans*-infect recipient CD4⁺ T cells (Figure 26) [634]. In an elegant study, Pino and colleagues compared the ability of myeloid cells to capture and transfer HIV-1. They found that both DC and macrophages expressed Siglec-1 at higher levels than monocytes, and they were able to bind similarly to HIV-1 particles. Similar to Akiyama and colleagues, they observed that Siglec-1-bound HIV-1 particles were internalized in intracellular compartments, and were able to *trans*-infect CD4⁺ T cells. Interestingly, the capture, internalization, and transfer of HIV-1 was abrogated in all myeloid populations upon Siglec-1 inhibition [635]. In isolated monocytes from HIV-1 infected patients, which expressed high levels of Siglec-1, HIV-1 was captured and efficiently transferred to CD4⁺ T cells. However, these events were reversed after successful cART [635], further supporting the importance of Siglec-1 in HIV-1 capture and cell-to-cell transfer.

b. The virological synapse

To date, formation of the so-called “virological synapse” is the cell-to-cell transfer mechanism most widely described. This structure was first defined between T cells, by the group of Quentin Sattentau, as a “cytoskeleton-dependent, stable adhesive junction, across which virus is transmitted by directed transfer” [636]. It is initiated upon established contact between a HIV-1 infected and non-infected T cell, a process dependent on the viral tropism, or in other words, dependent on the viral envelope. This interaction induces the recruitment of the HIV-1 envelope and core proteins on the infected cell, and CD4 and co-receptors, CXCR4 and CCR5, on the uninfected cell at the site of contact [637], [638]. The structure is then stabilized by the enrichment of adhesion molecules at the contact zone, including LFA-1, ICAM-1, and ICAM-3 [639], and requires intact lipid-rafts to be secured. Indeed, cholesterol depletion in the infected cell abolishes the viral protein clusters and prevents the assembly of the virological synapse and HIV-1 transfer [640]. Along with both host and viral protein clusterization, remodeling of the actin cytoskeleton, and reorganization of the microtubule organizing center are required in both donor and recipient cells to allow the viral transfer [641]. This allows the polarization of the site of virus assembly and budding at the contact zone, resulting in the rapid, highly efficient, and consequent infection of the target cell [642], [643].

Some studies have reported that infected DC and macrophages are able to infect T cells through a virological synapse-like structure [644], [645]. Yet, the mechanisms involved in the formation of these virological synapses are not completely characterized. Macrophage/T cell virological synapses present similarities with T/T cell synapses, for example, as they involve the rapid recruitment of macrophage VCC to the contact site [532], the enrichment of CD4, CCR5, Gag, and Env, and are stabilized by LFA-1 and ICAM-1 [573], [646]. However, it appears that viral gp120 is not necessary to form the virological synapse between macrophages and T cells, and that the multiplicity of HIV-1 transferred from macrophages is much higher than in T/T cell synapses. This structure also protects HIV-1 from reverse transcriptase inhibitors and neutralizing antibodies [532], [646]. In light of the differences observed between the varying T cells virological synapses, the possibility that macrophages can be infected through virological synapse transfer from infected T cells, DC or even macrophages is

not to be excluded. However, to the best of our knowledge, such structures have not yet been described.

c. Phagocytosis of infected T-cells by macrophages

One of the main functions of macrophages is to maintain tissue homeostasis, notably through recognition and engulfment of apoptotic cells *via* a process called efferocytosis [647]. In infection settings, this function is essential in the elimination of pathogen-infected cells, although certain pathogens are able to escape this killing and succeed to infect macrophages [648]. As discussed earlier, HIV-1 infection of CD4⁺ T cells induces high degrees of apoptotic cell death as well as that of bystander T cells. *In vitro*, only one study so far has evaluated the possibility that macrophages can become infected by HIV-1 after the engulfment of apoptotic infected-T cells. The team of Sattentau reported that macrophages selectively capture and phagocytose infected CD4⁺ T cells, regardless of their activation status. This process was found to be independent from HIV-1 entry receptors and co-receptors, and therefore distinct from virological synapse formation. However, this process was strongly dependent on the modulation of the actin cytoskeleton, concordant with the phagocytic process. Subsequently, macrophages were productively infected, especially when CCR5-tropic strains were used [649]. It is likely that this mechanism of macrophage infection exists *in vivo*. Indeed, in Asian Macaques and African Green Monkeys, both viral DNA and TCR γ/δ^{30} DNA (specific material of T cells) were detected in macrophages isolated from tissues where CD4⁺ T cells were not highly depleted, suggesting that phagocytosis of SIV-infected CD4⁺ T cells had occurred [650]. Histological observations reported by Orenstein and colleagues indicates the presence of p24⁺ cellular debris within the cytoplasm of paracortical macrophages in the lymphoid organs of HIV-1 infected patients, which results in a positive hybridization of HIV-1 RNA in macrophages, suggesting that these cells phagocytose viral particles from infected cells, and possibly become infected themselves [651]. Finally, in HIV-1 infected patients under cART for three years, DiNapoli and colleagues found viral DNA and TCR³¹ DNA in alveolar macrophages, further supporting the existence of this infection mechanism in the lung *in vivo* [652].

d. HIV-1-induced cell fusion mechanisms

Early after the discovery of HIV-1, MGC were found in several organs of HIV-1 infected individuals, most notably in the brain, lymph nodes, spleen and lungs [653]–[655], adding HIV-1 into the fusogenic viruses category. In 1986, Gartner and colleagues showed for the first time that HIV-1 infection of macrophages led to cell-to-cell fusion. Using infected monocyte-derived macrophages *in vitro*, from the healthy donor blood, bone marrow or cord blood, they showed that these cells produced large amounts of virus that persisted for at least 40 days, and in these cultures, MGC were frequently observed [495]. This observation led to the hypothesis that cell-cell fusion between infected

³⁰ TCR γ/δ : T cell receptor containing the γ and δ chains instead of α and β chains and expressed by a subtype of T cells.

³¹ TCR: T cell receptor recognizes fragments of antigen as peptides bound to major histocompatibility complex (MHC) molecules.

cells and non-infected cells could be an indirect mechanism for HIV-1 to infect new target cells. Early studies performed with T cells reported the formation of T cell giant syncytia, 5–100 times bigger than individual cells [656]. The fusion process was mediated by actin cytoskeleton rearrangements and depended upon the interaction between the viral envelope glycoproteins, expressed at the cell surface of infected cells, and the CD4 receptor, expressed by target cells [657]–[659]. Of note, it has been observed that HIV-1 infected individuals have small T-cell syncytia in their lymph node, containing no more than five nuclei [651]. More recent studies performed with HIV-1-infected humanized mouse models also reported the presence of motile infected syncytia in lymph nodes, smaller than those observed *in vitro* [660]. While T-cell syncytia are very rare *in vivo*, the fusion with infected macrophages is considered dominant [661]. Yet, the majority of infected MGC found in brains of patient, for example, may be bigger than the reported *in vivo* T cell syncytia, and display phagocytic properties, arguing that they derive from myeloid origins, particularly from macrophages. The cellular and molecular mechanisms related to their formation remain, to date, poorly understood. In my team, we aimed to elucidate the mechanisms that triggered macrophage-to-macrophage fusion upon HIV-1 infection. My PhD adviser demonstrated that the viral protein Nef, by modulating p61Hck, is responsible for macrophages fusion, due to the depletion of Nef from the viral genome or the blocking p61Hck reducing the number of MGC in culture [319]. Since CD4⁺ T cells are the main cell target for HIV-1, an interesting question is whether macrophages could become infected through heterotypic fusion between infected T cells and non-infected macrophages. This was assessed by the laboratory of S. Bénichou, who recently reported that formation of HIV-1 infected MGC occur in a 2-step fusion process, leading to productive cell-to-cell viral transfer. The initial contact between the infected T cells and the recipient macrophages was found to be necessary for efficient viral transfer and cell fusion. It was also dependent on the viral envelope glycoproteins. Subsequently, the heterocaryon acquired the ability to fuse with surrounding uninfected macrophages, leading to MGC formation in a short timeframe [592]. During my Masters' degree, I was able to show that the same mechanism occurs between infected CD4⁺ T cells and osteoclasts [323]. In our previous study, we also demonstrated that osteoclast infection was much more rapid and efficient through cell-to-cell transfer, while infection increased their size and nuclei numbers while also exacerbating their bone-degradation function in a Nef-dependent manner (Annex 3, [323]).

Altogether, these studies suggest that cell-to-cell transfer of HIV-1 can occur *via* cell-cell fusion, an efficient infection mechanism allowing the formation of long-lived infected macrophage-derived MGC that sustain viral replication and disseminate the infection in several organs of HIV-1 infected individuals.

e. Tunneling nanotubes: bridges for HIV-1 spread

Tunneling nanotubes (TNT) are a novel type of cell-to-cell communication machinery, allowing distant cells to exchange information on their environment's perturbations. They were first discovered in 2004 by Rustom and colleagues, who identified these transient actin-rich structures in rat kidney cells and human cell lines [662]. Since then, numerous cells have been reported to form TNT in cultures *in vitro*, including neuronal cells, astrocytes, and immune cells [663]. TNT are defined as F-actin rich structures connecting at least two cells without touching the substrate. At steady state, about 10% of cultured cells form TNT [664]. Two types of TNT have been reported in macrophages: thin TNT (or

short, with a diameter of less than 0.7 μm) which contain only F-actin, and thick (or long TNT with a diameter above 0.7 μm) that contain both F-actin and microtubules [534], [665]. Their principal function is to transfer cellular materials and signals (*e.g.* lysosomes, big proteins, and mitochondria by thick TNT; calcium flux and soluble factors including cytokines by thin TNT) [662]. In the TNT scientific community, it is commonly thought that these structures can, and are hijacked by pathogens, specifically HIV-1, which I will briefly introduce since it was the subject of a review I co-wrote and is presented hereafter [666].

Eugenin and colleagues were the first to report that HIV-1 infection of macrophages led to increased number of TNT without altering their length. They reported that short TNT likely transported single HIV-1 particles, while long TNT carried larger HIV-1 containing vesicles (maybe exosomes or VCC) either inside or outside the structure; a theme that could not be precisely determined [534]. In a recent study, connexin 43, a component of the gap junction, accumulated in intracellular compartments that localized both at the base and tip of the TNT formed from the infected cell. HIV-1-infected macrophages formed TNT that allowed gap junction communication between distant cells. Blocking these gap junctions resulted in inhibition of TNT formation and decreased HIV-1 spread in culture [667], supporting the important roles of both TNT and the gap junctions in HIV-1 cell-to-cell transfer. HIV-1 spread was also reported to happen between T cells [668]. Hashimoto and colleagues identified the viral protein Nef as a critical inducer of HIV-1-mediated TNT, through its interaction with the ubiquitous M-sec³² protein, an important molecular factor in TNT biology [669]. M-sec complexation with protein members of the exocyst complex have been shown to be part of the TNT formation mechanism [670]. Using tandem mass spectrometry performed in the Jurkat cell line, Nef was found to interact with five components of the exocyst complex. Depletion of one of these interactions led to a reduction in the number of TNT between the Jurkat cells [671]. Finally, a recent study reported the ability of Nef to induce TNT formation in infected macrophages in a myosin 10-dependent manner. It was described that Nef alone was transported from macrophages to T cells *via* TNT, a process that resulted in a decrease of CD4 expression in recipient T cells [672].

Taken together, these studies indicate that HIV-1, mainly through Nef-dependent interactions with host proteins, hijacks physiological structures to ensure its spread in the host, as well as a way to evade detection by the immune system and drug toxicity. Considering TNT as a potential target to inhibit viruses intercellular transport could be an interesting strategy to develop the next generation of HIV-1 treatment.

³² **M-sec:** 73 kDa cytosolic protein also known as TNF α -induced protein 2 that displays a central role in the formation of cell protrusions.



Tunneling Nanotubes: Intimate Communication between Myeloid Cells

Maeva Dupont^{1,2†}, Shanti Souriant^{1,2†}, Geanncarlo Lugo-Villarino^{1,2},
Isabelle Maridonneau-Parini^{1,2*} and Christel Vérollet^{1,2*}

¹ Institut de Pharmacologie et de Biologie Structurale, Université de Toulouse, CNRS, Université Toulouse III Paul Sabatier, Toulouse, France, ² Research Program “IM-TB/HIV” (1167), International Associated Laboratory (LIA), CNRS, Toulouse, France

OPEN ACCESS

Edited by:

Christoph Hölscher,
Forschungszentrum Borstel (LG),
Germany

Reviewed by:

Christian Bogdan,
University of Erlangen-
Nuremberg, Germany
Mario M. D’Elios,
University of Florence, Italy

*Correspondence:

Isabelle Maridonneau-Parini
maridono@ipbs.fr;
Christel Vérollet
verollet@ipbs.fr

[†]These authors have contributed
equally to this work.

Specialty section:

This article was submitted
to Microbial Immunology,
a section of the journal
Frontiers in Immunology

Received: 17 October 2017

Accepted: 08 January 2018

Published: 25 January 2018

Citation:

Dupont M, Souriant S, Lugo-
Villarino G, Maridonneau-Parini I and
Vérollet C (2018) Tunneling
Nanotubes: Intimate
Communication between
Myeloid Cells.
Front. Immunol. 9:43.
doi: 10.3389/fimmu.2018.00043

Tunneling nanotubes (TNT) are dynamic connections between cells, which represent a novel route for cell-to-cell communication. A growing body of evidence points TNT towards a role for intercellular exchanges of signals, molecules, organelles, and pathogens, involving them in a diverse array of functions. TNT form among several cell types, including neuronal cells, epithelial cells, and almost all immune cells. In myeloid cells (e.g., macrophages, dendritic cells, and osteoclasts), intercellular communication *via* TNT contributes to their differentiation and immune functions. Importantly, TNT enable myeloid cells to communicate with a targeted neighboring or distant cell, as well as with other cell types, therefore creating a complex variety of cellular exchanges. TNT also contribute to pathogen spread as they serve as “corridors” from a cell to another. Herein, we addressed the complexity of the definition and *in vitro* characterization of TNT in innate immune cells, the different processes involved in their formation, and their relevance *in vivo*. We also assess our current understanding of how TNT participate in immune surveillance and the spread of pathogens, with a particular interest for HIV-1. Overall, despite recent progress in this growing research field, we highlight that further investigation is needed to better unveil the role of TNT in both physiological and pathological conditions.

Keywords: tunneling nanotubes, myeloid cells, innate immunity, pathogens, HIV-1

INTRODUCTION

Tunneling nanotubes (TNT) represent a novel type of intercellular communication machinery, which differs from the secretion of signaling molecules and the signal transmission through gap or synaptic junctions between adjacent cells. Along with exosomes, TNT mediate long-range communication, independent of soluble factors. They are membranous structures displaying a remarkable capacity to communicate with selected neighbor or distant cells. There are recent reviews covering the broad biological role of TNT, which are able to form in multiple cell types (1–3). Here, our focus is exclusively on TNT formed by myeloid cells, including macrophages, osteoclasts, and dendritic cells (DC). Based on the nascent literature on TNT in these cells, we will discuss the definition of TNT, their mechanisms of formation, and their role in physiological and pathological contexts. We will also address the need of further investigation of these structures to better understand their

functions and improve their potential as therapeutic targets in pathological conditions.

DEFINITION AND FUNCTION OF TNT

The main obstacle in reviewing the emerging TNT field is the different names given to these structures: TNT, cellular and membrane nanotubes, filopodia bridges, conduits or tubes, and nanotubules. Also, the huge number of publications on carbon nanotubes impedes the track of developments on TNT. Unifying terminology for nanotubes would thus be beneficial. In this mini-review, the term TNT will be used as done previously (2, 4). TNT are membranous channels connecting two or more cells over short to long distances. Actually, these structures can extend up to 200 μm in length in macrophages (5). To define TNT, we adopted the three phenotypic criteria proposed in a recent elegant review: (i) they connect at least two cells, (ii) they contain F-actin, and (iii) they do not touch the substrate (2). This definition allows the discrimination of TNT with any other F-actin-rich structures, such as filopodia. Regarding their functional properties, TNT transfer cytoplasmic molecules from one cell to another such as calcium, proteins or miRNA, mitochondria, several vesicles (e.g., lysosomes), pathogens, and cell-surface molecules; this ability constitutes the main functional criterion for TNT definition (6). The end of the structure can form a junctional border with the targeted cell (close-ended TNT) or the cytoplasm of the two connected cells can be mixed (open-ended TNT). On the one hand, the transfer of large molecules such as the lipophilic dye DiO is used to identify open-ended TNT (7). On the other hand, close-ended TNT form a junction at their end which are visualized by scanning electron microscopy (8). To avoid the past arguments on the need of cytoplasmic interactions for TNT, we shall consider in this review both close-ended and open-ended TNT (**Figure 1A**). As close-ended TNT mediate signal transfer through distant gap junctions (8, 9), they meet the functional criterion to be considered as TNT. Also, close-ended TNT could represent an intermediary status in the process of open-ended TNT formation. Finally, the group of Davis demonstrated that one particularity of macrophages is their ability to form different classes of TNT: thin ones (<0.7 μm in diameter), containing only F-actin; and thick ones (>0.7 μm), containing F-actin and microtubules (7). These two types of TNT could have different functions, as large material (e.g., lysosomes, mitochondria) can only travel between macrophages *via* thick TNT on microtubules (7).

DISCOVERY OF TNT

The first description of functional TNT *in vitro* was made in rat kidney cells (PC12 cells) and human cell lines (10), followed immediately by the identification of similar structures in human monocytes and macrophages (11). It is now clear that TNT can form in several cell types, including cancer cells and most leukocytes. However, to our knowledge, TNT were not described in granulocytes. In DC, TNT appeared to be similar to those made by monocytes-derived macrophages (6, 12). However, unlike DC exposed to anti-inflammatory conditions, only those activated by pro-inflammatory conditions form complex network of TNT

able to transfer soluble molecules and pathogens (13). Likewise, macrophages undergo different activation programs within the broad spectrum of pro- (M1) and anti-inflammatory (M2) polarization. Yet, their activation state has not been linked to the formation of TNT. The only available data concern the early HIV-1 infection of macrophages, driving them toward M1 polarization (14) and inducing a significant increase in TNT formation (5, 15–18).

While the majority of studies in TNT biology has been performed in one cell type (homotypic TNT) at a time, TNT formation between different cell types (heterotypic TNT) is not rare. In fact, TNT frequently form between macrophages or DC with another cell type, enabling the exchange of lysosomes, mitochondria, or viral proteins (16, 19–21).

The reason why TNT were discovered quite recently could be attributed to their fragility. Indeed, they are poorly resistant to the existing shearing forces in culture media, as well as light exposure and classical fixation methods. Thus, an appropriate way of performing live imaging is necessary to study TNT. When working on fixed cells, gentle fixation (e.g., glutaraldehyde-based fixation) should help preserve these highly delicate structures (22, 23).

FORMATION OF TNT

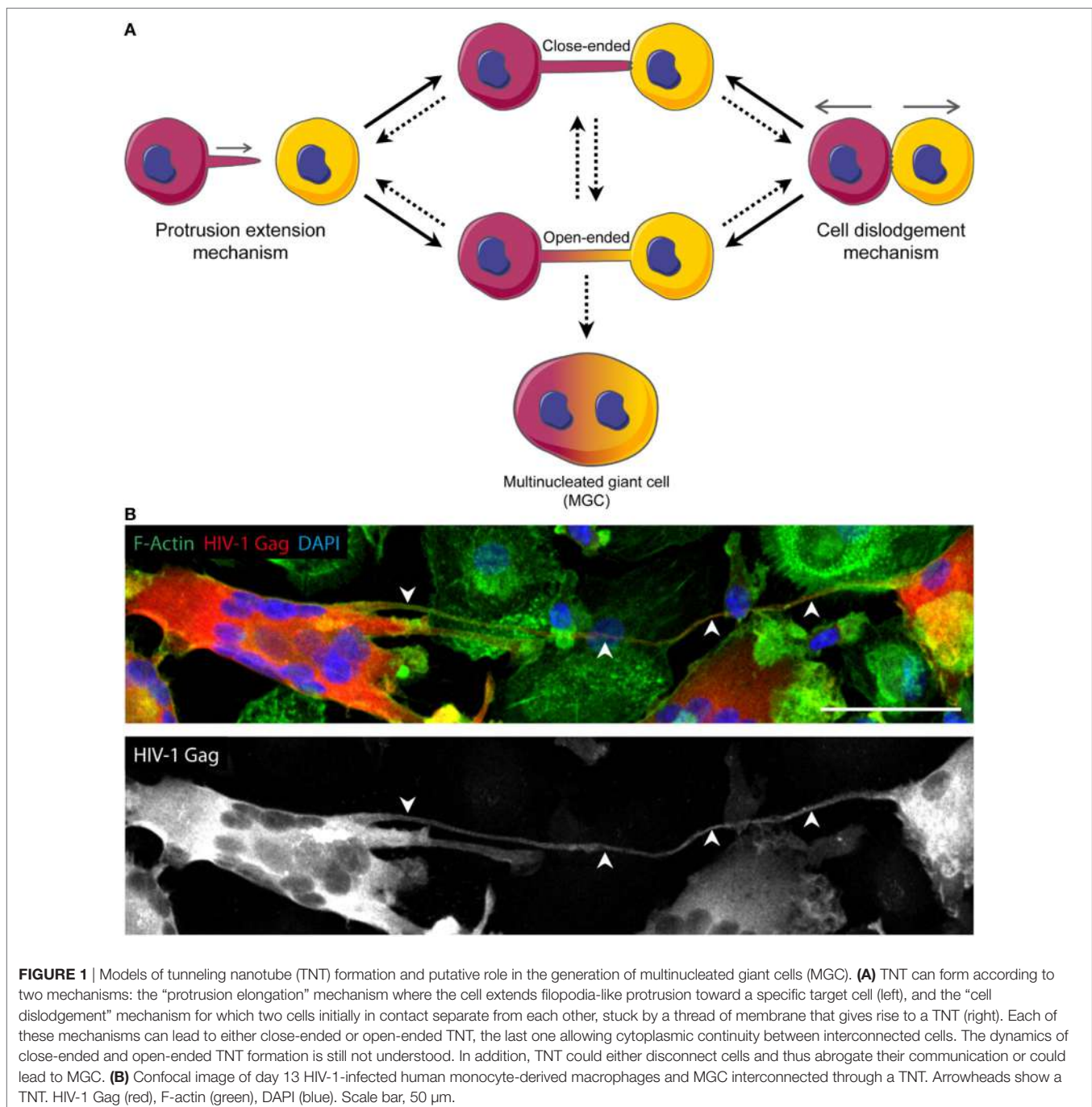
Mechanisms of Formation

Cell examination by time-lapse microscopy suggested two mechanisms of TNT formation could exist. The first one proposes that two cells initially in contact separate from each other, remaining connected through a thin thread of membrane, which will be elongated upon cell separation (**Figure 1A**, right). The second puts forward that a cell would first bulge filopodia and extend them until reaching a neighboring cell, then converting towards TNT after making contact (24, 25) (**Figure 1A**, left). While the former is the prevailing mechanism in lymphoid cells, the latter one is observed in DC as TNT were reported to develop mainly from conversion of their filopodia (13, 19). In the case of macrophages, while they can use both mechanisms (6), the murine macrophage cell line (RAW 264.7 cells) mainly forms TNT from actin-driven protrusions, also called TNT-precursors (26). Of note, these two processes are not necessarily exclusive and could both occur between a given pair of cells. In either case, the requirement of F-actin is not questioned since treatment with latrunculin or cytochalasin D is often used to abolish TNT formation (2, 27, 28).

Regarding the opening of the conduit, and the potential transition between close-ended and open-ended TNT (**Figure 1A**), there is no proposed mechanism available. It is likely that the formation of open-ended TNT involves a step similar to what occurs during virus-to-cell membrane fusion or cell-to-cell fusion (29, 30), eventually leading to the generation of multinucleated giant cells (MGC) (**Figure 1A**).

Molecular Actors

Few data are available to describe TNT at the molecular level. M-Sec, also known as tumor necrosis factor- α -induced protein, is one of the best characterized protein involved in TNT formation



in macrophages. Its depletion in Raw264.7 cells reduces the formation of *de novo* TNT and their associated function (transfer of calcium flux) (22). Using the same macrophage cell line, the group of D. Cox recently showed that actin polymerization factors including the Rho GTPases family Rac1 and Cdc42, and their downstream effectors WAVE and WASP, participate in TNT formation (26). In addition, functional TNT are induced by the expression of the leukocyte specific transcript 1 (LST1) protein in HeLa and HEK cell lines. LST1 recruits the actin cross-linking protein filamin and the small GTPase RalA to the

plasma membrane where it promotes RalA interaction with the exocyst complex, M-Sec, and myosin; these interactions trigger TNT formation (22, 23). Whether the mechanisms that operate in cell lines derived often from tumor origin apply to primary cells remains to be confirmed.

IN VIVO RELEVANCE OF TNT

A remaining question is to determine to what extent the *in vitro* data available in the literature are relevant *in vivo*. One of the

problems is to apply *in vivo* the criteria of *bona fide* TNT (see above), in particular the requirement not to touch the substrate, which seems unlikely in 3D environments. In addition, testing the functionality of TNT in the context of tissues is challenging. Therefore, the structures observed *in vivo* should be carefully indicated as “TNT-like structures.” Key evidence for TNT-like structures *in vivo* comes from the immunology field providing the first images of thick TNT connecting DC in inflamed mouse corneas (31). To our knowledge, macrophage TNT have not been observed *in vivo* yet. The identification of specific molecular markers for TNT would be a great tool to confirm the existence of these structures *in vivo*. M-Sec, which is involved in TNT formation, cannot be considered as a specific marker since this ubiquitous protein is expressed all over the cytoplasm (5, 18, 28, 32, 33). Thus, one of the priority to progress in the TNT field is to characterize markers allowing unambiguous identification of cell-to-cell tubular connections as TNT.

ROLE OF TNT IN PHYSIOLOGICAL CONTEXTS

One of the most studied functions of TNT is the propagation of calcium flux. Calcium signaling through TNT helps regulate cell metabolism and communication between neurons (34). Interestingly, DC present the ability to establish calcium fluxes *via* TNT transmitted within seconds to other DC as far as 500 μm away from the donor cell (12). When TNT are disturbed by M-Sec knockdown, this calcium flux is inhibited (12, 22). DC have also the particularity to form TNT networks allowing the intercellular exchange of antigens (13), including in the context of MHC molecules as described between Hela cells (19, 27). Therefore, TNT could contribute to a higher efficiency in the antigen presentation process to activate adaptive immunity (19).

Another physiological role for TNT concerns the differentiation of osteoclasts (5, 18, 28, 32, 33). Osteoclasts are MGC derived from a myeloid precursor that present the unique ability to degrade the bone matrix, and thus to regulate bone homeostasis. Inhibition of TNT either by latrunculin B or by M-Sec depletion significantly suppresses osteoclastogenesis, and the M-Sec expression level increases during osteoclastogenesis (28, 35). Dendritic cell-specific transmembrane protein, a receptor involved in cell-to-cell fusion, has been shown to be transferred *via* TNT. The authors proposed that this process could participate in cell fusion among osteoclast precursors (28, 35). Moreover, nuclei are found inside large TNT-like structures (36), inferring that they participate in cell-cell fusion to generate OC. Elucidating the role of TNT in differentiation of MGC such as placental trophoblast, myotubes, and osteoclasts could be a new research area.

ROLE OF TNT IN PATHOLOGICAL CONTEXTS

Tunneling nanotubes not only contribute to cell-to-cell communication in physiological conditions but also in pathological processes. For example, the transfer of lysosomes from macrophages

to fibroblasts, and of mitochondria from mesenchymal stromal cells to macrophages, are mediated by TNT and have important consequences in cystinosis and acute respiratory distress syndrome, respectively (20, 21).

Without the shadow of doubt, the most studied consequence of TNT in diseases is the transfer of pathogens, including prions, bacteria, and viruses [for review, see Ref. (1)]. One of the well-known example concerns the role of TNT in neurological diseases, especially when caused by prions (34). Actually, in addition to the TNT-dependent transfer of the infectious form of the prion protein (PrP^{Sc}) between neuronal cells, TNT support PrP^{Sc} transfer from DC to the neurons in which PrP^{Sc} is further synthesized and transferred to the rest of the central nervous system (37). Regarding bacteria and viruses, some publications propose that they “surf” along TNT to spread from one cell to another (7, 13, 38–41). For example, in macrophages, live experiments show that *Mycobacterium bovis* bacillus Calmette–Guerin can travel along the surface of thin TNT, toward another macrophage, which will ingest it (7).

Viruses, including HIV-1, are well known to hijack the cytoskeleton in order to enter and travel inside their host cell, as well as towards bystander neighbor cells (5, 33, 39, 41, 42). For example, HIV-1 can actively induce the generation of filopodia in DC to propel virus particles towards neighboring cells. As one of the mechanism of TNT formation starts with membrane extension, filopodia formed upon HIV-1 infection could lead to TNT formation (2), especially in DC that develop networks of TNT from elongation of their dendrites (13, 19). Importantly, the formation of TNT by DC favors trans-infection of targeted CD4⁺ T lymphocytes at a relatively long distance, similar to what happens between two distant CD4⁺ T lymphocytes (8).

In macrophages, HIV-1 induces TNT formation and potentially uses them to spread (18). Whether thin or thick TNT are formed is unknown. Assuming that thick TNT are induced, HIV-1 could travel inside these structures by using a microtubule-dependent movement, in addition to the described “surfing” of HIV-1 at the surface of TNT. Despite the fact that Gag and Nef proteins and HIV-1-containing vesicles have been detected inside TNT, there are no convincing experiments in living cells available to prove that HIV-1 travels inside TNT and infects the targeted cell (5, 15, 17, 18). Pushing live imaging to super-resolution microscopy techniques would be of great help to study how HIV-1 traffics using TNT.

In light of the importance of macrophages in HIV-1 pathogenesis (43–45), it is crucial to bridge the several gaps that blur our understanding of the role of TNT in macrophages during HIV-1 infection. First, it is important to determine whether HIV-1-induced TNT in macrophages are close- or open-ended to better understand how HIV-1 traffics *via* TNT. Second, whether TNT from a HIV-infected cell could target non-infected cells remains to be elucidated. It would be an efficient way for the virus to spread around without being detected. Finally, the molecular regulation of HIV-1-induced TNT in macrophages has only started to be elucidated. The HIV-1 Nef protein could play a central role in TNT formation by interacting with members of the exocyst complex (16, 18, 46, 47). Moreover, Nef modulates F-actin and cell migration (48), two effects which could participate in TNT

generation. Finally, a hallmark of HIV-1 infection is the formation of MGC, a process that can be driven by TNT in order to persist during late infection stages, when most infected macrophages are MGC (**Figure 1B**) (32, 33). Interestingly, both HIV-1-induced TNT and MGC are reduced when macrophages are infected with *nef*-deleted viruses (18, 32, 33).

Importantly, while TNT spread the virus among HIV-1 target cells (T lymphocytes, macrophages, and DC), TNT also affects the nature of infection by circumventing the need for classical receptor-mediated virus entry or transfer viral components to cells that are not susceptible to infection. As a matter of fact, the transfer of Nef *via* TNT between infected macrophages and B cells induces drastic B cell abnormalities at the systemic and mucosal level (16).

CONCLUSION

The TNT field requires the unification of the terminology and definition of TNT, as well as the development of new tools adapted for the detection and monitoring of these particular structures. The main challenge so far is to discover molecular markers to specifically identify TNT, especially *in vivo*. To this end, an automated siRNA-based screen could be used in *in vitro* conditions for which TNT formation is controlled, as performed for the virological synapse (49). Another issue is the fragility of TNT which complicates their manipulation. Thus, the use of specific experimental conditions or devices, such as microfluidic systems (50), is needed. Moreover, it would be helpful to study the opening of close-ended TNT in terms of molecular components and dynamics. Likewise, it is imperative to determine whether TNT formation and regulation can be influenced by extracellular stimuli and/or tissue microenvironment in pertinent *in vivo* physiological and pathological contexts. For example, during HIV-1 infection, TNT represent a new way for viral spread.

REFERENCES

- Sisakhtnezhad S, Khosravi L. Emerging physiological and pathological implications of tunneling nanotubes formation between cells. *Eur J Cell Biol* (2015) 94:429–43. doi:10.1016/j.ejcb.2015.06.010
- McCoy-Simandle K, Hanna SJ, Cox D. Exosomes and nanotubes: control of immune cell communication. *Int J Biochem Cell Biol* (2016) 71:44–54. doi:10.1016/j.biocel.2015.12.006
- Zaccard CR, Rinaldo CR, Mailliard RB. Linked in: immunologic membrane nanotube networks. *J Leukoc Biol* (2016) 100:81–94. doi:10.1189/jlb.4VMR0915-395R
- Baker M. How the Internet of cells has biologists buzzing. *Nature* (2017) 549:322–4. doi:10.1038/549322a
- Eugenin EA, Gaskill PJ, Berman JW. Tunneling nanotubes (TNT) are induced by HIV-infection of macrophages: a potential mechanism for intercellular HIV trafficking. *Cell Immunol* (2009) 254:142–8. doi:10.1016/j.cellimm.2008.08.005
- Gerdes HH, Carvalho RN. Intercellular transfer mediated by tunneling nanotubes. *Curr Opin Cell Biol* (2008) 20:470–5. doi:10.1016/j.ccb.2008.03.005
- Onfelt B, Nedvetzki S, Benninger RK, Purbhoo MA, Sowinski S, Hume AN, et al. Structurally distinct membrane nanotubes between human macrophages support long-distance vesicular traffic or surfing of bacteria. *J Immunol* (2006) 177:8476–83. doi:10.4049/jimmunol.177.12.8476
- Sowinski S, Jolly C, Berninghausen O, Purbhoo MA, Chauveau A, Kohler K, et al. Membrane nanotubes physically connect T cells over long distances presenting a novel route for HIV-1 transmission. *Nat Cell Biol* (2008) 10:211–9. doi:10.1038/ncb1682
- Wang X, Veruki ML, Bukoreshltiev NV, Hartveit E, Gerdes HH. Animal cells connected by nanotubes can be electrically coupled through interposed gap-junction channels. *Proc Natl Acad Sci U S A* (2010) 107:17194–9. doi:10.1073/pnas.1006785107
- Rustom A, Saffrich R, Markovic I, Walther P, Gerdes HH. Nanotubular highways for intercellular organelle transport. *Science* (2004) 303:1007–10. doi:10.1126/science.1093133
- Onfelt B, Nedvetzki S, Yanagi K, Davis DM. Cutting edge: membrane nanotubes connect immune cells. *J Immunol* (2004) 173:1511–3. doi:10.4049/jimmunol.173.3.1511
- Watkins SC, Salter RD. Functional connectivity between immune cells mediated by tunneling nanotubes. *Immunity* (2005) 23:309–18. doi:10.1016/j.immuni.2005.08.009
- Zaccard CR, Watkins SC, Kalinski P, Fecek RJ, Yates AL, Salter RD, et al. CD40L induces functional tunneling nanotube networks exclusively in dendritic cells programmed by mediators of type 1 immunity. *J Immunol* (2015) 194:1047–56. doi:10.4049/jimmunol.1401832
- Lugo-Villarino G, Verollet C, Maridonneau-Parini I, Neyrolles O. Macrophage polarization: convergence point targeted by mycobacterium tuberculosis and HIV. *Front Immunol* (2011) 2:43. doi:10.3389/fimmu.2011.00043
- Kadiu I, Ricardo-Dukelow M, Ciborowski P, Gendelman HE. Cytoskeletal protein transformation in HIV-1-infected macrophage giant cells. *J Immunol* (2007) 178:6404–15. doi:10.4049/jimmunol.178.10.6404

16. Xu W, Santini PA, Sullivan JS, He B, Shan M, Ball SC, et al. HIV-1 evades virus-specific IgG2 and IgA responses by targeting systemic and intestinal B cells via long-range intercellular conduits. *Nat Immunol* (2009) 10:1008–17. doi:10.1038/ni.1753
17. Kadiu I, Gendelman HE. Human immunodeficiency virus type 1 endocytic trafficking through macrophage bridging conduits facilitates spread of infection. *J Neuroimmune Pharmacol* (2011) 6:658–75. doi:10.1007/s11481-011-9298-z
18. Hashimoto M, Bhuyan F, Hiyoshi M, Noyori O, Nasser H, Miyazaki M, et al. Potential role of the formation of tunneling nanotubes in HIV-1 spread in macrophages. *J Immunol* (2016) 196:1832–41. doi:10.4049/jimmunol.1500845
19. Campana S, De Pasquale C, Carrega P, Ferlazzo G, Bonaccorsi I. Cross-dressing: an alternative mechanism for antigen presentation. *Immunol Lett* (2015) 168:349–54. doi:10.1016/j.imlet.2015.11.002
20. Naphade S, Sharma J, Gaide Chevronnay HP, Shook MA, Yeagy BA, Rocca CJ, et al. Brief reports: lysosomal cross-correction by hematopoietic stem cell-derived macrophages via tunneling nanotubes. *Stem Cells* (2015) 33:301–9. doi:10.1002/stem.1835
21. Jackson MV, Morrison TJ, Doherty DF, Mcauley DF, Matthay MA, Kissenpfennig A, et al. Mitochondrial transfer via tunneling nanotubes is an important mechanism by which mesenchymal stem cells enhance macrophage phagocytosis in the in vitro and in vivo models of ARDS. *Stem Cells* (2016) 34:2210–23. doi:10.1002/stem.2372
22. Hase K, Kimura S, Takatsu H, Ohmae M, Kawano S, Kitamura H, et al. M-Sec promotes membrane nanotube formation by interacting with Ral and the exocyst complex. *Nat Cell Biol* (2009) 11:1427–32. doi:10.1038/ncb1990
23. Schiller C, Diakopoulos KN, Rohwedder I, Kremmer E, Von Toerne C, Ueffing M, et al. LST1 promotes the assembly of a molecular machinery responsible for tunneling nanotube formation. *J Cell Sci* (2013) 126:767–77. doi:10.1242/jcs.114033
24. Kimura S, Hase K, Ohno H. Tunneling nanotubes: emerging view of their molecular components and formation mechanisms. *Exp Cell Res* (2012) 318:1699–706. doi:10.1016/j.yexcr.2012.05.013
25. Gerdes HH, Rustom A, Wang X. Tunneling nanotubes, an emerging intercellular communication route in development. *Mech Dev* (2013) 130:381–7. doi:10.1016/j.mod.2012.11.006
26. Hanna SJ, Mccoy-Simandle K, Miskolci V, Guo P, Cammer M, Hodgson L, et al. The role of Rho-GTPases and actin polymerization during macrophage tunneling nanotube biogenesis. *Sci Rep* (2017) 7:8547. doi:10.1038/s41598-017-08950-7
27. Schiller C, Huber JE, Diakopoulos KN, Weiss EH. Tunneling nanotubes enable intercellular transfer of MHC class I molecules. *Hum Immunol* (2013) 74:412–6. doi:10.1016/j.humimm.2012.11.026
28. Takahashi A, Kukita A, Li YJ, Zhang JQ, Nomiya H, Yamaza T, et al. Tunneling nanotube formation is essential for the regulation of osteoclastogenesis. *J Cell Biochem* (2013) 114:1238–47. doi:10.1002/jcb.24433
29. Chen EH, Olson EN. Unveiling the mechanisms of cell-cell fusion. *Science* (2005) 308:369–73. doi:10.1126/science.1104799
30. Chen EH, Grote E, Mohler W, Vignery A. Cell-cell fusion. *FEBS Lett* (2007) 581:2181–93. doi:10.1016/j.febslet.2007.03.033
31. Chinnery HR, Pearlman E, Mcmenamin PG. Cutting edge: membrane nanotubes in vivo: a feature of MHC class II+ cells in the mouse cornea. *J Immunol* (2008) 180:5779–83. doi:10.4049/jimmunol.180.9.5779
32. Verollet C, Zhang YM, Le Cabec V, Mazzolini J, Charriere G, Labrousse A, et al. HIV-1 Nef triggers macrophage fusion in a p61Hck- and protease-dependent manner. *J Immunol* (2010) 184:7030–9. doi:10.4049/jimmunol.0903345
33. Verollet C, Souriant S, Bonnaud E, Jolicœur P, Raynaud-Messina B, Kinnaer C, et al. HIV-1 reprograms the migration of macrophages. *Blood* (2015) 125:1611–22. doi:10.1182/blood-2014-08-596775
34. Victoria GS, Zurzolo C. The spread of prion-like proteins by lysosomes and tunneling nanotubes: Implications for neurodegenerative diseases. *J Cell Biol* (2017) 216(9):2633–44. doi:10.1083/jcb.201701047
35. Kukita T, Takahashi A, Zhang JQ, Kukita A. Membrane nanotube formation in osteoclastogenesis. *Methods Mol Biol* (2015) 1313:193–202. doi:10.1007/978-1-4939-2703-6_14
36. Penanen P, Alanne MH, Fazeli E, Deguchi T, Nareoja T, Peltonen S, et al. Diversity of actin architecture in human osteoclasts: network of curved and branched actin supporting cell shape and intercellular micrometer-level tubes. *Mol Cell Biochem* (2017) 432:131–9. doi:10.1007/s11010-017-3004-2
37. Goussset K, Schiff E, Langevin C, Marijanovic Z, Caputo A, Browman DT, et al. Prions hijack tunnelling nanotubes for intercellular spread. *Nat Cell Biol* (2009) 11:328–36. doi:10.1038/ncb1841
38. Hope TJ. Bridging efficient viral infection. *Nat Cell Biol* (2007) 9:243–4. doi:10.1038/ncb0307-243
39. Sherer NM, Lehmann MJ, Jimenez-Soto LF, Horensavitz C, Pypaert M, Mothes W. Retroviruses can establish filopodial bridges for efficient cell-to-cell transmission. *Nat Cell Biol* (2007) 9:310–5. doi:10.1038/ncb1544
40. Davis DM, Sowinski S. Membrane nanotubes: dynamic long-distance connections between animal cells. *Nat Rev Mol Cell Biol* (2008) 9:431–6. doi:10.1038/nrm2399
41. Sherer NM, Mothes W. Cytonemes and tunneling nanotubules in cell-cell communication and viral pathogenesis. *Trends Cell Biol* (2008) 18:414–20. doi:10.1016/j.tcb.2008.07.003
42. Nikolic DS, Lehmann M, Felts R, Garcia E, Blanchet FP, Subramaniam S, et al. HIV-1 activates Cdc42 and induces membrane extensions in immature dendritic cells to facilitate cell-to-cell virus propagation. *Blood* (2011) 118:4841–52. doi:10.1182/blood-2010-09-305417
43. Honeycutt JB, Wahl A, Baker C, Spagnuolo RA, Foster J, Zakharova O, et al. Macrophages sustain HIV replication in vivo independently of T cells. *J Clin Invest* (2016) 126:1353–66. doi:10.1172/JCI84456
44. Sattentau QJ, Stevenson M. Macrophages and HIV-1: an unhealthy constellation. *Cell Host Microbe* (2016) 19:304–10. doi:10.1016/j.chom.2016.02.013
45. Honeycutt JB, Thayer WO, Baker CE, Ribeiro RM, Lada SM, Cao Y, et al. HIV persistence in tissue macrophages of humanized myeloid-only mice during antiretroviral therapy. *Nat Med* (2017) 23(5):638–43. doi:10.1038/nm.4319
46. Mukerji J, Olivieri KC, Misra V, Agopian KA, Gabuzda D. Proteomic analysis of HIV-1 Nef cellular binding partners reveals a role for exocyst complex proteins in mediating enhancement of intercellular nanotube formation. *Retrovirology* (2012) 9:33. doi:10.1186/1742-4690-9-33
47. Imle A, Abraham L, Tsopoulidis N, Hoflack B, Saksela K, Fackler OT. Association with PAK2 enables functional interactions of lentiviral Nef proteins with the exocyst complex. *MBio* (2015) 6:e1309–15. doi:10.1128/mBio.01309-15
48. Verollet C, Le Cabec V, Maridonneau-Parini I. HIV-1 infection of T lymphocytes and macrophages affects their migration via Nef. *Front Immunol* (2015) 6:514. doi:10.3389/fimmu.2015.00514
49. Menager MM, Littman DR. Actin dynamics regulates dendritic cell-mediated transfer of HIV-1 to T cells. *Cell* (2016) 164:695–709. doi:10.1016/j.cell.2015.12.036
50. Xiao M, Xu N, Wang C, Pang DW, Zhang ZL. Dynamic monitoring of membrane nanotubes formation induced by vaccinia virus on a high throughput microfluidic chip. *Sci Rep* (2017) 7:44835. doi:10.1038/srep44835

Conflict of Interest Statement: The authors declare that the research was conducted in the absence of any commercial or financial relationships that could be construed as a potential conflict of interest.

Copyright © 2018 Dupont, Souriant, Lugo-Villarino, Maridonneau-Parini and Verollet. This is an open-access article distributed under the terms of the Creative Commons Attribution License (CC BY). The use, distribution or reproduction in other forums is permitted, provided the original author(s) or licensor are credited and that the original publication in this journal is cited, in accordance with accepted academic practice. No use, distribution or reproduction is permitted which does not comply with these terms.

TIMELINE OF HIV AND TB

Tuberculosis (TB) is the leading cause of illness and death among people living with HIV. TB can be cured.

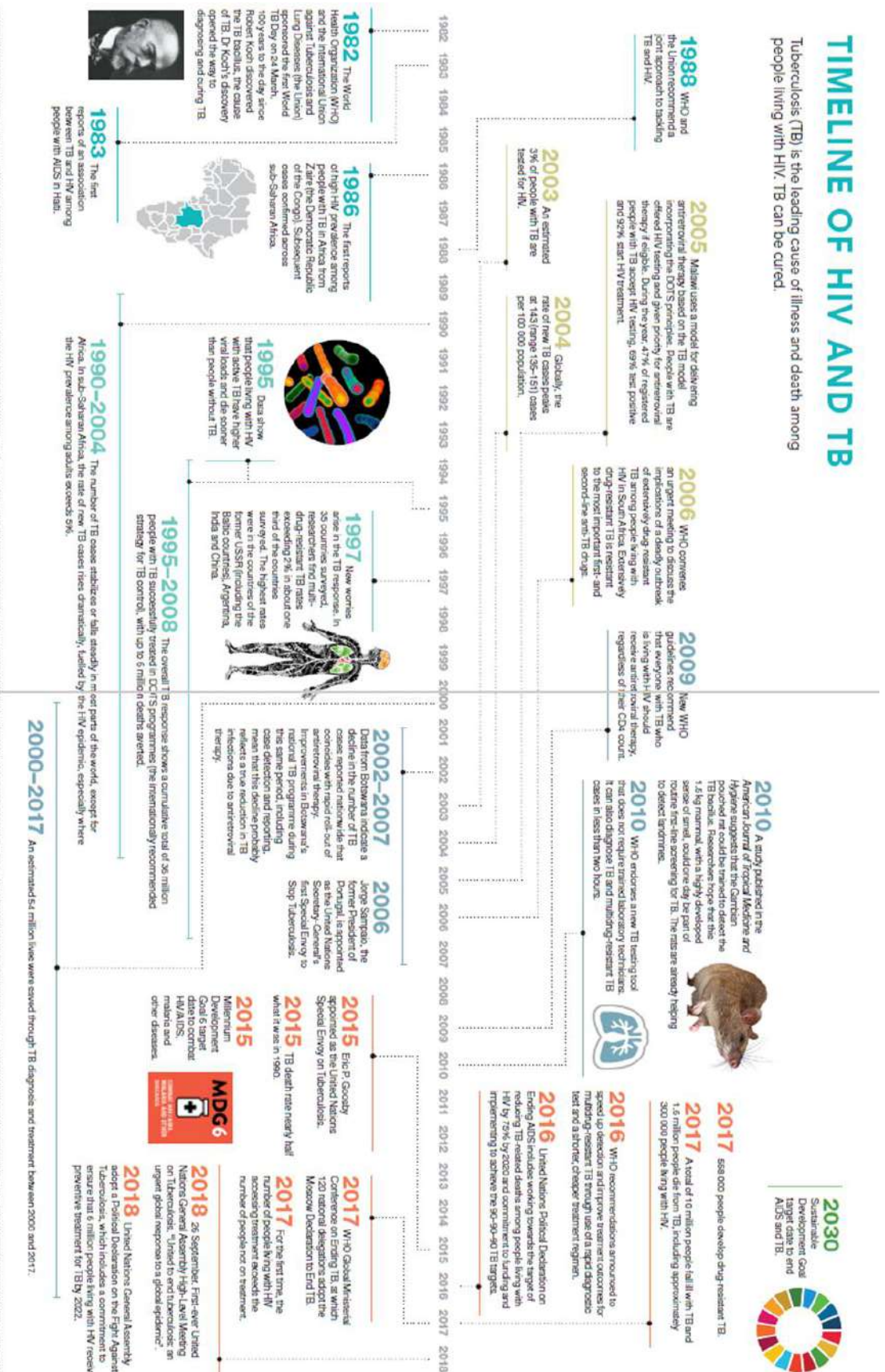


Figure 27: Historical timeline showing advances in the co-infection fight ([263])

Chapter III: *Mycobacterium tuberculosis*-HIV-1 co-infection - the deadly duo

The co-infection of Mtb and HIV-1 is still a major public health issue on a global scale, particularly in Africa and Eastern Europe where the TB-HIV “syndemic” converges. The risk of developing TB is estimated to be between 16 to 27 times higher in people living with HIV-1, compared to the general population, with 55% of TB notified patients also infected with HIV-1 [1]. Moreover, TB is the main aggravating factor and cause of AIDS-related deaths. In 2017, 464 633 (*i.e.* 51%) new TB cases were declared in HIV-1 infected patients, among which 86% were under cART; 300 000 people infected with HIV-1 died of TB, representing a quarter of all TB deaths worldwide [1]. In addition, HIV-1 infected people are particularly at risk of infection and death from multidrug-resistant Mtb infection. To answer this threat, the WHO guidelines recommend offering HIV-1 testing to all patients with presumptive and diagnosed TB. Likewise, routine TB symptom screening in people living with HIV-1 is to be developed in order to treat as quickly as possible new Mtb infections [1].

I. Clinical considerations of the co-infection

A. Historical overview

The first report of an association between TB and HIV-1 was established in Haiti in 1983 [673], and was followed by a high incidence of HIV-1 infection among people with TB in the Democratic Republic of Congo and in other sub-Saharan African regions in 1986 [263]. As soon as 1988, the increasing numbers of co-infection cases led to the WHO proposing a joint approach to tackling both HIV-1 and TB, and set the long-term goal to decrease the co-infection incidence. In 1995, the first evidence of pathogen synergy emerged when people living with HIV-1 and active TB tended to have higher viral load and died sooner of AIDS comorbidities than people living with HIV-1 alone [263]. At the beginning of 2000, the increasing number of TB cases, especially in Africa fueled by HIV-1 epidemics, made the diagnosis of co-infection more important than ever. In 2003, only 3% of people with TB were tested for HIV-1 co-infection, a number that increased to 22% by 2008 and that, thankfully is still increasing today, according to WHO recommendations [1]. For example, in Malawi, HIV-1 testing was offered to TB patients who were given cART in priority when eligible. In 2009, due to the high prevalence of co-infection in sub-Saharan Africa, and the fact that TB is officially the leading cause of AIDS-related deaths, the WHO actualized its guideline for co-infection treatment and recommended cART for all co-infected persons, independent of their CD4⁺ T cell count. The 2011 CAMELIA study, performed in Cambodia by the Pasteur Institute, showed that among 661 patients with TB and HIV-1, 35% were more likely to survive AIDS-related TB when they received cART as soon as two weeks post-antibiotherapy [674]. In 2016, the United Nation declaration to end AIDS included in its main goal the reduction of TB-related deaths in people living with HIV-1 by 75% by 2020. This

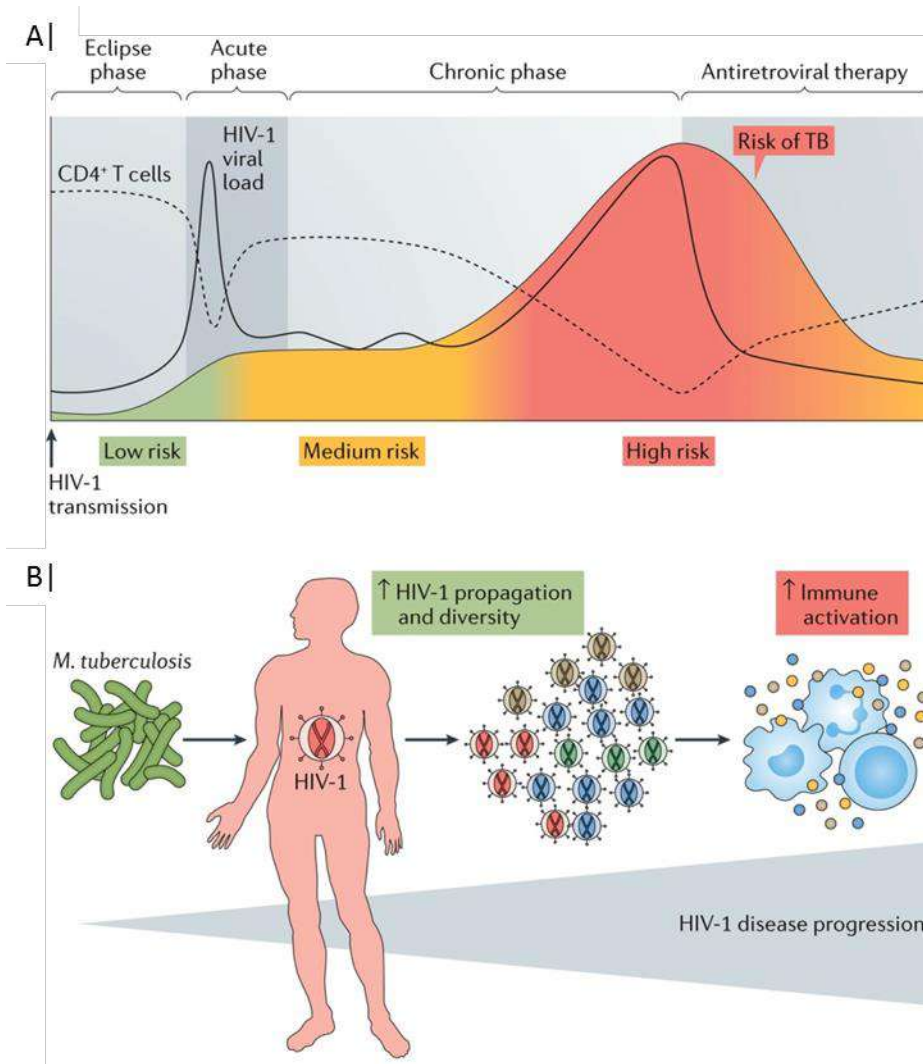


Figure 28: HIV-1 and Mtb synergy increases the risk of progression of both pathologies (from [675]).

A | Soon after HIV-1 infection, an individual has an increased (2- to 5- fold above baseline) risk of developing active TB. During the chronic HIV-1 infection phase, the risk to develop active TB dramatically increases, up to 20-fold compared to the general population, and is correlated with CD4⁺ T cell count drop. In addition, the initiation of antiretroviral therapy to control HIV-1 replication does not fully restore the active TB risk to baseline, which remains about 4-fold above baseline even after CD4⁺ T cell counts have recovered.

B | Infection with Mtb in individuals infected with HIV-1 increases the viral replication and consequently viral diversity. With the increased number of viruses, the immune system is strongly required and heavily activated. Therefore, Mtb infection potentiates the chronic immune activation observed in HIV-1⁺ individuals, accelerating the progression of HIV-1 disease towards AIDS.

goal has been reached by certain countries in Africa (e.g. Eritrea, Malawi, Djibouti, and Togo) and India. However, this goal is still far from being achieved in Western Europe where the reduction in TB-related deaths in co-infected patients was decreased by only 24%, instead of 75% (i.e. France, Poland, Turkey) [1], [263]). That is why the United Nations General Assembly adopted a new measure in the fight against TB in 2018, committing to the distribution of preventive TB treatment to at least 6 million people living with HIV-1 by 2022 (https://www.unaids.org/sites/default/files/media_asset/tuberculosis-and-hiv-progress-towards-the-2020-target_en.pdf).

All these facts and key dates were reported by UNAIDS and the WHO and are summarized in Figure 27.

B. Synergy between HIV-1 and Mtb

It is well-known now that both HIV-1 and Mtb act in synergy within the infected individuals, to dysregulate the host immune response and to accelerate each other's progression (Figure 28). HIV-1 influences the clinical outcomes and phenotype of TB disease in co-infected patients, whereby in advanced AIDS where CD4⁺ T cells depletion is at its highest level, Mtb frequently disseminates throughout the host, causing extra-pulmonary TB and mycobacteria circulation in the bloodstream [676], [677]. In fact, if HIV-1 patients are more likely to become Mtb infected (up to 27 times more susceptible to develop the disease), the risk of developing active TB is increased by HIV-1 co-infection [678], [679]. TB pathogenesis evolves with the HIV-1-caused immunosuppression, involving the main characteristic of HIV-1 pathology, CD4⁺ T cell loss, as an important element responsible for TB exacerbation for which mechanisms will be discussed further later in this chapter (section II). In patients with a CD4⁺ T cell count above 300 cells/mm³, no difference in the proportion of cavitation or disease seen in X-rays of the upper lungs was observed in co-infected patients compared to Mtb mono-infected patients. However, when the CD4⁺ T cell count declined to below 300 cells/mm³, lung adenopathy (miliary pattern), extension of the disease in the lower pulmonary cavitation, and high pleural effusion bacterial burden were more common manifestations of TB pathogenesis [680]. Post-mortem studies showed that in addition to aggravated lung pathology, co-infected patients displayed more disseminated TB than the mono-infected patients. The spleen, liver, lymph nodes, and bone marrow are the most commonly affected organs during extra-pulmonary TB (see Chapter I, section I.A.c.), which is the most common form of TB in HIV-1 infected people with low T cell counts [681].

Conversely, active TB is tightly linked to increased viral replication in co-infected hosts, as proven by an observed viral load of up to 160 times higher in the co-infected patient blood compared to that in the HIV-1-mono-infected patient. This increased viral load is even greater at the anatomical sites of co-infection [682]. Indeed, increased p24 HIV-1 antigen and viral loads (up to 200 fold) were not only found in BAL in co-infected patients compared to TB patients [683], [684] but also in pleural effusions [685], [686], where the virus titers were up to 35-fold higher than that found in the peripheral blood of the same patient [687], [688]. This observation of increased viral production is associated with macrophages rather than T cell infection [689]. In fact, it was shown that alveolar macrophages isolated from co-infected patients, the main target of Mtb and HIV-1 in the lung (see chapter I and II), exhibited upregulated viral replication *ex vivo* [690], [691]. The brain of co-infected patients is also an

important anatomical site of sustained HIV-1 replication and is often associated with the development of TB meningitis (see chapter I section I.A.c.). Patients presenting this extra-pulmonary TB form have a 10-fold increase in HIV-1 viral load in the cerebro-spinal fluid compared to the bloodstream, indicating that this organ is an important site for viral replication [692].

Altogether, these clinical data demonstrate the existing synergy between HIV-1 and Mtb, and further emphasize the gravity of the co-infection. As discussed in the next section, one of the biggest health challenges in the field of infectious diseases is to increase the prevention of TB infection in people living with HIV-1, and to ameliorate the diagnosis of this co-infection, in order to treat it as soon as possible to decrease the number of AIDS-TB deaths.

C. Clinical challenges raised by the co-infection

a. Difficulty to diagnosis

As co-infection with HIV-1 modulates TB clinical manifestations, it renders TB diagnosis (see chapter I section I.B.b.) quite complicated. Indeed, the usual tests to detect Mtb infection are less sensitive in HIV-1 co-infected patients. Both TST and IGRA tests become imprecise, if not obsolete due to Mtb-specific IFN γ ⁺ T cells depletion [693]. Moreover, TB disease often comes with atypical manifestation in co-infected patients, including disseminated bacterial loads [694], [695]. In addition, given that HIV-1-mediated immunosuppression is associated with reduced cavitation in the lungs, most co-infected patients have reduced sputum production compared to HIV-1 uninfected people [696]. In regions where resources are limited, the more common and fastest test used to diagnose TB is the smear microscopy. It consists of examining by microscopy the presence of acid-fast bacilli present in sputum. However, this test is poorly sensitive, particularly in HIV-1 co-infected patients since there are fewer bacilli in sputum [697]–[699]. Solid or liquid Mtb cultures remain the standard methods for TB diagnosis, however, both are still based on sputum bacilli load; this kind of test requires time and specific infrastructures, which are not available everywhere in low-income countries and delay the diagnosis. Yet, MTB/RIF detection method overcomes smear microscopy techniques, irrespective of HIV-1 status, and is fast enough to reduce the delay before TB treatment initiation [700], [701], but this method remains expensive to be routinely used in low-income countries where the co-infection burden is the highest.

b. Drug interactions and TB IRIS

In addition to the difficulty of TB diagnosis in HIV-1 co-infected individuals, the treatment is also complicated. Drugs interaction must be considered, since rifampicin interacts with NNRTIs and protease inhibitors, leading to sub-therapeutic efficiency of these antiviral drugs and to subsequent treatment failure [702]. Consequently, the antiretroviral regimen should be chosen on the basis of minimal drug interaction with the antibiotic regimen besides the need to be adapted to the patient viral infection characteristics [703]. An important challenge healthcare providers must face in the co-infection between HIV-1 and Mtb is the fact that people living with the virus are more susceptible to

become infected with MDR-TB or XDR-TB. This TB drug resistance in HIV-1 infection settings is thought to be due to two major mechanisms: first, rifampin and ethambutol display maladsorption in HIV-1 infected people, causing TB treatment failure; second, even in the case of low incidence, drug-resistant strains enable disease progression because of the immune-depression caused by HIV-1 and of the treatment inefficiency [704], [705]. Another problem in co-infection treatment is the order and timing of drug initiation. Several studies found that initiation of cART two weeks after TB treatment was more beneficial than delaying cART for 8 weeks as it reduced mortality [674], [706].

The main problem observed after cART initiation in co-infected patients is the risk to develop TB immune reconstitution inflammatory syndrome (TB-IRIS), an adverse consequence of the restoration of pathogen-specific T cell responses [707]. About 15.7% of the HIV-1-associated IRIS are caused by Mtb co-infection [708], [709]. TB-IRIS is an excessive inflammatory response that is manifested by high fever, respiratory and renal failures, worsening infection symptoms, and revealing new TB infection or reactivation of latent TB [710]. This symptom happens in up to 40% of the co-infected population, usually between 4 to 8 weeks after cART initiation [711], [712]. TB-IRIS is thought to be mainly caused by sustained Th1 responses, characterized by increased IFN γ -mediated responses against the mycobacterial antigens, dysregulation of cytokines secretions and recruitment of Mtb-specific T cells migration to the site of infection [713], [714]. However, cART has been shown to induce the macrophage hyperactivation in response to Mtb antigens, indicating that innate cells have a role in TB-IRIS occurrence [715]. More precisely, susceptibility to Th1 responses and higher bacterial loads in co-infected patients compared to Mtb-mono-infected patient could be related to innate immune responses, as they involve elevated production of IL-18 and CXCL10, favouring both Th1 cells polarization and attraction to Mtb-infection site [713].

To conclude, and despite the progress made in the last 10 years to combat either Mtb or HIV-1 infection, HIV-1/TB co-infection is still a major health issue at the global scale, and particularly in Africa where this burden is the highest [1]. This is due to the initial separation of strategies to fight individual infection instead of developing collaborative strategies to eradicate both pathogens at the same time. Improvement has been made to increase co-infected patients survival, notably by initiating cART regardless of the CD4⁺ T cell count status. Many efforts still remain to be made to efficiently fight this co-infection, starting with the understanding of the mechanisms leading to pathogen synergy and mutual exacerbation. I will now discuss what is known for HIV-1-mediated enhancement of Mtb infection, which have been better explored.

II. HIV-1 exacerbates Mtb growth

A. Depletion of Mtb-specific effector T cells

It is well established now that HIV-1 infection impairs the ability of the host to control Mtb growth (for review, see [2], [696], [675], [716]). Indeed, several clinical studies shed light to an increased risk of developing TB shortly after HIV-1 infection. For example, HIV-1 infected miners in South Africa were found to be 2 to 3 times more prone to develop TB within two years of HIV-1 seroconversion compared to HIV-1 uninfected miners [679], [717]. The most obvious mechanism

explaining this increased risk is the depletion of CD4⁺ T cells after HIV-1 infection. Indeed, enhanced propensity to develop both TB and extra-pulmonary TB is strongly correlated to CD4⁺ T cell counts in co-infected patients [675], [718]. In addition, several studies reported a decreased number of CD4⁺ T cells in co-infected patients, notably in BAL [719]–[721] and in the lung, more precisely around the granuloma [686], [721]. The remaining cells display altered functions, such as reduced ability to produce cytokines [719], [720], an issue that will be discussed in the next section. The observed T cell depletion in co-infected patients leads to granuloma structure disruption and promotes progression towards active TB [722]. Indeed, in the absence of CD4⁺ T cells, the repartition of CD8⁺ T cells is no longer maintained in the outer ring of the granuloma, but instead sparsely distributed in the malformed structure, showing the importance of CD4⁺ T cells in the granuloma maintenance [723]. Interestingly, Mtb-specific T cells are preferentially depleted during HIV-1 infection of patients with TB, as demonstrated by several reports. First, Mtb-specific T cells are particularly susceptible to HIV-1 infection as they frequently display HIV-1 DNA, a characteristic mainly due to their high IL-2 production [724], and to the increased expression level of the HIV-1 entry co-receptors CCR5 and CXCR4 after Mtb infection [725], [726]. Second, Geldmacher and colleagues reported that within 3 months after HIV-1 seroconversion, a drastic drop in peripheral Mtb-specific memory CD4⁺ T cells secreting IFN γ occurs in patients with latent TB, leading to TB reactivation [727]. Third, polyfunctional T cells that produce IFN γ , TNF α and IL-2, were found to be specifically depleted in HIV-1 infected individuals [719], as further shown by the diminished recruitment of IFN γ -producing cells in co-infected patients after TST challenge [728].

Collectively, these studies provide strong evidence that CD4⁺ T cells depletion, especially that of Mtb-specific T cells, is an important mechanism by which HIV-1 triggers Mtb growth in the co-infected host as it dampens Mtb-specific responses and alters the granuloma structure and function. In addition to this, T cells functions are also modified by HIV-1 infection, a topic discussed in the following section.

B. Functional changes in Mtb-reactive T cells

The main alteration in T cell function after HIV-1 infection is the modification of the cytokines they produce, together with their proliferation after efficient infection. Zhang and colleagues evaluated cytokine patterns in co-infected patients by *in vitro* stimulation of their PBMCs with heat-killed Mtb and found a decreased production of IFN γ and IL-2 by Mtb-specific Th1 cells compared to HIV-1 seronegative patients. In addition, these cells were less proliferative in co-infected patients, an effect independent of CD4⁺ T cell count. However, the reduced Th1 response was a direct result of CD4⁺ T cell depletion and to high IL-10 levels, indicating the negative impact of immunosuppressive cytokines on Mtb growth in co-infection settings [729]. Other studies also reported a defect in IFN γ production by T cells in co-infected patients both in the bloodstream [730] and in the airways [731]. In addition to IFN γ , T cells isolated from BAL in BCG-vaccinated people living with HIV-1 produce less IL-2 and TNF α after BCG-stimulation, compared to HIV-1 negative people [719]. Moreover, BAL T cells from TB-HIV-1 co-infected patients stimulated with avirulent Mtb strains were found to be less proliferative than the one from mono-infected patients, further supporting the HIV-1-mediated alterations on the T cell compartment [732].

Besides evident modification of the cytokine responses, HIV-1 is well known to induce chronic immune activation of T cells (see chapter II section II.B.b.). Indeed, during the chronic stage of the disease, HIV-1 is able to switch T cell memory profile towards an effector one, and induces high levels of activation markers expression on T cells such as HLA-DR, as well as exhaustion markers like CD57 and PD-1, particularly on effector memory subsets [733]. In active TB-HIV-1 co-infection settings, PD-1 expression is particularly elevated on Mtb-specific CD4⁺ T cells compared to HIV-1 negative persons [121]. Blocking the PD-1 interaction with its ligand marginally enhanced the proliferation of CD4⁺ T cells specific for Mtb [734], suggesting that PD-1 overexpression promotes T-cells exhaustion, leading to suboptimal Mtb-responses in co-infected individuals. In that same study, the authors evaluated the expression of PD-1 ligand (PD-L1) in monocytes and macrophages, which expressed high levels of this ligand in active-TB patients compared to healthy control. This high expression and interaction of PD-1 with PD-L1 decreased macrophages phagocytosis and intracellular killing of Mtb, showing that innate immunity is inhibited as well as the CD4⁺ T cell-mediated response against Mtb. In fact, this is not surprising since Th1 responses contribute actively to the recruitment of monocytes and macrophages to the site of Mtb infection, where they enhance the macrophage antimicrobial activity [696]. Considering this intricate relationship between the innate and adaptive immune responses, the importance of innate cells, and particularly of macrophages in HIV-1-mediated exacerbation of TB, should not be ignored.

C. Alteration of the macrophage response

HIV-1 infected people are more susceptible to develop TB, even before CD4⁺ T cell depletion [675], suggesting a role for innate immunity in the observed bacterial burden in co-infected patients. HIV-1 infects macrophages *in vivo* and efficiently establishes viral reservoirs out of these cells in almost all organs within the host. In the lung, alveolar macrophages are the main HIV-1-infected cells, a target shared by Mtb. Therefore, it is likely that macrophages are a central cellular population in HIV-1-mediated exacerbation of Mtb growth. Here, I will focus on the probable mechanisms explaining the loss of Mtb-growth control that favours TB reactivation in co-infected patients.

a. Alteration of cytokines responses and cell death

As the principal target for Mtb, macrophages are at the center of the immune response against Mtb (see chapter I section II.B.). They are essential to contain the bacteria, as they are the primary cells that phagocytize the bacillus targeting it for phagosomal degradation. Even if macrophages fail to kill all bacteria, they induce the recruitment of new macrophages and phagocytes to the site of infection, notably through secretion of TNF α and cell death apoptosis. This phenomenon leads to the final development of the granuloma to contain the bacteria, a structure highly depending on TNF α and Th1 responses [86], [98]. To determine (at the molecular level) the *in vivo* immune response against Mtb at the site of infection, Bell and colleagues performed a transcriptional profiling of patients with active TB and HIV-1 using cells recruited to the site of TST challenge. HIV-1⁺TST⁺ patients exhibited preserved Th1 responses but were deficient for IL-10-inducible immunoregulatory responses. On the contrary,

HIV-1⁺TST⁻ patients revealed a deep anergy of both innate and adaptive immune cells except for IFN- γ activity, which paired with the impairment of anti-mycobacterial responses [728].

Mtb-infected macrophages are high producers of TNF α , a key cytokine involved in the immune response to TB by the induction of granuloma formation (see chapter I section II.A.a.). Both alveolar macrophages isolated from HIV-1⁺ BAL and macrophages within the granuloma [735] were found to produce less TNF α in response to Mtb infection. This led to extensive lesions necrosis, poorly formed granulomas and neutrophils accumulation, indicating the deep alteration of the granuloma structure as a consequence for the dampened TNF α production [736]. In addition, co-infected macrophages were found to release lower levels of TNF α than Mtb-infected macrophages, which resulted in decreased frequency of TNF-mediated macrophages apoptosis [735], [737], [738]. Alveolar macrophages from healthy, *ex vivo* infected with HIV-1 [735], or from HIV-1 infected individuals [738] display a decrease in Mtb-mediated apoptosis after Mtb challenge compared to those mono-infected with Mtb. This effect was mediated by the viral protein Nef that can be found in the extracellular medium. Kumawat and colleagues found that exogenous Nef inhibits TNF α synthesis in Mtb-infected macrophages, due to cross-regulation of the individual signaling pathway that lead to TNF α production. More specifically, the authors identified the ability of Nef to inhibit the ASK1³³/p38 MAPK signaling pathway, resulting in TNF α mRNA instability in the co-infected cell, as the mechanism responsible for TNF α inhibition [737].

Contradictory results were obtained in other studies, reporting an increased level of TNF α in the co-infected patients. Indeed, it was reported that alveolar macrophages isolated from BAL of healthy controls, HIV-1 mono-infected or HIV-1 infected patients with suspected TB, spontaneously produce TNF α shortly after their isolation and were able to produce pro-inflammatory cytokines in response to lipopolysaccharide, indicating a retained ability to respond to danger signals *in vivo* [739]. Another study was conducted in hospitalized patients with severe disseminated TB in HIV-1 co-infection settings. The authors found that monocytes dysfunction was associated with mortality. In patients who died, high activation of the innate immune system was found. This elevated activation was characterized by an increased proportion of (i) CD14⁺CD16⁺ monocytes, (ii) IL-6, (iii) TNF α , and (iv) colony-stimulating factor 3 (CSF-3). Increased anti-inflammatory markers (increased IL-1R and lower monocyte and neutrophil responses to bacterial stimuli), were also found in dead patients [740]. Another study found equivalent numbers of granuloma in HIV-1⁺ co-infected patients compared to Mtb mono-infected ones, but those with HIV-1 expressed more IFN γ , TNF α , IL-12 and IL-4, which correlated with the increased number of necrotic granuloma in these patients [741]. Increased necrosis is deleterious in TB disease, since necrosis is one of the mechanism used by Mtb to escape macrophage killing (see chapter I section II.A.a.).

Despite the variance obtained in different studies, it is clear that macrophages play a major role in HIV-1-mediated exacerbation of Mtb growth by modulating their capacity to produce TNF α and by altering the granuloma formation and maintenance. Since differential stages of granuloma development can be observed for each subject [742], the contradictory results reported in the studies

³³ **ASK1:** Apoptosis signal-regulating kinase 1 (ASK1) is a member of MAP kinase kinase family. It activates c-Jun N-terminal kinase (JNK) and p38 mitogen-activated protein kinases in response to an array of stresses and calcium influx.

cited above may not have taken into account this granuloma heterogeneity. It is possible that in a single individual, some granuloma express high level of TNF α while others have decreased level of this cytokine. Nevertheless, the modulation of TNF α leads to a decrease in macrophage apoptosis, compensated by an increase in necrosis level, which must then participate to granuloma disruption and Mtb spread.

b. Inhibition of phagocytosis and autophagy

Macrophages are the main effector cell involved in Mtb killing. Consequently, the bacterium has evolved strategies to overcome macrophage-mediated killing. One of the main mechanisms for this escape is the inhibition of the phagosome maturation (see chapter I section II.B.c.i.). Mwandumba and colleagues studied the capacity of alveolar macrophages isolated from healthy or co-infected patient to phagocytize and acidify phagosomes. They found that alveolar macrophages from both healthy and co-infected individuals had equivalent capacity to phagocytize IgG-coated beads and to transport them to acidic compartment, but observed that Mtb was located in different vacuoles that failed to accumulate endosomal markers and to acidify [143]. To date, HIV-1 infected macrophages were reported to facilitate Mtb intracellular growth in *in vitro* experiments [743]. Indeed, HIV-1 impairs Mtb phagocytosis and phagosomes maturation (Figure 29). The team of Niedergang showed that macrophages phagocytosis by various receptors was inhibited by HIV-1 infection in a Nef-dependent manner, which has strong consequences on the control of opportunistic bacterial infection [744]. Nef prevented the recruitment of adaptor protein 1 (AP-1) expressing endosomes to the phagosome, thereby preventing the phagosome maturation [555]. This is supported by the impairment of phagocytosis by alveolar macrophages obtained from BAL from healthy or HIV-1 infected adults, and by the fact that patient treatment with cART for less than 4 years did not fully restore alveolar macrophages functions, as assessed by phagosomal proteolysis [480], [743]. In addition to impaired phagocytosis, HIV-1 infection of TB patients also negatively impacts autophagy in macrophages. Indeed, Nef is able to inhibit autophagosome maturation through interaction with the autophagy regulator protein beclin-1 [745], [746]. Altogether, the inhibition of phagocytosis and autophagy in HIV-1 infected macrophages is beneficial for Mtb in co-infection, since it further diminishes anti-bacterial functions, as shown by the increased bacterial burden in co-infected macrophages compared to Mtb-infected cells [743]. In addition to Mtb increased bacterial growth, Pathak and colleagues observed that co-infected macrophages were also more susceptible to HIV-1 infection, since they displayed enhanced viral replication; suggesting that both pathogens act in synergy within the same macrophage [743].

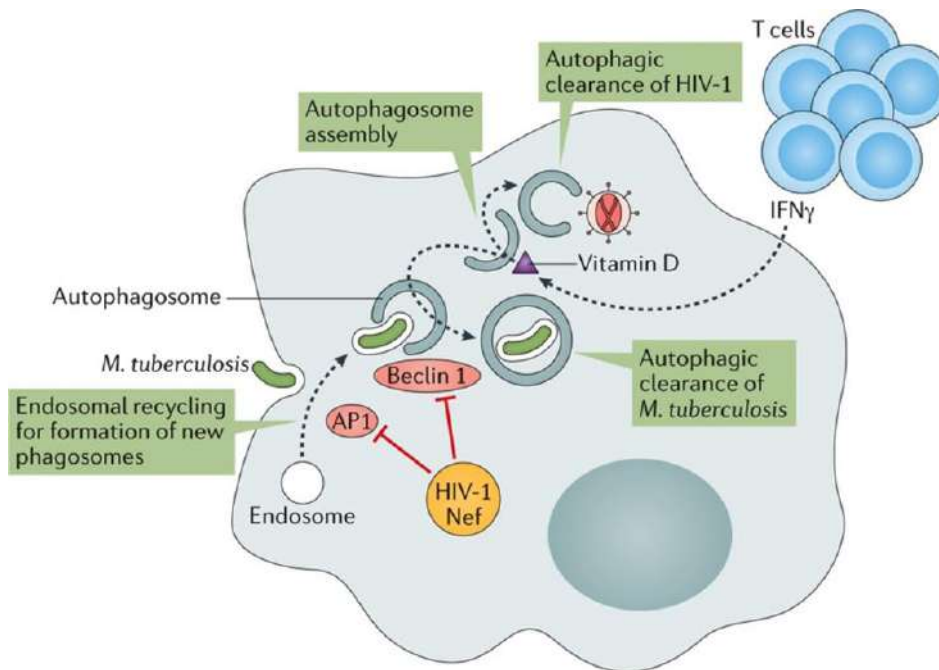


Figure 29: Nef impairs the macrophage phagosome maturation and alters the Mtb control (from [675]).

Macrophage control of Mtb is mainly mediated by bacterial phagocytosis and clearance by the phagosome and autophagosome, in a vitamin D-dependant manner. HIV-1 co-infection can undermine this host defence at multiple levels. Indeed, the viral accessory protein Nef reduces macrophage phagocytic capacity by inhibiting AP1-mediated endosomal recycling that is needed to form nascent phagosomes. Moreover, Nef interaction with Beclin 1 inhibits autophagosome maturation and fusion with lysosome, including Mtb-containing (auto)phagosome, therefore preventing bacterial clearance. Interestingly, vitamin D supplementation may overcome this inhibition of autophagosome maturation to improve both Mtb clearance and HIV-1 restriction by autophagy.

III. Mtb exacerbates HIV-1 replication

There is strong evidence supporting the capacity of Mtb to enhance HIV-1 replication *in vivo*. Indeed, increased viral loads are found in co-infected patients, both in the bloodstream [691] and at the anatomical site of co-infection, especially in the lungs [683], [688], [689]. However, the mechanisms explaining how Mtb exacerbates HIV-1 are just beginning to emerge. In this section, I will provide an overview of the few mechanisms that have been proposed to explain this phenomenon.

A. Mtb triggers viral transcription in infected cells

Importantly, HIV-1 replication is particularly enhanced in the lungs, pleural effusion and BAL of co-infected patients. In fact, high level of HIV-1 proteins were found in lung segments where Mtb is also detected compared to those lacking the bacillus from the same individual. This tendency correlated with high TNF α concentration in segments positive for both pathogens, arguing that HIV-1 replication is locally exacerbated in co-infected patients [683]. The enriched levels of TNF α that come with Mtb infection are in part responsible for enhanced HIV-1 transcription in co-infection settings. Indeed, 30 years ago, TNF α was reported to increase HIV-1 mRNA levels and transcription in a chronically infected T cell line. Using gel mobility shift assays, Duh and colleagues found an increased activation of HIV-1 LTR sequences because of NF κ B binding to these sequences, in response to TNF α stimulation [747]. In co-infected macrophages, for which the activation profile is determined in terms of HIV-1 permissiveness, the inhibition of C/EBP β transcription factor leads to increased activation of NF κ B that binds subsequently to HIV-1 LTR sequences to enhance viral transcription [748]. This inhibition of C/EBP β is mediated by Mtb infection. Alveolar macrophages from healthy tissue express high level of C/EBP β under its HIV-1 inhibitory form due to sustained IFN-I stimulation. However, this isoform is strongly downregulated at the site of infection with Mtb, allowing high HIV-1 replication levels [749]. These results also suggest that the pro-inflammatory milieu of active TB overcomes the IFN-I antiviral responses. Direct evidence of this hypothesis was shown in HIV-1 infected macrophages where co-infection with Mtb primarily inhibited viral transcription, but was followed by a substantial increase after IL-10 early responses were attenuated by the virus [750]. In fact, IL-10 was shown to inhibit HIV-1 transcription by inducing the expression of C/EBP β through STAT3 activation [751]. Conversely, pro-inflammatory cytokines such as TNF α , IL-6 and IL-1 β , all up-regulated during Mtb infection, have long been established to act synergistically to promote HIV-1 transcription [544], [545], [747], notably by modulating macrophages polarization and therefore permissiveness to HIV-1 infection [187]. It is likely that this bystander effect, *i.e.* the polarization of uninfected macrophages by the cytokines released upon Mtb-infection of some macrophages, is the main factor inducing susceptibility to HIV-1 infection. Indeed, the direct co-infection of macrophages by Mtb and HIV-1 has recently been observed *in vivo* in a model of TB-SIV co-infected NHP [752]. Moreover, Orenstein and colleagues observed the co-infection of multi-nucleated macrophages by HIV-1 and *Mycobacterium avium* [753] (Figure 30). However, the direct co-infection of macrophages with both pathogens remains a rare event, which excludes the direct interaction between HIV-1 and Mtb as the main mechanism by which infected macrophages become particularly permissive to the virus.

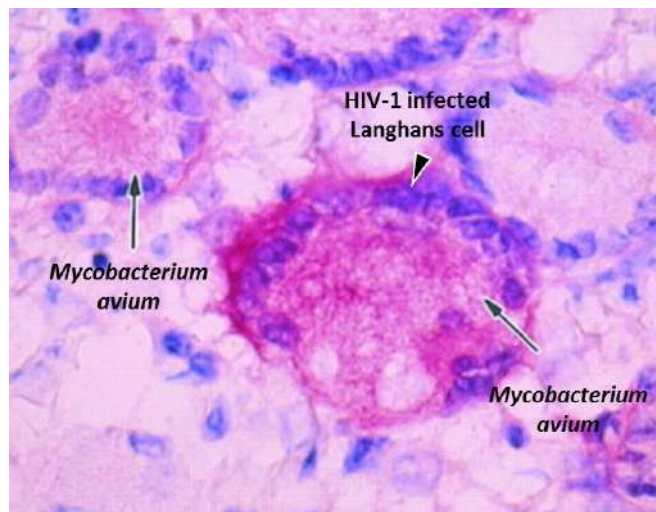


Figure 30: *In vivo* evidence of co-infected macrophages (from [753])

Deparaffinized sections of macrophages infected with HIV-1 and *Mycobacterium avium* complex (MAC). The immunohistochemical staining shows HIV p24–positive (red stain) MAC-infected multinucleated giant Langhans cells. The clear needle-like intracytoplasmic structures (arrows) represent negative-stained images of bacilli.

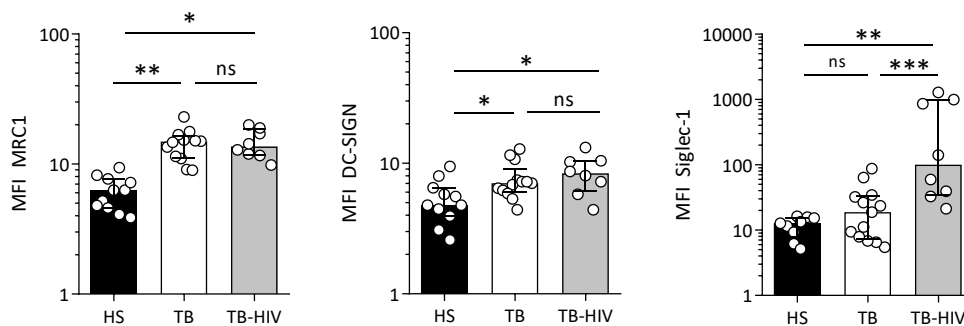


Figure 31: Mtb infection and TB-associated environment induce C-type lectin receptor expression on macrophages.

Peripheral blood monocytes from healthy, TB and TB-HIV individuals (thanks to our collaboration with Dr L. Balboa, IMEX-CONICET, Argentina) were stained for Siglec-1, DC-SIGN and MRC1. Monocytes isolated from TB and TB-HIV patients exhibited higher cell surface expression of the C-type lectin receptors (CLR), MRC1 and DC-SIGN, compared to that found in healthy donors, while Siglec-1 expression was upregulated in co-infected patients only. This data indicate that Mtb infection induces the expression of various CLR involved in HIV-1 binding, which could then be used by the virus to efficiently infect target myeloid cells.

B. Mtb accelerates the progression to AIDS by increasing HIV-1 strains diversity

In co-infected patients, Mtb not only supports HIV-1 replication and dissemination through dysregulation of host cells receptors, whose expression are modulated by environmental cytokines and chemokines, but it also favours HIV-1 heterogeneity both at the site of infection and systemically [754]. By increasing CXCR4 levels in alveolar macrophages, Mtb accelerates the progression to AIDS in co-infected people, by skewing the switch from R5 to X4 dominant HIV-1 strains [755]. Indeed, in HIV-1 pathology, disease progression is related to the evolution of HIV-1 strains towards those that use CXCR4 co-receptors to enter the cells, which are mainly T cell tropic strains. This switch is allowed by the high rate of error made by the viral reverse transcriptase that induces constant mutation of the viral genome (see chapter II section II.A.a.i.). In BAL fluids from TB infected patients, CXCR4 expression levels are higher than that of CCR5 [755]. Moreover, Mtb infection of macrophages enhances X4-tropic virus DNA but not that of R5 viruses, further supporting the selection of X4 tropism in co-infection settings. This is due notably to the natural CCR5 antagonist MIP-1 β , which is highly concentrated in BAL fluids from TB patients [278]. In addition, BAL from co-infected patients displayed a great number of HIV-1 gp120 V3 region substitutions that was associated with greater viral heterogeneity [683]. Supporting these findings, Collins and colleagues, as well as Biru *et al.*, found that Mtb-HIV-1 co-infection led to 2- to 3-fold greater mutation frequency in comparison with HIV-1 infection alone, resulting in greater diversity of viral strains [687], [756], [757].

All in all, these studies show that Mtb is able to influence HIV-1 mutations towards X4-tropic strains, however, the mechanisms explaining this selection pressure and the identity of the cells involved remain to be explored and understand.

C. Mtb renders cells permissive to HIV-1 infection and favours viral cell-to-cell transmission

During the constant activation of the immune system in chronic disease, both in HIV-1 and TB pathologies create an environment that polarizes macrophages towards more or less permissive target for intracellular pathogen. Previously, macrophages were thought to be terminally differentiated cells that were unable to replicate. However, mouse experiment showed that macrophages are able to re-enter the cell cycle in response to inflammatory stimuli such as helminth infection [758]. In TB granuloma, MGLC were found to do so as well, even if they do not complete cytokinesis [759]. It was shown that macrophages who enter the cell cycle, but get arrested in G1 phase, downregulate SAMHD1 expression, an important restriction factor of HIV-1. Consequently, these macrophages become more permissive to HIV-1 infection, as dividing cells are preferentially targeted by the virus [428]. In addition to decreased restriction factors expression, Mtb infection not only up-regulates the expression of CCR5 and CXCR4, HIV-1 main co-entry receptors [725], [726], but also the expression of alternate HIV-1 receptors such as DC-SIGN and MRC1 (Figure 31), both responsible for gp120 binding (see chapter II section III.D.a.i.). The induction of DC-SIGN expression by Mtb infection is likely to be detrimental to the host in the case of HIV-1 infection. Indeed, HIV-1 binding to DC-SIGN leads to the protection of HIV-1 particles in VCC and promote HIV-1 cell-to-cell transfer to T cells [760]. *In vitro* co-

culture experiment showed that co-infected macrophages expanded T cell proliferation and promoted HIV-1 transmission to these lymphocytes [761]. Mtb therefore promotes HIV-1 dissemination, not only by inducing HIV-1 receptors expression on DC and macrophages, but also by recruiting CD4⁺ target cells to the site of co-infection, and more particularly to the granuloma, where Mtb-specific T cells are constantly recruited to maintain the structure [675].

The diversity of models used to study the effect of direct macrophage co-infection, including the monocyte cell line THP-1 (which proliferates as opposed to monocyte-derived-macrophages), peripheral blood mononuclear cells (PBMC, rich in T cells) and different virulent, avirulent or killed strains of Mtb produced contradictory results. While the majority of studies reported an exacerbated viral replication in co-infected macrophages due to TNF α production in response to Mtb [683], [748], [749], few studies found the opposite, such as reduced HIV-1 replication [762] or TNF α -independent exacerbation mechanisms [761]. Moreover, these studies have been performed in co-infected macrophages. However, this event is rare, despite the proximity of Mtb- and HIV-1-infected areas in the co-infected lungs. Altogether, these observations suggest that the main mechanisms by which Mtb exacerbates HIV-1 replication in macrophages are due to bystander effects of Mtb infection, and more precisely to the microenvironment created by the bacterial infection (including notably cytokines, chemokines and bacterial products). Moreover, the bystander effect of Mtb infection has not been explored as much as the co-infected models of macrophages, despite the probability of this effect to be more physiological than direct co-infection. That is why, for my PhD work, I focused my research on the effect of TB-associated microenvironment on macrophage's susceptibility to HIV-1 infection, which I hope will be complementary to those found in the models of co-infected cells and help covering the full spectrum of what really happens in co-infected individuals.

Thesis objectives

As stated in the introduction, TB-HIV-1 co-infection is, to date, a major global health issue. HIV-1 infected individuals are more susceptible to develop active and extra-pulmonary TB, which is the major cause of death in HIV-1 infected people. The reason why co-infection is still a worldwide health concern is because of the synergy between HIV-1 and Mtb. The mechanisms by which HIV-1 infection enhance Mtb growth in the host have been well described. They are mostly related to the global CD4⁺ T cell loss and the modification of the cytokine profile within the co-infected lungs, causing granuloma disruption and allowing uncontrolled Mtb growth and spread. By contrast, clinical evidence shows that Mtb is responsible for the exacerbation of HIV-1 replication since co-infected patients present with increased viral load in their blood and at the anatomical site of co-infection. And yet, the mechanisms for this latter point remain poorly understood. As co-infection diagnosis and treatment is complicated due to drug interactions, a better understanding of the mechanisms contributing to the synergy between both pathogens, and the interplay with the host, is key for developing new treatment strategies.

The principal objective of my PhD project was to **identify and characterize novel factors participating in the exacerbation of HIV-1 infection by Mtb**. I focused on the role of macrophages because they are the cellular convergence point for both pathogens. In HIV-1 pathogenesis, macrophages are able to sustain HIV-1 replication independently of T cells, they are particularly long-lived after viral infection, and are part of the viral reservoir. Additionally, they actively participate in the dissemination of HIV-1 in the host.

To study the role of Mtb infection on HIV-1 replication in macrophages, I used a relevant *in vitro* model developed in the laboratory to mimic TB-associated microenvironments, which consist of harvested supernatants from either Mtb (cmMTB) or mock-infected (cmCTR) macrophages. These supernatants were used to differentiate healthy primary human monocytes towards macrophages. Alternatively, to validate the physiological pertinence of the cmMTB treatment, we also used acellular pleural effusion fluid from active TB patients (PE-TB), and made important correlations in lung biopsies of NHP co-infected with Mtb and SIV.

The first objective of my PhD project was to determine whether TB-associated microenvironments led to the exacerbation of HIV-1 replication in macrophages, and if so, to identify the cellular mechanisms involved. The completion of this objective is reflected in my first publication as a co-author, for which I made key contributions and is presented in the Results section, in chapter I. Briefly, we found that treatment with both cmMTB and PE-TB exacerbated HIV-1 infection in human macrophages. We deciphered that the induction of TNT, dependent on the IL-10/STAT3 axis, is the cellular mechanism responsible for this exacerbation. Indeed, inhibition of these structures reversed HIV-1 replication in cmMTB-treated macrophages to the level of control cells, which were less permissive to HIV-1 infection and spread.

To identify the molecular factors involved in the process described above, I assessed the gene expression landscape of cmCTR- *versus* cmMTB-treated cells by performing a genome-wide transcriptomic analysis. This approach revealed IFN-I/STAT1 as the main altered signaling pathways in

cmMTB-treated cells. Among the strongly upregulated ISG gene signature, Siglec-1 captured our attention due to it being known to enhance HIV-1 uptake and viral cell-to-cell transfer from myeloid cells to T cells. Therefore, the second objective of my PhD thesis was to understand **how the upregulation of Siglec-1 expression in a TB-associated environment participates in the exacerbation of HIV-1 infection in human macrophages** (Results section, chapter II).

For the third objective of my PhD, I focused on the IFN-I responses in cmMTB-treated macrophages. Indeed, our transcriptomic data showed that IFN-I/STAT1 pathway was the main modified signaling pathway upon cmMTB treatment. Surprisingly, cmMTB-treated cells were distinguished by the accentuation of an ISG-gene signature, which usually indicates an anti-viral state, but in our model, this signature appeared to be inefficient to control HIV-1 replication. Therefore, I tackled the unexpected ISG-gene signature obtained from the transcriptome analysis. While IFN-I are commonly thought to be antiviral, IFN-I are also recognized to be deleterious in chronic viral infections, as well as in Mtb-infection setting. Therefore, I investigated the **reasons why, in our model, IFN-I do not display their usual antiviral activity** (Results section, chapter III).

Part 2: Results

Chapter IV: Tuberculosis exacerbates HIV-1 infection through IL-10/STAT3-dependent tunneling nanotube formation in macrophages.

I. Paper summary

To date, HIV-1 infection is responsible for a global epidemic. Worsening this public health issue is the co-infection with Mtb, responsible for TB. Indeed, both pathogens act in synergy to weaken the host immune system, which leads to the acceleration of both pathogeneses. Moreover, the co-infection is difficult to diagnose since HIV-1 infection is asymptomatic and TB can present atypical features in co-infected patients [59], [694], [695]. It has been well established now that Mtb is an aggravating factor for HIV-1 pathogenesis, since co-infected patients have higher viral loads both in the blood, and at the site of co-infection [682]. While the general mechanisms explaining TB aggravation in HIV-1⁺ individuals are mainly attributed to CD4⁺ T cell depletion [675], [718], those explaining how Mtb exacerbates HIV-1 replication in co-infected hosts remain scarce.

Macrophages represent a convergent target for Mtb and HIV-1, and actively participate in the infection-associated pathogenesis. As previously mentioned in the introduction (Part I, chapter II), macrophages are important target cells for HIV-1 that strongly participate in the viral pathogenesis. Indeed, macrophages can be infected through different mechanisms, such as cell-free viruses, phagocytosis of infected cells, and cell-to-cell transfer of infectious virions [644]. Once infected, macrophages are able to actively produce new viruses, but also to store them in specific cellular compartments, the VCC [528]. Moreover, macrophages participate in the viral dissemination, since infected macrophages are found in several organs (*e.g.* brain, lungs, liver) and are part of the viral reservoir [482], [485], [491], [763]. These cells are particularly interesting due to their high plasticity: they are able to adapt to their microenvironment and to acquire certain functions, depending on the context (see preamble section I.B). Both Mtb and HIV-1 are able to manipulate the activation profile of macrophages, allowing the pathogens to thrive within the host and to escape the immune system [187], [188]. In the case of TB, my team at IPBS previously showed that TB-associated microenvironments induce the differentiation of monocytes towards “M2” macrophages [764]. More precisely, the phenotype acquired by these macrophages is driven by IL-10 present in the TB-associated microenvironment and characterized by the upregulation of CD16, CD163 and MerTK, a strong activation of STAT3, an increased capacity to migrate in dense matrices and a higher susceptibility to Mtb infection. Moreover, the team also showed that the abundance of these M(IL-10) macrophages in TB patients' blood and in the lung of Mtb-infected macaques correlated with TB disease severity [764].

Clinical evidence indicates that co-infected individuals have higher viral loads in their blood and at the anatomical site of co-infection. However, it is unknown if this phenomenon is due to the co-

infection with both Mtb and HIV-1 in the same macrophage, and such an observation has only been reported once *in vivo* in a model of NHP co-infection with Mtb and SIV [752], suggesting that this is a rare event. Therefore, we hypothesized that the exacerbation of the viral replication in macrophages is due to a bystander effect of Mtb-infection. In this first study, we asked whether the M(IL-10) activation profile of macrophages was sustained during subsequent HIV-1 infection and if it could affect the viral replication. We showed that TB-associated microenvironments, mimicked with either supernatant from Mtb-infected macrophages (cmMTB) or pleural effusion fluids from TB patient (PE-TB), increase both the rate of HIV-1 infection of macrophages (3x-fold) and the viral replication (4x-fold) compared to control cells. This phenomenon is specific of Mtb infection since the conditioning of monocytes with pleural effusion from patients with cancer or heart failure did not induce the exacerbation of HIV-1 replication in these cells. We also confirmed that the M(IL-10) phenotype is conserved after HIV-1 infection, and looked for the mechanism(s) involved in the exacerbation of the viral replication. First, we found that the viral entry was not enhanced in cmMTB-macrophages, while we observed an increase in CCR5 and CXCR4 cell-surface expression. Second, the expression level of the main restriction factors (*i.e.* IFITM, SAMHD1 and C/EBP β) were not affected in cmMTB-treated cells; neither was the autophagic response of these cells. By contrast, we finally observed that cmMTB conditioning triggered the formation of TNT (see chapter II, section III.D.e.). Both thin (F-actin containing TNT, usually with a diameter < 0.7 μ m) and thick (F-actin and microtubule-containing TNT, with a diameter > 0.7 μ m allowing them to transport small organelles such as mitochondria or vesicles) were induced by cmMTB, and further enhanced upon HIV-1 infection. This increased formation of TNT is responsible for the enhanced viral replication and dissemination, since the pharmacological inhibition of these structures by a published inhibitor (TNTi) [669] reversed the infection levels to that of cmCTR-cells (cells differentiated with the supernatant of mock-infected macrophages). Finally, by pharmacologically inhibiting STAT3, and by replacing cmMTB conditioning by an IL-10 treatment for 3 days prior to HIV-1 infection, we identified the IL-10/STAT3 axis as the pathway involved in TNT formation.

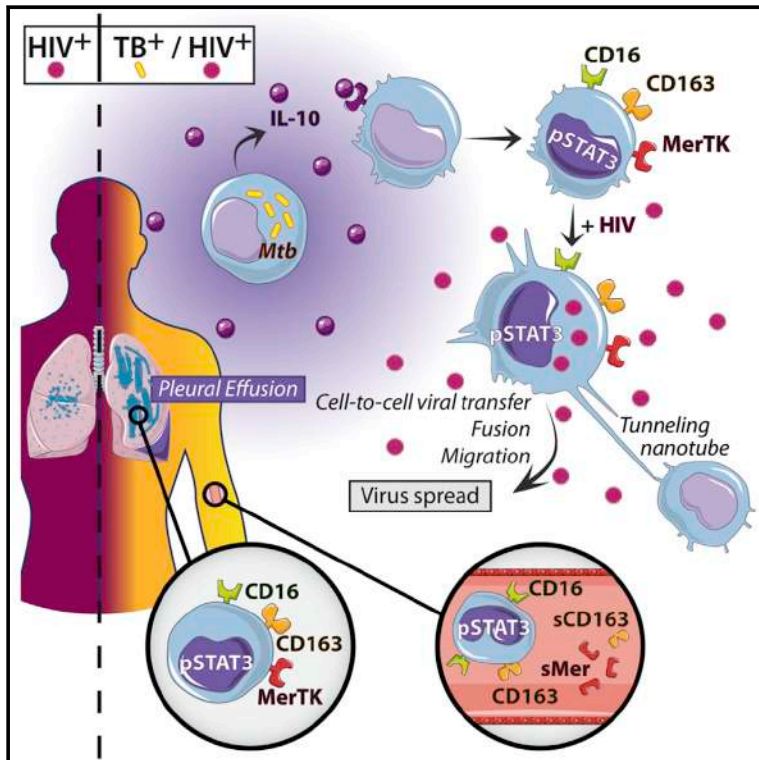
During TB pathogenesis, the number of CD14⁺CD16⁺ monocytes is increased in the blood of Mtb-infected [764]. Here, we assessed the presence of this population, and more particularly the presence of M(IL-10) by measuring the soluble form of MerTK and CD163 (sMerTK and sCD163 respectively), which are both subject to shedding and characteristic of M(IL-10) macrophages. We found an increased level of both soluble markers in the plasma of TB patient, which was further enhanced in TB-HIV-1 co-infected patients compared to healthy subjects. In addition, the number of CD163⁺ macrophages, which were also pSTAT3⁺, in the lungs of healthy, SIV-infected, Mtb-infected or Mtb-SIV co-infected macaques correlated with the disease severity, which was the strongest in co-infected animals. Therefore, the cmMTB-model is relevant to mimic the *in vivo* pathology in the context of co-infection.

In this study, we evidenced that in the context of TB-HIV-1 co-infection, the microenvironment associated to Mtb-infection renders macrophages highly susceptible to HIV-1 infection and replication through the formation of TNT, which favour the viral dissemination from one cell to another.

II. Results

Tuberculosis Exacerbates HIV-1 Infection through IL-10/STAT3-Dependent Tunneling Nanotube Formation in Macrophages

Graphical Abstract



Authors

Shanti Souriant, Luciana Balboa, Maeva Dupont, ..., Isabelle Maridonneau-Parini, Geanncarlo Lugo-Villarino, Christel V erollet

Correspondence

lugo@ipbs.fr (G.L.-V.), verollet@ipbs.fr (C.V.)

In Brief

Tuberculosis is a clear, yet confounding, risk factor for HIV-1-induced morbidity and mortality. In this issue, Souriant et al. reveal that a tuberculosis-associated microenvironment triggers IL-10/STAT3-dependent tunneling nanotube formation in M(IL-10) macrophages, which promotes HIV-1 exacerbation during co-infection. M(IL-10) macrophage accumulation is also observed *in vivo* in co-infected subjects.

Highlights

- TB-induced anti-inflammatory M(IL-10) macrophages are prone to HIV-1 overproduction
- Tunneling nanotubes between TB-induced M(IL-10) macrophages promote HIV-1 spread
- The IL-10/STAT3 axis triggers tunneling nanotube induction in the TB microenvironment
- M(IL-10) macrophages accumulate in TB/HIV co-infected patients and non-human primates



Tuberculosis Exacerbates HIV-1 Infection through IL-10/STAT3-Dependent Tunneling Nanotube Formation in Macrophages

Shanti Souriant,^{1,2} Luciana Balboa,^{2,3} Maeva Dupont,^{1,2} Karine Pingris,¹ Denise Kviatcovsky,^{2,3} Céline Cougoule,^{1,2} Claire Lastrucci,^{1,4} Aicha Bah,¹ Romain Gasser,⁵ Renaud Poincloux,¹ Brigitte Raynaud-Messina,¹ Talal Al Saati,⁶ Sandra Inwentarz,⁷ Susana Poggi,⁷ Eduardo Jose Moraña,⁷ Pablo González-Montaner,⁷ Marcelo Corti,⁸ Bernard Lagane,⁵ Isabelle Vergne,¹ Carolina Allers,^{9,10} Deepak Kaushal,^{9,10} Marcelo J. Kuroda,^{9,10,12} Maria del Carmen Sasiain,^{2,3} Olivier Neyrolles,^{1,2,11} Isabelle Maridonneau-Parini,^{1,2,11} Geanncarlo Lugo-Villarino,^{1,2,11,13,*} and Christel Vérollet^{1,2,11,*}

¹Institut de Pharmacologie et Biologie Structurale, IPBS, Université de Toulouse, CNRS, UPS, Toulouse, France

²International Associated Laboratory (LIA) CNRS “IM-TB/HIV” (1167), Toulouse, France, and Buenos Aires, Argentina

³Institute of Experimental Medicine–CONICET, National Academy of Medicine, Buenos Aires, Argentina

⁴Centre for Genomic Regulation, Barcelona, Spain

⁵Centre de Physiopathologie de Toulouse Purpan, INSERM UMR 1043, CNRS UMR 5282, Université Toulouse III Paul Sabatier, Toulouse, France

⁶INSERM/UPS/ENVT–US006/CREFRE, Service d’Histopathologie, CHU Purpan, 31024 Toulouse, France

⁷Instituto de Tisiología “Raúl F. Vaccarezza,” Universidad de Buenos Aires, Argentina

⁸Division de SIDA, Hospital de Infecciosas Dr. F.J. Muñiz, Buenos Aires, Argentina

⁹Tulane National Primate Research Center, Covington, LA 70433, USA

¹⁰Department of Microbiology and Immunology, School of Medicine, Tulane University, New Orleans, LA 70112, USA

¹¹These authors contributed equally

¹²Present address: Center for Comparative Medicine and California National Primate Research Center, University of California, Davis, Davis, CA 95616, USA

¹³Lead Contact

*Correspondence: lugo@ipbs.fr (G.L.-V.), verollet@ipbs.fr (C.V.)
<https://doi.org/10.1016/j.celrep.2019.02.091>

SUMMARY

The tuberculosis (TB) bacillus, *Mycobacterium tuberculosis* (Mtb), and HIV-1 act synergistically; however, the mechanisms by which Mtb exacerbates HIV-1 pathogenesis are not well known. Using *in vitro* and *ex vivo* cell culture systems, we show that human M(IL-10) anti-inflammatory macrophages, present in TB-associated microenvironment, produce high levels of HIV-1. *In vivo*, M(IL-10) macrophages are expanded in lungs of co-infected non-human primates, which correlates with disease severity. Furthermore, HIV-1/Mtb co-infected patients display an accumulation of M(IL-10) macrophage markers (soluble CD163 and MerTK). These M(IL-10) macrophages form direct cell-to-cell bridges, which we identified as tunneling nanotubes (TNTs) involved in viral transfer. TNT formation requires the IL-10/STAT3 signaling pathway, and targeted inhibition of TNTs substantially reduces the enhancement of HIV-1 cell-to-cell transfer and overproduction in M(IL-10) macrophages. Our study reveals that TNTs facilitate viral transfer and amplification, thereby promoting TNT formation as a mechanism to be explored in TB/AIDS potential therapeutics.

INTRODUCTION

Worldwide, individuals co-infected with *Mycobacterium tuberculosis* (Mtb), the agent of tuberculosis (TB), and the AIDS virus, HIV-1, pose particular clinical challenges not only because a significant proportion of co-infected patients remain sputum smear-negative, hampering TB diagnosis, but also because HIV-1 infection makes these individuals more prone to TB reactivation (World Health Organization [WHO] TB 2016, Joint United Nations Programme on HIV and AIDS [UNAIDS] Report 2016) (Getahun et al., 2007). At the heart of this problem is the synergy between HIV-1 and Mtb, which interferes with treatment and promotes the pathogenesis of both pathogens (Diedrich and Flynn, 2011; Diedrich et al., 2016). On the one hand, CD4⁺ T cell decay and other mechanisms induced by HIV-1 are a leading cause for reactivation of latent TB and progression to active TB disease in AIDS patients (Bell and Noursadeghi, 2018; Tomlinson et al., 2013). On the other hand, clinical and epidemiological data clearly identify TB as a risk factor amplifying HIV-1-associated morbidity and mortality (Toossi, 2003). However, the mechanisms by which Mtb exacerbates HIV-1 infection require further investigation (Charles and Shellito, 2016; Esmail et al., 2018; Toossi, 2003; Bell and Noursadeghi, 2018). Addressing this issue should help in developing strategies for the attenuation of viral activation in co-infected subjects and for a better control of the AIDS epidemic (Diedrich and Flynn, 2011).



Lung macrophages are the primary host cells for Mtb (O'Garra et al., 2013; Russell et al., 2010). While CD4⁺ T cells are the major target cells for HIV-1, macrophages, including those in the lungs, are also infected by HIV-1 in humans (Bell and Noursadeghi, 2018; Cribbs et al., 2015) and by simian immunodeficiency virus (SIV) in experimentally infected non-human primates (NHPs) (Avalos et al., 2016). Recent data indicate that macrophages play an important role in HIV-1 pathogenesis (Honeycutt et al., 2016, 2017; Sattentau and Stevenson, 2016) and may also be involved in HIV-1/Mtb co-infection (Khan and Divangahi, 2018; Kuroda et al., 2018). In HIV-1-infected individuals with active TB, for example, macrophages from the lungs and pleural effusions (PEs) exhibit high levels of HIV-1 infection (Lawn et al., 2001; Toossi, 2003). Furthermore, Mtb increases the level of HIV-1 infection either *in vitro* in monocyte-derived macrophages or *ex vivo* in lung macrophages obtained from patients with HIV-1 (Mancino et al., 1997; Toossi et al., 1997). It is presently unclear how a TB-associated microenvironment renders macrophages more susceptible to HIV-1.

Macrophages display considerable heterogeneity in tissues (Gordon et al., 2014). The broad spectrum of pro- (M1) and anti-inflammatory (M2) activation programs are a manifestation of the different levels of response to HIV-1 and Mtb infections (Cassol et al., 2009; Lugo-Villarino et al., 2011). We have shown that active TB skews human monocyte differentiation toward M2-like macrophages, distinguished by a CD16⁺CD163⁺MerTK⁺ phenotype, as well as by increased immunomodulatory activity and Mtb permissivity (Lastrucci et al., 2015). This phenotype is dependent on the interleukin-10 (IL-10)/STAT3 signaling axis and is closely related to the so-called "M(IL-10)" activation program (Murray et al., 2014). We further reported that the abundance of M(IL-10) cells correlates with TB severity in patients and NHPs (Lastrucci et al., 2015). Herein, we investigated whether the TB-induced M(IL-10) macrophage activation program also plays a role in promoting HIV-1 infection in co-infected individuals.

RESULTS

TB-Associated Microenvironment Increases HIV-1 Infection in Human Macrophages

To determine whether HIV-1 replication is modulated in TB-induced M(IL-10) macrophages, we employed our previously described *in vitro* model (Lastrucci et al., 2015), which uses conditioned medium from either mock-infected macrophages (CmCTR) or Mtb-infected macrophages (CmMTB). CmMTB triggered primary human monocytes to differentiate into M(IL-10) macrophages, which activated STAT3, as well as acquired a CD16⁺CD163⁺MerTK⁺PD-L1⁺ receptor signature, similar to differentiated M(IL-10) macrophages observed *in vivo* (Figure S1; Lastrucci et al., 2015). When macrophages treated with either CmCTR or CmMTB were then infected with HIV-1 ADA (Figure 1A) or NLAD8 strain (data not shown) (Raynaud-Messina et al., 2018), we observed a substantial increase in viral replication, as measured by the level of the viral protein p24 in culture supernatants, only in the CmMTB-treated M(IL-10) macrophages (Figures 1B and S2A). In addition, the number of HIV-1-infected cells increased by 3-fold, as measured by the expression of the HIV-1 Gag protein (Figures 1C and 1D). The M(IL-10) receptor signature

was maintained upon HIV-1 infection (Figure S1). HIV-1 infection of macrophages enhanced their migration capacity in dense 3-dimensional matrices, together with their fusion potential, forming multinucleated giant cells (MGCs) (Orenstein, 2000; Vérollet et al., 2010, 2015a). We found that these properties, known to contribute to viral dissemination (Vérollet et al., 2015a, 2015b), were further amplified specifically in M(IL-10) macrophages infected with HIV-1 (Figures S2B–S2E).

PE fluid from TB patients (PE-TB) was used as an *ex vivo* TB-associated microenvironment model (Genoula et al., 2018). PE is observed in up to 30% of TB patients and results from infection-induced local inflammation and recruitment of leukocytes into the pleural space (Vorster et al., 2015). In co-infected patients, the formation of PE is more common than in TB patients and PE contains high viral titers, compared to serum from the same patient (Collins et al., 2002; Toossi, 2003). Unlike control PE obtained from non-TB patients (PE-non-TB), differentiation of macrophages in the presence of PE-TB (Table S1; Figure 1A) yielded the M(IL-10) phenotype (Figures S3A and S3B), similar to macrophages isolated from PE-TB (Lastrucci et al., 2015). This M(IL-10) phenotype also correlated with the high level of soluble IL-10 contained in PE-TB compared to PE-non-TB (Figure S3C). We found that cell treatment with PE-TB increased the production of HIV-1 by 6-fold and increased the number of infected macrophages and MGCs (Figures 1E–1G and S3D).

Collectively, using CmMTB- and PE-TB-conditioned macrophages as model systems, we show that HIV-1 production by M(IL-10) macrophages is enhanced in a TB-associated microenvironment.

M(IL-10) Cells Accumulate in Co-infected NHPs and Patients

To investigate M(IL-10) cells in HIV-1/Mtb co-infections, we compared, by using CD163 and pSTAT3 staining (Lastrucci et al., 2015), the number of M(IL-10) macrophages in pulmonary samples from NHPs that had been (1) co-infected with Mtb (active or latent TB) and SIV; (2) mono-infected with Mtb (active or latent TB); (3) mono-infected with SIV (Cai et al., 2015; Kuroda et al., 2018); or (4) uninfected (Tables S2 and S3). Histological staining revealed abundant CD163⁺ and nuclear pSTAT3⁺ cells in co-infected NHPs (Figures 2A and 2B). While the detection of pSTAT3 is not specific to macrophages, double-staining analysis demonstrated that most CD163⁺ alveolar macrophages were also positive for nuclear pSTAT3 (Figure 2C). The increased abundance of CD163⁺ and pSTAT3⁺ cells was correlated with the severity of lung histopathology (Table S3) and the gross pathological status of the animals, as analyzed in 30 organs (Figures 2D and 2E).

We have previously shown that CD14⁺CD16⁺ circulating monocytes have a predisposition to differentiate into M(IL-10) macrophages in patients with active TB (Lastrucci et al., 2015). Here, we confirmed that CD14⁺CD16⁺ monocytes are expanded in the peripheral blood of TB, HIV-1, and co-infected patients, compared to healthy subjects (Balboa et al., 2011; Ellery et al., 2007; Ziegler-Heitbrock, 2007) (Table S1; Figure S4A). We examined two cell surface markers characteristic of the M(IL-10) phenotype, which are selectively expressed in the monocytic lineage, CD163 and MerTK, and which are both subjected to inflammation-driven shedding (Fabriek et al., 2005; Sather

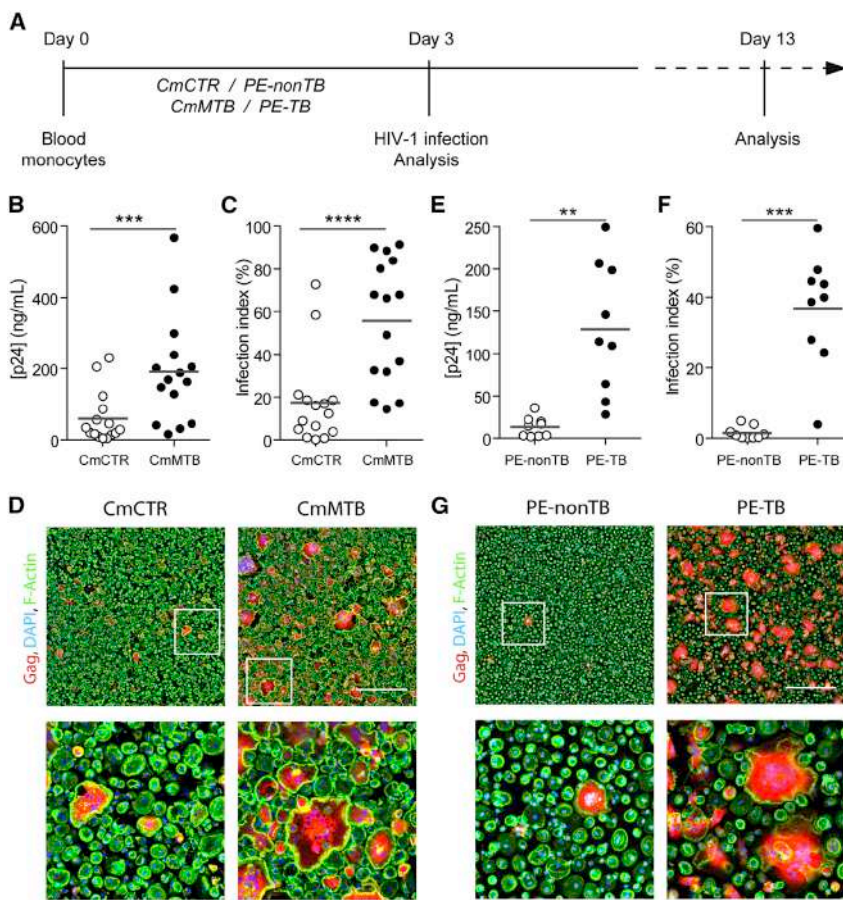


Figure 1. TB-Induced Microenvironment Exacerbates HIV-1 Infection of M(IL-10) Macrophages

(A) Representation of the experimental design of two *in vitro* models. Briefly, monocytes from healthy subjects were treated either with conditioned medium from mock-infected (CmCTR) or Mtb-infected macrophages (CmMTB), or with pleural effusions (PE) from TB (PE-TB) or non-TB (PE-nonTB) patients for 3 days. Cells were then infected with HIV-1 ADA strain at MOI of 0.1 and kept in culture for at least 10 more days.

(B) Vertical scatterplot showing p24 concentration from day 13 supernatants of HIV-1-infected macrophages treated with CmCTR or CmMTB.

(C) Vertical scatterplot showing the infection index of day 13 HIV-1-infected macrophages treated with CmCTR or CmMTB. Infection index was calculated as 100 × the ratio of the area covered by Gag⁺ cells over the total cell area, measured from immunofluorescence (IF) images.

(D) Representative IF images of day 13 HIV-1-infected macrophages treated with CmCTR or CmMTB. HIV-1 Gag (red), F-actin (green), and DAPI (blue). Scale bar, 500 μm. Insets are 4× zooms (lower panels).

(E) Vertical scatterplot showing p24 concentration from day 13 supernatants of HIV-1-infected macrophages treated with PE-TB or PE-nonTB.

(F) Vertical scatterplot showing the infection index of day 13 HIV-1-infected macrophages treated with PE-TB or PE-nonTB.

(G) Representative IF images of day 13 HIV-1-infected macrophages treated with PE-nonTB or PE-TB. HIV-1 Gag (red), F-actin (green), and DAPI (blue). Scale bar, 500 μm. Insets are 4× zooms

(lower panels). Each circle within vertical scatterplots represents a single donor. Mean value is represented as a dark gray line. In this figure, PE-nonTB are parapneumonic PE. Statistical analyses: two-tailed, Wilcoxon matched-paired signed rank test (B and C); paired t test (E and F). **p ≤ 0.005; ***p ≤ 0.0005; ****p ≤ 0.0001. See also Figures S1–S3.

et al., 2007). We found that the soluble forms of these receptors (sCD163 and sMer), but not their membrane-bound forms, were substantially increased in co-infected patients when compared to mono-infected patients and healthy subjects (Figure 3). The amount of these soluble factors correlated with one another (Figure S4B). Receiver operating characteristic (ROC) curve analyses for plasma concentration of sCD163 and sMer (Figures S4C and S4D) suggested both molecules may be useful biomarkers for co-infection.

Our findings reveal the extent of the *in vivo* expansion of TB-induced M(IL-10) cell population in co-infected individuals. They also identify potential biomarkers for diagnosis and monitoring TB in co-infected patients.

TB-Associated Microenvironments Enhance Tunneling Nanotube Formation

TB-associated microenvironment could increase the level of HIV-1 in M(IL-10) macrophages by modulating viral (1) entry, (2) replication, (3) clearance, (4) infectivity of the produced virions, and/or (5) cell-to-cell transmission. We tested each of these possibilities in turn. Although cell-surface expression of the HIV-1 entry receptors CD4, CCR5, and CXCR4 was increased in

CmMTB-treated cells compared to control cells (Figure 4A), virus entry was unchanged in these cells, as shown using the BlamVpr fusion assay (Cavrois et al., 2002) (Figure 4B). The expression level of several host factors known to be involved in HIV-1 replication (CEBP-β and CUGBP1) or restriction (IFITM proteins and SAMHD1) was not modified by CmMTB (Figures 4C–4F). As autophagy represents a viral clearance mechanism known to be inhibited by HIV-1 or Mtb infection in macrophages (Espert et al., 2015), we measured the autophagic flux and found it to be similar between CmMTB- and CmCTR-treated cells (Figure 4G). Furthermore, the infectivity of viruses produced in CmMTB conditions was comparable to those produced in CmCTR-treated cells (7.7% ± 2.1% of p24-positive TZM-bl [Vérollet et al., 2015a] for CmMTB-treated macrophages versus 10.3% ± 3.5% for CmCTR-treated cells; n = 3; p = 0.5066).

Finally, we investigated whether cell-to-cell virus transfer was influenced by TB-associated microenvironment. Tunneling nanotube (TNT) formation has been proposed as a macrophage-to-macrophage transmission process for host and microbial material (Dupont et al., 2018; Eugenin et al., 2009; Hashimoto et al., 2016; Okafo et al., 2017). Importantly, TNT formation is triggered by HIV-1 infection of macrophages and it has been associated with

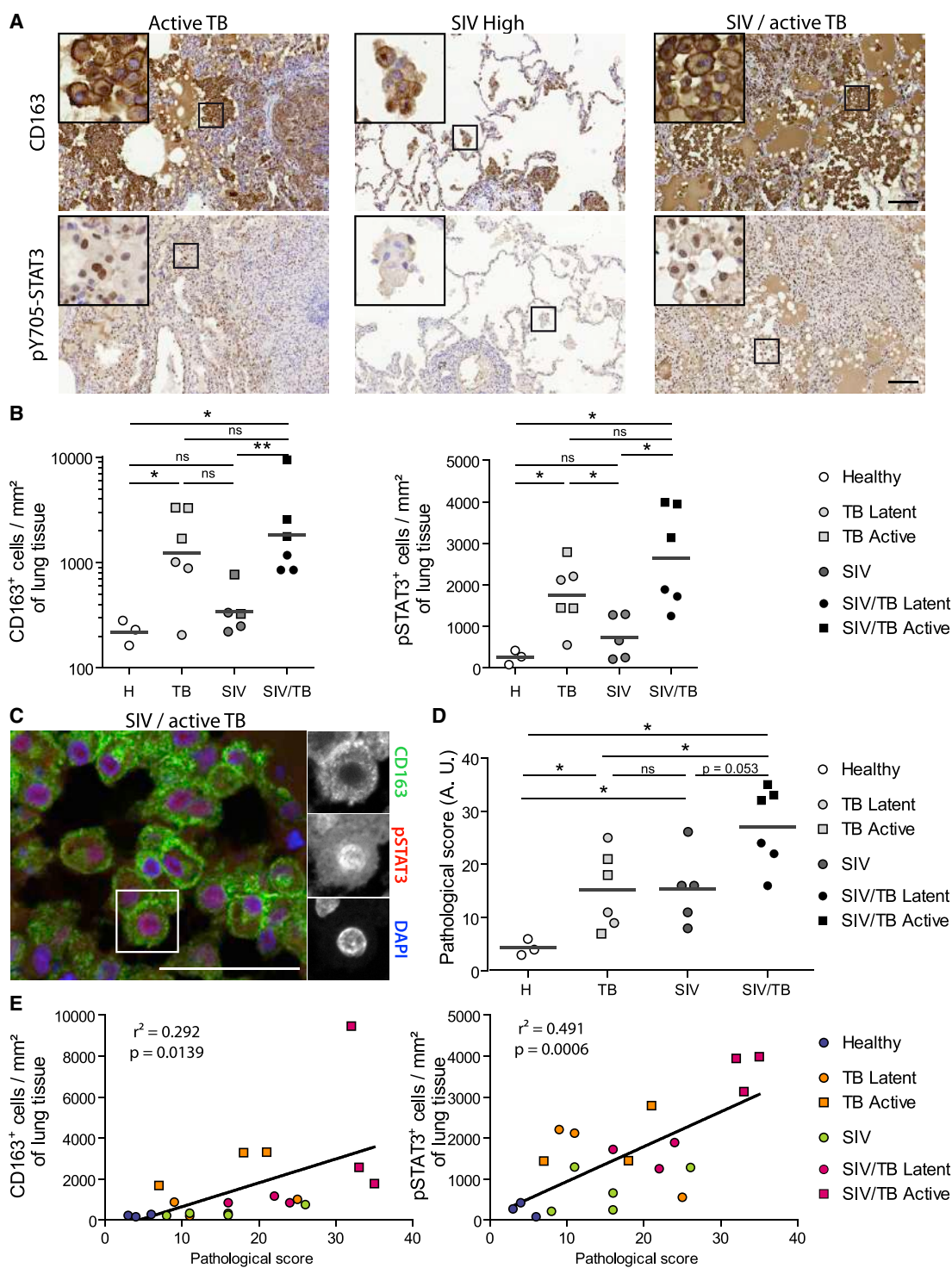


Figure 2. Accumulation of M(IL-10) Macrophages in the Lung of Co-infected NHPs Correlates with Pathology

(A) Representative immunohistochemical images illustrate higher number of CD163⁺ cells and p-STAT3⁺ cells in lung biopsies of SIV-Mtb-infected NHPs compared to Mtb or SIV mono-infected NHPs. Scale bar, 100 μ m. Insets are 4 \times zooms.

(B) Quantification of the number of CD163⁺ cells (left) and p-STAT3⁺ cells (right) per square millimeter of lung tissue of healthy (H), SIV-infected, Mtb-infected, and SIV-Mtb-co-infected NHPs.

(C) Immunohistochemistry staining of lung biopsy of SIV-Mtb co-infected NHP showing the nuclear localization of p-STAT3 (red, center) in CD163 alveolar macrophages (green, top). Nuclei are stained using DAPI (blue, bottom). Scale bar, 50 μ m. Insets are 1.3 \times zooms.

(legend continued on next page)

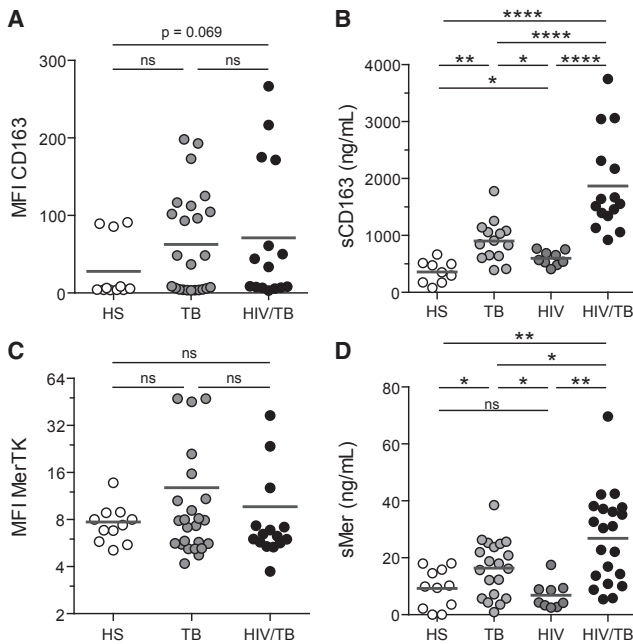


Figure 3. Systemic Expansion of the M(IL-10) Monocyte Population in Co-infected Patients

(A) Vertical scatterplots showing the median fluorescence intensity (MFI) of cell-surface marker CD163 on CD14⁺ monocytes from peripheral blood (PB) of healthy subjects, TB patients (TB), and HIV/Mtb co-infected patients (HIV/TB).

(B) Vertical scatterplots showing the amount of sCD163, the cleaved form of CD163 in the serum of healthy subjects and TB, HIV, and HIV/TB patients.

(C) Vertical scatterplots showing the MFI of cell-surface marker MerTK on CD14⁺ monocytes from PB of healthy subjects and TB and HIV/TB patients.

(D) Vertical scatterplots showing the amount of sMer, the cleaved form of MerTK, in the serum of healthy subjects and TB, HIV, and HIV/TB patients. Each circle within vertical scatterplots represents a single donor. Mean value is represented as a dark gray line.

Statistical analyses: two-tailed, Mann-Whitney (A–C); unpaired t test (D). * $p \leq 0.05$; ** $p \leq 0.005$; *** $p \leq 0.0005$; ns, not significant. See also Figure S4 and Table S1.

an increase in viral replication (Eugenin et al., 2009; Hashimoto et al., 2016). TNTs are long-range membranous F-actin-containing tubes, not in contact with the extracellular substrate, which are classified into two types based on their thickness and on whether they contain microtubules (Ariazi et al., 2017; Dupont et al., 2018; McCoy-Simandle et al., 2016; Onfelt et al., 2006) (Figure 5A). Treatment with CmMTB increased the percentage of cells forming both types of TNTs by more than 2-fold (Figures 5A and 5B), compared to CmCTR-treated cells, and HIV-1 infection further amplified this phenomenon (Figures 5B and 5C).

Using different microscopy approaches, we further characterized TNTs in macrophages as induced by TB-associated

microenvironment. TNTs are (1) long (up to 200 μm in length), actin-containing structures connecting two cells, which are above the surface of the substrate (Figures 5D, S5A, and S5B; Videos S1 and S2) (Dupont et al., 2018); (2) positive for M-Sec, a regulator of TNT formation (Hase et al., 2009) (Figure S5C; Video S4); and (3) inhibited by cytochalasin D treatment ($39\% \pm 5\%$ of TNTs in HIV-1-infected CmMTB-treated macrophages versus $6\% \pm 4\%$ upon 2 μM Cytochalasin D treatment; $n = 3$; $p = 0.0003$). We also observed that CmMTB-induced TNTs contained HIV-1 material and particles (Figures 5E and 5F; Video S3). Of note, we detected putative TNT-like structures in pulmonary samples from NHPs co-infected with Mtb and SIV, as revealed by H&E staining, or by immunohistochemistry targeting CD163-positive macrophages (Figure S5D).

Taken together, these data indicate that TB-associated microenvironments do not affect the entry, replication, or turnover of HIV-1. Instead, they trigger the formation of TNTs in M(IL-10) macrophages that appear to contain HIV-1 particles.

IL-10/STAT3 Promotes TNTs and Increased Viral Production in Macrophages

We have previously reported that the expansion of M(IL-10) macrophages relies on the IL-10/STAT3 signaling pathway (Lastrucci et al., 2015). To study how TB-associated microenvironment triggers the formation of TNTs in macrophages, we examined whether IL-10/STAT3 signaling was required for TNT formation and increased HIV-1 production induced by TB-associated microenvironment. Recombinant IL-10 triggered M(IL-10) macrophage differentiation (Lastrucci et al., 2015) (Figure S6A), increased TNT formation (Figure 6A) and recapitulated the TB-driven expansion of HIV-1 infection, as measured by p24 release, number of infected cells (Figure 6B), and formation of MGCs (Figure S6B). Depletion of IL-10 from CmMTB abolished enhanced TNT formation, the increase in HIV-1 replication in M(IL-10) cells, and the increase in MGCs (Figures 6C, 6D, and S6C). We examined the role of STAT3 activation by pharmacological inhibition with Stattic, which targets the STAT3 SH2 domain to prevent association with upstream kinases and abrogates STAT3 phosphorylation and the associated M(IL-10) phenotype (Lastrucci et al., 2015). Stattic treatment inhibited both the CmMTB-driven TNT formation and the increase in HIV-1 production (Figures 6E and 6F), along with enhanced cell migration and formation of MGCs (Figures S2E and S6D). Of note, treatment of monocytes with other cytokines prior to HIV-1 infection does not trigger TNT formation significantly, indicating that IL-10 is one of the main factors involved in this process (Figure S6E).

Our data demonstrate that TB-associated microenvironment controls TNT formation and increase HIV-1 infection in macrophages. In addition, they reveal the IL-10/STAT3 axis as a signaling pathway involved in TNT formation.

(D) Vertical scatterplot showing the pathological scoring of NHPs used in this study (see Table S3).

(E) Correlation between CD163⁺ cells (left) or p-STAT3⁺ cells (right) per square millimeter of lung tissue and pathological score in the indicated NHPs. Each symbol within vertical scatterplots represents a single animal. Mean value is represented as a dark gray line.

Statistical analyses: two-tailed Mann-Whitney (B and D). * $p \leq 0.05$; ** $p \leq 0.005$; ns, not significant. See also Tables S2 and S3.

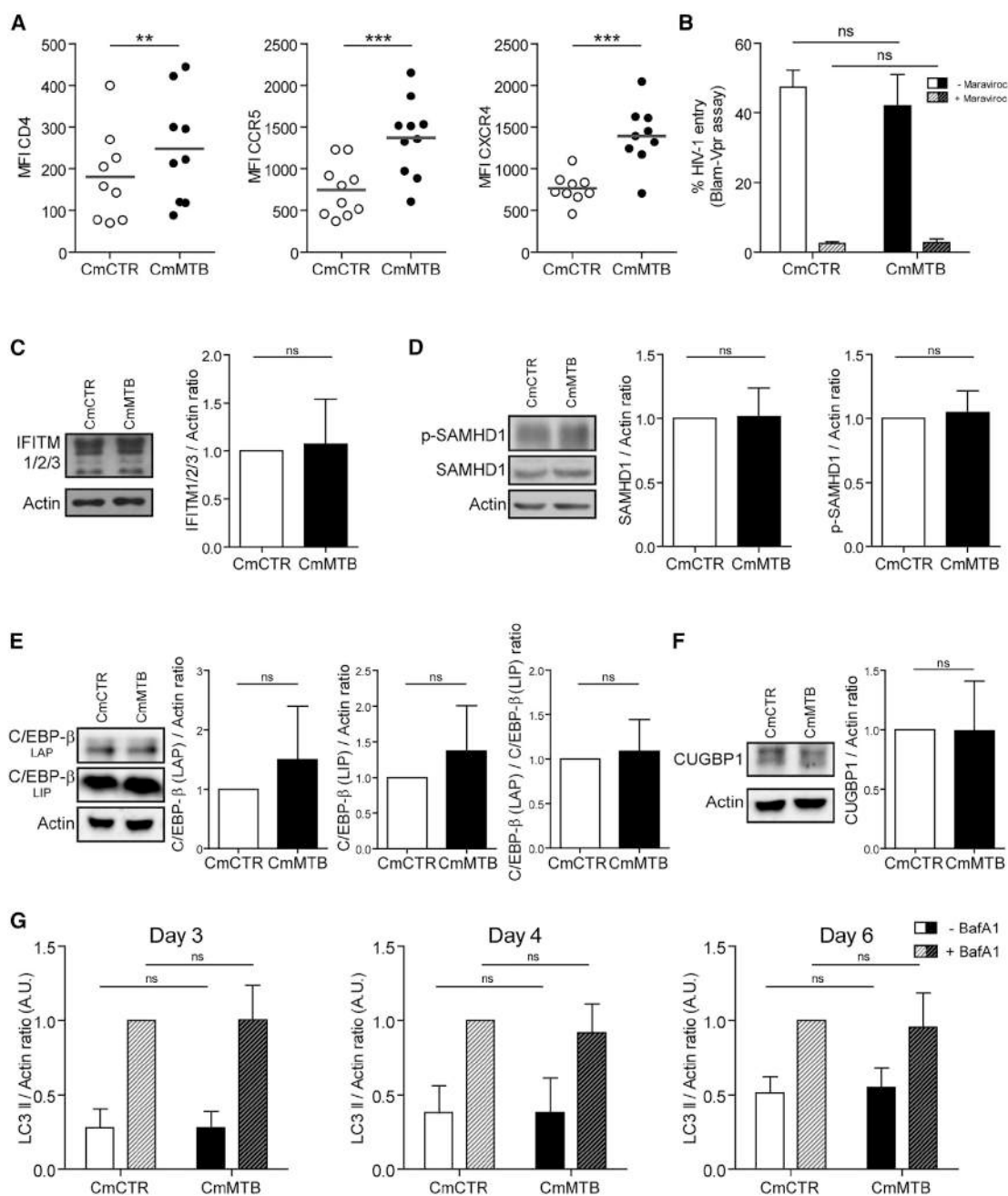


Figure 4. The TB-Driven Exacerbation of HIV-1 Infection in Macrophages Is Not Due to Modulation in Viral Entry, HIV-1-Related Activation or Restriction Factors, or Autophagy

(A) Vertical scatterplots showing the median fluorescence intensity (MFI) of cell-surface receptors involved in HIV-1 entry (CD4, CCR5, CXCR4) on monocytes differentiated for 3 days under the presence of CmCTR and CmMTB. Each circle within vertical scatterplots represents a single donor. Mean value is represented as a dark gray line.

(B) Histogram showing the percentage of HIV-1 fusion with CmCTR (white)- or CmMTB (black)-pre-treated cells, as determined using the Blam-Vpr assay in the presence of entry inhibitor Maraviroc (dashed bars).

(C) Left: representative images of western blot analysis illustrating the expression of IFITM1/2/3 and Actin as loading control. Right: quantification of IFITM1/2/3 expressed as a ratio related to actin of monocytes differentiated for 3 days into macrophages under the presence of CmCTR (white) and CmMTB (black). n = 6 donors.

(D) Representative images of western blot analysis illustrating the expression of SAMHD1 and its phosphorylated version (pSAMHD1), and Actin as loading control (left). Quantification of SAMHD1 (center) pSAMHD1 (right) expressed as a ratio related to actin of monocytes differentiated for 3 days into macrophages under the presence of CmCTR and CmMTB. n = 11 donors.

(legend continued on next page)

TNTs Participate in the High Viral Production in M(IL-10) Macrophages

To determine whether TNT formation is involved in the increased HIV-1 production in M(IL-10) macrophages, we used a previously described pharmacological inhibitor of TNT formation, TNTi (Hashimoto et al., 2016). We observed that TNTi inhibited the TNT-mediated transfer of fluorescent material between DiO-stained cells and CellTracker-positive cells (Figure S7A), without affecting macrophage viability, or F-actin-dependent processes like podosome formation and phagocytosis (Mardonneau-Parini, 2014) (Figures S7B–S7E). In TB-induced M(IL-10) macrophages infected with HIV-1, TNTi strongly inhibited TNT formation (Figure 7A), significantly diminished HIV-1 overproduction (Figure 7B), and reduced MGC formation (Figure S7F).

Unlike in T lymphocytes, the transfer of HIV-1 particles via TNTs has been suggested but not formally demonstrated in macrophages (Dupont et al., 2018; Eugenin et al., 2009; Hashimoto et al., 2016; Okafo et al., 2017). Thus, we set up a co-culture system between M(IL-10) macrophages to assess the transfer of the viral Gag protein from infected donor cells to uninfected recipient cells. Uninfected (recipient, CellTracker⁺, green) and HIV-1-infected (donor, Gag⁺, red) macrophages were either co-cultured or separated by a transwell membrane that blocks cell-to-cell connections (Figure 7C). Importantly, TNT quantification showed that productively infected macrophages preferentially formed TNT (38% ± 6% of TNT formation in Gag⁺ cells compared to 21% ± 7% in non-infected CellTracker⁺ cells; n = 5; p = 0.0003). After 24 h in co-culture, we observed that donor macrophages were able to transfer the virus to recipient macrophages, which became HIV-1 positive (Figure 7D; Videos S5 and S6). By contrast, the transfer of HIV-1 from donor to recipient macrophages was blocked in the transwell cultures (Figure 7E), showing that cell-to-cell contacts are involved in this process. In co-culture experiments, TNTi significantly diminished the capacity of M(IL-10) macrophages to transfer HIV-1 to recipient cells (Figure 7E), indicating that TNT formation is responsible for cell-to-cell viral spread.

These results establish a role for TNTs in spreading the virus between M(IL-10) macrophages, uncovering a key cellular mechanism responsible for HIV-1 overproduction in the context of TB.

DISCUSSION

TB is the most common co-infection among people living with HIV-1 and is a leading cause of AIDS-related deaths. Here, we

asked whether TB-associated microenvironment influences the control of HIV-1 infection in human macrophages. We report that M(IL-10) macrophages (CD163⁺MerTK⁺CD16⁺pSTAT3⁺), which accumulate in TB patients and can be derived *in vitro* from TB-associated microenvironment, are highly permissive for HIV-1 production. This exacerbation of HIV-1 infection involves the IL-10/STAT3 signaling axis, which controls TNT formation, thus enhancing cell-to-cell transfer of the virus in our experimental systems. *In vivo*, M(IL-10) cells are more abundant in co-infected individuals compared to mono-infection settings. We have identified potential biomarkers, sCD163 and sMer, in the blood of co-infected patients, which could be used to monitor disease progression, as their expression correlates with the severity of the pathology. All things considered, our study makes three important contributions to the general understanding of how TB exacerbates HIV-1 infection.

First, we show that M(IL-10) macrophages (CD163⁺pSTAT3⁺) accumulate in co-infected patients and NHPs. In co-infected NHPs, we observe M(IL-10) macrophages in great abundance in the lung environment, including the alveolar space and the lung interstitial tissue. M(IL-10) macrophage abundance in lungs is correlated with the pathological score of the animals, arguing for the physiological and pathological pertinence of these macrophages. These macrophages are likely driven by the IL-10/STAT3 signaling pathway and originate from CD14⁺CD16⁺ monocytes (Lastrucci et al., 2015), which are increased in the blood of patients with active TB, regardless of their HIV-1 infection status (Ziegler-Heitbrock, 2007). Monocytes are the only circulating leukocytes known to express membrane-bound CD163 and MerTK (Fabriek et al., 2005; Sather et al., 2007). As these membrane receptors are subjected to inflammation-driven shedding (Fabriek et al., 2005; Sather et al., 2007), their soluble form in the blood can be used as a proxy for estimating the abundance of CD14⁺CD16⁺ monocytes in the circulation. Here, we show that, in HIV-1⁺ patients with active TB, the plasma levels of both sCD163 and sMer are significantly higher than those found in healthy subjects, HIV-1- or Mtb-infected patients. sCD163 is already described as a clinical indicator of monocyte activation in HIV-1 patients (Burdo et al., 2011), as an indicator of lesions and accumulation of macrophages in the brain of SIV-infected NHPs (Burdo et al., 2010), and as an independent predictor of survival in TB (Knudsen et al., 2005). Although our findings will need to be expanded in larger cohorts, they nevertheless reveal both sCD163 and sMer as potential tools for the diagnosis and disease monitoring in HIV-1/Mtb co-infected patients. Because TB diagnosis in HIV-1-infected individuals remains a major

(E) Representative images of western blot analysis illustrating the expression of C/EBP-β (LAP), C/EBP-β (LIP), and Actin as loading control (left). Quantification of C/EBP-β (LAP, center left) and C/EBP-β (LIP, center right) expressed as a ratio related to actin, and LAP expressed as a ratio related to LIP (right), of monocytes differentiated for 3 days into macrophages under the presence of CmCTR and CmMTB. n = 9 donors. LAP is an activator of HIV-1-LTR, whereas LIP is a repressor of HIV-1-LTR.

(F) Representative images of western blot analysis illustrating the expression of CUGBP1 and Actin as loading control (left). Quantification of CUGBP1 expressed as a ratio related to actin (right) of monocytes differentiated for 3 days into macrophages under the presence of CmCTR and CmMTB. n = 9 donors.

(G) Quantification of LC3-II expression as a ratio to actin of monocytes differentiated for 3 days under the presence of CmCTR and CmMTB at the indicated time points after 2 h treatment with Bafilomycin A1 (BafA1) or DMSO as control, as measured by western blot analysis. Uninfected cells at day 3 of the experiment (left; n = 6 donors), and HIV-infected cells at 1 (day 4; center; n = 4 donors) and 3 (day 6; right; n = 6 donors) days post-infection. Each circle within vertical scatterplots represents a single donor. Mean value is represented as a dark gray line.

Data in histograms are represented as mean ± SD. *p ≤ 0.05; **p ≤ 0.005; ***p ≤ 0.0005; ****p ≤ 0.0001.

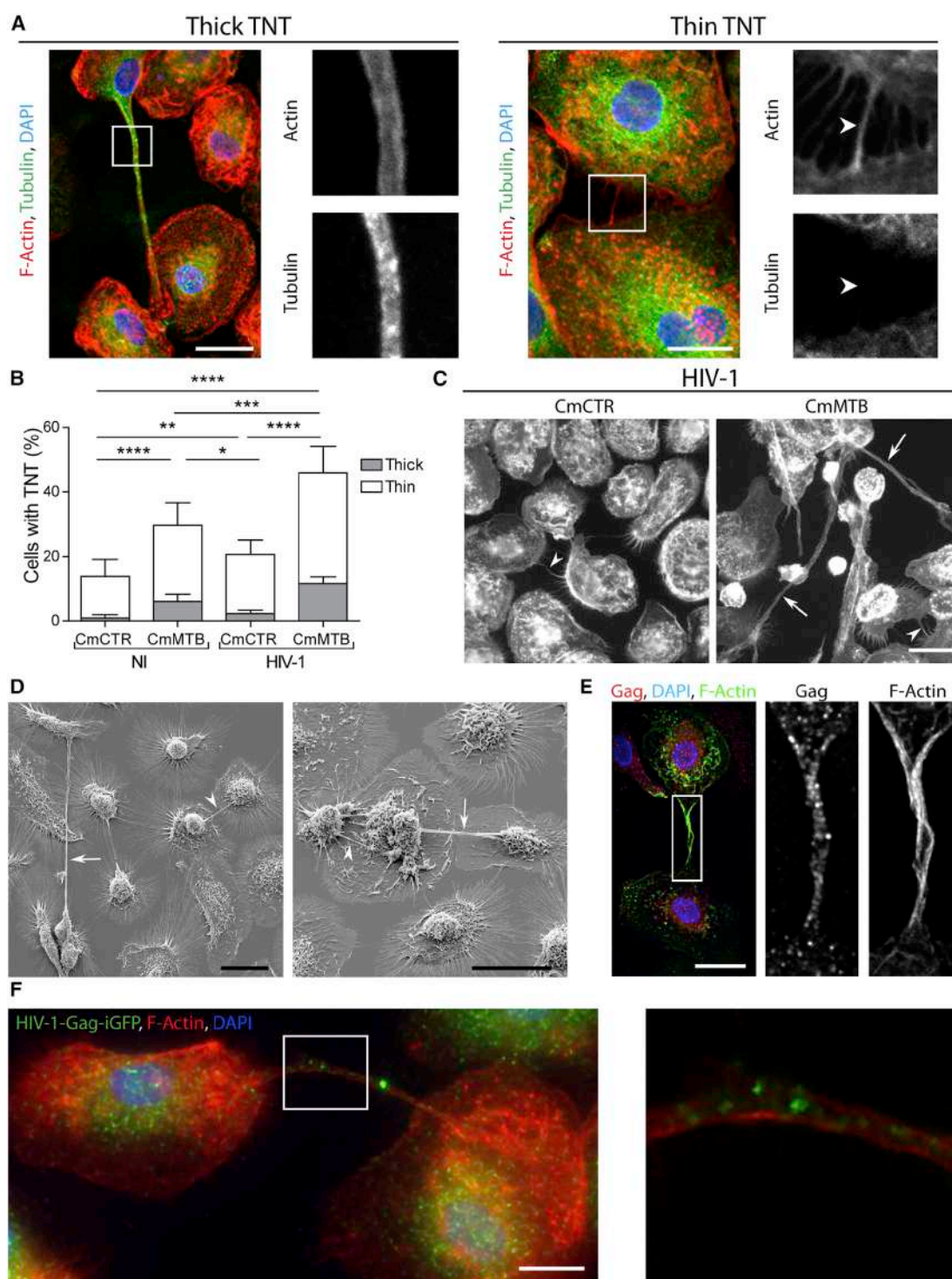


Figure 5. TB Enhances HIV-1-Induced TNT Formation

(A) Representative immunofluorescence image (IF) of macrophages interconnected through thick (left) and thin (right) TNTs. F-Actin (red), Tubulin (green), and DAPI (blue). Scale bar, 20 μ m. The arrows point at the thin TNT without microtubules.

(B) Stacked bars showing the percentage of cells with thick (gray) and thin (white) TNTs of day 6 uninfected or HIV-1-infected macrophages treated with CmCTR or CmMTB. Data in histograms are represented as mean \pm SD.

(C) Representative wide-field IF images showing F-actin staining in day 6 HIV-1-infected macrophages, treated with CmCTR or CmMTB. Arrows, thick TNTs; arrowheads, thin TNTs. Scale bar, 20 μ m.

(legend continued on next page)

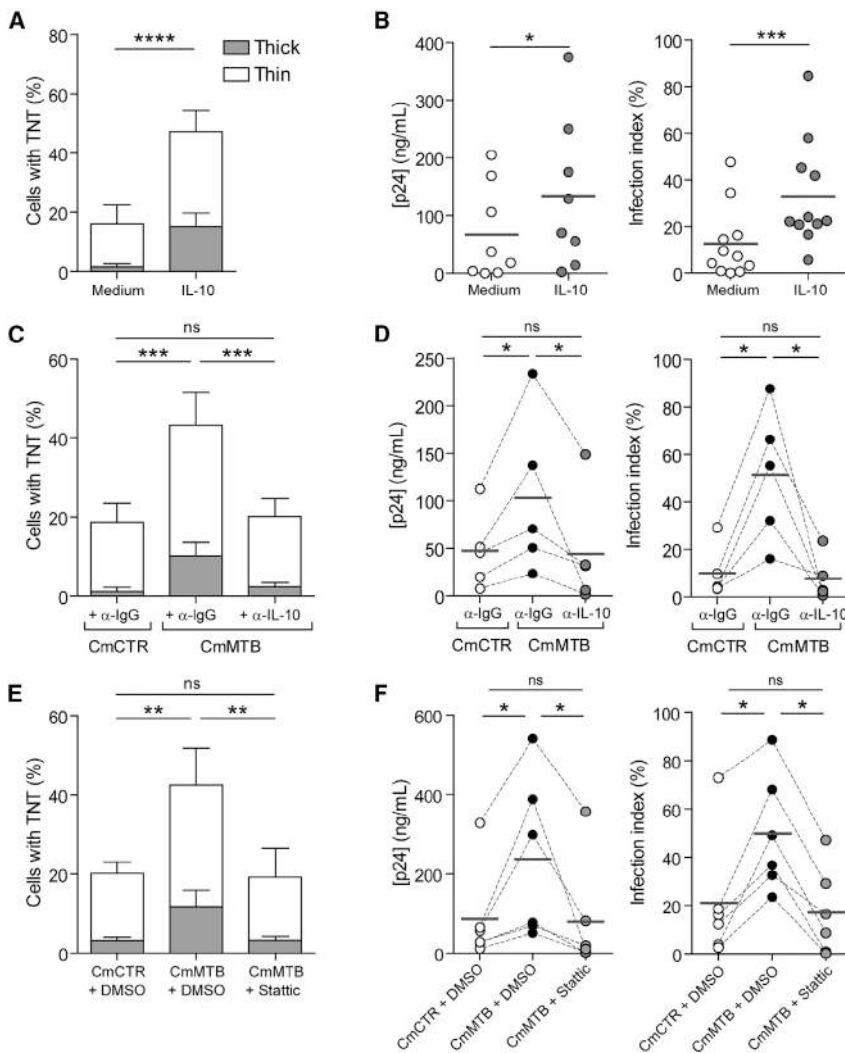


Figure 6. TB-Driven TNT Formation and Increased HIV-1 Infection Are Dependent on the IL-10/STAT3 Axis

(A) Stacked bars showing the percentage of cells with thick (gray) and thin (white) TNTs of day 6 HIV-1-infected macrophages untreated or treated with recombinant IL-10 (10 ng/mL).

(B) Vertical scatterplots showing p24 concentration (left) and infection index (right) of day 13 HIV-1-infected macrophages untreated or treated with recombinant IL-10 (10 ng/mL).

(C) Stacked bars showing the percentage of cells with thick (gray) and thin (white) TNTs of day 6 HIV-1-infected macrophages treated with IL-10-depleted (α -IL-10) CmMTB and mock depletion controls (α -IgG) of CmCTR and CmMTB.

(D) Vertical scatterplots showing p24 concentration (left) and infection index (right) of day 13 HIV-1-infected macrophages treated with IL-10-depleted (α -IL-10) CmMTB and mock depletion controls (α -IgG) of CmCTR and CmMTB.

(E) Stacked bars showing the percentage of cells with thick (gray) and thin (white) TNTs of day 6 HIV-1-infected macrophages treated with CmCTR, CmMTB, or CmMTB in the presence of the STAT3 activation inhibitor, Stattic (1 μ M).

(F) Vertical scatterplots showing p24 release (left) and infection index (right) of day 13 HIV-1-infected macrophages treated with CmCTR, CmMTB, or CmMTB in the presence of the STAT3 activation inhibitor, Stattic (1 μ M).

Statistical analyses: two-tailed, Wilcoxon matched-paired signed rank test (B and D, right, and F); paired t test (A–D, left, and E). * $p \leq 0.05$; ** $p \leq 0.005$; *** $p \leq 0.0005$; ns, not significant. See also Figures S2 and S6.

clinical challenge (Getahun et al., 2007), sCD163 and sMer may hold great promise as biomarkers in these populations.

Second, our study reveals that M(IL-10) macrophages are highly susceptible to HIV-1 infection. This is accompanied by enhanced MGC formation and protease-dependent migration capacity, which could play a role in HIV-1 dissemination (Vérollet et al., 2015b). All of these effects are fully dependent on the anti-inflammatory IL-10/STAT3 signaling pathway. Most of our work has been done with the ADA HIV-1 strain, which is a useful laboratory strain that can infect efficiently macrophages with low CD4 levels. However, these viruses are rather rare in the blood

(Joseph and Swanstrom, 2018). As infected macrophages are found in the lungs (Bell and Noursadeghi, 2018; Cribbs et al., 2015), the characterization of the types of viruses mainly found in this co-infection sites (lung and pleural cavity) (Collins et al., 2002; Nakata et al., 1997; Singh et al., 1999) would be of great interest as we would have the opportunity to assess their effect in our model. Other reports also show that Mtb infection increases HIV-1 replication *in vitro* (Diedrich and Flynn, 2011; Goletti et al., 1998; Hoshino et al., 2002; Lederman et al., 1994; Zhang et al., 1995). However, unlike our study, they show that Mtb induces a pro-inflammatory environment resulting in the auto-activation of NF- κ B, which ultimately binds the HIV-1 long terminal repeat (LTR) and initiates viral transcription in co-infected macrophages (Collins et al., 2002; Goletti et al., 1998,

(D) Scanning electron microscopy images showing TNTs of day 6 HIV-1-infected macrophages, treated with CmMTB. Arrows, thick TNTs; arrowheads, thin TNTs. Scale bar, 20 μ m.

(E) Deconvolution microscopy images showing HIV-1 Gag intra-TNT distribution in day 6 HIV-1-infected macrophages, treated with CmMTB. HIV-1 Gag (red), F-actin (green), and DAPI (blue). Scale bar, 20 μ m. Insets are 3 \times zooms.

(F) Immunofluorescence (IF) images showing viral particles in TNT of day 6 HIV-1-Gag-iGFP-infected macrophages previously treated with CmMTB. HIV-1-Gag-GFP (green), F-actin (red), and DAPI (blue). Scale bar, 10 μ m. Inset is 4 \times zoom.

Statistical analyses: two-tailed paired t test (B). * $p \leq 0.05$; ** $p \leq 0.005$; *** $p \leq 0.0005$; **** $p \leq 0.0001$; ns, not significant. See also Figure S5 and Video S3.

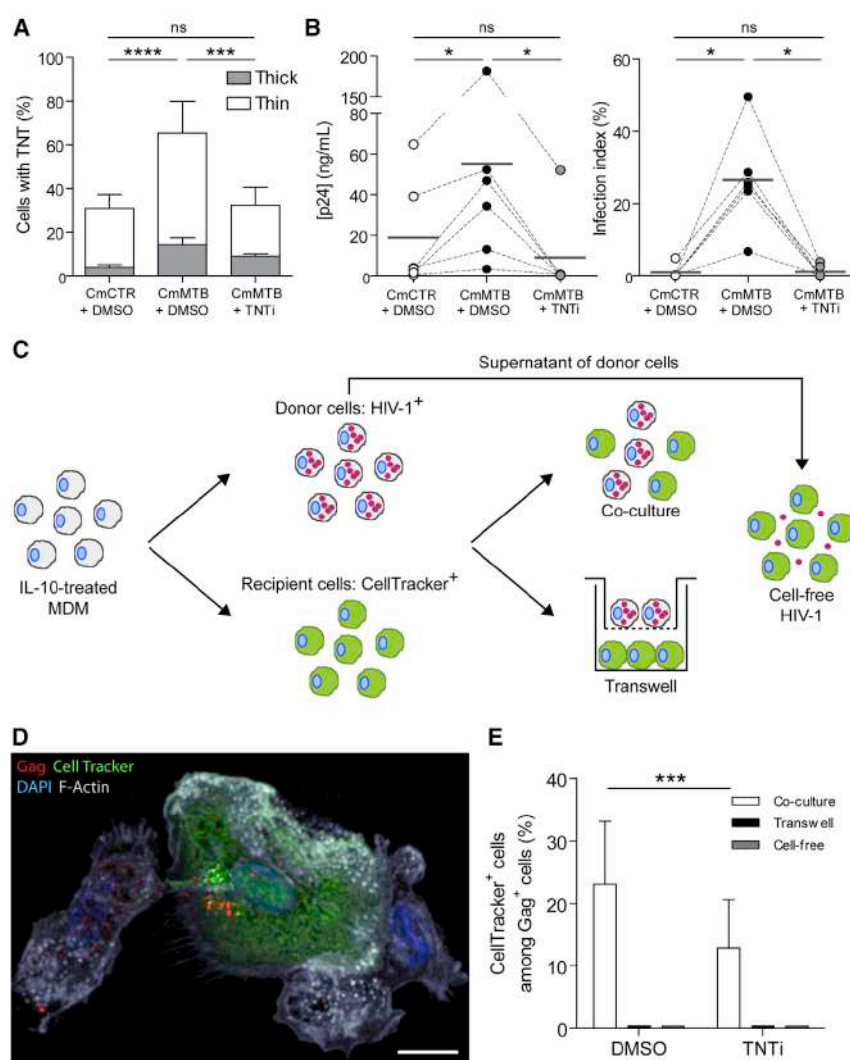


Figure 7. TB-Driven TNT Formation Is Necessary for Increased HIV-1 Infection

(A) Stacked bars showing the percentage of cells with thick (gray) and thin (white) TNTs of day 6 HIV-1-infected macrophages treated with CmCTR, CmMTB, or CmMTB in the presence of TNT inhibitor (TNTi, 20 μ M).

(B) Vertical scatterplots showing p24 release (left) and infection index (right) of day 13 HIV-1-infected macrophages treated with CmCTR, CmMTB, or CmMTB in the presence of TNTi.

(C) Experimental setup used for the co-culture (also referred to as a transfer assay), Transwell, and cell-free HIV-1 experiments. IL-10-treated macrophages were either infected with HIV-1 NLAD8-VSVG pseudotyped strain at a MOI of 5 for 48 h (donor cells) or stained with CellTracker (acceptor cells). For the co-culture experiment, donor cells were mixed with acceptor cells at a 1:1 ratio. The Transwell assay was designed to separate donor and acceptor cells to investigate the contribution of cell contact to transfer of HIV-1. The experiment was performed as described in the co-culture assay, with the exception that acceptor cells were plated in the well, and then a Transwell filter was placed containing the donor cells. Finally, to assess the contribution of cell-free infection in the propagation of HIV-1, the supernatant of donor cells (containing the virions produced during 48 h of infection) was incubated with acceptor cells. To assess the contribution of TNTs in HIV-1 transfer, all three experiments were performed in the presence or not of TNTi (20 μ M), and fixed after 24 h. The cells were stained for HIV-1 Gag protein, and the percentage of CellTracker⁺ cells among Gag⁺ cells was quantified.

(D) Deconvolution microscopy image showing HIV-1 Gag transfer into CellTracker⁺ acceptor cell after 24-h co-culture. HIV-1 Gag (red), Cell Tracker (green), F-actin (gray), and DAPI (blue). Scale bar, 10 μ m.

(E) Stacked bars showing the percentage of CellTracker⁺ cells among Gag⁺ cells after 24 h co-culture with or without TNTi (20 μ M). Data in

histograms are represented as mean \pm SD. Each circle within the vertical scatterplots represents a single donor. Mean value is represented as a dark gray line. Statistical analyses: two-tailed, paired t test (A and E); Wilcoxon matched-paired signed rank test (B). * $p \leq 0.05$; *** $p \leq 0.0005$; **** $p \leq 0.0001$; ns, not significant. See also Figure S7 and Videos S5 and S6.

2004; Hoshino et al., 2002; Lederman et al., 1994; Mancino et al., 1997; Nakata et al., 1997; Orenstein et al., 1997; Queval et al., 2016; Tanaka et al., 2005; Toossi, 2003; Zhang et al., 1995). Based on both these published observations and ours, we propose that TB exacerbates HIV-1 pathogenesis in a two-step manner: initially, by activating HIV-1 LTR transcription via short-lived pro-inflammatory signals in resident macrophages, and then by enhancing HIV-1 infection and spread in newly recruited monocytes predisposed toward the M(IL-10) phenotype, as a result of the anti-inflammatory signals induced by IL-10. This two-step model reconciles previous work done in co-infected cells and the results of our study, which is based on inherent susceptibility to HIV-1 infection observed in CD16⁺ monocytes (Ellery et al., 2007) and macrophages derived from these cells (Ancuta et al., 2006). In light of recent evidence for macrophages as targets for HIV-1 pathogenesis (Honeycutt et al., 2016, 2017;

Sattentau and Stevenson, 2016), together with the renewed appreciation of the importance of IL-10-driven anti-inflammatory program in macrophages (Ip et al., 2017), we believe that our *in vitro* model to generate M(IL-10) cells will help further characterize how TB influences viral infection of macrophages, and onward viral spread.

Third, based on our findings, we infer that TNT formation is likely a key cellular mechanism by which the IL-10/STAT3 signaling axis increases virus spread in human macrophages in a TB context. TNTs are transient membrane projections that facilitate intercellular communication to allow the transfer of endosomal cargo vesicles, calcium fluxes, and pathogens, such as bacteria, viruses, and prions (Davis and Sowinski, 2008; Dupont et al., 2018; Malik and Eugenin, 2016; McCoy-Simandle et al., 2016; Sherer and Mothes, 2008). In T cells, transmission of HIV-1 through TNTs is estimated to be approximately 100- to

1,000-fold more efficient than through classical cell-free viral infection (Sowinski et al., 2008). In macrophages, HIV-1 induces the formation of TNT via the protein Nef (Hashimoto et al., 2016; Xu et al., 2004). We confirmed that Nef is also involved in HIV-1-induced TNT formation in a TB-associated microenvironment (data not shown). Since the transmission of HIV-1 between macrophages via TNTs had not been formally demonstrated, we used here transwells to separate HIV-1-infected macrophages from uninfected macrophages, and we demonstrated that M(IL-10) macrophages are capable of transferring HIV-1 to non-infected macrophages through a cell-to-cell contact-dependent mechanism. While we cannot exclude the contribution of other cell-to-cell contact-dependent mechanisms of virus spread, such as virological synapse, cell fusion, phagocytosis, or efferocytosis (Baxter et al., 2014; Bracq et al., 2017; Jolly and Sattentau, 2004; Karaji and Sattentau, 2017), we clearly show that TNTs play a major role in this process. Pharmacological inhibition of TNT formation results in both reduced capacity of M(IL-10) macrophages to transfer viral particles and a substantial decrease of HIV-1 production. TNTs have been observed in several cell types and their formation is stimulated by different factors, including lipopolysaccharide (LPS) and interferon- γ (IFN- γ), pathogens, and oxidative stress, yet the signaling pathway(s) involved in TNT formation have not been identified (Ariazi et al., 2017; Dupont et al., 2018; Malik and Eugenin, 2016; Zhang, 2011). We reveal the IL-10/STAT3-axis as the main signaling pathway responsible for TNT formation between macrophages, providing an important contribution to this emerging field and paving the way for further elucidating the biology of TNTs. It would be interesting to find out whether TNTs could also form between M(IL-10) macrophages and other cell types, such as T or B cells, to transfer HIV-1 and/or viral material (Xu et al., 2009), which could participate in HIV-1 dissemination and pathogenesis within the co-infection context. Finally, whether TNTs are involved in MGC formation during HIV-1 infection of macrophages is suggested by a correlation between TNT formation and the number of MGCs that are formed ($r^2 = 0.7$ to 0.9). Another aspect that needs further improvement is the *in vivo* relevance of TNTs. Despite evidence for material transfer via TNT-like structures *in vivo* (Naphade et al., 2015; Rocca et al., 2017), the current lack of a specific TNT marker prevents the formal demonstration of existence of TNT *in vivo*. In pulmonary tissue lesions of co-infected NHPs, we observed TNT-like structures between CD163⁺ macrophages, suggesting that cell-to-cell transfer of HIV-1 via TNTs could also occur *in vivo*. Indeed, M(IL-10) macrophages are in close proximity to each other, particularly in the lungs of co-infected NHPs, a parameter that is critical for TNT formation and viral transmission. Taking together our results, we propose that enhanced TNT formation induced by TB-associated microenvironment in M(IL-10) macrophages favors HIV-1 cell-to-cell transmission and, consequently, could play a key role in the high HIV-1 levels usually observed at anatomical sites of co-infection (Toossi, 2003).

In conclusion, this study highlights the importance of TB-associated microenvironment in shaping the response of macrophages to HIV-1 infection. Our results are highly relevant to the investigation of the role of macrophages in the pathogenesis of HIV-1/Mtb co-infection, cell signaling pathways involved in

TNT formation, and the identification of potential biomarkers to monitor disease progression. Future research will reveal whether HIV-1 production and spread through TB-driven TNT formation occurs among M(IL-10) macrophages only, or also affects macrophage-to-T cell viral transmission (Groot et al., 2008), and whether TNT can be considered as a therapeutic target in co-infected patients.

STAR★METHODS

Detailed methods are provided in the online version of this paper and include the following:

- KEY RESOURCES TABLE
- CONTACT FOR REAGENT AND RESOURCE SHARING
- EXPERIMENTAL MODEL AND SUBJECT DETAILS
 - Human Subjects
 - NHPs
 - Bacteria
 - Viruses
 - Preparation of human monocytes and monocyte-derived macrophages
- METHODS DETAILS
 - Chemicals
 - Preparation of conditioned media and cytokine depletion
 - Conditioning of monocytes with the secretome of Mtb-infected macrophages or pleural effusions from TB patients
 - HIV-1 infection of cells
 - Blam-Vpr fusion assay
 - Flow cytometry
 - Immunofluorescence microscopy
 - HIV-1 and DiO transfer monitoring
 - Scanning electron microscopy
 - Immunoblot analyses
 - 3D migration assays
 - Protein quantifications in cell-free fluids by ELISA
 - Cytotoxicity assay
 - Phagocytosis assay
 - Histological analyses
- QUANTIFICATION AND STATISTICAL ANALYSIS

SUPPLEMENTAL INFORMATION

Supplemental Information can be found with this article online at <https://doi.org/10.1016/j.celrep.2019.02.091>.

ACKNOWLEDGMENTS

We greatly acknowledge F. Capilla and C. Salon (US006/CREFRE) and M. Ben Neji for histology analyses; M. Dubois, M. Cazabat, M. Requena, and J. Izopet (BIVic facility) and P. Constant, F. Levillain, F. Moreau, and C. Berrone (IPBS) (ASB3 and P3 multi-pathogens) for BSL3 facilities; I. Fourqueaux (CMEAB) for SEM imaging; T. Mangeat (LBCMCP) for deconvolution imaging; and A. Peixoto (IPBS) for imaging and flow cytometry analyses. The authors acknowledge the TRI-Genotoul and ANEXPLO facilities. We thank I. Gaillard and S. Caldirola (Immunology Division of the Hospital de Niños R. Gutiérrez, Buenos Aires) for their technical assistance. We greatly thank I. Staropoli and Z. Zhou (Pasteur Institute) for HIV-1 entry experiments, and C.A. Spinner

(IPBS), C. Gutierrez (IPBS), A. Moris (Cimi-Paris), and N. Iakobachvili (Maastricht University) for critical reading of the manuscript and helpful comments. This work was supported by Centre National de la Recherche Scientifique; Université Paul Sabatier; Agence Nationale de la Recherche (ANR 2010-01301, ANR14-CE11-0020-02, ANR16-CE13-0005-01, and ANR-11-EQUIPEX-0003); Agence Nationale de Recherche sur le Sida et les Hépatites Virales (ANRS2014-CI-2 and ANRS2014-049); the ECOS-Sud Program (A14S01); Fondation pour la Recherche Médicale (DEQ2016 0334894 and DEQ2016 0334902); Fondation Bettencourt Schueller, INSERM Plan Cancer; the Argentinian National Agency of Promotion of Science and Technology (PICT-2015-0055); and Alberto J. Roemmers Foundation (2016). We also thank the AIDS Research and Reference Reagent Program, Division of AIDS, NIAID. The NHP study was supported by NIH awards AI097059, AI110163, AI058609 and OD011104 to the Tulane National Primate Research Center and bridge fund by the Tulane Vice President for Research and awards by the Wetmore TB and Leprosy Foundation and the Louisiana Board of Regents. S.S. is supported by Sidaction and R.G. by ANRS.

AUTHOR CONTRIBUTIONS

Conceptualization & Methodology, S.S., L.B., M.d.C.S., O.N., I.M.-P., G.L.-V., and C.V.; Software, S.S. and R.P.; Investigation, S.S., L.B., M.D., K.P., C.L., D.K., C.C., A.B., R.G., R.P., and B.R.-M.; Resources, S.I., E.J.M., P.G.-M., S.P., and M.C.; Writing, S.S., O.N., I.M.-P., G.L.-V., and C.V.; Visualization, S.S.; Supervision, O.N., I.M.-P., G.L.-V., and C.V. Corresponding authors G.L.-V. and C.V. are responsible for ownership and responsibility that are inherent to aspects of tuberculosis (G.L.-V.) and HIV-1 (C.V.).

DECLARATION OF INTERESTS

The authors declare no competing interests.

Received: August 23, 2018
Revised: December 8, 2018
Accepted: February 21, 2019
Published: March 26, 2019

REFERENCES

Ancuta, P., Wang, J., and Gabuzda, D. (2006). CD16⁺ monocytes produce IL-6, CCL2, and matrix metalloproteinase-9 upon interaction with CX3CL1-expressing endothelial cells. *J. Leukoc. Biol.* *80*, 1156–1164.

Ariazi, J., Benowitz, A., De Biasi, V., Den Boer, M.L., Cherqui, S., Cui, H., Douillet, N., Eugenin, E.A., Favre, D., Goodman, S., et al. (2017). Tunneling nanotubes and gap junctions—their role in long-range intercellular communication during development, health, and disease conditions. *Front. Mol. Neurosci.* *10*, 333.

Avalos, C.R., Price, S.L., Forsyth, E.R., Pin, J.N., Shirk, E.N., Bullock, B.T., Queen, S.E., Li, M., Gellerup, D., O'Connor, S.L., et al. (2016). Quantitation of productively infected monocytes and macrophages of simian immunodeficiency virus-infected macaques. *J. Virol.* *90*, 5643–5656.

Balboa, L., Romero, M.M., Basile, J.I., Sabio y García, C.A., Schierloh, P., Yokobori, N., Geffner, L., Musella, R.M., Castagnino, J., Abbate, E., et al. (2011). Paradoxical role of CD16⁺CCR2⁺CCR5⁺ monocytes in tuberculosis: efficient APC in pleural effusion but also mark disease severity in blood. *J. Leukoc. Biol.* *90*, 69–75.

Baxter, A.E., Russell, R.A., Duncan, C.J., Moore, M.D., Willberg, C.B., Pablos, J.L., Finzi, A., Kaufmann, D.E., Ochsenbauer, C., Kappes, J.C., et al. (2014). Macrophage infection via selective capture of HIV-1-infected CD4⁺ T cells. *Cell Host Microbe* *16*, 711–721.

Bell, L.C.K., and Noursadeghi, M. (2018). Pathogenesis of HIV-1 and *Mycobacterium tuberculosis* co-infection. *Nat. Rev. Microbiol.* *16*, 80–90.

Bracq, L., Xie, M., Lambelé, M., Vu, L.T., Matz, J., Schmitt, A., Delon, J., Zhou, P., Randriamampita, C., Bouchet, J., and Benichou, S. (2017). T cell-macrophage fusion triggers multinucleated giant cell formation for HIV-1

spreading. *J. Virol.* Published online October 4, 2017. <https://doi.org/10.1128/JVI.01237-17>.

Burdo, T.H., Soulas, C., Orzechowski, K., Button, J., Krishnan, A., Sugimoto, C., Alvarez, X., Kuroda, M.J., and Williams, K.C. (2010). Increased monocyte turnover from bone marrow correlates with severity of SIV encephalitis and CD163 levels in plasma. *PLoS Pathog.* *6*, e1000842.

Burdo, T.H., Lentz, M.R., Autissier, P., Krishnan, A., Halpern, E., Letendre, S., Rosenberg, E.S., Ellis, R.J., and Williams, K.C. (2011). Soluble CD163 made by monocyte/macrophages is a novel marker of HIV activity in early and chronic infection prior to and after anti-retroviral therapy. *J. Infect. Dis.* *204*, 154–163.

Cai, Y., Sugimoto, C., Liu, D.X., Midkiff, C.C., Alvarez, X., Lackner, A.A., Kim, W.K., Didier, E.S., and Kuroda, M.J. (2015). Increased monocyte turnover is associated with interstitial macrophage accumulation and pulmonary tissue damage in SIV-infected rhesus macaques. *J. Leukoc. Biol.* *97*, 1147–1153.

Cassol, E., Cassetta, L., Rizzi, C., Alfano, M., and Poli, G. (2009). M1 and M2a polarization of human monocyte-derived macrophages inhibits HIV-1 replication by distinct mechanisms. *J. Immunol.* *182*, 6237–6246.

Cavrois, M., De Noronha, C., and Greene, W.C. (2002). A sensitive and specific enzyme-based assay detecting HIV-1 virion fusion in primary T lymphocytes. *Nat. Biotechnol.* *20*, 1151–1154.

Charles, T.P., and Shellito, J.E. (2016). Human immunodeficiency virus infection and host defense in the lungs. *Semin. Respir. Crit. Care Med.* *37*, 147–156.

Collins, K.R., Quiñones-Mateu, M.E., Wu, M., Luzze, H., Johnson, J.L., Hirsch, C., Toossi, Z., and Arts, E.J. (2002). Human immunodeficiency virus type 1 (HIV-1) quasispecies at the sites of *Mycobacterium tuberculosis* infection contribute to systemic HIV-1 heterogeneity. *J. Virol.* *76*, 1697–1706.

Cribbs, S.K., Lennox, J., Caliendo, A.M., Brown, L.A., and Guidot, D.M. (2015). Healthy HIV-1-infected individuals on highly active antiretroviral therapy harbor HIV-1 in their alveolar macrophages. *AIDS Res. Hum. Retroviruses* *31*, 64–70.

Davis, D.M., and Sowinski, S. (2008). Membrane nanotubes: dynamic long-distance connections between animal cells. *Nat. Rev. Mol. Cell Biol.* *9*, 431–436.

Diedrich, C.R., and Flynn, J.L. (2011). HIV-1/*Mycobacterium tuberculosis* coinfection immunology: how does HIV-1 exacerbate tuberculosis? *Infect. Immun.* *79*, 1407–1417.

Diedrich, C.R., O'Hern, J., and Wilkinson, R.J. (2016). HIV-1 and the *Mycobacterium tuberculosis* granuloma: a systematic review and meta-analysis. *Tuberculosis (Edinb.)* *98*, 62–76.

Dupont, M., Souriant, S., Lugo-Villarino, G., Maridonneau-Parini, I., and Vérollet, C. (2018). Tunneling nanotubes: intimate communication between myeloid cells. *Front. Immunol.* *9*, 43.

Ellery, P.J., Tippett, E., Chiu, Y.L., Paukovics, G., Cameron, P.U., Solomon, A., Lewin, S.R., Gorry, P.R., Jaworowski, A., Greene, W.C., et al. (2007). The CD16⁺ monocyte subset is more permissive to infection and preferentially harbors HIV-1 in vivo. *J. Immunol.* *178*, 6581–6589.

Esmail, H., Riou, C., du Bruyn, E., Lai, R.P., Harley, Y.X.R., Meintjes, G., Wilkinson, K.A., and Wilkinson, R.J. (2018). The immune response to *Mycobacterium tuberculosis* in HIV-1-coinfected persons. *Annu. Rev. Immunol.* *36*, 603–638.

Esper, L., Beaumelle, B., and Vergne, I. (2015). Autophagy in *Mycobacterium tuberculosis* and HIV infections. *Front. Cell. Infect. Microbiol.* *5*, 49.

Eugenin, E.A., Gaskill, P.J., and Berman, J.W. (2009). Tunneling nanotubes (TNT) are induced by HIV-infection of macrophages: a potential mechanism for intercellular HIV trafficking. *Cell. Immunol.* *254*, 142–148.

Fabrick, B.O., Dijkstra, C.D., and van den Berg, T.K. (2005). The macrophage scavenger receptor CD163. *Immunobiology* *210*, 153–160.

Foreman, T.W., Mehra, S., LoBato, D.N., Malek, A., Alvarez, X., Golden, N.A., Bucşan, A.N., Didier, P.J., Doyle-Meyers, L.A., Russell-Lodrigue, K.E., et al. (2016). CD4⁺ T-cell-independent mechanisms suppress reactivation of latent tuberculosis in a macaque model of HIV coinfection. *Proc. Natl. Acad. Sci. USA* *113*, E5636–E5644.

García-Perez, J., Staropoli, I., Azoulay, S., Heinrich, J.T., Cascajero, A., Colin, P., Lortat-Jacob, H., Arenzana-Seisdedos, F., Alcami, J., Kellenberger, E., and

- Lagane, B. (2015). A single-residue change in the HIV-1 V3 loop associated with maraviroc resistance impairs CCR5 binding affinity while increasing replicative capacity. *Retrovirology* 12, 50.
- Gaudin, R., Berre, S., Cunha de Alencar, B., Decalf, J., Schindler, M., Gobert, F.X., Jouve, M., and Benaroch, P. (2013). Dynamics of HIV-containing compartments in macrophages reveal sequestration of virions and transient surface connections. *PLoS ONE* 8, e69450.
- Genoula, M., Marín Franco, J.L., Dupont, M., Kviatcovsky, D., Miñillo, A., Schierloh, P., Moraña, E.J., Poggi, S., Palmero, D., Mata-Espinosa, D., et al. (2018). Formation of foamy macrophages by tuberculous pleural effusions is triggered by the interleukin-10/signal transducer and activator of transcription 3 axis through ACAT upregulation. *Front. Immunol.* 9, 459.
- Getahun, H., Harrington, M., O'Brien, R., and Nunn, P. (2007). Diagnosis of smear-negative pulmonary tuberculosis in people with HIV infection or AIDS in resource-constrained settings: informing urgent policy changes. *Lancet* 369, 2042–2049.
- Goletti, D., Weissman, D., Jackson, R.W., Collins, F., Kinter, A., and Fauci, A.S. (1998). The in vitro induction of human immunodeficiency virus (HIV) replication in purified protein derivative-positive HIV-infected persons by recall antigen response to *Mycobacterium tuberculosis* is the result of a balance of the effects of endogenous interleukin-2 and proinflammatory and antiinflammatory cytokines. *J. Infect. Dis.* 177, 1332–1338.
- Goletti, D., Carrara, S., Vincenti, D., Giacomini, E., Fattorini, L., Garbuglia, A.R., Capobianchi, M.R., Alonzi, T., Fimia, G.M., Federico, M., et al. (2004). Inhibition of HIV-1 replication in monocyte-derived macrophages by *Mycobacterium tuberculosis*. *J. Infect. Dis.* 189, 624–633.
- Gordon, S., Plüddemann, A., and Martínez Estrada, F. (2014). Macrophage heterogeneity in tissues: phenotypic diversity and functions. *Immunol. Rev.* 262, 36–55.
- Groot, F., Welsch, S., and Sattentau, Q.J. (2008). Efficient HIV-1 transmission from macrophages to T cells across transient virological synapses. *Blood* 111, 4660–4663.
- Hase, K., Kimura, S., Takatsu, H., Ohmae, M., Kawano, S., Kitamura, H., Ito, M., Watarai, H., Hazelett, C.C., Yeaman, C., and Ohno, H. (2009). M-Sec promotes membrane nanotube formation by interacting with Ral and the exocyst complex. *Nat. Cell Biol.* 11, 1427–1432.
- Hashimoto, M., Bhuyan, M., Hiyoshi, M., Noyori, O., Nasser, H., Miyazaki, M., Saito, T., Kondoh, Y., Osada, H., Kimura, S., et al. (2016). Potential role of the formation of tunneling nanotubes in HIV-1 spread in macrophages. *J. Immunol.* 196, 1832–1841.
- Honeycutt, J.B., Wahl, A., Baker, C., Spagnuolo, R.A., Foster, J., Zakharova, O., Wietgreffe, S., Caro-Vegas, C., Madden, V., Sharpe, G., et al. (2016). Macrophages sustain HIV replication in vivo independently of T cells. *J. Clin. Invest.* 126, 1353–1366.
- Honeycutt, J.B., Thayer, W.O., Baker, C.E., Ribeiro, R.M., Lada, S.M., Cao, Y., Cleary, R.A., Hudgens, M.G., Richman, D.D., and Garcia, J.V. (2017). HIV persistence in tissue macrophages of humanized myeloid-only mice during antiretroviral therapy. *Nat. Med.* 23, 638–643.
- Hoshino, Y., Nakata, K., Hoshino, S., Honda, Y., Tse, D.B., Shioda, T., Rom, W.N., and Weiden, M. (2002). Maximal HIV-1 replication in alveolar macrophages during tuberculosis requires both lymphocyte contact and cytokines. *J. Exp. Med.* 195, 495–505.
- Ip, W.K.E., Hoshi, N., Shouval, D.S., Snapper, S., and Medzhitov, R. (2017). Anti-inflammatory effect of IL-10 mediated by metabolic reprogramming of macrophages. *Science* 356, 513–519.
- Jolly, C., and Sattentau, Q.J. (2004). Retroviral spread by induction of virological synapses. *Traffic* 5, 643–650.
- Joseph, S.B., and Swanstrom, R. (2018). The evolution of HIV-1 entry phenotypes as a guide to changing target cells. *J. Leukoc. Biol.* 103, 421–431.
- Karaji, N., and Sattentau, Q.J. (2017). Efferocytosis of pathogen-infected cells. *Front. Immunol.* 8, 1863.
- Kaushal, D., Mehra, S., Didier, P.J., and Lackner, A.A. (2012). The non-human primate model of tuberculosis. *J. Med. Primatol.* 41, 191–201.
- Khan, N., and Divangahi, M. (2018). *Mycobacterium tuberculosis* and HIV co-infection brings fire and fury to macrophages. *J. Infect. Dis.* 217, 1851–1853.
- Knudsen, T.B., Gustafson, P., Kronborg, G., Kristiansen, T.B., Moestrup, S.K., Nielsen, J.O., Gomes, V., Aaby, P., Lisse, I., Moller, H.J., et al. (2005). Predictive value of soluble haemoglobin scavenger receptor CD163 serum levels for survival in verified tuberculosis patients. *Clin. Microbiol. Infect.* 11, 730–735.
- Kuroda, M.J., Sugimoto, C., Cai, Y., Merino, K.M., Mehra, S., Araínga, M., Roy, C.J., Midkiff, C.C., Alvarez, X., Didier, E.S., and Kaushal, D. (2018). High turnover of tissue macrophages contributes to tuberculosis reactivation in simian immunodeficiency virus-infected rhesus macaques. *J. Infect. Dis.* 217, 1865–1874.
- Laguette, N., Sobhian, B., Casartelli, N., Ringeard, M., Chable-Bessia, C., Ségéral, E., Yatim, A., Emiliani, S., Schwartz, O., and Benkirane, M. (2011). SAMHD1 is the dendritic- and myeloid-cell-specific HIV-1 restriction factor counteracted by Vpx. *Nature* 474, 654–657.
- Lastrucci, C., Bénard, A., Balboa, L., Pingris, K., Souriant, S., Poincloux, R., Al Saati, T., Rasolofo, V., González-Montaner, P., Inwentarz, S., et al. (2015). Tuberculosis is associated with expansion of a motile, permissive and immunomodulatory CD16⁺ monocyte population via the IL-10/STAT3 axis. *Cell Res.* 25, 1333–1351.
- Lawn, S.D., Pisell, T.L., Hirsch, C.S., Wu, M., Butera, S.T., and Toossi, Z. (2001). Anatomically compartmentalized human immunodeficiency virus replication in HLA-DR⁺ cells and CD14⁺ macrophages at the site of pleural tuberculosis coinfection. *J. Infect. Dis.* 184, 1127–1133.
- Le Cabec, V., and Maridonneau-Parini, I. (1994). Annexin 3 is associated with cytoplasmic granules in neutrophils and monocytes and translocates to the plasma membrane in activated cells. *Biochem. J.* 303, 481–487.
- Le Cabec, V., Cols, C., and Maridonneau-Parini, I. (2000). Nonopsonic phagocytosis of zymosan and *Mycobacterium kansasii* by CR3 (CD11b/CD18) involves distinct molecular determinants and is or is not coupled with NADPH oxidase activation. *Infect. Immun.* 68, 4736–4745.
- Lederman, M.M., Georges, D.L., Kusner, D.J., Mudido, P., Giam, C.Z., and Toossi, Z. (1994). *Mycobacterium tuberculosis* and its purified protein derivative activate expression of the human immunodeficiency virus. *J. Acquir. Immune Defic. Syndr.* 7, 727–733.
- Light, R.W. (2010). Update on tuberculous pleural effusion. *Respirology* 15, 451–458.
- Lugo-Villarino, G., Vélollet, C., Maridonneau-Parini, I., and Neyrolles, O. (2011). Macrophage polarization: convergence point targeted by *Mycobacterium tuberculosis* and HIV. *Front. Immunol.* 2, 43.
- Malik, S., and Eugenin, E.A. (2016). Mechanisms of HIV neuropathogenesis: role of cellular communication systems. *Curr. HIV Res.* 14, 400–411.
- Mancino, G., Placido, R., Bach, S., Mariani, F., Montesano, C., Ercoli, L., Zembala, M., and Colizzi, V. (1997). Infection of human monocytes with *Mycobacterium tuberculosis* enhances human immunodeficiency virus type 1 replication and transmission to T cells. *J. Infect. Dis.* 175, 1531–1535.
- Maridonneau-Parini, I. (2014). Control of macrophage 3D migration: a therapeutic challenge to limit tissue infiltration. *Immunol. Rev.* 262, 216–231.
- McCoy-Simandle, K., Hanna, S.J., and Cox, D. (2016). Exosomes and nanotubes: control of immune cell communication. *Int. J. Biochem. Cell Biol.* 71, 44–54.
- Mehra, S., Golden, N.A., Dutta, N.K., Midkiff, C.C., Alvarez, X., Doyle, L.A., Asher, M., Russell-Lodrigue, K., Monjure, C., Roy, C.J., et al. (2011). Reactivation of latent tuberculosis in rhesus macaques by coinfection with simian immunodeficiency virus. *J. Med. Primatol.* 40, 233–243.
- Murray, P.J., Allen, J.E., Biswas, S.K., Fisher, E.A., Gilroy, D.W., Goerdts, S., Gordon, S., Hamilton, J.A., Ivashkiv, L.B., Lawrence, T., et al. (2014). Macrophage activation and polarization: nomenclature and experimental guidelines. *Immunity* 41, 14–20.
- Nakata, K., Rom, W.N., Honda, Y., Condos, R., Kanegasaki, S., Cao, Y., and Weiden, M. (1997). *Mycobacterium tuberculosis* enhances human immunodeficiency virus-1 replication in the lung. *Am. J. Respir. Crit. Care Med.* 155, 996–1003.

- Naphade, S., Sharma, J., Gaide Chevronnay, H.P., Shook, M.A., Yeagy, B.A., Rocca, C.J., Ur, S.N., Lau, A.J., Courtoy, P.J., and Cherqui, S. (2015). Brief reports: lysosomal cross-correction by hematopoietic stem cell-derived macrophages via tunneling nanotubes. *Stem Cells* 33, 301–309.
- O'Garra, A., Redford, P.S., McNab, F.W., Bloom, C.I., Wilkinson, R.J., and Berry, M.P. (2013). The immune response in tuberculosis. *Annu. Rev. Immunol.* 31, 475–527.
- Okafo, G., Prevedel, L., and Eugenin, E. (2017). Tunneling nanotubes (TNT) mediate long-range gap junctional communication: implications for HIV cell to cell spread. *Sci. Rep.* 7, 16660.
- Onfelt, B., Nedvetzki, S., Benninger, R.K., Purbhoo, M.A., Sowinski, S., Hume, A.N., Seabra, M.C., Neil, M.A., French, P.M., and Davis, D.M. (2006). Structurally distinct membrane nanotubes between human macrophages support long-distance vesicular traffic or surfing of bacteria. *J. Immunol.* 177, 8476–8483.
- Orenstein, J.M. (2000). In vivo cytolysis and fusion of human immunodeficiency virus type 1-infected lymphocytes in lymphoid tissue. *J. Infect. Dis.* 182, 338–342.
- Orenstein, J.M. (2001). The macrophage in HIV infection. *Immunobiology* 204, 598–602.
- Orenstein, J.M., Fox, C., and Wahl, S.M. (1997). Macrophages as a source of HIV during opportunistic infections. *Science* 276, 1857–1861.
- Queval, C.J., Song, O.R., Deboosère, N., Delorme, V., Debrie, A.S., Iantomasi, R., Veyron-Churlat, R., Jouny, S., Redhage, K., Deloison, G., et al. (2016). STAT3 represses nitric oxide synthesis in human macrophages upon *Mycobacterium tuberculosis* infection. *Sci. Rep.* 6, 29297.
- Raynaud-Messina, B., Bracq, L., Dupont, M., Souriant, S., Usmani, S.M., Proag, A., Pingris, K., Soldan, V., Thibault, C., Capilla, F., et al. (2018). Bone degradation machinery of osteoclasts: an HIV-1 target that contributes to bone loss. *Proc. Natl. Acad. Sci. USA* 115, E2556–E2565.
- Rocca, C.J., Goodman, S.M., Dulin, J.N., Haquang, J.H., Gertsman, I., Blondelle, J., Smith, J.L.M., Heyser, C.J., and Cherqui, S. (2017). Transplantation of wild-type mouse hematopoietic stem and progenitor cells ameliorates deficits in a mouse model of Friedreich's ataxia. *Sci. Transl. Med.* 9, eaaj2347.
- Russell, D.G., Barry, C.E., 3rd, and Flynn, J.L. (2010). Tuberculosis: what we don't know can, and does, hurt us. *Science* 328, 852–856.
- Sather, S., Kenyon, K.D., Lefkowitz, J.B., Liang, X., Varnum, B.C., Henson, P.M., and Graham, D.K. (2007). A soluble form of the Mer receptor tyrosine kinase inhibits macrophage clearance of apoptotic cells and platelet aggregation. *Blood* 109, 1026–1033.
- Sattentau, Q.J., and Stevenson, M. (2016). Macrophages and HIV-1: an unhealthy constellation. *Cell Host Microbe* 19, 304–310.
- Schierloh, P., Yokobori, N., Alemán, M., Landoni, V., Geffner, L., Musella, R.M., Castagnino, J., Baldini, M., Abbate, E., de la Barrera, S.S., and Sasiain, M.C. (2007). *Mycobacterium tuberculosis*-induced gamma interferon production by natural killer cells requires cross talk with antigen-presenting cells involving Toll-like receptors 2 and 4 and the mannose receptor in tuberculous pleurisy. *Infect. Immun.* 75, 5325–5337.
- Sherer, N.M., and Mothes, W. (2008). Cytonemes and tunneling nanotubules in cell-cell communication and viral pathogenesis. *Trends Cell Biol.* 18, 414–420.
- Singh, A., Besson, G., Mobasher, A., and Collman, R.G. (1999). Patterns of chemokine receptor fusion cofactor utilization by human immunodeficiency virus type 1 variants from the lungs and blood. *J. Virol.* 73, 6680–6690.
- Sowinski, S., Jolly, C., Berninghausen, O., Purbhoo, M.A., Chauveau, A., Köhler, K., Oddos, S., Eissmann, P., Brodsky, F.M., Hopkins, C., et al. (2008). Membrane nanotubes physically connect T cells over long distances presenting a novel route for HIV-1 transmission. *Nat. Cell Biol.* 10, 211–219.
- Tanaka, N., Hoshino, Y., Gold, J., Hoshino, S., Martiniuk, F., Kurata, T., Pine, R., Levy, D., Rom, W.N., and Weiden, M. (2005). Interleukin-10 induces inhibitory C/EBPbeta through STAT-3 and represses HIV-1 transcription in macrophages. *Am. J. Respir. Cell Mol. Biol.* 33, 406–411.
- Tomlinson, G.S., Bell, L.C., Walker, N.F., Tsang, J., Brown, J.S., Breen, R., Lipman, M., Katz, D.R., Miller, R.F., Chain, B.M., et al. (2013). HIV-1 infection of macrophages dysregulates innate immune responses to *Mycobacterium tuberculosis* by inhibition of interleukin-10. *J. Infect. Dis.* 209, 1055–1065.
- Toossi, Z. (2003). Virological and immunological impact of tuberculosis on human immunodeficiency virus type 1 disease. *J. Infect. Dis.* 188, 1146–1155.
- Toossi, Z., Nicolacakis, K., Xia, L., Ferrari, N.A., and Rich, E.A. (1997). Activation of latent HIV-1 by *Mycobacterium tuberculosis* and its purified protein derivative in alveolar macrophages from HIV-infected individuals in vitro. *J. Acquir. Immune Defic. Syndr. Hum. Retrovirol.* 15, 325–331.
- Vérollet, C., Zhang, Y.M., Le Cabec, V., Mazzolini, J., Charrière, G., Labrousse, A., Bouchet, J., Medina, I., Biessen, E., Niedergang, F., et al. (2010). HIV-1 Nef triggers macrophage fusion in a p61Hck- and protease-dependent manner. *J. Immunol.* 184, 7030–7039.
- Vérollet, C., Souriant, S., Bonnaud, E., Jolicoeur, P., Raynaud-Messina, B., Kinnaer, C., Fourquaux, I., Imle, A., Benichou, S., Fackler, O.T., et al. (2015a). HIV-1 reprograms the migration of macrophages. *Blood* 125, 1611–1622.
- Vérollet, C., Souriant, S., Raynaud-Messina, B., and Maridonneau-Parini, I. (2015b). [HIV-1 drives the migration of macrophages]. *Med. Sci. (Paris)* 31, 730–733.
- Vorster, M.J., Allwood, B.W., Diacon, A.H., and Koegelenberg, C.F. (2015). Tuberculous pleural effusions: advances and controversies. *J. Thorac. Dis.* 7, 981–991.
- Xu, Y., Kulkosky, J., Acheampong, E., Nunnari, G., Sullivan, J., and Pomerantz, R.J. (2004). HIV-1-mediated apoptosis of neuronal cells: proximal molecular mechanisms of HIV-1-induced encephalopathy. *Proc. Natl. Acad. Sci. USA* 101, 7070–7075.
- Xu, W., Santini, P.A., Sullivan, J.S., He, B., Shan, M., Ball, S.C., Dyer, W.B., Ketas, T.J., Chadburn, A., Cohen-Gould, L., et al. (2009). HIV-1 evades virus-specific IgG2 and IgA responses by targeting systemic and intestinal B cells via long-range intercellular conduits. *Nat. Immunol.* 10, 1008–1017.
- Zhang, Y. (2011). Tunneling-nanotube: a new way of cell-cell communication. *Commun. Integr. Biol.* 4, 324–325.
- Zhang, Y., Nakata, K., Weiden, M., and Rom, W.N. (1995). *Mycobacterium tuberculosis* enhances human immunodeficiency virus-1 replication by transcriptional activation at the long terminal repeat. *J. Clin. Invest.* 95, 2324–2331.
- Ziegler-Heitbrock, L. (2007). The CD14⁺ CD16⁺ blood monocytes: their role in infection and inflammation. *J. Leukoc. Biol.* 81, 584–592.

STAR★METHODS

KEY RESOURCES TABLE

REAGENT or RESOURCE	SOURCE	IDENTIFIER
Antibodies		
Anti-human CD14	Biologend	Clone M5E2; RRID:AB_893250
Anti-human CD16	Biologend	Clone 3G8; RRID:AB_314206
Anti-human CD163	Biologend	Clone GHI/61; RRID:AB_1134002
Anti-human CD184 (CXCR4)	Biologend	Clone 12G5; RRID:AB_10642818
Anti-human CD195 (CCR5)	Biologend	Clone J418F1; RRID:AB_2564073
Anti-human CD274 (B7-H1, PD-L1)	Biologend	Clone 29E.2A3; RRID:AB_940366
Anti-human CD4	Biologend	Clone RPA-T4; RRID:AB_314082
Anti-human CD64	Biologend	Clone 10.1; RRID:AB_2734691
Anti-human CD86	Biologend	Clone IT2.2; RRID:AB_2074981
Anti-human HLA-DR	Biologend	Clone L243; RRID:AB_2572101
Anti-human MerTK	Biologend	Clone 590H11G1E3; RRID:AB_2687286
Anti-human STAT3	Cell Signaling Technology	Clone D1A5; https://media.cellsignal.com/pdf/8768.pdf
Anti-human phosphoTyr705-STAT3	Cell Signaling Technology	Clone D3A7; https://media.cellsignal.com/pdf/9145.pdf
Anti-human SAMHD1	Gift from Dr. O Schwartz Institut Pasteur, Paris, France	Laguette et al., 2011
Anti-human phosphoThr592-SAMHD1	ProSci	Cat# 8005; RRID:AB_2316381
Anti-human IFITM1/2/3	Santa Cruz Biotechnology	Clone FL-125; http://datasheets.scbt.com/sc-66827.pdf
Anti-human C/EBP- β	Santa Cruz Biotechnology	Clone H-7; https://datasheets.scbt.com/sc-7962.pdf
Anti-human CUGBP1	Santa Cruz Biotechnology	Clone 3B1; RRID:AB_627319
Anti-human Actin	Sigma-Aldrich	Clone 20-33; RRID:AB_476738
Anti-human LC3	Sigma-Aldrich	Cat# L8918; RRID:AB_1079382
Anti-human Gag-RD1	Beckman Coulter	Clone KC57; https://www.bc-cytometry.com/PDF/DataSheet/6604665&6604667%20D.S.pdf
Anti-human CD163	Leica/Novocastra	Clone 10D6; RRID:AB_2756375
Anti-human alpha-tubulin	Sigma-Aldrich	clone B-5-1-2; RRID:AB_477582
LEAF purified anti-human IL-10	Biologend	Clone JES3-19F1; RRID:AB_315460
LEAF purified rat anti-human IgG2a	Biologend	Clone RTK2758; RRID:AB_326523
Goat anti-rabbit IgG, AlexaFluor 555	Thermo Fisher Scientific	Cat# A-21430; RRID:AB_2535851
Goat anti-mouse IgG, AlexaFluor 488	Thermo Fisher Scientific	Cat# A-10684; RRID:AB_2534064
Goat anti-Mouse IgG, AlexaFluor 555	Cell Signaling Technology	Cat# 4409; RRID:AB_1904022
Goat anti-rabbit IgG, HRP	Thermo Fisher Scientific	Cat# 32460; RRID:AB_1185567
Goat anti-mouse IgG, HRP	Thermo Fisher Scientific	Cat# 31430; RRID:AB_228307
Bacterial and Virus Strains		
<i>M. tuberculosis</i> H37Rv	N/A	N/A
HIV-1 ADA strain	Gift from Dr. S Benichou Institut Cochin, Paris, France	Vérollet et al., 2015a
HIV-1 ADA Gag-iGFP strain	Gift from Dr P. Benaroch Institut Pasteur, Paris, France	Gaudin et al., 2013
HIV-1 NLAD8-VSVG	Gift from Dr. S Benichou Institut Cochin, Paris, France	Bracq et al., 2017
HIV-1 ADA (BlaM-Vpr)	N/A	N/A

(Continued on next page)

Continued

REAGENT or RESOURCE	SOURCE	IDENTIFIER
Biological Samples		
Buffy Coat	Etablissement Français du Sang, Toulouse, France	N/A
Patients-derived pleural effusions	División de Tisioneumonología at the Instituto de Tisioneumonología Vaccarezza-University of Buenos Aires, Argentina	N/A
TB patients-derived peripheral blood	División de Tisioneumonología at the Instituto de Tisioneumonología Vaccarezza-University of Buenos Aires, Argentina	N/A
HIV/TB patients-derived peripheral blood	Division de SIDA at the Hospital F.J Muñiz, Buenos Aires, Argentina	N/A
Healthy subjects-derived peripheral blood	Blood Transfusion Service, <i>Hospital Fernandez</i> , Buenos Aires, Argentina	N/A
Histological slides of lung biopsies from rhesus macaques	Tulane National Primate Research Center	N/A
Chemicals, Peptides, and Recombinant Proteins		
Human M-CSF	Peptotech	Cat# 300-25
Stattic	Sigma-Aldrich	Cat# S7947
TNTi	Pharmeks	N/A
Cytochalasin D	Sigma-Aldrich	Cat# 22144-77-0
Maraviroc	Sigma-Aldrich	Cat# 376348-65-1
Bafilomycin A1	Sigma-Aldrich	Cat# 88899-55-2
Critical Commercial Assays		
Mouse anti-human CD14 microbeads	Miltenyi Biotec	Cat# 130-050-201
LS magnetic columns	Miltenyi Biotec	Cat# 130-042-401
Protein G Agarose, Fast Flow	Millipore	Cat# 16-266
Renilla Luciferase Assay	Promega	Cat# E2810
Amersham ECL Prisma Western Blotting Detection Reagent	GE Healthcare	Cat# RPN2232
SuperSignal WestPico Chemiluminescent Substrate	Thermo Scientific	Cat# 34080
Matrigel	BD Bioscience	Cat# 356234
IL-10 ELISA set	BD Bioscience	Cat# 555157
Human CD163 ELISA kit	BD Bioscience	Cat# DY1607-05
Human Mer ELISA kit	BD Bioscience	Cat# DY6488
Human TruStain FcX	Biolegend	Cat#422302
Cell Dissociation Buffer	Thermo Fisher Scientific	Cat# 13151014
Phalloidin AlexaFluor 488	Thermo Fisher Scientific	Cat# A12379
DAPI	Sigma Aldrich	Cat# D9542
Vybrant® DiO	Thermo Fisher Scientific	Cat# V22886
CellTracker Red CMPTX Dye	Thermo Fisher Scientific	Cat# C34552
CellTracker Green CMFDA Dye	Thermo Fisher Scientific	Cat# C7025
Fluorescence Mounting Medium	Agilent Technologies	Cat# S302380-2
Prolong anti-fade reagent	Thermo Fisher Scientific	Cat# P10144
Experimental Models: Cell Lines		
TZM-bl cell line	NIH AIDS Reagent Program	Cat# 8129
Software and Algorithms		
ImageJ	ImageJ	https://www.imagej.nih.gov/ij/
Prism (v5)	GraphPad	https://www.graphpad.com/
Photoshop CS3	Adobe	https://www.adobe.com/
Illustrator CS3	Adobe	https://www.adobe.com/

(Continued on next page)

Continued

REAGENT or RESOURCE	SOURCE	IDENTIFIER
Huygens Professional Version 16.10	Scientific Volume Imaging	https://svi.nl/Huygens-Professional
FACS DIVA	BD Bioscience	http://www.bdbiosciences.com/
FlowJo 7.6.5	TreeStar	https://www.flowjo.com/
FCS Express V3	DeNovo Software	http://www.denovosoftware.com
Image Lab	Bio-Rad Laboratories	http://www.bio-rad.com

CONTACT FOR REAGENT AND RESOURCE SHARING

Further information and requests for reagents should be directed to and will be fulfilled by the Lead Contact, Geanncarlo Lugo-Vilarino (lugo@ipbs.fr). Sharing of antibodies and other reagents with academic researchers may require UBMTA agreements.

EXPERIMENTAL MODEL AND SUBJECT DETAILS

Human Subjects

Monocytes from healthy subjects (HS) were provided by Etablissement Français du Sang, Toulouse, France, under contract 21/PLER/TOU/IPBS01/20130042. According to articles L12434 and R124361 of the French Public Health Code, the contract was approved by the French Ministry of Science and Technology (agreement number AC 2009921). Written informed consents were obtained from the donors before sample collection. The sex of HS is unknown.

Tuberculous (TB) patients from the División de Tisioneumonología at the Instituto de Tisioneumonología Vaccarezza-University of Buenos Aires, Argentina and co-infected HIV/TB patients from the Division de SIDA at the Hospital F.J Muñiz, from 2015 to 2016, were diagnosed by the presence of recent clinical respiratory symptoms, abnormal chest radiography and positive sputum smear test for acid-fast bacilli. The research was carried out in accordance with the Declaration of Helsinki (2013) of the World Medical Association, and was approved by the Ethics Committees of the institutes mentioned above (protocol numbers: NIN-1671-12 and proceedings 37/38). Written informed consent was obtained before sample collection. Exclusion criteria included the presence of concurrent infectious diseases or non-infectious conditions (cancer, diabetes, or steroid therapy). Blood samples were collected at 3 to 10 days after start of TB treatment. The diagnosis of tuberculous pleurisy was based on a positive Ziehl–Nielsen stain or Lowenstein–Jensen culture from pleural effusion (PE) and/or histopathology of pleural biopsy, and was further confirmed by an *Mycobacterium tuberculosis*-induced IFN- γ response and an ADA-positive test (Light, 2010). Effusions were classified as exudates according to Light (2010). PE and peripheral blood (PB) samples were obtained as described previously (Schierloh et al., 2007). PB samples from HS were provided by the Blood Transfusion Service, Hospital Fernandez, Buenos Aires (agreement number CEIANM-52-5-2012). All HS had received BCG vaccination in childhood and their tuberculin-test status (TTS) was unknown. Clinical features and sex of the experimental groups are summarized in Table S1.

Strategy for randomization and/or stratification

Blood samples from enrolled patients were classified in 3 groups of individuals: 1) TB patients with abnormal chest radiography and positive sputum smear test for acid-fast bacilli, who received less than one week of anti-TB therapy (TB); 2) HIV-1 infected patients with active TB, who received less than one week of anti-TB therapy (HIV/TB); and 3) Bacillus Calmette-Guerin-vaccinated healthy donors (HS). Pleural effusions samples from enrolled patients were classified in 2 groups of individuals: 1) TB pleurisy based on a positive Ziehl–Nielsen stain or Lowenstein–Jensen culture from PE and/or histopathology of pleural biopsy, and confirmed by an Mtb-induced IFN- γ response and an adenosine deaminase-positive test; and 2) no-TB pleurisy including the following etiologies: malignant effusions (mesothelioma, lung carcinoma or metastatic patients), parapneumonic effusions and heart failure associated effusions.

Inclusion and Exclusion criteria for blood samples

Inclusion: person > 21 years old diagnosed with TB (clinical or laboratory criteria) having HIV⁺ serology (HIV/TB) or not and who consent to participate. Exclusion: the presence of concurrent infectious diseases, except HIV, or non-infectious conditions (cancer, diabetes, or steroid therapy) and patients who do not provide consent.

Inclusion and Exclusion criteria for pleural effusion samples

Inclusion: person > 21 years old having a pleural effusion requiring drainage by therapeutic thoracentesis and who consent to participate. Exclusion: the presence of empyema, pleural effusion that does not require therapeutic drainage and patients who do not provide consent.

The GPower software was used for sample-size estimation and statistics. No replicates and no blinding were done.

NHPs

All animal procedures were approved by the Institutional Animal Care and Use Committee of Tulane University, New Orleans, LA, and were performed in strict accordance with NIH guidelines. The twenty adult rhesus macaques used in this study (Table S2) were bred

and housed at Tulane National Primate Research Center (TNPRC). The sex of animals is specified in [Table S2](#). All macaques were infected as previously described ([Foreman et al., 2016](#); [Mehra et al., 2011](#)). Briefly, macaques were aerosol-exposed to a low dose (25 CFU implanted) of Mtb CDC1551 and a subset of the macaques were also exposed 9 weeks later to 300 TCID₅₀ of SIVmac239 administered intravenously in 1 mL saline. The control subset received an equal volume of saline intravenously. Criteria for killing included presentation of four or more of the following conditions: (i) body temperatures consistently greater than 2°F above preinfection values for 3 or more weeks in a row; (ii) 15% or more loss in body weight; (iii) serum CRP values higher than 10 mg/mL for 3 or more consecutive weeks, CRP being a marker for systemic inflammation that exhibits a high degree of correlation with active TB in macaques ([Kaushal et al., 2012](#); [Mehra et al., 2011](#)); (iv) CXR values higher than 2 on a scale of 0–4; (v) respiratory discomfort leading to vocalization; (vi) significant or complete loss of appetite; and (vii) detectable bacilli in BAL samples.

Bacteria

Mtb H37Rv strain was grown in 7H9 media at 37°C, as described ([Lastrucci et al., 2015](#)). Exponentially growing Mtb was centrifuged (460 g) and resuspended in PBS (MgCl₂, CaCl₂ free, GIBCO). Clumps were dissociated by 20 passages through a 26-G needle then resuspended in RPMI-1640 containing 10% FBS. Bacterial concentration was determined by measuring OD₆₀₀.

Viruses

Proviral infectious clones of the macrophage-tropic HIV-1 isolate ADA ([Vérollet et al., 2015a](#)) was kindly provided by Serge Benichou (Institut Cochin, Paris, France). Virions were produced by transient transfection of 293T cells with proviral plasmids, as previously described ([Vérollet et al., 2015a](#)). HEK293 T cells (the sex of original cells is unknown) were maintained in DMEM, 20% FBS, 5% CO₂. HIV-1 p24 antigen concentration of viral stocks was assessed by an home-made ELISA. HIV-1 infectious units were quantified, as reported ([Vérollet et al., 2015a](#)) using TZM-bl cells. TZM-bl cells are HeLa cell lines (female origin) that were obtained through NIH AIDS Reagent Program, Division of AIDS, NIAID, NIH from Dr. John C. Kappes, Dr. Xiaoyun Wu and Tranzyme Inc). In some experiments, we used Betalactamase (BlaM)-Vpr-containing ADA virus and NLAD8-VSVG pseudotyped viruses and HIV-1 ADA Gag-iGFP strain (see [Key Resources Table](#)).

Preparation of human monocytes and monocyte-derived macrophages

Monocytes from healthy subjects (HS) were isolated and differentiated into macrophages as previously described ([Balboa et al., 2011](#); [Lastrucci et al., 2015](#); [Vérollet et al., 2015a](#)). Briefly, purified CD14⁺ monocytes from HS were differentiated for 5–7 days in RPMI-1640 medium (GIBCO), 10% Fetal Bovine Serum (FBS, Sigma-Aldrich) and human M-CSF (Peprotech) at 20 ng/mL. Differentiated macrophages were used as the cellular source to prepare the CmMTB after infection with Mtb. The cell medium was renewed every 3 or 4 days.

For the human samples of peripheral blood and pleural effusion (PE) from nonTB, TB and HIV/TB patients and HS, mononuclear cells were isolated by Ficoll-Hypaque gradient centrifugation (Pharmacia, Uppsala, Sweden), as described previously ([Balboa et al., 2011](#); [Lastrucci et al., 2015](#)). Isolated monocytes from patients were allowed to adhere to 24-well plates, at 5 × 10⁵ cells/well for 1 h at 37°C in warm RPMI-1640 medium. The medium was then supplemented to a final concentration of 10% FBS and human recombinant M-CSF at 10 ng/mL. Flow cytometry analysis was performed in mononuclear cells, gating within the CD14⁺ population.

METHODS DETAILS

Chemicals

When stated, monocytes (day 0) are treated with STAT3 activation inhibitor Stattic (1 μM, kindly provided by Fabienne Meggetto from CRCT, INSERM Toulouse). In some conditions, monocytes (day 0) were treated with an inhibitor of TNT formation (TNTi, 20 μM, Pharmeks), which was renewed after HIV-1 infection. In some experiments, macrophages were treated with Cytochalasin D (Sigma-Aldrich) at 2 μM. DMSO alone was used as vehicle control.

Preparation of conditioned media and cytokine depletion

The preparation of the conditioned medium of Mtb-infected macrophages (CmMTB) has been reported previously ([Lastrucci et al., 2015](#)). Briefly, macrophages were infected with Mtb H37Rv at a MOI of 3. The conditioned control medium (CmCTR) was obtained from uninfected macrophages. After incubation at 37°C for 18h, culture media were collected, sterilized by double filtration (0.2 μm pores) and aliquots were stored at –80°C. For cytokine depletion experiments, CmCTR or CmMTB were incubated with 10 μg/mL of control IgG or neutralizing IL-10 antibody (JES3-19F1, Biolegend) for 1h at 4°C. Afterwards, 50 μg/mL of 50% slurry Protein G agarose beads (EMD Millipore) were added and incubated for 1h at 4°C. Conditioned media were centrifuged (300 g) to remove antibody-bead complexes and then filtered (0.2 μm pores) before use. The depletion was controlled by ELISA.

Conditioning of monocytes with the secretome of Mtb-infected macrophages or pleural effusions from TB patients

Freshly isolated CD14⁺ monocytes from HS were allowed to adhere in the absence of serum (4 × 10⁵ cells/24-well in 500 μL or 2 × 10⁶ cells/6-well in 1.5 mL). After 1h of culture, 80% CmMTB or CmCTR supplemented with 20 ng/mL M-CSF and 20% FBS were added to the cells (vol/vol). For experiments with PE, samples were collected in heparin tubes and centrifuged at 300 g for 10 minutes at room

temperature without brake. The cell-free supernatant was transferred into new plastic tubes, further centrifuged at 12000 g for 10 minutes and aliquots were stored at -80°C . After having the diagnosis of the PE, pools were prepared by mixing same amounts of individual PE associated to a specific etiology. The pools were de-complemented at 56°C for 30 minutes, and filtered by $0.22\ \mu\text{m}$ in order to remove any remaining debris or residual bacteria. Particularly, we studied 21 patients with PE that were divided according their etiology. First group had 8 patients with tuberculous PE (PE-TB), second group had 8 patients with parapneumonic PE (PE-NPI), and third group had 5 patients with transudates secondary to heart failure (PE-HF). PE-TB or PE-nonTB (PE-NPI and PE-HF) supplemented with 40ng/mL M-CSF and 40% FBS were added to the cells (25% vol/vol). Cells were then cultured for 3 days. Monocytes were also conditioned in presence of 10 ng/mL M-CSF and 10 ng/mL recombinant human Interleukin-10 (IL-10) (PeproTech). Cell-surface expression of macrophage activation markers was measured by flow cytometry using standard procedures detailed in [Star Methods](#).

HIV-1 infection of cells

Cells were infected with HIV-1 ADA strain at day 3 of culture at MOI 0.1. HIV-1 infection and replication were assessed 10 days post-infection by measuring p24-positive cells by immunostaining and the level of p24 released in culture media by ELISA.

Blam-Vpr fusion assay

Experiments were carried out as described previously ([Garcia-Perez et al., 2015](#)). Briefly, monocytes adhered on glass coverslips were conditioned for 3 days with CmMTB or CmCTR medium and then collected with cell dissociation buffer (Thermo Fisher Scientific). Then, 1.5×10^5 cells were incubated for 3 h at 37°C with 100 ng p24 of a Betalactamase (Blam)-vpr-containing ADA virus. Infected cells were next incubated for 2 h with the CCF2/AM dye according to the manufacturer's instructions (Invitrogen). After washing, cells were fixed in 2% paraformaldehyde. Enzymatic cleavage of CCF2 by Blam, which causes a blue-shift in the CCF2 fluorescence emission spectrum, was measured by flow cytometry (FACSCanto, BD Biosciences).

Flow cytometry

Staining of conditioned monocytes-to-macrophage population was performed as previously described ([Lastrucci et al., 2015](#)). Adherent cells were harvested using Cell Dissociation Buffer (Life Technologies), centrifuged for 5 min at 340 g, incubated in staining buffer (PBS, 2mM EDTA, 0.5% FBS) with a 1:100 dilution of Human TruStain FcX (Biolegend) for 5 minutes at room temperature. Cells were then stained in cold staining buffer for 25 min with fluorophore-conjugated antibodies (see [Key Resources Table](#)) and, in parallel, with the corresponding isotype control antibody using a general dilution of 1:400. After staining, the cells were washed with cold staining buffer, centrifuged for 5 min at 340g at 4°C (twice), and analyzed by flow cytometry using LSR-II flow cytometer (BD Biosciences) and the associated BD FACSDiva software. Data was then analyzed using the FlowJo 7.6.5 software (TreeStar). The monocyte-to-macrophage population was first gated according to its Forward Scatter (FSC) and Size Scatter (SSC) properties before singlet selection and analysis of the percentage of positive cells and the median fluorescence intensity (MFI) for each staining.

Cells from nonTB, TB and HIV/TB patients and related controls from HS (2×10^5 cells) were labeled as described above and acquired in a FACSria II cytometer (BD Biosciences) and analyzed using FCS Express V3 software (*De Novo Software*, Los Angeles, CA, USA).

Immunofluorescence microscopy

Cells were fixed with PFA 3.7%, Sucrose 30mM in PBS. Stainings were performed as described ([Vérollet et al., 2015a](#)). Briefly, cells were permeabilized with Triton X-100 0.3% for 10 minutes, and saturated with PBS BSA 1% for 30 minutes. Cells were incubated with anti-Gag KC57 antibody (1:100, Beckman Coulter) in PBS BSA 1% for 1 hour, washed and then incubated with Alexa Fluor 555 Goat anti-Mouse IgG secondary antibody (1:1000, Cell Signaling Technology), Alexa Fluor 488 Phalloidin (1:500, Thermo Fisher Scientific) and DAPI (500 ng/mL, Sigma Aldrich) in PBS BSA 1% for 30 minutes. Coverslips were mounted on a glass slide using Fluorescence Mounting Medium (Dako). Slides were visualized with a Leica DM-RB fluorescence microscope or a FV1000 confocal microscope (Olympus). For deconvolution images shown in [Figures 5E, S5A, and S5C](#), macrophages were imaged over nine planes at 100 nm intervals with a 100x/1.49 Nikon objective mounted on a Nikon Eclipse Ti-E and an Hamamatsu Orca flash 4.0 LT sCMOS. All images were deconvolved with Huygens Professional version 16.10 (Scientific Volume Imaging, the Netherlands), using the CMLE algorithm, with SNR:20 and 40 iterations.

For the deconvolution image shown in [Figure 7D](#), imaging was performed using a dragonfly multimodal imaging platform in three-dimensional fast confocal mode using a 63x/1.47 objective and a Zyla 4.2 PLUS sCMOS camera (Andor).

TNTs were detected and counted using Phalloidin and microtubules staining. We quantified both thick and thin nanotubes: thin membrane nanotubes contained only F-actin, whereas thick TNTs contained both F-actin and microtubules.

As HIV-1 infection of macrophages makes them fuse into MGCs ([Orenstein, 2001; Vérollet et al., 2010](#)), the number of infected cells largely underestimates the rate of infection. Thus, to better reflect the rate of infection, we quantified HIV infection index (HIV-stained area divided by total cell area \times 100), percentage of nuclei in multinucleated cells and percentage of multinucleated cells. These parameters were assessed by using semi-automatic quantification with home-made ImageJ macros, allowing the study of more than 5,000 cells per condition in at least five independent donors.

HIV-1 and DiO transfer monitoring

Freshly isolated CD14⁺ monocytes from HS were allowed to adhere in the absence of serum (2×10^6 cells/6-well in 1.5 mL). After 1 h of culture, RPMI medium supplemented with 20 ng/mL M-CSF and 20% FBS and 20 ng/mL IL-10 were added to the cells (vol/vol). At day 3, half cells are infected with 120 ng p24 of a HIV-1 NLAD8 strain pseudotyped with a VSVG envelope. The other half cells are stained with CellTracker Green CMFDA Dye at day 5 (Thermo Fisher Scientific). Briefly, cells are washed with Mg²⁺/Ca²⁺-containing PBS and stained for 30 minutes in Mg²⁺/Ca²⁺-containing PBS supplemented with 500 ng/mL CellTracker, then washed with FBS-containing RPMI medium. HIV⁺ and CellTracker⁺ were then detached using accutase and co-cultured at a 1:1 ratio. In order to co-culture HIV⁺ and CellTracker⁺ cells in conditions that allow their physical separation, HIV⁺ cells were plated on 6.5-mm transwell filters with 0.4 μ m pore polyester membrane insert (Sigma-Aldrich) while CellTracker⁺ cells were plated on coverslips at the bottom of 24-well plates holding the transwell filters. The cells therefore shared only the culture medium but were unable to physically contact each other. For the cell-free HIV-1 control, CellTracker⁺ cells were incubated with the supernatant of HIV⁺ cells containing produced virions. After 24 h, cells were fixed, stained and imaged.

For DiO transfer monitoring, cells were stained either with CellTracker Red CMPTX Dye (Thermo Fisher Scientific) as described above, or with a lipophilic tracer Vybrant® DiO (Thermo Fisher Scientific), according to manufacturer's instructions. Then, cells were detached using accutase, co-cultured at a 1:1 ratio in 8-well Lab-Tek® chambers for 24 h and imaged.

Scanning electron microscopy

Scanning electron microscopy observations were performed as previously described (Lastrucci et al., 2015). Briefly, HIV-1-infected macrophages were fixed in 2.5% glutaraldehyde/3.7% PFA/0.1 M sodium cacodylate (pH 7.4), post-fixed in 1% osmium tetroxide (in 0.2 M cacodylate buffer), dehydrated in a series of increasing ethanol. Critical point was dried using carbon dioxide in a Leica EMCPD300. After coating with gold, cells were examined with a FEI Quanta FEG250 scanning electron microscope.

Immunoblot analyses

Total protein lysates were extracted as previously described (Lastrucci et al., 2015; Vérollet et al., 2015a). Total proteins were separated through SDS-polyacrylamide gel electrophoresis, transferred and immunoblotted overnight at 4°C with indicated primary antibodies (See Key Resources Table). Secondary antibodies were the following: Anti-rabbit and anti-mouse IgG, HRP-linked Antibody (Cell Signaling Technology). Proteins were visualized with Amersham ECL Prime Western Blotting Detection Reagent (GE Healthcare). Chemiluminescence was detected with ChemiDoc Touch Imaging System (Bio-Rad Laboratories) and quantified using Image Lab software (Bio-Rad Laboratories).

For the detection of LC3 autophagy protein, monocytes were seeded on 12-well plates at a density of 0.8×10^6 cells by well. After infection and treatment with Bafilomycin A1 (100 nM) or DMSO vehicle control for 2 h, cells were lysed. Proteins harvested were subjected to a SDS-polyacrylamide gel electrophoresis, 4%–15% gradient (Biorad). Blots were blocked with 5% dried milk in PBS, incubated with LC3 primary antibody and then with the corresponding horseradish peroxidase-conjugated secondary antibody (ThermoScientific). Staining was detected with SuperSignal WestPico Chemiluminescent Substrate (ThermoScientific), and immunostained proteins were visualized using the ChemiDoc Touch Imaging System (Biorad). Densitometric LC3-II/actin ratios were measured using the ImageJ software.

3D migration assays

3D migration assays of cells in Matrigel (10–12 mg/mL, BD Biosciences) were performed as described (Vérollet et al., 2015a) and quantified at 48 h. Briefly, pictures of cells were taken automatically with a 10X objective at constant intervals using the motorized stage of an inverted microscope (Leica DMIRB, Leica Microsystems). Cells were counted using ImageJ software as described previously (Vérollet et al., 2015a). The number of cells inside the matrix (% of migration measured after 48 h of migration) was quantified.

Protein quantifications in cell-free fluids by ELISA

Soluble protein concentration was measured in cell supernatants by ELISA using kits from BD Bioscience (IL-10) and R&D Systems (sCD163 and sMer), according to manufacturer's instructions.

Cytotoxicity assay

To exclude any impact of cytotoxicity of TNTi used in this study we measured lactate dehydrogenase (LDH) activity released from the cytosol of damaged cells into the supernatant. LDH release was measured using the Cytotoxicity Detection kit (Roche, Mannheim, Germany) according to the manufacturer's instructions. Monocytes were treated with TNTi (20 μ M) or DMSO as a control for 13 days. Cell-free culture supernatants were collected and incubated with LDH assay solution at 25°C for 30 min. The optical density values were analyzed at 490 nm by subtracting the reference value at 620 nm.

Phagocytosis assay

IgG-opsonized zymosan was prepared by incubating particles in suspension in PBS with human IgG (13 mg/mL, 30 min at 37°C) and washing as described (Le Cabec and Maridonneau-Parini, 1994). The number of particles was counted in a Malassez chamber. FITC-labeled zymosan particles were then added at a MOI of 5 and incubated for 30 minutes at 37°C. Cells were then extensively washed

with PBS and fixed in 3.7% PFA. To exclusively quantify phagocytosis and not binding, extracellular zymosan was stained as described (Le Cabec et al., 2000).

Histological analyses

Paraffin embedded tissue samples were sectioned and stained with hematoxylin and eosin for histomorphological analysis. Immunohistochemical staining was performed on paraffin-embedded tissue sections, using anti-CD163 (10D6, mouse mAb, Leica/Novocastra) and anti-pSTAT3 (D3A7 rabbit mAb, Cell Signaling Technology). Immunostaining of paraffin sections was preceded by different antigen unmasking methods. After incubation with primary antibodies, sections were incubated with biotin-conjugated polyclonal anti-mouse or anti-rabbit immunoglobulin antibodies followed by the streptavidin-biotin-peroxidase complex (ABC) method (Vector Laboratories) and then were counter-stained with hematoxylin. Slides were scanned with the Panoramic 250 Flash II (3DHISTECH). Virtual slides were automatically quantified for macrophage distribution as previously described (Lastrucci et al., 2015; Vérollet et al., 2015a). For confocal microscopy, samples were stained with primary antibodies as described above and followed by anti-mouse IgG isotype specific or anti-rabbit IgG antibodies labeled with Alexa488 and Alexa555 (Molecular Probes). Samples were mounted with Prolong® Antifade reagent (Molecular Probes) and examined using a 60x/1.40N.A. objective of an Olympus FV1000 confocal microscope.

QUANTIFICATION AND STATISTICAL ANALYSIS

Information on the statistical tests used, and the exact values of n (number of donors) can be found in the Figure Legends. All statistical analyses were performed using GraphPad Prism 6.0 (GraphPad Software Inc.). The statistical tests were chosen according to the following. Two-tailed paired or unpaired t test was applied on datasets with a normal distribution (determined using Kolmogorov-Smirnov test), whereas two-tailed Mann-Whitney (unpaired test) or Wilcoxon matched-paired signed rank tests were used otherwise. $p < 0.05$ was considered as the level of statistical significance (* $p \leq 0.05$; ** $p \leq 0.005$; *** $p \leq 0.0005$; **** $p \leq 0.0001$).

Cell Reports, Volume 26

Supplemental Information

Tuberculosis Exacerbates HIV-1 Infection

through IL-10/STAT3-Dependent

Tunneling Nanotube Formation in Macrophages

Shanti Souriant, Luciana Balboa, Maeva Dupont, Karine Pingris, Denise Kviatcovsky, Céline Cougoule, Claire Lastrucci, Aicha Bah, Romain Gasser, Renaud Poincloux, Brigitte Raynaud-Messina, Talal Al Saati, Sandra Inwentarz, Susana Poggi, Eduardo Jose Moraña, Pablo González-Montaner, Marcelo Corti, Bernard Lagane, Isabelle Vergne, Carolina Allers, Deepak Kaushal, Marcelo J. Kuroda, Maria del Carmen Sasiain, Olivier Neyrolles, Isabelle Maridonneau-Parini, Geanncarlo Lugo-Villarino, and Christel Vérolet

SUPPLEMENTAL FIGURES

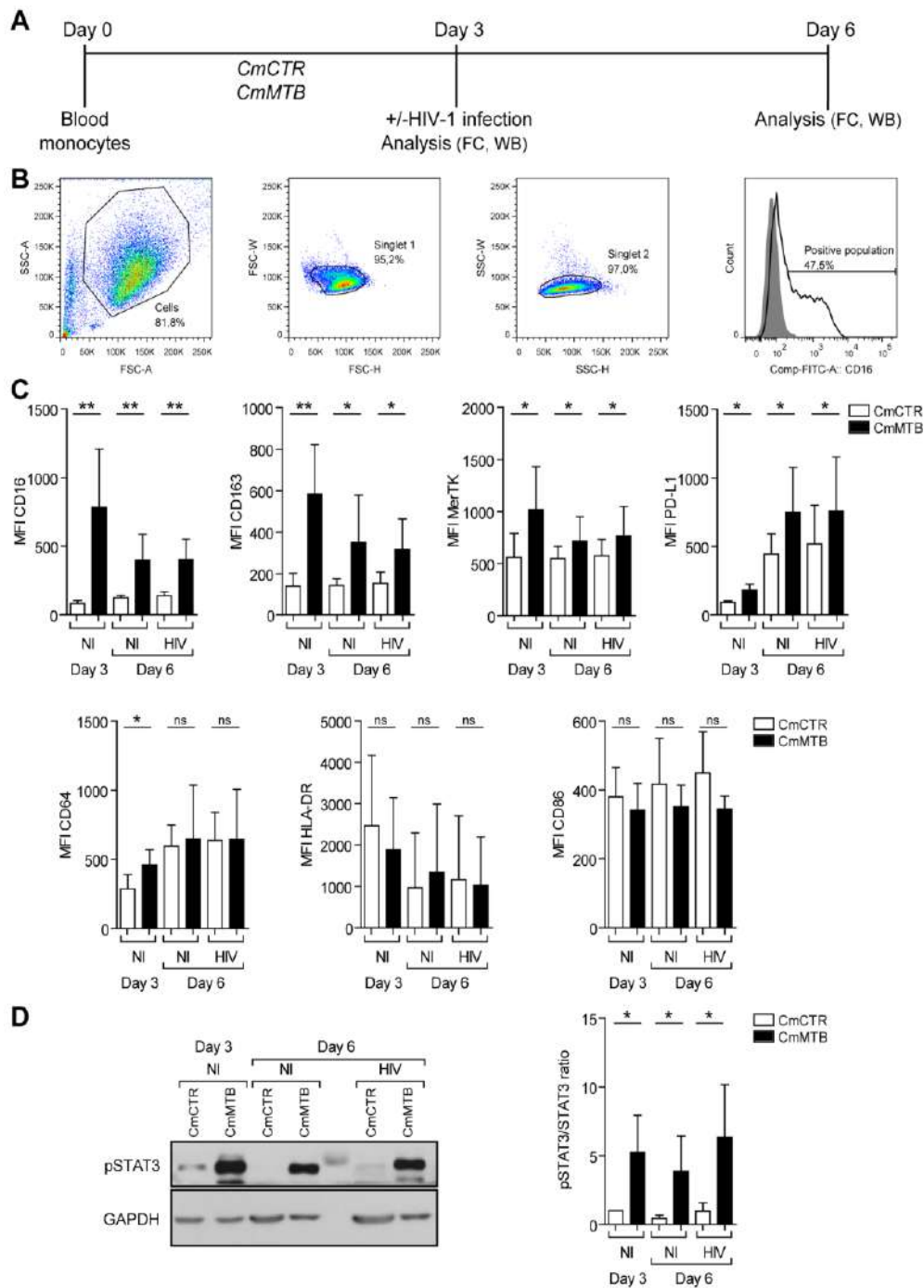


Figure S1 (Related to Figure 1). M(IL-10) phenotype of cells conditioned with CmCTR or CmMTB is conserved upon HIV-1 infection.

(A) Representation of the experimental design. Briefly, monocytes from healthy subjects were treated with conditioned medium from mock- (CmCTR) or Mtb-infected macrophages (CmMTB) for 3 days. Cells were then infected with HIV-1 ADA strain at MOI of 0.1 or left uninfected and kept in culture for 3 more days. (B) Flow cytometry gating strategy of representative sample of monocytes treated for 3 days with CmCTR or CmMTB. (C) Histograms showing the Median Fluorescence Intensity (MFI) of anti-inflammatory cell-surface markers CD16, CD163, MerTK and PD-L1 (top) and pro-inflammatory markers CD64, HLA-DR and CD86 (bottom) on cells treated with CmCTR and CmMTB at day 3, and HIV-1-infected or uninfected at day 6. $n = 7$ donors. (D) Left: Representative images of Western Blot illustrating the expression of p^{Y705}-STAT3, STAT3 and GAPDH as loading control. Right: Histogram showing the quantification of the p^{Y705}-STAT3 on total STAT3 ratio of cells treated

with CmCTR and CmMTB at day 3, and HIV-1-infected or uninfected at day 6. n = 6 donors. Data in histograms are represented as mean \pm SD. * $p \leq 0.05$; ** $p \leq 0.005$; ns, not significant.

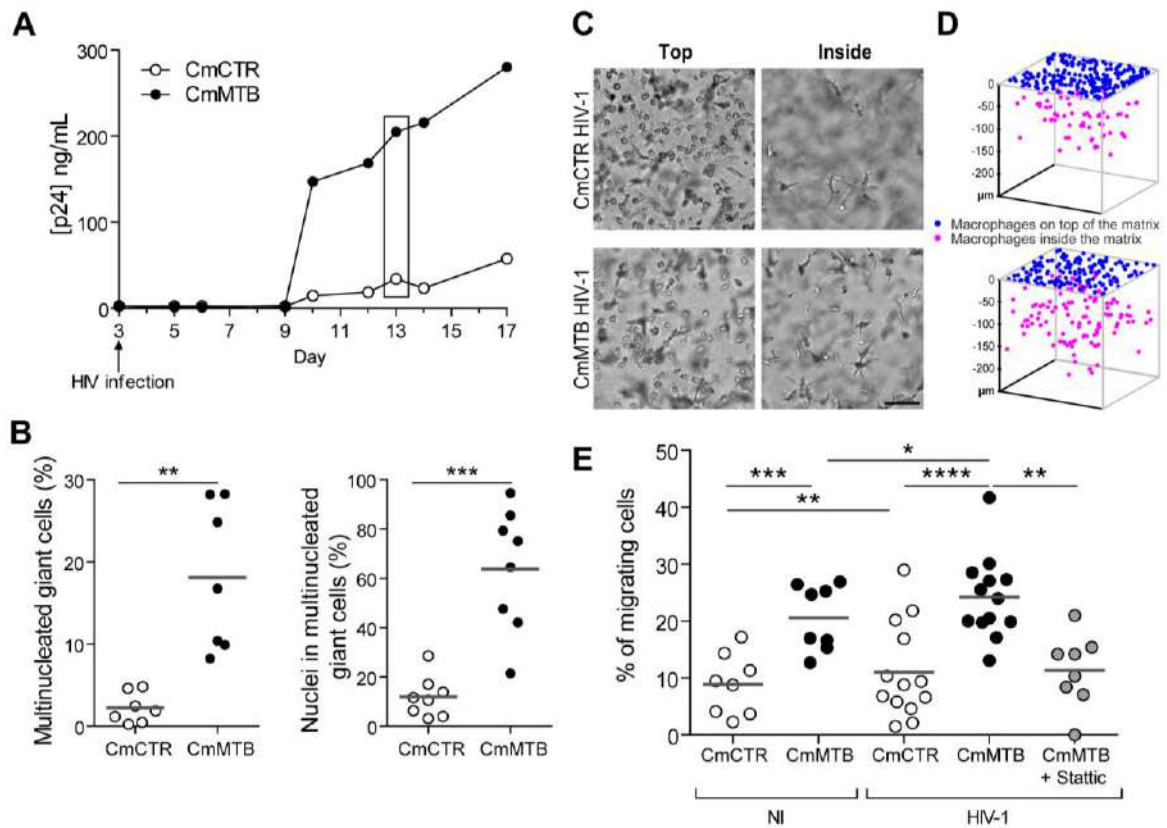


Figure S2 (Related to Figure 1 and 6). TB-associated microenvironment increased HIV-induced multinucleated giant cells (MGC) formation and HIV-induced cell migration (in a STAT3-dependent manner).

(A) Kinetics of HIV-1 protein p24 release in the supernatant of cells from a representative donor, treated with either CmCTR or CmMTB. (B) Vertical scatter plots showing the percentages of MGC (left) and nuclei within MGC (right) of day 13 HIV-1 infected macrophages treated with CmCTR or CmMTB. (C-E) Day 5 uninfected (NI) or HIV-1 infected macrophages, previously treated with CmCTR, CmMTB and CmMTB in the presence of Stattic were seeded on the top of Matrigel matrices and allowed to migrate for 48h. (C) Representative brightfield images of HIV-1 infected macrophages previously treated either with CmCTR (top) or CmMTB (bottom), and visualized either on top (left) or inside (right) the matrix. Scale bar, 50 μ m. (D) 3D positions of migrating HIV-1 infected macrophages, previously treated with CmCTR, CmMTB, for a representative donor, reported using TopCat software. (E) Vertical scatter plot showing the percentage of migrating cells after 48h. Each circle within vertical scatter plots represents a single donor. Mean value is represented as a dark grey line. * $p \leq 0.05$; ** $p \leq 0.005$; *** $p \leq 0.0005$; **** $p \leq 0.0001$.

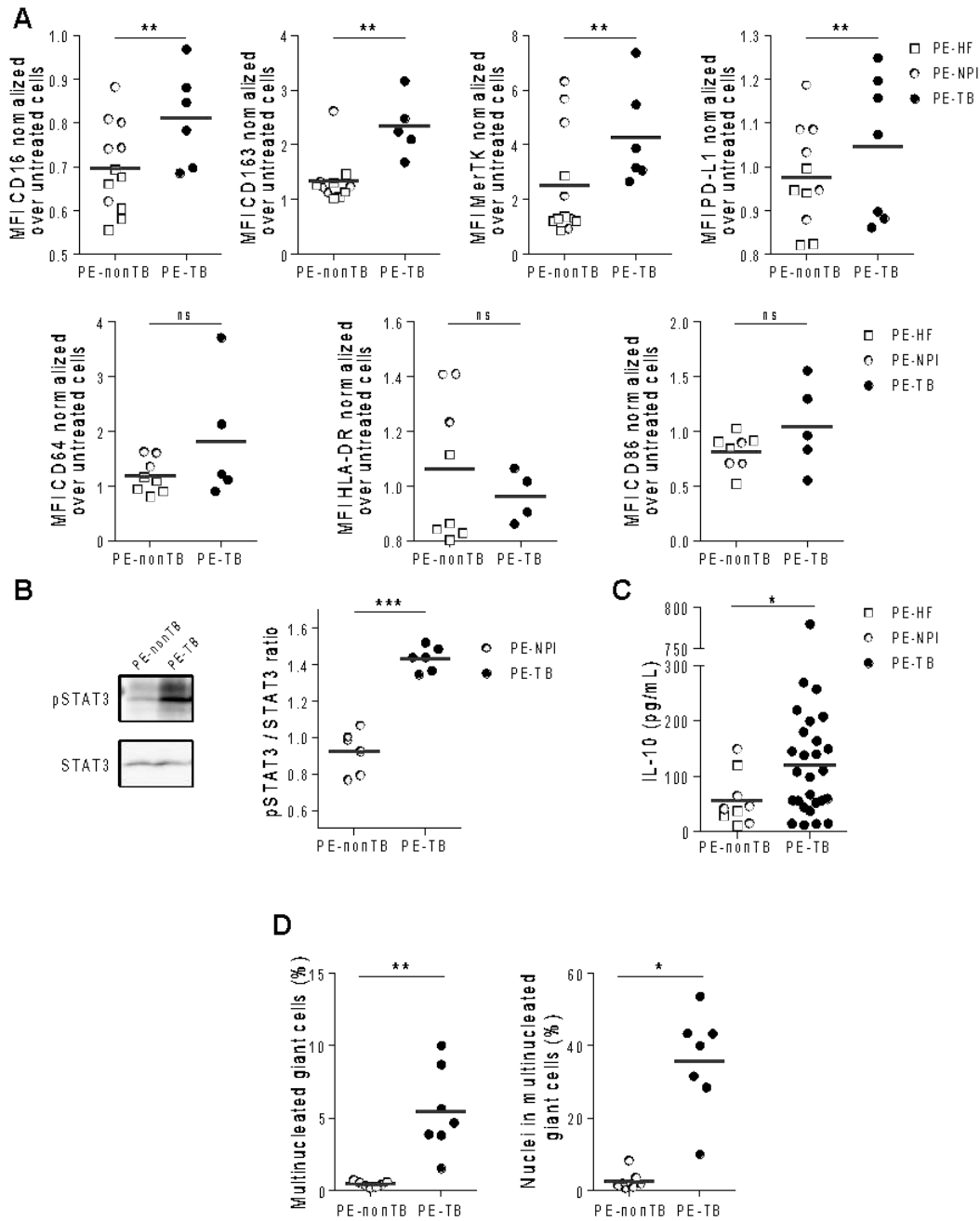


Figure S3 (Related to Figure 1). Monocytes treated with pleural effusions (PE) from TB patients exhibit a M(IL-10) phenotype, STAT3 activation and high HIV-induced multinucleated giant cells (MGC) formation.

(A) Vertical scatter plots showing the Median Fluorescence Intensity (MFI) of cell-surface markers characteristic of the M(IL-10) phenotype, including CD16, CD163, MerTK and PD-L1 (top), and markers typical of M1 phenotype such as CD64, HLA-DR and CD86 (bottom), on monocytes differentiated 3 days into macrophages under the presence of PE-TB or PE-nonTB (normalized over the corresponding MFI of untreated cells). (B) Left: Representative images of Western Blot illustrating the expression of p^{Y705}-STAT3, STAT3 and GAPDH as loading control. Right: Quantification of the p^{Y705}-STAT3 on total STAT3 ratio of monocytes differentiated 3 days in the presence of PE-TB or PE-nonTB. (C) Vertical scatter plots showing the dosage of interleukin-10 (IL-10) in PE-TB and PE-nonTB. (D) Vertical scatter plots showing the percentages of MGC (left panel) and nuclei within MGC (right) of day 13 HIV-1 infected macrophages treated with PE-nonTB or PE-TB. Each circle within vertical scatter plots represents a single donor. Mean value is represented as a dark grey line. In this figure, PE-nonTB are parapneumonic PEs (PE-NPI, empty circle) and Heart Failure PEs (PE-HF, empty square). * p < 0.05; ** p < 0.005; *** p < 0.0005; ns, not significant.

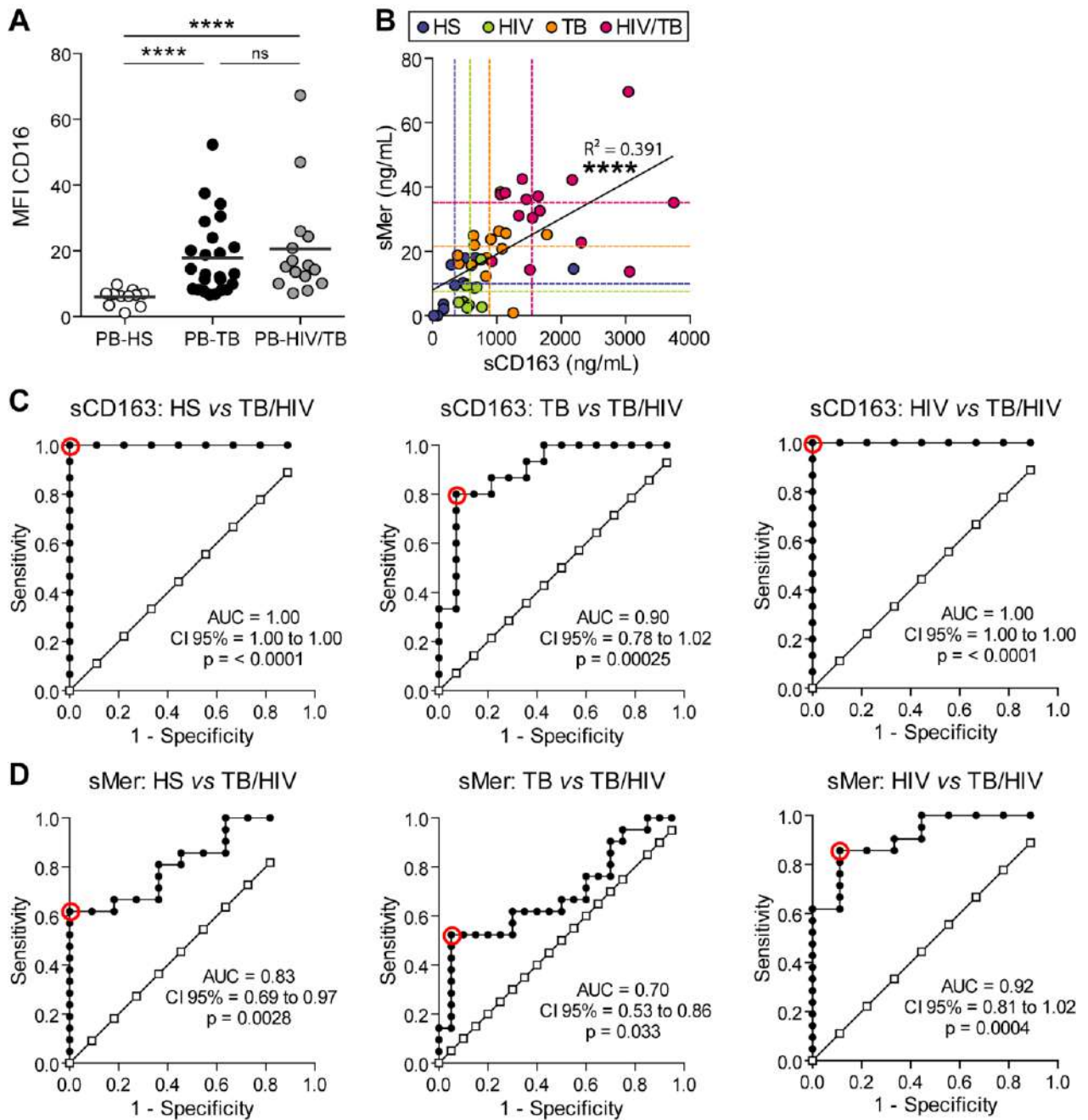


Figure S4 (Related to Figure 3). **Systemic expansion of the M(IL-10) monocyte population in co-infected patients.**

(A) Vertical scatter plots showing the Median Fluorescence Intensity (MFI) of cell-surface marker CD16 on CD14⁺ monocytes from peripheral blood (PB) of healthy subjects (PB-HS), tuberculous patients (PB-TB) and HIV/Mtb co-infected patients (PB-HIV/TB). (B) Vertical scatter plot showing sMer vs sCD163 in HS (blue), HIV (green), TB (orange) and HIV/TB (pink) patients. Median values are indicated as a dashed line. (C) Receiver Operating Characteristic (ROC) curve of sCD163 concentration in the serum of HS (left), TB (middle), HIV (right) compared to HIV/TB patients. The red circle represents the optimal cut point. (D) ROC curve of sMer concentration in the serum of HS (left), TB (middle), HIV (right) compared to HIV/TB patients. The red circle represents the optimal cut point. Each circle within vertical scatter plots represents a single donor. Mean value is represented as a dark grey line. Abbreviation: AUC, area under the curve; CI, confidence interval. **** $p < 0.0001$; ns, not significant.

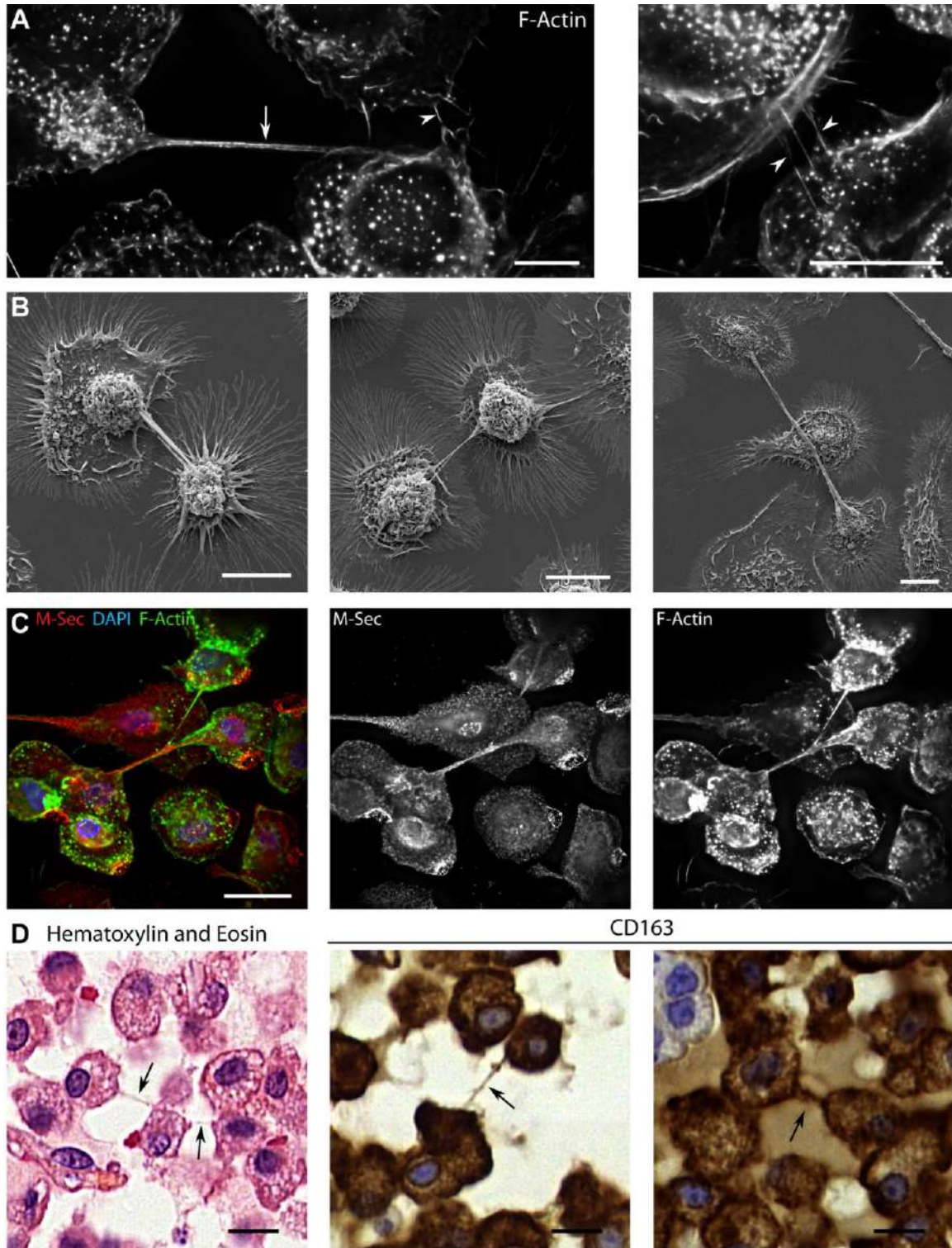


Figure S5 (Related to Figure 5, and Movies 1, 2 and 4). TB-induced microenvironment increases tunneling nanotube (TNT) formation.

(A) Deconvolution microscopy images showing F-actin staining in day 6 HIV-1 infected macrophages, treated with CmMTB. Arrow: thick TNT (left, see Movie 1); arrowheads: thin TNTs (right, see Movie 2). Scale bars, 20 μ m. (B) Representative scanning electron microscopy images, showing TNTs on day 6 HIV-infected macrophages previously treated with CmMTB. Scale bars, 10 μ m. (C) Deconvolution microscopy images showing M-Sec distribution in day 6 HIV-1 infected macrophages, treated with CmMTB. M-Sec (red), F-actin (green), DAPI (blue). Scale bar, 20 μ m. See movie 4. (D) Immunohistochemical images illustrate TNT-like structures (arrows) in lung biopsy of a SIV/Mtb co-infected NHP stained with Eosin (left) or CD163 (middle and right). Nuclei are counterstained with Hematoxylin. Scale bar, 10 μ m.

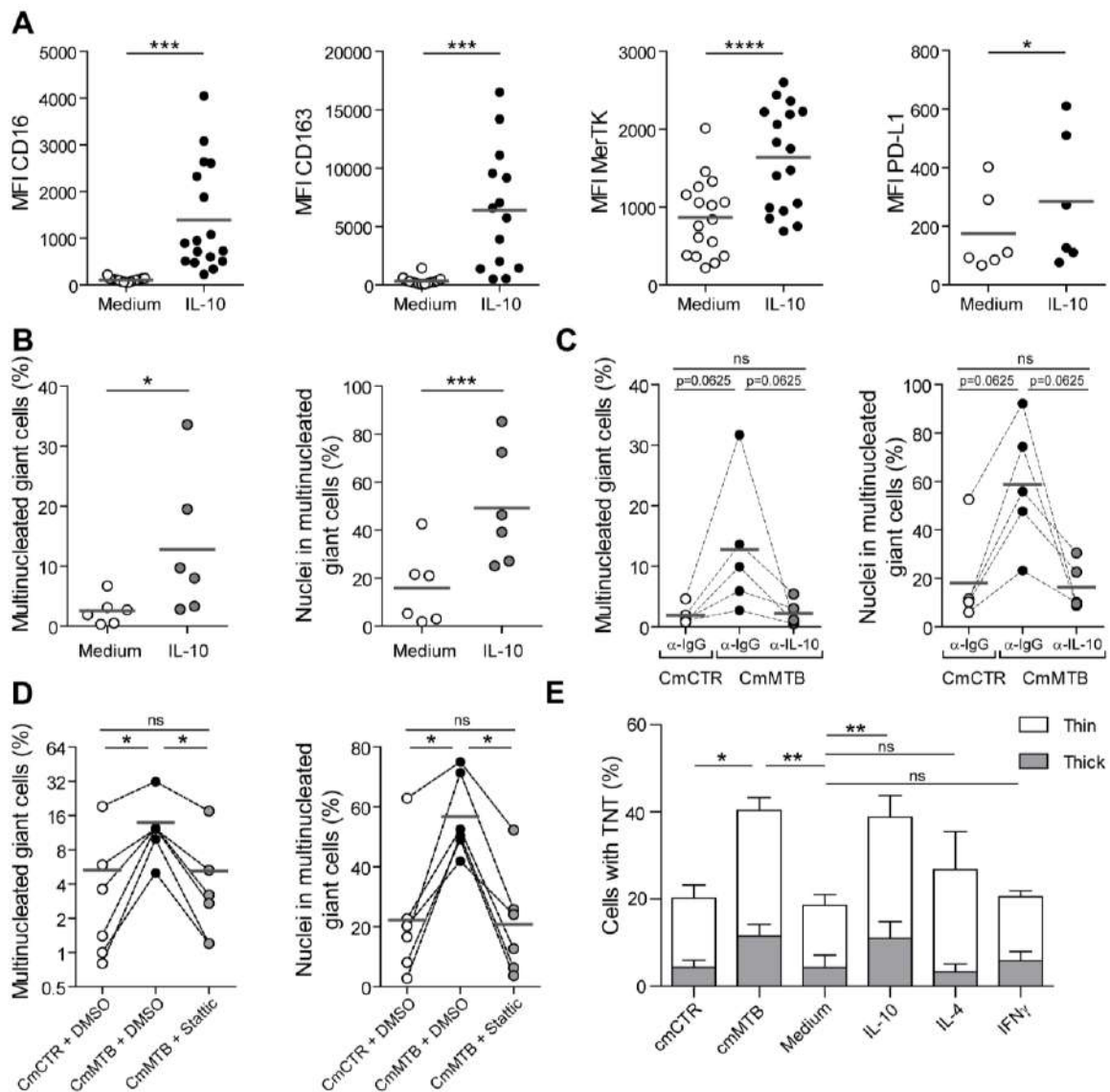


Figure S6 (Related to Figure 6). The IL-10/STAT3 axis is responsible for the M(IL-10) phenotype as well as increased HIV-1- induced multinucleated giant cells (MGC) and tunneling nanotubes (TNT) formation.

(A) Vertical scatter plots showing the Median Fluorescence Intensity (MFI) of M(IL-10) cell-surface markers such as CD16, CD163, MerTK and PD-L1 on monocytes differentiated 3 days in culture medium or culture medium supplemented with recombinant IL-10. (B) Vertical scatter plots showing the percentages of multinucleated giant cells (MGC) (left) and nuclei within MGC (right) of day 13 HIV-1 infected macrophages treated with IL-10 or not. (C) Vertical scatter plots showing the percentages of MGC (left) and nuclei within MGC (right) of day 13 HIV-1 infected macrophages treated with IL-10-depleted (α-IL-10) CmMTB, or mock-depleted (α-IgG) CmCTR and CmMTB. (D) Vertical scatter plots showing the percentages of multinucleated giant cells (MGC) (left) and nuclei within MGC (right) of day 13 HIV-1 infected macrophages treated with CmCTR, CmMTB and Stattic. Each circle within vertical scatter plots represents a single donor. Mean value is represented as a dark grey line. (E) Stacked bars showing the percentage of cells with thick (grey) and thin (white) TNTs of day 6 HIV-1 infected macrophages untreated (Medium) or treated with CmCTR, CmMTB, recombinant IL-10 (10ng/mL), recombinant IL-4 (20ng/mL), recombinant IFN-γ (2ng/mL). * p < 0.05; ** p < 0.005; *** p < 0.0005; **** p < 0.0001; ns, not significant.

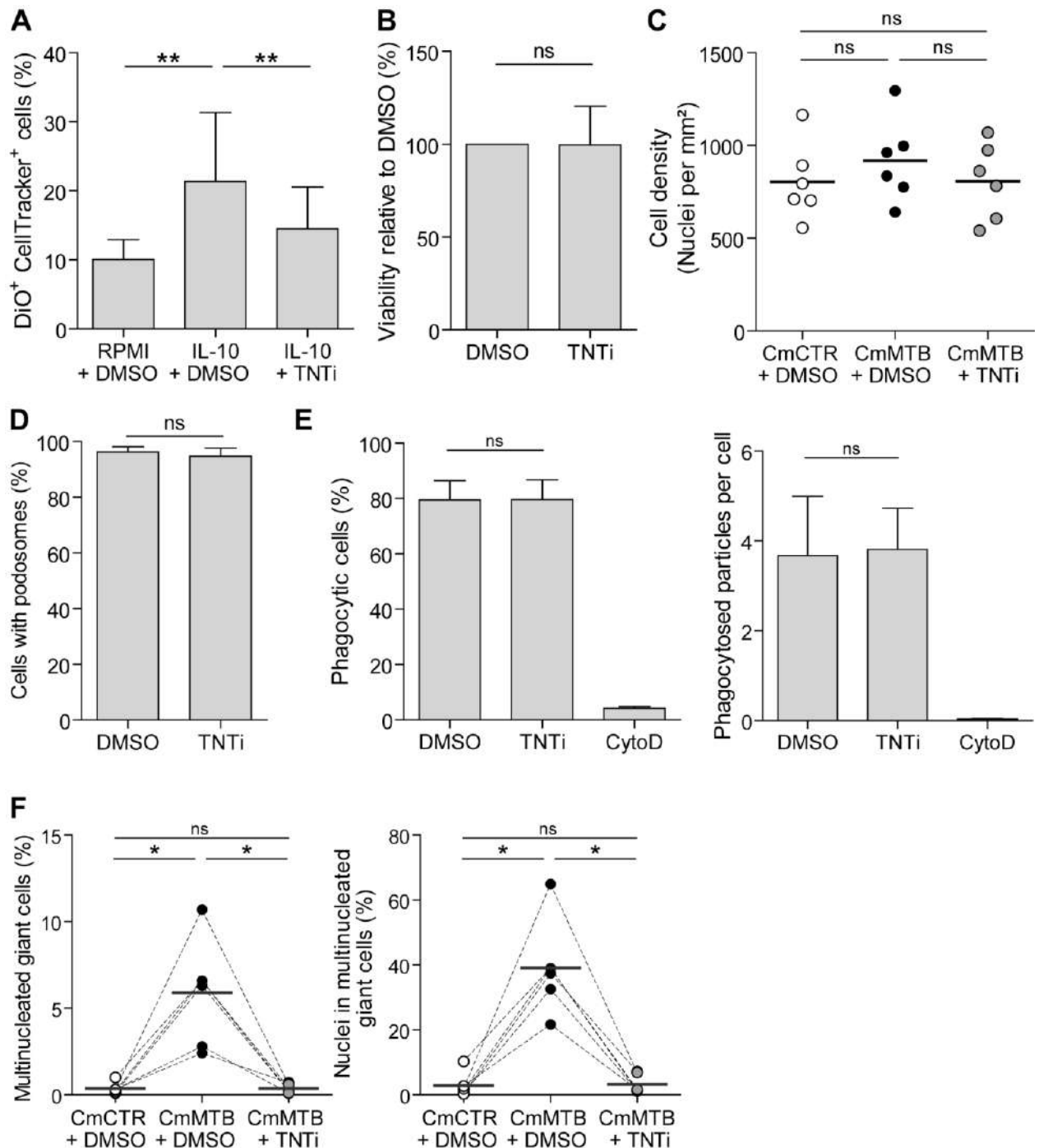


Figure S7 (Related to Figure 7). Effects of TNTi (20 μ M) on several macrophage characteristics and functions.

(A) Histograms showing the effect of TNTi on fluorescent material transfer between DiO- and CellTracker-stained cells, in macrophages treated (or not) with IL-10 or IL-10 + TNTi, measured using live cell imaging. More than 1300 cells per condition were analyzed. $n = 3$ donors. (B) Histograms showing the viability of TNTi-treated macrophages relative to DMSO-treated cells, as measured with LDH assay. $n = 6$ donors. (C) Vertical scatter plot showing the cell density of day 13 HIV-1 infected macrophages treated with CmCTR, CmMTB or CmMTB + TNTi, measured on immunofluorescence images. More than 3000 cells per conditions were analyzed. (D) Histograms showing the percentage of cells with podosomes of TNTi-treated macrophages compared to DMSO-treated cells, as measured on immunofluorescence images. More than 500 cells per conditions were analyzed. $n = 6$ donors. (E) Histograms showing the percentage of phagocytic cells (left) and the number of phagocytosed particles per cell (right) of TNTi-treated macrophages compared to DMSO-treated cells, as measured on immunofluorescence images. $n = 4$ donors. Cytochalasin D was used at 2 μ M ($n = 2$ donors). (F) Vertical scatter plots showing the percentages of multinucleated giant cells (MGC) (left) and nuclei within MGC (right) of day 13 HIV-1 infected macrophages treated with CmCTR, CmMTB or CmMTB + TNTi. Each circle within vertical

scatter plots represents a single donor. Mean value is represented as a dark grey line. Data in histograms are represented as mean \pm SD. * $p \leq 0.05$; ** $p \leq 0.005$; ns, not significant.

SUPPLEMENTAL TABLES

Table S1 (Related to Figure 3). **Clinical data of tuberculous (TB), co-infected (HIV/TB) Patients and Healthy Subjects (HS) from Argentina.**

	PB-HS	PB-TB	PB-HIV/TB	PE-TB	PE-nonTB
Age, years (range)	37 (21-65)	38 (19-66)	37 (31-58)	37 (19-58)	46 (27-69)
Gender, %	M, 84%	M, 92%	M, 100%	M, 96%	M, 67%
Nationality, %	Arg., 100%	Arg., 70% Bol., 23% Peru, 7%	Arg., 88% Bol., 12%	Arg., 45% Bol., 44% Peru, 11%	Bol., 67% Arg., 33%
TB disease localization, %	-	Pulmonary, 100 % (Pleural, 46%)	Pulmonary, 88% (Pleural, 43%) Ganglionar, 12%	Pleural, 100%	-
AFB in sputum, %	-	3+, 56% 2+, 12% 1+, 30% -, 2%	3+, 50% 2+, 25% 1+, 25% -, 0%	ND	-
ART treatment, %	-	-	21 %	-	-
Leukocyte count, mean ± SEM, cell/μL	9348 ± 954	8965 ± 1247	5356 ± 788,3	ND	ND
Lymphocyte mean ± SEM, %	25 ± 5	23 ± 6	21 ± 4	ND	ND
Monocyte mean ± SEM, %	7 ± 3	7 ± 3	16 ± 3	ND	ND

Abbreviations: M.: Male, Arg.: Argentina, Bol.: Bolivia, ND: No data

Table S2 (Related to Figure 2). **Clinical data of NHPs.**

Animals	Status	Sex	Age of death (years)	Days after infection*	Viral load**
EC61	-	M	8.99	-	-
GI53	-	M	5.02	-	-
IT02	-	M	4.69	-	-
BK48	SIV	M	12.06	322	8.58 x 10 ⁶
DD87	SIV	F	9.84	540	3.03 x 10 ⁴
DT18	SIV	M	8.85	764	4.40 x 10 ⁴
BA34	SIV	M	16.79	750	1.91 x 10 ⁵
DR28	SIV	M	8.84	120	1.48 x 10 ⁷
CA75	LTB	M	11.7	106	-
FE10	LTB	M	7	166	-
FJ05	LTB	M	6.81	181	-
CL10	ATB	M	13.84	51	-
CG58	ATB	M	7.71	75	-
GK87	ATB	F	7.76	38	-
ER44	SIV/LTB	M	8.61	167	1.93 x 10 ⁵
HB12	SIV/LTB	M	4.97	167	1.04 x 10 ⁶
ID01	SIV/LTB	M	3.58	153	2.17 x 10 ⁶
HP22	SIV/ATB	M	3.79	113	3.7 x 10 ⁸
HP41	SIV/ATB	M	3.78	111	6 x 10 ⁵
HT09	SIV/ATB	M	3.72	104	7.5 x 10 ⁶

* Infection 1: Mtb CDC1551 and infection 2: SIVmac239. For co-infected macaques, days after first Mtb infection. Abbreviations: LTB: latent TB, ATB: active TB, M: male, F: female.

Table S3 (Related to Figure 2): Histopathological scoring of lung lesions in NHPs.

Animals	Status	Lung Disease severity	Granulomatous lesions				Non- Granulomatous lesions
			Granuloma Size	Type of granuloma	Distribution pattern	Cellular composition	
EC61	-	None	-	-	-	-	- Few & small perivascular lymphohistiocytic infiltrates, PMN+
GI53	-	None	-	-	-	-	- Few & small perivascular lymphohistiocytic infiltrates, PMN+
IT02	-	None	-	-	-	-	- Few & small perivascular lymphohistiocytic infiltrates -PMN+ -peribronchial iBALT
BK48	SIV	Minimal	-	-	-	-	- small perivascular lymphohistiocytic infiltrates
DD87	SIV	Minimal	-	-	-	-	- small perivascular lymphohistiocytic infiltrates
DT18	SIV	Minimal	-	-	-	-	-polymorph infiltrates
BA34	SIV	Mild	-	-	-	-	- Focal interstitial pneumonia, - interstitial lymphohistiocytic infiltrates, - thickening of the alveolar wall, - collagen deposit, - type-2 pneumocyte hyperplasia
DR28	SIV	Minimal	-	-	-	-	thickening of the alveolar wall closed to the pleura
CA75	LTB	Mild	small	Non Necrotizing, Poorly organized	multifocal	- Lymphocytic cuff - Epithelioid & Foamy Mφ - MGC, - Fibrosis [+]	Interstitial pneumopathy
FE10	LTB	Mild	large	Nonnecrotizing Suppurative	focal solid coalescent	- Lymphocytic cuff - Epithelioid & Foamy Mφ - MGC	Thickening of the alveolar wall
FJ05	LTB	Mild	medium	caseous	multifocal	- Lymphocytic cuff - peripheral fibrosis	Strong interstitial pneumopathy
CL10	ATB	Moderate	Small & medium	Caseous & solid	Multifocal coalescent	- Lymphocytic cuff	- Strong interstitial pneumopathy

						- Epithelioid Mφ, - MGC++	& haemorrhage
CG58	ATB	Mild	Small, medium & large	Necrotic & solid	Multifocal coalescent	- Lymphocytic cuff - Epithelioid Mφ, - MGC++	-
GK87	ATB	Moderate	Medium & large	Necrotic, caseous and suppurative	Multifocal coalescent	- Lymphocytic cuff - Epithelioid Mφ, MGC++, PMN++	-transudat in the alveolar space, - collagen deposits -Interstitial pneumopathy
ER44	SIV/LTB	Mild	large	Necrotic & caseous	focal	2 coalescent follicles, Loss of the lymphocytic cuff, Epithelioid Mφ- MGC++,	-Interstitial pneumopathy, - haemorrhage & fibrosis
HB12	SIV/LTB	Severe	none	-	-	-	-Interstitial pneumopathy, iBALT - haemorrhage & alveolitis, - fibrosis, syncytia and PMN++
ID01	SIV/LTB	Moderate	none	-	-	-	-Interstitial pneumopathy, iBALT - haemorrhage & alveolitis,
HP22	SIV/ATB	Moderate	medium	Solid, necrotic, fibrotic & mineralized	multifocal	- Lymphocytic cuff - Epithelioid Mφ, MGC++	-Interstitial pneumopathy - haemorrhage & syncytia
HP41	SIV/ATB	Severe	large	Necrotic	coalescent	- Lymphocytic cuff - Epithelioid Mφ, MGC++	-strong Interstitial pneumopathy, - haemorrhage & alveolitis, fibrosis, PMN++
HT09	SIV/ATB	Severe	large	Suppurative	Multifocal, coalescent & invasive	Loss of the lymphocytic cuff, Epithelioid Mφ, MGC++, PMN++ fibrosis	- Interstitial pneumopathy, - haemorrhage

Abbreviations: PMN: polymorphonuclear leukocytes, iBALT: inducible Bronchus-associated lymphoid tissue, Mφ: Macrophages, MGC: Multinucleated giant cells.

III. Scientific contribution to the paper

In this paper, where we show that cmMTB-induced TNT are responsible for the increased viral replication and dissemination observed in macrophages in the context of co-infection, my main contribution was to reproduce the experiments showing the exacerbation of HIV-1 replication in cmMTB macrophages and to perform the experiments requested during the revision process of the manuscript in October-November 2018.

One of the main points raised by the reviewers concerned the use of HIV-1_{ADA} strain, which infects efficiently macrophages but is not sexually transmitted. The reviewers argued that HIV-1-infected patients are poorly infected with macrophage-tropic strains, therefore the use of HIV-1_{ADA} might represent a caveat in our study. It is true that most transmitted/founder viruses are generally non-macrophage tropic, albeit most of them are R5-tropic. Actually, Swanstrom and colleagues described that M-tropic viruses are enriched in the brain, where they efficiently infect the microglia through their high affinity for CD4. These viruses are rather rare in the blood, where T-cell tropic viruses are predominant [327]. However, T-tropic viruses showing a certain degree of infection of macrophages have also been described [765]–[767]. In addition, macrophage tropism is a relative and complex concept that greatly depends on how viruses are transferred into the macrophages. For instance, it has been shown that T/F viruses can infect macrophages through phagocytosis of infected T-cells [649]. In humanized mouse, some M-tropic T/F viruses such as CHO40 are able to sustain systemic replication and are found in various tissues including the lung [768]. Altogether, these studies strongly suggest that under certain circumstances, T-tropic viruses (including T/F viruses) with a certain capacity to infect macrophages (though less efficiently than infection of T cell) are less rare in patients than thought. To answer the reviewers' concerns, we performed additional experiments using the T/F HIV-1 strain SUMA. Our preliminary results showed that, in macrophages, the replication of this virus is quite low (around 0.1 ng/mL of p24 was measured at 10 days post-infection), but 3x-fold enhanced in cells conditioned with cmMTB, indicating that independently of the viral strain used, Mtb-environment enhances HIV-1 replication. It is likely that restriction at the viral entry step explains why the replication of SUMA remains low in macrophages, despite cmMTB treatment. This is consistent with our finding that cmMTB conditioning has no effects on the viral entry efficiency in macrophages (Figure 4B).

Another interesting question asked by the reviewers was to know whether TNT formation is specific of M(IL-10) macrophages or if other phenotypes could also form such structures. To answer that question, I differentiated monocytes from 6 independent healthy donors into macrophages with IL-4, IFN γ and LPS, IL-10, cmMTB or left untreated and compared their capacity to form TNT after 3 days of infection with HIV-1. Only IL-10 and cmMTB treatment increased the number of cells forming TNT significantly, while IL-4 treatment showed a tendency to increase TNT formation (Figure 32A), suggesting that TNT induction is not specific of M(IL-10) macrophages. I also assessed whether fully differentiated macrophages with different activation profiles (M(IL-4), M(IL-10), and M(IFN γ)) could form TNT, at day 8 of differentiation and in absence of HIV-1 infection. I found that cmMTB-macrophages and M(IL-10) macrophages could still form TNT, but it was M(IFN γ) that was more efficient at forming TNT (Figure 32B, n=4 independent donors), suggesting that these macrophages are

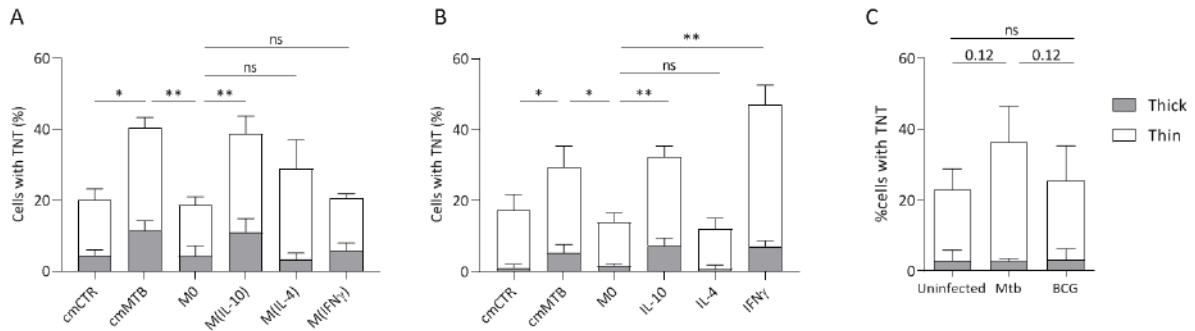


Figure 32: Quantification of tunneling nanotube (TNT) formation in several conditions.

A | Freshly isolated monocytes were treated with M-CSF alone (M0), or M-CSF with cmCTR, cmMTB, IL-10 (20 ng/mL), IL-4 (20 ng/mL) or IFN γ (2 ng/mL) and infected at day 3 with HIV-1_{ADA}. Stacked bars shows the quantification of the percentage of cells with thick (grey) and thin (white) TNTs at day 6 (3 days post-infection). n = 6 donors.

B | Freshly isolated monocytes were cultured with M-CSF for 6 days to obtain macrophages. Then, cells were treated with M-CSF (M0), cmCTR, cmMTB, IL-10 (20 ng/mL), IL-4 (20 ng/mL) or IΦN γ (2 ng/mL) for 48h. Stacked bars shows the quantification of the percentage of cells with thick (grey) and thin (white) TNTs at day 8. n = 4 donors. Histograms are represented as mean \pm SD.

C | Differentiated macrophages were infected with BCG-mCherry or Mtb (H37Rv) for 24h at a MOI of 1. After washing, cells were fixed and stained for TNT. Stacked bars shows the quantification of the percentage of cells with thick (grey) and thin (white) TNTs at day 8. n = 4 donors. Histograms are represented as mean \pm SD.

Statistical analyses: Two-tailed, Wilcoxon unpaired signed rank test (A), paired t-test (B). * p \leq 0.05; ** p \leq 0.005; ns, not significant.

strongly involved in cell-to-cell communication. In addition, we evaluated the capacity of Mtb and BCG to induce TNT formation after infection. We infected non-polarized, differentiated macrophages with either BCG or Mtb at an MOI of 1. After 24h of infection, we observed that Mtb infection induces a 2x-fold increase in the number of cells with TNT, while BCG infection did not (Figure 32C), suggesting that TNT induction in infectious context is dependent on the pathogen.

The findings obtained in this study constitute the basis of my PhD project, which was to identify novel factors involved in the exacerbation of HIV-1 replication in a co-infection context. To do so, we performed a transcriptomic analysis of cmCTR- and cmMTB-macrophages, and identified the lectin receptor Siglec-1 as a strong candidate. In the first part of my PhD, I assessed the role of this lectin in the viral exacerbation observed in cmMTB-cells, and found it to be expressed by a subset of thick TNT, which were identified in the present article as one of the mechanism participating to the dissemination of HIV-1 in the context of co-infection. The results obtained during my thesis are presented in the next chapter.

Chapter V: Tuberculosis-associated IFN-I induces Siglec-1 on microtubule-containing tunneling nanotubes and favours HIV-1 spread in macrophages.

I. Paper summary

As discussed in the introduction, chapter III, and in the previous article, co-infection with Mtb and HIV-1 remains a challenging global health issue, difficult to diagnose and to treat, especially in low-income countries where the centers able to detect Mtb-infection are rare.

The present work, for which I am the first author of a manuscript just submitted, follows the one presented in the result section, chapter IV; and is currently under review process in a peer-review journal. In the previous study, we found that in the context of co-infection with Mtb, the exacerbation of HIV-1 infection and replication in macrophages was mediated by the IL-10/STAT3-dependent induction of TNT. Here, to assess the gene expression landscape of cmMTB-cells and identify specific factors involved in the exacerbation of the viral infection and replication, we performed a genome-wide transcriptomic analysis. We defined a 60 gene-transcript signature in cmMTB-macrophages, among which 9 were down-regulated and 51 were upregulated compared to cmCTR-cells. Among those, we focused on the lectin Siglec-1 that was strongly induced in cmMTB-treated cells. We verified that Siglec-1 was also upregulated at the protein level by cmMTB conditioning, and found that the abundance of Siglec-1⁺ alveolar macrophages was increased in the lung of TB and TB-SIV co-infected NHP compared to SIV or healthy animals. Moreover, the abundance of these cells correlated with the disease severity. As an ISG [769], we validated that Siglec-1 expression was induced by the IFN-I present in cmMTB conditioning media, and that its expression was not due to IL-10, as observed in the previous study for the CD163 and MerTK markers (Chapter IV). In our NHP model, the number of Siglec-1⁺ alveolar macrophages also correlated with the number of IFN-I activated macrophages, as measured by immunohistology detection of phosphorylated STAT1 in the nucleus. Therefore, in this study, we evidenced that the IFN-I/STAT1 axis, together with the IL-10/STAT3 axis (Chapter IV), is involved in the viral exacerbation observed in the co-infection context.

Siglec-1, whose expression is restricted to myeloid cells (*i.e.* DC, monocytes and macrophages), has been previously described for its role in HIV-1 pathogenesis. Indeed, Siglec-1 efficiently binds to the gangliosides present at the viral envelope of retroviruses and, upon uptake, induces the internalization of captured virions into VCC in DC and macrophages [536], [634]. Moreover, Siglec-1 expressed by DC and macrophages has been shown to actively increase HIV-1 trans-infection of CD4⁺ T cells [633], [635]. As Siglec-1 is upregulated by cmMTB treatment, we suspected an increased viral uptake by cmMTB-macrophages. We found that was the case, and reversed the viral uptake by the lectin using a blocking antibody. These observations led us to suspect the expression of Siglec-1 on

TNT, which could increase the number of molecule and the surface perimeter accessible for viral uptake, thereby explaining the increase in Siglec-1 expression and HIV-1 capture in cmMTB-cells that could result in higher viral entry efficiency, independently of the entry receptor. We found that a subtype of thick TNT (containing microtubules) expressed Siglec-1 and were longer than Siglec-1⁻ TNT. At the functional level, we observed that Siglec-1⁺ TNT contained higher HIV-1 and mitochondria cargos, suggesting that Siglec-1⁺ TNT are preferentially used by HIV-1 to spread in distant cells. Finally, we found that the depletion of Siglec-1 had no impact on TNT formation but had a significant effect on their length. Siglec-1 inhibition also led to a decrease uptake of viral particle, a diminished transfer of HIV-1 from macrophage to macrophage (independently of the entry efficiency) and to a strong reduction in HIV-1 replication.

In this work, we further characterized the mechanisms involved in the exacerbation of the viral replication in the co-infection context by identifying Siglec-1 as a novel marker of a subtype of thick TNT, which are preferentially used by HIV-1 to disseminate from one macrophage to another.

II. Results

Tuberculosis-associated type I interferon induces Siglec-1 expression on microtubule-containing tunneling nanotubes and favours HIV-1 spread among macrophages

Maeva Dupont^{1,2}, Shanti Souriant^{1,2,14}, Luciana Balboa^{2,3,14}, Thien-Phong Vu Manh⁴, Karine Pingris¹, Stella Rousset^{1,5}, Céline Cougoule^{1,2}, Yoann Rombouts¹, Renaud Poincloux¹, Myriam Ben Neji¹, Carolina Allers⁶, Deepak Kaushal^{6,7}, Marcelo J. Kuroda^{6,8}, Susana Benet^{9,10}, Javier Martinez-Picado^{9,11,12}, Nuria Izquierdo-Useros^{9,13}, Maria del Carmen Sasiain^{2,3}, Isabelle Maridonneau-Parini^{1,2,15}, Olivier Neyrolles^{1,2,15}, Christel Vérollet^{1,2,15*} and Geanncarlo Lugo-Villarino^{1,2, 15, 16*}

¹ Institut de Pharmacologie et Biologie Structurale, IPBS, Université de Toulouse, CNRS, UPS, Toulouse, France

² International associated laboratory (LIA) CNRS "IM-TB/HIV" (1167), Toulouse, France and Buenos Aires, Argentina

³ Institute of Experimental Medicine-CONICET, National Academy of Medicine, Buenos Aires, Argentina

⁴ Aix Marseille Univ, CNRS, INSERM, CIML, Marseille, France

⁵ Present address: Department of infectious and tropical diseases, Toulouse University Hospital, Place du Docteur Baylac, TSA 40031, 31059 Toulouse CEDEX 9, France

⁶ Tulane National Primate Research Center, Covington, LA 70433; Department of Microbiology and Immunology, School of Medicine, Tulane University, New Orleans, LA 70112

⁷ Present address: Southwest National Primate Research Center, Texas Biomedical Research Institute, San Antonio, TX, 78227, USA

⁸ Present address: Center for Comparative Medicine and California National Primate Research Center, University of California, Davis, Davis, CA 95616, USA

⁹ IrsiCaixa AIDS Research Institute, Department of Retrovirology, Badalona, Spain

¹⁰ Universitat Autònoma de Barcelona, Barcelona, Spain

¹¹ University of Vic-Central University of Catalonia (UVic-UCC), Vic, Spain.

¹² Catalan Institution for Research and Advanced Studies (ICREA), Barcelona, Spain

¹³ Institut d'Investigació en Ciències de la Salut Germans Trias i Pujol, Badalona, Spain

¹⁴ These authors contributed equally to this work

¹⁵ These senior authors contributed equally to this work

¹⁶ Lead contact

*Correspondance: Geanncarlo Lugo-Villarino (lugo@ipbs.fr), Christel Vérollet (verollet@ipbs.fr)

Summary

While tuberculosis (TB) is a risk factor in HIV-1-infected individuals, the mechanisms by which *Mycobacterium tuberculosis* worsens HIV-1 pathogenesis remain poorly understood. Recently, we showed that HIV-1 spread is exacerbated in macrophages exposed to TB-associated microenvironments due to tunneling nanotube (TNT) formation. To identify factors associated with TNT function, we performed a transcriptomic analysis in these macrophages, and revealed the up-regulation of Siglec-1 receptor, which is dependent on TB-mediated production of type I interferon (IFN-I). In co-infected non-human primates, Siglec-1 is highly expressed by alveolar macrophages, whose abundance correlates with pathology and activation of IFN-I/STAT1 pathway. Intriguingly, Siglec-1 expression localizes exclusively on long microtubule-containing TNT that carry HIV-1 cargo. Siglec-1 depletion in macrophages decreases TNT length, HIV-1 capture and cell-to-cell transfer, and abrogates TB-driven exacerbation of HIV-1 infection. Altogether, we uncover a deleterious role for Siglec-1 in TB-HIV-1 co-infection, and its localization on TNT opens avenues to understand viral spread.

Keywords

Tuberculosis, AIDS, *Mycobacterium tuberculosis*, HIV-1, co-infection, macrophages, monocytes, Siglec-1, CD169, TNT, type I Interferon

INTRODUCTION

Co-infection with *Mycobacterium tuberculosis* (Mtb) and the human immunodeficiency virus (HIV-1), the agents of tuberculosis (TB) and acquired immunodeficiency syndrome (AIDS), respectively, is a major health issue. Indeed, TB is the most common illness in HIV-1-infected individuals, about 55% of TB notified patients are also infected with HIV-1, and about a fifth of the TB death toll occurs in HIV-1 co-infected individuals (WHO health report 2017). Clinical studies evidence a synergy between these two pathogens, which is associated with a spectrum of aberration in immune function (Esmail et al., 2018). Yet, while progress has been made towards understanding how HIV-1 enhances Mtb growth and spread, the mechanisms by which Mtb exacerbates HIV-1 infection require further investigation (Bell and Noursadeghi, 2018; Deffur et al., 2013; Diedrich and Flynn, 2011).

Besides CD4⁺ T cells, macrophages are infected by HIV-1 in humans and by the simian immunodeficiency virus (SIV), the most closely related lentivirus to HIV, in non-human primates (NHP) (Cribbs et al., 2015; Rodrigues et al., 2017). Recently, using a humanized mouse model, macrophages were shown to sustain HIV-1 infection and replication, even in the absence of T cells (Honeycutt et al., 2017; Honeycutt et al., 2016). This is in line with several studies characterizing tissue macrophages, such as alveolar, microglia and gut macrophages, as reservoirs in HIV-1 patients undergoing antiretroviral therapy (Ganor et al., 2019; Jambo et al., 2014; Mathews et al., 2019; Sattentau and Stevenson, 2016).

Macrophages are key host cells for Mtb (O'Garra et al., 2013; VanderVen et al., 2016). We recently reported the importance of macrophages in HIV-1 exacerbation within the TB co-infection context (Souriant et al., 2019). Using relevant *in vitro* and *in vivo* models, we showed that TB-associated microenvironments activate macrophages towards an M(IL-10) profile, distinguished by a CD16⁺CD163⁺MerTK⁺ phenotype. Acquisition of this phenotype is dependent on the IL-10/STAT3 signaling pathway (Lastrucci et al., 2015). M(IL-10) macrophages are highly susceptible not only to Mtb infection (Lastrucci et al., 2015), but also to HIV-1 infection and spread (Souriant et al., 2019). At the functional level, we demonstrated that TB-associated microenvironments stimulate the formation of tunneling nanotubes (TNT), membranous channels connecting two or more cells over short to long distances above substrates. TNT are subdivided in two classes based on their thickness and cytoskeleton composition: "thin" TNT (<0.7 μm in diameter) containing F-actin, and "thick" TNT (>0.7 μm in diameter) are enriched in F-actin and microtubules (MTs) (Souriant et al., 2019). Thick TNT are functionally distinguished by the transfer of large organelles, such as lysosomes and mitochondria (Dupont et al., 2018; Eugenin et al., 2009; Hashimoto et al., 2016). While the contribution for each TNT class to HIV-1 pathogenesis has not been explored (Dupont et al., 2018; Eugenin et al., 2009; Hashimoto et al., 2016), we reported that total inhibition of TNT formation in M(IL-10) macrophages resulted in the abrogation of HIV-1 exacerbation induced by Mtb (Souriant et al., 2019). Factors influencing TNT function in M(IL-10) macrophages remain unknown at large.

In this study, global mapping of the M(IL-10) macrophage transcriptome revealed Siglec-1 (CD169, or sialoadhesin) as a potential factor responsible for HIV-1 dissemination in the co-infection context with TB. As a type I transmembrane lectin receptor, Siglec-1 possesses a large extracellular domain

composed of 17 immunoglobulin-like domains, including the N-terminal V-set domain, which allows the *trans* recognition of terminal α 2,3-linked sialic acid residues in *O*- and *N*-linked glycans and glycolipids, such as those surface-exposed in HIV-1 and SIV particles (Izquierdo-Useros et al., 2012a; Puryear et al., 2012). While Siglec-1 has yet to be implicated in the TB context, it is clearly involved in the pathogenesis of HIV-1, SIV and other retroviruses (Martinez-Picado et al., 2017). Siglec-1 is mainly expressed in myeloid cells (macrophages and dendritic cells) and participates in HIV-1 transfer from myeloid cells to T cells, as well as in the initiation of virus-containing compartment (VCC) formation in macrophages (Izquierdo-Useros et al., 2012a; Izquierdo-Useros et al., 2012b; Puryear et al., 2013; Puryear et al., 2012), and in the viral dissemination *in vivo* (Akiyama et al., 2017; Izquierdo-Useros et al., 2012a; Sewald et al., 2015). Indeed, HIV-1 and other retroviruses have evolved the capacity to hijack the immune surveillance and housekeeping immunoregulatory functions of Siglec-1 (Izquierdo-Useros et al., 2014; O'Neill et al., 2013). Here, we investigate how Siglec-1 expression is induced by TB, and the role it has in the capture and transfer of HIV-1 by TB-induced M(IL-10) macrophages, in particular in the context of TNT.

RESULTS

Tuberculosis-associated microenvironments induce Siglec-1 in macrophages

TB-induced M(IL-10) macrophages are highly susceptible to HIV-1 infection and spread (Souriant et al., 2019). To assess the global gene expression landscape in these cells, we performed a genome-wide transcriptome analysis. To this end, we employed our published *in vitro* model (Lastrucci et al., 2015), which relies on the use of conditioned medium from either mock- (cmCTR) or Mtb-infected (cmMTB) human macrophages. As we described and observed before and herein, cmMTB-treated cells were positive for the M(IL-10) markers (CD16⁺CD163⁺MerTK⁺ and phosphorylated STAT3), and displayed a high rate of HIV-1 infection, as compared to those treated with cmCTR (Lastrucci et al., 2015; Souriant et al., 2019). A distinct 60 gene-transcript signature was defined in cmMTB-treated cells, using a combination of the expression level, statistical filters and hierarchical clustering; 51 genes were up-regulated and 9 genes were down-regulated in cmMTB- compared to cmCTR-treated cells (Figure 1A). We compared expression data of cmMTB- and cmCTR-treated cells to public genesets available from MSigDB (Broad Institute) using the gene set enrichment analysis (GSEA) algorithm (Subramanian et al., 2005). As shown in Figure S1A, a significant fraction of genes that were up-regulated in response to interferon (IFN) type I (*e.g.* IFN α) and II (*i.e.* IFN γ), were also found, as a group, significantly up-regulated in cmMTB-treated cells in comparison to control samples (FDR q-value: < 10E-3). IFN-stimulated genes (ISG) usually exert antiviral activities (McNab et al., 2015; Schneider et al., 2014) and cannot be inferred as obvious candidates to facilitate HIV-1 infection. However, among this ISG signature, the up-regulation of Siglec-1 (7.4-fold, adjusted p value of 0.0162) in cmMTB-treated cells captured our attention due to its known role in HIV-1 pathogenesis (Izquierdo-Useros et al., 2014; O'Neill et al., 2013). We confirmed high Siglec-1 expression in cmMTB-treated macrophages at the mRNA (Figure 1B) and cell-surface protein (Figure 1C, Figure S1B) levels, which was superior to the level obtained in HIV-1-infected cells (Figure S1C). Particularly, cmMTB-treated macrophages displayed high density of Siglec-1 surface expression applying a quantitative FACS assay that determines the absolute number of Siglec-1 antibody binding sites per cell (Figure 1D).

These data indicate that Siglec-1 is highly expressed in human macrophages exposed to TB-associated microenvironments and potentially in the context of TB-HIV co-infection.

Siglec-1⁺ alveolar macrophage abundance correlates with pathology in co-infected primates

NHP has been an invaluable *in vivo* model to better understand the role of macrophages in SIV/HIV pathogenesis (Merino et al., 2017). Considering Siglec-1 binds sialylated lipids present in the envelop of HIV-1 and SIV (Izquierdo-Useros et al., 2012a; Puryear et al., 2012), we examined the presence of Siglec-1 positive alveolar macrophages in lung biopsies obtained from different NHP groups: (i) co-infected with Mtb (active or latent TB) and SIV, (ii) mono-infected with Mtb (active or latent TB), (iii) mono-infected with SIV, and (iv) healthy (Table S1, Figure S2A) (Cai et al., 2015; Kuroda et al., 2018; Souriant et al., 2019). Histological immuno-staining confirmed the presence of Siglec-1⁺ alveolar macrophages in the lungs of healthy NHP (Figure 1E-F and S2A), and revealed its significant increase in NHP mono-infected with either Mtb or SIV (Figure 1E-F and S2A). Strikingly, we noticed a massive abundance of these cells in co-infected NHP (Figure 1E-F and S2A). Concerning the overall abundance of Siglec-1⁺ leukocytes in lungs, we observed a significant increased in all infected NHP in comparison to healthy, with a higher tendency in active TB or co-infected NHP (Figure 1G and S2A). In fact, the number of Siglec-1⁺ leukocytes correlated positively with the severity of NHP pathology (Figure 1H, Table S2). Based on their cell morphology, localization in alveoli, and co-expression with the macrophage marker CD163 (Figure S2A-C), Siglec-1⁺ cells were identified as alveolar macrophages.

Collectively, these data show that Siglec-1 is up-regulated in alveolar macrophages in the context of a retroviral co-infection with active TB.

Siglec-1 expression is dependent on TB-mediated type I IFN signaling

Siglec-1 is an ISG whose expression is induced by IFN-I in myeloid cells (Hartnell et al., 2001). In addition to viral infection, IFN-I is also induced in TB and known to mainly play a detrimental role (McNab et al., 2015; Moreira-Teixeira et al., 2018). Siglec-1 expression has not been described in the TB context or in co-infection with retroviruses such as SIV or HIV-1, therefore we assessed whether IFN-I stimulates Siglec-1 expression in TB-associated microenvironments. First, we found that cmMTB contains high amounts of IFN-I compared to cmCTR (Figure 2A). Next, we showed that recombinant IFN β significantly increased Siglec-1 cell-surface expression in macrophages, close to the level induced by cmMTB (Figure 2B). Interestingly, we observed a modest, albeit significant, induction of Siglec-1 expression in cells treated with interleukin 10 (IL-10), a cytokine we have previously showed to be abundant in cmMTB (Lastrucci et al., 2015) and that renders macrophages highly susceptible to HIV-1 infection (Souriant et al., 2019). However, IL-10 depletion had no effect on Siglec-1 expression by cmMTB-treated cells (Figure 2C). By contrast, blocking the IFN-I receptor (IFNAR2) during cmMTB treatment fully abolished expression of Siglec-1 (Figure 2D), indicating that IFN-I is the responsible factor for Siglec-1 up-regulation in cmMTB-treated cells.

IFN-I binding to IFNAR leads to the phosphorylation and nuclear translocation of the transcription factor STAT1, whose role is essential for transcription of ISG (Ivashkiv and Donlin, 2014). We thus

examined the status of STAT1 activation in co-infected NHP lung tissue. Histological staining of serial sections of co-infected lungs revealed that zones rich in Siglec-1⁺ leukocytes also exhibited positivity for nuclear phosphorylated STAT1 (pSTAT1) (Figure 2E), and the abundance of these two markers strongly correlated with the active status of TB in the different NHP groups (Figure 2F). Moreover, we found that the majority of Siglec-1⁺ alveolar macrophages were also positive for nuclear pSTAT1 in the infected NHP groups compared to healthy (Figure 2E and 2G). In fact, there was a higher number of pSTAT1⁺ alveolar macrophages in TB-SIV co-infected lungs when compared to those from mono-infected NHP (Figure 2G-H).

Altogether, these data demonstrate that Siglec-1 expression in human macrophages is controlled by IFN-I in a TB-associated microenvironment, and suggest the involvement of the IFN-I/STAT1/Siglec-1 axis in the pathogenesis of TB and co-infection with retroviruses.

Siglec-1 localization on thick TNT is associated with their length and HIV-1 cargo

TNT formation is responsible for the increase in HIV-1 spread between human macrophages in TB-associated microenvironments (Souriant et al., 2019). To investigate whether Siglec-1 expression is involved in this process, we first examined its localization in the context of TNT formed by cmMTB-treated cells infected by HIV-1. We observed that Siglec-1 is localized exclusively on microtubule (MT)-positive thick TNT, and not on thin TNT (Figure 3A and Movie 1). Semi-automatic quantification of hundreds of TNT showed that about 50% of thick TNT were positive for Siglec-1 (Figure 3B and S3A). These TNT exhibited a greater length compared to those lacking Siglec-1 (Figure 3C). Importantly, unlike thin TNT, HIV-1 viral proteins are found mainly inside Siglec-1⁺ thick TNT (Figure 3D-E and Movie 2). In addition, these thick TNT also contain large organelles such as mitochondria (Figure 3F and S3B), another characteristic distinguishing thick from thin TNT (Dupont et al., 2018; Onfelt et al., 2006). In general, we also noticed that the incidence of Siglec-1⁺ thick TNT between HIV-1 infected macrophages persisted for more than one week upon HIV-1 infection (Figure S3C), suggesting a high degree of stability for these TNT.

These findings reveal an exclusive localization of Siglec-1 on MT-positive thick TNT that correlates positively with a greater length and high cargo of HIV-1 and mitochondria, arguing for a functional capacity of Siglec-1⁺ TNT to transfer material to recipient cells over long distances.

TB-driven exacerbation of HIV-1 infection and spread in macrophages requires Siglec-1

To demonstrate a functional role for Siglec-1 in the susceptibility of macrophages to HIV-1 infection and spread induced by TB, Siglec-1 was depleted in cmMTB-treated cells by siRNA-mediated gene silencing (Figure 4A and S4A). While this depletion did not affect the total number of thick TNT (Figure 4B and S4B), we observed a 2-fold shortening of thick TNT in cells lacking Siglec-1 when compared to control cells (Figure 4C). Then, we performed a viral uptake assay in these cells using HIV-1 Gag-eGFP virus-like particles (GFP VLP) lacking the viral envelope glycoprotein but bearing sialylated lipids that interact with Siglec-1 on myeloid cells (Izquierdo-Useros et al., 2012b; Puryear et al., 2013). We consistently observed binding of VLP along Siglec-1⁺ thick TNT (Figure S4C). Yet, in the absence of

Siglec-1, we noticed a significant reduction of VLP binding in comparison to control cells (Figure S4D). We confirmed this functional observation using a blocking monoclonal antibody against Siglec-1, showing that this receptor is involved in HIV-1 binding in cmMTB-treated cells (Figure S4E).

We then assessed the role of Siglec-1 in HIV-1 transfer between macrophages, as this receptor is also important for the transfer of the virus to CD4⁺ T cells, (Akiyama et al., 2015; Izquierdo-Useros et al., 2012a; Puryear et al., 2013). We used an established co-culture system between cmMTB-treated macrophages that allows the transfer of the viral Gag protein from infected (donor, Gag⁺, red) to uninfected (recipient, CellTracker⁺, green) cells over 24 hours (Souriant et al., 2019) (Figure S4F). Of note, since Siglec-1 facilitates the infection of macrophages (Zou et al., 2011), we used VSV-G pseudotyped viruses to avoid any effect on HIV-1 primo-infection. Like this, we ensured the viral content was equal in cells at the time of the co-culture despite the loss of Siglec-1 (Figure S4G). The siRNA-mediated depletion of Siglec-1 significantly diminished the capacity of cmMTB-treated macrophages to transfer HIV-1 to recipient cells (Figure 4D), indicating that this receptor is involved in TB-driven macrophage-to-macrophage viral spread (Souriant et al., 2019). Intriguingly, there was a decreasing tendency for the capacity of Siglec-1-depleted cmMTB-treated macrophages to transfer mitochondria to recipient cells compared to controls (Figure 4E and S4F), alluding to a possible defect in mechanisms involved in intercellular material transfer including through thick TNT (Torralba et al., 2016). Remarkably, using replicative HIV-1 ADA strain (Figure 4A), we showed that silencing Siglec-1 expression in cmMTB-treated cells abolished the exacerbation of HIV-1 infection and production, as well as the enhanced formation of multinucleated giant cells (Figures 4F-G), which are pathological hallmarks of HIV-1 infection of macrophages (Verollet et al., 2015; Verollet et al., 2010).

These results determine that TB-induced Siglec-1 expression plays a key part in HIV-1 uptake and efficient cell-to-cell transfer, resulting in the exacerbation of HIV-1 infection and production in M(IL-10) macrophages.

DISCUSSION

In this study, we investigated potential mechanisms by which Mtb exacerbates HIV-1 infection in macrophages, and uncovered a deleterious role for Siglec-1 in this process. These findings have different contributions to our understanding of this receptor in the synergy between Mtb and distinct retroviral infections, and also for TNT biology in host-pathogen interactions.

Our global transcriptomic approach revealed the up-regulation of Siglec-1, as part of an ISG-signature enhanced in macrophages exposed to a TB-associated microenvironment. Although pulmonary active TB has been characterized as an IFN-I-driven disease (Berry et al., 2010; McNab et al., 2015; Moreira-Teixeira et al., 2018), there are no reports in the literature about a role for Siglec-1 in TB or in Mtb co-infection with retroviruses. Expression of Siglec-1 is restricted to myeloid cells except circulating monocytes (Crocker et al., 2007), and is enhanced by IFN-I (Puryear et al., 2013; Rempel et al., 2008) and during HIV-1 infection (Pino et al., 2015). In addition, human alveolar macrophages are distinguished from lung interstitial macrophages by Siglec-1 expression (Yu et al., 2016). In this study, we determined that IFN-I present in TB-associated environments is responsible for Siglec-1

overexpression in human macrophages, which resembled that obtained in HIV-1-infected cells. While we saw a modest induction of Siglec-1 in macrophages upon IL-10 treatment, its depletion from the TB-associated microenvironment had no effect on Siglec-1 expression. This could be explained by the fact that IL-10 induces the autocrine production of IFN-I (Ziegler-Heitbrock et al., 2003) to indirectly modulate Siglec-1 expression in M(IL-10), which then contributes to the exacerbation of HIV-1 infection as we previously reported (Souriant et al., 2019). In the context of the most closely related lentivirus to HIV, namely SIV, we not only confirmed the presence of Siglec-1⁺ alveolar macrophages in SIV-infected NHP, but also reported the high abundance of these cells in active TB and in co-infected NHP groups, when compared to healthy ones. Importantly, we associated the high abundance of Siglec-1⁺ leukocytes with the increase NHP pathological scores, and it correlated positively to the detection of pSTAT1⁺ macrophage nuclei in histological staining of serial sections of lung biopsies from co-infected NHP. This is in line with a recent report on the presence of IFN-I, IFNAR and different ISGs in alveolar and lung interstitial tissue from NHP with active TB (Mattila, 2019), and with the fact that the *in vivo* expression of Siglec-1 is up-regulated early in myeloid cells after SIV infection and maintained thereafter in the pathogenic NHP model (Jaroenpool et al., 2007). In TB-SIV co-infection, we hypothesized that IFN-I is not exerting the expected antiviral effect, but instead is concomitant with chronic immune activation and attenuated by the high expression of Siglec-1 in myeloid cells, as recently proposed in the HIV-1 context (Akiyama et al., 2017). Altogether, these findings uncover the IFN-I/STAT1/Siglec-1 axis as a mechanism established by Mtb to exacerbate HIV-1 infection in myeloid cells, and call for the need to further investigate this signaling pathway in TB pathogenesis.

Another aspect worth highlighting is the impact that Siglec-1 expression has in the capture and transfer of HIV-1 by M(IL-10) macrophages, in particular in the context of TNT. First, we reported that Siglec-1 is located on MT-positive thick (and not on thin) TNT, correlating positively with increased length and HIV-1 cargo. To our knowledge, no receptor has been described so far to be present exclusively on thick TNT, making Siglec-1 an unprecedented potential marker for this subtype of TNT (Dupont et al., 2018). Second, viral uptake assays demonstrated the functional capacity of Siglec-1, including on thick TNT, to interact with viral-like particles bearing sialylated lipids; loss-of-function approaches showed Siglec-1 is important in the capture of these viral particles. Third, Siglec-1 depletion correlated with a decrease in thick TNT length, but had no effect in the total number of thick TNT. This suggests that, while the IFN-I/STAT1 axis is responsible for Siglec-1 expression in M(IL-10) macrophages, it does not contribute to TNT formation. This is in line with our previous report where TNT formation induced by TB-associated microenvironments depends on the IL-10/STAT3 axis (Souriant et al., 2019). Concerning the shortening of thick TNT length, we infer that it may reflect a fragile state due to an altered cell membrane composition in the absence of Siglec-1; TNT are known for their fragility towards light exposure, shearing force and chemical fixation (Rustom et al., 2004). We hypothesize that the longer the TNT is, the more rigidity it requires to be stabilized. Cholesterol and lipids are known to increase membrane rigidity (Redondo-Morata et al., 2012) and are thought to be critical for TNT stability (Lokar et al., 2012; Thayanithy et al., 2014). Thus, the presence of Siglec-1 in thick TNT may affect the cholesterol and lipid composition *via* the recruitment of GM1/GM3 glycosphingolipid-enriched microvesicles (Halasz et al., 2018). In fact, TNT formation depends on GM1/GM3 ganglioside and cholesterol content (Kabaso et al., 2011; Lokar et al., 2012; Osteikoetxea-Molnar et al., 2016; Toth et al., 2017). Since GM1 and GM3 glycosphingolipids are *bona fide* ligands for Siglec-1 (Puryear et al.,

2013), it is likely that Siglec-1⁺ thick TNT exhibit a higher lipid and cholesterol content, and hence an increase of membrane rigidity that favours the stability of longer TNT. Fourth, Siglec-1-depleted donor macrophages were less capable to transfer HIV-1, and to some extent mitochondria, to recipient cells. While infectious synapse and exosome release are mechanisms attributed to Siglec-1 that contribute to cell-to-cell transfer of HIV-1 (Bracq et al., 2018; Gummuluru et al., 2014; Izquierdo-Useros et al., 2014), they accomplish so extracellularly. Here, we speculate that Siglec-1 participates indirectly in the intracellular HIV-1 transfer *via* TNT as a tunnel over long distance, suggesting that factors affecting TNT rigidity favour distal viral dissemination while ensuring protection against immune detection. Finally, the depletion of Siglec-1 abrogated the exacerbation of HIV-1 infection and production induced by TB in M(IL-10) macrophages. This is likely to result from an accumulative effect of deficient capture and transfer of HIV-1 in the absence of Siglec-1. However, these results do not discern the specific contribution of Siglec-1 to the cell-to-cell transmission of HIV-1 *via* TNT from that obtained through other mechanisms (Bracq et al., 2018). Future studies will address whether the contribution of Siglec-1 to cell-to-cell transfer mechanisms has an impact in Mtb dissemination (Onfelt et al., 2006).

In conclusion, our study identifies Siglec-1 as a key TB-driven factor for the exacerbation of HIV-1 infection in macrophages, and as a new potential therapeutic target to limit viral dissemination in the co-infection context. It also sheds light on yet another housekeeping function for Siglec-1 with the potential to be hijacked by pathogens including HIV-1, such as intercellular communication facilitated by TNT. We argue that Siglec-1 localization on thick TNT has a physiological significance to macrophage biology in health and disease.

ACKNOWLEDGMENTS

We greatly acknowledge F. Capilla and T. Al Saati, US006/CREFRE for histology analyses; P. Constant, F. Levillain, F. Moreau and C. Berrone, IPBS and Genotoul Anexplo-IPBS, for accessing the BSL3 facilities; E. Näser, E. Vega, A. Peixoto, S. Mazeret and the Genotoul TRI-IPBS facilities for imaging and flow cytometry. We thank F. Quiroga and C. del Carmen Melucci Ganzarain, Instituto de Investigaciones Biomédicas en Retrovirus y SIDA, INBIRS UBA - CONICET, Buenos Aires, Argentina, for the technical help and advice provided. We greatly thank Y-M. Boudehen for technical expertise provided in molecular biology, M. Dalod and B. Raynaud-Messina for fruitful discussions, and S. Benichou for providing HIV-1 strains. We are grateful to D. Hudrisier, C. Gutierrez, C. A. Spinner, L. Bernard, and B. Raymond for critical reading of the manuscript and helpful comments. This work was supported by the *Centre National de la Recherche Scientifique, Université Paul Sabatier*, the *Agence Nationale de la Recherche* (ANR14-CE11-0020-02, ANR16-CE13-0005-01, ANR-11-EQUIPEX-0003), the *Agence Nationale de Recherche sur le Sida et les hépatites virales* (ANRS2014-CI-2, ANRS2014-049, ANRS2018-01), the ECOS-Sud program (A14S01), the *Fondation pour la Recherche Médicale* (DEQ2016 0334894 ; DEQ2016 0334902), the *Fondation Bettencourt Schueller*, INSERM Plan Cancer, the Argentinean National Agency of Promotion of Science and Technology (PICT-2015-0055 and PICT-2017-1317). We also thank the AIDS Research and Reference Reagent Program, Division of AIDS, NIAID. The NHP study was supported by NIH award OD011104, AI058609, AI111943 and AI111914. The genetic analyses were realized within the framework of the Swiss HIV Cohort Study (SHCS Project number 717), which is supported by the Swiss National Science Foundation (Grant Number 148522) and by the SHCS research foundation. M.D. is supported by an ATP (*Axes Thématiques Prioritaires*) doctoral scholarship from *Université Paul Sabatier*, S.S. by a 4th-year doctoral scholarship from Sidaction, and S. R. by a scholarship from Toulouse University Hospital to perform a Master's degree. J.M.-P and NI-U are supported by the Spanish Secretariat of State of Research, Development and Innovation through grant SAF2016-80033-R, J.M.-P. by the Spanish AIDS network *Red Temática Cooperativa de Investigación en SIDA*, and S.B. by the *Rio Hortega programme* funded by the Spanish Health Institute Carlos III (No. CM17/00242).

AUTHOR CONTRIBUTIONS

Conceptualization & methodology: MD, LB, YR, NI-U, ON, IMP, GL-V, CV. Software: MD, RP, and TPVM. Investigation: MD, LB, SS, KP, SR, CC, MBN, SB, NI-U, CV and GL-V. Resources: TPVM, CA, DK, MC, JM-P, NI-U and MdCS. Writing: MD, ON, IMP, CV and GL-V. Visualization: MD and CV. Supervision: CV and GL-V. Corresponding authors: GL-V is responsible for ownership and responsibility that are inherent to aspects on tuberculosis, and CV on HIV-1.

DECLARATION OF INTERESTS

The authors have declared that no conflict of interest exists.

REFERENCES

- Akiyama, H., Ramirez, N.G., Gudheti, M.V., and Gummuluru, S. (2015). CD169-mediated trafficking of HIV to plasma membrane invaginations in dendritic cells attenuates efficacy of anti-gp120 broadly neutralizing antibodies. *PLoS pathogens* *11*, e1004751.
- Akiyama, H., Ramirez, N.P., Gibson, G., Kline, C., Watkins, S., Ambrose, Z., and Gummuluru, S. (2017). Interferon-Inducible CD169/Siglec1 Attenuates Anti-HIV-1 Effects of Alpha Interferon. *Journal of virology* *91*.
- Bell, L.C.K., and Noursadeghi, M. (2018). Pathogenesis of HIV-1 and Mycobacterium tuberculosis co-infection. *Nature reviews Microbiology* *16*, 80-90.
- Berry, M.P., Graham, C.M., McNab, F.W., Xu, Z., Bloch, S.A., Oni, T., Wilkinson, K.A., Banchereau, R., Skinner, J., Wilkinson, R.J., *et al.* (2010). An interferon-inducible neutrophil-driven blood transcriptional signature in human tuberculosis. *Nature* *466*, 973-977.
- Bracq, L., Xie, M., Benichou, S., and Bouchet, J. (2018). Mechanisms for Cell-to-Cell Transmission of HIV-1. *Frontiers in immunology* *9*, 260.
- Cai, Y., Sugimoto, C., Liu, D.X., Midkiff, C.C., Alvarez, X., Lackner, A.A., Kim, W.K., Didier, E.S., and Kuroda, M.J. (2015). Increased monocyte turnover is associated with interstitial macrophage accumulation and pulmonary tissue damage in SIV-infected rhesus macaques. *Journal of leukocyte biology* *97*, 1147-1153.
- Cribbs, S.K., Lennox, J., Caliendo, A.M., Brown, L.A., and Guidot, D.M. (2015). Healthy HIV-1-infected individuals on highly active antiretroviral therapy harbor HIV-1 in their alveolar macrophages. *AIDS research and human retroviruses* *31*, 64-70.
- Crocker, P.R., Paulson, J.C., and Varki, A. (2007). Siglecs and their roles in the immune system. *Nature reviews Immunology* *7*, 255-266.
- Deffur, A., Mulder, N.J., and Wilkinson, R.J. (2013). Co-infection with Mycobacterium tuberculosis and human immunodeficiency virus: an overview and motivation for systems approaches. *Pathogens and disease* *69*, 101-113.
- Diedrich, C.R., and Flynn, J.L. (2011). HIV-1/mycobacterium tuberculosis coinfection immunology: how does HIV-1 exacerbate tuberculosis? *Infection and immunity* *79*, 1407-1417.
- Dupont, M., Souriant, S., Lugo-Villarino, G., Maridonneau-Parini, I., and Verollet, C. (2018). Tunneling Nanotubes: Intimate Communication between Myeloid Cells. *Frontiers in immunology* *9*, 43.
- Esmail, H., Riou, C., Bruyn, E.D., Lai, R.P., Harley, Y.X.R., Meintjes, G., Wilkinson, K.A., and Wilkinson, R.J. (2018). The Immune Response to Mycobacterium tuberculosis in HIV-1-Coinfected Persons. *Annual review of immunology* *36*, 603-638.
- Eugenin, E.A., Gaskill, P.J., and Berman, J.W. (2009). Tunneling nanotubes (TNT) are induced by HIV-infection of macrophages: a potential mechanism for intercellular HIV trafficking. *Cellular immunology* *254*, 142-148.
- Ganor, Y., Real, F., Sennepin, A., Dutertre, C.A., Prevedel, L., Xu, L., Tudor, D., Charmeteau, B., Couedel-Courteille, A., Marion, S., *et al.* (2019). HIV-1 reservoirs in urethral macrophages of patients under suppressive antiretroviral therapy. *Nature microbiology* *4*, 633-644.
- Gummuluru, S., Pina Ramirez, N.G., and Akiyama, H. (2014). CD169-dependent cell-associated HIV-1 transmission: a driver of virus dissemination. *The Journal of infectious diseases* *210 Suppl 3*, S641-647.
- Halasz, H., Ghadaksaz, A.R., Madarasz, T., Huber, K., Harami, G., Toth, E.A., Osteikoetxea-Molnar, A., Kovacs, M., Balogi, Z., Nyitrai, M., *et al.* (2018). Live cell superresolution-structured illumination microscopy imaging analysis of the intercellular transport of microvesicles and costimulatory proteins via nanotubes between immune cells. *Methods and applications in fluorescence* *6*, 045005.
- Hartnell, A., Steel, J., Turley, H., Jones, M., Jackson, D.G., and Crocker, P.R. (2001). Characterization of human sialoadhesin, a sialic acid binding receptor expressed by resident and inflammatory macrophage populations. *Blood* *97*, 288-296.

- Hashimoto, M., Bhuyan, F., Hiyoshi, M., Noyori, O., Nasser, H., Miyazaki, M., Saito, T., Kondoh, Y., Osada, H., Kimura, S., *et al.* (2016). Potential Role of the Formation of Tunneling Nanotubes in HIV-1 Spread in Macrophages. *Journal of immunology* *196*, 1832-1841.
- Honeycutt, J.B., Thayer, W.O., Baker, C.E., Ribeiro, R.M., Lada, S.M., Cao, Y., Cleary, R.A., Hudgens, M.G., Richman, D.D., and Garcia, J.V. (2017). HIV persistence in tissue macrophages of humanized myeloid-only mice during antiretroviral therapy. *Nature medicine* *23*, 638-643.
- Honeycutt, J.B., Wahl, A., Baker, C., Spagnuolo, R.A., Foster, J., Zakharova, O., Wietgreffe, S., Caro-Vegas, C., Madden, V., Sharpe, G., *et al.* (2016). Macrophages sustain HIV replication in vivo independently of T cells. *The Journal of clinical investigation* *126*, 1353-1366.
- Ivashkiv, L.B., and Donlin, L.T. (2014). Regulation of type I interferon responses. *Nature reviews Immunology* *14*, 36-49.
- Izquierdo-Useros, N., Lorizate, M., Contreras, F.X., Rodriguez-Plata, M.T., Glass, B., Erkizia, I., Prado, J.G., Casas, J., Fabrias, G., Krausslich, H.G., *et al.* (2012a). Sialyllactose in viral membrane gangliosides is a novel molecular recognition pattern for mature dendritic cell capture of HIV-1. *PLoS biology* *10*, e1001315.
- Izquierdo-Useros, N., Lorizate, M., McLaren, P.J., Telenti, A., Krausslich, H.G., and Martinez-Picado, J. (2014). HIV-1 capture and transmission by dendritic cells: the role of viral glycolipids and the cellular receptor Siglec-1. *PLoS pathogens* *10*, e1004146.
- Izquierdo-Useros, N., Lorizate, M., Puertas, M.C., Rodriguez-Plata, M.T., Zangger, N., Erikson, E., Pino, M., Erkizia, I., Glass, B., Clotet, B., *et al.* (2012b). Siglec-1 is a novel dendritic cell receptor that mediates HIV-1 trans-infection through recognition of viral membrane gangliosides. *PLoS biology* *10*, e1001448.
- Jambo, K.C., Banda, D.H., Kankwatira, A.M., Sukumar, N., Allain, T.J., Heyderman, R.S., Russell, D.G., and Mwandumba, H.C. (2014). Small alveolar macrophages are infected preferentially by HIV and exhibit impaired phagocytic function. *Mucosal immunology* *7*, 1116-1126.
- Jaroenpool, J., Rogers, K.A., Pattanapanyasat, K., Villinger, F., Onlamoon, N., Crocker, P.R., and Ansari, A.A. (2007). Differences in the constitutive and SIV infection induced expression of Siglecs by hematopoietic cells from non-human primates. *Cellular immunology* *250*, 91-104.
- Kabaso, D., Lokar, M., Kralj-Iglic, V., Veranic, P., and Iglic, A. (2011). Temperature and cholera toxin B are factors that influence formation of membrane nanotubes in RT4 and T24 urothelial cancer cell lines. *International journal of nanomedicine* *6*, 495-509.
- Kuroda, M.J., Sugimoto, C., Cai, Y., Merino, K.M., Mehra, S., Arainga, M., Roy, C.J., Midkiff, C.C., Alvarez, X., Didier, E.S., *et al.* (2018). High Turnover of Tissue Macrophages Contributes to Tuberculosis Reactivation in Simian Immunodeficiency Virus-Infected Rhesus Macaques. *The Journal of infectious diseases* *217*, 1865-1874.
- Lastrucci, C., Benard, A., Balboa, L., Pingris, K., Souriant, S., Poincloux, R., Al Saati, T., Rasolofo, V., Gonzalez-Montaner, P., Inwentarz, S., *et al.* (2015). Tuberculosis is associated with expansion of a motile, permissive and immunomodulatory CD16(+) monocyte population via the IL-10/STAT3 axis. *Cell research* *25*, 1333-1351.
- Lokar, M., Kabaso, D., Resnik, N., Sepcic, K., Kralj-Iglic, V., Veranic, P., Zorec, R., and Iglic, A. (2012). The role of cholesterol-sphingomyelin membrane nanodomains in the stability of intercellular membrane nanotubes. *International journal of nanomedicine* *7*, 1891-1902.
- Martinez-Picado, J., McLaren, P.J., Telenti, A., and Izquierdo-Useros, N. (2017). Retroviruses As Myeloid Cell Riders: What Natural Human Siglec-1 "Knockouts" Tell Us About Pathogenesis. *Frontiers in immunology* *8*, 1593.
- Mathews, S., Branch Woods, A., Katano, I., Makarov, E., Thomas, M.B., Gendelman, H.E., Poluektova, L.Y., Ito, M., and Gorantla, S. (2019). Human Interleukin-34 facilitates microglia-like cell differentiation and persistent HIV-1 infection in humanized mice. *Molecular neurodegeneration* *14*, 12.
- Mattila, J.T. (2019). Type 1 interferon expression and signaling occur in spatially-distinct regions in granulomas from *Mycobacterium tuberculosis*-infected cynomolgus macaques. *The Journal of Immunology* *202*, 62.19-62.19.

- McNab, F., Mayer-Barber, K., Sher, A., Wack, A., and O'Garra, A. (2015). Type I interferons in infectious disease. *Nature reviews Immunology* *15*, 87-103.
- Moreira-Teixeira, L., Mayer-Barber, K., Sher, A., and O'Garra, A. (2018). Type I interferons in tuberculosis: Foe and occasionally friend. *The Journal of experimental medicine* *215*, 1273-1285.
- O'Garra, A., Redford, P.S., McNab, F.W., Bloom, C.I., Wilkinson, R.J., and Berry, M.P. (2013). The immune response in tuberculosis. *Annual review of immunology* *31*, 475-527.
- O'Neill, A.S., van den Berg, T.K., and Mullen, G.E. (2013). Sialoadhesin - a macrophage-restricted marker of immunoregulation and inflammation. *Immunology* *138*, 198-207.
- Onfelt, B., Nedvetzki, S., Benninger, R.K., Purbhoo, M.A., Sowinski, S., Hume, A.N., Seabra, M.C., Neil, M.A., French, P.M., and Davis, D.M. (2006). Structurally distinct membrane nanotubes between human macrophages support long-distance vesicular traffic or surfing of bacteria. *Journal of immunology* *177*, 8476-8483.
- Osteikoetxea-Molnar, A., Szabo-Meleg, E., Toth, E.A., Oszvald, A., Izsepi, E., Kremlitzka, M., Biri, B., Nyitray, L., Bozo, T., Nemeth, P., *et al.* (2016). The growth determinants and transport properties of tunneling nanotube networks between B lymphocytes. *Cellular and molecular life sciences : CMLS* *73*, 4531-4545.
- Pino, M., Erkizia, I., Benet, S., Erikson, E., Fernandez-Figueras, M.T., Guerrero, D., Dalmau, J., Ouchi, D., Rausell, A., Ciuffi, A., *et al.* (2015). HIV-1 immune activation induces Siglec-1 expression and enhances viral trans-infection in blood and tissue myeloid cells. *Retrovirology* *12*, 37.
- Puryear, W.B., Akiyama, H., Geer, S.D., Ramirez, N.P., Yu, X., Reinhard, B.M., and Gummuluru, S. (2013). Interferon-inducible mechanism of dendritic cell-mediated HIV-1 dissemination is dependent on Siglec-1/CD169. *PLoS pathogens* *9*, e1003291.
- Puryear, W.B., Yu, X., Ramirez, N.P., Reinhard, B.M., and Gummuluru, S. (2012). HIV-1 incorporation of host-cell-derived glycosphingolipid GM3 allows for capture by mature dendritic cells. *Proceedings of the National Academy of Sciences of the United States of America* *109*, 7475-7480.
- Redondo-Morata, L., Giannotti, M.I., and Sanz, F. (2012). Influence of cholesterol on the phase transition of lipid bilayers: a temperature-controlled force spectroscopy study. *Langmuir : the ACS journal of surfaces and colloids* *28*, 12851-12860.
- Rempel, H., Calosing, C., Sun, B., and Pulliam, L. (2008). Sialoadhesin expressed on IFN-induced monocytes binds HIV-1 and enhances infectivity. *PLoS One* *3*, e1967.
- Rodrigues, V., Ruffin, N., San-Roman, M., and Benaroch, P. (2017). Myeloid Cell Interaction with HIV: A Complex Relationship. *Frontiers in immunology* *8*, 1698.
- Rustom, A., Saffrich, R., Markovic, I., Walther, P., and Gerdes, H.H. (2004). Nanotubular highways for intercellular organelle transport. *Science* *303*, 1007-1010.
- Sattentau, Q.J., and Stevenson, M. (2016). Macrophages and HIV-1: An Unhealthy Constellation. *Cell host & microbe* *19*, 304-310.
- Schneider, W.M., Chevillotte, M.D., and Rice, C.M. (2014). Interferon-stimulated genes: a complex web of host defenses. *Annual review of immunology* *32*, 513-545.
- Sewald, X., Ladinsky, M.S., Uchil, P.D., Beloor, J., Pi, R., Herrmann, C., Motamedi, N., Murooka, T.T., Brehm, M.A., Greiner, D.L., *et al.* (2015). Retroviruses use CD169-mediated trans-infection of permissive lymphocytes to establish infection. *Science* *350*, 563-567.
- Souriant, S., Balboa, L., Dupont, M., Pingris, K., Kviatcovsky, D., Cougoule, C., Lastrucci, C., Bah, A., Gasser, R., Poincloux, R., *et al.* (2019). Tuberculosis Exacerbates HIV-1 Infection through IL-10/STAT3-Dependent Tunneling Nanotube Formation in Macrophages. *Cell reports* *26*, 3586-3599 e3587.

- Subramanian, A., Tamayo, P., Mootha, V.K., Mukherjee, S., Ebert, B.L., Gillette, M.A., Paulovich, A., Pomeroy, S.L., Golub, T.R., Lander, E.S., *et al.* (2005). Gene set enrichment analysis: a knowledge-based approach for interpreting genome-wide expression profiles. *Proceedings of the National Academy of Sciences of the United States of America* *102*, 15545-15550.
- Thayanithy, V., Babatunde, V., Dickson, E.L., Wong, P., Oh, S., Ke, X., Barlas, A., Fujisawa, S., Romin, Y., Moreira, A.L., *et al.* (2014). Tumor exosomes induce tunneling nanotubes in lipid raft-enriched regions of human mesothelioma cells. *Experimental cell research* *323*, 178-188.
- Torralba, D., Baixauli, F., and Sanchez-Madrid, F. (2016). Mitochondria Know No Boundaries: Mechanisms and Functions of Intercellular Mitochondrial Transfer. *Frontiers in cell and developmental biology* *4*, 107.
- Toth, E.A., Oszvald, A., Peter, M., Balogh, G., Osteikoetxea-Molnar, A., Bozo, T., Szabo-Meleg, E., Nyitrai, M., Derenyi, I., Kellermayer, M., *et al.* (2017). Nanotubes connecting B lymphocytes: High impact of differentiation-dependent lipid composition on their growth and mechanics. *Biochimica et biophysica acta Molecular and cell biology of lipids* *1862*, 991-1000.
- VanderVen, B.C., Huang, L., Rohde, K.H., and Russell, D.G. (2016). The Minimal Unit of Infection: Mycobacterium tuberculosis in the Macrophage. *Microbiology spectrum* *4*.
- Verollet, C., Souriant, S., Bonnaud, E., Jolicoeur, P., Raynaud-Messina, B., Kinnaer, C., Fourquaux, I., Imle, A., Benichou, S., Fackler, O.T., *et al.* (2015). HIV-1 reprograms the migration of macrophages. *Blood* *125*, 1611-1622.
- Verollet, C., Zhang, Y.M., Le Cabec, V., Mazzolini, J., Charriere, G., Labrousse, A., Bouchet, J., Medina, I., Biessen, E., Niedergang, F., *et al.* (2010). HIV-1 Nef triggers macrophage fusion in a p61Hck- and protease-dependent manner. *Journal of immunology* *184*, 7030-7039.
- Yu, Y.R., Hotten, D.F., Malakhau, Y., Volker, E., Ghio, A.J., Noble, P.W., Kraft, M., Hollingsworth, J.W., Gunn, M.D., and Tighe, R.M. (2016). Flow Cytometric Analysis of Myeloid Cells in Human Blood, Bronchoalveolar Lavage, and Lung Tissues. *American journal of respiratory cell and molecular biology* *54*, 13-24.
- Ziegler-Heitbrock, L., Lotzerich, M., Schaefer, A., Werner, T., Frankenberger, M., and Benkhart, E. (2003). IFN-alpha induces the human IL-10 gene by recruiting both IFN regulatory factor 1 and Stat3. *Journal of immunology* *171*, 285-290.
- Zou, Z., Chastain, A., Moir, S., Ford, J., Trandem, K., Martinelli, E., Cicala, C., Crocker, P., Arthos, J., and Sun, P.D. (2011). Siglecs facilitate HIV-1 infection of macrophages through adhesion with viral sialic acids. *PLoS One* *6*, e24559.

FIGURE

Dupont et al., Figure 1

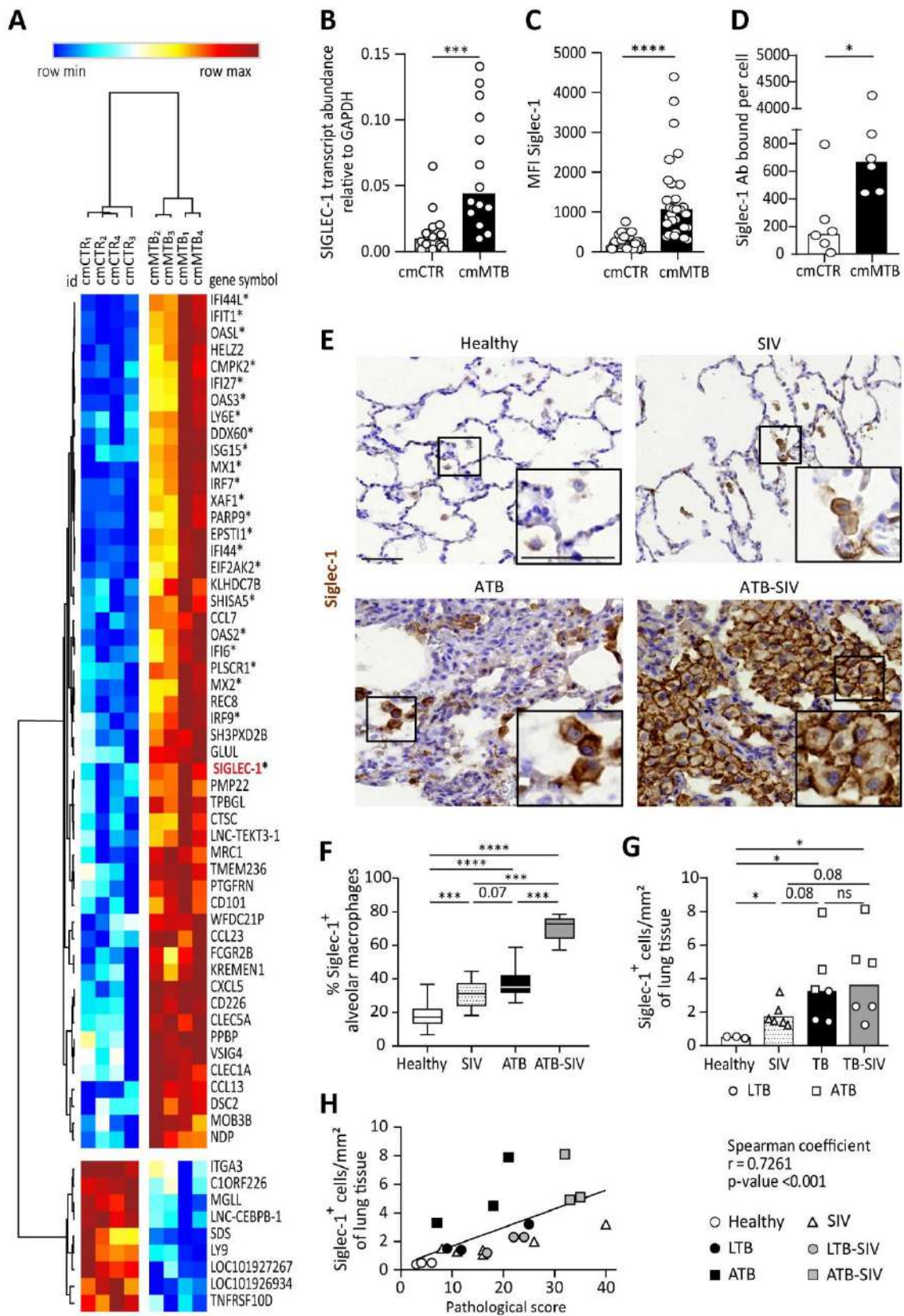


Figure 1. Tuberculosis-associated microenvironment induces Siglec-1 expression in macrophages (see also Figure S1 and S2).

(A-D) For 3 days, human monocytes were differentiated into macrophages with cmCTR (white) or cmMTB (black) supernatants.

(A) Heatmap from a transcriptomic analysis illustrating the top 60 differentially expressed genes (DEGs) between cmCTR- or cmMTB-cells. Selection of the top DEGs was performed using an adjusted p-value ≤ 0.05 , a fold change of at least 2, and a minimal expression of 6 in a \log_2 scale. Hierarchical clustering was performed using the complete linkage method and the Pearson correlation metric with Morpheus (Broad Institute). Interferon-stimulated genes (ISG) are labelled with an asterisk and Siglec-1 is indicated in red.

(B-D) Validation of Siglec-1 expression in cmMTB-treated macrophages. Vertical scatter plots showing the relative abundance to mRNA (B), median fluorescent intensity (MFI) (C), and mean number of Siglec-1 antibody binding sites per cell (D). Each circle represents a single donor and histograms median values.

(E) Representative immunohistochemical images of Siglec-1 staining (brown) in lung biopsies of healthy, SIV infected (SIV), active TB (ATB), and co-infected (ATB-SIV) non-human primates (NHP). Scale bar, 100 μm . Insets are 2x zoom.

(F) Vertical Box and Whisker plot indicating the distribution of the percentage of Siglec-1⁺ alveolar macrophages in lung biopsies from the indicated NHP groups. n=800 alveolar macrophages analyzed per condition from one representative animal per NHP group.

(G) Vertical scatter plots displaying the number of cells that are positive for Siglec-1 per mm^2 of lung biopsies from the indicated NHP groups. Each symbol represents a single animal per NHP group.

(H) Correlation between Siglec-1⁺ cells per mm^2 of lung tissue and the pathological score for healthy (white circle), SIV⁺ (white triangles), latent (black circle) or active (black square) TB, and SIV⁺ with latent (grey circle) or active (grey square) TB. Each symbol represents a single animal per NHP group. Mean value is represented as a black line.

Statistical analyses: Two-tailed, Wilcoxon signed-rank test (B-D), Mann-Whitney unpaired test (F-G), Spearman correlation (H). *P < 0.05, **P < 0.01, ***P < 0.001, ****P < 0.0001. ns: not significant.

Dupont et al., Figure 2

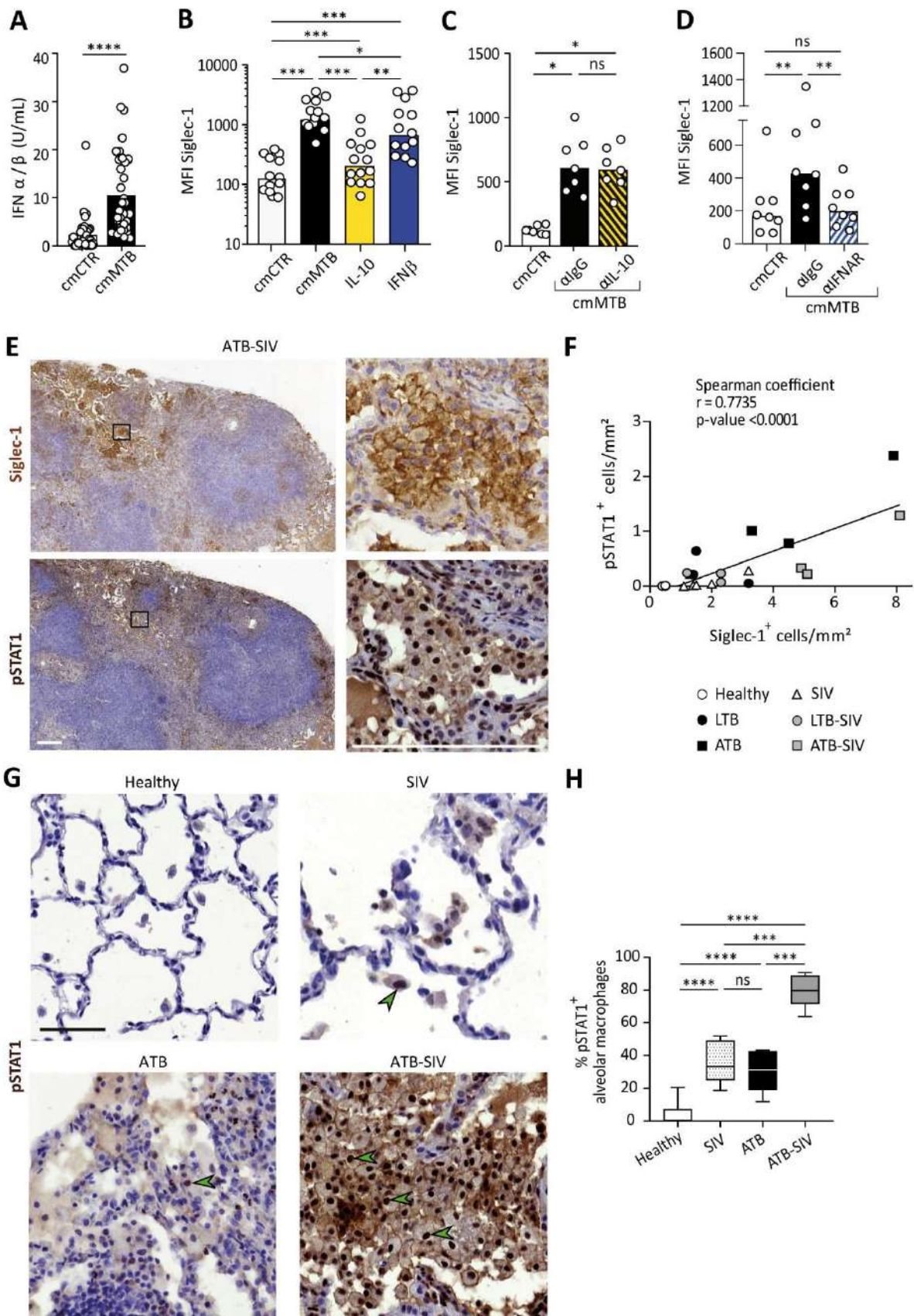


Figure 2. Siglec-1 expression is dependent on TB-mediated type I IFN signaling.

(A) Vertical scatter plot showing the relative abundance of IFN-I in cmCTR (white) and cmMTB (black) media, as measured indirectly after 24h exposure to the HEK-Blue IFN- γ / γ reporter cell line yielding reporter activity in units (U) per mL.

(B-D) For 3 days, monocytes were differentiated into macrophages either with cmMTB (black) or cmCTR (white), the indicated recombinant cytokines (B), the presence of an IL-10 depletion (α -IL-10) or a control (α -IgG) antibodies (C), or the presence of an IFNAR-2 blocking (α -IFNAR) or control (α -IgG) antibodies (D).

(E) Representative serial immunohistochemical images of lung biopsies of a co-infected (ATB-SIV) NHP stained for Siglec-1 (brown, top) and pSTAT1 (brown, bottom). Scale bar, 250 μ m. Insets are 10x zooms.

(F) Correlation of the percentage of cells positive for Siglec-1 and pSTAT1, as measured per mm² of lung tissue from the indicated NHP groups. Mean value is represented as a black line.

(G) Representative immunohistochemical images of lung biopsies from the indicated NHP group stained for pSTAT1 (brown). Arrowheads show pSTAT1-positive nuclei. Scale bar, 500 μ m.

(H) Vertical Box and Whisker plot illustrating the percentage of pSTAT1⁺ alveolar macrophages in lung biopsies from the indicated NHP groups. N=450 alveolar macrophages analyzed per condition from one representative animal per NHP group.

(A-D) Each circle within vertical scatter plots represents a single donor and histograms median value.

(B-D) Vertical scatter plots displaying the median fluorescent intensity (MFI) of Siglec-1 cell-surface expression. Statistical analyses: Two-tailed, Wilcoxon signed-rank test (A-D), Spearman correlation (F), and Mann-Whitney unpaired test (H). *P < 0.05, **P < 0.01, ***P < 0.001, ****P < 0.0001. ns: not significant.

Dupont et al., Figure 3

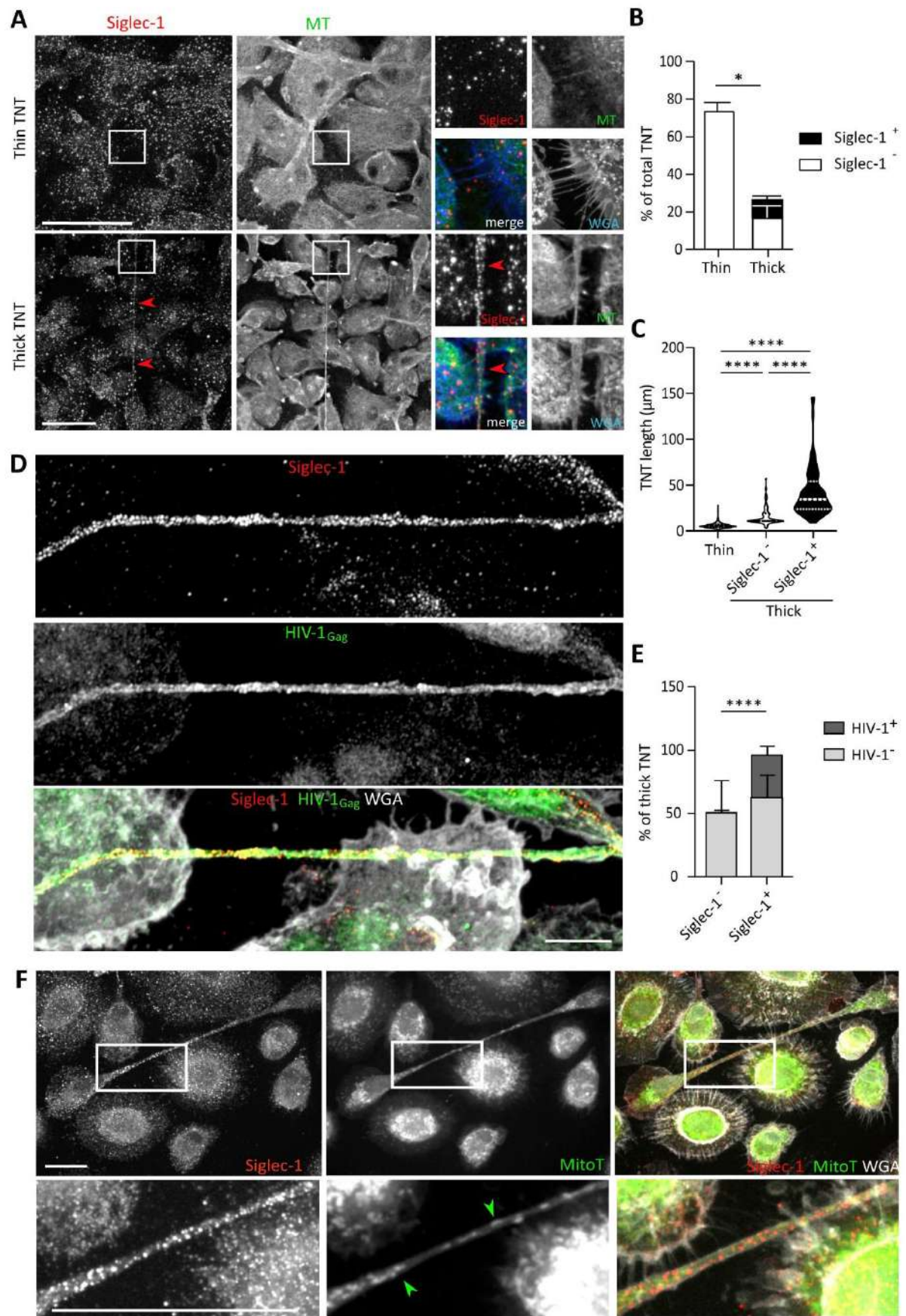


Figure 3. Siglec-1 localization on thick TNT is associated with their length and HIV/mitochondria cargo (see also Figure S3).

(A-F) Human monocytes were differentiated into macrophages with cmMTB for 3 days, and then infected with HIV-1-ADA strain (unless indicated otherwise) and fixed 3 days post-infection.

(A) Representative immunofluorescence images of cmMTB-treated macrophages infected with HIV-1-ADA, and stained for extracellular Siglec-1 (red), intracellular tubulin (MT, green) and Wheat Germ Agglutinin (WGA, blue). Inserts are 3x zooms. Red arrowheads show Siglec-1 localization on TNT. Scale bar, 20 μm .

(B) Vertical bar plot showing the semi-automatic quantification of Siglec-1⁺ TNT (black) and Siglec-1⁻ TNT (white) in thick (WGA⁺, MT⁺) and thin (WGA⁺, MT⁻) TNT. 400 TNT were analyzed from 2 independent donors.

(C) Siglec-1⁺ TNT exhibit a larger length index. Violin plots displaying the semi-automatic quantification of TNT length (in μm) for thin (WGA⁺, MT⁻), and thick TNT (WGA⁺, MT⁺) expressing Siglec-1 or not. 400 TNT were analyzed per condition from two independent donors.

(D) Representative immunofluorescence images of cmMTB-treated macrophages 3-day post-infection with HIV-1-NLAD8-VSVG strain, and stained for extracellular Siglec-1 (red), intracellular HIV-1_{Gag} (green) and WGA (grey). Scale bar, 10 μm .

(E) Vertical bar plots indicating the quantification of presence (dark grey) or absence (light grey) of HIV-1_{Gag} in thick TNT (WGA⁺, MT⁺) expressing Siglec-1 or not. 120 TNT in at least 1000 cells were analyzed from four independent donors.

(F) Representative immunofluorescence images of cmMTB-treated macrophages infected with HIV-1-ADA loaded with MitoTracker (MitoT, green), and stained for extracellular Siglec-1 (red) and WGA (grey). Inserts are 3x zooms. Green arrowheads show mitochondria inside TNT. Scale bar, 10 μm .

Statistical analyses: Two-way ANOVA comparing the presence of Siglec-1 in thin and thick TNT (B), and two-tailed Mann-Whitney unpaired test comparing TNT length (C) and the presence of HIV-1 in TNT (E). *P < 0.05, ****P < 0.0001.

Dupont et al., Figure 4

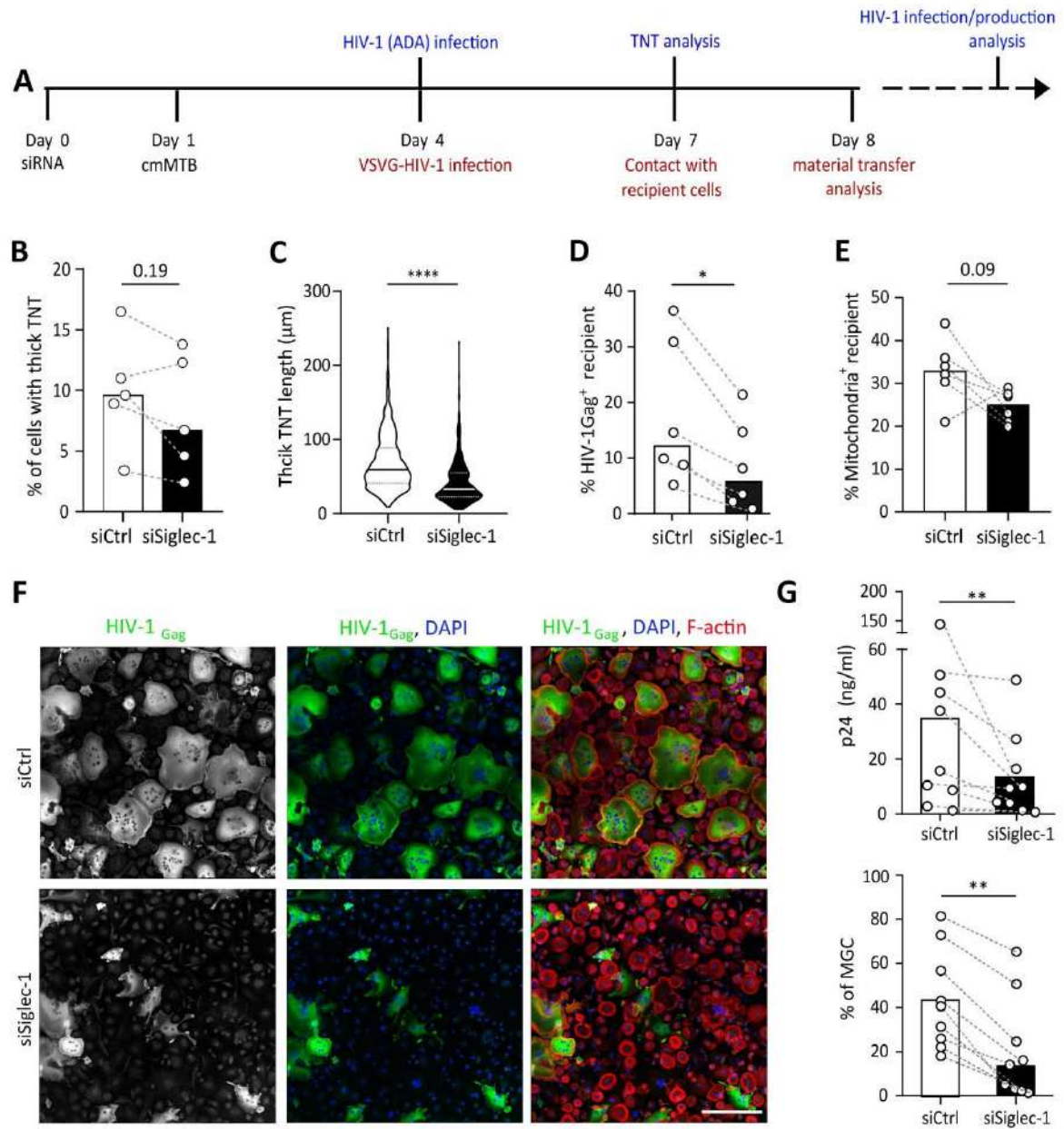


Figure 4. TB-driven exacerbation of HIV-1 infection and spread in macrophages requires Siglec-1 (see also Figure S4).

(A) Experimental design. Monocytes from healthy subjects were transfected with siRNA targeting of Siglec-1 (siSiglec-1, black) or not (siCtrl, white). A day after, monocytes were differentiated into macrophages with cmMTB for 3 days. Cells were then infected with HIV-1-ADA (blue protocol) to measure the formation (B) and length (C) of TNT at day 7, or assess HIV-1 production and multinucleated giant cell (MGC) formation at day 14 (F-G). In parallel, cells were either infected with HIV-NLAD8-VSVG or labelled with mitoTracker to measure the transfer (red protocol) of HIV-1 (D) or mitochondria (E), respectively.

(B) Before-and-after plots showing the percentage of cells forming thick TNT (F-actin⁺, WGA⁺, MT⁺).

(C) Violin plots displaying the semi-automatic quantification of TNT length (in μm) for thick (WGA⁺, MT⁺) TNT; 300 TNT were analyzed per condition from two independent donors.

(D-E) Before-and-after plots indicating the percentage of HIV-1_{Gag}⁺ cells (D) or MitoTracker⁺ cells (E) among CellTracker⁺ cells after 24h co-culture.

(F) Representative immunofluorescence images of siRNA transfected cells, treated with cmMTB 14 days post-HIV-1 infection. Cells were stained for intracellular HIV-1_{Gag} (green), F-actin (red) and DAPI (blue). Scale bar, 500 μm .

(G) Vertical scatter plots showing HIV-1-p24 concentration in cell supernatants (upper panel) and percentage of MGC (lower panel) at day 14 post-HIV-1 infection in cells represented in F (siSiglec-1, black; siCtrl, white).

(B, D, E and G) Each circle represents a single donor and histograms median value. Statistical analyses: Two-tailed, Wilcoxon signed-rank test (B-E, G). *P < 0.05, **P < 0.01, ****P < 0.0001.

STAR METHODS

CONTACT FOR REAGENT AND RESOURCE SHARING

Further information and requests for reagents should be directed to and will be fulfilled by the Lead Contact, Geanncarlo Lugo-Villarino (lugo@ipbs.fr). Sharing of antibodies and other reagents with academic researchers may require UBMTA agreements.

EXPERIMENTAL MODEL AND SUBJECT DETAILS

Human Subjects

Monocytes from healthy subjects were provided by Etablissement Français du Sang (EFS), Toulouse, France, under contract 21/PLER/TOU/IPBS01/20130042. According to articles L12434 and R124361 of the French Public Health Code, the contract was approved by the French Ministry of Science and Technology (agreement number AC 2009921). Written informed consents were obtained from the donors before sample collection.

Non-Human Primate (NHP) samples

All animal procedures were approved by the Institutional Animal Care and Use Committee of Tulane University, New Orleans, LA, and were performed in strict accordance with NIH guidelines. The twenty adult rhesus macaques used in this study (Table S1 and S2) were bred and housed at the Tulane National Primate Research Center (TNPRC). All macaques were infected as previously described ([Foreman et al., 2016](#); [Mehra et al., 2011](#); [Souriant et al., 2019](#)). Briefly, aerosol infection was performed on macaques using a low dose (25 CFU implanted) of Mtb CDC1551. Nine weeks later, a subgroup of the animals was additionally intravenously injected with 300 TCID₅₀ of SIVmac239 in 1mL saline, while controls received an equal volume of saline solution. Euthanasia criteria were presentation of four or more of the following conditions: (i) body temperatures consistently greater than 2°F above pre-infection values for 3 or more weeks in a row; (ii) 15% or more loss in body weight; (iii) serum CRP values higher than 10 mg/mL for 3 or more consecutive weeks, CRP being a marker for systemic inflammation that exhibits a high degree of correlation with active TB in macaques ([Kaushal et al., 2012](#); [Mehra et al., 2011](#)); (iv) CXR values higher than 2 on a scale of 0–4; (v) respiratory discomfort leading to vocalization; (vi) significant or complete loss of appetite; and (vii) detectable bacilli in BAL samples.

METHODS DETAILS

Bacteria

Mtb H37Rv strain was grown in suspension in Middlebrook 7H9 medium (Difco) supplemented with 10% albumin-dextrose-catalase (ADC, Difco) and 0.05% Twen-80 (Sigma-Aldrich) ([Lastrucci et al., 2015](#)). For infection, growing Mtb was centrifuged (3000 RPM) at exponential phase stage and resuspended in PBS (MgCl₂, CaCl₂ free, Gibco). Twenty passages through a 26-G needle were done for dissociation of bacterial aggregates. Bacterial suspension concentration was then determined by measuring OD₆₀₀, and then resuspended in RPMI-1640 containing 10% FBS for infection.

Viruses

Virus stocks were generated by transient transfection of 293T cells with proviral plasmids coding for HIV-1 ADA and HIV-1 NLAD8-VSVG isolates, kindly provided by Serge Benichou (Institut Cochin, Paris, France), as previously described ([Verollet et al., 2015](#)). Supernatant were harvested 2 days post-transfection and HIV-1 p24 antigen concentration was assessed by a homemade enzyme-linked immunosorbent assay (ELISA). HIV-1 infectious units were quantified, as reported ([Souriant et al., 2019](#)) using TZM-bl cells (NIH AIDS Reagent Program, Division of AIDS, NIAID, NIH from Dr. John C. Kappes, Dr. Xiaoyun Wu and Tranzyme Inc).

HIV-VLP stock (GFP VLP) was generated by transfecting the molecular clone pGag-eGFP obtained from the NIH AIDS Research and Reference Reagent Program. HEK-293 T cells were transfected with calcium phosphate (CalPhos, Clontech) in T75 flasks using 30 µg of plasmid DNA. Supernatants containing VLPs were filtered (Millex HV, 0.45 µm; Millipore) and frozen at -80°C until use. The p24 Gag content of the VLPs was determined by an ELISA (Perkin-Elmer).

Preparation of human monocytes and monocyte-derived macrophages

Human monocytes were isolated from healthy subject (HS) buffy coat (from EFS) and differentiated towards macrophages as described ([Souriant et al., 2019](#)). Briefly, peripheral blood mononuclear cells (PBMCs) were recovered by gradient centrifugation on Ficoll-Paque Plus (GE Healthcare). CD14⁺ monocytes were then isolated by positive selection magnetic sorting, using human CD14 Microbeads and LS columns (Miltenyi Biotec). Cells were then plated at 1.6×10^6 cells per 6-well and allowed to differentiate for 5-7 days in RPMI-1640 medium (GIBCO), 10% Fetal Bovine Serum (FBS, Sigma-Aldrich) and human M-CSF (20 ng/mL) Peprotech) before infection with Mtb H37Rv for conditioned-media preparation. The cell medium was renewed every 3 or 4 days.

Preparation of conditioned media

Conditioned-media from Mtb-infected macrophages (cmMTB) has been reported previously ([Lastrucci et al., 2015](#); [Souriant et al., 2019](#)). Succinctly, hMDM were infected with Mtb H37Rv at a MOI of 3. After 18h of infection at 37°C, culture supernatants were collected, sterilized by double filtration (0.2µm pores) and aliquots were stored at -80°C. We then tested the capacity of individual cmMTB to differentiate freshly isolated CD14⁺ monocytes towards the M(IL-10) cell-surface marker phenotype, as assessed by FACS analyses. Those supernatants yielding a positive readout were then pooled together (5-10 donors) to minimize the inter-variability obtained between donors. Control media (cmCTR) was obtained from uninfected macrophages supernatant. When specified, IL-10 was eliminated from cmMTB by antibody depletion as described previously ([Lastrucci et al., 2015](#); [Souriant et al., 2019](#)). The depletion was verified by ELISA (BD-Bioscience), according to manufacturer's protocol.

Conditioning of monocytes with the secretome of Mtb-infected macrophages or cytokines

Human CD14⁺ sorted monocytes from HS buffy coat were allowed to adhere in the absence of serum (0.4×10^6 cells / 24-well in 500 µL) on glass coverslips, and then cultured for 3 days with 40% dilution (vol/vol) of cmCTR or cmMTB supplemented with 20% FBS and M-CSF (20 ng/mL, Peprotech). Blocking IFNAR receptor was performed by pre-incubation with mouse anti-IFNAR antibody (20 µg/mL, Thermo

Fischer Scientific) in a 200 μ L for 30 min prior to conditioning. After 3 days, cells were washed and collected for phenotyping.

When specified, monocytes were also conditioned in presence of 20 ng/mL M-CSF and 10 ng/mL recombinant human IL-10 (PeproTech) or 10 U/mL of IFN γ (PeproTech). Cell-surface expression of Siglec-1 was measured by flow cytometry using standard procedures detailed hereafter.

RNA extraction and transcriptomic analysis

Cells conditioned with cmCTR and cmMTB supernatants (approximately 1.5 million cells) were treated with TRIzol Reagent (Invitrogen) and stored at -80°C. Total RNA was extracted from the TRIzol samples using the RNeasy mini kit (Qiagen). RNA amount and purity (absorbance at 260/280 nm) was measured with the Nanodrop ND-1000 apparatus (Thermo Scientific). According to the manufacturer's protocol, complementary DNA was then reverse transcribed from 1 μ g total RNA with Moloney murine leukemia virus reverse transcriptase (Invitrogen), using random hexamer oligonucleotides for priming. The microarray analysis was performed using the Agilent Human GE 4x44 v2 (single color), as previously described (Lugo-Villarino et al., 2018). Briefly, we performed hybridization with 2 μ g Cy3-cDNA and the hybridization kit (Roche NimbleGen). The samples were then incubated for 5 min at 65°C, and 5 min at 42°C before loading for 17h at 42°C, according to manufacturer's protocol. After washing, the microarrays were scanned with MS200 microarray scanner (Roche NimbleGen), and using Feature Extraction software, the Agilent raw files were extracted and then processed through Bioconductor (version 3.1) in the R statistical environment (version 3.6.0). Using the limma package, raw expression values were background corrected in a 'normexp' fashion and then quantile normalized and log₂ transformed (Ritchie et al., 2015). Density plots, boxplots, principal component analyses, and hierarchical clustering assessed the quality of the hybridizations. Differentially expressed genes between macrophages exposed to cmCTR or cmMTB supernatants were extracted based on the p-value corrected using the Benjamini-Hochberg procedure. The log₂ normalized expression values were used to perform Gene Set Enrichment Analyses (GSEA). The GSEA method allows to statistically test whether a set of genes of interest (referred to as a geneset) is distributed randomly or not in the list of genes that were pre-ranked according to their differential expression ratio between macrophages exposed to cmCTR or cmMTB supernatants. The output of GSEA is a GeneSet enrichment plot. The vertical black lines represent the projection onto the ranked GeneList of the individual genes of the GeneSet. The top curve in green corresponds to the calculation of the enrichment score (ES). The more the ES curve is shifted to the upper left of the graph, the more the GeneSet is enriched in the red cell population. Conversely, the more the ES curve is shifted to the lower right of the graph, the more the GeneSet is enriched in the blue cell population.

siRNA silencing

Targets silencing in monocytes was performed using reverse transfection protocol as previously described (Troegeler et al., 2014). Shortly, human primary monocytes were transfected with 200 nM of ON-TARGETplus SMARTpool siRNA targeting Siglec-1 (Horizon Discovery) or non-targeting siRNA (control) using HiPerfect transfection system (Qiagen). Four hours post-transfection, transfected cells were incubated for 24h in RPMI-1640 medium, 10% FBS, 20 ng/mL of M-CSF, before addition of cmMTB media (40% vol/vol). After 3 additional days, cells were infected with HIV-1 ADA or HIV-1- NLAD8-VSV-

G strain and kept in culture for 10 more days (48h, respectively). As soon as 3-day post-transfection, this protocol led to the efficient depletion of Siglec-1 between a range of 50-95%, as measured by flow cytometry.

HIV-1 infection

For HIV-1 infection, at day 3 of differentiation, 0.4×10^6 human monocytes-derived macrophages (hMDM) were infected with HIV-1 ADA strain (or specified) at MOI 0.1. HIV-1 infection and replication were assessed 10-day post-infection by measuring p24-positive cells by immunostaining and the level of p24 released in culture media by ELISA. For the infection and TNT quantification at day 6 post-infection, the same protocol was used. For HIV-1 transfer, higher MOI of HIV-1 VSVG pseudotyped NLAD8 virus was used, as described below (see section *HIV-1 and cell-to-cell transfer*) and in ([Souriant et al., 2019](#)).

Uptake of Virus-Like Particles

Uptake experiment were performed as previously described ([Izquierdo-Useros et al., 2012](#); [Izquierdo-Useros et al., 2014](#); [Pino et al., 2015](#)) using p24^{Gag} HIV-1_{Gag-eGFP} VLP (GFP VLP). Briefly, monocytes transfected or not with control siRNA or with siRNA directed against Siglec-1 and differentiated for 3 days in cmCTR or cmMTB were washed once with PBS prior to addition of 2 ng/mL of GFP VLP. Binding was performed during 3.5h at 37°C in a 5 % CO₂ incubator. Cells were then detached with cell dissociation buffer (Gibco) and prepared for flow cytometry analysis on a BD LSRFortessa (TRI-Genotoul platform). Same experiment was also performed blocking monocyte-derived macrophages at RT for 15 min with 10 µg/ml of mAb α-Siglec-1 7–239 (Abcam), IgG1 isotype control (BD Biosciences) or leaving cells untreated before VLP addition.

Flow cytometry and Siglec-1 quantitation

Staining of conditioned macrophages was performed as previously described ([Souriant et al., 2019](#)). Adherent cells were harvested after 5 min incubation in trypsin 0.05% EDTA (Gibco) and washes with PBS (Gibco). After 10 min centrifugation at 320g, pellets were resuspended in cold staining buffer (PBS, 2mM EDTA, 0.5% FBS) with fluorophore-conjugated antibodies (See Key Resource Table) and in parallel, with the corresponding isotype control antibody using a general concentration of 1 µg/mL. After staining, cells were washed with cold staining buffer, centrifuged for 2 min at 320g at 4°C, and analyzed by flow cytometry using BD LSRFortessa flow cytometer (BD Biosciences, TRI Genotoul platform) and the associated BD FACSDiva software. Data were then analyzed using the FlowJo_V10 software (FlowJo, LLC). Gating on macrophage population was set according to its Forward Scatter (FSC) and Size Scatter (SSC) properties before doublet exclusion and analysis of the median fluorescence intensity (MFI) for each staining.

To determine Siglec-1 expression we applied a quantitative FACS assay. Briefly, cmCTR- and cmMTB-treated macrophages were detached using Accutase solution (Gibco) for 10 min at 37°C, washed, blocked with 1 mg/mL human IgG (Privigen, Behring CSL) and stained with mAb 7–239 α-Siglec-1-PE or matched isotype-PE control (Biolegend) at 4°C for 30 min. The mean number of Siglec-1 mAb binding sites per cell was obtained with a Quantibrite kit (Becton Dickinson) as previously described ([Izquierdo-](#)

Users et. al 2012b). Samples were analyzed with FACSCalibur using CellQuest software to evaluate collected data.

Immunofluorescence microscopy

Cells were fixed with PFA 3.7%, Sucrose 30 mM in PBS. After washing with PBS, cells were saturated with blocking buffer (PBS-BSA 1%). Membrane proteins were then stained for 2h with primary antibodies: anti-Siglec-1 (10 µg/mL, Novus Biologicals). Cells were then incubated with appropriate secondary antibodies for 1h: Alexa Fluor 488 or 555 or 647 Goat anti-Mouse IgG (2 µg/mL, Cell Signaling Technology). Cells were then permeabilized as previously described ([Souriant et al., 2019](#)) with Triton X-100 0,3% for 10 minutes, washed in PBS before saturation with 0.6 µg/mL mouse IgG2 diluted in Dako Antibody Reducing Background buffer (Dako) for 30 min. Intracellular proteins were then stained with anti-Gag KC57 RD1 antibody (1/100, Beckman Coulter) and/or anti- α -tubulin (5 µg/mL, Abcam) for 2h. Cells were washed and finally incubated with Alexa Fluor 488, 555 or 647 Goat anti-Mouse or Goat anti-Rabbit IgG secondary antibodies (2 µg/mL, Cell Signaling Technology), Alexa Fluor 488 or 555 Phalloidin (33 mM, Thermo Fisher Scientific), Wheat Germ Agglutinin (CF[®]350 WGA, Thermofischer) and DAPI (500 ng/mL, Sigma Aldrich) in blocking buffer for 1h. Coverslips were mounted on a glass slide using Fluorescence Mounting Medium (Dako) and visualized with a spinning disk (Olympus) (Fig. S2C; 3A; 3F; S3A, S3B, S3C; movie 1), a Zeiss confocal LSM880 with Airyscan (Fig. 3D, Movie 2) and a FV1000 confocal microscope (Olympus) (Fig. 4F).

TNT were identified by WGA or phalloidin and tubulin staining, and counted on at least 1000 cells per condition and per donor.

As HIV-1 infection induces macrophages fusion into MGC ([Verollet et al., 2010](#)) the number of infected cells largely underestimates the rate of infection. Thus, to better reflect the rate of infection, we quantified the percentage of multinucleated cells. Using semi-automatic quantification with homemade Image J macros, allowing the study of more than 5,000 cells per condition in at least five independent donors, assessed these parameters.

HIV-1 and cell-to-cell transfer

Freshly isolated CD14⁺ monocytes from HS transfected with siRNA against Siglec-1 or siRNA control were allowed to adhere in the absence of serum (2×10^6 cells/6-well in 1.5 mL). After 4h of culture, RPMI-1640 supplemented with 20 ng/mL M-CSF and 20% FBS were added to the cells (vol/vol). After 24h, cells were conditioned with cmMTB media. At day 4, 120 ng p24 of a HIV-1 NLAD8 strain pseudotyped with a VSVG envelope was used to infect half of the cells, kept in culture for 2 more days. At day 6, before co-culture, uninfected cells were stained with CellTracker Green CMFDA Dye (Thermo Fisher Scientific). For mitochondria transfer, half of the macrophages were pre-stained with Green CellTracker, and the other half, uninfected, was stained with mitoTracker Deep-Red prior to co-culture. Briefly, cells were washed with PBS Mg²⁺/Ca²⁺ and stained for 30 min with 500 ng/mL CellTracker or mitoTracker, before washing with RPMI-1640 10% FBS. HIV-1⁺ or mitoTracker⁺ and CellTracker⁺ cells were then detached using accutase (Sigma) and co-cultured at a 1:1 ratio on glass coverslips in 24-well.

Histological analyses

Paraffin embedded tissue samples were sectioned and stained with hematoxylin and eosin for histomorphological analysis. Different antigen unmasking methods were used on tissue slides for immunohistochemical staining, which was performed using anti-CD163 (Leica/Novocastra), anti-Siglec-1 (Novus Biologicals) and anti-pSTAT1 (Cell Signaling Technology). Sections were then incubated with biotin-conjugated polyclonal anti-mouse or anti-rabbit immunoglobulin antibodies followed by the streptavidin-biotin-peroxidase complex (ABC) method (Vector Laboratories). Finally, sections were counter-stained with hematoxylin. Slides were scanned with the Panoramic 250 Flash II (3DHISTECH). Virtual slides were automatically quantified for macrophage distribution as previously described ([Souriant et al., 2019](#)). Immunofluorescence staining of the sections was performed as described above and followed by anti-mouse IgG isotype specific or anti-rabbit IgG antibodies labelled with Alexa488 and Alexa555 (Molecular Probes). Samples were mounted with Prolong® Antifade reagent (Molecular Probes) and examined using a 60x/1.40N.A. objective of an Olympus spinning disk microscope.

QUANTIFICATION AND STATISTICAL ANALYSIS

Information on the statistical tests used and the exact values of n (donors) can be found in the Figure Legends. All statistical analyses were performed using GraphPad Prism 8.0.0 (GraphPad Software Inc.). Two-tailed paired or unpaired t-test was applied on data sets with a normal distribution (determined using Kolmogorov-Smirnov test), whereas two-tailed Mann-Whitney (unpaired test) or Wilcoxon matched-paired signed rank tests were used otherwise. $p < 0.05$ was considered as the level of statistical significance (* $p \leq 0.05$; ** $p \leq 0.005$; *** $p \leq 0.0005$; **** $p \leq 0.0001$).

KEY RESOURCES TABLE

REAGENT or RESOURCE	SOURCE	IDENTIFIER
Antibodies		
Mouse monoclonal anti-human Siglec-1 (clone 7-293)	Biologend	Cat# 346008; RRID:AB_11147948
Mouse monoclonal anti-human CD16 (clone 3G8)	Biologend	Cat# 302019 and 302018; RRID:AB_492974 and AB_314218
Mouse monoclonal anti-human CD163 (clone GHI/61)	Biologend	Cat# 333608; RRID:AB_2228986
Mouse monoclonal anti-human MerTK (clone 590H11G1E3)	Biologend	Cat# 367607; RRID:AB_2566400
Rabbit monoclonal anti-human STAT1 (clone 42H3)	Cell Signaling Technology	Cat# 9175; RRID:AB_2197984
Rabbit anti-human actin (a.a. 20-33)	Sigma-Aldrich	Cat# A5060; RRID:AB_476738
Rabbit polyclonal anti- β -tubulin	Abcam	Cat# ab18251; RRID:AB_2210057
Mouse monoclonal anti-Siglec-1 (clone hsn 7D2)	Novus Biologicals	Cat# NB 600-534; RRID:AB_526814
Mouse monoclonal anti-Gag RD1 (clone KC57)	NIH AIDS Reagent program	Cat# 13449
Monoclonal mouse anti-HIV p24 (clone Kal-1)	Dako Agilent technologies	Cat# M0857, RRID:AB_2335686
Mouse monoclonal anti-HIV-1 p24 (clone 183-H12-5C)	NIH AIDS Reagent Program	Cat# 3537
Human polyclonal anti-HIV Immune Globulin (HIVIG)	NIH AIDS Reagent Program	Cat# 3957
Polyclonal goat anti-human IgG	Sigma-Aldrich	Cat# A0170
Mouse monoclonal anti-human CD163 (clone 10D6)	Leica/Novocastra	Cat# NCL-L-CD163; RRID:AB_2756375
Anti-pSTAT1	Cell Signaling Technology	Cat# 9167 RRID:AB_561284
Mouse monoclonal anti-IFNAR2 (clone MMHAR-2)	Thermo Fisher Scientific	Cat# 213851; RRID:AB_223508
Mouse IgG2a isotype control	Thermo Fisher Scientific	Cat# 02-6200; RRID:AB_2532943
Polyclonal F(ab) ₂ goat anti-rabbit IgG, AlexaFluor 555	Thermo Fisher Scientific	Cat# A-21430, RRID:AB_2535851
Polyclonal F(ab) ₂ goat anti-mouse IgG, AlexaFluor 488	Thermo Fisher Scientific	Cat# A-10684, RRID:AB_2534064

Pyclonal F(ab)2 goat anti-mouse IgG, AlexaFluor 555	Cell Signaling Technology	Cat# 4409, RRID:AB_1904022
Polyclonal goat anti-rabbit IgG, HRP	Thermo Fisher Scientific	Cat# 32460; RRID:AB_1185567
Polyclonal goat anti-mouse IgG, HRP	Thermo Fisher Scientific	Cat# 31430; RRID:AB_228307
Bacterial and Virus Strains		
<i>M. tuberculosis</i> H37Rv	N/A	N/A
HIV-1 ADA	Gift from Dr. S Benichou	Institut Cochin, Paris, France
HIV-1 ADA Gag-iGFP	Gift from Dr P. Benaroch and Dr. M. Schindler	Institu Pasteur, Paris, France Institute of Virology, Munich, Germany
HIV-1 NLAD8-VSVG	Gift from Dr. S Benichou	Institut Cochin, Paris, France
HIV-1 ADA Gag-iGFP-VSVG	N/A	N/A
HIV-1 ADA-VSVG	Gift from Dr. S Benichou	Institut Cochin, Paris, France
HIV-1 Gag-eGFP	NIH research reagent program	Catalogue number 11468 Lot number: 2 070514
Biological Samples		
Buffy Coat	Etablissement Français du Sang, Toulouse, France	N/A
Histological slides of lung biopsies from rhesus macaques	Tulane National Primate Research Center	N/A
Chemicals, Peptides, and Recombinant Proteins		
Human recombinant M-CSF	Peprtech	Cat# 300-25
Human recombinant IFN γ	Peprtech	Cat# 300-02BC
Human recombinant IL-10	Peprtech	Cat# 200-10
Critical Commercial Assays		
Mouse anti-human CD14 microbeads	Miltenyi Biotec	Cat# 130-050-201
LS magnetic columns	Miltenyi Biotec	Cat# 130-042-401
Amersham ECL Prisme Western Blotting Detection Reagent	GE Healthcare	Cat# RPN2232
SuperSignal WestPico Chemiluminescent Substrate	Thermo Scientific	Cat# 34080
IL-10 ELISA set	BD Bioscience	Cat# 555157
Trypsin EDTA 0.05%	Thermo Fisher Scientific	Cat# 25200072

Accutase	Sigma-Aldrich	Cat# A-6964
Phalloidin AlexaFluor 488	Thermo Fisher Scientific	Cat# A12379
Phalloidin Alexa Fluor 647	Thermo Fisher Scientific	Cat# A22287
DAPI	Sigma Aldrich	Cat# D9542
CellTracker Red CMPTX Dye	Thermo Fisher Scientific	Cat# C34552
CellTracker Green CMFDA Dye	Thermo Fisher Scientific	Cat# C7025
MitoTracker Deep Red FM	Invitrogen	Cat# M22426
Fluorescence Mounting Medium	Agilent Technologies	Cat# S302380-2
Antibody diluent, Background reducing	DAKO, Agilent Technologies	Cat# S302283-2
Experimental Models: Cell Lines		
TZM-bl cell line	NIH AIDS Reagent Program	Cat# 8129
HEK 293T cell line	NIH AIDS Reagent Program	Cat# 3318
HKB-IFNAB	Invivogen	Cat# hb-detE
Software and Algorithms		
ImageJ	ImageJ	http://www.imagej.nih.gov/ij
Prism (v8.0.0)	GraphPad	http://www.graphpad.com
Photoshop CS3	Adobe	http://www.adobe.com
Adobe Illustrator CS5	Adobe	https://www.adobe.com/fr/products/illustrator.html
Huygens Professional Version 16.10	Scientific Volume Imaging	https://svi.nl/HuygensProfessional
FACS DIVA	BD Bioscience	http://www.bdbiosciences.com/
FlowJo_v10	FlowJo	https://www.flowjo.com/
FCS Express V3	DeNovo Software	http://www.denovosoftware.com
Image Lab	Bio-Rad Laboratories	http://www.bio-rad.com
Pannoramic Viewer	3DHISTECH	https://www.3dhitech.com/pannорamic_viewer

REFERENCES

- Foreman, T.W., Mehra, S., LoBato, D.N., Malek, A., Alvarez, X., Golden, N.A., Bucsan, A.N., Didier, P.J., Doyle-Meyers, L.A., Russell-Lodrigue, K.E., *et al.* (2016). CD4+ T-cell-independent mechanisms suppress reactivation of latent tuberculosis in a macaque model of HIV coinfection. *Proceedings of the National Academy of Sciences of the United States of America* *113*, E5636-5644.
- Izquierdo-Useros, N., Lorizate, M., Contreras, F.X., Rodriguez-Plata, M.T., Glass, B., Erkizia, I., Prado, J.G., Casas, J., Fabrias, G., Krausslich, H.G., *et al.* (2012). Sialyllactose in viral membrane gangliosides is a novel molecular recognition pattern for mature dendritic cell capture of HIV-1. *PLoS biology* *10*, e1001315.
- Izquierdo-Useros, N., Lorizate, M., McLaren, P.J., Telenti, A., Krausslich, H.G., and Martinez-Picado, J. (2014). HIV-1 capture and transmission by dendritic cells: the role of viral glycolipids and the cellular receptor Siglec-1. *PLoS pathogens* *10*, e1004146.
- Kaushal, D., Mehra, S., Didier, P.J., and Lackner, A.A. (2012). The non-human primate model of tuberculosis. *Journal of medical primatology* *41*, 191-201.
- Lastrucci, C., Benard, A., Balboa, L., Pingris, K., Souriant, S., Poincloux, R., Al Saati, T., Rasolofoa, V., Gonzalez-Montaner, P., Inwentarz, S., *et al.* (2015). Tuberculosis is associated with expansion of a motile, permissive and immunomodulatory CD16(+) monocyte population via the IL-10/STAT3 axis. *Cell research* *25*, 1333-1351.
- Mehra, S., Golden, N.A., Dutta, N.K., Midkiff, C.C., Alvarez, X., Doyle, L.A., Asher, M., Russell-Lodrigue, K., Monjure, C., Roy, C.J., *et al.* (2011). Reactivation of latent tuberculosis in rhesus macaques by coinfection with simian immunodeficiency virus. *Journal of medical primatology* *40*, 233-243.
- Pino, M., Erkizia, I., Benet, S., Erikson, E., Fernandez-Figueras, M.T., Guerrero, D., Dalmau, J., Ouchi, D., Rausell, A., Ciuffi, A., *et al.* (2015). HIV-1 immune activation induces Siglec-1 expression and enhances viral trans-infection in blood and tissue myeloid cells. *Retrovirology* *12*, 37.
- Ritchie, M.E., Phipson, B., Wu, D., Hu, Y., Law, C.W., Shi, W., and Smyth, G.K. (2015). limma powers differential expression analyses for RNA-sequencing and microarray studies. *Nucleic acids research* *43*, e47.
- Souriant, S., Balboa, L., Dupont, M., Pingris, K., Kviatcovsky, D., Cougoule, C., Lastrucci, C., Bah, A., Gasser, R., Poincloux, R., *et al.* (2019). Tuberculosis Exacerbates HIV-1 Infection through IL-10/STAT3-Dependent Tunneling Nanotube Formation in Macrophages. *Cell reports* *26*, 3586-3599 e3587.
- Troegeler, A., Lastrucci, C., Duval, C., Tanne, A., Cougoule, C., Maridonneau-Parini, I., Neyrolles, O., and Lugo-Villarino, G. (2014). An efficient siRNA-mediated gene silencing in primary human monocytes, dendritic cells and macrophages. *Immunology and cell biology* *92*, 699-708.
- Verollet, C., Souriant, S., Bonnaud, E., Jolicoeur, P., Raynaud-Messina, B., Kinnaer, C., Fourquaux, I., Imle, A., Benichou, S., Fackler, O.T., *et al.* (2015). HIV-1 reprograms the migration of macrophages. *Blood* *125*, 1611-1622.
- Verollet, C., Zhang, Y.M., Le Cabec, V., Mazzolini, J., Charriere, G., Labrousse, A., Bouchet, J., Medina, I., Biessen, E., Niedergang, F., *et al.* (2010). HIV-1 Nef triggers macrophage fusion in a p61Hck- and protease-dependent manner. *Journal of immunology* *184*, 7030-7039.

SUPPLEMENTAL INFORMATION

Dupont et al., Figure S1

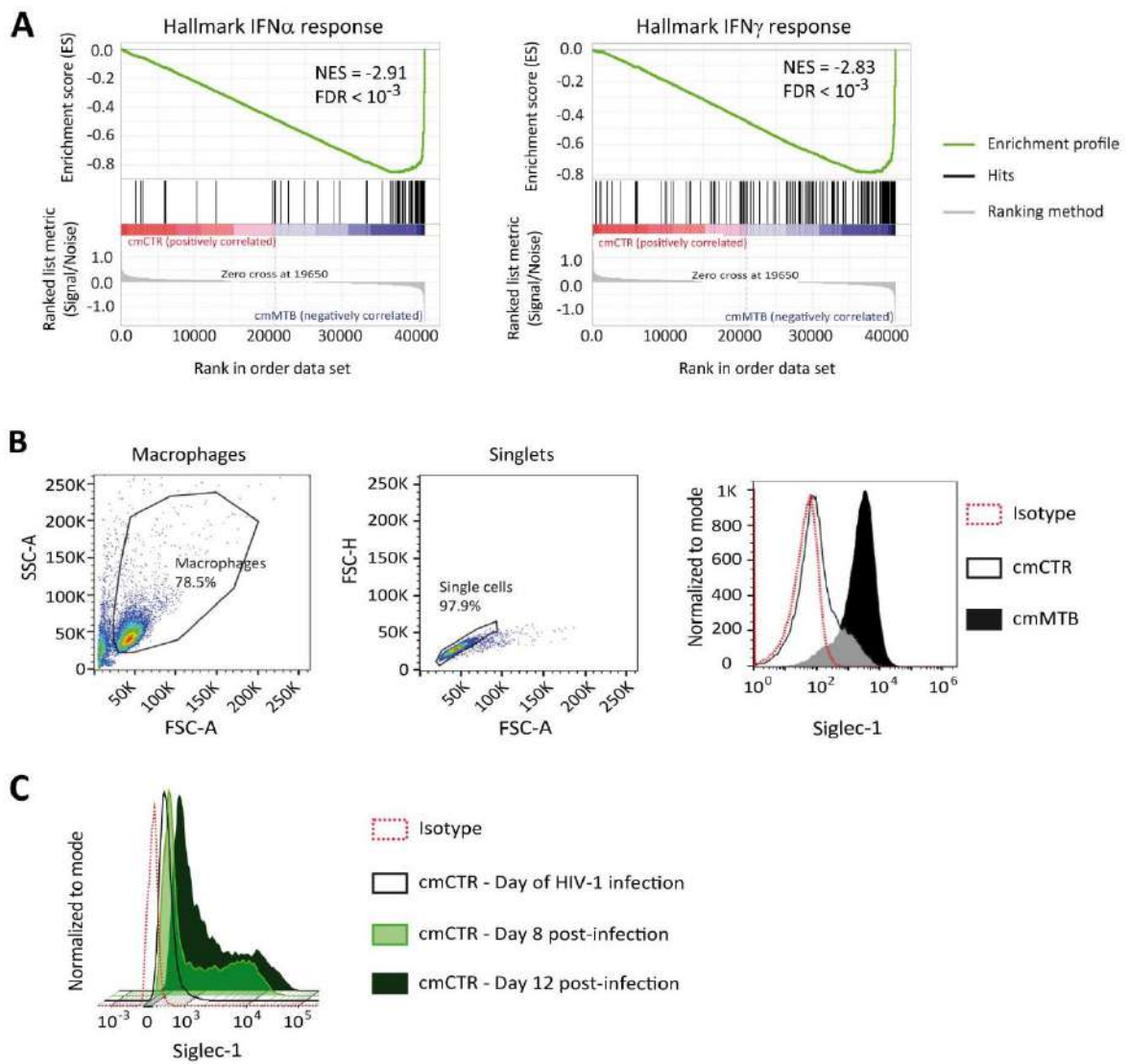


Figure S1. Tuberculosis-associated microenvironment increases Siglec-1 expression in human macrophages (see also Figure 1).

(A-C) For 3 days, human monocytes were differentiated into macrophages with cmCTR (white) or cmMTB (black) supernatants.

(A) (Left) Gene set enrichment plot of the interferon alpha (IFN α) response (hallmark collection of MSigDB). This plot shows the distribution of the barcode between macrophages exposed to cmCTR (red) *versus* cmMTB (blue) supernatants. Each bar of the barcode corresponds to a signature gene of the gene set. The skewing to the right indicates enrichment in macrophages exposed to cmMTB *versus* cmCTR supernatant of genes up-regulated in response to IFN α . (Right) Gene set enrichment plot of the IFN α response (hallmark collection of MSigDB).

(B-C) Flow cytometry gating strategy to assess Siglec-1 cell-surface expression in human macrophages exposed to cmCTR (white) and cmMTB (black) (B), or cmCTR-treated cells infected with HIV-1 (C). (B) Left: Based on size (FCS-A) and granularity (SSC-A), a gate was created to separate human macrophages from cell debris and dying cells. Macrophages were then subjected through a second gate based FSC Area Scaling (FCS-A and FCS-H) to separate singlets from doublets. Right: Based on the singlet gate, the histogram plot illustrates Siglec-1 expression that is higher in cmMTB- than in cmCTR-treated macrophages. (C) The histogram plot illustrates the time-course of Siglec-1 expression that is upregulated after HIV-1 infection in cmCTR-treated cells compared to uninfected ones.

Dupont et al., Figure S2

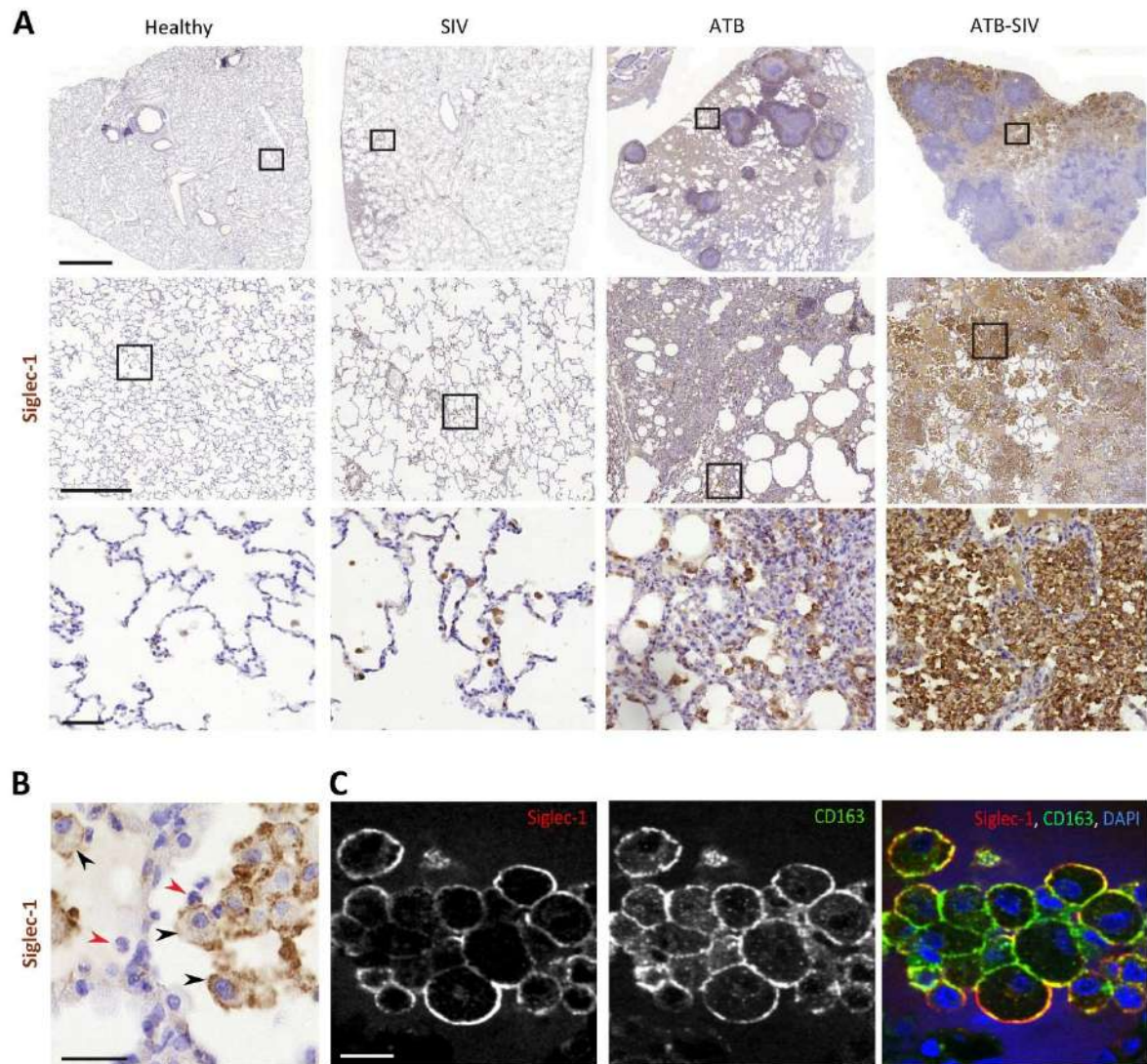


Figure S2. Tuberculosis-associated microenvironment increases Siglec-1 expression in non-human primate alveolar macrophages (see also Figure 1).

(A) Accumulation of Siglec-1⁺ alveolar macrophages in the lung of co-infected non-human primates (NHP). Representative immunohistochemical images of Siglec-1 staining (brown) in lung biopsies of healthy, SIV-infected (SIV), active tuberculosis (ATB) and co-infected with SIV (ATB-SIV) NHP. Scale bars from top to bottom: 2 mm, 500 μ m and 50 μ m.

(B-C) Siglec-1⁺ cells display the alveolar macrophage morphology. (B) Representative immunohistochemistry image from lung biopsy of an ATB-SIV NHP stained for Siglec-1 (brown). Siglec-1⁺ cells display a cell morphology with a single nucleus and large cytoplasm reminiscent of macrophage (black arrowhead); Siglec-1⁻ cells display a different nucleus morphology and small cytoplasm reminiscent of neutrophils (red arrowhead). Scale bar, 20 μ m. (C) Representative immunofluorescence images of alveolar macrophages found in lung biopsy of a representative ATB-SIV NHP stained for Siglec-1 (red), CD163 (green) and DAPI (nuclei, blue). Scale bar, 20 μ m.

Dupont et al., Figure S3

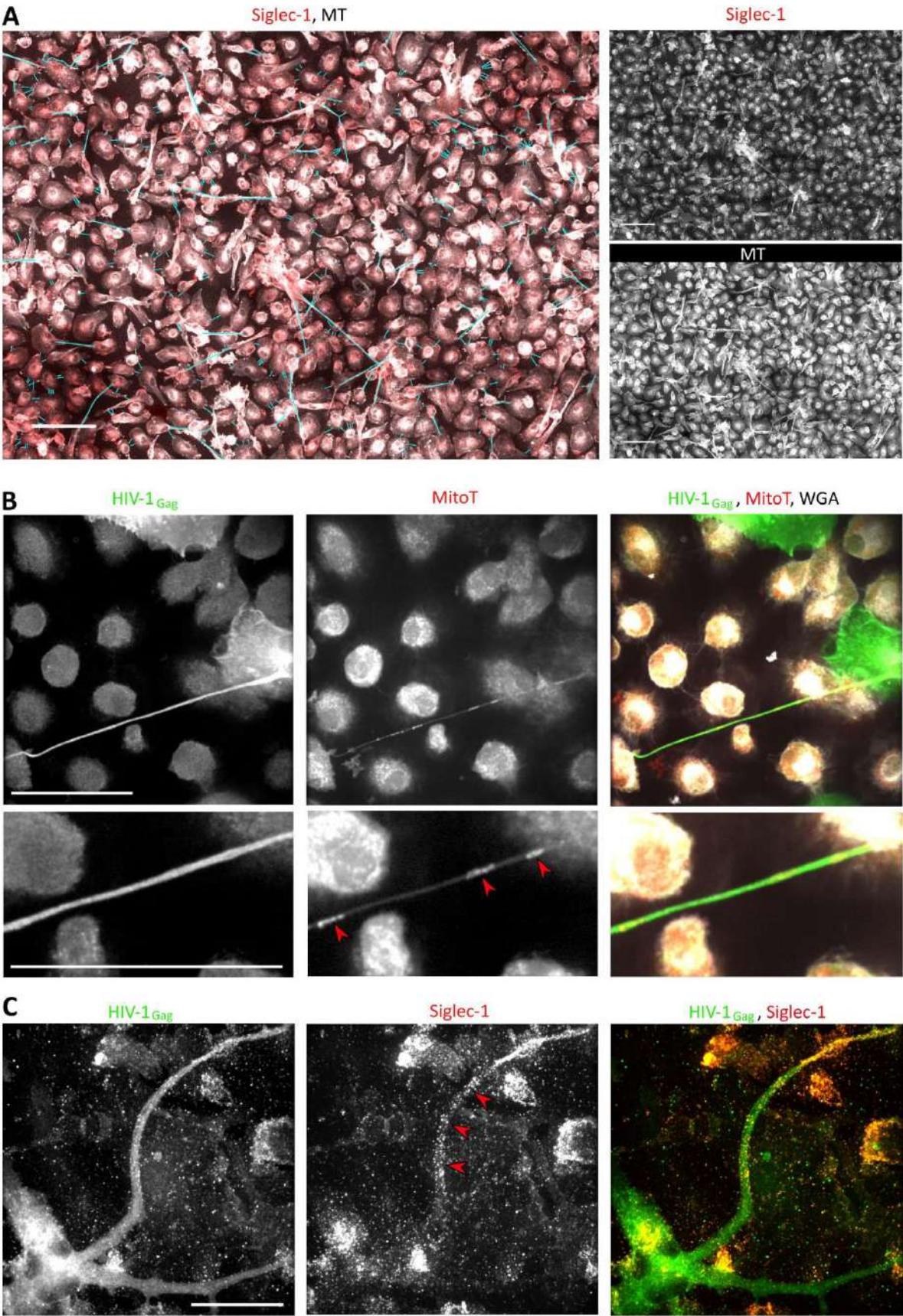


Figure S3. Siglec-1 localizes specifically on thick tunneling nanotubes that contain HIV-1 Gag and mitochondria (see also Figure 3).

(A-C) Human monocytes were differentiated into macrophages with cmMTB for 3 days, infected with HIV-1-ADA strain (unless indicated otherwise) and then fixed at day 3 (A-B) or 10 (C) post-infection.

(A) Representative immunofluorescence images used for semi-automatic quantification of TNT in cmMTB-treated macrophages infected with HIV-1. Cells were stained for extracellular Siglec-1 (red), intracellular tubulin (MT, grey) and Wheat Germ Agglutinin (WGA, not shown). Blue lines show all TNT considered. Thick (WGA⁺, MT⁺) and thin (WGA⁺, MT⁻) TNT were assessed for Siglec-1 positivity by applying a threshold and measured in length. Scale bar, 20 μ m.

(B) Representative immunofluorescence images of cmMTB-treated macrophages infected with HIV-1-NLAD8-VSVG, loaded with Mitotracker (MitoT, red) and stained for intracellular HIV-1 Gag (green) and WGA (grey). Red arrowheads show mitochondria inside HIV-1 Gag-containing TNT. Inserts are 2x zoom. Scale bar, 20 μ m.

(C) Representative immunofluorescence images of cmMTB-treated macrophages infected with HIV-1 and kept in culture until day 10 post-infection. Cells were fixed and stained for intracellular HIV-1 Gag (green), extracellular Siglec-1 (red) and WGA (grey). Red arrowheads show Siglec-1 on HIV-1 Gag-containing TNT emanating from an infected multinucleated giant cell (MGC). Scale bar, 20 μ m

Dupont et al., Figure S4

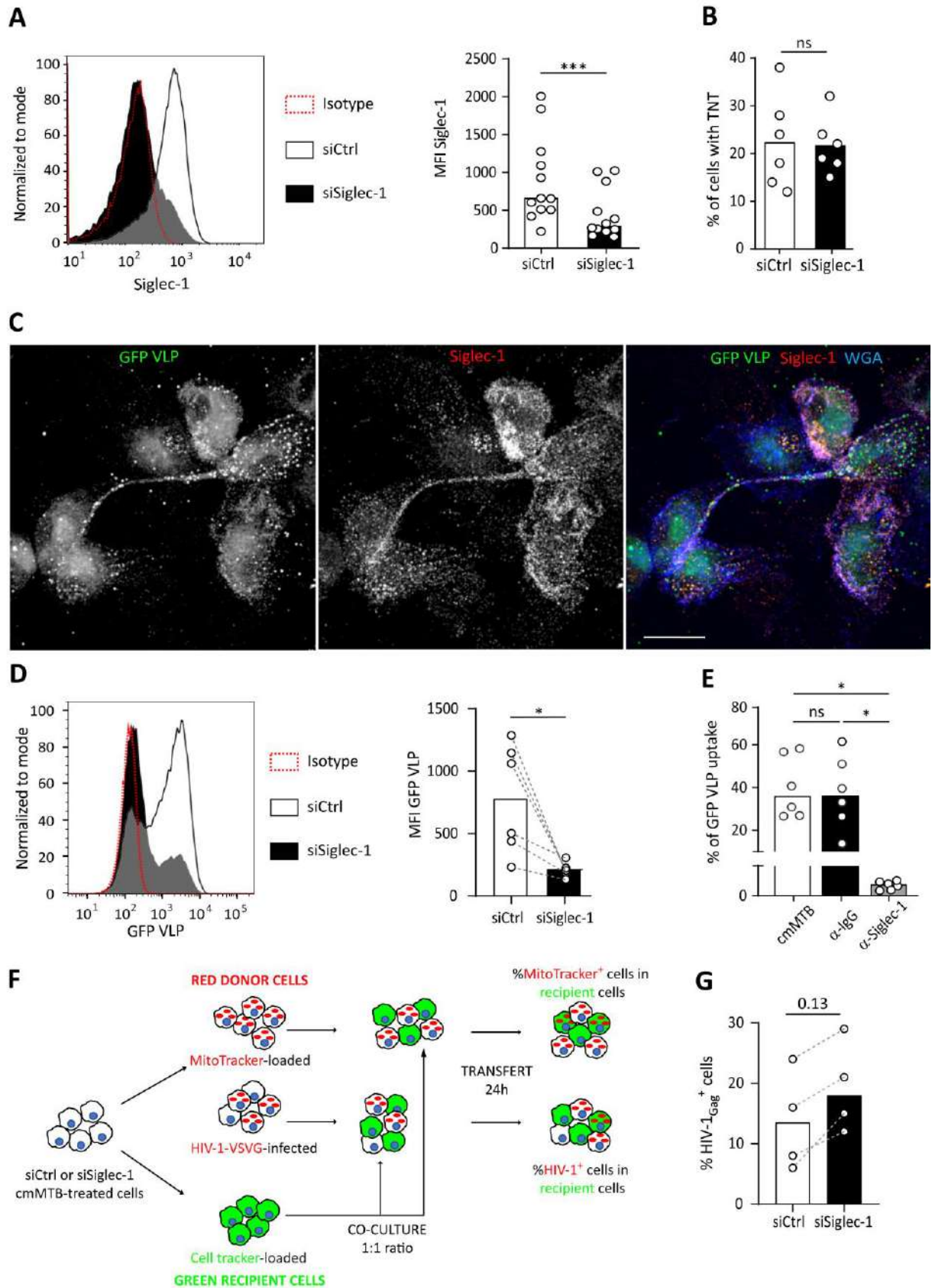


Figure S4. Siglec-1 is required for the capture and transfer of HIV-1 in cmMTB-treated macrophages (see also Figure 4).

(A-D, F-G) Monocytes from healthy subjects were transfected with siRNA targeting of Siglec-1 (siSiglec-1, black) or not (siCtrl, white). A day after, monocytes were differentiated into macrophages with cmMTB for 3 days.

(A) Representative histogram (left) and vertical scatter plot showing the median fluorescent intensity (MFI) (right) of Siglec-1 expression on the indicated cell populations.

(B) Vertical scatter plot indicating the percentage of cells forming TNT in cells.

(C-E) Inhibition of Siglec-1 reduces binding of HIV-1 Gag-eGFP VLP (GFP VLP). (C) Representative immunofluorescence (IF) images of cmMTB-treated cells incubated with GFP VLP (green) for 3.5h. Cells were fixed and stained for Siglec-1 (red) and Wheat Germ Agglutinin (WGA, blue). Scale bar, 500 μ m.

(D) Representative histogram (left) and vertical scatter plot showing the median fluorescent intensity (MFI) (right) displaying of GFP VLP binding in the indicated cell populations.

(E) Vertical scatter plot showing the percentage of GFP VLP binding in cmMTB treated cells pre-incubated with specific anti-Siglec-1 (α -Siglec-1, grey), isotype control antibody (α -IgG, black) or mock (white).

(F) Experimental model for the cell-to-cell transfer experiment. siRNA-transfected donor (red) cells were either labelled with MitoTracker (1h prior co-culture) or infected with HIV-1-NLAD8-VSVG (48h prior to co-culture), while autologous recipient cells (green) were stained with cell tracker (1h prior co-culture). Both donor and recipient cells were co-culture for 24h. Red fluorescence was then measured in recipient cells by IF.

(G) Vertical scatter plot showing the percentage of HIV-1_{Gag}⁺ cells at the time of co-culture experiment in the indicated cells.

Statistical analyses: Two-tailed, Wilcoxon matched-pairs signed rank test (A, B, D-E, G). *P < 0.05, ***P < 0.001. ns: not significant.

SUPPLEMENTAL TABLES

Table S1. Clinical data of NHPs (related to Figure 1E-H and 2E-H, and Figure S2A).

Animals	Status	Sex	Age of death (years)	Days after infection*	Viral load**
EC61	-	M	8.99	-	-
GI53	-	M	5.02	-	-
IT02	-	M	4.69	-	-
BK48	SIV	M	12.06	322	8.58×10^6
DD87	SIV	F	9.84	540	3.03×10^4
DT18	SIV	M	8.85	764	4.40×10^4
BA34	SIV	M	16.79	750	1.91×10^5
DR28	SIV	M	8.84	120	1.48×10^7
CA75	LTB	M	11.7	106	-
FE10	LTB	M	7	166	-
FJ05	LTB	M	6.81	181	-
CL10	ATB	M	13.84	51	-
CG58	ATB	M	7.71	75	-
GK87	ATB	F	7.76	38	-
ER44	SIV/LTB	M	8.61	167	1.93×10^5
HB12	SIV/LTB	M	4.97	167	1.04×10^6
ID01	SIV/LTB	M	3.58	153	2.17×10^6
HP22	SIV/ATB	M	3.79	113	3.7×10^8
HP41	SIV/ATB	M	3.78	111	6×10^5
HT09	SIV/ATB	M	3.72	104	7.5×10^6

* Infection 1: Mtb CDC1551 and infection 2: SIVmac239. For co-infected macaques, days after first Mtb infection. Abbreviations: LTb: latent TB, ATb: active TB, M: male, F: female.

Table S2. Histopathological scoring of lung lesions in NHPs (related to Figure 1E-H and 2E-H, and Figure S2A).

Animals	Status	Lung Disease severity	Granulomatous lesions				Non-Granulomatous lesions
			Granuloma Size	Type of granuloma	Distribution pattern	Cellular composition	
EC61	-	None	-	-	-	-	- Few & small perivascular lymphohistiocytic infiltrates, PMN+
GI53	-	None	-	-	-	-	- Few & small perivascular lymphohistiocytic infiltrates, PMN+
IT02	-	None	-	-	-	-	- Few & small perivascular lymphohistiocytic infiltrates -PMN+ -peribronchial iBALT
BK48	SIV	Minimal	-	-	-	-	- small perivascular lymphohistiocytic infiltrates
DD87	SIV	Minimal	-	-	-	-	- small perivascular lymphohistiocytic infiltrates
DT18	SIV	Minimal	-	-	-	-	- polymorph infiltrates
BA34	SIV	Mild	-	-	-	-	- Focal interstitial pneumonia, - interstitial lymphohistiocytic infiltrates, - thickening of the alveolar wall,

							- collagen deposit, - type-2 pneumocyte hyperplasia
DR28	SIV	Minimal	-	-	-	-	thickening of the alveolar wall closed to the pleura
CA75	LTB	Mild	small	Non Necrotizing, Poorly organized	multifocal	- Lymphocytic cuff - Epithelioid & Foamy Mφ - MGC, - Fibrosis [+]	Interstitial pneumopathy
FE10	LTB	Mild	large	Nonnecro tizing Suppurative	focal solid coalescent	- Lymphocytic cuff - Epithelioid & Foamy Mφ - MGC	Thickening of the alveolar wall
FJ05	LTB	Mild	medium	caseous	multifocal	- Lymphocytic cuff - peripheral fibrosis	Strong interstitial pneumopathy
CL10	ATB	Moderate	Small & medium	Caseous & solid	Multifocal coalescent	- Lymphocytic cuff - Epithelioid Mφ, - MGC++	- Strong interstitial pneumopathy & haemorrhage
CG58	ATB	Mild	Small , medium & large	Necrotic & solid	Multifocal coalescent	- Lymphocytic cuff - Epithelioid Mφ, - MGC++	-
GK87	ATB	Moderate	Medium & large	Necrotic, caseous and suppurative	Multifocal coalescent	- Lymphocytic cuff - Epithelioid Mφ, MGC++, PMN++	-transudate in the alveolar space, - collagen deposits -Interstitial pneumopathy

ER44	SIV/LT B	Mild	large	Necrotic & caseous	focal	2 coalescent follicles, Loss of the lymphocytic cuff, Epithelioid Mφ- MGC++,	-Interstitial pneumopathy, - haemorrhage & fibrosis
HB12	SIV/LT B	Severe	none	-	-	-	-Interstitial pneumopathy, iBALT - haemorrhage & alveolitis, - fibrosis, syncytia and PMN++
ID01	SIV/LT B	Moderate	none	-	-	-	-Interstitial pneumopathy, iBALT - haemorrhage & alveolitis,
HP22	SIV/A TB	Moderate	medium	Solid, necrotic, fibrotic & mineralized	multifocal	- Lymphocytic cuff - Epithelioid Mφ, MGC++	-Interstitial pneumopathy - haemorrhage & syncytia
HP41	SIV/A TB	Severe	large	Necrotic	coalescent	- Lymphocytic cuff - Epithelioid Mφ, MGC++	-strong Interstitial pneumopathy, - haemorrhage & alveolitis, fibrosis, PMN++
HT09	SIV/A TB	Severe	large	Suppurative	Multifocal, coalescent & invasive	Loss of the lymphocytic cuff, Epithelioid Mφ, MGC++, PMN++ fibrosis	- Interstitial pneumopathy, - haemorrhage

Abbreviations: PMN: polymorphonuclear leukocytes, iBALT: inducible Bronchus-associated lymphoid tissue, Mφ: Macrophages, MGC: Multinucleated giant cells.

SUPPLEMENTAL REFERENCES

- Foreman, T.W., Mehra, S., LoBato, D.N., Malek, A., Alvarez, X., Golden, N.A., Bucsan, A.N., Didier, P.J., Doyle-Meyers, L.A., Russell-Lodrigue, K.E., *et al.* (2016). CD4+ T-cell-independent mechanisms suppress reactivation of latent tuberculosis in a macaque model of HIV coinfection. *Proceedings of the National Academy of Sciences of the United States of America* *113*, E5636-5644.
- Izquierdo-Useros, N., Lorizate, M., Contreras, F.X., Rodriguez-Plata, M.T., Glass, B., Erkizia, I., Prado, J.G., Casas, J., Fabrias, G., Krausslich, H.G., *et al.* (2012). Sialyllactose in viral membrane gangliosides is a novel molecular recognition pattern for mature dendritic cell capture of HIV-1. *PLoS biology* *10*, e1001315.
- Izquierdo-Useros, N., Lorizate, M., McLaren, P.J., Telenti, A., Krausslich, H.G., and Martinez-Picado, J. (2014). HIV-1 capture and transmission by dendritic cells: the role of viral glycolipids and the cellular receptor Siglec-1. *PLoS pathogens* *10*, e1004146.
- Kaushal, D., Mehra, S., Didier, P.J., and Lackner, A.A. (2012). The non-human primate model of tuberculosis. *Journal of medical primatology* *41*, 191-201.
- Lastrucci, C., Benard, A., Balboa, L., Pingris, K., Souriant, S., Poincloux, R., Al Saati, T., Rasolofo, V., Gonzalez-Montaner, P., Inwentarz, S., *et al.* (2015). Tuberculosis is associated with expansion of a motile, permissive and immunomodulatory CD16(+) monocyte population via the IL-10/STAT3 axis. *Cell research* *25*, 1333-1351.
- Mehra, S., Golden, N.A., Dutta, N.K., Midkiff, C.C., Alvarez, X., Doyle, L.A., Asher, M., Russell-Lodrigue, K., Monjure, C., Roy, C.J., *et al.* (2011). Reactivation of latent tuberculosis in rhesus macaques by coinfection with simian immunodeficiency virus. *Journal of medical primatology* *40*, 233-243.
- Pino, M., Erkizia, I., Benet, S., Erikson, E., Fernandez-Figueras, M.T., Guerrero, D., Dalmau, J., Ouchi, D., Rausell, A., Ciuffi, A., *et al.* (2015). HIV-1 immune activation induces Siglec-1 expression and enhances viral trans-infection in blood and tissue myeloid cells. *Retrovirology* *12*, 37.
- Ritchie, M.E., Phipson, B., Wu, D., Hu, Y., Law, C.W., Shi, W., and Smyth, G.K. (2015). limma powers differential expression analyses for RNA-sequencing and microarray studies. *Nucleic acids research* *43*, e47.
- Souriant, S., Balboa, L., Dupont, M., Pingris, K., Kviatcovsky, D., Cougoule, C., Lastrucci, C., Bah, A., Gasser, R., Poincloux, R., *et al.* (2019). Tuberculosis Exacerbates HIV-1 Infection through IL-10/STAT3-Dependent Tunneling Nanotube Formation in Macrophages. *Cell reports* *26*, 3586-3599 e3587.
- Troegeler, A., Lastrucci, C., Duval, C., Tanne, A., Cougoule, C., Maridonneau-Parini, I., Neyrolles, O., and Lugo-Villarino, G. (2014). An efficient siRNA-mediated gene silencing in primary human monocytes, dendritic cells and macrophages. *Immunology and cell biology* *92*, 699-708.
- Verollet, C., Souriant, S., Bonnaud, E., Jolicœur, P., Raynaud-Messina, B., Kinnaer, C., Fourquaux, I., Imle, A., Benichou, S., Fackler, O.T., *et al.* (2015). HIV-1 reprograms the migration of macrophages. *Blood* *125*, 1611-1622.
- Verollet, C., Zhang, Y.M., Le Cabec, V., Mazzolini, J., Charriere, G., Labrousse, A., Bouchet, J., Medina, I., Biessen, E., Niedergang, F., *et al.* (2010). HIV-1 Nef triggers macrophage fusion in a p61Hck- and protease-dependent manner. *Journal of immunology* *184*, 7030-7039.

III. Discussion

Here, we evidence that the TB-associated microenvironment induces the formation of TNT, together with the IFN-I inducible receptor Siglec-1 that was previously shown to efficiently capture and transfer HIV-1 from DC to CD4⁺ T cells. We found that Siglec-1 was specifically expressed by a subtype of thick TNT, longer than Siglec-1⁻ TNT, which contained high HIV-1 and mitochondria cargos. In addition, Siglec-1⁺ alveolar macrophage abundance in the lung of Mtb-SIV co-infected macaques correlated with the disease severity and the activation of the IFN-I/STAT1 pathway. We also observed that the depletion of Siglec-1 decreased HIV-1 capture, while the viral replication dropped to the levels observed in control cells. Therefore, Siglec-1 is a key factor involved in the exacerbation of HIV-1 replication in the context of co-infection with Mtb, at least in part in a TNT-dependent manner.

By means of co-culture experiments, we showed that Siglec-1 depletion reduced the intracellular cell-to-cell transfer of HIV-1, since we used a VSVG-pseudotyped strain of HIV-1 to avoid differences of viral uptake in presence or absence of Siglec-1. Moreover, prior to co-culture, infected cells were washed to remove viruses that did not infect the cells, and the production of new virions in macrophages is longer than 24h. We correlated this diminution with the reduced TNT length and the diminished capacity of silenced cells to transfer mitochondria. However, we could not prove that the decreased transfer of both HIV-1 and mitochondria in Siglec-1-depleted macrophages was due to TNT transport inhibition. Indeed, HIV-1 proteins, full viruses and mitochondria elements, such as DNA, can also be transferred from one cell to another through the exosome pathway. To assess to what extent TNT or exosome-like particle, secreted through the exosome pathway, are involved in cell-to-cell transfer of HIV-1 and mitochondria, co-culture experiments combining the depletion of Siglec-1 and use of TNT inhibitor [550], [669] could be performed. In addition, proper exosomes secreted by Mtb-infected cells could also be filtered and extracted from cmMTB conditioning media, and used in independent culture of non-polarized macrophages infected with HIV-1 to evaluate the role of cmMTB-exosome in the enhancement of HIV-1 dissemination. In parallel, exosome-free and vesicles-free cmMTB could be used to differentiate monocytes and to reiterate the co-culture experiment, in comparison with “complete” cmMTB treatment. I would expect that exosomes and vesicles play a minor role in the exacerbation of HIV-1 replication and spread. Indeed, we previously performed the co-culture experiment of infected macrophages with uninfected one using transwells, of which pores are large enough to allow exosome to pass from one side of the transwell to the other ([550], Chapter IV). Donor macrophages separated by a transwell from uninfected recipient cells failed to transfer HIV-1, as compared to co-culture where TNT were strongly induced. Moreover, this transfer was inhibited when TNTi was used during the co-culture ([550], Chapter IV), suggesting that the main mechanism through which HIV-1 spread from one macrophage to the other is dependent on cell-to-cell contact.

In this study, we observed that Siglec-1 expression had an impact on the length of TNT. Moreover, we observed that Siglec-1⁺ TNT were still present in the culture after 10 days of infection with HIV-1, whereas Siglec-1⁻ thick TNT were rarer, suggesting that Siglec-1⁺ TNT are possibly more stable than other TNT. Interestingly, Siglec-1 binds both in *cis* and *trans* to α 2,3-sialic acid expressed at the cell surface [621], [622]. One of its ligand, GM3, is strongly expressed both at the cell surface

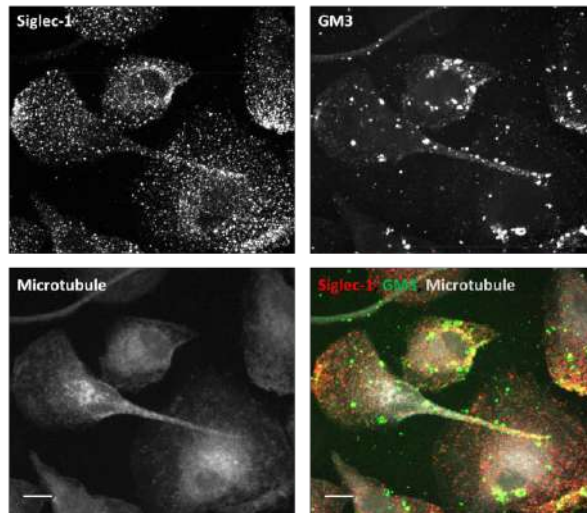


Figure 33: Siglec-1 and GM3 are localized on thick TNTs.

Representative immunofluorescence images of cmMTB-treated macrophages differentiated for 3 days prior to HIV-1_{ADA} infection and fixation 3 days post-infection. Cells were stained for extracellular Siglec-1 (red), GM3 (green) and intracellular tubulin (microtubule, grey). *Scale bar: 100 μm.*

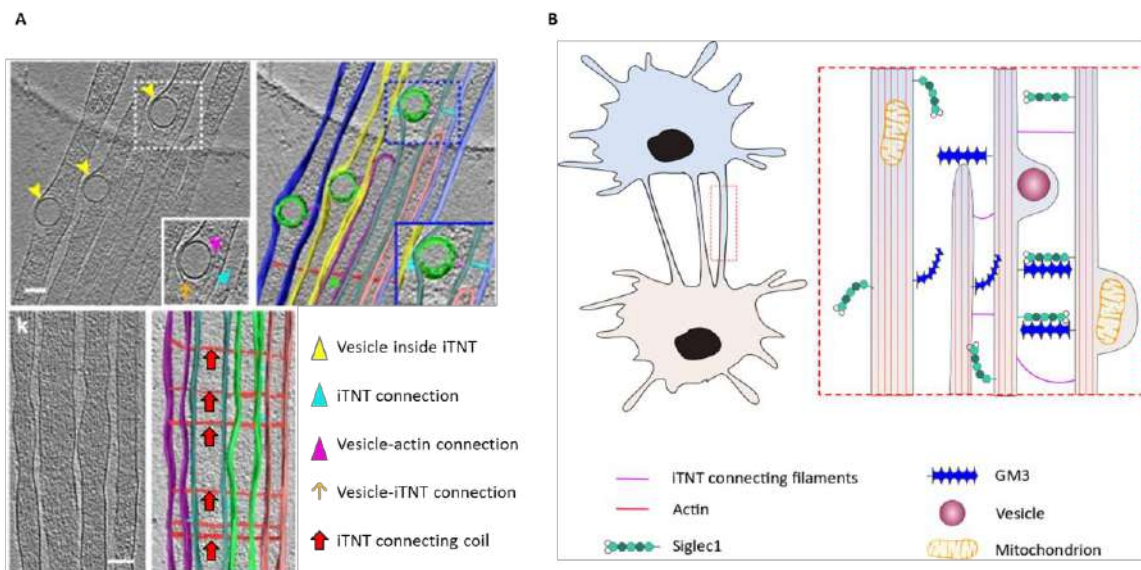


Figure 34: Structure and stability of TNT.

A | Schematic diagram depicting the structure of TNT. TNT formed between two cells can either be single thick connections or an association between thinner individual TNT. Both type of TNT structure can contain intracellular cargos, such as small vesicles, mitochondria for the bigger ones, and pathogens. Vesicles trafficking inside TNT are connected to the TNT plasma membrane through thin connecting coil composed of actin filaments. Individual TNT are connected with one another through actin and N-cadherin proteins that act as membrane anchors (not represented). Adapted from [770].

B | Schematic representation of Siglec-1-GM3 bound TNT in the context of HIV-1 infection. Individual TNT are connected to one another through the interaction of Siglec-1 and GM3 expressed all along TNT; stabilizing the structure for a longer period of time or longer distance, allowing for enhanced viral transport.

and on HIV-1 virion when budding from infected cells [633]. In a preliminary experiment, I observed that GM3 is the main ganglioside present at the surface of cmMTB-treated macrophages, and more specifically, I found that both Siglec-1 and GM3 are present on TNT (Figure 33). According to these observations, one can hypothesize that the expression of Siglec-1 and GM3 on TNT are involved in the stability of these structures and would therefore allow the transport of soluble factors, organelles and pathogens for longer period of time or to longer distance. However, Siglec-1 is also able to bind several ligands, including mucin-1 and CD43, which were suggested previously to be putative ligands for Siglec-1 in breast cancer and T cells respectively [822], and could be, as much as GM3, part of the molecules stabilizing Siglec-1⁺ TNT. Importantly, counter receptors, such as MRC1, are also capable of binding to Siglec-1 [830]. Considering that MRC1 is highly expressed by macrophages (especially in the TB context) and its involvement in the capture of HIV-1 (see chapter II section D.a.i.), it would be interesting to find out the role of MRC1-Siglec-1 interactions in the enhanced capture of HIV-1 virions and potential role in the stabilization of TNT structures.

The group of Dr C. Zurzolo have identified the structure of neuronal cell TNT using highly resolutive cryo-electron microscopy technique and found that a single TNT observed by immunofluorescence is in fact constituted of several individual small TNT (diameter comprised between 145 and 700 nm) (Figure 34A), connected with one another by actin filament and N-cadherin anchors. Individual TNT were found to contain small vesicles and mitochondria that efficiently transferred from one cell to another, unidirectionally [770]. It would be interesting to study if macrophages TNT display the same organization, and what are the proteins involved in the connection between individual TNT. My hypothesis is that, under physiological conditions, macrophages TNT are composed of several individual TNT and that are maintained by adhesion molecules, such as ICAM or integrin. However, in pathological condition such as Mtb-HIV-1 mono- or co-infection, the upregulation of Siglec-1 could strengthen the stability of TNT by providing an additional anchor between individual TNT. Indeed, it is possible that one individual TNT expresses GM3, or another ligand or counter-receptor (*e.g.* MRC1), while the other expresses Siglec-1, which bind to each other and stabilize the entire structure (Figure 34B). To verify this hypothesis, the same methodology than that used by Dr C. Zurzolo could be used. In addition, to establish the role of Siglec-1 in TNT stabilization, video-microscopy experiment following the same TNT for several hours, or maximum few days, could be performed on cmMTB-macrophages depleted or not for Siglec-1. To go further with TNT stability, it could be interesting to investigate the involvement of lipid-rafts, and more particularly on cholesterol function in TNT formation and/or stabilization. Indeed, GM3 are inserted in lipid rafts rich in cholesterol [771]. In addition, cholesterol was previously reported to be involved in TNT stabilization [772], [773]. To do so, we could study the formation of TNT in cells where cholesterol was depleted with β -methylcyclodextrin, and evaluate the capacity of cholesterol replenishment to induce TNT formation. In terms of stability, live cell imaging experiments following the same principle as for Siglec-1⁺ cells could be performed, with or without cholesterol.

Another interesting question relative to TNT-mediated exacerbation of HIV-1 replication in the context of TB co-infection would be to assess the part of HIV-1 trafficking inside TNT and the part of external Siglec-1-bound HIV-1 particles in the infection mechanisms of macrophages. Indeed, it was previously suggested that HIV-1 proteins [669], [774] and particles [668], [775] were present inside

TNT and spread from one cell to another by intracellular trafficking. However, the clear demonstration of internal viral transfer remains to be done and is a quite challenging question in the field since even super-resolution microscopy has a resolution range of about the diameter of TNT. One technique that could answer the question whether HIV-1 virus are inside or outside TNT is to use electron microscopy where a TNT can be found and cut to see the inside. Here, we found that Siglec-1 is mainly expressed at the cell surface and on TNT membrane. Moreover, we saw that Siglec-1 present on TNT captured efficiently the viral-like particles through GM3 recognition. Therefore, and considering that cell membranes are highly dynamic structures, it is highly possible that HIV-1 particles bound to Siglec-1 are transported from the infected to the non-infected cell through Siglec-1 membrane “sliding”, as previously observed with BCG [665]. This process could also be enhanced by the expression of other lectins on TNT. In the context of Mtb infection, we found that DC-SIGN, MRC1 and DCIR, all described to bind to the viral protein gp120, were induced by cmMTB in macrophages. Assessing whether these lectins are also involved in TNT stabilization or HIV-1 TNT-mediated transfer could further help to characterize certain subtype of TNT, which actively transport HIV-1 particles. For instance, if DC-SIGN or MRC1 are expressed on TNT, it could represent an increased binding site for the virus, just like Siglec-1, and therefore participate to the increase viral capture and transfer from one cell to another. I suspect that DC-SIGN and MRC1 would display similar role than Siglec-1 in stabilizing the transfer, notably through interaction with their ligand on another individual TNT. For example, it has been shown that a decrease in cholesterol levels in HIV-1 non-progressors resulted in the absence of HIV-1 trans-infection between target cells. This was directly linked to the number of DC-SIGN⁺ macrophages, which were low in non-progressors [776]. Considering that cholesterol was shown to stabilize TNT [773], [777], it is likely that DC-SIGN interacts with cholesterol-enriched membrane region, and thereby participate in TNT stabilization. Combining cholesterol deprivation and DC-SIGN depletion could be a way to evaluate their combined role in TNT biology and function. At a larger scale, several studies have reported the competitive interaction of DC-SIGN with HIV-1 or other molecules, including the C-type lectin surfactant protein D [608], lactoferrin present in colorectal mucus [778], or Lewis antigens glycans [779] which all prevented HIV-1 uptake and transfer. Hence, enrichment or administration of such molecules in cell culture or in patient could prevent DC-SIGN-mediated HIV-1 spread.

Beside from their role in molecules and organelles transport, few things are known about TNT physiology. In the infection context, the mechanisms of TNT formation are unknown other than the implication by the viral protein Nef [669] and the IL-10/STAT3 axis ([550], Chapter IV). VCC represent an intracellular compartment where the virus can assemble and bud safely from the immune system detection [528]. Hammonds and colleagues have reported that upon capture by Siglec-1, HIV-1 particles are internalized into pre-existing VCC [536]. First, it would be interesting to assess if in the co-infection context, the size and volume of VCC are increased in cmMTB-macrophages, and if this is dependent on Siglec-1 expression. This could be performed by immunofluorescence experiments and/or video-microscopy, in the presence or absence of Siglec-1 (siRNA depletion or use of blocking antibodies to prevent VCC formation upon HIV-1 capture). Second, it was previously showed that Siglec-1-bound HIV-1 particles stored in VCC in DC were then transferred efficiently to CD4⁺ T cells in a cell-to-cell contact dependent manner [633]. Considering that cmMTB induces the expression of TNT, it would be interesting to evaluate if the formation of VCC or if pre-existing VCC could lead to the

formation of TNT, providing HIV-1-infected cells with a rapid and efficient mechanism to transport HIV-1 from one cell to another.

Finally, a key issue to address is the existence and importance of Siglec-1⁺ TNT *in vivo*. The existence and characterization of such structures *in vivo* is quite complicated since no specific marker of TNT has been described yet. Moreover, the definition of TNT *in vitro* ((i) connect at least two cells, (ii) contain F-actin and (iii) do not touch the substrate), cannot be fully applied to *in vivo* systems; the criteria of not touching the substrate is not applicable in 3D organisms or cultures. Few studies though report the existence of TNT-like structure *in vivo*, notably during the embryo development or in the eye. Indeed, Chinnery and colleagues evidenced the formation of long and thin protrusions connecting MHC-II⁺ DC in the cornea of mice [780]. Other developmental studies also reported TNT-like structures during the embryogenesis of mice [781], chicken [782], zebrafish [783] and sea urchin [784]. In the context of cancer, notably in the brain, microtubes have been observed between cancerous cells by intravital microscopy [785]. In humans, TNT have been mainly studied *ex vivo* in tumor explant, stained with hematoxylin and eosin [786], but such structures were also observed in ovarian cancer explants by phase contrast imaging [787]. Taken together, these studies suggest that TNT are not cell culture artefact and do exist *in vivo*. However, an applicable definition of these structures in 3D context and specific markers are required to precisely prove their existence. Moreover, most human studies focused on the cancer cell ability to form TNT, along with their function of mitochondria transfer, but none has shown the formation of TNT between macrophages. We observed the first evidence of TNT-like structure existence between macrophages *ex vivo*, in the lung of Mtb-SIV co-infected NHP, which we reported in ([550]; Chapter IV). However, the strict demonstration of the existence of TNT *in vivo* has yet to be made. Here, we propose that Siglec-1 could help to define and to demonstrate the existence of TNT *in vivo*. For example, we could use previously published models of mice infection with murine-leukemia virus (MLV) or use GFP-HIV-1 virus like particles (GFP-HIV-1-VLP) to study the formation and function of TNT *in vivo* in Siglec-1⁺ macrophages of the spleen or lymph node by intravital microscopy [629]. To establish the relevance of Siglec-1⁺ TNT *in vivo*, comparative experiments of GFP-MLV or GFP-HIV-1-VLP infection in WT or Siglec-1^{-/-} mice could be performed.

Chapter VI: Dysregulation of the Type-I Interferon signaling pathway by *Mycobacterium tuberculosis* leads to HIV-1 exacerbation in human macrophages

I will here discuss the unpublished data obtained for the second part of my PhD project, which will be submitted for publication early in 2020.

I. Introduction

As seen in the last chapter of the introduction, the co-infection between Mtb and HIV-1 is, to date, a global health issue due to pathogen synergy. Indeed, it is well known that HIV-1 infection enhances Mtb growth and increases the risk of developing active TB, however, the mechanisms by which the bacilli exacerbates HIV-1 replication need further investigation.

In the laboratory, we have been studying this issue, using an *in vitro* model that mimics a TB-associated environment. The model consists in differentiating primary human monocytes towards macrophages by incubating them with supernatant harvested from Mtb- or mock-infected macrophages (cmMTB and cmCTR, respectively). We previously showed that this TB-associated microenvironment orients macrophages towards an anti-inflammatory “M2-like” polarization distinguished by a CD16⁺CD163⁺MerTK⁺ phenotype and an increased Mtb permissiveness, both of which were dependent on the IL-10/STAT3 signaling pathway [764]. Moreover, we found that cmMTB-macrophages were highly susceptible to HIV-1 infection and replication. The exacerbation of HIV-1 replication in these cells depends on the induction of TNT, which favours the HIV-1 cell-to-cell transfer and feed the viral infection and dissemination (Chapter IV, [550]). We later identified the upregulated lectin receptor Siglec-1 as part of the IFN-I transcriptomic signature of cmMTB-macrophages, together with another 50 upregulated interferon inducible genes (ISG). We showed that this molecule is present on Mtb-induced TNT in which HIV-1 cargos are abundant and are crucial for the exacerbation of the viral replication in cmMTB-macrophages (Chapter V). We also found that Siglec-1 expression is mediated by the IFN-I present in the cmMTB media, and its expression on alveolar macrophages in Mtb-SIV co-infected macaques correlated with both the disease severity and the activation of STAT1, the first transcription factor involved in IFN-I signaling pathway.

Our previous results suggested that the activation of the IFN-I signaling pathway promotes HIV-1 replication in our model. However, IFN-I are historically well known for their antiviral functions [788], [789], including during HIV-1 infection of monocytes and macrophages [790], [791]. For the second axis of my PhD work, I focused on this pathway to understand why IFN-I pre-exposure of macrophages during cmMTB conditioning did not induce antiviral immunity against HIV-1. We hypothesized that

IFN-I production by Mtb infected macrophages could be deleterious to the control of the viral infection in bystander HIV-1-infected macrophages, as it is observed in TB pathogenesis [18], [27]. By analysing the cmMTB-macrophage response to exogenous IFN-I stimuli, we found here that cmMTB-treated cells are hypo-responsive to exogenous IFN-I, a phenomenon that prevents macrophage activation against HIV-1. We also identified the negative regulator of IFN-I signaling, USP18, as a key factor involved in cmMTB-treated macrophage hypo-responsiveness to IFN-I.

II. Results

The global gene landscape in cmMTB-treated macrophages displays an enrichment of the IFN-I response signature, matching that described in active TB patients

To assess the gene expression landscape of cmMTB-treated macrophages and to identify potential factors involved in the exacerbation of HIV-1 replication in these cells, a genome-wide transcriptomic analysis was performed. Compared to cmCTR-conditioned cells, cmMTB-treated macrophages displayed a distinct gene transcript signature, comprising 51 genes upregulated, most of which belonged to the ISG family (Chapter V, Figure 1, S1). We compared this gene signature to those obtained from transcriptome analyses performed in whole blood and monocytes from active TB patients [221], using the gene set enrichment analysis (GSEA) algorithm. All genes analyzed in cmMTB-treated cells were used as a signature to compare transcriptomic data from healthy *versus* active TB patients. As shown in figure 35A, the group of genes upregulated in cmMTB-treated macrophages were significantly enriched in monocytes of TB patients (left, FDR q-value: $< 10^{-3}$) or in their whole blood (right, FDR q-value: $< 10^{-3}$), indicating that the gene signature obtained in cmMTB-treated cells is similar to that found in active TB patient leukocytes. These results confirmed that cmMTB is a relevant model to mimic TB-associated microenvironment and active TB patient monocytes activation profile *in vitro*. We confirmed the upregulation of several ISG in cmMTB-treated cells compared to cmCTR-treated macrophages, including three antiviral genes: MX1, which blocks viruses integration to the host genome; MX2, known to block HIV-1 entry in the host nucleus; and ISG15 that induces ISGylation of viral proteins, rendering them non-functional. We also included Siglec-1 as internal control (Table 4, Figure 35B). All genes analyzed were significantly upregulated in cmMTB-treated cells by a 3-10-fold. In addition, we analyzed the corresponding protein levels, and found increased levels of MX1, MX2 (Figure 35C), Siglec-1 (Figure 1C, D, chapter V) and STAT1, confirming the activation of IFN-I signaling (Chapter V, figure 1C, D) in cmMTB-differentiated cells.

It has been described previously that the time of exposure and quantity of IFN-I strongly impacts the response of cells to this stimulus [406], [457]. Moreover, as cmMTB contains both IL-10, responsible for the CD16⁺CD163⁺MerTK⁺ phenotype [261], and IFN-I, responsible for Siglec-1 induction among other ISG (Chapter V, Figure 2), we asked whether cmMTB-treated macrophage gene signature and phenotype is dependent on the time of exposure to cmMTB. To address that question, primary

human monocytes were either incubated with RPMI-10% FCS for two days, followed by 12h of cmMTB conditioning, or differentiated in cmMTB for 72h (Figure 36A). Interestingly, all ISG transcripts analyzed were highly expressed after 12h of conditioning with cmMTB compared to cmCTR (Figure 36B). Moreover, we observed a significant induction of MX2 and a tendency of higher induction of the antiviral ISG MX1 and ISG15 at 12h of conditioning compared to 72h in cmMTB condition, suggesting that the antiviral state established in cmMTB-macrophages is stronger when IFN-I exposure is shorter. The reduction in antiviral ISG transcript levels suggests that after 3 days of cmMTB conditioning, macrophages are no longer protected against viral infection. By contrast, Siglec-1 transcript abundance was maintained after 72h of treatment (Figure 36B), supporting its deleterious role in TB-HIV-1 co-infection (Chapter V, Figure 4). As 72h of cmMTB conditioning activate macrophages towards a M(IL-10) profile, characterized by the upregulation of CD16, CD163, MerTK [550], [764] and Siglec-1 (Chapter V, Figure 1C, D), we next assessed the phenotype of cmMTB-treated cells after 12h or 72h of conditioning by flow cytometry. As expected, with the exception of CD163, M(IL-10) markers were significantly upregulated in cmMTB after 12h and 72h of treatment, but the expression level of each marker was higher at 72h than at 12h, indicating that a relatively long exposure to TB-microenvironment is necessary to obtain the M(IL-10)-like phenotype (Figure 36C).

Collectively, these data indicate that the IFN-I signature displayed by cmMTB-treated cells, which reproduces that found in leukocytes from active TB patients, and coincides with the M(IL-10) phenotype, is specific to long-term exposure to the TB-associated microenvironment.

Precocious activation of the IFN-I/STAT-1 signaling in cmMTB-cells is deleterious for the control of HIV-1 replication

Despite a historical protective and antiviral function, recent studies point at the deleterious effect of IFN-I in chronic diseases [457], [792]. Indeed, in a viral chronic infection, IFN-I are pro-viral since they favour the systemic inflammation, which enhances viral replication [18], [406]. Therefore, it is currently thought that IFN-I effects are dependent on the dose and timing at which they are induced, a theory that applies to the results found in figure 36. As TB is also a chronic disease, and considering the exacerbation of HIV-1 replication in the TB co-infection context [775], we next asked if IFN-I signaling could also have a detrimental role in HIV-1 disease. We inhibited the IFN-I signaling pathway during cmMTB conditioning by depleting the transcription factor STAT1 by siRNA-mediated gene silencing (Figure 37A). This was confirmed by western blot analysis showing that STAT1 protein was efficiently depleted at the time of HIV-1 infection (Figure 37B). Noticeably, we found that depletion of STAT1 during cmMTB-conditioning dampened the exacerbation of HIV-1 infection, as indicated by the decrease in the viral production measured by the level of the viral protein p24 released in the cell supernatant (Figure 37C).

Together, these data indicate that the constant activation of the IFN-I signaling during cmMTB treatment is deleterious for the control of HIV-1 replication in macrophages.

IFN-I present in cmMTB conditioning media renders macrophages hypo-responsive to stimulation to exogenous IFN β

As mentioned in the introduction chapter I II.C. and II. II.C.b.ii., prolonged IFN-I exposure and signaling is associated with negative outcome in chronic diseases, notably by inducing immune cell exhaustion and apoptosis [793]. As cmMTB-treated macrophages are unable to control their viral load due to IFN-I signaling occurring during their conditioning, we hypothesized that cmMTB-treated cells are hypo-responsive to further IFN-I stimulation, which is produced in response to HIV-1 infection [794], after 3 days of conditioned-media treatment. To mimic the production of IFN-I in response to viral infection, we used recombinant IFN-I. Specifically, we stimulated cells with IFN β since it displays a higher affinity to IFNAR than the majority of IFN α subtypes and potently inhibits HIV-1 replication in peripheral mononuclear cells *in vitro* [393], [795]. First, we evaluated the capacity of exogenous IFN β to activate STAT1 and STAT2, the main transcription factors involved in IFN-I signaling pathway (Figure 2 in preamble). After 3 days of cmCTR or cmMTB differentiation, macrophages were stimulated with 100 U/ml of recombinant IFN β (Figure 38A). Upon IFN-I stimulation, we found that STAT1 activation was significantly reduced in cmMTB-treated macrophages compared to control cells (Figure 38B), indicating that cmMTB pre-exposure decreases the macrophage capacity to elicit an IFN-I-mediated response. This decreased activation was specific of STAT1 since no significant diminution of STAT2 was observed (Figure 38C). Second, we assessed the capacity of IFN β stimulation to induce the expression of the ISG signature defined in figure 35. Without IFN β stimulation, we obtained the same increase in the ISG expression in cmMTB-treated cells as described earlier (Figure 38D, bars on the left), thereby reproducing the results obtained in the transcriptome validation. Upon IFN β stimulation, ISG expression in cmCTR-treated macrophages were all induced by 3-80-fold (Figure 38D, white bars). In cmMTB-cells, ISG were upregulated as well after IFN β stimulation, but to a lesser extent than in cmCTR-cells (maximum fold change of 17, Figure 38D, black bars), suggesting a reduced sensitivity to IFN-I stimuli.

Finally, we confirmed that the reduced response to further IFN-I stimulation in cmMTB-macrophages was due to the pre-exposure to IFN-I. We differentiated monocytes for 3 days with cmCTR in the presence (or absence) of 20 or 100 U/ml of recombinant IFN β to mimic cmMTB media. Indeed, IFN β is the major subtype of IFN-I induced by Mtb infection in macrophages, thereby appropriate to mimic cmMTB [796]. After an extra-stimulation with 100 U/ml of IFN β , we measured STAT1 activation levels and found that it was down-modulated in cells treated with cmCTR media supplemented with IFN-I in a dose-dependent manner, as shown by the reduced level of pSTAT1 (Figure 38E). Moreover, MX1, MX2, and Siglec-1 gene expression were also downregulated in cells treated with cmCTR supplemented with IFN β (Figure 38F), further supporting the induction of hypo-responsiveness to IFN-I observed in cmMTB-cells.

Altogether, we showed here that IFN-I desensitization of macrophages is mediated by the IFN-I present in cmMTB media, which can be reproduced by supplementing cmCTR media with exogenous IFN β , and that the induced hypo-responsiveness to further stimuli is dependent on the dose of IFN-I present in the conditioning media.

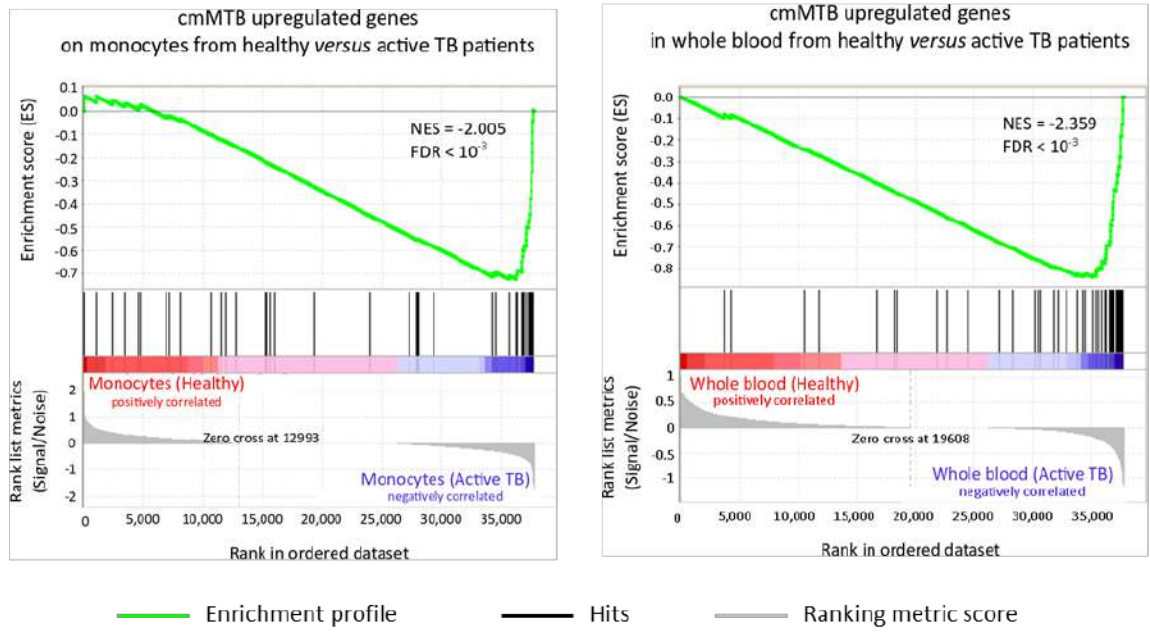
The IFN-I-inducible USP18 regulatory factor is a potential actor involved in the exacerbation of HIV-1 replication in cmMTB-macrophages.

To uncover how the IFN-I exposure during cmMTB treatment renders macrophages hypo-responsive to further IFN-I stimulation, we looked for a potential negative regulator of IFN-I signaling pathway induced by cmMTB. Indeed, as many other pathways, IFN-I needs to be tightly controlled to avoid excessive inflammation or auto-immune diseases such as interferonopathies [19]. Therefore, it is common that cells become desensitized to IFN-I for a short time, in order to recover from sustained IFN-I signaling [425], [797]. The desensitization state established by the cells occurs through several mechanisms, some of them being intrinsic and others being mediated by the action of ISG [425]. The IFN-I-induced negative regulator Ubiquitin specific peptidase 18 (USP18) was previously shown to be upregulated in the context of bacterial infection in mice [798], where it plays a deleterious role in the control of the bacteria. Here, we found that cmMTB-conditioning of macrophages induces the expression of USP18 at the mRNA level and was part of the ISG signature found in the transcriptome of cmMTB macrophages (Fold change: 4.3; adjusted p-value: 0.06) (Figure 39A and Chapter V, Figure 1A).

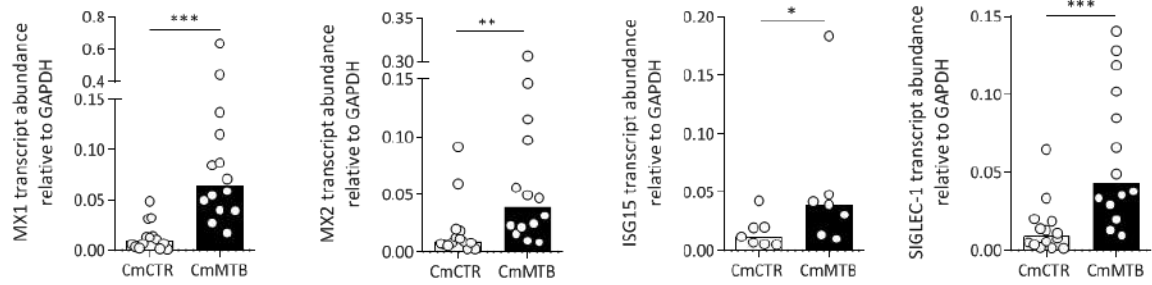
We then asked whether USP18 could have a deleterious role on HIV-1 replication control in the context of co-infection with Mtb. Indeed, it was previously shown that HIV-1 infection of monocyte-derived macrophages upregulates USP18, allowing HIV-1 replication. This phenomenon was due to the minimized IFN-I response of infected cells, which displayed low antiviral responses due to USP18 upregulation [799]. We reproduced on two independent donors the induction of USP18 after HIV-1 infection in cmCTR- and cmMTB-treated cells (Figure 39B). Interestingly, USP18 expression was enhanced in cells from both donors by cmMTB treatment, and even further by HIV-1 infection in these cells. Consequently, we suspected a role for USP18 in the control of HIV-1 replication. To address this question, we silenced USP18 gene expression by siRNA-mediated gene silencing during cmMTB-treatment, before infecting these cells with HIV-1_{ADA}, using the same protocol as described in Figure 37A. Ten days post-infection, we found that USP18 silencing reduced the number of HIV-1 infected MGC (Figure 39C, left), along with the exacerbation of HIV-1 replication in cmMTB macrophages (Figure 39C, right). However, we were not able to confirm USP18 depletion by western blot (data not shown). Consequently, these experiments need to be repeated to confirm that the restoration of the control of HIV-1 replication is mediated by USP18 depletion.

Considering the reduced viral replication in siUSP18 condition, it is likely that inhibition of USP18 would restore the macrophage capacity to elicit antiviral response to IFN-I stimuli.

A



B



C

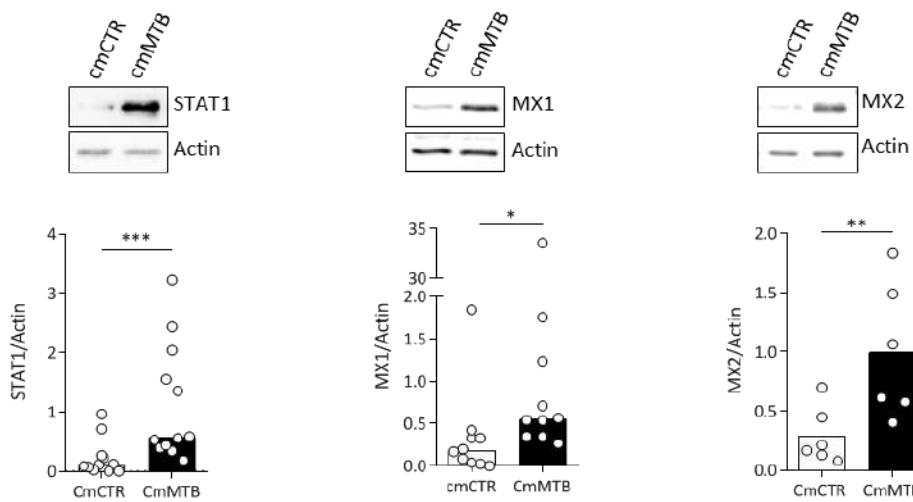


Figure 35: The cmMTB-treated macrophages are characterized by an IFN-I signature, which is also found in TB patient monocytes and whole blood.

(A-C) For three days, human monocytes were differentiated into macrophages with cmCTR (white) or cmMTB (black).

(A) *Left.* Gene set enrichment plot obtained with the GSEA software, using as a signature the genes found significantly (FDR<0.05) upregulated in cmMTB-treated cells as compared to control cells. The plot shows the distribution of the signature genes (barcode) in the comparison between monocytes from healthy (red) *versus* active TB (blue) patients. The skewing to the right indicates an (significant, FDR<0.001) enrichment of cmMTB-upregulated genes as a group, in the monocytes from active TB patients. *Right.* Gene set enrichment plot using the same signature applied to the comparison between the whole blood of healthy *versus* active TB patients.

(B) Validation of the four ISG expression induced in cmMTB-treated cells. Vertical scatter plot showing the relative transcript abundance to GAPDH mRNA. Each circle represents a single donor and histogram median value.

(C) *Top.* Representative images of western blot analysis illustrating the expression of STAT1 (*left*), MX1 (*middle*) and MX2 (*right*), with actin as a loading control. *Bottom.* Quantification of protein levels expressed as the ratio related to actin expression. Each circle represents a single donor and histogram mean value.

Statistical analyses: When data display a normal distribution according to Kolmogorov-Smirnov normality test, paired student t-test (C, *right*), otherwise two-tailed, Wilcoxon signed-rank test (B-C, *left, middle*). *P<0.05, **P<0.01, P***<0.001.

	Fold Change compared to cmCTR	Adjusted p-value	Comment
MX1	29.3	0.013	Restriction factor involved in the inhibition of viruses
MX2	9.42	0.027	HIV-1 resistance factor inhibiting HIV-1 DNA to enter the host nucleus
ISG15	9.18	0.028	Antiviral factor involved in the proteasomal degradation of viral proteins through ISGylation
SIGLEC-1	7.37	0.016	Internal control. Involved in HIV-1 capture and transfer; potential role in the negative regulation of IFN-I signaling

Table 4: Gene transcriptomic signature and expression in cmMTB-treated cells compared to control.

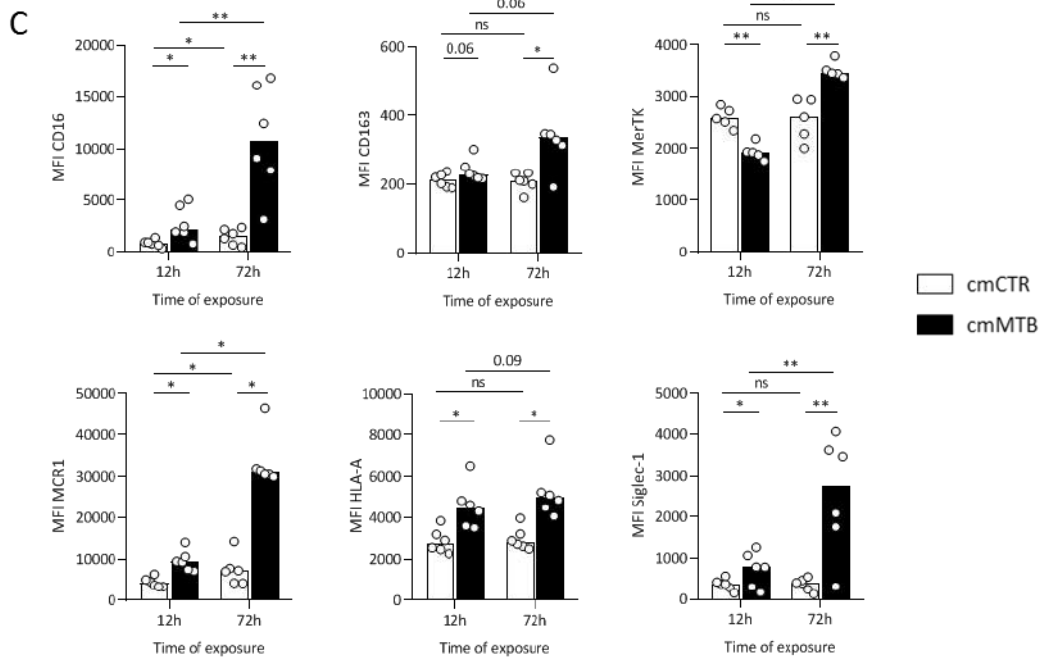
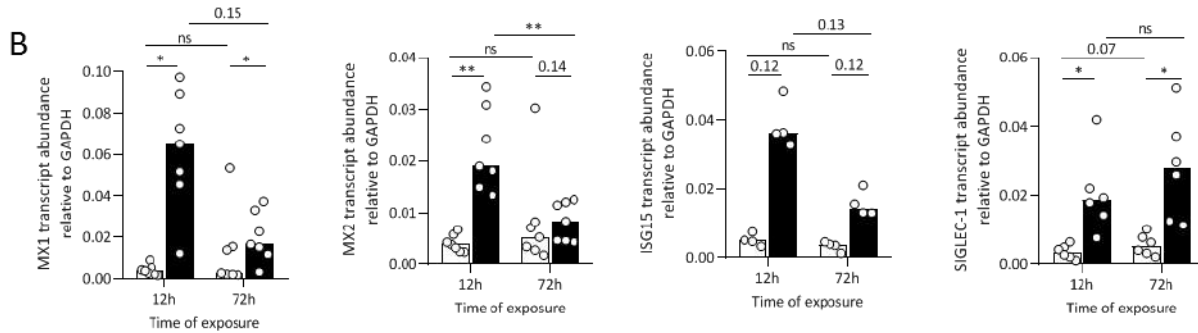
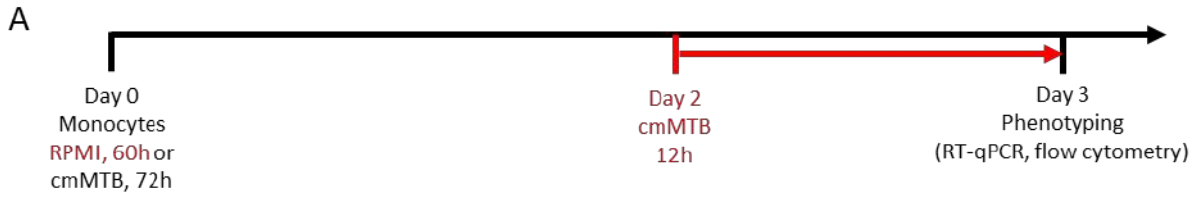


Figure 36: The interferon-stimulated gene signature obtained in the transcriptome and cell phenotype depend on the timing of cmMTB conditioning.

(A) Experimental design. Monocytes from healthy subjects were isolated and treated with cmMTB (black) or cmCTR (white) for either 72h or 12h prior phenotyping by RT-qPCR and flow cytometry.

(B) Gene expression of four ISG normally induced in cmMTB-treated cells. Vertical scatter plot showing the relative transcript abundance to GAPDH mRNA. Each circle represents a single donor and histogram median value.

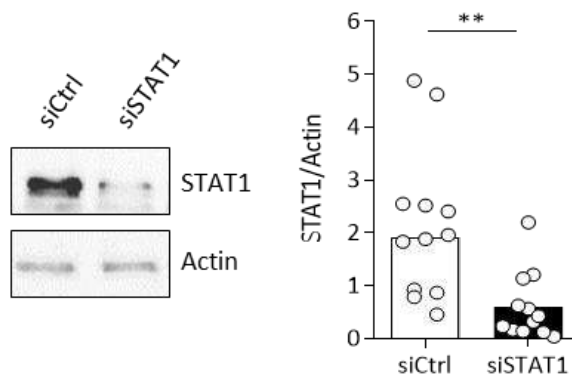
(C) Median fluorescent intensity (MFI) of cmMTB-treated cells markers. Each circle represents a single donor and histogram mean value.

Statistical analyses: When data display a normal distribution according to Kolmogorov-Smirnov normality test, paired student t-test (C, *top middle, bottom left and right*), otherwise two-tailed, Wilcoxon signed-rank test (B-C, *top left and right, bottom middle*). *P<0.05, **P<0.01, P***<0.001. ns: not significant (p-value > 0.2)

A



B



C

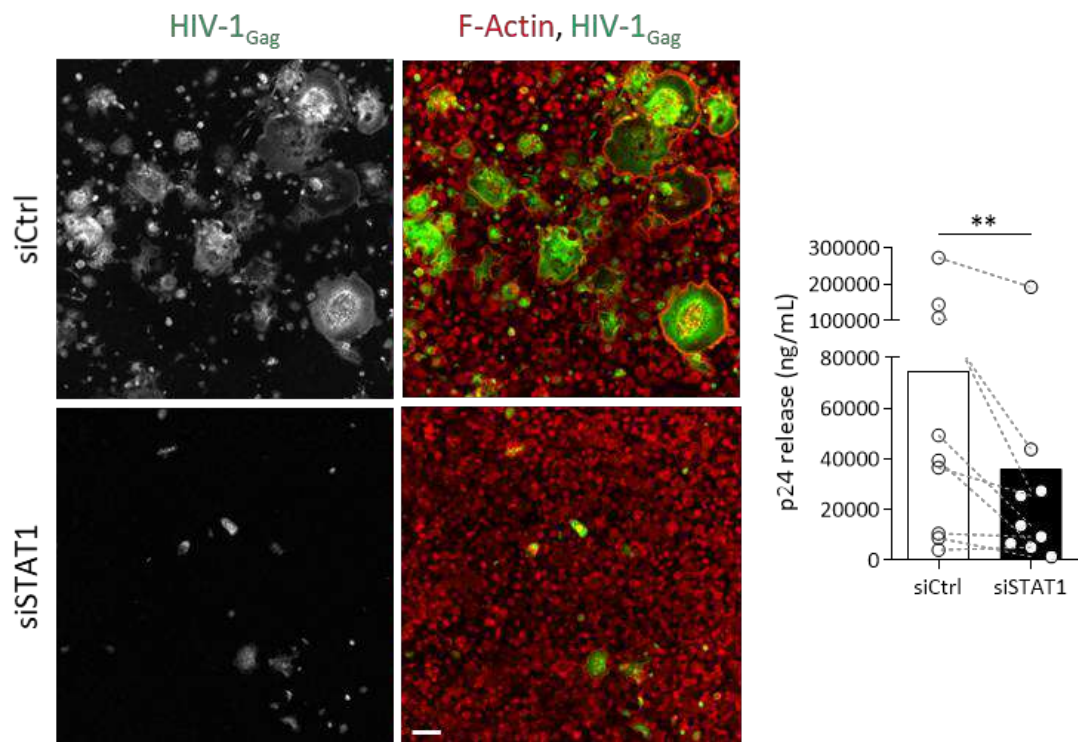


Figure 37: The interferon-stimulated gene signature of cmMTB cells is deleterious for the control of HIV-1 replication.

(A) Experimental design. Monocytes from healthy subjects were transfected with siRNA targeting STAT1 (siSTAT1, black) or off target mRNA (siCtrl, white). One day later, monocytes were differentiated into macrophages with cmMTB for 3 days. Cells were then infected with HIV-1_{ADA} and viral replication was measured by ELISA at day 15.

(B) *Left*. Representative images of western blot analysis illustrating the expression of STAT1 with actin as a loading control. *Right*. Quantification of protein levels expressed as the ratio related to actin expression. Each circle represents a single donor and histogram median value.

(C) *Left*. Representative immunofluorescence images of cmMTB-treated macrophages transfected siCtrl (top) or siSTAT1 (bottom) and infected with HIV-1_{ADA} at day 4. Staining show HIV-1_{Gag} (green) and F-actin (red). Scale bar: 200 μ m. *Right*. Vertical scatter plot showing HIV-1-p24 concentration in cell supernatant at day 15 post-HIV-1 infection in STAT1-depleted cells. Each circle represents a single donor and histogram median value.

Statistical analyses: When data display a normal distribution according to Kolmogorov-Smirnov normality test, paired student t-test (B, C). *P<0.05, **P<0.01, P***<0.001. ns: not significant (p-value > 0.2)

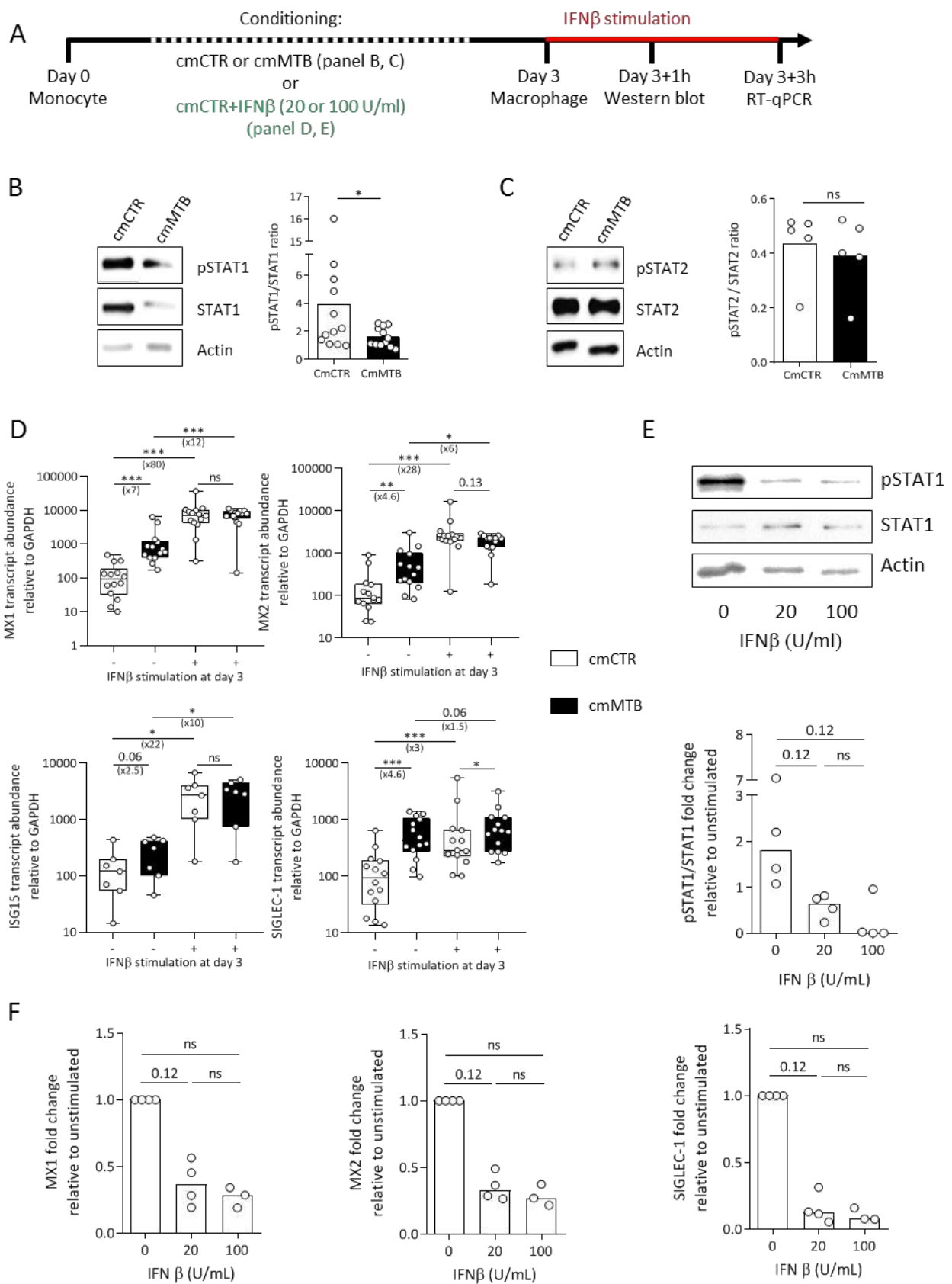


Figure 38: IFN-I exposure upon cmMTB treatment renders cells hypo-responsive to additional stimulation with IFN β .

(A) Experimental design. Monocytes from healthy subjects were treated with cmMTB (black) or cmCTR (white, black line) (panel B, C) or with conditioned media supplemented with recombinant IFN β (panel D, E). After 3 days, cells were stimulated with IFN β and their response was evaluated by Western blot (1h) and RT-qPCR (3h) after stimulation.

(B) *Left*. Representative images of western blot analysis illustrating the expression of pSTAT1 and STAT1 with actin as loading control. *Right*. Quantification of the ratio of pSTAT1/STAT1 after IFN β stimulation.

(C) *Left*. Representative images of western blot analysis illustrating the expression of pSTAT2 and STAT2 with actin as loading control. *Right*. Quantification of the ratio of pSTAT2/STAT2 after IFN β stimulation.

(D) Vertical scatter plot showing the transcript abundance of cmCTR or cmMTB cells with (+) or without (-) IFN β stimulation at day 3. The number in brackets represents the fold change of gene expression between conditions.

(E) *Top*. Representative images of western blot analysis illustrating the expression of pSTAT1 and STAT1 with actin as a loading control in cells conditioned with cmCTR supplemented (or not) with recombinant IFN β . *Bottom*. The quantification of protein levels is expressed as the ratio of pSTAT1 over STAT1 after normalization to actin.

(F) Vertical scatter plot showing the expression of MX1 (*left*), MX2 (*center*) and Siglec-1 (*right*) protein levels in cells treated with cmCTR supplemented (or not) with IFN β .

(B-E) Each circle represents a single donor and histogram median value.

Statistical analyses: When data display a normal distribution according to Kolmogorov-Smirnov normality test, paired student t-test (B, *right*), otherwise two-tailed, Wilcoxon signed-rank test (B, *left*, C). *P<0.05, **P<0.01, P***<0.001. ns: not significant (p-value > 0.2)

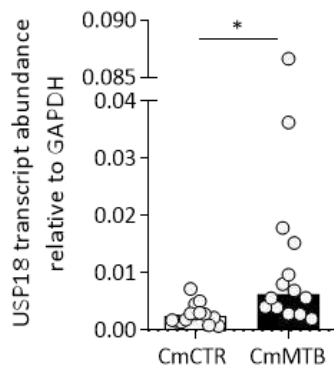
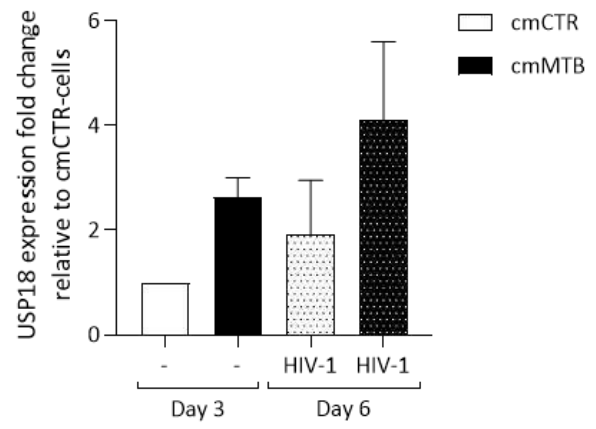
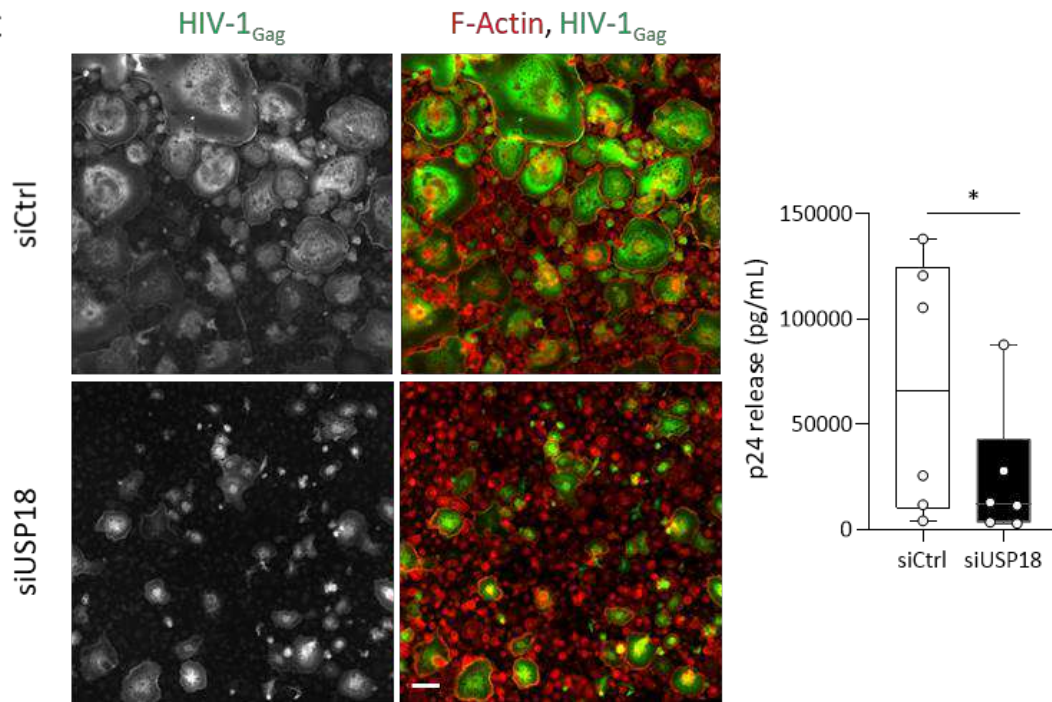
A**B****C**

Figure 39: The IFN-I inducible USP18 regulatory factor seems responsible for the exacerbation of HIV-1 replication in cmMTB cells.

(A) Vertical scatter plot showing USP18 gene expression in human macrophages after 3 days of cmCTR (white) or cmMTB (black) conditioning.

(B) Monocytes were differentiated for 3 days with cmCTR (white) or cmMTB (black) and infected with HIV-1_{ADA}. USP18 gene expression was assessed prior HIV-1 infection (day 3) and 3 days post-infection (day 6). Vertical scatter plot showing the fold change of USP18 expression compared to uninfected cmCTR condition. n=2 independent donors.

(C) Monocytes from healthy subjects were transfected with siRNA targeting USP18 (siUSP18, black) or off target mRNA (siCtrl, white). One day later, monocytes were differentiated into macrophages with cmMTB for 3 days. Cells were then infected with HIV-1_{ADA} and viral replication was measured by ELISA at day 14. Representative immunofluorescence images showing HIV-1 infected macrophages transfected with siCtrl (top) or siUSP18 (bottom) after 14 days in culture. Staining show HIV-1_{Gag} (green) and F-actin (red). Scale bar 200 μ m. *Right*. Vertical scatter plot showing HIV-1-p24 concentration in cell supernatant at day 10 post-HIV-1 infection in USP18-depleted cells. Each circle represents a single donor and histogram median value.

Statistical analyses: Wilcoxon signed-rank test (C). *P<0.05.

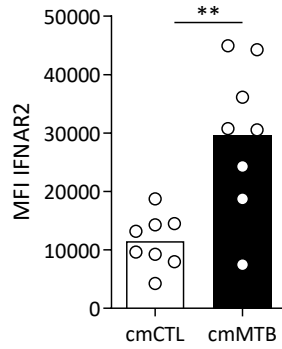


Figure 40: cmMTB-treatment induces the expression of the IFN-I receptor IFNAR.

Monocytes from healthy donors were isolated and differentiated for 3 days with cmCTR or cmMTB prior to phenotyping by flow cytometry. Vertical scatter plot showing the median fluorescent intensity (MFI) of IFNAR2 surface expression. Each circle represents a single donor and histograms median value.

Statistical analysis: passed Kolmogorov-Smirnov normality test, paired student t-test. * $P < 0.05$, ** $P < 0.01$.

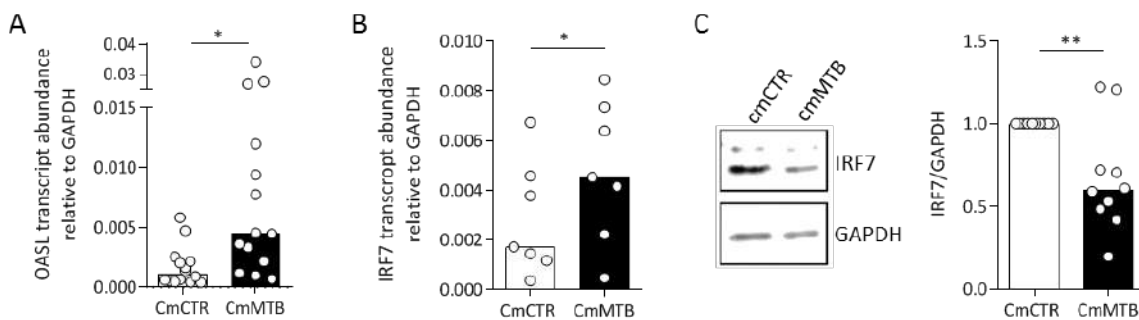


Figure 41: cmMTB upregulates OASL and IRF7 gene expression, but not IRF7 protein level.

Monocytes from healthy donors were isolated and differentiated for 3 days with cmCTR or cmMTB prior to gene expression assessment by RT-qPCR and protein level evaluation by western blot.

(A) Vertical scatter plot showing OASL gene transcript abundance relative to GAPDH in cmCTR- (white) or cmMTB-treated cells (black). Each circle represents a single donor and histograms median value.

(B) Vertical scatter plot showing IRF7 gene transcript abundance relative to GAPDH in cmCTR- (white) or cmMTB-treated cells (black). Each circle represents a single donor and histograms median value.

(C) *Left*. Representative images of western blot analysis illustrating the expression of IRF7 with GAPDH as a loading control. *Right*. Quantification of IRF7 protein level are represented as IRF7/GAPDH ratio. Each circle represents a single donor and histograms median value.

Statistical analysis: When data display a normal distribution according to Kolmogorov-Smirnov normality test, paired student t-test (A), otherwise, Wilcoxon matched-pairs signed rank test (B, *right*). * $P < 0.05$, ** $P < 0.01$.

III. Discussion

In this part of my PhD project, I investigated the implication of IFN-I in the exacerbation of HIV-1 replication in macrophages in the context of co-infection with Mtb. I found that cmMTB-conditioning renders macrophages hypo-responsive to further stimulation with IFN β , and that inhibiting the IFN-I signaling by blocking the transcription factor STAT1 restored the control of the viral replication in macrophages. To confirm these results, experiments are currently being performed using IFNAR blocking antibodies during cmMTB conditioning to prevent the precocious activation IFN-I signaling prior to HIV-1 infection. Moreover, the genes signature and cell phenotype rendering cells hypo-responsive to IFN-I and highly susceptible to HIV-1 infection was dependent on the time of exposure to cmMTB. Indeed, 72h of cmMTB conditioning were necessary to induce the expression of M(IL-10) markers. Concerning the gene signature, cells treated with cmMTB for 12h displayed strong induction of antiviral ISG compared to cells treated for 72h. However, this experiment needs to be reproduced to confirm our observation, since we found a strong tendency of MX2 and ISG15 induction by cmMTB treatment (albeit not significant) compared to cmCTR-macrophages at 72h. One reason that could explain this is the low quantity of mRNA available for the RT-qPCR, which renders gene induction analysis delicate. Moreover, despite the use of pool of cmMTB media to attenuate donor response variability during media preparation, the answer of healthy donor to cmMTB conditioning remains also highly variable and might explain why we could not observe a significant induction of MX2 and ISG15 in cmMTB-cells.

Most cells are able to respond to IFN-I stimulation. However, to avoid strong inflammation and associated tissue damage, IFN-I responding cells can enter a desensitized state that can last for several days [797]. This state allows cells to recover from IFN-I signaling and is tightly regulated. Desensitization establishment in cells can be induced by intrinsic mechanisms or by action of negative regulator of the IFN signaling pathway [425]. For example, receptor endocytosis and turnover have an important role in rapidly inhibiting the activation of JAK and STAT proteins, which consequently reduces ISG expression. To assess if cmMTB-macrophages displayed an endocytosis process of IFNAR during the conditioning, we evaluated at day 3 the cell surface expression of the receptor in cmCTR *versus* cmMTB-cells by flow cytometry. Interestingly, IFNAR2 expression was upregulated in cmMTB-macrophages (Figure 40), suggesting that the desensitization of cmMTB cells is not due to IFN-I receptor recycling process.

To demonstrate that cmMTB-treated macrophages are hypo-responsive to IFN-I stimulation, we assessed the induction of ISG after 3 days of conditioning, in response to exogenous IFN β . We found a strong upregulation of ISG in control cells compared to cmMTB-treated macrophages, yet, there was no significant difference in the overall ISG expression between cmCTR- and cmMTB-macrophages stimulated with IFN β . In the present case, it is possible that the difference in gene induction fold change obtained after IFN β stimulation is due to the saturation of the system, mRNA levels having reached a plateau of maximum expression in cmMTB-stimulated cells. Nevertheless, we also found a decreased activation of STAT1 in response to IFN β stimulation, and were able to induce cell hypo-responsiveness upon conditioning with cmCTR media supplemented with IFN-I, which provide further

evidence of cmMTB-induced desensitization to IFN-I. Considering that HIV-1 infection of macrophages induces IFN-I synthesis [794], we hypothesize that this new wave of IFN-I upon HIV-1 infection of cmMTB-macrophages will not induce the antiviral function related to IFN-I signaling, due to Mtb-mediated desensitization to IFN-I. This may be a mechanism explaining why cmMTB-macrophages are unable to contain HIV-1 replication (Chapter IV and V).

A potential mechanism explaining the IFN-I desensitization and loss of antiviral function observed in cmMTB-macrophages is the induction of USP18, which is the most important factor in the establishment and maintenance of IFN-I long-term desensitization. It has been shown that USP18^{-/-} mice are hypersensitive to IFN-I, and consequently, more resistant to viral infections [800]. Moreover, studies performed in USP18-deficient murine cell culture revealed that STAT1 activation and subsequent ISG induction were prolonged in response to IFN β in comparison to WT cells, further supporting the role of this factor in the negative regulation of IFN-I signaling [801]. In a mouse model of infection with vesicular stomatitis virus, Honke and colleagues found that USP18 expression was upregulated in Siglec-1⁺ macrophages of the marginal zone in the kidney. These cells locally supported an enhanced viral replication [802], suggesting a deleterious role of USP18 in the control of the virus life cycle. Similarly, we found USP18 to be induced at the mRNA level, both by cmMTB treatment (Figure 39A) and after HIV-1 infection (Figure 39B). By inhibiting USP18, we partially restored the control of the viral replication in cmMTB-macrophages, indicating that the IFN-I antiviral effect was partially recovered. However, this experiment needs to be reproduced, in order to validate the gene depletion efficiency. In addition, to confirm that the inhibition of HIV-1 replication is mediated by the reconstruction of IFN-I signaling, we need to verify that in the absence of USP18, the activation of STAT1 along with the induction of ISG upon exogenous IFN β stimulation are equivalent to that found in cmCTR-cells. It is likely that the IFN-I response will not be fully restored by silencing USP18, for two reasons. First, siRNA-silencing efficiency is usually comprised between 50 to 95%. Therefore, the remaining mRNA can still be actively translated and produce sufficient levels of protein to exert the negative regulation feedback loop on IFN-I signaling. Second, USP18 needs STAT2 to efficiently downregulate IFN-I signaling [803]. Arimoto and colleagues showed that STAT2 recruits USP18 to IFNAR2 intracytoplasmic chain, where it favours the replacement of JAK1 from its IFNAR2-binding site by USP18, therefore preventing the initiation of IFN-I/STAT signaling pathway [803]. We found here that STAT2 activation is not affected by the long exposure to IFN-I during cmMTB conditioning, and as such, could be part of the desensitization process observed in cmMTB-macrophages (Figure 38C). To verify this hypothesis, a double inhibition of STAT2 and USP18 could be performed prior to cmMTB conditioning. If the hypothesis is correct, the double knock-down strategy should restore IFN-I signaling after cmMTB treatment and abolish HIV-1 replication in macrophages, although the IFN-I signaling observed will activate STAT2-independent signaling (see Figure 2 in preamble). Finally, USP18 is an isopeptidase, *i.e.* an enzyme responsible for the deubiquitination of ISGylated proteins, that could also down-modulate IFN-I signaling through its enzymatic activity. Another important molecule to study, when considering USP18, is Siglec-1. Indeed, since USP18 expression was induced in infected Siglec-1⁺ macrophages in mice spleen [802], it is legitimate to ask whether Siglec-1 expression could modulate IFN-I responses probably *via* USP18 expression. In fact, the group of Gumuluru recently showed that infection of a macrophages cell line (THP-1), or of primary MDM, with HIV-1 or pseudotyped HIV-1

particles with the MLV envelope was enhanced after cell exposure to IFN α . This observation was dependent on Siglec-1, and supported by the enhanced *in vivo* expression of Siglec-1 in pigtail macaque lymph nodes after infection with SHIV (a modified HIV-1 virus expressing SIV envelope). Interestingly, there was an important co-localization of the viral protein Gag and Siglec-1 in these organs, suggesting a productive infection of Siglec-1⁺ myeloid cells *in vivo*. This enhanced replication of HIV in Siglec-1⁺ cells was due to the fact that the lectin counteracted the protective antiviral function of IFN α by enhancing viral capture and transfer to CD4⁺ T cells [831]. In addition, a study conducted by Zheng and colleagues indicated that Siglec-1 might be responsible for inducing the downregulation of IFN-I signaling cascade upon viral infection (*i.e.* VSV, Sendai virus and HSV). The mechanism behind this observation seemed to involve Siglec1 association with DAP12, which consequently induced the recruitment and activation of the scaffolding function of SHP2. Upon activation, SHP2 recruited the E3 ubiquitin ligase TRIM27, leading to TBK1 degradation *via* ubiquitination. Altogether, these findings demonstrated that the upregulation of Siglec-1 induced by the viral infection led to a feedback loop, which inhibited IFN-I production and suppressed antiviral innate immune responses [832]. Therefore, it would be interesting to evaluate whether the IFN-I signaling of cmMTB-treated cells is restored upon Siglec-1 silencing, along with a reduced expression of USP18.

Other molecules known as ISG can also negatively regulate the IFN-I signaling pathway through actions downstream of STAT activation. An example of such factor is OASL, which we found to be strongly upregulated in the transcriptome of cmMTB-treated cells (Figure 41A). OASL is known to bind to IRF7 mRNA in mice, and inhibits its translation [804], thereby preventing activated IRF7 to translocate into the nucleus to activate IFN-I synthesis and subsequent antiviral responses (Figure 42). Depletion of OASL1 gene in mice was shown to induce stronger IFN-I responses and to diminish viral replication *in vivo* [804]. However, the human OASL does not seem to share this binding property. Actually, Zhu and colleagues found opposing results to that observed in mice and proposed that human OASL enhances RIG-I-mediated signaling, supporting strong antiviral responses [805]. Our preliminary data on the expression of IRF7 in cmMTB-macrophages are in contradiction with these findings. Indeed, despite the increased expression of IRF7 mRNA after 3 days of cmMTB-conditioning (Figure 41B), we found that the protein level was lower in these cells compared to cmCTR-cells (Figure 41C). This observation suggests that OASL, in the context of co-infection with Mtb, is negatively affecting the IFN-I-mediated antiviral responses. It would be interesting to inhibit OASL function, either by pharmacological inhibition or by siRNA-mediated silencing, to evaluate if the expression of IRF7 at the protein level is restored in cmMTB-macrophages. To confirm the negative regulation of IFN-I by OASL, silenced cells should be then evaluated for their capacity to translocate activated IRF7 into the nucleus, along with their ability to express antiviral ISG. Finally, if OASL is involved in cell hypo-responsiveness of cmMTB-macrophages, its inhibition should lead to an increased control of HIV-1 replication in the context of co-infection.

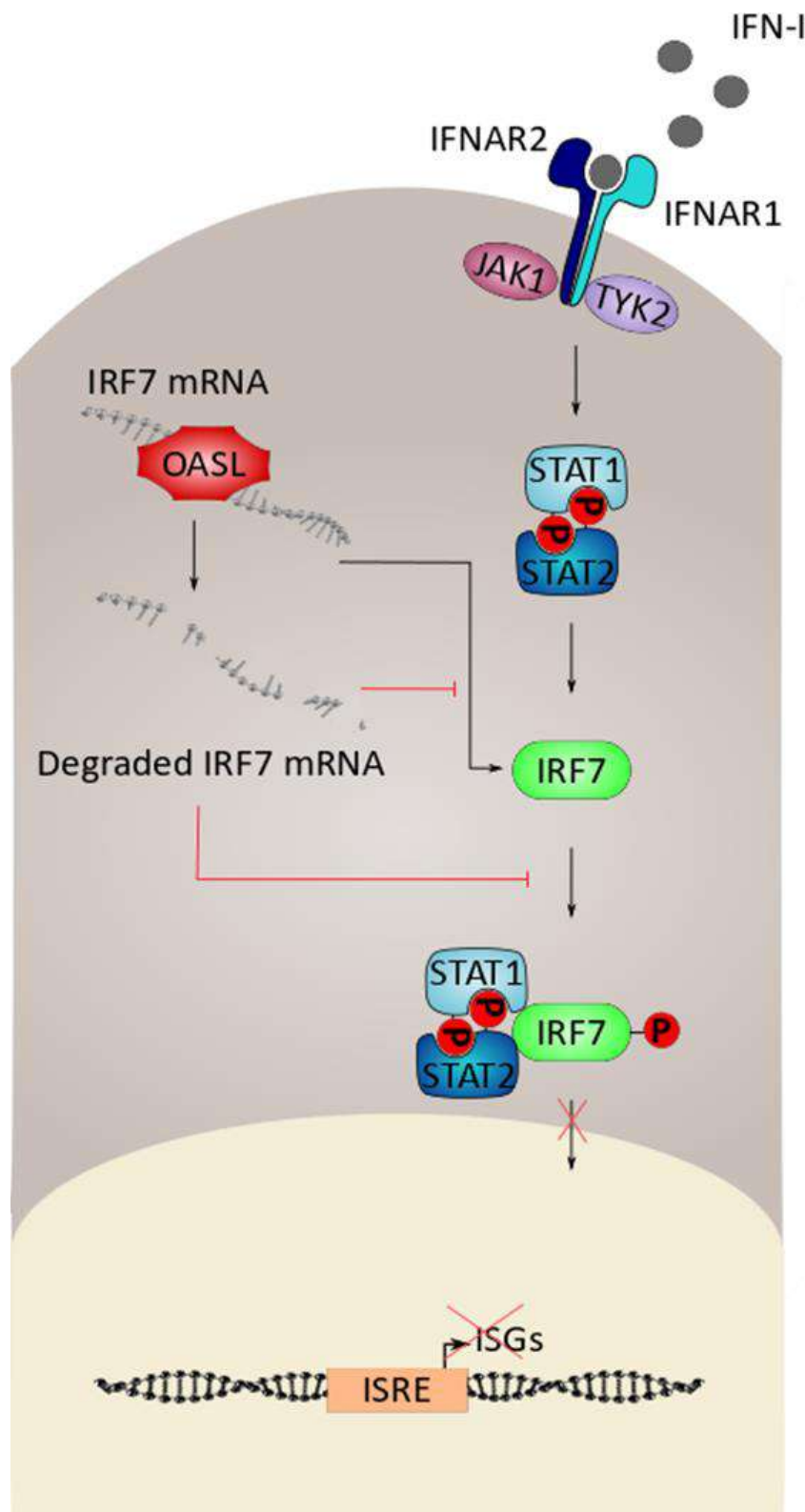


Figure 42: OASL inhibits type I interferon signaling by degrading IRF7 mRNA (inspired from [804]).

In mouse, OASL has been described to bind to IRF7 mRNA and to prevent its translation [801]. Consequently, less IRF7 proteins are available for recruitment to STAT1-STAT2 heterodimers. This prevents further translocation of STAT1-STAT2-IRF7 complexes to the nucleus, which leads to a decreased binding to interferon-stimulated response element (ISRE) promoter and result in a reduction of the activation of interferon-stimulated genes (ISG).

Here, we found that the IFN-I/STAT1 axis induces the expression of molecular factors involved in cmMTB-macrophages hypo-responsiveness to IFN β , preventing macrophages from establishing an efficient antiviral response. We also published that the IL-10/STAT3 axis induces the formation of TNT that participate to HIV-1 infection and dissemination in the co-infection context (Chapter IV). Since IL-10 is produced downstream of IFN-I signaling as an immuno-modulatory cytokine, we propose that both axis act in synergy to favour HIV-1 replication in cmMTB-treated macrophages. This synergy would occur both at the cellular and molecular levels. At the cellular scale, IL-10 induces TNT and IFN-I induces Siglec-1, both enhancing all crucial steps in the viral cycle success. To begin with, Siglec-1 favours the viral uptake, which is more important in cmMTB-treated cells because the area and number of Siglec-1 molecules is higher than in cmCTR-treated macrophages (Chapter V Figure 1B-D). Then, Mtb-induced TNT enhance the viral spread between macrophages, increasing the number of productively infected cells (Chapter IV Figure 6A and 7E). The IFN-I/IL-10 synergy could also occur at the molecular level, since both signaling pathways are interconnected [550]. First, STAT1 and STAT3 can heterodimerize. Increased amount of activated STAT3 can therefore sequester STAT1 molecules, preventing them from homodimerizing or heterodimerizing with STAT2, subsequently inhibiting the induction of ISG by ISGF3 [806]. Second, STAT3 can induce factors such as phospholipid scramblase 2 (PLSCR2) to suppress the recruitment of ISGF3 to the ISRE promoter sequence of ISG [807]. Third, STAT3 itself is able to suppress the expression of various component of the ISGF3 complex (*i.e.* STAT1, STAT2, IRF9), but also the expression of IRF7 [808], which could be degraded by STAT3- and OASL-dependent mechanisms. Finally, STAT3 inhibits IFN-I signal transduction by inducing negative regulators such as SOCS3, which prevents the activation of the janus kinases JAK1 and TYK2 by targeting them to proteasomal degradation through poly-ubiquitination [425], [809]. Importantly, SOCS3 has been described to prevent human macrophages IFN-I-antiviral responses following HIV-1 infection [421]. In addition, SOCS3 expression was reported to be induced in response to *Mycobacterium avium* infection [810]. We found that SOCS3, which is part of the transcriptomic signature (Fold change: 3.1; adjusted p-value: 0.07), is induced by cmMTB treatment in macrophages, both at the mRNA (Figure 43A) and protein level (Figure 43B). Moreover, we found that SOCS3 expression is further increased days after HIV-1 infection in cmMTB-macrophages (Figure 43B, left), and is equally induced in macrophages treated with cmMTB and stimulated with IFN γ prior to HIV-1 infection (Figure 43B, right). These preliminary data were performed in two independent donors and suggest that SOCS3 upregulation by a TB-associated microenvironment might have a role in the desensitization of macrophages to IFN-I. Moreover, we found that the expression of the restriction factor MX2 decreases during the course of HIV-1 infection (Figure 43C, left) in cmMTB-treated cells, as well as in cells pre-treated with IFN γ prior to infection (Figure 43C, right). Taken together, these observations suggest that the negative regulation of IFN-I signaling in cmMTB-macrophages is mediated by either SOCS3, OASL, USP18, or as a combination. These results must be reproduced in the near future. Also, we cannot exclude additional factors that could lead to macrophages hypo-responsiveness to IFN-I produced in response to HIV-1 infection. As a result, protective antiviral ISG expression like MX2 is inhibited, causing a defect in the restriction of HIV-1 replication.

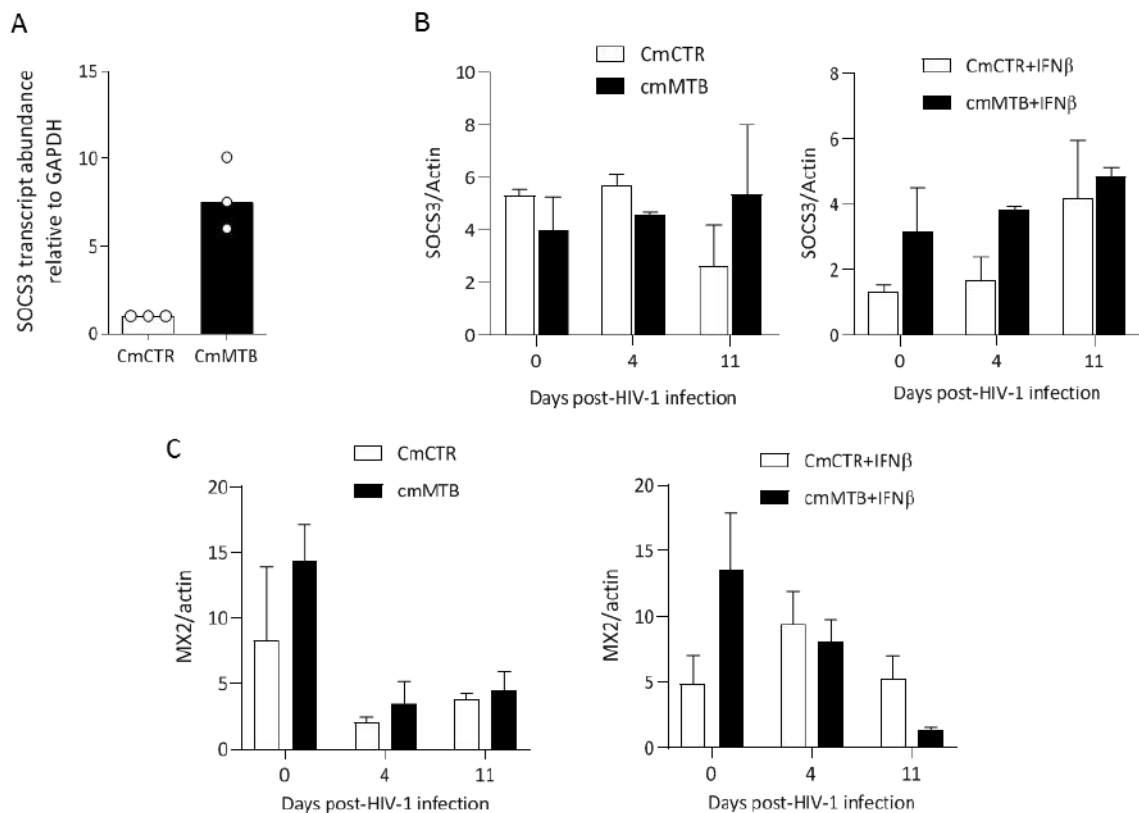


Figure 43: IFN-I negative regulators are enhanced by cmMTB during the course of HIV-1 infection, while restriction factors are downregulated.

Monocytes from healthy donors were isolated and differentiated for 3 days with cmCTR or cmMTB and stimulated (*Right. B, C*) or not (*A, Left, B, C*) with 100 U/ml of recombinant IFN β for 30 min prior to infection with HIV-1_{ADA}. Cell lysates were collected at day 0, 4 and 11 post-HIV-1 infection to assess the expression of ISG. (A) Vertical scatter plot showing SOCS3 gene transcript abundance relative to GAPDH in cmCTR- (white) or cmMTB-treated cells (black) after 3 days of conditioning, prior to HIV-1 infection. Each circle represents a single donor and histograms median value. (B) Vertical histograms showing SOCS3 expression after HIV-1 infection with (*right*) or without (*left*) IFN β stimulation. n= 2 independent donors. (C) Vertical histograms showing MX2 expression after HIV-1 infection in presence (*right*) or absence (*left*) of IFN β stimulation. n= 2 independent donors.

To conclude, a better understanding of the modulation of the IFN-I response triggered by Mtb infection is required to improve our comprehension on how these cytokines favour HIV-1 replication instead of the expected antiviral state. Also, this study promotes the need for *in vivo* investigation of the IFN-I/STAT1 axis as a potential contributor to pathogenesis in co-infected patients, suggesting the modulation of this signaling pathway as a suitable target for treatment and disease outcome.

Part 3: Discussion and perspectives

To date, the co-infection between HIV-1 and Mtb remains a major public health problem at the global scale, and more particularly in world regions like Africa, India, and China, where the burden of the epidemic associated to each pathogen is the strongest. Since the first report of co-infection event in Haiti in 1983, many efforts have been made to diagnose and treat co-infection, both of which are particularly challenging due to atypical presentation of TB symptoms and drug interactions. Despite the progresses made the last 10 years, TB-HIV-1 co-infection remains a challenging threat to human health, mainly because of the separated strategies applied to treat either TB or HIV-1 infection. The improvements necessary to fight co-infection will require a joint-effort on TB and HIV-1 eradication strategies, which will most likely rely on the better understanding of Mtb and HIV-1 synergy. It is well known that HIV-1 infected patients are more susceptible to develop active TB, mainly because of the depletion of Mtb-specific CD4⁺ T cells responses and the disruption of the granuloma structure that usually contain the bacteria in a latent, dormant replicative state (Introduction – Chapter 1). In addition, clinical evidence indicates increased viral loads in co-infected patients, both in the blood and at the anatomical site of co-infection, arguing for an Mtb-driven exacerbation of the viral replication. However, the mechanisms explaining this enhanced replication of HIV-1 remain to be investigated.

In the collaborative project between the team composing the LIA agreement, one of the main objective was to understand how Mtb-associated microenvironment exacerbates HIV-1 replication in its host. We focused our research on the role of macrophages in the co-infection, since they are the main target for Mtb and important cells in HIV-1 pathogenesis. Indeed, together with CD4⁺ T cells, macrophages are the principal cells capable of efficiently produce HIV-1 *in vivo* [768], are long-lived after infection since they are resistant to the cytopathogenic effect of the infection [485] and are part of the viral reservoir established in many tissues, including the brain and the lungs [480], [491], which are difficult to reach with cART.

My contribution to the field of co-infection during my PhD was to identify novel factors involved in the exacerbation of HIV-1 replication in macrophages, in a context of co-infection with Mtb. I used relevant *in vitro* models of TB-associated microenvironments (cmMTB or PE-TB) to mimic the bystander effect of Mtb-infection on surrounding cells. Indeed, direct co-infection of macrophages with Mtb and HIV-1 has never been described *in vivo* but does exist as recently shown by the co-staining of Mtb and SIV in alveolar macrophages in a NHP model of co-infection [811]. Yet, it is likely that this event is quite rare. Consequently, the major consequence of Mtb-infection must be indirect and involve the activation of bystander cells, depending on the cytokines present in their environment. In our model, we found that monocytes differentiated with cmMTB displayed an IFN-I signature, supposed to be antiviral. This correlates with the recent evidence that Mtb infection of macrophages induces IFN-I responses to set an antiviral state and distract the host from establishing an efficient antibacterial state [812]. Yet, in the context of TB, IFN-I are mainly detrimental to the control of the disease. Indeed, the dominant IFN-I-dependent ISG signature in active TB patients was found to positively correlate to the disease severity, and diminished after successful treatment [221]. In addition, the early overexpression of several IFN-I inducible genes in the blood of apparently healthy individuals in contact with TB patients correlated with the development of the active disease in these persons [222], [223]. Moreover, mice deficient for IFN-I signaling (e.g. IFNAR^{-/-}, WT mice injected with blocking IFN-I antibodies) have decreased bacterial loads and improved survival compared to WT counterparts [217]–[219]. In patients infected with HCV virus receiving IFN α therapy, TB reactivation

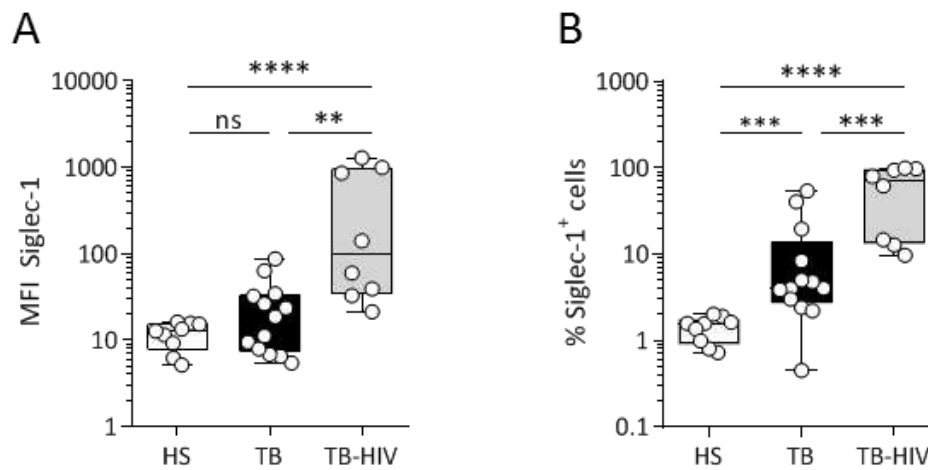


Figure 44: The number of Siglec-1⁺ blood monocytes is increased in TB and TB-HIV-1 patients.

Siglec-1 expression was assessed by flow cytometry on freshly isolated peripheral blood monocytes of healthy, TB or TB-HIV-1 patients.

(A) Vertical scatter plot showing the median fluorescent intensity (MFI) of Siglec-1. Each circle represents a single donor and histogram median value.

(B) Vertical scatter plot showing the percentage of blood monocytes expressing Siglec-1. Each circle represents a single donor and histogram median value.

Statistical analysis: When data display a normal distribution according to Kolmogorov-Smirnov normality test, paired student t-test (A), otherwise, Wilcoxon matcher-pairs signed rank test (B, right). *P<0.05, **P<0.01.

has been well reported [224], [225], and further supports the deleterious outcome of IFN-I in TB pathogenesis. Similarly, IFN-I have a deleterious impact on the host global immune response in the context of chronic viral infections, including HIV-1 pathology. In SIV natural host, the induction of IFN-I responses is quickly shut down, as opposed to non-natural host infection, where IFN-I responses are maintained and correlate with the immune system hyperactivation and CD4⁺ T cell loss [402], [403], a phenomenon also observed between HIV-1 non-progressors and HIV-1 progressors patients. Moreover, IFN α therapy used at the beginning of the epidemic was poorly efficient (few HIV-1 individuals responded to this treatment) and only transient [385]. Considering these facts, it is likely that IFN-I are highly detrimental to the host in the co-infection context. Therefore, developing strategies to reverse IFN-I negative effect on the host could improve the patient quality of life. One option to do so would be to treat patients with blocking antibodies against IFN-I or their receptor IFNAR, in combination with antibiotics and cART, in order to diminish the chronic immune activation in TB-HIV-1 co-infected patients. Changes in blood transcriptomic analysis, or a in a pre-established gene list part of the general signature by qPCR (to reduce costs for low-income countries) could be then used to monitor patient's reaction to treatment and to modulate it accordingly [813]. Another strategy to improve co-infected patient treatment is to optimize the balance between the immune system reaction to clear both pathogens and the immune-regulation dampening IFN-I responses. One possibility would be to increase eicosanoid levels in the blood circulation of patients in order to decrease IFN-I responses. In a mouse model of TB infection, Dorhoi and colleagues found that IL-1 conferred mice resistance to deleterious IFN-I during TB infection by inducing eicosanoids. Consequently, mice were able to better contain bacterial growth. The authors further showed that both in mouse and human, reduced IL-1 responses and excessive IFN-I induction were linked to an imbalance in eicosanoids, and led to TB disease exacerbation [242]. Among eicosanoids, PGE2 was previously shown to be a critical mediator of TB resistance, notably by preventing macrophage necrosis upon Mtb infection [27]. The use of host-directed immunotherapy clinically approved drugs improved the disease outcome in TB mice model of Mtb infection [242]. Interestingly, PGE2 was also part of the transcriptomic signature of cmMTB-macrophages (fold change: 1.4; adjusted p-value: 0.6). To assess the potential protective role of this molecule in the co-infection context, we will need to validate its upregulation at the protein level in our model. If, like IRF7, it is decreased, it would be interesting to add PGE2 in our culture system to see if we can prevent HIV-1 infection and spread. Depending on the result, the use of PGE2, maybe in combination with blocking IFN-I induction by IFNAR blocking antibody in co-infected patient could limit the replication of both Mtb and HIV-1 by inducing apoptosis of infected macrophages.

In addition to the direct deleterious effect of IFN-I responses in the co-infection context, these cytokines are responsible for the upregulation of detrimental factors for the control of HIV-1. Among those, we identified Siglec-1, a lectin receptor previously shown to be involved in HIV-1 uptake and transfer to CD4⁺ T cells [629], [633]. In HIV-1⁺ individuals, Siglec-1 expression is increased in circulating monocytes, a phenomenon reversed after successful cART [631]. In addition, its expression in SIV natural host remains low compared to non-natural host [814], indicating that Siglec-1 has a role in the disease progression, either as a marker of progression or as a factor enhancing viral spread. In our model, we found that cmMTB treatment increases the expression of Siglec-1 at the mRNA and protein levels in macrophages. Thanks to the LIA collaboration consortium with L. Balboa in Argentina, we could assess the expression of Siglec-1 in peripheral blood monocytes and pleural effusion cells from

TB or TB-HIV-1 co-infected patients. We found that the median fluorescent intensity of Siglec-1 was increased in co-infected patients only, compared to healthy subject or TB patients (Figure 44A). However, when comparing the percentage of cells positive for the lectin, we found it significantly increased in TB patient compared to healthy subjects, and even further increased in co-infected individuals (Figure 44B). These results are in accordance with our observations in NHP lungs, where we found an increased number of Siglec-1⁺ alveolar macrophages in Mtb-infected animals, further enhanced in co-infected NHP (Chapter V, figure 1E-H). However, in pleural effusion CD14⁺ cells, we failed to observe an increase in Siglec-1 expression, compared to pleural effusion cells from heart failure. It is possible that in the lungs and in peripheral blood monocytes from TB patients, Siglec-1 is shed, just like MerTK and CD163. Indeed, a soluble form of Siglec-1 has been reported previously in patients with systemic lupus erythematosus and used as a potential biomarker of the disease [815]. To evaluate the potential use of soluble Siglec-1 as a biomarker of TB-HIV-1 co-infection, ELISA measurement of Siglec-1 present in patient's plasma could be performed. In the case where Siglec-1 is indeed shed in TB or co-infection settings, Siglec-1 plasma levels, along with soluble MerTK and CD163 could represent a novel valuable diagnostic tool and marker to monitor co-infection progression. Nevertheless, additional fundamental research on this lectin is required, since its role in TB disease has never been reported, apart from one single study that associated one particular Siglec-1 polymorphism with a decreased production of IL-1 β in active TB patient, suggesting a role of the lectin in the inflammasome pathway [816]. Another polymorphism causing Siglec-1 loss of function (the GluTer88 truncation mutation) was reported in the context of HIV-1-infected individuals. *Ex vivo*, cells haplo-insufficient³⁴ or null for Siglec-1 function were unable to capture and transfer the virus to bystander CD4⁺ T cells. In patients, this null mutation only delayed HIV-1 acquisition or AIDS progression in infected patients, suggesting that classical route of infection and, potentially other molecules involved in HIV-1 capture and transfer to other cells (*e.g.* the C-type lectin receptors DC-SIGN or MRC1), may compensate for the lack of Siglec-1 in fuelling the viral dissemination [817]. In collaboration with us, the same group has assessed the effect of Siglec-1 GluTer88 polymorphism on HIV-1 co-infection into two large cohorts (> 6 200 individuals) and found a significant association between Siglec-1 loss-of-function and extrapulmonary dissemination of Mtb. They confirmed these findings in Siglec-1 knocked-out mice, who presented with larger and less structured pulmonary lesions upon Mtb infection compared to WT mice [818]. As Siglec-1's role at steady state is to regulate immune responses by modulating antigen presentation, it is possible that the null mutation in Siglec-1 gene leads to a delay in Mtb-induced immunity, by limiting antigen spread and T cell responses, thereby allowing an early dissemination of the virus. As a result, in the co-infection setting, it is more likely that Siglec-1 represents a promising diagnostic tool rather than a potential drug target, since its inhibition will probably reduce HIV-1 spread, but favour Mtb dissemination.

Last but not least, my PhD work allowed the identification of TNT as a major mechanism through which HIV-1 infection is exacerbated in the context of co-infection. Both cmMTB conditioning and HIV-1 infection of macrophages induced these structures, and inhibiting them decreased the viral replication and spread. Several studies report that cell-to-cell transfer is the most efficient mechanism of HIV-1 infection, especially compared to cell-free viruses [323], [592]–[594]. Cell-to-cell transfer also protects the virus from immune detection and neutralization by anti-HIV-1 antibodies [612] and even

³⁴ Haplo-insufficient: one allele is encoded by the WT gene while the other allele is mutated and non-functional.

from cART drugs [570]. Moreover, it has been reported that the antiviral properties of IFN-I have moderate effect on viral cell-to-cell transfer [819]. Vendrame and colleagues have reported that T cells pre-treated with IFN-I control the viral replication, but that the number of infected cells increased with time, despite the low production of virus by the infected cells, indicating that IFN-I are not as efficient as previously thought in inhibiting the global life cycle of HIV-1 [819]. However, other studies have shown that antiviral factors and more specifically IFN α -induced ISG can be transferred from one cell to another through exosome release and subsequent capture and endocytosis [820]. Hence, combining TNT capacity to transfer material and blocking HIV-1 trafficking represent a potential strategy to enhance antiviral factors from one cell to another, particularly in those desensitized to IFN-I. TNT function could also be used as tools for delivering drugs in specific cell target, notably HIV-1 reservoirs such as macrophages or CD4⁺ memory T cells, and help to eliminate them. Combined to cART, TNT-delivered drugs to viral reservoir might allow the elimination of HIV-1 from the organism. However, to reach such promising goals, further research on TNT biology is needed. First, it is necessary to validate TNT existence *in vivo*, particularly their formation and function between immune cells. Evidence obtained from mice model suggest the existence of functional TNT *in vivo*, notably in the eye during embryonic development [780] or in tumor brain cancers [785]. Second, once the formal demonstration of their formation done, TNT functions *in vivo* should be addressed but represent a quite challenging question on the technical level. For example, it will be difficult to distinguish materials transfer from inside TNT or outside of these structures, a key element in the design of potential use of TNT for drug delivery. Finally, instead of being used to spread chemical compounds, TNT could be blocked to reduce pathogen transfer from one cell to another in infectious context. To do so, drugs like TNTi [669] could be evaluated for their *in vivo* potency at inhibiting pathogen transfer, including HIV-1 or Mtb. Importantly, TNT specific markers, such as Siglec-1 and potentially others (*e.g.* DC-SIGN and MRC1), should be carefully studied, in order to optimize drug-designed strategies and specifically target pathways involved in auto-immune disease, cancers, or pathogen exacerbation and spread.

Altogether, the work realized during my PhD thesis contributes to a better understanding of the synergy between Mtb and HIV-1 and proposes Siglec-1, TNT and IFN-I-dependent signaling as potential diagnostic tools to follow the disease progression, along with possible new targets to prevent viral dissemination and replication in co-infected patients.

References

- [1] Global tuberculosis report., *Global Health TB Report*. 2018.
- [2] C. R. Diedrich and J. L. Flynn, "HIV-1/ Mycobacterium tuberculosis Coinfection Immunology: How Does HIV-1 Exacerbate Tuberculosis?," *Infect. Immun.*, vol. 79, no. 4, pp. 1407–1417, 2011.
- [3] V. Rodrigues, N. Ruffin, M. San-Roman, and P. Benaroch, "Myeloid cell interaction with HIV: A complex relationship," *Front. Immunol.*, vol. 8, no. NOV, pp. 1–16, 2017.
- [4] N. K. Saksena, B. Wang, L. Zhou, M. Soedjono, Y. S. Ho, and V. Conceicao, "HIV reservoirs in vivo and new strategies for possible eradication of HIV from the reservoir sites.," *HIV. AIDS. (Auckl)*., vol. 2, pp. 103–22, 2010.
- [5] S. Sprangers, T. J. D. Vries, and V. Everts, "Monocyte Heterogeneity: Consequences for Monocyte-Derived Immune Cells," *Journal of Immunology Research*, vol. 2016. Hindawi Limited, 2016.
- [6] P. J. Murray *et al.*, "Macrophage Activation and Polarization: Nomenclature and Experimental Guidelines," *Immunity*, vol. 41, no. 1. Cell Press, pp. 14–20, 17-Jul-2014.
- [7] S. J. Jenkins and D. A. Hume, "Homeostasis in the mononuclear phagocyte system," *Trends in Immunology*, vol. 35, no. 8. Elsevier Ltd, pp. 358–367, 2014.
- [8] G. M. Barton, "A calculated response: Control of inflammation by the innate immune system," *Journal of Clinical Investigation*, vol. 118, no. 2. pp. 413–420, 01-Feb-2008.
- [9] S. Gordon and P. R. Taylor, "Monocyte and macrophage heterogeneity," *Nature Reviews Immunology*, vol. 5, no. 12. pp. 953–964, Dec-2005.
- [10] K. L. Wong, W. H. Yeap, J. J. Y. Tai, S. M. Ong, T. M. Dang, and S. C. Wong, "The three human monocyte subsets: Implications for health and disease," *Immunol. Res.*, vol. 53, no. 1–3, pp. 41–57, Sep. 2012.
- [11] P. J. Ellery *et al.*, "The CD16 + Monocyte Subset Is More Permissive to Infection and Preferentially Harbors HIV-1 In Vivo ," *J. Immunol.*, vol. 178, no. 10, pp. 6581–6589, May 2007.
- [12] G. Fingerle, A. Pforte, B. Passlick, M. Blumenstein, M. Ströbel, and H. W. Ziegler-Heitbrock, "The novel subset of CD14+/CD16+ blood monocytes is expanded in sepsis patients.," *Blood*, vol. 82, no. 10, pp. 3170–6, Nov. 1993.
- [13] B. Passlick, D. Flieger, and H. W. Ziegler-Heitbrock, "Identification and characterization of a novel monocyte subpopulation in human peripheral blood.," *Blood*, vol. 74, no. 7, pp. 2527–34, Nov. 1989.
- [14] P. J. Murray and T. A. Wynn, "Protective and pathogenic functions of macrophage subsets," *Nature Reviews Immunology*, vol. 11, no. 11. pp. 723–737, Nov-2011.
- [15] F. Ginhoux and M. Guilliams, "Tissue-Resident Macrophage Ontogeny and Homeostasis," *Immunity*, vol. 44, no. 3. Cell Press, pp. 439–449, 15-Mar-2016.
- [16] C. D. Mills, K. Kincaid, J. M. Alt, M. J. Heilman, and A. M. Hill, "M-1/M-2 Macrophages and the Th1/Th2 Paradigm," *J. Immunol.*, vol. 164, no. 12, pp. 6166–6173, Jun. 2000.
- [17] M. C. Orme J1, "Macrophage subpopulations in systemic lupus erythematosus.," *Discov. Med.*, 2012.
- [18] F. McNab, K. Mayer-Barber, A. Sher, A. Wack, and A. O'Garra, "Type I interferons in infectious disease," *Nat. Rev. Immunol.*, vol. 15, no. 2, pp. 87–103, 2015.
- [19] J. Taft and D. Bogunovic, "The Goldilocks Zone of Type I IFNs: Lessons from Human Genetics.," *J. Immunol.*, vol. 201, no. 12, pp. 3479–3485, 2018.
- [20] H. Knüpfer and R. Preiß, "Significance of interleukin-6 (IL-6) in breast cancer (review)," *Breast Cancer*

Research and Treatment, vol. 102, no. 2. pp. 129–135, Apr-2007.

- [21] J. Lu *et al.*, “Discrete functions of M 2a and M 2c macrophage subsets determine their relative efficacy in treating chronic kidney disease,” *Kidney Int.*, vol. 84, no. 4, pp. 745–755, 2013.
- [22] D. Goubau, S. Deddouche, and C. Reis e Sousa, “Cytosolic Sensing of Viruses,” *Immunity*, vol. 38, no. 5. pp. 855–869, 23-May-2013.
- [23] L. O. Moreira and D. S. Zamboni, “NOD1 and NOD2 signaling in infection and inflammation,” *Frontiers in Immunology*, vol. 3, no. NOV. 2012.
- [24] M. Divangahi, I. L. King, and E. Pernet, “Alveolar macrophages and type I IFN in airway homeostasis and immunity,” *Trends Immunol.*, vol. 36, no. 5, pp. 307–314, 2015.
- [25] T. Tamura, H. Yanai, D. Savitsky, and T. Taniguchi, “The IRF Family Transcription Factors in Immunity and Oncogenesis,” *Annu. Rev. Immunol.*, vol. 26, no. 1, pp. 535–584, Apr. 2008.
- [26] K. Honda, A. Takaoka, and T. Taniguchi, “Type I Interferon Gene Induction by the Interferon Regulatory Factor Family of Transcription Factors,” *Immunity*, vol. 25, no. 3. Cell Press, pp. 349–360, 2006.
- [27] L. Moreira-Teixeira, K. Mayer-Barber, A. Sher, and A. O’Garra, “Type I interferons in tuberculosis: Foe and occasionally friend,” *J. Exp. Med.*, vol. 215, no. 5, pp. 1273–1285, 2018.
- [28] N. Yan and Z. J. Chen, “Intrinsic antiviral immunity,” *Nature Immunology*, vol. 13, no. 3. pp. 214–222, Mar-2012.
- [29] I. Hershkovitz *et al.*, “Tuberculosis origin: The Neolithic scenario,” *Tuberculosis*, vol. 95, no. S1, pp. S122–S126, Jun. 2015.
- [30] T. M. Daniel, “The history of tuberculosis,” *Respir. Med.*, vol. 100, no. 11, pp. 1862–1870, Nov. 2006.
- [31] M. R. Zimmerman, “Pulmonary and osseous tuberculosis in an Egyptian mummy,” *Bull. N. Y. Acad. Med.*, vol. 55, no. 6, pp. 604–8, Jun. 1979.
- [32] E. Cambau and M. Drancourt, “Steps towards the discovery of Mycobacterium tuberculosis by Robert Koch, 1882,” *Clinical Microbiology and Infection*, vol. 20, no. 3. Blackwell Publishing Ltd, pp. 196–201, 2014.
- [33] Z. A. Grange JM, Gandy M, Farmer P, “Historical declines in tuberculosis: nature, nurture and the biosocial model,” *Int. J. Tuberc. Lung Dis.*, 2001.
- [34] K. Stýblo, J. Meijer, and I. Sutherland, “[The transmission of tubercle bacilli: its trend in a human population].,” *Bull. World Health Organ.*, vol. 41, no. 1, pp. 137–78, 1969.
- [35] R. M. Pai M, Behr MA, Dowdy D, Dheda K, Divangahi M, Boehme CC, Ginsberg A, Swaminathan S, Spigelman M, Getahun H, Menzies D, “Tuberculosis,” *Nat. Rev. Dis. Prim.*, 2016.
- [36] D. B. Young, H. P. Gideon, and R. J. Wilkinson, “Eliminating latent tuberculosis,” *Trends Microbiol.*, vol. 17, no. 5, pp. 183–188, May 2009.
- [37] J. R. Andrews, F. Noubary, R. P. Walensky, R. Cerda, E. Losina, and C. R. Horsburgh, “Risk of progression to active tuberculosis following reinfection with Mycobacterium tuberculosis,” *Clin. Infect. Dis.*, vol. 54, no. 6, pp. 784–791, Mar. 2012.
- [38] J. Mazza-Stalder, L. Nicod, and J. P. Janssens, “La tuberculose extrapulmonaire,” *Revue des Maladies Respiratoires*, vol. 29, no. 4. Elsevier Masson SAS, pp. 566–578, 2012.
- [39] N. Mlika-Cabanne *et al.*, “Radiographic abnormalities in tuberculosis and risk of coexisting human immunodeficiency virus infection: Methods and preliminary results from Bujumbura, Burundi,” *Am. J. Respir. Crit. Care Med.*, vol. 152, no. 2, pp. 794–799, 1995.
- [40] A. M. Saks and R. Posner, “Tuberculosis in HIV positive patients in south africa: A comparative radiological study with HIV negative patients,” *Clin. Radiol.*, vol. 46, no. 6, pp. 387–390, 1992.

- [41] R. J. Wilkinson *et al.*, "Tuberculous meningitis," *Nature Reviews Neurology*, vol. 13, no. 10. Nature Publishing Group, pp. 581–598, 01-Oct-2017.
- [42] S. Gagneux, "Ecology and evolution of Mycobacterium tuberculosis," *Nature Reviews Microbiology*, vol. 16, no. 4. Nature Publishing Group, pp. 202–213, 01-Apr-2018.
- [43] M. Gengenbacher and S. H. E. Kaufmann, "Mycobacterium tuberculosis: Success through dormancy," *FEMS Microbiology Reviews*, vol. 36, no. 3. pp. 514–532, May-2012.
- [44] S. T. Cole *et al.*, "Deciphering the biology of mycobacterium tuberculosis from the complete genome sequence," *Nature*, vol. 393, no. 6685. pp. 537–544, 11-Jun-1998.
- [45] T. Dos Vultos *et al.*, "Evolution and diversity of clonal bacteria: The paradigm of Mycobacterium tuberculosis," *PLoS One*, vol. 3, no. 2, Feb. 2008.
- [46] J. L. Flint, J. C. Kowalski, P. K. Karnati, and K. M. Derbyshire, "The RD1 virulence locus of Mycobacterium tuberculosis regulates DNA transfer in Mycobacterium smegmatis," *Proc. Natl. Acad. Sci. U. S. A.*, vol. 101, no. 34, pp. 12598–12603, Aug. 2004.
- [47] O. Neyrolles and C. Guilhot, "Recent advances in deciphering the contribution of Mycobacterium tuberculosis lipids to pathogenesis," *Tuberculosis*, vol. 91, no. 3. pp. 187–195, May-2011.
- [48] S. Goyal, T. E. Klassert, and H. Slevogt, "C-type lectin receptors in tuberculosis: what we know," *Medical Microbiology and Immunology*, vol. 205, no. 6. Springer Verlag, pp. 513–535, 01-Dec-2016.
- [49] M. Daffé and H. Marrakchi, "Unraveling the Structure of the Mycobacterial Envelope," *Microbiol. Spectr.*, vol. 7, no. 4, Jul. 2019.
- [50] M. Daffé, "The cell envelope of tubercle bacilli," *Tuberculosis*, vol. 95, no. S1, pp. S155–S158, Jun. 2015.
- [51] E. C. Hett and E. J. Rubin, "Bacterial Growth and Cell Division: a Mycobacterial Perspective," *Microbiol. Mol. Biol. Rev.*, vol. 72, no. 1, pp. 126–156, Mar. 2008.
- [52] D. Kaur, M. E. Guerin, H. Škovierová, P. J. Brennan, and M. Jackson, "Chapter 2 Biogenesis of the Cell Wall and Other Glycoconjugates of Mycobacterium tuberculosis," *Advances in Applied Microbiology*, vol. 69. pp. 23–78, 2009.
- [53] A. Zvi, N. Ariel, J. Fulkerson, J. C. Sadoff, and A. Shafferman, "Whole genome identification of Mycobacterium tuberculosis vaccine candidates by comprehensive data mining and bioinformatic analyses," *BMC Med. Genomics*, vol. 1, no. 1, Dec. 2008.
- [54] M. Jackson, "The mycobacterial cell envelope-lipids," *Cold Spring Harb. Perspect. Med.*, vol. 4, no. 10, 2014.
- [55] A. Roy *et al.*, "Effect of BCG vaccination against Mycobacterium tuberculosis infection in children: Systematic review and meta-analysis," *BMJ*, vol. 349, Aug. 2014.
- [56] B. B. Trunz, P. Fine, and C. Dye, "Effect of BCG vaccination on childhood tuberculous meningitis and miliary tuberculosis worldwide: a meta-analysis and assessment of cost-effectiveness," *Lancet*, vol. 367, no. 9517, pp. 1173–1180, Apr. 2006.
- [57] G. A. Colditz *et al.*, "Efficacy of BCG vaccine in the prevention of tuberculosis. Meta-analysis of the published literature.," *JAMA*, vol. 271, no. 9, pp. 698–702, Mar. 1994.
- [58] H. McShane *et al.*, "BCG: Myths, realities, and the need for alternative vaccine strategies," *Tuberculosis*, vol. 92, no. 3. pp. 283–288, May-2012.
- [59] L. Scott, P. Da Silva, C. C. Boehme, W. Stevens, and C. M. Gilpin, "Diagnosis of opportunistic infections: HIV co-infections-tuberculosis," *Current Opinion in HIV and AIDS*, vol. 12, no. 2. Lippincott Williams and Wilkins, pp. 129–138, 01-Mar-2017.
- [60] M. L. Moro *et al.*, "An outbreak of multidrug-resistant tuberculosis involving HIV-infected patients of two hospitals in Milan, Italy. Italian Multidrug-Resistant Tuberculosis Outbreak Study Group.," *AIDS*, vol. 12,

no. 9, pp. 1095–102, Jun. 1998.

- [61] S. H. E. Kaufmann and A. J. McMichael, “Annulling a dangerous liaison: Vaccination strategies against aids and tuberculosis,” *Nat. Med.*, vol. 11, no. 4S, p. S33, 2005.
- [62] A. M. Cadena *et al.*, “Concurrent infection with Mycobacterium tuberculosis confers robust protection against secondary infection in macaques,” *PLoS Pathog.*, vol. 14, no. 10, Oct. 2018.
- [63] P. J. Cardona *et al.*, “Extended safety studies of the attenuated live tuberculosis vaccine SO2 based on phoP mutant,” *Vaccine*, vol. 27, no. 18, pp. 2499–2505, Apr. 2009.
- [64] L. Grode *et al.*, “Increased vaccine efficacy against tuberculosis of recombinant Mycobacterium bovis bacille Calmette-Guérin mutants that secrete listeriolysin,” *J. Clin. Invest.*, vol. 115, no. 9, pp. 2472–2479, 2005.
- [65] H. McShane, A. A. Pathan, C. R. Sander, N. P. Goonetilleke, H. A. Fletcher, and A. V. S. Hill, “Boosting BCG with MVA85A: The first candidate subunit vaccine for tuberculosis in clinical trials,” *Tuberculosis*, vol. 85, no. 1–2 SPEC.ISS., pp. 47–52, 2005.
- [66] P. Andersen and S. H. E. Kaufmann, “Novel vaccination strategies against tuberculosis,” *Cold Spring Harb. Perspect. Med.*, vol. 4, no. 6, 2014.
- [67] T. R. Hawn *et al.*, “Tuberculosis Vaccines and Prevention of Infection,” *Microbiol. Mol. Biol. Rev.*, vol. 78, no. 4, pp. 650–671, Dec. 2014.
- [68] S. H. E. Kaufmann, “Tuberculosis vaccine development: Strength lies in tenacity,” *Trends in Immunology*, vol. 33, no. 7. pp. 373–379, Jul-2012.
- [69] S. H. E. Kaufmann, J. Weiner, and C. F. von Reyn, “Novel approaches to tuberculosis vaccine development,” *International Journal of Infectious Diseases*, vol. 56. Elsevier B.V., pp. 263–267, 01-Mar-2017.
- [70] A. M. Cadena, S. M. Fortune, and J. L. Flynn, “Heterogeneity in tuberculosis,” *Nature Reviews Immunology*, vol. 17, no. 11. Nature Publishing Group, pp. 691–702, 27-Oct-2017.
- [71] A. O’Garra, P. S. Redford, F. W. McNab, C. I. Bloom, R. J. Wilkinson, and M. P. R. Berry, “The Immune Response in Tuberculosis,” *Annu. Rev. Immunol.*, vol. 31, no. 1, pp. 475–527, Mar. 2013.
- [72] G. Gualano *et al.*, “Tuberculin skin test – Outdated or still useful for Latent TB infection screening?,” *Int. J. Infect. Dis.*, vol. 80, pp. S20–S22, Mar. 2019.
- [73] L. B. Reichman, “Tuberculin Skin Testing,” *Chest*, vol. 76, no. 6, pp. 764–770, Dec. 1979.
- [74] D. Shingadia, “The diagnosis of tuberculosis,” *Pediatr. Infect. Dis. J.*, vol. 31, no. 3, pp. 302–5, Mar. 2012.
- [75] P. Hepple, N. Ford, and R. McNerney, “Microscopy compared to culture for the diagnosis of tuberculosis in induced sputum samples: A systematic review,” *International Journal of Tuberculosis and Lung Disease*, vol. 16, no. 5. pp. 579–588, 01-May-2012.
- [76] K. R. Steingart *et al.*, “Fluorescence versus conventional sputum smear microscopy for tuberculosis: a systematic review,” *Lancet Infectious Diseases*, vol. 6, no. 9. Lancet Publishing Group, pp. 570–581, 2006.
- [77] A. O. Ankrah *et al.*, “Ankrah, Alfred O. Glaudemans, Andor W.J.M. Maes, Alex Van de Wiele, Christophe Dierckx, Rudi A.J.O. Vorster, Mariza.Tuberculosis,” *Semin. Nucl. Med.*, vol. 48, no. 2, pp. 108–130, 2018.
- [78] J. C. Palomino, “Current developments and future perspectives for TB diagnostics,” *Future Microbiology*, vol. 7, no. 1. pp. 59–71, Jan-2012.
- [79] J. J. Dunn, J. R. Starke, and P. A. Revell, “Laboratory diagnosis of mycobacterium tuberculosis infection and disease in children,” *Journal of Clinical Microbiology*, vol. 54, no. 6. American Society for Microbiology, pp. 1434–1441, 01-Jun-2016.
- [80] P. Nahid *et al.*, “Executive Summary: Official American Thoracic Society/Centers for Disease Control and Prevention/Infectious Diseases Society of America Clinical Practice Guidelines: Treatment of Drug-

- Susceptible Tuberculosis," *Clinical Infectious Diseases*, vol. 63, no. 7. Oxford University Press, pp. 853–867, 01-Oct-2016.
- [81] and C. L. C. Robert Horsburgh, Jr., M.D., Clifton E. Barry III, Ph.D., "Treatment of Tuberculosis — NEJM Review."
- [82] V. Eldholm and F. Balloux, "Antimicrobial Resistance in Mycobacterium tuberculosis: The Odd One Out," *Trends in Microbiology*, vol. 24, no. 8. Elsevier Ltd, pp. 637–648, 01-Aug-2016.
- [83] C. for D. C. and P. (CDC), "Emergence of Mycobacterium tuberculosis with extensive resistance to second-line drugs--worldwide, 2000-2004.," *MMWR Morb. Mortal. Wkly. Rep.*, 2006.
- [84] Y. Zhao *et al.*, "National survey of drug-resistant tuberculosis in China," *N. Engl. J. Med.*, vol. 366, no. 23, pp. 2161–2170, Jun. 2012.
- [85] Z. F. Udawadia, R. A. Amale, K. K. Ajbani, and C. Rodrigues, "Totally drug-resistant tuberculosis in India," *Clinical Infectious Diseases*, vol. 54, no. 4. pp. 579–581, 15-Feb-2012.
- [86] L. Ramakrishnan, "Revisiting the role of the granuloma in tuberculosis," *Nature Reviews Immunology*, vol. 12, no. 5. pp. 352–366, May-2012.
- [87] C. Bussi and M. G. Gutierrez, "Mycobacterium tuberculosis infection of host cells in space and time," *FEMS Microbiol. Rev.*, vol. 43, no. 4, pp. 341–361, Jul. 2019.
- [88] J. B. Torrelles and L. S. Schlesinger, "Integrating Lung Physiology, Immunology, and Tuberculosis," *Trends in Microbiology*, vol. 25, no. 8. Elsevier Ltd, pp. 688–697, 01-Aug-2017.
- [89] T. R. Lerner, S. Borel, and M. G. Gutierrez, "The innate immune response in human tuberculosis," *Cell. Microbiol.*, vol. 17, no. 9, pp. 1277–1285, 2015.
- [90] J. Tang, W. C. Yam, and Z. Chen, "Mycobacterium tuberculosis infection and vaccine development," *Tuberculosis*, vol. 98. Churchill Livingstone, pp. 30–41, 01-May-2016.
- [91] C. J. Cambier, S. Falkow, and L. Ramakrishnan, "Host evasion and exploitation schemes of Mycobacterium tuberculosis," *Cell*, vol. 159, no. 7. Cell Press, pp. 1497–1509, 18-Dec-2014.
- [92] V. Quesniaux *et al.*, "Toll-like receptor pathways in the immune responses to mycobacteria," *Microbes and Infection*, vol. 6, no. 10. Elsevier Masson SAS, pp. 946–959, 2004.
- [93] S. B. Cohen *et al.*, "Alveolar Macrophages Provide an Early Mycobacterium tuberculosis Niche and Initiate Dissemination," *Cell Host Microbe*, vol. 24, no. 3, p. 439–446.e4, 2018.
- [94] L. Huang, E. V. Nazarova, S. Tan, Y. Liu, and D. G. Russell, "Growth of Mycobacterium tuberculosis in vivo segregates with host macrophage metabolism and ontogeny," *J. Exp. Med.*, vol. 215, no. 4, pp. 1135–1152, Apr. 2018.
- [95] S. L. Rajaram M, Dodd C, "Macrophage immunoregulatory pathways in tuberculosis," *Bone*, vol. 23, no. 1, pp. 1–7, 2008.
- [96] C. J. Martin, A. F. Carey, and S. M. Fortune, "A bug's life in the granuloma," *Seminars in Immunopathology*, vol. 38, no. 2. Springer Verlag, pp. 213–220, 01-Mar-2016.
- [97] D. G. Russell, C. E. Barry, and J. L. Flynn, "Tuberculosis: What we don't know can, and does, hurt us," *Science*, vol. 328, no. 5980. pp. 852–856, 14-May-2010.
- [98] D. G. Russell, "Who puts the tubercle in tuberculosis?," *Nature Reviews Microbiology*, vol. 5, no. 1. pp. 39–47, Jan-2007.
- [99] A. M. Cooper, "Cell-Mediated Immune Responses in Tuberculosis," *Annu. Rev. Immunol.*, vol. 27, no. 1, pp. 393–422, Apr. 2009.
- [100] W. P. Gill, N. S. Harik, M. R. Whiddon, R. P. Liao, J. E. Mittler, and D. R. Sherman, "A replication clock for Mycobacterium tuberculosis," *Nat. Med.*, vol. 15, no. 2, pp. 211–214, Feb. 2009.

- [101] A. M. Gallegos, E. G. Pamer, and M. S. Glickman, "Delayed protection by ESAT-6-specific effector CD4+ T cells after airborne *M. tuberculosis* infection.," *J. Exp. Med.*, vol. 205, no. 10, pp. 2359–68, Sep. 2008.
- [102] A. J. Wolf *et al.*, "Initiation of the adaptive immune response to *Mycobacterium tuberculosis* depends on antigen production in the local lymph node, not the lungs," *J. Exp. Med.*, vol. 205, no. 1, pp. 105–115, Jan. 2008.
- [103] H. E. Volkman, H. Clay, D. Beery, J. C. W. Chang, D. R. Sherman, and L. Ramakrishnan, "Tuberculous granuloma formation is enhanced by a *Mycobacterium* virulence determinant," *PLoS Biol.*, vol. 2, no. 11, Nov. 2004.
- [104] L. E. Swaim, L. E. Connolly, H. E. Volkman, O. Humbert, D. E. Born, and L. Ramakrishnan, "*Mycobacterium marinum* infection of adult zebrafish causes caseating granulomatous tuberculosis and is moderated by adaptive immunity," *Infect. Immun.*, vol. 74, no. 11, pp. 6108–6117, Nov. 2006.
- [105] A. Iliopoulos, K. Psathakis, S. Aslanidis, L. Skagias, and P. P. Sfikakis, "Tuberculosis and granuloma formation in patients receiving anti-TNF therapy.," *Int. J. Tuberc. Lung Dis.*, vol. 10, no. 5, pp. 588–90, May 2006.
- [106] J. Harris and J. Keane, "How tumour necrosis factor blockers interfere with tuberculosis immunity.," *Clin. Exp. Immunol.*, vol. 161, no. 1, pp. 1–9, Jul. 2010.
- [107] J. Keane *et al.*, "Tuberculosis associated with infliximab, a tumor necrosis factor α -neutralizing agent," *N. Engl. J. Med.*, vol. 345, no. 15, pp. 1098–1104, Oct. 2001.
- [108] P. L. Lin *et al.*, "Tumor necrosis factor neutralization results in disseminated disease in acute and latent *Mycobacterium tuberculosis* infection with normal granuloma structure in a cynomolgus macaque model.," *Arthritis Rheum.*, vol. 62, no. 2, pp. 340–50, Feb. 2010.
- [109] J. L. Flynn and J. Chan, "IMMUNOLOGY OF TUBERCULOSIS," *Annu. Rev. Immunol.*, vol. 19, no. 1, pp. 93–129, Apr. 2001.
- [110] J. A. L. Flynn *et al.*, "Tumor necrosis factor- α is required in the protective immune response against *mycobacterium tuberculosis* in mice," *Immunity*, vol. 2, no. 6, pp. 561–572, 1995.
- [111] T. Botha and B. Ryffel, "Reactivation of latent tuberculosis infection in TNF-deficient mice.," *J. Immunol.*, vol. 171, no. 6, pp. 3110–8, Sep. 2003.
- [112] V. P. Mohan *et al.*, "Effects of tumor necrosis factor alpha on host immune response in chronic persistent tuberculosis: possible role for limiting pathology.," *Infect. Immun.*, vol. 69, no. 3, pp. 1847–55, Mar. 2001.
- [113] H. Kaneko *et al.*, "Role of tumor necrosis factor-alpha in *Mycobacterium*-induced granuloma formation in tumor necrosis factor-alpha-deficient mice.," *Lab. Invest.*, vol. 79, no. 4, pp. 379–86, Apr. 1999.
- [114] J. G. Egen, A. G. Rothfuchs, C. G. Feng, N. Winter, A. Sher, and R. N. Germain, "Macrophage and T Cell Dynamics during the Development and Disintegration of *Mycobacterial* Granulomas," *Immunity*, vol. 28, no. 2, pp. 271–284, Feb. 2008.
- [115] E. A. Miller and J. D. Ernst, "Illuminating the Black Box of TNF Action in Tuberculous Granulomas," *Immunity*, vol. 29, no. 2, pp. 175–177, 15-Aug-2008.
- [116] A. M. Cooper, K. D. Mayer-Barber, and A. Sher, "Role of innate cytokines in mycobacterial infection.," *Mucosal Immunol.*, vol. 4, no. 3, pp. 252–60, May 2011.
- [117] J. L. Flynn, J. Chan, K. J. Triebold, D. K. Dalton, T. A. Stewart, and B. R. Bloom, "An essential role for interferon gamma in resistance to *Mycobacterium tuberculosis* infection.," *J. Exp. Med.*, vol. 178, no. 6, pp. 2249–54, Dec. 1993.
- [118] A. M. Cooper, J. Magram, J. Ferrante, and I. M. Orme, "Interleukin 12 (IL-12) is crucial to the development of protective immunity in mice intravenously infected with *mycobacterium tuberculosis*," *J. Exp. Med.*, vol. 186, no. 1, pp. 39–45, Jul. 1997.
- [119] S. Boisson-Dupuis *et al.*, "IL-12Rbeta1 deficiency in two of fifty children with severe tuberculosis from

- Iran, Morocco, and Turkey," *PLoS One*, vol. 6, no. 4, p. e18524, 2011.
- [120] J. T. Mattila, C. R. Diedrich, P. L. Lin, J. Phuah, and J. L. Flynn, "Simian Immunodeficiency Virus-Induced Changes in T Cell Cytokine Responses in Cynomolgus Macaques with Latent Mycobacterium tuberculosis Infection Are Associated with Timing of Reactivation," *J. Immunol.*, vol. 186, no. 6, pp. 3527–3537, Mar. 2011.
- [121] K. M. Pollock *et al.*, "PD-1 expression and cytokine secretion profiles of Mycobacterium tuberculosis-specific Cd4+ T-cell subsets; potential correlates of containment in HIV-TB co-infection," *PLoS One*, vol. 11, no. 1, Jan. 2016.
- [122] E. Mortaz *et al.*, "Interaction of Pattern Recognition Receptors with Mycobacterium Tuberculosis," *J. Clin. Immunol.*, vol. 35, no. 1, 2015.
- [123] M. H. Zaman, "The role of engineering approaches in analysing cancer invasion and metastasis," *Nature Reviews Cancer*, vol. 13, no. 8. pp. 596–603, Aug-2013.
- [124] C. A. Scanga, A. Bafica, C. G. Feng, A. W. Cheever, S. Hieny, and A. Sher, "MyD88-Deficient Mice Display A Profound Loss in Resistance to Mycobacterium tuberculosis Associated with Partially Impaired Th1 Cytokine and Nitric Oxide Synthase 2 Expression," *Infect. Immun.*, vol. 72, no. 4, pp. 2400–2404, Apr. 2004.
- [125] S. J. Lee *et al.*, "Mannose receptor-mediated regulation of serum glycoprotein homeostasis," *Science (80-.)*, vol. 295, no. 5561, pp. 1898–1901, Mar. 2002.
- [126] G. Lugo-Villarino, D. Hudrisier, A. Tanne, and O. Neyrolles, "C-type lectins with a sweet spot for Mycobacterium tuberculosis," *Eur. J. Microbiol. Immunol.*, vol. 1, no. 1, pp. 25–40, Mar. 2011.
- [127] E. K. Jo, "Mycobacterial interaction with innate receptors: TLRs, C-type lectins, and NLRs," *Current Opinion in Infectious Diseases*, vol. 21, no. 3. pp. 279–286, Jun-2008.
- [128] J. B. Torrelles and L. S. Schlesinger, "Diversity in Mycobacterium tuberculosis mannosylated cell wall determinants impacts adaptation to the host," *Tuberculosis*, vol. 90, no. 2. pp. 84–93, Mar-2010.
- [129] J. Nigou, C. Zelle-Rieser, M. Gilleron, M. Thurnher, and G. Puzo, "Mannosylated Lipoarabinomannans Inhibit IL-12 Production by Human Dendritic Cells: Evidence for a Negative Signal Delivered Through the Mannose Receptor," *J. Immunol.*, vol. 166, no. 12, pp. 7477–7485, Jun. 2001.
- [130] C. Astarie-Dequeker, E. N. N'Diaye, V. Le Cabec, M. G. Rittig, J. Prandi, and I. Maridonneau-Parini, "The mannose receptor mediates uptake of pathogenic and nonpathogenic mycobacteria and bypasses bactericidal responses in human macrophages," *Infect. Immun.*, vol. 67, no. 2, pp. 469–77, Feb. 1999.
- [131] E. Guirado *et al.*, "Deletion of PPAR γ in lung macrophages provides an immunoprotective response against M. tuberculosis infection in mice," *Tuberculosis*, vol. 111, pp. 170–177, Jul. 2018.
- [132] T. B. H. Geijtenbeek *et al.*, "DC-SIGN, a dendritic cell-specific HIV-1-binding protein that enhances trans-infection of T cells," *Cell*, vol. 100, no. 5, pp. 587–597, Mar. 2000.
- [133] B. M. Curtis, S. Scharnowske, and A. J. Watson, "Sequence and expression of a membrane-associated C-type lectin that exhibits CD4-independent binding of human immunodeficiency virus envelope glycoprotein gp120," *Proc. Natl. Acad. Sci. U. S. A.*, vol. 89, no. 17, pp. 8356–8360, 1992.
- [134] O. Neyrolles, B. Gicquel, and L. Quintana-Murci, "Towards a crucial role for DC-SIGN in tuberculosis and beyond," *Trends Microbiol.*, vol. 14, no. 9, pp. 383–387, Sep. 2006.
- [135] L. Tailleux *et al.*, "DC-SIGN is the major Mycobacterium tuberculosis receptor on human dendritic cells," *J. Exp. Med.*, vol. 197, no. 1, pp. 121–7, Jan. 2003.
- [136] T. B. H. Geijtenbeek *et al.*, "Mycobacteria target DC-SIGN to suppress dendritic cell function," *J. Exp. Med.*, vol. 197, no. 1, pp. 7–17, Jan. 2003.
- [137] L. Tailleux *et al.*, "DC-SIGN induction in alveolar macrophages defines privileged target host cells for mycobacteria in patients with tuberculosis," *PLoS Med.*, vol. 2, no. 12, pp. 1269–1279, 2005.

- [138] G. Lugo-Villarino *et al.*, "The C-type lectin receptor DC-SIGN has an anti-inflammatory role in Human M(IL-4) macrophages in response to *Mycobacterium tuberculosis*," *Front. Immunol.*, vol. 9, no. JUN, pp. 1–15, 2018.
- [139] D. M. E. Bowdish *et al.*, "MARCO, TLR2, and CD14 are required for macrophage cytokine responses to mycobacterial trehalose dimycolate and *Mycobacterium tuberculosis*," *PLoS Pathog.*, vol. 5, no. 6, p. e1000474, Jun. 2009.
- [140] L. C. Hsu *et al.*, "A NOD2-NALP1 complex mediates caspase-1-dependent IL-1 β secretion in response to *Bacillus anthracis* infection and muramyl dipeptide," *Proc. Natl. Acad. Sci. U. S. A.*, vol. 105, no. 22, pp. 7803–7808, Jun. 2008.
- [141] M. N. Brooks *et al.*, "NOD2 controls the nature of the inflammatory response and subsequent fate of *Mycobacterium tuberculosis* and *M. bovis* BCG in human macrophages," *Cell. Microbiol.*, vol. 13, no. 3, pp. 402–18, Mar. 2011.
- [142] O. H. Vandal, C. F. Nathan, and S. Ehrt, "Acid Resistance in *Mycobacterium tuberculosis* Acid Resistance in *Mycobacterium tuberculosis* □," vol. 191, no. May, 2009.
- [143] H. C. Mwandumba *et al.*, "Mycobacterium tuberculosis Resides in Nonacidified Vacuoles in Endocytically Competent Alveolar Macrophages from Patients with Tuberculosis and HIV Infection," *J. Immunol.*, vol. 172, no. 7, pp. 4592–4598, Apr. 2004.
- [144] I. Vergne, R. A. Fratti, P. J. Hill, J. Chua, J. Belisle, and V. Deretic, "Mycobacterium tuberculosis Phagosome Maturation Arrest: Mycobacterial Phosphatidylinositol Analog Phosphatidylinositol Mannoside Stimulates Early Endosomal Fusion," *Mol. Biol. Cell*, vol. 15, no. 2, pp. 751–760, Feb. 2004.
- [145] I. Vergne, J. Chua, S. B. Singh, and V. Deretic, "Cell biology of mycobacterium tuberculosis phagosome," *Annu. Rev. Cell Dev. Biol.*, vol. 20, pp. 367–94, 2004.
- [146] L. E. Via, D. Deretic, R. J. Ulmer, N. S. Hibler, L. A. Huber, and V. Deretic, "Arrest of mycobacterial phagosome maturation is caused by a block in vesicle fusion between stages controlled by rab5 and rab7," *J. Biol. Chem.*, vol. 272, no. 20, pp. 13326–31, May 1997.
- [147] O. H. Vandal, J. A. Roberts, T. Odaira, D. Schnappinger, C. F. Nathan, and S. Ehrt, "Acid-susceptible mutants of *Mycobacterium tuberculosis* share hypersusceptibility to cell wall and oxidative stress and to the host environment," *J. Bacteriol.*, vol. 191, no. 2, pp. 625–31, Jan. 2009.
- [148] R. D. Xu S1, Cooper A, Sturgill-Koszycki S, van Heyningen T, Chatterjee D, Orme I, Allen P, "Intracellular trafficking in *Mycobacterium tuberculosis* and *Mycobacterium avium*-infected macrophages," *J. Immunol.*, 1994.
- [149] A. Härtlova *et al.*, "LRRK2 is a negative regulator of *Mycobacterium tuberculosis* phagosome maturation in macrophages," *EMBO J.*, vol. 37, no. 12, 2018.
- [150] H. Botella *et al.*, "Mycobacterium tuberculosis protease MarP activates a peptidoglycan hydrolase during acid stress," *EMBO J.*, vol. 36, no. 4, pp. 536–548, 2017.
- [151] J. L. Small *et al.*, "Substrate specificity of MarP, a periplasmic protease required for resistance to acid and oxidative stress in *Mycobacterium tuberculosis*," *J. Biol. Chem.*, vol. 288, no. 18, pp. 12489–99, May 2013.
- [152] D. G. Russell, H. C. Mwandumba, and E. E. Rhoades, "Mycobacterium and the coat of many lipids," *Journal of Cell Biology*, vol. 158, no. 3. pp. 421–426, 2002.
- [153] L. Schnettger *et al.*, "A Rab20-Dependent Membrane Trafficking Pathway Controls M. tuberculosis Replication by Regulating Phagosome Spaciousness and Integrity," *Cell Host Microbe*, vol. 21, no. 5, p. 619–628.e5, May 2017.
- [154] M. I. De Jonge *et al.*, "ESAT-6 from *Mycobacterium tuberculosis* dissociates from its putative chaperone CFP-10 under acidic conditions and exhibits membrane-lysing activity," *J. Bacteriol.*, vol. 189, no. 16, pp. 6028–6034, Aug. 2007.

- [155] J. Augenstreich *et al.*, "ESX-1 and phthiocerol dimycocerosates of *Mycobacterium tuberculosis* act in concert to cause phagosomal rupture and host cell apoptosis," *Cell. Microbiol.*, vol. 19, no. 7, Jul. 2017.
- [156] Z. Chen *et al.*, "Inhibition of autophagy by MiR-30A induced by *Mycobacteria tuberculosis* as a possible mechanism of immune escape in human macrophages," *Jpn. J. Infect. Dis.*, vol. 68, no. 5, pp. 420–424, Sep. 2015.
- [157] A. R. Martineau *et al.*, "Reciprocal seasonal variation in vitamin D status and tuberculosis notifications in Cape Town, South Africa," *Proc. Natl. Acad. Sci. U. S. A.*, vol. 108, no. 47, pp. 19013–19017, Nov. 2011.
- [158] A. R. Martineau, F. U. Honecker, R. J. Wilkinson, and C. J. Griffiths, "Vitamin D in the treatment of pulmonary tuberculosis," *Journal of Steroid Biochemistry and Molecular Biology*, vol. 103, no. 3–5, pp. 793–798, Mar-2007.
- [159] C. Bogdan, M. Röllinghoff, and A. Diefenbach, "Reactive oxygen and reactive nitrogen intermediates in innate and specific immunity," *Current Opinion in Immunology*, vol. 12, no. 1. Current Biology Ltd, pp. 64–76, 01-Feb-2000.
- [160] A. J. Olive and C. M. Sasseti, "Tolerating the Unwelcome Guest; How the Host Withstands Persistent *Mycobacterium tuberculosis*," *Front. Immunol.*, vol. 9, p. 2094, 2018.
- [161] A. S. Davis, I. Vergne, S. S. Master, G. B. Kyei, J. Chua, and V. Deretic, "Mechanism of inducible nitric oxide synthase exclusion from mycobacterial phagosomes," *PLoS Pathog.*, vol. 3, no. 12, pp. 1887–1894, Dec. 2007.
- [162] M. I. Voskuil *et al.*, "Inhibition of respiration by nitric oxide induces a *Mycobacterium tuberculosis* dormancy program," *J. Exp. Med.*, vol. 198, no. 5, pp. 705–13, Sep. 2003.
- [163] C. D. Sohaskey and L. G. Wayne, "Role of narK2X and narGHJ in hypoxic upregulation of nitrate reduction by *Mycobacterium tuberculosis*," *J. Bacteriol.*, vol. 185, no. 24, pp. 7247–56, Dec. 2003.
- [164] F. Levillain *et al.*, "Horizontal acquisition of a hypoxia-responsive molybdenum cofactor biosynthesis pathway contributed to *Mycobacterium tuberculosis* pathoadaptation," *PLoS Pathog.*, vol. 13, no. 11, Nov. 2017.
- [165] R. Appelberg, "Macrophage nutriprive antimicrobial mechanisms," *J. Leukoc. Biol.*, vol. 79, no. 6, pp. 1117–1128, Mar. 2006.
- [166] X. W. Li *et al.*, "SLC11A1 (NRAMP1) polymorphisms and tuberculosis susceptibility: Updated systematic review and meta-analysis," *PLoS ONE*, vol. 6, no. 1. 2011.
- [167] C. M. Jones and M. Niederweis, "Mycobacterium tuberculosis can utilize heme as an iron source," *J. Bacteriol.*, vol. 193, no. 7, pp. 1767–1770, Apr. 2011.
- [168] M. Luo, E. A. Fadeev, and J. T. Groves, "Mycobactin-mediated iron acquisition within macrophages," *Nat. Chem. Biol.*, vol. 1, no. 3, pp. 149–153, 2005.
- [169] J. Gobin and M. A. Horwitz, "Exochelins of *Mycobacterium tuberculosis* remove iron from human iron-binding proteins and donate iron to mycobactins in the M. tuberculosis cell wall," *J. Exp. Med.*, vol. 183, no. 4, pp. 1527–1532, Apr. 1996.
- [170] U. E. Schaible, H. L. Collins, F. Priem, and S. H. E. Kaufmann, "Correction of the iron overload defect in β -2-microglobulin knockout mice by lactoferrin abolishes their increased susceptibility to tuberculosis," *J. Exp. Med.*, vol. 196, no. 11, pp. 1507–1513, Dec. 2002.
- [171] J. Daniel, H. Maamar, C. Deb, T. D. Sirakova, and P. E. Kolattukudy, "Mycobacterium tuberculosis uses host triacylglycerol to accumulate lipid droplets and acquires a dormancy-like phenotype in lipid-loaded macrophages," *PLoS Pathog.*, vol. 7, no. 6, Jun. 2011.
- [172] P. Peyron *et al.*, "Foamy macrophages from tuberculous patients' granulomas constitute a nutrient-rich reservoir for M. tuberculosis persistence," *PLoS Pathog.*, vol. 4, no. 11, 2008.
- [173] A. K. Pandey and C. M. Sasseti, "Mycobacterial persistence requires the utilization of host cholesterol,"

Proc. Natl. Acad. Sci. U. S. A., vol. 105, no. 11, pp. 4376–4380, Mar. 2008.

- [174] A. Gouzy *et al.*, “Mycobacterium tuberculosis nitrogen assimilation and host colonization require aspartate,” *Nat. Chem. Biol.*, vol. 9, no. 11, pp. 674–676, 2013.
- [175] A. Gouzy *et al.*, “Mycobacterium tuberculosis Exploits Asparagine to Assimilate Nitrogen and Resist Acid Stress during Infection,” *PLoS Pathog.*, vol. 10, no. 2, 2014.
- [176] U. Babu and M. L. Failla, “Respiratory burst and candidacidal activity of peritoneal macrophages are impaired in copper-deficient rats,” *J. Nutr.*, vol. 120, no. 12, pp. 1692–1699, 1990.
- [177] U. Babu and M. L. Failla, “Copper status and function of neutrophils are reversibly depressed in marginally and severely copper-deficient rats,” *J. Nutr.*, vol. 120, no. 12, pp. 1700–1709, 1990.
- [178] F. Wolschendorf *et al.*, “Copper resistance is essential for virulence of Mycobacterium tuberculosis,” *Proc. Natl. Acad. Sci. U. S. A.*, vol. 108, no. 4, pp. 1621–1626, Jan. 2011.
- [179] J. M. Rybicka, D. R. Balce, M. F. Khan, R. M. Krohn, and R. M. Yates, “NADPH oxidase activity controls phagosomal proteolysis in macrophages through modulation of the luminal redox environment of phagosomes,” *Proc. Natl. Acad. Sci. U. S. A.*, vol. 107, no. 23, pp. 10496–10501, Jun. 2010.
- [180] J. M. Rybicka, D. R. Balce, S. Chaudhuri, E. R. O. Allan, and R. M. Yates, “Phagosomal proteolysis in dendritic cells is modulated by NADPH oxidase in a pH-independent manner,” *EMBO J.*, vol. 31, no. 4, pp. 932–944, Feb. 2012.
- [181] R. Ballestín *et al.*, “Ethanol reduces zincosome formation in cultured astrocytes,” *Alcohol Alcohol.*, vol. 46, no. 1, pp. 17–25, Jan. 2011.
- [182] O. Neyrolles, F. Wolschendorf, A. Mitra, and M. Niederweis, “Mycobacteria, metals, and the macrophage,” *Immunol. Rev.*, vol. 264, no. 1, pp. 249–263, Mar. 2015.
- [183] S. K. Ward, B. Abomoelak, E. A. Hoye, H. Steinberg, and A. M. Talaat, “CtpV: A putative copper exporter required for full virulence of Mycobacterium tuberculosis,” *Mol. Microbiol.*, vol. 77, no. 5, pp. 1096–1110, Sep. 2010.
- [184] H. Botella *et al.*, “Mycobacterial P 1 -Type ATPases mediate resistance to Zinc poisoning in human macrophages,” *Cell Host Microbe*, vol. 10, no. 3, pp. 248–259, Sep. 2011.
- [185] L. Quintana-Murci, A. Alcaïs, L. Abel, and J. L. Casanova, “Immunology in natura: Clinical, epidemiological and evolutionary genetics of infectious diseases,” *Nat. Immunol.*, vol. 8, no. 11, pp. 1165–1171, Nov. 2007.
- [186] M. Benoit, B. Desnues, and J.-L. Mege, “Macrophage Polarization in Bacterial Infections,” *J. Immunol.*, vol. 181, no. 6, pp. 3733–3739, Sep. 2008.
- [187] G. Lugo-Villarino, C. Vérollet, I. Maridonneau-Parini, and O. Neyrolles, “Macrophage polarization: Convergence point targeted by Mycobacterium tuberculosis and HIV,” *Frontiers in Immunology*, vol. 2, no. SEP. 2011.
- [188] G. Lugo-Villarino and O. Neyrolles, “Manipulation of the mononuclear phagocyte system by mycobacterium tuberculosis,” *Cold Spring Harb. Perspect. Med.*, vol. 4, no. 11, 2014.
- [189] T. Schreiber *et al.*, “Autocrine IL-10 Induces Hallmarks of Alternative Activation in Macrophages and Suppresses Antituberculosis Effector Mechanisms without Compromising T Cell Immunity,” *J. Immunol.*, vol. 183, no. 2, pp. 1301–1312, Jul. 2009.
- [190] A. Kahnert *et al.*, “Alternative activation deprives macrophages of a coordinated defense program to Mycobacterium tuberculosis,” *Eur. J. Immunol.*, vol. 36, no. 3, pp. 631–647, Mar. 2006.
- [191] K. C. El Kasmi *et al.*, “Toll-like receptor-induced arginase 1 in macrophages thwarts effective immunity against intracellular pathogens,” *Nat. Immunol.*, vol. 9, no. 12, pp. 1399–1406, 2008.
- [192] C. Verollet *et al.*, “HIV-1 Nef Triggers Macrophage Fusion in a p61Hck- and Protease-Dependent Manner,”

- J. Immunol.*, vol. 184, no. 12, pp. 7030–7039, 2010.
- [193] M. Silva Miranda, A. Breiman, S. Allain, F. Deknuydt, and F. Altare, “The tuberculous granuloma: An unsuccessful host defence mechanism providing a safety shelter for the bacteria?,” *Clinical and Developmental Immunology*, vol. 2012. 2012.
- [194] H. Sakai *et al.*, “The CD40-CD40L axis and IFN- γ play critical roles in Langhans giant cell formation,” *Int. Immunol.*, vol. 24, no. 1, pp. 5–15, 2012.
- [195] M.-P. Puissegur *et al.*, “Mycobacterial Lipomannan Induces Granuloma Macrophage Fusion via a TLR2-Dependent, ADAM9- and β 1 Integrin-Mediated Pathway,” *J. Immunol.*, vol. 178, no. 5, pp. 3161–3169, Mar. 2007.
- [196] G. Lay *et al.*, “Langhans giant cells from M. Tuberculosis-induced human granulomas cannot mediate mycobacterial uptake,” *J. Pathol.*, vol. 211, no. 1, pp. 76–85, Jan. 2007.
- [197] D. G. Russell, P. J. Cardona, M. J. Kim, S. Allain, and F. Altare, “Foamy macrophages and the progression of the human tuberculosis granuloma,” *Nature Immunology*, vol. 10, no. 9, pp. 943–948, 2009.
- [198] P. Santucci *et al.*, “Experimental models of foamy macrophages and approaches for dissecting the mechanisms of lipid accumulation and consumption during dormancy and reactivation of tuberculosis,” *Frontiers in Cellular and Infection Microbiology*, vol. 6, no. OCT. Frontiers Media S.A., 07-Oct-2016.
- [199] D. S. Ridley and M. J. Ridley, “Rationale for the histological spectrum of tuberculosis. A basis for classification,” *Pathology*, vol. 19, no. 2, pp. 186–192, 1987.
- [200] R. L. Hunter, C. Jagannath, and J. K. Actor, “Pathology of postprimary tuberculosis in humans and mice: Contradiction of long-held beliefs,” *Tuberculosis*, vol. 87, no. 4, pp. 267–278, Jul. 2007.
- [201] R. Dhouib, A. Ducret, P. Hubert, F. Carrière, S. Dukan, and S. Canaan, “Watching intracellular lipolysis in mycobacteria using time lapse fluorescence microscopy,” *Biochim. Biophys. Acta - Mol. Cell Biol. Lipids*, vol. 1811, no. 4, pp. 234–241, 2011.
- [202] M. Datta *et al.*, “Mathematical Model of Oxygen Transport in Tuberculosis Granulomas,” *Ann. Biomed. Eng.*, vol. 44, no. 4, pp. 863–872, Apr. 2016.
- [203] M. J. Kim *et al.*, “Caseation of human tuberculosis granulomas correlates with elevated host lipid metabolism,” *EMBO Mol. Med.*, vol. 2, no. 7, pp. 258–274, 2010.
- [204] J. Korf, A. Stoltz, J. Verschoor, P. De Baetselier, and J. Grooten, “The Mycobacterium tuberculosis cell wall component mycolic acid elicits pathogen-associated host innate immune responses,” *Eur. J. Immunol.*, vol. 35, no. 3, pp. 890–900, Mar. 2005.
- [205] M. Genoula *et al.*, “Formation of foamy macrophages by tuberculous pleural effusions is triggered by the interleukin-10/signal transducer and activator of transcription 3 axis through ACAT upregulation,” *Front. Immunol.*, vol. 9, no. MAR, 2018.
- [206] J. D. MacMicking, “Interferon-inducible effector mechanisms in cell-autonomous immunity,” *Nature Reviews Immunology*, vol. 12, no. 5, pp. 367–382, May-2012.
- [207] T. Ishihara *et al.*, “Inhibition of chlamydia trachomatis growth by human interferon-alpha: mechanisms and synergistic effect with interferon-gamma and tumor necrosis factor-alpha,” *Biomed. Res.*, vol. 26, no. 4, pp. 179–85, Aug. 2005.
- [208] J. Kazar, J. D. Gillmore, and F. B. Gordon, “Effect of Interferon and Interferon Inducers on Infections with a Nonviral Intracellular Microorganism, Chlamydia trachomatis,” *Infect. Immun.*, vol. 3, no. 6, pp. 825–32, Jun. 1971.
- [209] A. G. Rothfuchs, D. Gigliotti, K. Palmblad, U. Andersson, H. Wigzell, and M. E. Rottenberg, “IFN-alpha beta-dependent, IFN-gamma secretion by bone marrow-derived macrophages controls an intracellular bacterial infection,” *J. Immunol.*, vol. 167, no. 11, pp. 6453–61, Dec. 2001.
- [210] C. R. Plumlee, C. Lee, A. A. Beg, T. Decker, H. A. Shuman, and C. Schindler, “Interferons direct an effective

- innate response to *Legionella pneumophila* infection," *J. Biol. Chem.*, vol. 284, no. 44, pp. 30058–30066, Oct. 2009.
- [211] V. Auerbuch, D. G. Brockstedt, N. Meyer-Morse, M. O’Riordan, and D. A. Portnoy, "Mice lacking the type I interferon receptor are resistant to *Listeria monocytogenes*," *J. Exp. Med.*, vol. 200, no. 4, pp. 527–533, Aug. 2004.
- [212] J. A. Carrero, B. Calderon, and E. R. Unanue, "Type I interferon sensitizes lymphocytes to apoptosis and reduces resistance to *Listeria* infection," *J. Exp. Med.*, vol. 200, no. 4, pp. 535–540, Aug. 2004.
- [213] R. M. O’Connell *et al.*, "Type I interferon production enhances susceptibility to *Listeria monocytogenes* infection," *J. Exp. Med.*, vol. 200, no. 4, pp. 437–445, Aug. 2004.
- [214] K. Al Moussawi, E. Ghigo, U. Kalinke, L. Alexopoulou, J. L. Mege, and B. Desnues, "Type I interferon induction is detrimental during infection with the Whipple’s disease bacterium, *Tropheryma whipplei*," *PLoS Pathog.*, vol. 6, no. 1, Jan. 2010.
- [215] D. Ordway *et al.*, "The Hypervirulent *Mycobacterium tuberculosis* Strain HN878 Induces a Potent TH1 Response followed by Rapid Down-Regulation," *J. Immunol.*, vol. 179, no. 1, pp. 522–531, Jul. 2007.
- [216] S. A. Stanley, J. E. Johndrow, P. Manzanillo, and J. S. Cox, "The Type I IFN Response to Infection with *Mycobacterium tuberculosis* Requires ESX-1-Mediated Secretion and Contributes to Pathogenesis," *J. Immunol.*, vol. 178, no. 5, pp. 3143–3152, Mar. 2007.
- [217] C. Manca *et al.*, "Hypervirulent *M. tuberculosis* W/Beijing strains upregulate Type I IFNs and increase expression of negative regulators of the jak-stat pathway," *J. Interf. Cytokine Res.*, vol. 25, no. 11, pp. 694–701, Nov. 2005.
- [218] J. M. Kimmey, J. A. Campbell, L. A. Weiss, K. J. Monte, D. J. Lenschow, and C. L. Stallings, "The impact of ISGylation during *Mycobacterium tuberculosis* infection in mice," *Microbes Infect.*, vol. 19, no. 4–5, pp. 249–258, Apr. 2017.
- [219] A. Dorhoi *et al.*, "Type I IFN signaling triggers immunopathology in tuberculosis-susceptible mice by modulating lung phagocyte dynamics," *Eur. J. Immunol.*, vol. 44, no. 8, pp. 2380–2393, 2014.
- [220] K. D. Mayer-Barber *et al.*, "Innate and Adaptive Interferons Suppress IL-1 α and IL-1 β Production by Distinct Pulmonary Myeloid Subsets during *Mycobacterium tuberculosis* Infection," *Immunity*, vol. 35, no. 6, pp. 1023–1034, Dec. 2011.
- [221] M. P. R. Berry *et al.*, "An interferon-inducible neutrophil-driven blood transcriptional signature in human tuberculosis," *Nature*, vol. 466, no. 7309, pp. 973–977, Aug. 2010.
- [222] T. J. Scriba *et al.*, "Sequential inflammatory processes define human progression from *M. tuberculosis* infection to tuberculosis disease," *PLoS Pathog.*, vol. 13, no. 11, Nov. 2017.
- [223] A. Singhanian *et al.*, "A modular transcriptional signature identifies phenotypic heterogeneity of human tuberculosis infection," *Nat. Commun.*, vol. 9, no. 1, Dec. 2018.
- [224] S. N. de Oliveira Uehara *et al.*, "High incidence of tuberculosis in patients treated for hepatitis C chronic infection," *Brazilian J. Infect. Dis.*, vol. 20, no. 2, pp. 205–209, Mar. 2016.
- [225] S. Matsuoka, H. Fujikawa, H. Hasegawa, T. Ochiai, Y. Watanabe, and M. Moriyama, "Onset of tuberculosis from a pulmonary latent tuberculosis infection during antiviral triple therapy for chronic hepatitis C," *Intern. Med.*, vol. 55, no. 15, pp. 2011–2017, 2016.
- [226] F. W. McNab *et al.*, "Type I IFN Induces IL-10 Production in an IL-27-Independent Manner and Blocks Responsiveness to IFN- γ for Production of IL-12 and Bacterial Killing in *Mycobacterium tuberculosis* – Infected Macrophages," *J. Immunol.*, vol. 193, no. 7, pp. 3600–3612, Oct. 2014.
- [227] L. Moreira-Teixeira *et al.*, "T Cell-Derived IL-10 Impairs Host Resistance to *Mycobacterium tuberculosis* Infection," *J. Immunol.*, vol. 199, no. 2, pp. 613–623, Jul. 2017.
- [228] P. S. Redford, P. J. Murray, and A. O’Garra, "The role of IL-10 in immune regulation during *M. tuberculosis*

- infection," *Mucosal Immunol.*, vol. 4, no. 3, pp. 261–270, May 2011.
- [229] F. Bouchonnet, N. Boechat, M. Bonay, and A. J. Hance, "Alpha/beta interferon impairs the ability of human macrophages to control growth of *Mycobacterium bovis* BCG," *Infect. Immun.*, vol. 70, no. 6, pp. 3020–3025, 2002.
- [230] C. Manca *et al.*, "Virulence of a *Mycobacterium tuberculosis* clinical isolate in mice is determined by failure to induce Th1 type immunity and is associated with induction of IFN- α/β ," *Proc. Natl. Acad. Sci. U. S. A.*, vol. 98, no. 10, pp. 5752–5757, May 2001.
- [231] L. R. V. Antonelli *et al.*, "Intranasal poly-IC treatment exacerbates tuberculosis in mice through the pulmonary recruitment of a pathogen-permissive monocyte/macrophage population," *J. Clin. Invest.*, vol. 120, no. 5, pp. 1674–1682, May 2010.
- [232] S. M. Dauphinee *et al.*, "Contribution of increased ISG15, ISGylation and deregulated type I IFN signaling in Usp18 mutant mice during the course of bacterial infections," *Genes Immun.*, vol. 15, no. 5, pp. 282–292, 2014.
- [233] Lúcia Moreira-Teixeira, K. Mayer-Barber, A. Sher, and A. O'Garra, "Type I interferons in tuberculosis: Foe and occasionally friend," *Journal of Experimental Medicine*, vol. 215, no. 5. Rockefeller University Press, pp. 1273–1285, 01-May-2018.
- [234] A. Bénard *et al.*, "B cells producing type I IFN modulate macrophage polarization in tuberculosis," *Am. J. Respir. Crit. Care Med.*, vol. 197, no. 6, pp. 801–813, 2018.
- [235] F. W. McNab *et al.*, "TPL-2–ERK1/2 Signaling Promotes Host Resistance against Intracellular Bacterial Infection by Negative Regulation of Type I IFN Production," *J. Immunol.*, vol. 191, no. 4, pp. 1732–1743, Aug. 2013.
- [236] P. Zarogoulidis *et al.*, "The effect of combination IFN-alpha-2a with usual antituberculosis chemotherapy in non-responding tuberculosis and diabetes mellitus: A case report and review of the literature," *J. Chemother.*, vol. 24, no. 3, pp. 173–177, Jun. 2012.
- [237] D. Palmero, K. Eiguchi, P. Rendo, L. Castro Zorrilla, E. Abbate, and L. J. González Montaner, "Phase II trial of recombinant interferon-alpha2b in patients with advanced intractable multidrug-resistant pulmonary tuberculosis: long-term follow-up.," *Int. J. Tuberc. Lung Dis.*, vol. 3, no. 3, pp. 214–8, Mar. 1999.
- [238] L. Moreira-Teixeira *et al.*, "Type I IFN Inhibits Alternative Macrophage Activation during *Mycobacterium tuberculosis* Infection and Leads to Enhanced Protection in the Absence of IFN- γ Signaling," *J. Immunol.*, vol. 197, no. 12, pp. 4714–4726, Dec. 2016.
- [239] L. Desvignes, A. J. Wolf, and J. D. Ernst, "Dynamic Roles of Type I and Type II IFNs in Early Infection with *Mycobacterium tuberculosis*," *J. Immunol.*, vol. 188, no. 12, pp. 6205–6215, Jun. 2012.
- [240] K. D. Mayer-Barber *et al.*, "Caspase-1 independent IL-1beta production is critical for host resistance to mycobacterium tuberculosis and does not require TLR signaling in vivo.," *J. Immunol.*, vol. 184, no. 7, pp. 3326–30, Apr. 2010.
- [241] G. Guarda *et al.*, "Type I Interferon Inhibits Interleukin-1 Production and Inflammasome Activation," *Immunity*, vol. 34, no. 2, pp. 213–223, Feb. 2011.
- [242] K. D. Mayer-Barber *et al.*, "Host-directed therapy of tuberculosis based on interleukin-1 and type I interferon crosstalk," *Nature*, vol. 511, no. 7507, pp. 99–103, 2014.
- [243] M. Divangahi, D. Desjardins, C. Nunes-Alves, H. G. Remold, and S. M. Behar, "Eicosanoid pathways regulate adaptive immunity to *Mycobacterium tuberculosis*," *Nat. Immunol.*, vol. 11, no. 8, pp. 751–758, Aug. 2010.
- [244] M. Divangahi *et al.*, "Mycobacterium tuberculosis evades macrophage defenses by inhibiting plasma membrane repair," *Nat. Immunol.*, vol. 10, no. 8, pp. 899–906, 2009.
- [245] M. Chen *et al.*, "Lipid mediators in innate immunity against tuberculosis: Opposing roles of PGE 2 and LXA 4 in the induction of macrophage death," *J. Exp. Med.*, vol. 205, no. 12, pp. 2791–2801, Nov. 2008.

- [246] S. Yan *et al.*, "Deficiency of the AIM2–ASC Signal Uncovers the STING-Driven Overreactive Response of Type I IFN and Reciprocal Depression of Protective IFN- γ Immunity in Mycobacterial Infection," *J. Immunol.*, vol. 200, no. 3, pp. 1016–1026, Feb. 2018.
- [247] K. D. Mayer-Barber and A. Sher, "Cytokine and lipid mediator networks in tuberculosis," *Immunol. Rev.*, vol. 264, no. 1, pp. 264–275, Mar. 2015.
- [248] D. E. Furst, R. Wallis, M. Broder, and D. O. Beenhouwer, "Tumor Necrosis Factor Antagonists: Different Kinetics and/or Mechanisms of Action May Explain Differences in the Risk for Developing Granulomatous Infection," *Semin. Arthritis Rheum.*, vol. 36, no. 3, pp. 159–167, Dec. 2006.
- [249] T. R. Lerner *et al.*, "Mycobacterium tuberculosis replicates within necrotic human macrophages," *J. Cell Biol.*, vol. 216, no. 3, pp. 583–594, 2017.
- [250] D. Castaño, L. F. García, and M. Rojas, "Increased frequency and cell death of CD16 + monocytes with Mycobacterium tuberculosis infection," *Tuberculosis*, vol. 91, no. 5, pp. 348–360, Sep. 2011.
- [251] L. Balboa *et al.*, "Paradoxical role of CD16+CCR2+CCR5+ monocytes in tuberculosis: efficient APC in pleural effusion but also mark disease severity in blood," *J. Leukoc. Biol.*, vol. 90, no. 1, pp. 69–75, 2011.
- [252] L. Balboa *et al.*, "Diverging biological roles among human monocyte subsets in the context of tuberculosis infection," *Clin. Sci.*, vol. 129, no. 4, pp. 319–330, 2015.
- [253] L. Balboa *et al.*, "Impaired dendritic cell differentiation of CD16-positive monocytes in tuberculosis: Role of p38 MAPK," *Eur. J. Immunol.*, vol. 43, no. 2, pp. 335–347, 2013.
- [254] J. Xie, J. Qian, J. Yang, S. Wang, M. E. Freeman, and Q. Yi, "Critical roles of Raf/MEK/ERK and PI3K/AKT signaling and inactivation of p38 MAP kinase in the differentiation and survival of monocyte-derived immature dendritic cells," *Exp. Hematol.*, vol. 33, no. 5, pp. 564–572, 2005.
- [255] J. L. Flynn, J. Chan, and P. L. Lin, "Macrophages and control of granulomatous inflammation in tuberculosis," *Mucosal Immunology*, vol. 4, no. 3, pp. 271–278, May-2011.
- [256] S. Ehrt *et al.*, "Reprogramming of the macrophage transcriptome in response to interferon- γ and mycobacterium tuberculosis: Signaling roles of nitric oxide synthase-2 and phagocyte oxidase," *J. Exp. Med.*, vol. 194, no. 8, pp. 1123–1139, Oct. 2001.
- [257] F. O. Martinez, L. Helming, and S. Gordon, "Alternative Activation of Macrophages: An Immunologic Functional Perspective," *Annu. Rev. Immunol.*, vol. 27, no. 1, pp. 451–483, Apr. 2009.
- [258] E. F. Redente, D. M. Higgins, L. D. Dwyer-Nield, I. M. Orme, M. Gonzalez-Juarrero, and A. M. Malkinson, "Differential polarization of alveolar macrophages and bone marrow-derived monocytes following chemically and pathogen-induced chronic lung inflammation," *J. Leukoc. Biol.*, vol. 88, no. 1, pp. 159–168, Jul. 2010.
- [259] A. Verbon, N. Juffermans, S. J. H. Van Deventer, P. Speelman, H. Van Deutekom, and T. Van Der Poll, "Serum concentrations of cytokines in patients with active tuberculosis (TB) and after treatment," *Clin. Exp. Immunol.*, vol. 115, no. 1, pp. 110–113, 1999.
- [260] S. K. Pathak *et al.*, "Corrigendum: Direct extracellular interaction between the early secreted antigen ESAT-6 of Mycobacterium tuberculosis and TLR2 inhibits TLR signaling in macrophages," *Nat. Immunol.*, vol. 16, no. 3, p. 326, Mar. 2015.
- [261] C. Lastrucci *et al.*, "Tuberculosis is associated with expansion of a motile, permissive and immunomodulatory CD16+ monocyte population via the IL-10/STAT3 axis," *Cell Res.*, vol. 25, no. 12, pp. 1333–1351, 2015.
- [262] "WHO progress reports HIV," 2019. [Online]. Available: <https://www.who.int/hiv/strategy2016-2021/progress-report-2019/en/>.
- [263] "UNAIDS," 2019. [Online]. Available: <https://aidsinfo.unaids.org>.
- [264] Center for Disease Control, "Kaposi's Center for Disease Control. (1981). Kaposi's sarcoma and

- Pneumocystis pneumonia among homosexual men--New York City and California. MMWR. Morbidity and Mortality Weekly Report. <https://doi.org/10.1056/AC200106010000008> sarcoma and Pneumocystis pne," *MMWR. Morb. Mortal. Wkly. Rep.*, 1981.
- [265] J. C. F. Barré-Sinoussi, Chermann *et al.*, "Isolation of a T-Lymphotropic Retrovirus from a Patient at Risk for Acquired Immune Deficiency Syndrome (AIDS) Isolation of a T-Lymphotropic Retrovirus from a Patient at Risk for Acquired Immune Deficiency Syndrome (AIDS)," *Science (80-)*, vol. 220, no. 4599, pp. 868–871, 1983.
- [266] D. Klatzmann *et al.*, "Selective tropism of lymphadenopathy associated virus (LAV) for helper-inducer T lymphocytes," *Science (80-)*, vol. 225, no. 4657, pp. 59–63, 1984.
- [267] M. Popovic, M. G. Sarngadharan, E. Read, and R. C. Gallo, "Detection, isolation, and continuous production of cytopathic retroviruses (HTLV-III) from patients with AIDS and pre-AIDS," *Science (80-)*, vol. 224, no. 4648, pp. 497–500, 1984.
- [268] J. A. Levy, A. D. Hoffman, S. M. Kramer, J. A. Landis, J. M. Shimabukuro, and L. S. Oshiro, "Isolation of lymphocytopathic retroviruses from San Francisco patients with AIDS," *Science (80-)*, vol. 225, no. 4664, pp. 840–842, 1984.
- [269] T. S. Alexander, "Human Immunodeficiency Virus Diagnostic Testing: 30 Years of Evolution," *Clin. Vaccine Immunol.*, vol. 23, no. 4, pp. 249–253, Apr. 2016.
- [270] L. Ratner *et al.*, "Complete nucleotide sequence of the AIDS virus, HTLV-III," *Nature*, vol. 313, no. 6000, pp. 277–284, 1985.
- [271] R. Sanchez-Pescador *et al.*, "Nucleotide sequence and expression of an AIDS-Associated Retrovirus (ARV-2)," *Science (80-)*, vol. 227, no. 4686, pp. 484–492, 1985.
- [272] S. Wain-Hobson, P. Sonigo, O. Danos, S. Cole, and M. Alizon, "Nucleotide sequence of the AIDS virus, LAV," *Cell*, vol. 40, no. 1, pp. 9–17, 1985.
- [273] S. Broder, "The development of antiretroviral therapy and its impact on the HIV-1/AIDS pandemic," *Antiviral Research*, vol. 85, no. 1, pp. 1–18, Jan-2010.
- [274] A. Wlodawer *et al.*, "Conserved folding in retroviral proteases: Crystal structure of a synthetic HIV-1 protease," *Science (80-)*, vol. 245, no. 4918, pp. 616–621, 1989.
- [275] P. W. Berman *et al.*, "Protection of chimpanzees from infection by HIV-1 after vaccination with recombinant glycoprotein gp120 but not gp160," *Nature*, vol. 345, no. 6276, pp. 622–625, 1990.
- [276] M. Piatak *et al.*, "High levels of HIV-1 in plasma during all stages of infection determined by competitive PCR," *Science (80-)*, vol. 259, no. 5102, pp. 1749–1754, 1993.
- [277] P. Borrow, H. Lewicki, B. H. Hahn, G. M. Shaw, and M. B. Oldstone, "Virus-specific CD8+ cytotoxic T-lymphocyte activity associated with control of viremia in primary human immunodeficiency virus type 1 infection," *J. Virol.*, vol. 68, no. 9, pp. 6103–10, Sep. 1994.
- [278] H. K. Deng *et al.*, "Identification of a major co-receptor for primary isolates of HIV-1," *Nature*, vol. 381, no. 6584, pp. 661–666, 1996.
- [279] T. Dragic *et al.*, "HIV-1 entry into CD4+ cells is mediated by the chemokine receptor CC-CKR-5," *Nature*, vol. 381, no. 6584, pp. 667–673, 1996.
- [280] D. Finzi *et al.*, "Identification of a reservoir for HIV-1 in patients on highly active antiretroviral therapy," *Science (80-)*, vol. 278, no. 5341, pp. 1295–1300, Nov. 1997.
- [281] F. Clavel *et al.*, "Isolation of a new human retrovirus from West African patients with AIDS," *Science (80-)*, vol. 233, no. 4761, pp. 343–346, 1986.
- [282] P. M. Sharp and B. H. Hahn, "Origins of HIV and the AIDS pandemic," *Cold Spring Harb. Perspect. Med.*, vol. 1, no. 1, Sep. 2011.

- [283] T. Huet, R. Cheynier, A. Meyerhans, G. Roelants, and S. Wain-Hobson, "Genetic organization of a chimpanzee lentivirus related to HIV-1," *Nature*, vol. 345, no. 6273, pp. 356–359, 1990.
- [284] V. M. Hirsch, R. A. Olmsted, M. Murphey-Corb, R. H. Purcell, and P. R. Johnson, "An African primate lentivirus (SIVsmclosely related to HIV-2)," *Nature*, vol. 339, no. 6223, pp. 389–392, 1989.
- [285] B. H. Hahn, G. M. Shaw, K. M. De Cock, and P. M. Sharp, "AIDS as a zoonosis: Scientific and public health implications," *Science*, vol. 287, no. 5453, pp. 607–614, 28-Jan-2000.
- [286] M. Worobey *et al.*, "Island biogeography reveals the deep history of SIV," *Science*, vol. 329, no. 5998, American Association for the Advancement of Science, p. 1487, 17-Sep-2010.
- [287] E. L. B. John G. Robinson, Kent H. Redford, "Wildlife Harvest in Logged Tropical Forests," *Science (80-.)*, 1999.
- [288] M. Worobey *et al.*, "Direct evidence of extensive diversity of HIV-1 in Kinshasa by 1960," *Nature*, vol. 455, no. 7213, pp. 661–664, Oct. 2008.
- [289] M. S. Cohen, G. M. Shaw, A. J. McMichael, and B. F. Haynes, "Acute HIV-1 infection," *New England Journal of Medicine*, vol. 364, no. 20, Massachusetts Medical Society, pp. 1943–1954, 19-May-2011.
- [290] F. M. Koehlin *et al.*, "Values and Preferences on the Use of Oral Pre-exposure Prophylaxis (PrEP) for HIV Prevention Among Multiple Populations: A Systematic Review of the Literature," *AIDS Behav.*, vol. 21, no. 5, pp. 1325–1335, May 2017.
- [291] M. Fearon, "The Laboratory Diagnosis of HIV Infections," *Can. J. Infect. Dis. Med. Microbiol.*, vol. 16, no. 1, pp. 26–30, 2005.
- [292] F. J. Palella *et al.*, "Declining morbidity and mortality among patients with advanced human immunodeficiency virus infection," *N. Engl. J. Med.*, vol. 338, no. 13, pp. 853–860, Mar. 1998.
- [293] B. Larder, "Mechanisms of hiv-1 drug resistance," *AIDS*, vol. 15, no. SUPPL. 5, Lippincott Williams and Wilkins, 2001.
- [294] A. G. Cotter and P. W. G. Mallon, "HIV infection and bone disease: Implications for an aging population," *Sex. Health*, vol. 8, no. 4, pp. 493–501, 2011.
- [295] B. Liang, H. Li, L. Li, R. W. Omange, Y. Hai, and M. Luo, "Current advances in HIV vaccine preclinical studies using Macaque models," *Vaccine*, vol. 37, no. 26, Elsevier Ltd, pp. 3388–3399, 06-Jun-2019.
- [296] G. Alter and D. Barouch, "Immune Correlate-Guided HIV Vaccine Design," *Cell Host and Microbe*, vol. 24, no. 1, Cell Press, pp. 25–33, 11-Jul-2018.
- [297] M. Medina-Ramírez, R. W. Sanders, and Q. J. Sattentau, "Stabilized HIV-1 envelope glycoprotein trimers for vaccine use," *Current Opinion in HIV and AIDS*, vol. 12, no. 3, Lippincott Williams and Wilkins, pp. 241–249, 01-May-2017.
- [298] Q. Sattentau, "Envelope Glycoprotein Trimers as HIV-1 Vaccine Immunogens," *Vaccines*, vol. 1, no. 4, pp. 497–512, Oct. 2013.
- [299] Q. Sattentau, "Envelope Glycoprotein Trimers as HIV-1 Vaccine Immunogens," *Vaccines*, vol. 1, no. 4, pp. 497–512, 2013.
- [300] D. L. Robertson, "HIV-1 Nomenclature Proposal," *Science (80-.)*, vol. 288, no. 5463, p. 55d–55, Apr. 2000.
- [301] J. C. Plantier *et al.*, "A new human immunodeficiency virus derived from gorillas," *Nat. Med.*, vol. 15, no. 8, pp. 871–872, Aug. 2009.
- [302] E. O. Freed, "HIV-1 replication.," *Somat. Cell Mol. Genet.*, vol. 26, no. 1–6, pp. 13–33, Nov. 2001.
- [303] T. A. White *et al.*, "Molecular architectures of trimeric SIV and HIV-1 envelope glycoproteins on intact viruses: Strain- dependent variation in quaternary structure," *PLoS Pathog.*, vol. 6, no. 12, 2010.
- [304] E. Chertova *et al.*, "Envelope Glycoprotein Incorporation, Not Shedding of Surface Envelope Glycoprotein

- (gp120/SU), Is the Primary Determinant of SU Content of Purified Human Immunodeficiency Virus Type 1 and Simian Immunodeficiency Virus," *J. Virol.*, vol. 76, no. 11, pp. 5315–5325, Jun. 2002.
- [305] R. Blumenthal, S. Durell, and M. Viard, "HIV entry and envelope glycoprotein-mediated fusion," *Journal of Biological Chemistry*, vol. 287, no. 49, pp. 40841–40849, 30-Nov-2012.
- [306] W. C. Greene and B. M. Peterlin, "Charting HIV's remarkable voyage through the cell: Basic science as a passport to future therapy," *Nature Medicine*, vol. 8, no. 7, pp. 673–680, 2002.
- [307] F. Pereyra *et al.*, "Genetic and Immunologic Heterogeneity among Persons Who Control HIV Infection in the Absence of Therapy," *J. Infect. Dis.*, vol. 197, no. 4, pp. 563–571, Feb. 2008.
- [308] M. H. Malim and M. Emerman, "HIV-1 Accessory Proteins-Ensuring Viral Survival in a Hostile Environment," *Cell Host and Microbe*, vol. 3, no. 6, pp. 388–398, 12-Jun-2008.
- [309] G. Raposo *et al.*, "Human macrophages accumulate HIV-1 particles in MHC II compartments," *Traffic*, vol. 3, no. 10, pp. 718–729, 2002.
- [310] C. B. Wilen, J. C. Tilton, and R. W. Doms, "HIV: Cell binding and entry," *Cold Spring Harb. Perspect. Med.*, vol. 2, no. 8, 2012.
- [311] Y. Ghiglione and G. Turk, "Nef performance in macrophages: the master orchestrator of viral persistence and spread," *Curr. HIV Res.*, vol. 9, no. 7, pp. 505–13, Oct. 2011.
- [312] N. J. Arhel and F. Kirchhoff, "Implications of Nef: Host Cell Interactions in Viral Persistence and Progression to AIDS," 2009, pp. 147–175.
- [313] M. Geyer, O. T. Fackler, and B. M. Peterlin, "Structure-function relationships in HIV-1 Nef," *EMBO Reports*, vol. 2, no. 7, pp. 580–585, 2001.
- [314] S. Benichou and A. Benmerah, "[The HIV nef and the Kaposi-sarcoma-associated virus K3/K5 proteins: 'parasites' of the endocytosis pathway]," *Med Sci*, vol. 19, no. 1, pp. 100–106, 2003.
- [315] B. Stolp and O. T. Fackler, "How HIV takes advantage of the cytoskeleton in entry and replication," *Viruses*, vol. 3, no. 4, pp. 293–311, Apr-2011.
- [316] O. T. Fackler and H. G. Kräusslich, "Interactions of human retroviruses with the host cell cytoskeleton," *Current Opinion in Microbiology*, vol. 9, no. 4, pp. 409–415, Aug-2006.
- [317] C. Vérollet, V. Le Cabec, and I. Maridonneau-Parini, "HIV-1 infection of T lymphocytes and macrophages affects their migration via Nef," *Front. Immunol.*, vol. 6, no. OCT, 2015.
- [318] C. Vérollet *et al.*, "HIV-1 reprograms the migration of macrophages," *Blood*, vol. 125, no. 10, pp. 1611–1622, 2015.
- [319] C. Vérollet *et al.*, "HIV-1 Nef Triggers Macrophage Fusion in a p61Hck- and Protease-Dependent Manner," *J. Immunol.*, vol. 184, no. 12, pp. 7030–7039, Jun. 2010.
- [320] J. S. McDougal, J. K. Nicholson, G. D. Cross, S. P. Cort, M. S. Kennedy, and A. C. Mawle, "Binding of the human retrovirus HTLV-III/LAV/ARV/HIV to the CD4 (T4) molecule: conformation dependence, epitope mapping, antibody inhibition, and potential for idiotypic mimicry," *J. Immunol.*, vol. 137, no. 9, pp. 2937–44, Nov. 1986.
- [321] Q. J. Sattentau and R. A. Weiss, "The CD4 antigen: Physiological ligand and HIV receptor," *Cell*, vol. 52, no. 5, pp. 631–633, 11-Mar-1988.
- [322] J. Gohda *et al.*, "HIV-1 replicates in human osteoclasts and enhances their differentiation in vitro," *Retrovirology*, vol. 12, no. 1, Feb. 2015.
- [323] B. Raynaud-Messina *et al.*, "Bone degradation machinery of osteoclasts: An HIV-1 target that contributes to bone loss," *Proc. Natl. Acad. Sci. U. S. A.*, vol. 115, no. 11, pp. E2556–E2565, 2018.
- [324] A. G. Dalgleish, P. C. L. Beverley, P. R. Clapham, D. H. Crawford, M. F. Greaves, and R. A. Weiss, "The CD4 (T4) antigen is an essential component of the receptor for the AIDS retrovirus," *Nature*, vol. 312, no.

5996, pp. 763–767, 1984.

- [325] D. Klatzmann *et al.*, “IMMUNE STATUS OF AIDS PATIENTS IN FRANCE: RELATIONSHIP WITH LYMPHADENOPATHY ASSOCIATED VIRUS TROPISM,” *Ann. N. Y. Acad. Sci.*, vol. 437, no. 1, pp. 228–237, 1984.
- [326] G. Alkhatib, “The biology of CCR5 and CXCR4,” *Current Opinion in HIV and AIDS*, vol. 4, no. 2. pp. 96–103, Mar-2009.
- [327] S. B. Joseph and R. Swanstrom, “The evolution of HIV-1 entry phenotypes as a guide to changing target cells,” *Journal of Leukocyte Biology*, vol. 103, no. 3. Wiley-Blackwell, pp. 421–431, 01-Mar-2018.
- [328] M. Carrington, M. Dean, M. P. Martin, and S. J. O’Brien, “Genetics of HIV-1 infection: Chemokine receptor CCR5 polymorphism and its consequences,” *Human Molecular Genetics*, vol. 8, no. 10. pp. 1939–1945, 1999.
- [329] D. Schols, “HIV Co-receptors as Targets for Antiviral Therapy,” *Curr. Top. Med. Chem.*, vol. 4, no. 9, pp. 883–893, Mar. 2005.
- [330] S. Ledger *et al.*, “Analysis and dissociation of anti-HIV effects of shRNA to CCR5 and the fusion inhibitor C46,” *J. Gene Med.*, vol. 20, no. 2–3, Feb. 2018.
- [331] G. Pantaleo, C. Graziosi, and A. S. Fauci, “The role of lymphoid organs in the pathogenesis of hiv infection,” *Semin. Immunol.*, vol. 5, no. 3, pp. 157–163, 1993.
- [332] J. Cohen, “Has a second person with HIV been cured?,” *Science (80-.)*, 2019.
- [333] J. Kou and Y. Q. Kuang, “Mutations in chemokine receptors and AIDS,” in *Progress in Molecular Biology and Translational Science*, vol. 161, Elsevier B.V., 2019, pp. 113–124.
- [334] Y. Ganor and M. Bomsel, “HIV-1 Transmission in the Male Genital Tract,” *American Journal of Reproductive Immunology*, vol. 65, no. 3. pp. 284–291, Mar-2011.
- [335] P. Delobel *et al.*, “R5 to X4 switch of the predominant HIV-1 population in cellular reservoirs during effective highly active antiretroviral therapy,” *J. Acquir. Immune Defic. Syndr.*, vol. 38, no. 4, pp. 382–392, Apr. 2005.
- [336] E. W. Fiebig *et al.*, “Dynamics of HIV viremia and antibody seroconversion in plasma donors: Implications for diagnosis and staging of primary HIV infection,” *AIDS*, vol. 17, no. 13, pp. 1871–1879, Sep. 2003.
- [337] M. S. Cohen, C. L. Gay, M. P. Busch, and F. M. Hecht, “The Detection of Acute HIV Infection,” *J. Infect. Dis.*, vol. 202, no. S2, pp. S270–S277, Oct. 2010.
- [338] A. J. McMichael, P. Borrow, G. D. Tomaras, N. Goonetilleke, and B. F. Haynes, “The immune response during acute HIV-1 infection: Clues for vaccine development,” *Nature Reviews Immunology*, vol. 10, no. 1. pp. 11–23, Jan-2010.
- [339] H. Hocini and M. Bomsel, “Infectious Human Immunodeficiency Virus Can Rapidly Penetrate a Tight Human Epithelial Barrier by Transcytosis in a Process Impaired by Mucosal Immunoglobulins,” *J. Infect. Dis.*, vol. 179, no. s3, pp. S448–S453, May 1999.
- [340] A. Nazli *et al.*, “Exposure to HIV-1 directly impairs mucosal epithelial barrier integrity allowing microbial translocation.,” *PLoS Pathog.*, vol. 6, no. 4, p. e1000852, Apr. 2010.
- [341] C. Chu and P. A. Selwyn, “Diagnosis and initial management of acute HIV infection.,” *Am. Fam. Physician*, vol. 81, no. 10, pp. 1239–44, May 2010.
- [342] D. Douek, “HIV disease progression: immune activation, microbes, and a leaky gut.,” *Top. HIV Med.*, vol. 15, no. 4, pp. 114–7.
- [343] M. T. May and S. M. Ingle, “Life expectancy of HIV-positive adults: A review,” *Sexual Health*, vol. 8, no. 4. pp. 526–533, 2011.
- [344] M. Février, K. Dorgham, and A. Rebollo, “CD4 +T cell depletion in human immunodeficiency virus (HIV)

- infection: Role of apoptosis," *Viruses*, vol. 3, no. 5. pp. 586–612, May-2011.
- [345] A. E. Sousa, J. Carneiro, M. Meier-Schellersheim, Z. Grossman, and R. M. M. Victorino, "CD4 T Cell Depletion Is Linked Directly to Immune Activation in the Pathogenesis of HIV-1 and HIV-2 but Only Indirectly to the Viral Load," *J. Immunol.*, vol. 169, no. 6, pp. 3400–3406, Sep. 2002.
- [346] "hiv.gov." .
- [347] D. C. Douek, M. Roederer, and R. A. Koup, "Emerging Concepts in the Immunopathogenesis of AIDS," *Annu. Rev. Med.*, vol. 60, no. 1, pp. 471–484, 2009.
- [348] D. P. Kotler, H. P. Gaetz, M. Lange, E. B. Klein, and P. R. Holt, "Enteropathy associated with the acquired immunodeficiency syndrome," *Ann. Intern. Med.*, vol. 101, no. 4, pp. 421–428, 1984.
- [349] S. Kewenig *et al.*, "Rapid mucosal CD4+ T-cell depletion and enteropathy in simian immunodeficiency virus-infected rhesus macaques," *Gastroenterology*, vol. 116, no. 5, pp. 1115–1123, 1999.
- [350] J. M. Brenchley *et al.*, "CD4+ T cell depletion during all stages of HIV disease occurs predominantly in the gastrointestinal tract," *J. Exp. Med.*, vol. 200, no. 6, pp. 749–759, Sep. 2004.
- [351] Q. Li *et al.*, "Peak SIV replication in resting memory CD4 + T cells depletes gut lamina propria CD4 + T cells," *Nature*, vol. 434, no. 7037, pp. 1148–1152, Apr. 2005.
- [352] S. Mehandru *et al.*, "Primary HIV-1 infection is associated with preferential depletion of CD4+ T lymphocytes from effector sites in the gastrointestinal tract," *J. Exp. Med.*, vol. 200, no. 6, pp. 761–770, Sep. 2004.
- [353] M. Guadalupe *et al.*, "Severe CD4+ T-Cell Depletion in Gut Lymphoid Tissue during Primary Human Immunodeficiency Virus Type 1 Infection and Substantial Delay in Restoration following Highly Active Antiretroviral Therapy," *J. Virol.*, vol. 77, no. 21, pp. 11708–11717, Nov. 2003.
- [354] R. S. Veazey *et al.*, "Gastrointestinal tract as a major site of CD4+ T cell depletion and viral replication in SIV infection," *Science (80-.)*, vol. 280, no. 5362, pp. 427–431, Apr. 1998.
- [355] V. Cecchinato *et al.*, "Altered balance between Th17 and Th1 cells at mucosal sites predicts AIDS progression in simian immunodeficiency virus-infected macaques," *Mucosal Immunol.*, vol. 1, no. 4, pp. 279–288, Jul. 2008.
- [356] S. Sankaran *et al.*, "Gut mucosal T cell responses and gene expression correlate with protection against disease in long-term HIV-1-infected nonprogressors," *Proc. Natl. Acad. Sci. U. S. A.*, vol. 102, no. 28, pp. 9860–9865, Jul. 2005.
- [357] A. F. Suffredini, H. D. Hochstein, and F. G. McMahon, "Dose-Related Inflammatory Effects of Intravenous Endotoxin in Humans: Evaluation of a New Clinical Lot of Escherichia coli O:113 Endotoxin," *J. Infect. Dis.*, vol. 179, no. 5, pp. 1278–1282, May 1999.
- [358] T. Sokoya, H. C. Steel, M. Nieuwoudt, and T. M. Rossouw, "HIV as a Cause of Immune Activation and Immunosenescence," *Mediators of Inflammation*, vol. 2017. Hindawi Limited, 2017.
- [359] P. Ye, D. E. Kirschner, and A. P. Kourtis, "The thymus during HIV disease: role in pathogenesis and in immune recovery.," *Curr. HIV Res.*, vol. 2, no. 2, pp. 177–83, Apr. 2004.
- [360] M. Dagarag, H. Ng, R. Lubong, R. B. Effros, and O. O. Yang, "Differential Impairment of Lytic and Cytokine Functions in Senescent Human Immunodeficiency Virus Type 1-Specific Cytotoxic T Lymphocytes," *J. Virol.*, vol. 77, no. 5, pp. 3077–3083, Mar. 2003.
- [361] V. Appay and S. L. Rowland-Jones, "Premature ageing of the immune system: the cause of AIDS?," *Trends Immunol.*, vol. 23, no. 12, pp. 580–5, Dec. 2002.
- [362] L. Meyaard, S. A. Otto, R. R. Jonker, M. J. Mijster, R. P. M. Keet, and F. Miedema, "Programmed death of T cells in HIV-1 infection," *Science (80-.)*, vol. 257, no. 5067, pp. 217–219, 1992.
- [363] M. Massanella *et al.*, "CD4 T-cell hyperactivation and susceptibility to cell death determine poor CD4 T-

- cell recovery during suppressive HAART," *AIDS*, vol. 24, no. 7, pp. 959–968, Apr. 2010.
- [364] L. Zheng, G. Fisher, R. E. Miller, J. Peschon, D. H. Lynch, and M. J. Lenardo, "Induction of apoptosis in mature T cells by tumour necrosis factor," *Nature*, vol. 377, no. 6547, pp. 348–351, Sep. 1995.
- [365] U. Mählkecht and G. Herbein, "Macrophages and T-cell apoptosis in HIV infection: a leading role for accessory cells?," *Trends Immunol.*, vol. 22, no. 5, pp. 256–60, May 2001.
- [366] J. E. Schmitz *et al.*, "Control of viremia in simian immunodeficiency virus infection by CD8+ lymphocytes," *Science (80-.)*, vol. 283, no. 5403, pp. 857–860, Feb. 1999.
- [367] R. A. Koup *et al.*, "Temporal association of cellular immune responses with the initial control of viremia in primary human immunodeficiency virus type 1 syndrome.," *J. Virol.*, vol. 68, no. 7, pp. 4650–5, Jul. 1994.
- [368] S. C. Zimmerli, A. Harari, C. Cellera, F. Vallelian, P. A. Bart, and G. Pantaleo, "HIV-1-specific IFN- γ /IL-2-secreting CD8 T cells support CD4-independent proliferation of HIV-1-specific CD8 T cells," *Proc. Natl. Acad. Sci. U. S. A.*, vol. 102, no. 20, pp. 7239–7244, May 2005.
- [369] J. W. Critchfield *et al.*, "Multifunctional Human Immunodeficiency Virus (HIV) Gag-Specific CD8+ T-Cell Responses in Rectal Mucosa and Peripheral Blood Mononuclear Cells during Chronic HIV Type 1 Infection," *J. Virol.*, vol. 81, no. 11, pp. 5460–5471, Jun. 2007.
- [370] C. Petrovas *et al.*, "PD-1 is a regulator of virus-specific CD8+ T cell survival in HIV infection," *J. Exp. Med.*, vol. 203, no. 10, pp. 2281–2292, 2006.
- [371] J. Y. Zhang *et al.*, "PD-1 up-regulation is correlated with HIV-specific memory CD8+ T-cell exhaustion in typical progressors but not in long-term nonprogressors," *Blood*, vol. 109, no. 11, pp. 4671–4678, Jun. 2007.
- [372] G. D. Gaiha *et al.*, "Dysfunctional HIV-specific CD8+ T cell proliferation is associated with increased caspase-8 activity and mediated by necroptosis," *Immunity*, vol. 41, no. 6, pp. 1001–1012, Dec. 2014.
- [373] L. Trautmann *et al.*, "Upregulation of PD-1 expression on HIV-specific CD8+ T cells leads to reversible immune dysfunction," *Nat. Med.*, vol. 12, no. 10, pp. 1198–1202, 2006.
- [374] A. Khaitan and D. Unutmaz, "Revisiting immune exhaustion during HIV infection," *Current HIV/AIDS Reports*, vol. 8, no. 1, pp. 4–11, Mar-2011.
- [375] S. Neri, J. Leung, G. Besutti, A. Santoro, L. M. Fabbri, and G. Guaraldi, "Chronic lung disease in HIV patients," *AIDS Rev.*, vol. 20, no. 3, pp. 150–157, Jul. 2018.
- [376] B. S. Staitieh, E. E. Egea, and D. M. Guidot, "Pulmonary innate immune dysfunction in human immunodeficiency virus," *American Journal of Respiratory Cell and Molecular Biology*, vol. 56, no. 5. American Thoracic Society, pp. 563–567, 01-May-2017.
- [377] T. R. Kiderlen, J. Siehl, and M. Hentrich, "HIV-Associated Lung Cancer," *Oncology Research and Treatment*, vol. 40, no. 3. S. Karger AG, pp. 88–92, 01-Mar-2017.
- [378] I. Ofotokun, "Deciphering how HIV-1 weakens and cracks the bone," *Proceedings of the National Academy of Sciences of the United States of America*, vol. 115, no. 11. National Academy of Sciences, pp. 2551–2553, 13-Mar-2018.
- [379] J. J. Yang *et al.*, "Autoimmune diseases-related arthritis in HIV-infected patients in the era of highly active antiretroviral therapy," *J. Microbiol. Immunol. Infect.*, vol. 48, no. 2, pp. 130–136, Apr. 2015.
- [380] N. Ntusi *et al.*, "HIV-1-Related Cardiovascular Disease Is Associated with Chronic Inflammation, Frequent Pericardial Effusions, and Probable Myocardial Edema," *Circ. Cardiovasc. Imaging*, vol. 9, no. 3, Mar. 2016.
- [381] P. Chan, J. Hellmuth, S. Spudich, and V. Valcour, "Cognitive Impairment and Persistent CNS Injury in Treated HIV," *Current HIV/AIDS Reports*, vol. 13, no. 4. Current Medicine Group LLC 1, pp. 209–217, 01-Aug-2016.

- [382] R. De Wit, C. A. B. Boucher, K. H. N. Veenhof, J. K. M. E. Schattenkerk, P. J. M. Bakker, and S. A. Danner, "CLINICAL AND VIROLOGICAL EFFECTS OF HIGH-DOSE RECOMBINANT INTERFERON- α IN DISSEMINATED AIDS-RELATED KAPOSI'S SARCOMA," *Lancet*, vol. 332, no. 8622, pp. 1214–1217, Nov. 1988.
- [383] H. C. Lane *et al.*, "Anti-retroviral effects of interferon-alpha in AIDS-associated Kaposi's sarcoma.," *Lancet (London, England)*, vol. 2, no. 8622, pp. 1218–22, Nov. 1988.
- [384] H. C. Lane *et al.*, "Interferon- α in patients with asymptomatic human immunodeficiency virus (HIV) infection. A randomized, placebo-controlled trial," *Ann. Intern. Med.*, vol. 112, no. 11, pp. 805–811, 1990.
- [385] N. Noël, B. Jacquelin, N. Huot, C. Goujard, O. Lambotte, and M. Müller-Trutwin, "Interferon-associated therapies towards HIV control: The back and forth," *Cytokine Growth Factor Rev.*, vol. 40, pp. 99–112, 2018.
- [386] D. M. Asmuth *et al.*, "Safety, Tolerability, and Mechanisms of Antiretroviral Activity of Pegylated Interferon Alfa-2a in HIV-1–Monoinfected Participants: A Phase II Clinical Trial," *J. Infect. Dis.*, vol. 201, no. 11, pp. 1686–1696, Jun. 2010.
- [387] F. Boué *et al.*, "Alpha interferon administration during structured interruptions of combination antiretroviral therapy in patients with chronic HIV-1 infection: INTERVAC ANRS 105 trial," *AIDS*, vol. 25, no. 1, pp. 115–118, 02-Jan-2011.
- [388] C. Goujard *et al.*, "Continuous versus intermittent treatment strategies during primary HIV-1 infection: The randomized ANRS INTERPRIM Trial," *AIDS*, vol. 26, no. 15, pp. 1895–1905, Sep. 2012.
- [389] L. Azzoni *et al.*, "Pegylated interferon alfa-2a monotherapy results in suppression of HIV type 1 replication and decreased cell-associated HIV DNA integration," *J. Infect. Dis.*, vol. 207, no. 2, pp. 213–222, 2013.
- [390] C. Scagnolari and G. Antonelli, "Type I interferon and HIV: Subtle balance between antiviral activity, immunopathogenesis and the microbiome," *Cytokine and Growth Factor Reviews*, vol. 40. Elsevier Ltd, pp. 19–31, 01-Apr-2018.
- [391] M. S. Harper *et al.*, "Interferon- α Subtypes in an Ex Vivo Model of Acute HIV-1 Infection: Expression, Potency and Effector Mechanisms," *PLoS Pathog.*, vol. 11, no. 11, Nov. 2015.
- [392] K. J. Lavender *et al.*, "Interferon Alpha Subtype-Specific Suppression of HIV-1 Infection In Vivo," *J. Virol.*, vol. 90, no. 13, pp. 6001–6013, Jul. 2016.
- [393] S. Abraham, J. G. Choi, N. M. Ortega, J. Zhang, P. Shankar, and N. M. Swamy, "Gene therapy with plasmids encoding IFN- β or IFN- α 14 confers long-term resistance to HIV-1 in humanized mice," *Oncotarget*, vol. 7, no. 48, pp. 78412–78420, 2016.
- [394] H. Hofmann, B. Vanwalscappel, N. Bloch, and N. R. Landau, "TLR7/8 agonist induces a post-entry SAMHD1-independent block to HIV-1 infection of monocytes," *Retrovirology*, vol. 13, no. 1, Dec. 2016.
- [395] E. Poteet *et al.*, "Toll-like receptor 3 adjuvant in combination with virus-like particles elicit a humoral response against HIV," *Vaccine*, vol. 34, no. 48, pp. 5886–5894, Nov. 2016.
- [396] C. Gavegnano, M. Detorio, C. Montero, A. Bosque, V. Planelles, and R. F. Schinazi, "Ruxolitinib and tofacitinib are potent and selective inhibitors of HIV-1 replication and virus reactivation in vitro," *Antimicrob. Agents Chemother.*, vol. 58, no. 4, pp. 1977–1986, 2014.
- [397] W. B. Haile, C. Gavegnano, S. Tao, Y. Jiang, R. F. Schinazi, and W. R. Tyor, "The Janus kinase inhibitor ruxolitinib reduces HIV replication in human macrophages and ameliorates HIV encephalitis in a murine model," *Neurobiol. Dis.*, vol. 92, pp. 137–143, Aug. 2016.
- [398] A. T. Haase, "Targeting early infection to prevent HIV-1 mucosal transmission," *Nature*, vol. 464, no. 7286, pp. 217–223, 11-Mar-2010.
- [399] C. Scagnolari and G. Antonelli, "Type I interferon and HIV: Subtle balance between antiviral activity, immunopathogenesis and the microbiome," *Cytokine Growth Factor Rev.*, vol. 40, pp. 19–31, 2018.
- [400] R. S. Veazey *et al.*, "Prevention of SHIV transmission by topical IFN- β treatment," *Mucosal Immunol.*, vol.

9, no. 6, pp. 1528–1536, Nov. 2016.

- [401] N. G. Sandler *et al.*, “Type I interferon responses in rhesus macaques prevent SIV infection and slow disease progression,” *Nature*, vol. 511, no. 7511, pp. 601–605, 2014.
- [402] B. Jacquelin *et al.*, “Nonpathogenic SIV infection of African green monkeys induces a strong but rapidly controlled type I IFN response,” *J. Clin. Invest.*, vol. 119, no. 12, pp. 3544–3555, Dec. 2009.
- [403] J. N. Mandl *et al.*, “Divergent TLR7 and TLR9 signaling and type I interferon production distinguish pathogenic and nonpathogenic AIDS virus infections,” *Nat. Med.*, vol. 14, no. 10, pp. 1077–1087, Oct. 2008.
- [404] M. Rotger *et al.*, “Comparative transcriptomics of extreme phenotypes of human HIV-1 infection and SIV infection in sooty mangabey and rhesus macaque,” *J. Clin. Invest.*, vol. 121, no. 6, pp. 2391–2400, Jun. 2011.
- [405] A. Zhen *et al.*, “Targeting type I interferon-mediated activation restores immune function in chronic HIV infection,” *J. Clin. Invest.*, vol. 127, no. 1, pp. 260–268, Jan. 2017.
- [406] T. Doyle, C. Goujon, and M. H. Malim, “HIV-1 and interferons: Who’s interfering with whom?,” *Nat. Rev. Microbiol.*, vol. 13, no. 7, pp. 403–413, 2015.
- [407] A. Soper *et al.*, “Type I interferon responses by HIV-1 infection: Association with disease progression and control,” *Front. Immunol.*, vol. 8, no. JAN, pp. 1–11, 2018.
- [408] Y. Kumagai *et al.*, “Alveolar Macrophages Are the Primary Interferon- α Producer in Pulmonary Infection with RNA Viruses,” *Immunity*, vol. 27, no. 2, pp. 240–252, Aug. 2007.
- [409] K. M. Monroe *et al.*, “IFI16 DNA sensor is required for death of lymphoid CD4 T cells abortively infected with HIV,” *Science (80-.)*, vol. 343, no. 6169, pp. 428–432, 2014.
- [410] M. R. Jakobsen *et al.*, “IFI16 senses DNA forms of the lentiviral replication cycle and controls HIV-1 replication,” *Proc. Natl. Acad. Sci. U. S. A.*, vol. 110, no. 48, Nov. 2013.
- [411] G. Doitsh *et al.*, “Cell death by pyroptosis drives CD4 T-cell depletion in HIV-1 infection,” *Nature*, vol. 505, no. 7484, pp. 509–514, 2014.
- [412] D. Gao *et al.*, “Cyclic GMP-AMP synthase is an innate immune sensor of HIV and other retroviruses,” *Science (80-.)*, vol. 341, no. 6148, pp. 903–906, 2013.
- [413] X. Lahaye *et al.*, “The Capsids of HIV-1 and HIV-2 Determine Immune Detection of the Viral cDNA by the Innate Sensor cGAS in Dendritic Cells,” *Immunity*, vol. 39, no. 6, pp. 1132–1142, Dec. 2013.
- [414] T. Bruel *et al.*, “Plasmacytoid Dendritic Cell Dynamics Tune Interferon- α Production in SIV-Infected Cynomolgus Macaques,” *PLoS Pathog.*, vol. 10, no. 1, Jan. 2014.
- [415] M. Kader *et al.*, “Blocking TLR7- and TLR9-mediated IFN- α Production by Plasmacytoid Dendritic Cells Does Not Diminish Immune Activation in Early SIV Infection,” *PLoS Pathog.*, vol. 9, no. 7, Jul. 2013.
- [416] N. Manel and D. R. Littman, “Hiding in plain sight: How HIV evades innate immune responses,” *Cell*, vol. 147, no. 2, pp. 271–274, 14-Oct-2011.
- [417] J. Tsang *et al.*, “HIV-1 infection of macrophages is dependent on evasion of innate immune cellular activation,” *AIDS*, vol. 23, no. 17, pp. 2255–2263, Nov. 2009.
- [418] N. Yan, A. D. Regalado-Magdos, B. Stiggelbout, M. A. Lee-Kirsch, and J. Lieberman, “The cytosolic exonuclease TREX1 inhibits the innate immune response to human immunodeficiency virus type 1,” *Nat. Immunol.*, vol. 11, no. 11, pp. 1005–1013, Nov. 2010.
- [419] A. N. Harman *et al.*, “HIV infection of dendritic cells subverts the IFN induction pathway via IRF-1 and inhibits type I IFN production,” *Blood*, vol. 118, no. 2, pp. 298–308, Jul. 2011.
- [420] A. Okumura, T. Alce, B. Lubyova, H. Ezelle, K. Strebel, and P. M. Pitha, “HIV-1 accessory proteins VPR and Vif modulate antiviral response by targeting IRF-3 for degradation,” *Virology*, vol. 373, no. 1, pp. 85–97,

Mar. 2008.

- [421] L. N. Akhtar *et al.*, "Suppressor of Cytokine Signaling 3 Inhibits Antiviral IFN- β Signaling To Enhance HIV-1 Replication in Macrophages," *J. Immunol.*, vol. 185, no. 4, pp. 2393–2404, Aug. 2010.
- [422] T. Pertel *et al.*, "TRIM5 is an innate immune sensor for the retrovirus capsid lattice," *Nature*, vol. 472, no. 7343, pp. 361–365, Apr. 2011.
- [423] R. P. Galão, A. Le Tortorec, S. Pickering, T. Kueck, and S. J. D. Neil, "Innate sensing of HIV-1 assembly by tetherin induces NF κ B-dependent proinflammatory responses," *Cell Host Microbe*, vol. 12, no. 5, pp. 633–644, Nov. 2012.
- [424] L. B. Ivashkiv and L. T. Donlin, "Regulation of type I interferon responses," *Nature Reviews Immunology*, vol. 14, no. 1, pp. 36–49, Jan-2014.
- [425] W. M. Schneider, M. D. Chevillotte, and C. M. Rice, "Interferon-Stimulated Genes: A Complex Web of Host Defenses," *Annu. Rev. Immunol.*, vol. 32, no. 1, pp. 513–545, 2014.
- [426] R. S. Harris, J. F. Hultquist, and D. T. Evans, "The restriction factors of human immunodeficiency virus," *J. Biol. Chem.*, vol. 287, no. 49, pp. 40875–40883, 2012.
- [427] N. Laguette *et al.*, "SAMHD1 is the dendritic- and myeloid-cell-specific HIV-1 restriction factor counteracted by Vpx," *Nature*, vol. 474, no. 7353, pp. 654–657, Jun. 2011.
- [428] P. Mlcochova *et al.*, "A G1-like state allows HIV-1 to bypass SAMHD1 restriction in macrophages," *EMBO J.*, vol. 36, no. 5, pp. 604–616, Mar. 2017.
- [429] B. Descours *et al.*, "SAMHD1 restricts HIV-1 reverse transcription in quiescent CD4 + T-cells," *Retrovirology*, vol. 9, Oct. 2012.
- [430] H. M. Baldauf *et al.*, "SAMHD1 restricts HIV-1 infection in resting CD4 + T cells," *Nat. Med.*, vol. 18, no. 11, pp. 1682–1687, Nov. 2012.
- [431] D. C. Goldstone *et al.*, "HIV-1 restriction factor SAMHD1 is a deoxynucleoside triphosphate triphosphohydrolase," *Nature*, vol. 480, no. 7377, pp. 379–382, Dec. 2011.
- [432] S. M. Amie, E. Noble, and B. Kim, "Intracellular nucleotide levels and the control of retroviral infections," *Virology*, vol. 436, no. 2, pp. 247–254, 20-Feb-2013.
- [433] J. Ryoo *et al.*, "The ribonuclease activity of SAMHD1 is required for HIV-1 restriction," *Nat. Med.*, vol. 20, no. 8, pp. 936–941, 2014.
- [434] I. Puigdomenech, N. Casartelli, F. Porrot, and O. Schwartz, "SAMHD1 Restricts HIV-1 Cell-to-Cell Transmission and Limits Immune Detection in Monocyte-Derived Dendritic Cells," *J. Virol.*, vol. 87, no. 5, pp. 2846–2856, Mar. 2013.
- [435] D. Ayinde *et al.*, "SAMHD1 Limits HIV-1 Antigen Presentation by Monocyte-Derived Dendritic Cells," *J. Virol.*, vol. 89, no. 14, pp. 6994–7006, Jul. 2015.
- [436] M. Aebi *et al.*, "cDNA structures and regulation of two interferon-induced human Mx proteins," *Mol. Cell. Biol.*, vol. 9, no. 11, pp. 5062–5072, Nov. 1989.
- [437] E. Gordien, O. Rosmorduc, C. Peltekian, F. Garreau, C. Brechot, and D. Kremsdorf, "Inhibition of Hepatitis B Virus Replication by the Interferon-Inducible MxA Protein," *J. Virol.*, vol. 75, no. 6, pp. 2684–2691, Mar. 2001.
- [438] C. Goujon *et al.*, "Human MX2 is an interferon-induced post-entry inhibitor of HIV-1 infection," *Nature*, vol. 502, no. 7472, pp. 559–562, 2013.
- [439] M. Kane *et al.*, "MX2 is an interferon-induced inhibitor of HIV-1 infection," *Nature*, vol. 502, no. 7472, pp. 563–566, 2013.
- [440] K. Melén, P. Keskinen, T. Ronni, T. Sareneva, K. Lounatmaa, and I. Julkunen, "Human MxB protein, an interferon- α -inducible GTPase, contains a nuclear targeting signal and is localized in the heterochromatin

- region beneath the nuclear envelope," *J. Biol. Chem.*, vol. 271, no. 38, pp. 23478–23486, 1996.
- [441] C. Goujon, O. Moncorge, H. Bauby, T. Doyle, W. S. Barclay, and M. H. Malim, "Transfer of the Amino-Terminal Nuclear Envelope Targeting Domain of Human MX2 Converts MX1 into an HIV-1 Resistance Factor," *J. Virol.*, vol. 88, no. 16, pp. 9017–9026, 2014.
- [442] J. Rasaiyaah *et al.*, "HIV-1 evades innate immune recognition through specific cofactor recruitment," *Nature*, vol. 503, no. 7476, pp. 402–405, 2013.
- [443] K. A. Matreyek and A. Engelman, "Viral and cellular requirements for the nuclear entry of retroviral preintegration nucleoprotein complexes," *Viruses*, vol. 5, no. 10, pp. 2483–2511, 07-Oct-2013.
- [444] Z. Liu *et al.*, "The interferon-inducible MxB protein inhibits HIV-1 infection," *Cell Host Microbe*, vol. 14, no. 4, pp. 398–410, Oct. 2013.
- [445] S. J. D. Neil, T. Zang, and P. D. Bieniasz, "Tetherin inhibits retrovirus release and is antagonized by HIV-1 Vpu," *Nature*, vol. 451, no. 7177, pp. 425–430, Jan. 2008.
- [446] N. Van Damme *et al.*, "The Interferon-Induced Protein BST-2 Restricts HIV-1 Release and Is Downregulated from the Cell Surface by the Viral Vpu Protein," *Cell Host Microbe*, vol. 3, no. 4, pp. 245–252, Apr. 2008.
- [447] S. Kupzig, V. Korolchuk, R. Rollason, A. Sugden, A. Wilde, and G. Banting, "Bst-2/HM1.24 is a raft-associated apical membrane protein with an unusual topology," *Traffic*, vol. 4, no. 10, pp. 694–709, Oct. 2003.
- [448] D. Perez-Caballero *et al.*, "Tetherin Inhibits HIV-1 Release by Directly Tethering Virions to Cells," *Cell*, vol. 139, no. 3, pp. 499–511, Oct. 2009.
- [449] K. Miyakawa *et al.*, "BCA2/rabring7 promotes tetherin-dependent HIV-1 restriction," *PLoS Pathog.*, vol. 5, no. 12, Dec. 2009.
- [450] K. Strebel, T. Klimkait, and M. A. Martin, "A novel gene of HIV-1, vpu, and its 16-kilodalton product," *Science (80-.)*, vol. 241, no. 4870, pp. 1221–1223, 1988.
- [451] H. Chu *et al.*, "Tetherin/BST-2 is essential for the formation of the intracellular virus-containing compartment in HIV-infected macrophages," *Cell Host Microbe*, vol. 12, no. 3, pp. 360–372, Sep. 2012.
- [452] O. Leymarie *et al.*, "Contribution of the Cytoplasmic Determinants of Vpu to the Expansion of Virus-Containing Compartments in HIV-1-Infected Macrophages," *J. Virol.*, vol. 93, no. 11, Mar. 2019.
- [453] T. Kobayashi *et al.*, "Identification of Amino Acids in the Human Tetherin Transmembrane Domain Responsible for HIV-1 Vpu Interaction and Susceptibility," *J. Virol.*, vol. 85, no. 2, pp. 932–945, Jan. 2011.
- [454] Y. Iwabu *et al.*, "HIV-1 accessory protein Vpu internalizes cell-surface BST-2/tetherin through transmembrane interactions leading to lysosomes," *J. Biol. Chem.*, vol. 284, no. 50, pp. 35060–35072, Dec. 2009.
- [455] R. Vigan and S. J. D. Neil, "Determinants of Tetherin Antagonism in the Transmembrane Domain of the Human Immunodeficiency Virus Type 1 Vpu Protein," *J. Virol.*, vol. 84, no. 24, pp. 12958–12970, Dec. 2010.
- [456] M. Caillet *et al.*, "Rab7A is required for efficient production of infectious HIV-1," *PLoS Pathog.*, vol. 7, no. 11, Nov. 2011.
- [457] K. Nganou-Makamdop and D. C. Douek, "Manipulating the Interferon Signaling Pathway: Implications for HIV Infection," *Virologica Sinica*, vol. 34, no. 2, Science Press, pp. 192–196, 01-Apr-2019.
- [458] S. E. Bosinger and N. S. Uday, "Type I Interferon: Understanding Its Role in HIV Pathogenesis and Therapy," *Current HIV/AIDS Reports*, vol. 12, no. 1, Current Medicine Group LLC 1, pp. 41–53, 22-Mar-2015.
- [459] R. Hughes, G. Towers, and M. Noursadeghi, "Innate immune interferon responses to Human immunodeficiency virus-1 infection," *Reviews in Medical Virology*, vol. 22, no. 4, pp. 257–266, Jul-2012.

- [460] I. C. Anthony and P. J. E. Bell, "The Neuropathology of HIV/AIDS," *Int. Rev. Psychiatry*, vol. 20, no. 1, pp. 15–24, Jan. 2008.
- [461] P. D. Bieniasz and B. R. Cullen, "Multiple Blocks to Human Immunodeficiency Virus Type 1 Replication in Rodent Cells," *J. Virol.*, vol. 74, no. 21, pp. 9868–9877, Nov. 2000.
- [462] M. D. Marsden and J. A. Zack, "Studies of retroviral infection in humanized mice," *Virology*, vol. 479–480. Academic Press Inc., pp. 297–309, 01-May-2015.
- [463] Z. Hanna, D. G. Kay, N. Rebai, A. Guimond, S. Jothy, and P. Jolicoeur, "Nef harbors a major determinant of pathogenicity for an AIDS-like disease induced by HIV-1 in transgenic mice," *Cell*, vol. 95, no. 2, pp. 163–175, Oct. 1998.
- [464] B. L. Wei, V. K. Arora, J. L. Foster, D. L. Sodora, and J. V. Garcia, "In vivo analysis of Nef function.," *Curr. HIV Res.*, vol. 1, no. 1, pp. 41–50, Jan. 2003.
- [465] M. D. Marsden and J. A. Zack, "Humanized Mouse Models for Human Immunodeficiency Virus Infection," *Annu. Rev. Virol.*, vol. 4, no. 1, pp. 393–412, Sep. 2017.
- [466] J. B. Honeycutt *et al.*, "Macrophages sustain HIV replication in vivo independently of T cells," *J. Clin. Invest.*, vol. 126, no. 4, pp. 1353–1366, Apr. 2016.
- [467] J. B. Honeycutt *et al.*, "HIV persistence in tissue macrophages of humanized myeloid-only mice during antiretroviral therapy," *Nat. Med.*, vol. 23, no. 5, pp. 638–643, May 2017.
- [468] K. M. Merino, C. Allers, E. S. Didier, and M. J. Kuroda, "Role of monocyte/macrophages during HIV/SIV infection in adult and pediatric acquired immune deficiency syndrome," *Front. Immunol.*, vol. 8, no. DEC, pp. 1–16, 2017.
- [469] A. Hasegawa *et al.*, "The level of monocyte turnover predicts disease progression in the macaque model of AIDS," *Blood*, vol. 114, no. 14, pp. 2917–2925, 2009.
- [470] T. H. Burdo *et al.*, "Increased Monocyte Turnover from Bone Marrow Correlates with Severity of SIV Encephalitis and CD163 Levels in Plasma," *PLoS Pathog.*, vol. 6, no. 4, p. e1000842, Apr. 2010.
- [471] J. A. Walker, M. L. Sulciner, K. D. Nowicki, A. D. Miller, T. H. Burdo, and K. C. Williams, "Elevated numbers of CD163+ macrophages in hearts of simian immunodeficiency virus-infected monkeys correlate with cardiac pathology and fibrosis," *AIDS Res. Hum. Retroviruses*, vol. 30, no. 7, pp. 685–694, 2014.
- [472] Y. Cai *et al.*, "Increased monocyte turnover is associated with interstitial macrophage accumulation and pulmonary tissue damage in SIV-infected rhesus macaques," *J. Leukoc. Biol.*, vol. 97, no. 6, pp. 1147–1153, Jun. 2015.
- [473] Y. Cai *et al.*, "Preferential Destruction of Interstitial Macrophages over Alveolar Macrophages as a Cause of Pulmonary Disease in Simian Immunodeficiency Virus–Infected Rhesus Macaques," *J. Immunol.*, vol. 195, no. 10, pp. 4884–4891, Nov. 2015.
- [474] C. R. Avalos *et al.*, "Brain macrophages in simian immunodeficiency virus-infected, antiretroviral-suppressed macaques: A functional latent reservoir," *MBio*, vol. 8, no. 4, Jul. 2017.
- [475] E. Masliah, R. M. DeTeresa, M. E. Mallory, and L. A. Hansen, "Changes in pathological findings at autopsy in AIDS cases for the last 15 years," *AIDS*, vol. 14, no. 1, pp. 69–74, 2000.
- [476] Y. Cai, C. Sugimoto, M. Arainga, X. Alvarez, E. S. Didier, and M. J. Kuroda, "In Vivo Characterization of Alveolar and Interstitial Lung Macrophages in Rhesus Macaques: Implications for Understanding Lung Disease in Humans," *J. Immunol.*, vol. 192, no. 6, pp. 2821–2829, Mar. 2014.
- [477] F. T. Hufert, J. Schmitz, M. Schreiber, H. Schmitz, P. Rácz, and D. D. von Laer, "Human Kupffer cells infected with HIV-1 in vivo.," *J. Acquir. Immune Defic. Syndr.*, vol. 6, no. 7, pp. 772–7, Jul. 1993.
- [478] M. J. Churchill *et al.*, "Use of laser capture microdissection to detect integrated HIV-1 DNA in macrophages and astrocytes from autopsy brain tissues," *J. Neurovirol.*, vol. 12, no. 2, pp. 146–152, Apr. 2006.

- [479] A. Zalar *et al.*, "Macrophage HIV-1 infection in duodenal tissue of patients on long term HAART," *Antiviral Res.*, vol. 87, no. 2, pp. 269–271, Aug. 2010.
- [480] K. C. Jambo *et al.*, "Small alveolar macrophages are infected preferentially by HIV and exhibit impaired phagocytic function," *Mucosal Immunol.*, vol. 7, no. 5, pp. 1116–1126, 2014.
- [481] V. Rodrigues, N. Ruffin, M. San-Roman, and P. Benaroch, "Myeloid cell interaction with HIV: A complex relationship," *Frontiers in Immunology*, vol. 8, no. NOV. Frontiers Media S.A., 30-Nov-2017.
- [482] S. K. Cribbs, J. Lennox, A. M. Caliendo, L. A. Brown, and D. M. Guidot, "Healthy HIV-1-infected individuals on highly active antiretroviral therapy harbor HIV-1 in their alveolar macrophages," *AIDS Res. Hum. Retroviruses*, vol. 31, no. 1, pp. 64–70, Jan. 2015.
- [483] K. McIntosh *et al.*, "Age- and time-related changes in extracellular viral load in children vertically infected by human immunodeficiency virus," *Pediatr. Infect. Dis. J.*, vol. 15, no. 12, pp. 1087–1091, 1996.
- [484] J. M. Milush *et al.*, "Virally Induced CD4 + T Cell Depletion Is Not Sufficient to Induce AIDS in a Natural Host," *J. Immunol.*, vol. 179, no. 5, pp. 3047–3056, Sep. 2007.
- [485] V. Le Douce, G. Herbein, O. Rohr, and C. Schwartz, "Molecular mechanisms of HIV-1 persistence in the monocyte-macrophage lineage," *Retrovirology*, vol. 7. 09-Apr-2010.
- [486] M. E. Wong, A. Jaworowski, and A. C. Hearps, "The HIV reservoir in monocytes and macrophages," *Frontiers in Immunology*, vol. 10, no. JUN. Frontiers Media S.A., 2019.
- [487] J. Rappaport and D. J. Volsky, "Role of the macrophage in HIV-associated neurocognitive disorders and other comorbidities in patients on effective antiretroviral treatment," *Journal of NeuroVirology*, vol. 21, no. 3. Springer New York LLC, pp. 235–241, 16-Jun-2015.
- [488] V. Valcour *et al.*, "Central nervous system viral invasion and inflammation during acute HIV infection," *J. Infect. Dis.*, vol. 206, no. 2, pp. 275–282, Jul. 2012.
- [489] A. B. Ragin *et al.*, "Structural brain alterations can be detected early in HIV infection," *Neurology*, vol. 79, no. 24, pp. 2328–2334, Dec. 2012.
- [490] T. Ernst and L. Chang, "Effect of aging on brain metabolism in antiretroviral-naive HIV patients.," *AIDS*, vol. 18 Suppl 1, pp. S61-7, Jan. 2004.
- [491] V. Dahl *et al.*, "An example of genetically distinct HIV type 1 variants in cerebrospinal fluid and plasma during suppressive therapy.," *J. Infect. Dis.*, vol. 209, no. 10, pp. 1618–22, May 2014.
- [492] Y. Li *et al.*, "SIV infection of lung macrophages," *PLoS One*, vol. 10, no. 5, May 2015.
- [493] C. T. Costiniuk and M. A. Jenabian, "The lungs as anatomical reservoirs of HIV infection," *Reviews in Medical Virology*, vol. 24, no. 1. pp. 35–54, Jan-2014.
- [494] Y. Ganor *et al.*, "HIV-1 reservoirs in urethral macrophages of patients under suppressive antiretroviral therapy," *Nat. Microbiol.*, vol. 4, no. 4, pp. 633–644, Apr. 2019.
- [495] S. Gartner, P. Markovits, D. M. Markovitz, M. H. Kaplan, R. C. Gallo, and M. Popovic, "The role of mononuclear phagocytes in HTLV-III/LAV infection," *Science (80-.)*, vol. 233, no. 4760, pp. 215–219, 1986.
- [496] V. Marechal, M.-C. Prevost, C. Petit, E. Perret, J.-M. Heard, and O. Schwartz, "Human Immunodeficiency Virus Type 1 Entry into Macrophages Mediated by Macropinocytosis," *J. Virol.*, vol. 75, no. 22, pp. 11166–11177, Nov. 2001.
- [497] K. Miyauchi, Y. Kim, O. Latinovic, V. Morozov, and G. B. Melikyan, "HIV Enters Cells via Endocytosis and Dynamin-Dependent Fusion with Endosomes," *Cell*, vol. 137, no. 3, pp. 433–444, May 2009.
- [498] P. D. Uchil and W. Mothes, "HIV Entry Revisited," *Cell*, vol. 137, no. 3. pp. 402–404, 01-May-2009.
- [499] Y. J. Zhang *et al.*, "Use of coreceptors other than CCR5 by non-syncytium-inducing adult and pediatric isolates of human immunodeficiency virus type 1 is rare in vitro.," *J. Virol.*, vol. 72, no. 11, pp. 9337–44,

Nov. 1998.

- [500] M. Samson *et al.*, "Resistance to HIV-1 infection in caucasian individuals bearing mutant alleles of the CCR-5 chemokine receptor gene," *Nature*, vol. 382, no. 6593, pp. 722–726, 1996.
- [501] Y. Yi, S. Rana, J. D. Turner, N. Gaddis, and R. G. Collman, "CXCR-4 is expressed by primary macrophages and supports CCR5-independent infection by dual-tropic but not T-tropic isolates of human immunodeficiency virus type 1.," *J. Virol.*, vol. 72, no. 1, pp. 772–7, Jan. 1998.
- [502] H. Schmidtmayerova, M. Alfano, G. Nuovo, and M. Bukrinsky, "Human immunodeficiency virus type 1 T-lymphotropic strains enter macrophages via a CD4- and CXCR4-mediated pathway: replication is restricted at a postentry level.," *J. Virol.*, vol. 72, no. 6, pp. 4633–42, Jun. 1998.
- [503] A. Valentin, H. Trivedi, W. Lu, L. G. Kostrikis, and G. N. Pavlakis, "CXCR4 mediates entry and productive infection of syncytia-inducing (x4) hiv-1 strains in primary macrophages," *Virology*, vol. 269, no. 2, pp. 294–304, Apr. 2000.
- [504] G. Simmons *et al.*, "CXCR4 as a functional coreceptor for human immunodeficiency virus type 1 infection of primary macrophages.," *J. Virol.*, vol. 72, no. 10, pp. 8453–7, Oct. 1998.
- [505] A. Verani *et al.*, "CXCR4 is a functional coreceptor for infection of human macrophages by CXCR4-dependent primary HIV-1 isolates.," *J. Immunol.*, vol. 161, no. 5, pp. 2084–8, Sep. 1998.
- [506] C. K. Lapham, M. B. Zaitseva, S. Lee, T. Romanstseva, and H. Golding, "Fusion of monocytes and macrophages with HIV-1 correlates with biochemical properties of CXCR4 and CCR5," *Nat. Med.*, vol. 5, no. 3, pp. 303–308, 1999.
- [507] D. G. Nguyen and J. E. K. Hildreth, "Involvement of macrophage mannose receptor in the binding and transmission of HIV by macrophages," pp. 483–493, 2003.
- [508] M. V. Nermut and A. Fassati, "Structural Analyses of Purified Human Immunodeficiency Virus Type 1 Intracellular Reverse Transcription Complexes," *J. Virol.*, vol. 77, no. 15, pp. 8196–8206, Aug. 2003.
- [509] W. A. O'Brien, A. Namazi, H. Kalhor, S. H. Mao, J. A. Zack, and I. S. Chen, "Kinetics of human immunodeficiency virus type 1 reverse transcription in blood mononuclear phagocytes are slowed by limitations of nucleotide precursors.," *J. Virol.*, vol. 68, no. 2, pp. 1258–63, Feb. 1994.
- [510] M. D. Miller, C. M. Farnet, and F. D. Bushman, "Human immunodeficiency virus type 1 preintegration complexes: studies of organization and composition.," *J. Virol.*, vol. 71, no. 7, pp. 5382–90, Jul. 1997.
- [511] M. I. Bukrinsky *et al.*, "Active nuclear import of human immunodeficiency virus type 1 preintegration complexes.," *Proc. Natl. Acad. Sci.*, vol. 89, no. 14, pp. 6580–6584, Jul. 1992.
- [512] G. Zybarth, N. Reiling, H. Schmidtmayerova, B. Sherry, and M. Bukrinsky, "Activation-induced resistance of human macrophages to HIV-1 infection in vitro.," *J. Immunol.*, vol. 162, no. 1, pp. 400–6, Jan. 1999.
- [513] A. Sirven, M. Titeux, W. Vainchenker, L. Coulombel, A. Dubart-kupperschmitt, and P. Charneau, "The human immunodeficiency virus type-1 central DNA flap is a crucial determinant for lentiviral vector nuclear import and gene transduction of human hematopoietic stem cells," *Blood*, vol. 96, no. 13, pp. 4103–4111, 2000.
- [514] P. Gallay, T. Hope, D. Chin, and D. Trono, "HIV-1 infection of nondividing cells through the recognition of integrase by the importin/karyopherin pathway," *Proc. Natl. Acad. Sci. U. S. A.*, vol. 94, no. 18, pp. 9825–9830, Sep. 1997.
- [515] Y. Jenkins, M. McEntee, K. Weis, and W. C. Greene, "Characterization of HIV-1 Vpr nuclear import: Analysis of signals and pathways," *J. Cell Biol.*, vol. 143, no. 4, pp. 875–885, Nov. 1998.
- [516] S. Welsch, O. T. Keppler, A. Habermann, I. Allespach, J. Krijnse-Locker, and H. G. Kräusslich, "HIV-1 buds predominantly at the plasma membrane of primary human macrophages," *PLoS Pathog.*, vol. 3, no. 3, 2007.
- [517] S. Kinoshita, L. Su, M. Amano, L. A. Timmerman, H. Kaneshima, and G. P. Nolan, "The T cell activation

- factor NF-ATc positively regulates HIV-1 replication and gene expression in T cells," *Immunity*, vol. 6, no. 3, pp. 235–244, 1997.
- [518] Z. Yang and J. D. Engel, "Human T cell transcription factor gata-3 stimulates HIV-1 expression," *Nucleic Acids Res.*, vol. 21, no. 12, pp. 2831–2836, Jun. 1993.
- [519] M. Weiden *et al.*, "Differentiation of Monocytes to Macrophages Switches the Mycobacterium tuberculosis Effect on HIV-1 Replication from Stimulation to Inhibition: Modulation of Interferon Response and CCAAT/Enhancer Binding Protein Expression," *J. Immunol.*, vol. 165, no. 4, pp. 2028–2039, 2000.
- [520] Y. Honda *et al.*, "Type I Interferon Induces Inhibitory 16-kD CCAAT/ Enhancer Binding Protein (C/EBP) β , Repressing the HIV-1 Long Terminal Repeat in Macrophages: Pulmonary Tuberculosis Alters C/EBP Expression, Enhancing HIV-1 Replication," *J. Exp. Med.*, vol. 188, no. 7, pp. 1255–1265, 2002.
- [521] A. J. Henderson and K. L. Calame, "CCAAT/enhancer binding protein (C/EBP) sites are required for HIV-1 replication in primary macrophages but not CD4+ T cells," *Proc. Natl. Acad. Sci. U. S. A.*, vol. 94, no. 16, pp. 8714–8719, Aug. 1997.
- [522] O. Rohr, C. Marban, D. Aunis, and E. Schaeffer, "Regulation of HIV-1 gene transcription: from lymphocytes to microglial cells," *J. Leukoc. Biol.*, vol. 74, no. 5, pp. 736–749, Nov. 2003.
- [523] C. Floderer *et al.*, "Single molecule localisation microscopy reveals how HIV-1 Gag proteins sense membrane virus assembly sites in living host CD4 T cells," *Sci. Rep.*, vol. 8, no. 1, Dec. 2018.
- [524] S. Welsch, A. Habermann, S. Jäger, B. Müller, J. Krijnse-Locker, and H. G. Kräusslich, "Ultrastructural analysis of ESCRT proteins suggests a role for endosome-associated tubular-vesicular membranes in ESCRT function," *Traffic*, vol. 7, no. 11, pp. 1551–1566, Nov. 2006.
- [525] J. M. Orenstein, M. S. Meltzer, T. Phipps, and H. E. Gendelman, "Cytoplasmic assembly and accumulation of human immunodeficiency virus types 1 and 2 in recombinant human colony-stimulating factor-1-treated human monocytes: an ultrastructural study," *J. Virol.*, vol. 62, no. 8, pp. 2578–86, Aug. 1988.
- [526] M. Jouve, N. Sol-Foulon, S. Watson, O. Schwartz, and P. Benaroch, "HIV-1 Buds and Accumulates in 'Nonacidic' Endosomes of Macrophages," *Cell Host Microbe*, vol. 2, no. 2, pp. 85–95, 2007.
- [527] M. Deneka, A. Pelchen-Matthews, R. Byland, E. Ruiz-Mateos, and M. Marsh, "In macrophages, HIV-1 assembles into an intracellular plasma membrane domain containing the tetraspanins CD81, CD9, and CD53," *J. Cell Biol.*, vol. 177, no. 2, pp. 329–341, Apr. 2007.
- [528] J. Tan and Q. J. Sattentau, "The HIV-1-containing macrophage compartment: A perfect cellular niche?," *Trends in Microbiology*, vol. 21, no. 8, pp. 405–412, Aug-2013.
- [529] P. Benaroch, E. Billard, R. Gaudin, M. Schindler, and M. Jouve, "HIV-1 assembly in macrophages," *Retrovirology*, vol. 7, 07-Apr-2010.
- [530] F. Groot, H.-G. Krausslich, S. Welsch, Q. J. Sattentau, and O. T. Keppler, "Architecture and Regulation of the HIV-1 Assembly and Holding Compartment in Macrophages," *J. Virol.*, vol. 85, no. 15, pp. 7922–7927, 2011.
- [531] J. M. Orenstein, "Replication of HIV-1 in vivo and in vitro," *Ultrastruct. Pathol.*, vol. 31, no. 2, pp. 151–167, Apr. 2007.
- [532] K. Gousset *et al.*, "Real-time visualization of HIV-1 GAG trafficking in infected macrophages," *PLoS Pathog.*, vol. 4, no. 3, Mar. 2008.
- [533] I. Kadiu and H. E. Gendelman, "Macrophage bridging conduit trafficking of HIV-1 through the endoplasmic reticulum and golgi network," *J. Proteome Res.*, vol. 10, no. 7, pp. 3225–3238, Jul. 2011.
- [534] E. A. Eugenin, P. J. Gaskill, and J. W. Berman, "Tunneling nanotubes (TNT) are induced by HIV-infection of macrophages: A potential mechanism for intercellular HIV trafficking," *Cell. Immunol.*, vol. 254, no. 2, pp. 142–148, 2009.

- [535] R. Gaudin *et al.*, "Critical role for the kinesin KIF3A in the HIV life cycle in primary human macrophages," *J. Cell Biol.*, vol. 199, no. 3, pp. 467–479, Oct. 2012.
- [536] J. E. Hammonds *et al.*, "Siglec-1 initiates formation of the virus-containing compartment and enhances macrophage-to-T cell transmission of HIV-1," *PLoS Pathog.*, vol. 13, no. 1, pp. 1–28, 2017.
- [537] H. Akiyama, N. G. P. Ramirez, M. V. Gudheti, and S. Gummuluru, "CD169-Mediated Trafficking of HIV to Plasma Membrane Invaginations in Dendritic Cells Attenuates Efficacy of Anti-gp120 Broadly Neutralizing Antibodies," *PLoS Pathog.*, vol. 11, no. 3, pp. 1–23, Mar. 2015.
- [538] H. Koppensteiner, C. Banning, C. Schneider, H. Hohenberg, and M. Schindler, "Macrophage Internal HIV-1 Is Protected from Neutralizing Antibodies," *J. Virol.*, vol. 86, no. 5, pp. 2826–2836, Mar. 2012.
- [539] K. Kedzierska, R. Azzam, P. Ellery, J. Mak, A. Jaworowski, and S. M. Crowe, "Defective phagocytosis by human monocyte/macrophages following HIV-1 infection: underlying mechanisms and modulation by adjunctive cytokine therapy.," *J. Clin. Virol.*, vol. 26, no. 2, pp. 247–63, Feb. 2003.
- [540] F. Porcheray, B. Samah, C. Léone, N. Dereuddre-Bosquet, and G. Gras, "Macrophage activation and human immunodeficiency virus infection: HIV replication directs macrophages towards a pro-inflammatory phenotype while previous activation modulates macrophage susceptibility to infection and viral production," *Virology*, vol. 349, no. 1, pp. 112–120, May 2006.
- [541] D. L. Birx, R. R. Redfield, K. Tencer, A. Fowler, D. S. Burke, and G. Tosato, "Induction of interleukin-6 during human immunodeficiency virus infection.," *Blood*, vol. 76, no. 11, pp. 2303–10, Dec. 1990.
- [542] E. Cassol, L. Cassetta, M. Alfano, and G. Poli, "Macrophage polarization and HIV-1 infection," *J. Leukoc. Biol.*, vol. 87, no. 4, pp. 599–608, Apr. 2010.
- [543] E. Cassol, L. Cassetta, C. Rizzi, M. Alfano, and G. Poli, "M1 and M2a Polarization of Human Monocyte-Derived Macrophages Inhibits HIV-1 Replication by Distinct Mechanisms," *J. Immunol.*, vol. 182, no. 10, pp. 6237–6246, May 2009.
- [544] G. Poli, A. L. Kinter, and A. S. Fauci, "Interleukin 1 induces expression of the human immunodeficiency virus alone and in synergy with interleukin 6 in chronically infected U1 cells: inhibition of inductive effects by the interleukin 1 receptor antagonist.," *Proc. Natl. Acad. Sci.*, vol. 91, no. 1, pp. 108–112, Jan. 1994.
- [545] G. Poli *et al.*, "Interleukin 6 induces human immunodeficiency virus expression in infected monocytic cells alone and in synergy with tumor necrosis factor α by transcriptional and post-transcriptional mechanisms," *J. Exp. Med.*, vol. 172, no. 1, pp. 151–158, Jul. 1990.
- [546] G. Herbein and A. Varin, "The macrophage in HIV-1 infection: From activation to deactivation?," *Retrovirology*, vol. 7. 09-Apr-2010.
- [547] D. Weissman, G. Poli, and A. S. Fauci, "Interleukin 10 Blocks HIV Replication in Macrophages by Inhibiting the Autocrine Loop of Tumor Necrosis Factor α and Interleukin 6 Induction of Virus," *AIDS Res. Hum. Retroviruses*, vol. 10, no. 10, pp. 1199–1206, 1994.
- [548] L. J. Montaner, P. Griffin, and S. Gordon, "Interleukin-10 inhibits initial reverse transcription of human immunodeficiency virus type 1 and mediates a virostatic latent state in primary blood-derived human macrophages in vitro," *J. Gen. Virol.*, vol. 75, no. 12, pp. 3393–3400, Dec. 1994.
- [549] Y. R. Saville MW1, Taga K, Foli A, Broder S, Tosato G, "Interleukin-10 suppresses human immunodeficiency virus-1 replication in vitro in cells of the monocyte/macrophage lineage.," *Blood*, 1994.
- [550] S. Souriant *et al.*, "Tuberculosis Exacerbates HIV-1 Infection through IL-10/STAT3-Dependent Tunneling Nanotube Formation in Macrophages," *Cell Rep.*, vol. 26, no. 13, p. 3586–3599.e7, Mar. 2019.
- [551] J. Wang, K. Crawford, M. Yuan, H. Wang, P. R. Gorry, and D. Gabuzda, "Regulation of CC Chemokine Receptor 5 and CD4 Expression and Human Immunodeficiency Virus Type 1 Replication in Human Macrophages and Microglia by T Helper Type 2 Cytokines," *J. Infect. Dis.*, vol. 185, no. 7, pp. 885–897, Apr. 2002.

- [552] W. Bacrellini *et al.*, "Interleukin-10-induced HIV-1 expression is mediated by induction of both membrane-bound tumour necrosis factor (TNF)- α receptor type 1 in a promonocytic cell line," *AIDS*, vol. 10, no. 8, pp. 835–842, Jul. 1996.
- [553] J. B. Angel, B. M. Saget, M. Z. Wang, A. Wang, C. A. Dinarello, and P. R. Skolnik, "Interleukin-10 enhances human immunodeficiency virus type 1 expression in a chronically infected promonocytic cell line (U1) by a tumor necrosis factor alpha-independent mechanism.," *J. Interferon Cytokine Res.*, vol. 15, no. 6, pp. 575–84, Jun. 1995.
- [554] K. Kedzierska, P. Ellery, J. Mak, S. R. Lewin, S. M. Crowe, and A. Jaworowski, "HIV-1 Down-Modulates γ Signaling Chain of Fc γ R in Human Macrophages: A Possible Mechanism for Inhibition of Phagocytosis," *J. Immunol.*, vol. 168, no. 6, pp. 2895–2903, Mar. 2002.
- [555] J. Mazzolini, F. Herit, J. Bouchet, A. Benmerah, S. Benichou, and F. Niedergang, "Inhibition of phagocytosis in HIV-1-infected macrophages relies on Nef-dependent alteration of focal delivery of recycling compartments," *Blood*, vol. 115, no. 21, pp. 4226–4236, May 2010.
- [556] R. G. Lima, J. Van Weyenbergh, E. M. B. Saraiva, M. Barral-Netto, B. Galvão-Castro, and D. C. Bou-Habib, "The Replication of Human Immunodeficiency Virus Type 1 in Macrophages Is Enhanced after Phagocytosis of Apoptotic Cells," *J. Infect. Dis.*, vol. 185, no. 11, pp. 1561–1566, Jun. 2002.
- [557] D. Persaud, Y. Zhou, J. M. Siliciano, and R. F. Siliciano, "Latency in Human Immunodeficiency Virus Type 1 Infection: No Easy Answers," *J. Virol.*, vol. 77, no. 3, pp. 1659–1665, Feb. 2003.
- [558] M. K. Tripathy, W. Abbas, and G. Herbein, "Epigenetic regulation of HIV-1 transcription," *Epigenomics*, vol. 3, no. 4, pp. 487–502, Aug-2011.
- [559] E. Eisele and R. F. Siliciano, "Redefining the Viral Reservoirs that Prevent HIV-1 Eradication," *Immunity*, vol. 37, no. 3, pp. 377–388, 21-Sep-2012.
- [560] T. C. Pierson, Y. Zhou, T. L. Kieffer, C. T. Ruff, C. Buck, and R. F. Siliciano, "Molecular Characterization of Preintegration Latency in Human Immunodeficiency Virus Type 1 Infection," *J. Virol.*, vol. 76, no. 17, pp. 8518–8531, Sep. 2002.
- [561] S. Pang, Y. Koyanagi, S. Miles, C. Wiley, H. V. Vinters, and I. S. Y. Chen, "High levels of unintegrated HIV-1 DNA in brain tissue of AIDS dementia patients," *Nature*, vol. 343, no. 6253, pp. 85–89, 1990.
- [562] C. Van Lint, S. Bouchat, and A. Marcello, "HIV-1 transcription and latency: An update," *Retrovirology*, vol. 10, no. 1, 26-Jun-2013.
- [563] A. Kumar, W. Abbas, and G. Herbein, "HIV-1 latency in monocytes/macrophages," *Viruses*, vol. 6, no. 4, MDPI AG, pp. 1837–1860, 22-Apr-2014.
- [564] S. D. Barr, A. Ciuffi, J. Leipzig, P. Shinn, J. R. Ecker, and F. D. Bushman, "HIV Integration Site Selection: Targeting in Macrophages and the Effects of Different Routes of Viral Entry," *Mol. Ther.*, vol. 14, no. 2, pp. 218–225, Aug. 2006.
- [565] L. Redel *et al.*, "HIV-1 regulation of latency in the monocyte-macrophage lineage and in CD4+ T lymphocytes," *J. Leukoc. Biol.*, vol. 87, no. 4, pp. 575–588, Apr. 2010.
- [566] A. Brown, H. Zhang, P. Lopez, C. A. Pardo, and S. Gartner, "In vitro modeling of the HIV-macrophage reservoir," *J. Leukoc. Biol.*, vol. 80, no. 5, pp. 1127–1135, Nov. 2006.
- [567] E. Caselli, M. Galvan, E. Cassai, A. Caruso, L. Sighinolfi, and D. Di Luca, "Human herpesvirus 8 enhances human immunodeficiency virus replication in acutely infected cells and induces reactivation in latently infected cells," *Blood*, vol. 106, no. 8, pp. 2790–2797, Oct. 2005.
- [568] S. Welsch, F. Groot, H.-G. Krausslich, O. T. Keppler, and Q. J. Sattentau, "Architecture and Regulation of the HIV-1 Assembly and Holding Compartment in Macrophages," *J. Virol.*, vol. 85, no. 15, pp. 7922–7927, Aug. 2011.
- [569] R. Gaudin *et al.*, "Dynamics of HIV-Containing Compartments in Macrophages Reveal Sequestration of Virions and Transient Surface Connections," *PLoS One*, vol. 8, no. 7, Jul. 2013.

- [570] F. Graziano, E. Vicenzi, and G. Poli, "Immuno-Pharmacological Targeting of Virus-Containing Compartments in HIV-1-Infected Macrophages," *Trends in Microbiology*, vol. 24, no. 7. Elsevier Ltd, pp. 558–567, 01-Jul-2016.
- [571] S. Berre *et al.*, "CD36-specific antibodies block release of HIV-1 from infected primary macrophages and its transmission to T cells," *J. Exp. Med.*, vol. 210, no. 12, pp. 2523–2538, Nov. 2013.
- [572] G. Herbein, G. Gras, K. A. Khan, and W. Abbas, "Macrophage signaling in HIV-1 infection," *Retrovirology*, vol. 7. 09-Apr-2010.
- [573] F. Groot *et al.*, "Efficient HIV-1 transmission from macrophages to T cells across transient virological synapses Brief report Efficient HIV-1 transmission from macrophages to T cells across transient virological synapses," vol. 111, no. 9, pp. 4660–4663, 2011.
- [574] N. Sharova, C. Swingler, M. Sharkey, and M. Stevenson, "Macrophages archive HIV-1 virions for dissemination in trans," *EMBO J.*, vol. 24, no. 13, pp. 2481–2489, Jul. 2005.
- [575] J. M. Carr, H. Hocking, P. Li, and C. J. Burrell, "Rapid and efficient cell-to-cell transmission of human immunodeficiency virus infection from monocyte-derived macrophages to peripheral blood lymphocytes," *Virology*, vol. 265, no. 2, pp. 319–329, Dec. 1999.
- [576] G. Herbein *et al.*, "Apoptosis of CD8+T cells is mediated by macrophages through interaction of HIV gp120 with chemokine receptor CXCR4," *Nature*, vol. 395, no. 6698, pp. 189–194, Sep. 1998.
- [577] A. D. Badley *et al.*, "Macrophage-dependent apoptosis of CD4+ T lymphocytes from HIV-infected individuals is mediated by FasL and tumor necrosis factor," *J. Exp. Med.*, vol. 185, no. 1, pp. 55–64, Jan. 1997.
- [578] U. Mahlknecht *et al.*, "Resistance to Apoptosis in HIV-Infected CD4 + T Lymphocytes Is Mediated by Macrophages: Role for Nef and Immune Activation in Viral Persistence," *J. Immunol.*, vol. 165, no. 11, pp. 6437–6446, Dec. 2000.
- [579] A. Verani, G. Gras, and G. Pancino, "Macrophages and HIV-1: Dangerous liaisons," *Molecular Immunology*, vol. 42, no. 2. Elsevier Ltd, pp. 195–212, 2005.
- [580] K. L. Clayton *et al.*, "Resistance of HIV-infected macrophages to CD8 + T lymphocyte-mediated killing drives activation of the immune system article," *Nat. Immunol.*, vol. 19, no. 5, pp. 475–486, May 2018.
- [581] W. Stoorvogel, M. J. Kleijmeer, H. J. Geuze, and G. Raposo, "The biogenesis and functions of exosomes.," *Traffic*, vol. 3, no. 5, pp. 321–30, May 2002.
- [582] A. Finzi, A. Brunet, Y. Xiao, J. Thibodeau, and E. A. Cohen, "Major Histocompatibility Complex Class II Molecules Promote Human Immunodeficiency Virus Type 1 Assembly and Budding to Late Endosomal/Multivesicular Body Compartments," *J. Virol.*, vol. 80, no. 19, pp. 9789–9797, Oct. 2006.
- [583] E. Garcia *et al.*, "HIV-1 trafficking to the dendritic cell-T-cell infectious synapse uses a pathway of tetraspanin sorting to the immunological synapse," *Traffic*, vol. 6, no. 6, pp. 488–501, Jun. 2005.
- [584] N. Mukhamedova *et al.*, "Exosomes containing HIV protein Nef reorganize lipid rafts potentiating inflammatory response in bystander cells," *PLOS Pathog.*, vol. 15, no. 7, p. e1007907, Jul. 2019.
- [585] M. Lenassi *et al.*, "HIV Nef is secreted in exosomes and triggers apoptosis in bystander CD4+ T cells," *Traffic*, vol. 11, no. 1, pp. 110–122, Jan. 2010.
- [586] A. M. Booth *et al.*, "Exosomes and HIV Gag bud from endosome-like domains of the T cell plasma membrane," *J. Cell Biol.*, vol. 172, no. 6, pp. 923–935, Mar. 2006.
- [587] D. G. Nguyen, A. Booth, S. J. Gould, and J. E. K. Hildreth, "Evidence That HIV Budding in Primary Macrophages Occurs through the Exosome Release Pathway," *J. Biol. Chem.*, vol. 278, no. 52, pp. 52347–52354, Dec. 2003.
- [588] A. K. Khatua, H. E. Taylor, J. E. K. Hildreth, and W. Popik, "Exosomes Packaging APOBEC3G Confer Human Immunodeficiency Virus Resistance to Recipient Cells," *J. Virol.*, vol. 83, no. 2, pp. 512–521, Jan. 2009.

- [589] M. Mack *et al.*, "Transfer of the chemokine receptor CCR5 between cells by membrane- derived microparticles: A mechanism for cellular human immunodeficiency virus 1 infection," *Nat. Med.*, vol. 6, no. 7, pp. 769–775, Jul. 2000.
- [590] S. J. Gould, A. M. Booth, and J. E. K. Hildreth, "The Trojan exosome hypothesis," *Proceedings of the National Academy of Sciences of the United States of America*, vol. 100, no. 19. pp. 10592–10597, 16-Sep-2003.
- [591] C. A. Carter and L. S. Ehrlich, "Cell Biology of HIV-1 Infection of Macrophages," *Annu. Rev. Microbiol.*, vol. 62, no. 1, pp. 425–443, Oct. 2008.
- [592] L. Bracq *et al.*, "T Cell-Macrophage Fusion Triggers Multinucleated Giant Cell Formation for HIV-1 Spreading," *J. Virol.*, vol. 91, no. 24, Dec. 2017.
- [593] N. Casartelli, "HIV-1 Cell-to-Cell Transmission and Antiviral Strategies: An Overview," *Curr. Drug Targets*, vol. 17, no. 1, pp. 65–75, Dec. 2015.
- [594] S. Iwami *et al.*, "Cell-to-cell infection by HIV contributes over half of virus infection," *Elife*, vol. 4, pp. 1–16, 2015.
- [595] M. Borggren and M. Jansson, "The evolution of hiv-1 interactions with coreceptors and mannose C-type lectin receptors," in *Progress in Molecular Biology and Translational Science*, vol. 129, Elsevier B.V., 2015, pp. 109–140.
- [596] L. Wu and V. N. KewalRamani, "Dendritic-cell interactions with HIV: Infection and viral dissemination," *Nature Reviews Immunology*, vol. 6, no. 11. pp. 859–868, 13-Nov-2006.
- [597] Y. Van Kooyk and T. B. H. Geijtenbeek, "DC-SIGN: Escape mechanism for pathogens," *Nature Reviews Immunology*, vol. 3, no. 9. pp. 697–709, Sep-2003.
- [598] P. W.-P. Hong, S. Nguyen, S. Young, S. V. Su, and B. Lee, "Identification of the Optimal DC-SIGN Binding Site on Human Immunodeficiency Virus Type 1 gp120," *J. Virol.*, vol. 81, no. 15, pp. 8325–8336, Aug. 2007.
- [599] J. Lai, O. K. Bernhard, S. G. Turville, A. N. Harman, J. Wilkinson, and A. L. Cunningham, "Oligomerization of the macrophage mannose receptor enhances gp120-mediated binding of HIV-1," *J. Biol. Chem.*, vol. 284, no. 17, pp. 11027–11038, Apr. 2009.
- [600] T. Hirbod, T. Kaldensjö, and K. Broliden, "In situ distribution of HIV-binding CCR5 and C-type lectin receptors in the human endocervical mucosa," *PLoS One*, vol. 6, no. 9, Sep. 2011.
- [601] T. Hirbod *et al.*, "Abundant and superficial expression of C-type lectin receptors in ectocervix of women at risk of HIV infection," *J. Acquir. Immune Defic. Syndr.*, vol. 51, no. 3, pp. 239–247, Jul. 2009.
- [602] K. B. Gurney *et al.*, "Binding and Transfer of Human Immunodeficiency Virus by DC-SIGN+ Cells in Human Rectal Mucosa," *J. Virol.*, vol. 79, no. 9, pp. 5762–5773, May 2005.
- [603] E. J. Soilleux *et al.*, "Placental expression of DC-SIGN may mediate intrauterine vertical transmission of HIV," *J. Pathol.*, vol. 195, no. 5, pp. 586–592, 2001.
- [604] G. Boily-Larouche *et al.*, "Naturally-occurring genetic variants in human DC-SIGN increase HIV-1 capture, cell-transfer and risk of mother-to-child transmission," *PLoS One*, vol. 7, no. 7, Jul. 2012.
- [605] S. I. Gringhuis, M. Van Der Vlist, L. M. Van Den Berg, J. Den Dunnen, M. Litjens, and T. B. H. Geijtenbeek, "HIV-1 exploits innate signaling by TLR8 and DC-SIGN for productive infection of dendritic cells," *Nat. Immunol.*, vol. 11, no. 5, pp. 419–426, May 2010.
- [606] M. Van Der Vlist, A. M. G. Van Der Aar, S. I. Gringhuis, and T. B. H. Geijtenbeek, "Innate signaling in HIV-1 infection of dendritic cells," *Current Opinion in HIV and AIDS*, vol. 6, no. 5. pp. 348–352, Sep-2011.
- [607] W. Jin, C. Li, T. Du, K. Hu, X. Huang, and Q. Hu, "DC-SIGN plays a stronger role than DCIR in mediating HIV-1 capture and transfer," *Virology*, vol. 458–459, no. 1, pp. 83–92, 2014.

- [608] E. Dodagatta-Marri *et al.*, "Protein-protein interaction between surfactant protein D and DC-SIGN via C-Type lectin domain can suppress HIV-1 transfer," *Front. Immunol.*, vol. 8, no. JUL, Jul. 2017.
- [609] J. Hu, M. B. Gardner, and C. J. Miller, "Simian Immunodeficiency Virus Rapidly Penetrates the Cervicovaginal Mucosa after Intravaginal Inoculation and Infects Intraepithelial Dendritic Cells," *J. Virol.*, vol. 74, no. 13, pp. 6087–6095, Jul. 2000.
- [610] J. Hu, C. J. Miller, U. O'Doherty, P. A. Marx, and M. Pope, "The dendritic cell-T cell milieu of the lymphoid tissue of the tonsil provides a locale in which SIV can reside and propagate at chronic stages of infection," *AIDS Res. Hum. Retroviruses*, vol. 15, no. 14, pp. 1305–1314, Sep. 1999.
- [611] A. I. Spira *et al.*, "Cellular targets of infection and route of viral dissemination after an intravaginal inoculation of simian immunodeficiency virus into rhesus macaques," *J. Exp. Med.*, vol. 183, no. 1, pp. 215–225, Jan. 1996.
- [612] L. Ganesh *et al.*, "Infection of Specific Dendritic Cells by CCR5-Tropic Human Immunodeficiency Virus Type 1 Promotes Cell-Mediated Transmission of Virus Resistant to Broadly Neutralizing Antibodies," *J. Virol.*, vol. 78, no. 21, pp. 11980–11987, Nov. 2004.
- [613] D. S. Kwon, G. Gregorio, N. Bitton, W. A. Hendrickson, and D. R. Littman, "DC-SIGN-mediated internalization of HIV is required for trans-enhancement of T cell infection," *Immunity*, vol. 16, no. 1, pp. 135–144, 2002.
- [614] J. Chehimi *et al.*, "HIV-1 transmission and cytokine-induced expression of DC-SIGN in human monocyte-derived macrophages," *J. Leukoc. Biol.*, vol. 74, no. 5, pp. 757–763, Nov. 2003.
- [615] D. G. Nguyen and J. E. K. Hildreth, "Involvement of macrophage mannose receptor in the binding and transmission of HIV by macrophage," *European Journal of Immunology*, vol. 33, no. 2, pp. 483–493, 01-Feb-2003.
- [616] S. E. Fanibunda, D. N. Modi, J. S. Gokral, and A. H. Bandivdekar, "HIV gp120 Binds to Mannose Receptor on Vaginal Epithelial Cells and Induces Production of Matrix Metalloproteinases," vol. 6, no. 11, pp. 1–9, 2011.
- [617] J. R. Trujillo *et al.*, "Noninfectious entry of HIV-1 into peripheral and brain macrophages mediated by the mannose receptor," 2007.
- [618] J. Lai, O. K. Bernhard, S. G. Turville, A. N. Harman, J. Wilkinson, and A. L. Cunningham, "Oligomerization of the Macrophage Mannose Receptor Enhances gp120-mediated Binding of HIV-1," vol. 284, no. 17, pp. 11027–11038, 2009.
- [619] S. Sukegawa, E. Miyagi, F. Bouamr, H. Farkašová, and K. Strebel, "Mannose Receptor 1 Restricts HIV Particle Release from Infected Macrophages," *Cell Rep.*, vol. 22, no. 3, pp. 786–795, Jan. 2018.
- [620] D. J. Vigerust, B. S. Egan, and V. L. Shepherd, "HIV-1 Nef mediates post-translational down-regulation and redistribution of the mannose receptor," *J. Leukoc. Biol.*, vol. 77, no. 4, pp. 522–534, Apr. 2005.
- [621] S. Pillai, I. A. Netravali, A. Cariappa, and H. Mattoo, "Siglecs and Immune Regulation," *Annu. Rev. Immunol.*, vol. 30, no. 1, pp. 357–392, Apr. 2012.
- [622] P. R. Crocker, J. C. Paulson, and A. Varki, "Siglecs and their roles in the immune system," *Nature Reviews Immunology*, vol. 7, no. 4, pp. 255–266, Apr-2007.
- [623] P. R. Crocker and S. Gordon, "Properties and distribution of a lectin-like hemagglutinin differentially expressed by murine stromal tissue macrophages," *J. Exp. Med.*, vol. 164, no. 6, pp. 1862–1875, Dec. 1986.
- [624] N. Kawasaki *et al.*, "Targeted delivery of lipid antigen to macrophages via the CD169/sialoadhesin endocytic pathway induces robust invariant natural killer T cell activation," *Proc. Natl. Acad. Sci. U. S. A.*, vol. 110, no. 19, pp. 7826–7831, May 2013.
- [625] C. Oetke, M. C. Vinson, C. Jones, and P. R. Crocker, "Sialoadhesin-Deficient Mice Exhibit Subtle Changes in B- and T-Cell Populations and Reduced Immunoglobulin M Levels," *Mol. Cell. Biol.*, vol. 26, no. 4, pp.

1549–1557, Feb. 2006.

- [626] L. Chávez-galán, M. L. Olleros, D. Vesin, I. Garcia, and R. A. Harris, “Much more than M1 and M2 macrophages , there are also CD169 + and TCR + macrophages,” vol. 6, no. May, pp. 1–15, 2015.
- [627] S. C. Saunderson, A. C. Dunn, P. R. Crocker, and A. D. McLellan, “CD169 mediates the capture of exosomes in spleen and lymph node,” *Blood*, vol. 123, no. 2, pp. 208–216, Jan. 2014.
- [628] D. Perez-Zsolt *et al.*, “Anti-Siglec-1 antibodies block Ebola viral uptake and decrease cytoplasmic viral entry,” *Nat. Microbiol.*, 2019.
- [629] X. Sewald *et al.*, “Retroviruses use CD169-mediated trans-infection of permissive lymphocytes to establish infection,” *Science (80-.)*, vol. 350, no. 6260, pp. 563–567, Oct. 2015.
- [630] J. E. Hammonds *et al.*, “Siglec-1 initiates formation of the virus-containing compartment and enhances macrophage-to-T cell transmission of HIV-1,” *PLoS Pathog.*, vol. 13, no. 1, Jan. 2017.
- [631] H. Rempel, C. Calosing, B. Sun, and L. Pulliam, “Sialoadhesin expressed on IFN-induced monocytes binds HIV-1 and enhances infectivity,” *PLoS One*, vol. 3, no. 4, Apr. 2008.
- [632] Z. Zou *et al.*, “Siglecs facilitate HIV-1 infection of macrophages through adhesion with viral sialic acids,” *PLoS One*, vol. 6, no. 9, Sep. 2011.
- [633] N. Izquierdo-Useros *et al.*, “Siglec-1 Is a Novel Dendritic Cell Receptor That Mediates HIV-1 Trans-Infection Through Recognition of Viral Membrane Gangliosides,” *PLoS Biol.*, vol. 10, no. 12, Dec. 2012.
- [634] H. Akiyama, N. P. Ramirez, and M. V. Gudheti, “CD169-Mediated Trafficking of HIV to Plasma Membrane Invaginations in Dendritic Cells Attenuates Efficacy of Anti-gp120 Broadly Neutralizing Antibodies,” 2015.
- [635] M. Pino *et al.*, “HIV-1 immune activation induces Siglec-1 expression and enhances viral trans-infection in blood and tissue myeloid cells,” *Retrovirology*, vol. 12, p. 37, May 2015.
- [636] C. Jolly and Q. J. Sattentau, “Retroviral spread by induction of virological synapses,” *Traffic*, vol. 5, no. 9, pp. 643–650, Sep-2004.
- [637] N. Martin, S. Welsch, C. Jolly, J. A. G. Briggs, D. Vaux, and Q. J. Sattentau, “Virological Synapse-Mediated Spread of Human Immunodeficiency Virus Type 1 between T Cells Is Sensitive to Entry Inhibition,” *J. Virol.*, vol. 84, no. 7, pp. 3516–3527, Apr. 2010.
- [638] C. Jolly, K. Kashefi, M. Hollinshead, and Q. J. Sattentau, “HIV-1 Cell to Cell Transfer across an Env-induced, Actin-dependent Synapse,” *J. Exp. Med.*, vol. 199, no. 2, pp. 283–293, Jan. 2004.
- [639] C. Jolly, I. Mitar, and Q. J. Sattentau, “Adhesion Molecule Interactions Facilitate Human Immunodeficiency Virus Type 1-Induced Virological Synapse Formation between T Cells,” *J. Virol.*, vol. 81, no. 24, pp. 13916–13921, Dec. 2007.
- [640] C. Jolly and Q. J. Sattentau, “Human Immunodeficiency Virus Type 1 Virological Synapse Formation in T Cells Requires Lipid Raft Integrity,” *J. Virol.*, vol. 79, no. 18, pp. 12088–12094, Sep. 2005.
- [641] C. Jolly, I. Mitar, and Q. J. Sattentau, “Requirement for an Intact T-Cell Actin and Tubulin Cytoskeleton for Efficient Assembly and Spread of Human Immunodeficiency Virus Type 1,” *J. Virol.*, vol. 81, no. 11, pp. 5547–5560, 2007.
- [642] D. Rudnicka *et al.*, “Simultaneous Cell-to-Cell Transmission of Human Immunodeficiency Virus to Multiple Targets through Polysynapses,” *J. Virol.*, vol. 83, no. 12, pp. 6234–6246, Jun. 2009.
- [643] W. Hübner *et al.*, “Quantitative 3D video microscopy of HIV transfer across T cell virological synapses,” *Science (80-.)*, vol. 323, no. 5922, pp. 1743–1747, Mar. 2009.
- [644] L. Bracq, M. Xie, S. Benichou, and J. Bouchet, “Mechanisms for cell-to-cell transmission of HIV-1,” *Frontiers in Immunology*, vol. 9, no. FEB. Frontiers Media S.A., 19-Feb-2018.
- [645] K. M. Law, N. Satija, A. M. Esposito, and B. K. Chen, “Cell-to-Cell Spread of HIV and Viral Pathogenesis,” in *Advances in Virus Research*, vol. 95, Academic Press Inc., 2016, pp. 43–85.

- [646] C. J. A. Duncan *et al.*, "High-Multiplicity HIV-1 Infection and Neutralizing Antibody Evasion Mediated by the Macrophage-T Cell Virological Synapse," *J. Virol.*, vol. 88, no. 4, pp. 2025–2034, 2013.
- [647] C. J. Martin, K. N. Peters, and S. M. Behar, "Macrophages clean up: Efferocytosis and microbial control," *Current Opinion in Microbiology*, vol. 17, no. 1, pp. 17–23, Feb-2014.
- [648] M. A. Czuczman *et al.*, "Listeria monocytogenes exploits efferocytosis to promote cell-to-cell spread," *Nature*, vol. 509, no. 7499, pp. 230–234, 2014.
- [649] A. E. Baxter *et al.*, "Macrophage infection via selective capture of HIV-1-infected CD4+T cells," *Cell Host Microbe*, vol. 16, no. 6, pp. 711–721, 2014.
- [650] N. Calantone *et al.*, "Tissue myeloid cells in SIV-infected primates acquire viral DNA through phagocytosis of infected T cells," *Immunity*, vol. 41, no. 3, pp. 493–502, 2014.
- [651] J. M. Orenstein, "In Vivo Cytolysis and Fusion of Human Immunodeficiency Virus Type 1–Infected Lymphocytes in Lymphoid Tissue," *J. Infect. Dis.*, vol. 182, no. 1, pp. 338–342, Jul. 2000.
- [652] S. R. DiNapoli *et al.*, "Tissue-resident macrophages can contain replication-competent virus in antiretroviral-naive, SIV-infected Asian macaques," *JCI Insight*, vol. 2, no. 4, Feb. 2017.
- [653] J. L. Dargent, L. Lespagnard, A. Kornreich, P. Hermans, N. Clumeck, and A. Verhest, "HIV-associated multinucleated giant cells in lymphoid tissue of the waldeyer's ring: A detailed study," *Mod. Pathol.*, vol. 13, no. 12, pp. 1293–1299, 2000.
- [654] M. Lewin-Smith, S. M. Wahl, and J. M. Orenstein, "Human immunodeficiency virus-rich multinucleated giant cells in the colon: a case report with transmission electron microscopy, immunohistochemistry, and in situ hybridization.," *Mod. Pathol.*, vol. 12, no. 1, pp. 75–81, Jan. 1999.
- [655] J. M. Ward *et al.*, "Immunohistochemical localization of human and simian immunodeficiency viral antigens in fixed tissue sections," *Am. J. Pathol.*, vol. 127, no. 2, pp. 199–205, May 1987.
- [656] A. Sylwester *et al.*, "HIV-induced syncytia of a T cell line form single giant pseudopods and are motile.," *J. Cell Sci.*, vol. 106 (Pt 3), pp. 941–53, Nov. 1993.
- [657] D. R. Soll and R. C. Kennedy, "The Role of T Cell Motility and Cytoskeletal Reorganization in HIV-Induced Syncytium Formation," *AIDS Res. Hum. Retroviruses*, vol. 10, no. 4, pp. 325–327, 1994.
- [658] D. Schols, R. Pauwels, M. Baba, J. Desmyter, and E. De Clercq, "Syncytium formation and destruction of bystander CD4+ cells cocultured with T cells persistently infected with human immunodeficiency virus as demonstrated by flow cytometry," *J. Gen. Virol.*, vol. 70, no. 9, pp. 2397–2408, 1989.
- [659] J. D. Lifson *et al.*, "Induction of CD4-dependent cell fusion by the HTLV-III/LAV envelope glycoprotein," *Nature*, vol. 323, no. 6090, pp. 725–728, 1986.
- [660] T. T. Murooka *et al.*, "HIV-infected T cells are migratory vehicles for viral dissemination," *Nature*, vol. 490, no. 7419, pp. 283–289, Oct. 2012.
- [661] A. A. Compton and O. Schwartz, "They Might Be Giants: Does Syncytium Formation Sink or Spread HIV Infection?," *PLoS Pathogens*, vol. 13, no. 2. Public Library of Science, 01-Feb-2017.
- [662] A. Rustom, R. Saffrich, I. Markovic, P. Walther, and H. H. Gerdes, "Nanotubular Highways for Intercellular Organelle Transport," *Science (80-.)*, vol. 303, no. 5660, pp. 1007–1010, Feb. 2004.
- [663] E. E. Malik S, "Mechanisms of HIV Neuropathogenesis: Role of Cellular Communication Systems.," *Curr. HIV Res.*, 2016.
- [664] K. McCoy-Simandle, S. J. Hanna, and D. Cox, "Exosomes and nanotubes: Control of immune cell communication," *International Journal of Biochemistry and Cell Biology*, vol. 71. Elsevier Ltd, pp. 44–54, 01-Feb-2016.
- [665] B. Önfelt *et al.*, "Structurally Distinct Membrane Nanotubes between Human Macrophages Support Long-Distance Vesicular Traffic or Surfing of Bacteria," *J. Immunol.*, vol. 177, no. 12, pp. 8476–8483, Dec.

2006.

- [666] M. Dupont, S. Souriant, G. Lugo-Villarino, I. Maridonneau-Parini, and C. Vérollet, "Tunneling nanotubes: Intimate communication between myeloid cells," *Frontiers in Immunology*, vol. 9, no. JAN. Frontiers Media S.A., 25-Jan-2018.
- [667] G. Okafo, L. Prevedel, and E. Eugenin, "Tunneling nanotubes (TNT) mediate long-range gap junctional communication: Implications for HIV cell to cell spread," *Sci. Rep.*, vol. 7, no. 1, Dec. 2017.
- [668] S. Sowinski *et al.*, "Sowinski2008_cell_tubes.pdf," vol. 10, no. 2, 2008.
- [669] M. Hashimoto *et al.*, "Potential Role of the Formation of Tunneling Nanotubes in HIV-1 Spread in Macrophages," *J. Immunol.*, vol. 196, no. 4, pp. 1832–1841, Feb. 2016.
- [670] K. Hase *et al.*, "M-Sec promotes membrane nanotube formation by interacting with Ral and the exocyst complex," *Nat. Cell Biol.*, vol. 11, no. 12, pp. 1427–1432, Dec. 2009.
- [671] J. Mukerji, K. C. Olivieri, V. Misra, K. A. Agopian, and D. Gabuzda, "Proteomic analysis of HIV-1 Nef cellular binding partners reveals a role for exocyst complex proteins in mediating enhancement of intercellular nanotube formation," *Retrovirology*, vol. 9, Apr. 2012.
- [672] J. Uhl, S. Gujarathi, A. A. Waheed, A. Gordon, E. O. Freed, and K. Gousset, "Myosin-X is essential to the intercellular spread of HIV-1 Nef through tunneling nanotubes," *J. Cell Commun. Signal.*, vol. 13, no. 2, pp. 209–224, Jun. 2019.
- [673] A. E. Pitchenik *et al.*, "Opportunistic infections and Kaposi's sarcoma among Haitians: Evidence of a new acquired immunodeficiency state," *Ann. Intern. Med.*, vol. 98, no. 3, pp. 277–284, 1983.
- [674] F. X. Blanc *et al.*, "Earlier versus later start of antiretroviral therapy in HIV-infected adults with tuberculosis," *N. Engl. J. Med.*, vol. 365, no. 16, pp. 1471–1481, Oct. 2011.
- [675] L. C. K. Bell and M. Noursadeghi, "Pathogenesis of HIV-1 and mycobacterium tuberculosis co-infection," *Nat. Rev. Microbiol.*, vol. 16, no. 2, pp. 80–90, 2018.
- [676] C. Naing, J. W. Mak, M. Maung, S. F. Wong, and A. I. B. M. Kassim, "Meta-analysis: The association between HIV infection and extrapulmonary tuberculosis," *Lung*, vol. 191, no. 1, pp. 27–34, Feb. 2013.
- [677] S. D. Lawn, A. J. Evans, P. M. Sedgwick, and J. W. Acheampong, "Pulmonary tuberculosis: radiological features in west Africans coinfecting with HIV.," *Br. J. Radiol.*, vol. 72, no. 856, pp. 339–344, Apr. 1999.
- [678] H. Esmail *et al.*, "The Immune Response to Mycobacterium tuberculosis in HIV-1-Coinfected Persons," *Annu. Rev. Immunol.*, vol. 36, no. 1, Apr. 2018.
- [679] P. Sonnenberg, J. R. Glynn, K. Fielding, J. Murray, P. Godfrey-Faussett, and S. Shearer, "How Soon after Infection with HIV Does the Risk of Tuberculosis Start to Increase? A Retrospective Cohort Study in South African Gold Miners," *J. Infect. Dis.*, vol. 191, no. 2, pp. 150–158, Jan. 2005.
- [680] G. Chamie, A. Luetkemeyer, E. Charlebois, and D. V. Havlir, "Tuberculosis as Part of the Natural History of HIV Infection in Developing Countries," *Clin. Infect. Dis.*, vol. 50, no. s3, pp. S245–S254, May 2010.
- [681] R. K. Gupta, S. B. Lucas, K. L. Fielding, and S. D. Lawn, "Prevalence of tuberculosis in post-mortem studies of HIV-infected adults and children in resource-limited settings: A systematic review and meta-analysis," *AIDS*, vol. 29, no. 15, pp. 1987–2002, Sep. 2015.
- [682] F. G. Imperiali, A. Zaninoni, L. La Maestra, P. Tarsia, F. Blasi, and W. Barcellini, "Increased Mycobacterium tuberculosis growth in HIV-1-infected human macrophages: Role of tumour necrosis factor- α ," *Clin. Exp. Immunol.*, vol. 123, no. 3, pp. 435–442, 2001.
- [683] K. Nakata *et al.*, "Mycobacterium tuberculosis enhances human immunodeficiency virus-1 replication in the lung," *Am. J. Respir. Crit. Care Med.*, vol. 155, no. 3, pp. 996–1003, 1997.
- [684] Y. Zhang, K. Nakata, M. Weiden, and W. N. Rom, "Mycobacterium tuberculosis enhances human immunodeficiency virus-1 replication by transcriptional activation at the long terminal repeat," *J. Clin.*

- Invest.*, vol. 95, no. 5, pp. 2324–2331, 1995.
- [685] Y. Hoshino *et al.*, “Maximal HIV-1 replication in alveolar macrophages during tuberculosis requires both lymphocyte contact and cytokines,” *J. Exp. Med.*, vol. 195, no. 4, pp. 495–505, Feb. 2002.
- [686] S. D. Lawn, S. T. Butera, and T. M. Shinnick, “Tuberculosis unleashed: the impact of human immunodeficiency virus infection on the host granulomatous response to *Mycobacterium tuberculosis*,” *Microbes Infect.*, vol. 4, no. 6, pp. 635–46, May 2002.
- [687] K. R. Collins *et al.*, “Human Immunodeficiency Virus Type 1 (HIV-1) Quasispecies at the Sites of *Mycobacterium tuberculosis* Infection Contribute to Systemic HIV-1 Heterogeneity,” *J. Virol.*, vol. 76, no. 4, pp. 1697–1706, Feb. 2002.
- [688] Z. Toossi *et al.*, “Increased replication of HIV-1 at sites of *Mycobacterium tuberculosis* infection: Potential mechanisms of viral activation,” *J. Acquir. Immune Defic. Syndr.*, vol. 28, no. 1, pp. 1–8, Sep. 2001.
- [689] S. D. Lawn, T. L. Pisell, C. S. Hirsch, M. Wu, S. T. Butera, and Z. Toossi, “Anatomically Compartmentalized Human Immunodeficiency Virus Replication in HLA-DR + Cells and CD14 + Macrophages at the Site of Pleural Tuberculosis Coinfection,” *J. Infect. Dis.*, vol. 184, no. 9, pp. 1127–1133, Nov. 2001.
- [690] S. D. Lawn *et al.*, “Screening for HIV-associated tuberculosis and rifampicin resistance before antiretroviral therapy using the Xpert MTB/RIF assay: A prospective study,” *PLoS Med.*, vol. 8, no. 7, Jul. 2011.
- [691] D. Goletti *et al.*, “Effect of *Mycobacterium tuberculosis* on HIV replication. Role of immune activation,” *J. Immunol.*, vol. 157, no. 3, pp. 1271–8, Aug. 1996.
- [692] L. Morris *et al.*, “High Human Immunodeficiency Virus Type 1 RNA Load in the Cerebrospinal Fluid from Patients with Lymphocytic Meningitis,” *J. Infect. Dis.*, vol. 177, no. 2, pp. 473–476, Feb. 1998.
- [693] M. X. Rangaka *et al.*, “Effect of HIV-1 infection on T-cell-based and skin test detection of tuberculosis infection,” *Am. J. Respir. Crit. Care Med.*, vol. 175, no. 5, pp. 514–520, Mar. 2007.
- [694] A. Y. Vittor, J. M. Garland, and D. Schlossberg, “Improving the diagnosis of tuberculosis: From quantiferon to new techniques to diagnose tuberculosis infections,” *Curr. HIV/AIDS Rep.*, vol. 8, no. 3, pp. 153–163, Sep. 2011.
- [695] S. K. Sharma, A. Mohan, and T. Kadiravan, “HIV-TB co-infection: epidemiology, diagnosis & management,” *Indian J. Med. Res.*, vol. 121, no. 4, pp. 550–67, Apr. 2005.
- [696] H. Esmail *et al.*, “The Immune Response to *Mycobacterium tuberculosis* in HIV-1-Coinfected Persons,” *Annu. Rev. Immunol.*, vol. 36, no. 1, pp. 1–36, 2018.
- [697] S. Swaminathan, C. Padmapriyadarsini, and G. Narendran, “Diagnosis & treatment of tuberculosis in HIV co-infected patients,” *Indian J. Med. Res.*, vol. 134, no. 6, p. 850, 2011.
- [698] P. Monkongdee *et al.*, “Yield of acid-fast smear and mycobacterial culture for tuberculosis diagnosis in people with human immunodeficiency virus,” *Am. J. Respir. Crit. Care Med.*, vol. 180, no. 9, pp. 903–908, Nov. 2009.
- [699] F. W. Mugusi F1, Villamor E, Urassa W, Saathoff E, Bosch RJ, “HIV co-infection, CD4 cell counts and clinical correlates of bacillary density in pulmonary tuberculosis,” *Int. J. Tuberc. Lung Dis.*, 2006.
- [700] S. D. Lawn *et al.*, “Advances in tuberculosis diagnostics: The Xpert MTB/RIF assay and future prospects for a point-of-care test,” *The Lancet Infectious Diseases*, vol. 13, no. 4, pp. 349–361, Apr-2013.
- [701] C. C. Boehme *et al.*, “Feasibility, diagnostic accuracy, and effectiveness of decentralised use of the Xpert MTB/RIF test for diagnosis of tuberculosis and multidrug resistance: A multicentre implementation study,” *Lancet*, vol. 377, no. 9776, pp. 1495–1505, Apr. 2011.
- [702] G. M. Varghese, J. Janardhanan, R. Ralph, and O. C. Abraham, “The twin epidemics of tuberculosis and HIV,” *Curr. Infect. Dis. Rep.*, vol. 15, no. 1, pp. 77–84, Feb. 2013.

- [703] V. A. Londhey, "HIV and tuberculosis--a 'cursed duo' in the HAART era.," *J. Assoc. Physicians India*, vol. 57, pp. 681–2, Oct. 2009.
- [704] S. Suchindran, E. S. Brouwer, and A. Van Rie, "Is HIV infection a risk factor for multi-drug resistant tuberculosis? A systematic review," *PLoS ONE*, vol. 4, no. 5. 15-May-2009.
- [705] K. B. Patel, R. Belmonte, and H. M. Crowe, "Drug Malabsorption and Resistant Tuberculosis in HIV-Infected Patients," *New England Journal of Medicine*, vol. 332, no. 5. pp. 336–337, 02-Feb-1995.
- [706] D. V. Havlir *et al.*, "Timing of antiretroviral therapy for HIV-1 infection and tuberculosis," *N. Engl. J. Med.*, vol. 365, no. 16, pp. 1482–1491, Oct. 2011.
- [707] N. Kumarasamy *et al.*, "Incidence of immune reconstitution syndrome in HIV/tuberculosis-coinfected patients after initiation of generic antiretroviral therapy in India," *J. Acquir. Immune Defic. Syndr.*, vol. 37, no. 5, pp. 1574–1576, Dec. 2004.
- [708] M. Müller, S. Wandel, R. Colebunders, S. Attia, H. Furrer, and M. Egger, "Immune reconstitution inflammatory syndrome in patients starting antiretroviral therapy for HIV infection: a systematic review and meta-analysis," *The Lancet Infectious Diseases*, vol. 10, no. 4. pp. 251–261, Apr-2010.
- [709] S. D. Lawn, L. G. Bekker, and R. F. Miller, "Immune reconstitution disease associated with mycobacterial infections in HIV-infected individuals receiving antiretrovirals," *Lancet Infectious Diseases*, vol. 5, no. 6. pp. 361–373, Jun-2005.
- [710] R. P. J. Lai, G. Meintjes, and R. J. Wilkinson, "HIV-1 tuberculosis-associated immune reconstitution inflammatory syndrome," *Seminars in Immunopathology*, vol. 38, no. 2. Springer Verlag, pp. 185–198, 01-Mar-2016.
- [711] L. J. Haddow, M. Y. S. Moosa, A. Mosam, P. Moodley, R. Parboosing, and P. J. Easterbrook, "Incidence, Clinical Spectrum, Risk Factors and Impact of HIV-Associated Immune Reconstitution Inflammatory Syndrome in South Africa," *PLoS One*, vol. 7, no. 11, Nov. 2012.
- [712] D. M. Murdoch, W. D. F. Venter, C. Feldman, and A. Van Rie, "Incidence and risk factors for the immune reconstitution inflammatory syndrome in HIV patients in South Africa: A prospective study," *AIDS*, vol. 22, no. 5, pp. 601–610, Mar. 2008.
- [713] R. Vignesh *et al.*, "TB-IRIS after initiation of antiretroviral therapy is associated with expansion of preexistent th1 responses against mycobacterium tuberculosis antigens," in *Journal of Acquired Immune Deficiency Syndromes*, 2013, vol. 64, no. 3, pp. 241–248.
- [714] A. Bourgarit *et al.*, "Explosion of tuberculin-specific Th1-responses induces immune restoration syndrome in tuberculosis and HIV co-infected patients," *AIDS*, vol. 20, no. 2, Jan. 2006.
- [715] R. Van Den Bergh, G. Vanham, G. Raes, P. De Baetselier, R. Colebunders, and S. D. Lawn, "Mycobacterium-associated immune reconstitution disease: Macrophages running wild?," *Lancet Infectious Diseases*, vol. 6, no. 1. Lancet Publishing Group, pp. 2–3, 2006.
- [716] E. M. Shankar *et al.*, "HIV-Mycobacterium tuberculosis co-infection: A 'danger-couple model' of disease pathogenesis," *Pathogens and Disease*, vol. 70, no. 2. Blackwell Publishing Ltd, pp. 110–118, 2014.
- [717] J. R. Glynn, J. Murray, A. Bester, G. Nelson, S. Shearer, and P. Sonnenberg, "Effects of duration of HIV infection and secondary tuberculosis transmission on tuberculosis incidence in the South African gold mines," *AIDS*, vol. 22, no. 14, pp. 1859–1867, Sep. 2008.
- [718] S. D. Lawn, L. Myer, D. Edwards, L. G. Bekker, and R. Wood, "Short-term and long-term risk of tuberculosis associated with CD4 cell recovery during antiretroviral therapy in South Africa," *AIDS*, vol. 23, no. 13, pp. 1717–1725, Aug. 2009.
- [719] B. Kalsdorf *et al.*, "HIV-1 infection impairs the bronchoalveolar T-cell response to mycobacteria," *Am. J. Respir. Crit. Care Med.*, vol. 180, no. 12, pp. 1262–1270, Dec. 2009.
- [720] R. A. M. Breen, G. Janossy, S. M. Barry, I. Cropley, M. A. Johnson, and M. C. I. Lipman, "Detection of mycobacterial antigen responses in lung but not blood in HIV-tuberculosis co-infected subjects," *AIDS*,

vol. 20, no. 9, pp. 1330–1332, Jun. 2006.

- [721] K. F. Law, J. Jagirdar, M. D. Weiden, M. Bodkin, and W. N. Rom, "Tuberculosis in HIV-positive patients: Cellular response and immune activation in the lung," *Am. J. Respir. Crit. Care Med.*, vol. 153, no. 4, pp. 1377–1384, 1996.
- [722] C. Geldmacher, A. Zumla, and M. Hoelscher, "Interaction between HIV and Mycobacterium tuberculosis: HIV-1-induced CD4 T-cell depletion and the development of active tuberculosis," *Current Opinion in HIV and AIDS*, vol. 7, no. 3, pp. 268–275, May-2012.
- [723] J. Y. Shen, P. F. Barnes, T. H. Rea, and P. R. Meyer, "Immunohistology of tuberculous adenitis in symptomatic HIV infection.," *Clin. Exp. Immunol.*, vol. 72, no. 2, pp. 186–9, May 1988.
- [724] C. Geldmacher *et al.*, "Preferential infection and depletion of Mycobacterium tuberculosis-specific CD4 T cells after HIV-1 infection," *J. Exp. Med.*, vol. 207, no. 13, pp. 2869–2881, Dec. 2010.
- [725] A. G. Rosas-Taraco, A. Y. Arce-Mendoza, G. Caballero-Olín, and M. C. Salinas-Carmona, "Mycobacterium tuberculosis upregulates coreceptors CCR5 and CXCR4 while HIV modulates CD14 favouring concurrent infection," *AIDS Res. Hum. Retroviruses*, vol. 22, no. 1, pp. 45–51, Jan. 2006.
- [726] N. P. Juffermans *et al.*, "Patients with Active Tuberculosis Have Increased Expression of HIV Coreceptors CXCR4 and CCR5 on CD4+ T Cells," *Clin. Infect. Dis.*, vol. 32, no. 4, pp. 650–652, Feb. 2001.
- [727] C. Geldmacher *et al.*, "Early Depletion of Mycobacterium tuberculosis –Specific T Helper 1 Cell Responses after HIV-1 Infection ," *J. Infect. Dis.*, vol. 198, no. 11, pp. 1590–1598, Dec. 2008.
- [728] L. C. K. Bell *et al.*, "In Vivo Molecular Dissection of the Effects of HIV-1 in Active Tuberculosis," *PLoS Pathog.*, vol. 12, no. 3, Mar. 2016.
- [729] M. Zhang, J. Gong, D. V. Iyer, B. E. Jones, R. L. Modlin, and P. F. Barnes, "T cell cytokine responses in persons with tuberculosis and human immunodeficiency virus infection," *J. Clin. Invest.*, vol. 94, no. 6, pp. 2435–2442, 1994.
- [730] M. Mendonça *et al.*, "Deficient in vitro anti-mycobacterial immunity despite successful long-term highly active antiretroviral therapy in HIV-infected patients with past history of tuberculosis infection or disease," *Clin. Immunol.*, vol. 125, no. 1, pp. 60–66, Oct. 2007.
- [731] R. Condos, W. N. Rom, and M. Weiden, "Lung-specific immune response in tuberculosis.," *Int. J. Tuberc. Lung Dis.*, vol. 4, no. 2 Suppl 1, pp. S11-7, Feb. 2000.
- [732] M. Da Glória Bonecini-Almeida *et al.*, "Functional activity of alveolar and peripheral cells in patients with human acquired immunodeficiency syndrome and pulmonary tuberculosis," *Cell. Immunol.*, vol. 190, no. 2, pp. 112–120, Dec. 1998.
- [733] L. Papagno *et al.*, "Immune activation and CD8+ T-cell differentiation towards senescence in HIV-1 infection," *PLoS Biol.*, vol. 2, no. 2, 2004.
- [734] L. Shen *et al.*, "PD-1/PD-L pathway inhibits M.tb-specific CD4 + T-cell functions and phagocytosis of macrophages in active tuberculosis," *Sci. Rep.*, vol. 6, Dec. 2016.
- [735] N. R. Patel *et al.*, " HIV Impairs TNF- α Mediated Macrophage Apoptotic Response to Mycobacterium tuberculosis ," *J. Immunol.*, vol. 179, no. 10, pp. 6973–6980, Nov. 2007.
- [736] A. L. L. de Noronha, A. Báfica, L. Nogueira, A. Barral, and M. Barral-Netto, "Lung granulomas from Mycobacterium tuberculosis/HIV-1 co-infected patients display decreased in situ TNF production," *Pathol. Res. Pract.*, vol. 204, no. 3, pp. 155–161, Mar. 2008.
- [737] K. Kumawat, S. K. Pathak, A. L. Spetz, M. Kundu, and J. Basu, "Exogenous Nef is an inhibitor of Mycobacterium tuberculosis-induced tumor necrosis factor- α production and macrophage apoptosis," *J. Biol. Chem.*, vol. 285, no. 17, pp. 12629–12637, Apr. 2010.
- [738] N. R. Patel, K. Swan, X. Li, S. D. Tachado, and H. Koziel, " Impaired M. tuberculosis -mediated apoptosis in alveolar macrophages from HIV+ persons: potential role of IL-10 and BCL-3 ," *J. Leukoc. Biol.*, vol. 86,

no. 1, pp. 53–60, Jul. 2009.

- [739] H. C. Mwandumba *et al.*, “Alveolar macrophages from HIV-infected patients with pulmonary tuberculosis retain the capacity to respond to stimulation by lipopolysaccharide,” *Microbes Infect.*, vol. 9, no. 9, pp. 1053–1060, Jul. 2007.
- [740] S. Janssen *et al.*, “Mortality in Severe Human Immunodeficiency Virus-Tuberculosis Associates with Innate Immune Activation and Dysfunction of Monocytes,” *Clin. Infect. Dis.*, vol. 65, no. 1, pp. 73–82, 2017.
- [741] J. Bezuidenhout, T. Roberts, L. Muller, P. van Helden, and G. Walzl, “Pleural tuberculosis in patients with early HIV infection is associated with increased TNF-alpha expression and necrosis in granulomas,” *PLoS One*, vol. 4, no. 1, Jan. 2009.
- [742] A. Lenaerts, C. E. Barry, and V. Dartois, “Heterogeneity in tuberculosis pathology, microenvironments and therapeutic responses,” *Immunol. Rev.*, vol. 264, no. 1, pp. 288–307, Mar. 2015.
- [743] S. Pathak, T. Wentzel-Larsen, and B. Åsjö, “Effects of in vitro HIV-1 infection on mycobacterial growth in peripheral blood monocyte-derived macrophages,” *Infect. Immun.*, vol. 78, no. 9, pp. 4022–4032, Sep. 2010.
- [744] G. Lê-Bury and F. Niedergang, “Defective phagocytic properties of HIV-infected macrophages: How might they be implicated in the development of invasive *Salmonella Typhimurium*?,” *Frontiers in Immunology*, vol. 9, no. MAR. Frontiers Media S.A., 23-Mar-2018.
- [745] G. B. Kyei *et al.*, “Autophagy pathway intersects with HIV-1 biosynthesis and regulates viral yields in macrophages,” *J. Cell Biol.*, vol. 186, no. 2, pp. 255–268, Jul. 2009.
- [746] V. Deretic *et al.*, “Endosomal membrane traffic: Convergence point targeted by *Mycobacterium tuberculosis* and HIV,” *Cellular Microbiology*, vol. 6, no. 11, pp. 999–1009, Nov-2004.
- [747] E. J. Duh, W. J. Maury, T. M. Folks, A. S. Fauci, and A. B. Rabson, “Tumor necrosis factor α activates human immunodeficiency virus type 1 through induction of nuclear factor binding to the NF- κ B sites in the long terminal repeat,” *Proc. Natl. Acad. Sci. U. S. A.*, vol. 86, no. 15, pp. 5974–5978, 1989.
- [748] Y. Hoshino *et al.*, “Mechanisms of Polymorphonuclear Neutrophil-Mediated Induction of HIV-1 Replication in Macrophages during Pulmonary Tuberculosis,” *J. Infect. Dis.*, vol. 195, no. 9, pp. 1303–1310, May 2007.
- [749] Y. Honda *et al.*, “Type I interferon induces inhibitory 16-kD CCAAT/enhancer binding protein (C/EBP) β , repressing the HIV-1 long terminal repeat in macrophages: Pulmonary tuberculosis alters C/EBP expression, enhancing HIV-1 replication,” *J. Exp. Med.*, vol. 188, no. 7, pp. 1255–1265, Oct. 1998.
- [750] G. S. Tomlinson *et al.*, “HIV-1 infection of macrophages dysregulates innate immune responses to *Mycobacterium tuberculosis* by inhibition of interleukin-10,” *J. Infect. Dis.*, vol. 209, no. 7, pp. 1055–65, Apr. 2014.
- [751] N. Tanaka *et al.*, “Interleukin-10 induces inhibitory C/EBP β through STAT-3 and represses HIV-1 transcription in macrophages,” *Am. J. Respir. Cell Mol. Biol.*, vol. 33, no. 4, pp. 406–411, 2005.
- [752] M. J. Kuroda *et al.*, “High Turnover of Tissue Macrophages Contributes to Tuberculosis Reactivation in Simian Immunodeficiency Virus-Infected Rhesus Macaques,” no. February, pp. 1–10, 2018.
- [753] J. M. Orenstein, C. Fox, and S. M. Wahl, “Macrophages as a source of hiv during opportunistic infections,” *Science (80-.)*, vol. 276, no. 5320, pp. 1857–1860, Jun. 1997.
- [754] Z. Toossi, “Virological and Immunological Impact of Tuberculosis on Human Immunodeficiency Virus Type 1 Disease,” *J. Infect. Dis.*, vol. 188, no. 8, pp. 1146–1155, Oct. 2003.
- [755] Y. Hoshino *et al.*, “*Mycobacterium tuberculosis*-induced CXCR4 and chemokine expression leads to preferential X4 HIV-1 replication in human macrophages,” *J. Immunol.*, vol. 172, no. 10, pp. 6251–8, May 2004.

- [756] K. R. Collins, H. Mayanja-Kizza, B. A. Sullivan, M. E. Quiñones-Mateu, Z. Toossi, and E. J. Arts, "Greater Diversity of HIV-1 Quasispecies in HIV-Infected Individuals With Active Tuberculosis," *JAIDS J. Acquir. Immune Defic. Syndr.*, vol. 24, no. 5, pp. 408–417, Aug. 2000.
- [757] T. Biru *et al.*, "Human immunodeficiency virus type-1 group M quasispecies evolution: Diversity and divergence in patients co-infected with active tuberculosis," *Med. Microbiol. Immunol.*, vol. 199, no. 4, pp. 323–332, Nov. 2010.
- [758] S. J. Jenkins *et al.*, "Local macrophage proliferation, rather than recruitment from the blood, is a signature of T H2 inflammation," *Science (80-.)*, vol. 332, no. 6035, pp. 1284–1288, Jun. 2011.
- [759] L. Herrtwich *et al.*, "DNA Damage Signaling Instructs Polyploid Macrophage Fate in Granulomas," *Cell*, vol. 167, no. 5, p. 1264–1280.e18, Nov. 2016.
- [760] Y. Van Kooyk, B. Appelmek, and T. B. H. Geijtenbeek, "A fatal attraction : Mycobacterium tuberculosis and HIV-1 target DC-SIGN to escape immune surveillance," vol. 9, no. 4, pp. 153–159, 2003.
- [761] G. Mancino *et al.*, " Infection of Human Monocytes with Mycobacterium tuberculosis Enhances Human Immunodeficiency Virus Type 1 Replication and Transmission to T Cells ," *J. Infect. Dis.*, vol. 175, no. 6, pp. 1531–1535, Jun. 1997.
- [762] D. Goletti *et al.*, "Inhibition of HIV-1 Replication in Monocyte-Derived Macrophages by Mycobacterium tuberculosis," vol. 189, 2004.
- [763] N. K. Saksena, B. Wang, L. Zhou, M. Soedjono, Y. Shwen Ho, and V. Conceicao, "HIV reservoirs in vivo and new strategies for possible eradication of HIV from the reservoir sites," *HIV/AIDS - Res. Palliat. Care*, vol. 2, pp. 103–122, 2010.
- [764] C. Lastrucci *et al.*, "Tuberculosis is associated with expansion of a motile, permissive and immunomodulatory CD16+ monocyte population via the IL-10/STAT3 axis," *Cell Res.*, vol. 25, no. 12, pp. 1333–1351, Dec. 2015.
- [765] M. P. Gonzalez-Perez *et al.*, "Independent evolution of macrophage-tropism and increased charge between HIV-1 R5 envelopes present in brain and immune tissue," *Retrovirology*, vol. 9, Mar. 2012.
- [766] S. B. Joseph *et al.*, "Quantification of entry phenotypes of macrophage-tropic HIV-1 across a wide range of CD4 densities.," *J. Virol.*, vol. 88, no. 4, pp. 1858–69, Feb. 2014.
- [767] G. Schnell, S. Joseph, S. Spudich, R. W. Price, and R. Swanstrom, "HIV-1 replication in the central nervous system occurs in two distinct cell types," *PLoS Pathog.*, vol. 7, no. 10, Oct. 2011.
- [768] J. B. Honeycutt *et al.*, "Macrophages sustain HIV replication in vivo independently of T cells Find the latest version : Macrophages sustain HIV replication in vivo independently of T cells," vol. 126, no. 4, pp. 1353–1366, 2016.
- [769] M. R. York, T. Nagai, A. J. Mangini, R. Lemaire, J. M. Van Seventer, and R. Lafyatis, "A macrophage marker, siglec-1, is increased on circulating monocytes in patients with systemic sclerosis and induced by type I interferons and toll-like receptor agonists," *Arthritis Rheum.*, vol. 56, no. 3, pp. 1010–1020, Mar. 2007.
- [770] A. Sartori-Rupp *et al.*, "Correlative cryo-electron microscopy reveals the structure of TNTs in neuronal cells."
- [771] H. Halász *et al.*, "Live cell superresolution-structured illumination microscopy imaging analysis of the intercellular transport of microvesicles and costimulatory proteins via nanotubes between immune cells," *Methods Appl. Fluoresc.*, vol. 6, no. 4, Aug. 2018.
- [772] A. Osteikoetxea-Molnár *et al.*, "The growth determinants and transport properties of tunneling nanotube networks between B lymphocytes," *Cell. Mol. Life Sci.*, vol. 73, no. 23, pp. 4531–4545, Apr. 2016.
- [773] M. Weszl *et al.*, "Investigation of the mechanical and chemical characteristics of nanotubular and nano-pitted anodic films on grade 2 titanium dental implant materials," *Mater. Sci. Eng. C*, vol. 78, pp. 69–78, Sep. 2017.

- [774] E. a Eugenin, P. J. Gaskill, and J. W. Berman, "A potential mechanism for intercellular HIV trafficking," *Commun. Integr. Biol.*, vol. 2, no. June, pp. 243–244, 2009.
- [775] S. Souriant *et al.*, "Tuberculosis Exacerbates HIV-1 Infection through IL-10/STAT3-Dependent Tunneling Nanotube Formation in Macrophages.," *Cell Rep.*, vol. 26, no. 13, p. 3586–3599.e7, Mar. 2019.
- [776] D. C. DeLucia, C. R. Rinaldo, and G. Rappocciolo, " Inefficient HIV-1 trans Infection of CD4 + T Cells by Macrophages from HIV-1 Nonprogressors Is Associated with Altered Membrane Cholesterol and DC-SIGN ," *J. Virol.*, vol. 92, no. 13, Apr. 2018.
- [777] A. Osteikoetxea-Moln??r *et al.*, "The growth determinants and transport properties of tunneling nanotube networks between B lymphocytes," *Cell. Mol. Life Sci.*, vol. 73, no. 23, pp. 4531–4545, 2016.
- [778] M. J. Stax *et al.*, "Colorectal mucus binds DC-SIGN and inhibits HIV-1 trans-infection of CD4+ T-lymphocytes," *PLoS One*, vol. 10, no. 3, Mar. 2015.
- [779] P. Hong, M. R. Ninonuevo, B. Lee, C. Lebrilla, and L. Bode, "Human milk oligosaccharides reduce HIV-1-gp120 binding to dendritic cell-specific ICAM3-grabbing non-integrin (DC-SIGN)," *Br. J. Nutr.*, vol. 101, no. 4, pp. 482–486, 2009.
- [780] H. R. Chinnery, E. Pearlman, and P. G. McMenamin, "Cutting edge: Membrane nanotubes in vivo: a feature of MHC class II+ cells in the mouse cornea.," *J. Immunol.*, vol. 180, no. 9, pp. 5779–83, May 2008.
- [781] C. Pyrgaki, P. Trainor, A. K. Hadjantonakis, and L. Niswander, "Dynamic imaging of mammalian neural tube closure," *Dev. Biol.*, vol. 344, no. 2, pp. 941–947, 2010.
- [782] J. M. Teddy and P. M. Kulesa, "In vivo evidence for short- and long-range cell communication in cranial neural crest cells," *Development*, vol. 131, no. 24, pp. 6141–6151, Dec. 2004.
- [783] L. Caneparo, P. Pantazis, W. Dempsey, and S. E. Fraser, "Intercellular bridges in vertebrate gastrulation," *PLoS One*, vol. 6, no. 5, 2011.
- [784] M. D. Miller J1, Fraser SE, "Dynamics of thin filopodia during sea urchin gastrulation.," *Development*, 1995.
- [785] M. Osswald *et al.*, "Brain tumour cells interconnect to a functional and resistant network," *Nature*, vol. 528, no. 7580, pp. 93–98, Dec. 2015.
- [786] J. W. Ady *et al.*, "Intercellular communication in malignant pleural mesothelioma: properties of tunneling nanotubes," *Front. Physiol.*, vol. 5, Oct. 2014.
- [787] J. Pasquier *et al.*, "Preferential transfer of mitochondria from endothelial to cancer cells through tunneling nanotubes modulates chemoresistance," *J. Transl. Med.*, vol. 11, no. 1, Apr. 2013.
- [788] J. Lindenmann and G. E. Gifford, "Studies on vaccinia virus plaque formation and its inhibition by interferon," *Virology*, vol. 19, no. 3, pp. 283–293, Mar. 1963.
- [789] J. LINDENMANN, D. C. BURKE, and A. ISAACS, "Studies on the production, mode of action and properties of interferon.," *Br. J. Exp. Pathol.*, vol. 38, no. 5, pp. 551–562, Oct. 1957.
- [790] L. Baca-Regen, N. Heinzinger, M. Stevenson, and H. E. Gendelman, "Alpha interferon-induced antiretroviral activities: restriction of viral nucleic acid synthesis and progeny virion production in human immunodeficiency virus type 1-infected monocytes.," *J. Virol.*, vol. 68, no. 11, pp. 7559–65, Nov. 1994.
- [791] P. R. A. Meylan, J. C. Guatelli, J. R. Munis, D. D. Richman, and R. S. Kornbluth, "Mechanisms for the inhibition of hiv replication by interferons- α , - β , and - γ in primary human macrophages," *Virology*, vol. 193, no. 1, pp. 138–148, Jan. 1993.
- [792] L. M. Snell, T. L. McGaha, and D. G. Brooks, "Type I Interferon in Chronic Virus Infection and Cancer," *Trends in Immunology*, vol. 38, no. 8. Elsevier Ltd, pp. 542–557, 01-Aug-2017.
- [793] A. Zhen, D. G. Brooks, and S. G. Kitchen, "Targeting type I interferon-mediated activation restores immune function in chronic HIV infection The Journal of Clinical Investigation," *J Clin Invest*, vol. 127, no.

- 1, pp. 260–268, 2017.
- [794] J. Decalf *et al.*, “Sensing of HIV-1 Entry Triggers a Type I Interferon Response in Human Primary Macrophages,” *J. Virol.*, vol. 91, no. 15, 2017.
- [795] B. Michaelis and J. A. Levy, “HIV replication can be blocked by recombinant human interferon beta,” *AIDS*, vol. 3, no. 1, pp. 27–31, Jan. 1989.
- [796] A. Novikov *et al.*, “Mycobacterium tuberculosis Triggers Host Type I IFN Signaling To Regulate IL-1 β Production in Human Macrophages,” *J. Immunol.*, vol. 187, no. 5, pp. 2540–2547, Sep. 2011.
- [797] D. J. J. Larner AC, Chaudhuri A, “Transcriptional induction by interferon. New protein(s) determine the extent and length of the induction,” *J. Biol. Chem.*, 1986.
- [798] N. Shaabani *et al.*, “The probacterial effect of type I interferon signaling requires its own negative regulator USP18,” *Sci. Immunol.*, vol. 3, no. 27, 2018.
- [799] J. P. Taylor, M. N. Cash, K. E. Santostefano, M. Nakanishi, N. Terada, and M. A. Wallet, “CRISPR/Cas9 knockout of USP18 enhances type I IFN responsiveness and restricts HIV-1 infection in macrophages,” *J. Leukoc. Biol.*, vol. 103, no. 6, pp. 1225–1240, 2018.
- [800] K. J. Ritchie *et al.*, “Role of ISG15 protease UBP43 (USP18) in innate immunity to viral infection,” *Nat. Med.*, vol. 10, no. 12, pp. 1374–1378, Dec. 2004.
- [801] O. A. Malakhova *et al.*, “Protein ISGylation modulates the JAK-STAT signaling pathway,” *Genes Dev.*, vol. 17, no. 4, pp. 455–460, Feb. 2003.
- [802] N. Honke *et al.*, “Enforced viral replication activates adaptive immunity and is essential for the control of a cytopathic virus,” *Nat. Immunol.*, vol. 13, no. 1, pp. 51–57, Jan. 2012.
- [803] K. I. Arimoto *et al.*, “STAT2 is an essential adaptor in USP18-mediated suppression of type I interferon signaling,” *Nat. Struct. Mol. Biol.*, vol. 24, no. 3, pp. 279–289, 2017.
- [804] M. S. Lee, B. Kim, G. T. Oh, and Y. J. Kim, “OASL1 inhibits translation of the type I interferon-regulating transcription factor IRF7,” *Nat. Immunol.*, vol. 14, no. 4, pp. 346–355, Apr. 2013.
- [805] J. Zhu *et al.*, “Antiviral Activity of Human OASL Protein Is Mediated by Enhancing Signaling of the RIG-I RNA Sensor,” *Immunity*, vol. 40, no. 6, pp. 936–948, Jun. 2014.
- [806] H. H. Ho and L. B. Ivashkiv, “Role of STAT3 in type I interferon responses: Negative regulation of STAT1-dependent inflammatory gene activation,” *J. Biol. Chem.*, vol. 281, no. 20, pp. 14111–14118, May 2006.
- [807] M. H. Tsai and C. K. Lee, “STAT3 cooperates with phospholipid scramblase 2 to suppress Type I interferon response,” *Front. Immunol.*, vol. 9, no. AUG, Aug. 2018.
- [808] L. Lu *et al.*, “Gene regulation and suppression of type I interferon signaling by STAT3 in diffuse large B cell lymphoma,” *Proc. Natl. Acad. Sci. U. S. A.*, vol. 115, no. 3, pp. E498–E505, Jan. 2018.
- [809] J. J. Babon and N. A. Nicola, “The biology and mechanism of action of suppressor of cytokine signaling 3,” *Growth Factors*, vol. 30, no. 4, pp. 207–219, Aug. 2012.
- [810] N. Vázquez, T. Greenwell-Wild, S. Rekka, J. M. Orenstein, and S. M. Wahl, “Mycobacterium avium - induced SOCS contributes to resistance to IFN- γ -mediated mycobactericidal activity in human macrophages,” *J. Leukoc. Biol.*, vol. 80, no. 5, pp. 1136–1144, Nov. 2006.
- [811] M. J. Kuroda *et al.*, “High Turnover of Tissue Macrophages Contributes to Tuberculosis Reactivation in Simian Immunodeficiency Virus-Infected Rhesus Macaques,” *J. Infect. Dis.*, vol. 217, no. 12, pp. 1865–1874, May 2018.
- [812] B. H. Penn *et al.*, “An Mtb-Human Protein-Protein Interaction Map Identifies a Switch between Host Antiviral and Antibacterial Responses,” *Mol. Cell*, vol. 71, no. 4, p. 637–648.e5, 2018.
- [813] J. M. Cliff, S. H. E. Kaufmann, H. McShane, P. van Helden, and A. O’Garra, “The human immune response to tuberculosis and its treatment: a view from the blood,” *Immunol. Rev.*, vol. 264, no. 1, pp. 88–102,

Mar. 2015.

- [814] L. Pulliam, "Cognitive consequences of a sustained monocyte type 1 IFN response in HIV-1 infection.," *Curr. HIV Res.*, vol. 12, no. 2, pp. 77–84, 2014.
- [815] J. J. Oliveira *et al.*, "The plasma biomarker soluble SIGLEC-1 is associated with the type I interferon transcriptional signature, ethnic background and renal disease in systemic lupus erythematosus," *Arthritis Res. Ther.*, vol. 20, no. 1, Jul. 2018.
- [816] D. Souza de Lima, V. C. L. Nunes, M. M. Ogusku, A. Sadahiro, A. Pontillo, and B. de C. Alencar, "Polymorphisms in SIGLEC1 contribute to susceptibility to pulmonary active tuberculosis possibly through the modulation of IL-1 β ," *Infect. Genet. Evol.*, vol. 55, pp. 313–317, Nov. 2017.
- [817] J. Martinez-Picado *et al.*, "Identification of siglec-1 null individuals infected with HIV-1," *Nat. Commun.*, vol. 7, Aug. 2016.
- [818] J. M.-P. Susana Benet, Cristina Galvez, Irina Kontsevaya, Lilibeth Arias, Marta Monguió-Tortajada, Francis Drobniowski, Itziar Erkizia, Victor Urrea, Ruo-Yan Ong, Marina Luquin, Maeva Dupont, Judith Dalmau, Paula Cardona, Geancarlo Lugo, Christel Verollet, Esther, "Dissemination of Mycobacterium tuberculosis is associated to a SIGLEC-1 null variant that limits antigen exchange via trafficking extracellular vesicles," *Unpublished*.
- [819] D. Vendrame, M. Sourisseau, V. Perrin, O. Schwartz, and F. Mammano, "Partial Inhibition of Human Immunodeficiency Virus Replication by Type I Interferons: Impact of Cell-to-Cell Viral Transfer," *J. Virol.*, vol. 83, no. 20, pp. 10527–10537, Oct. 2009.
- [820] J. Li *et al.*, "Exosomes mediate the cell-to-cell transmission of IFN- α -induced antiviral activity," *Nat. Immunol.*, vol. 14, no. 8, pp. 793–803, Aug. 2013.
- [821] K. Hrecka *et al.*, "Vpx relieves inhibition of HIV-1 infection of macrophages mediated by the SAMHD1 protein," *Nature*, vol 474, pp 658-661, Apr 2011.
- [822] PR. Crocker, JC Paulson, and A. Varki, "Siglecs and their roles in the immune system", *Nat. Rev. Immunol.*, vol. 7, pp 255-266, Apr 2007.
- [823] AS. O'Neil, TK. Ven den Berg, and GE. Mullen, "Sialoadhesin – a macrophage-restricted marker of immunoregulation and inflammation", *Immunology*, vol 138, pp 198-207, Mar 2013.
- [824] BE. Collins, O. Blixt, AR. DeSieno, N. Bovin, JD. Marth, and JC. Paulson, "Masking of CD22 by cis ligands does not prevent redistribution of CD22 to sites of cell contact", *Proc. Natl. Acad. USA.*, vol 101, no 16, pp 6104-6109, Apr 2004.
- [825] A. Hartnell, J. Steel, H. Turley, M. Jones, DG. Jackson, and PR. Crocker, "Characterization of human sialoadhesin, a sialic acid binding receptor expressed by resident and inflammatory macrophage populations", *Blood*, vol 97, pp 288-296, Jan 2001.
- [826] C. Oetke, MC. Vinson, C. Jones, and PR. Crocker, "Sialoadhesin-deficient mice exhibit subtle changes in B- and T-cell populations and reduced immunoglobulin M levels", *Mol. Cell Biol.*, Feb 2006.
- [827] C. Wu *et al.*, "Sialoadhesin-positive macrophages bind regulatory T cells, negatively controlling their expansion and autoimmune disease progression", *J. Immunol.*, vol 182, no 10, pp 6508-6516, May 2009.
- [828] HR. Jiang, L. Hwenda, K. Makinen, C. Oetke, PR. Crocker, and JV. Forrester, "Sialoadhesin promotes the inflammatory response in experimental autoimmune uveoretinitis", *J. Immunol.*, vol 177, no 4, pp 2258-2264, Aug 2006.
- [829] ER. Vim, KA, Kalivoda, EL. Deszo, and SM. Steenbergen, "Diversity of microbial sialic acid metabolism", *Microbiol. Mol. Biol. Rev.*, Mar 2004.

- [830] L. Martinez-Pomares *et al.*, "Cell-specific glycoforms of sialoadhesin and CD45 are counter-receptors for the cysteine-rich domain of the mannose receptor", *J. Biol. Chem.*, vol 274, pp 35211-35218, Dec 1999.
- [831] H. Akiyama *et al.*, "Interferon-Inducible CD169/Siglec1 Attenuates Anti-HIV-1 Effects of Alpha Interferon", *J. Virol.*, vol 91, no 21, Oct 2017.
- [832] Q. Zheng, J. Hou, Y. Zhou, Y. Yang, B. Xie, and X. Cao, "Siglec1 suppresses antiviral innate immune response by inducing TBK1 degradation via the ubiquitin ligase TRIM27", *Cell Res.*, vol 25, no 10, pp 1121-1136, Oct 2015.

Annex

- I. Formation of Foamy Macrophages by Tuberculous Pleural Effusions Is Triggered by the Interleukin-10/Signal Transducer and Activator of Transcription 3 Axis through ACAT Upregulation.

- II. Tuberculosis is associated with expansion of a motile, permissive and immunomodulatory CD16(+) monocyte population via the IL-10/STAT3 axis.

- III. Bone degradation machinery of osteoclasts: An HIV-1 target that contributes to bone loss.



OPEN ACCESS

Edited by:

Christoph Hölscher,
Forschungszentrum Borstel (LG),
Germany

Reviewed by:

Peter Murray,
Max Planck Institute of
Biochemistry (MPG), Germany
Joseph E. Qualls,
Cincinnati Children's Research
Foundation, United States

Robin James Flynn,
University of Liverpool,
United Kingdom

***Correspondence:**

Luciana Balboa
luciana_balboa@hotmail.com

[†]These authors have contributed
equally to this work.

Specialty section:

This article was submitted to
Microbial Immunology,
a section of the journal
Frontiers in Immunology

Received: 30 November 2017

Accepted: 20 February 2018

Published: 09 March 2018

Citation:

Genoula M, Marín Franco JL,
Dupont M, Kviatcovsky D, Milillo A,
Schierloh P, Moraña EJ, Poggi S,
Palmero D, Mata-Espinosa D,
González-Domínguez E,
León Contreras JC, Barrionuevo P,
Rearte B, Córdoba Moreno MO,
Fontanals A, Crotta Asis A, Gago G,
Cougoule C, Neyrolles O,
Maridonneau-Parini I, Sánchez-
Torres C, Hernández-Pando R,
Vérollet C, Lugo-Villarino G,
Sasiain MdC and Balboa L (2018)
Formation of Foamy Macrophages by
Tuberculous Pleural Effusions Is
Triggered by the Interleukin-10/Signal
Transducer and Activator of
Transcription 3 Axis through
ACAT Upregulation.
Front. Immunol. 9:459.
doi: 10.3389/fimmu.2018.00459

Formation of Foamy Macrophages by Tuberculous Pleural Effusions Is Triggered by the Interleukin-10/Signal Transducer and Activator of Transcription 3 Axis through ACAT Upregulation

Melanie Genoula^{1,2,3}, José Luis Marín Franco^{1,2,3†}, Maeva Dupont^{2,3,4†}, Denise Kviatcovsky^{1,2,3}, Ayelén Milillo⁵, Pablo Schierloh^{1,2,3}, Eduardo Jose Moraña⁶, Susana Poggi⁶, Domingo Palmero⁶, Dulce Mata-Espinosa⁷, Erika González-Domínguez⁸, Juan Carlos León Contreras⁷, Paula Barrionuevo⁵, Bárbara Rearte⁵, Marlina Olyssa Córdoba Moreno⁵, Adriana Fontanals⁹, Agostina Crotta Asis¹⁰, Gabriela Gago¹⁰, Céline Cougoule^{2,3,4}, Olivier Neyrolles^{2,3,4}, Isabelle Maridonneau-Parini^{2,3,4}, Carmen Sánchez-Torres⁸, Rogelio Hernández-Pando⁷, Christel Vérollet^{2,3,4†}, Geanncarlo Lugo-Villarino^{2,3,4†}, María del Carmen Sasiain^{1,2,3†} and Luciana Balboa^{1,2,3*}

¹Laboratorio de Inmunología de Enfermedades Respiratorias, Instituto de Medicina Experimental (IMEX)-CONICET, Academia Nacional de Medicina, Buenos Aires, Argentina, ²International Associated Laboratory (LIA) CNRS IM-TB/HIV (1167), Toulouse, France, ³International Associated Laboratory (LIA) CNRS IM-TB/HIV (1167), Buenos Aires, Argentina, ⁴Institut de Pharmacologie et de Biologie Structurale, Université de Toulouse, CNRS, UPS, Toulouse, France, ⁵Laboratorio de Fisiología de los Procesos Inflamatorios, Instituto de Medicina Experimental (IMEX)-CONICET, Academia Nacional de Medicina, Buenos Aires, Argentina, ⁶Instituto Prof. Dr. Raúl Vaccarezza, Hospital de Infecciosas Dr. F. J. Muñiz, Buenos Aires, Argentina, ⁷Sección de Patología Experimental, Departamento de Patología, Instituto Nacional de Ciencias Médicas y Nutrición Salvador Zubirán, Mexico City, Mexico, ⁸Departamento de Biomedicina Molecular, Centro de Investigación y de Estudios Avanzados del Instituto Politécnico Nacional, Mexico City, Mexico, ⁹Fundación Instituto Leloir, CABA, Buenos Aires, Argentina, ¹⁰Laboratory of Physiology and Genetics of Actinomycetes, Instituto de Biología Molecular y Celular de Rosario (IBR-CONICET), Facultad de Ciencias Bioquímicas y Farmacéuticas, Universidad Nacional de Rosario, Rosario, Argentina

The ability of *Mycobacterium tuberculosis* (Mtb) to persist in its human host relies on numerous immune evasion strategies, such as the deregulation of the lipid metabolism leading to the formation of foamy macrophages (FM). Yet, the specific host factors leading to the foamy phenotype of Mtb-infected macrophages remain unknown. Herein, we aimed to address whether host cytokines contribute to FM formation in the context of Mtb infection. Our approach is based on the use of an acellular fraction of tuberculous pleural effusions (TB-PE) as a physiological source of local factors released during Mtb infection. We found that TB-PE induced FM differentiation as observed by the increase in lipid bodies, intracellular cholesterol, and expression of the scavenger receptor CD36, as well as the enzyme acyl CoA:cholesterol acyl transferase (ACAT). Importantly, interleukin-10 (IL-10) depletion from TB-PE prevented the augmentation of all these parameters. Moreover, we observed a positive correlation between the levels of IL-10 and the number of lipid-laden CD14⁺ cells among the pleural cells in TB patients, demonstrating that FM differentiation occurs within the pleural environment. Downstream of IL-10 signaling, we

noticed that the transcription factor signal transducer and activator of transcription 3 was activated by TB-PE, and its chemical inhibition prevented the accumulation of lipid bodies and ACAT expression in macrophages. In terms of the host immune response, TB-PE-treated macrophages displayed immunosuppressive properties and bore higher bacillary loads. Finally, we confirmed our results using bone marrow-derived macrophage from IL-10^{-/-} mice demonstrating that IL-10 deficiency partially prevented foamy phenotype induction after Mtb lipids exposure. In conclusion, our results evidence a role of IL-10 in promoting the differentiation of FM in the context of Mtb infection, contributing to our understanding of how alterations of the host metabolic factors may favor pathogen persistence.

Keywords: ACAT, interleukin-10, foamy macrophages, lipids, signal transducer and activator of transcription 3, tuberculosis

INTRODUCTION

Tuberculosis (TB) is a highly contagious disease caused by *Mycobacterium tuberculosis* (Mtb) infection. Even though the treatment of the disease has been standardized for a while, TB still remains one of the top 10 causes of death worldwide with 10.4 million new cases and 1.3 million deaths from TB among HIV-negative people in 2016 (1). Chronic host-pathogen interaction in TB leads to extensive metabolic remodeling in both the host and the pathogen (2). In fact, the success of Mtb as a pathogen derives from its efficient adaptation to the intracellular milieu of human macrophages. An important strategy to reach this metabolic adaptation is the promotion of lipid body accumulation by the host macrophage leading to foamy macrophages (FM) differentiation. The formation of lipid-laden macrophages is caused by infectious agents through deregulation in the balance between the influx and efflux of lipids. Key for the biogenesis of lipid bodies is the enzyme acyl CoA:cholesterol acyltransferase (ACAT), which represents an ideal target for pathogens (3).

Lipid body accumulation within leukocytes is a common feature in both clinical and experimental infections, especially in mycobacterial infections (4, 5). Mtb infection leads to the induction of FM, a process which is promoted by several mycobacterial lipids (6–8). This event enables the fusion between Mtb-containing phagosomes and lipid bodies resulting in an abundant supply of lipids for the pathogen (7), allowing Mtb to switch into a dormancy phenotype and to become tolerant to several front-line antibiotics (9). For this reason, lipid bodies are considered to be a secure niche for Mtb conferring protection from bactericidal mechanisms, such as respiratory burst (10). Moreover, the presence of FM within granulomatous structures was demonstrated in both experimentally infected animals and patients, especially in individuals developing secondary TB (5, 11). Therefore, FM may play a central role in mycobacterial persistence and reactivation (12, 13).

Concerning the impact of FM on the host immunity against Mtb, it was shown that human macrophages exposed to lipids prior to Mtb infection failed to produce TNF- α and to clear the infection (14, 15). Taking into account that FM generated prior to Mtb infection impair the host immune response,

there is a keen interest to identify the host-derived cytokines released at the site of Mtb infection, and to understand how these signals contribute to FM differentiation and alter host defense against Mtb. In this regard, it is well known that different activation programs in macrophages driven by pro or anti-inflammatory cytokines are associated to changes in the lipid metabolism (16). Therefore, it is likely that host cytokines produced in response to Mtb infection contribute to lipids turnover promoting FM formation, and consequently lead to Mtb persistence.

In this work, we report that a TB-associated microenvironment induces FM differentiation program dependent partially on the interleukin-10 (IL-10)/signal transducer and activator of transcription 3 (STAT3) axis through ACAT upregulation. Our approach was to model a genuine TB-associated microenvironment by employing a physiological relevant sample derived from active TB patients, such as the acellular fraction of tuberculous pleural effusions (TB-PE). Indeed, TB-PE are manifested in up to 30% of patients with TB, and they are caused by the spread of Mtb into the pleural space and subsequent local inflammation and recruitment of leukocytes (17). Based on this, we show that the acquisition of the foamy phenotype with immunosuppressive properties involves high IL-10 release, low TNF- α production, impaired Th1 activation, and high bacillary loads. We also confirmed that IL-10-deficiency in bone marrow-derived macrophages (BMDM) prevented partially foamy phenotype induction upon exposure to Mtb lipids. In conclusion, our results provide evidence for a role of IL-10 in promoting foamy differentiation of macrophages in the context of Mtb infection.

MATERIALS AND METHODS

Bacterial Strain and Antigens

Mycobacterium tuberculosis H37Rv strain was grown at 37°C in Middlebrook 7H9 medium (Difco) supplemented with 10% albumin-dextrose-catalase (Difco) and 0.05% Tween-80 (Sigma-Aldrich). The Mtb γ -irradiated H37Rv strain (NR-49098) and its total lipids' preparation (NR-14837) were obtained from BEI Resource, USA.

Preparation of Human Monocyte-Derived Macrophages (MDM)

Buffy coats from healthy donors were prepared at *Centro Regional de Hemoterapia Garrahan* (Buenos Aires, Argentina) according to institutional guidelines (resolution number CEIANM-664/07). Informed consent was obtained from each donor before blood collection. Peripheral blood mononuclear cells were obtained by Ficoll gradient separation on Ficoll-Paque (GE Healthcare). Then, monocytes were purified by centrifugation on a discontinuous Percoll gradient (Amersham) as previously described (18). After that, monocytes were allowed to adhere to 24-well plates (Costar) at 5×10^5 cells/well for 1 h at 37°C in warm RPMI-1640 medium (GIBCO). The cells were then washed with warm PBS twice. The final purity was checked by fluorescence-activated cell sorting analysis using an anti-CD14 monoclonal antibody (mAb) and was found to be >90%. The medium was then supplemented to a final concentration of 10% fetal bovine serum (FBS, Sigma-Aldrich) and human recombinant Macrophage Colony-Stimulating Factor (M-CSF, Peprotech) at 10 ng/ml. Cells were allowed to differentiate for 5–7 days.

Preparation of Pleural Effusion (PE) Pools

Pleural effusions were obtained by therapeutic thoracentesis by physicians at the *Hospital F. J. Muñiz* (Buenos Aires, Argentina). The research was carried out in accordance with the Declaration of Helsinki (2013) of the World Medical Association, and was approved by the Ethics Committees of the *Hospital F. J. Muñiz* and the *Academia Nacional de Medicina de Buenos Aires* (protocol number: NIN-1671-12). Written informed consent was obtained before sample collection. We collected a total of 43 PE samples which were classified according to their etiology, being 38 of them associated to TB (TB-PE) and 5 to heart failure (HF-PE). Individual samples of confirmed TB patients were used for correlation analysis. A group of samples ($n = 10$) were pooled and used for *in vitro* assays to treat macrophages. The selection of these samples was based merely on practical reasons, involving those samples that have been collected earlier through the course of this study. The diagnosis of TB pleurisy was based on a positive Ziehl–Nielsen stain or Lowenstein–Jensen culture from PE and/or histopathology of pleural biopsy, and was further confirmed by an Mtb-induced IFN- γ response and an ADA-positive test (19). Exclusion criteria included a positive HIV test, and the presence of concurrent infectious diseases or non-infectious conditions (cancer, diabetes, or steroid therapy). None of the patients had multidrug-resistant TB. Those PE samples derived from patients with pleural transudates secondary to heart failure (HF-PE, $n = 5$) were employed to prepare a second pool of PE, used as control of non-infectious inflammatory PE. The PE were collected in heparin tubes and centrifuged at 300 g for 10 min at room temperature without brake. The cell-free supernatant was transferred into new plastic tubes, further centrifuged at 12,000 g for 10 min and aliquots were stored at -80°C . After having the diagnosis of the PE, pools were prepared by mixing same amounts of individual PE associated to a specific etiology. The pools were decontaminated at 56°C for 30 min, and filtered by 0.22 μm in order to remove any remaining debris or residual bacteria.

FM Induction

Macrophages were plated on glass coverslips within a 24-well tissue culture plate (Costar) at a density of 5×10^5 cells/ml per well with or without 20% v/v of PE, 10 $\mu\text{g/ml}$ of Mtb lipids (BEI resources) or infected with Mtb (MOI 2:1) for 24 h. When indicated, cells were pre-incubated with either Cucurbitacin I (50–100 nM, Sigma-Aldrich), or the STAT3 inhibitor Stattic (1–20 μM , Sigma-Aldrich), or the ACAT inhibitor Sandoz 58-035 (5–50 $\mu\text{g/ml}$, Sigma-Aldrich) for 2 h prior TB-PE addition and for further 24 h during TB-PE incubation. DMSO alone was used as control. Alternatively, cells were treated with recombinant human IL-10 (Peprotech) at the indicated doses. Foam cell formation was followed by Oil Red O (ORO) staining (Sigma-Aldrich) as previously described (20) at 37°C for 1–5 min, and washed with water three times. For the visualization of the lipid bodies, slides were prepared using the aqueous mounting medium Poly-Mount (Polysciences), observed *via* light microscope (Leica) and finally photographed using the Leica Application Suite software. Alternatively, after fixation, cells were labeled with 1 $\mu\text{g/ml}$ of BODIPY 493/503 (Life technologies) for 15 min in order to visualize the lipid bodies by green fluorescence emission using a confocal microscope (Olympus BX51).

Infection of Human Macrophages with Mtb

Infections were performed in the biosafety level 3 laboratory at the *Unidad Operativa Centro de Contención Biológica, ANLIS-MALBRAN* (Buenos Aires), according to the biosafety institutional guidelines. Macrophages seeded on glass coverslips within a 24-well tissue culture plate (Costar) at a density of 5×10^5 cells/ml were infected with Mtb H37Rv strain at a MOI of 2:1 during 1 h at 37°C. Then, extracellular bacteria were removed gently by washing with pre-warmed PBS, and cells were cultured in RPMI-1640 medium supplemented with 10% FBS and gentamicin (50 $\mu\text{g/ml}$) for 24 h. The glass coverslips were fixed with PFA 4% and stained with ORO, as was previously described.

Quantification of Total Cholesterol

Total cholesterol was determined in TB-PE or cell lysates using the *Colestat Enzimatico kit* according to manufacturer instructions (Wiener Lab, Argentina). This assay is based in Trinder reaction in which cholesterol in the sample is quantified by enzymatic hydrolysis of cholesterol esters (21).

Lipid Analysis

Total lipids were extracted from the same number of macrophages with methanol/chloroform (2:1 v/v) as described by Bligh and Dyer (22). After extraction, lipids were dried and analyzed by thin layer chromatography on silica gel 60 F254 plates (Merck), using hexane/diethyl ether/acetic acid (75:25:1, v/v/v) as the developing solvent. Chemical staining with Cu-phosphoric was used for detection.

Phenotypic Characterization by Flow Cytometry

Macrophages were centrifuged for 7 min at 1,200 rpm and then stained for 40 min at 4°C with fluorophore-conjugated antibodies

FITC-anti-CD36 (clone 5-271), PerCP.Cy5.5-anti-CD14 (clone HCD14), PE-anti-CD163 (clone GHI/61), FITC-anti-CD206 (clone C068C2) (Biolegend), FITC-anti-HLA-DR (clone G46-6), or PE-anti-CD274 (clone MIH1) (BD Biosciences), and in parallel, with the corresponding isotype control antibody. After staining, the cells were washed with PBS 1×, centrifuged and analyzed by flow cytometry using FACSCalibur cytometer (BD Biosciences). The median fluorescence intensity were analyzed using FCS Express V3 software (*De Novo* Software, Los Angeles, CA, USA). The mean of the median fluorescence intensities (MFI) of the independent assays were used for comparisons between experimental conditions.

Soluble Cytokine Determinations

The amounts of human TNF- α , IL-1 β , IL-10, IL-6, IFN- γ , and IL-4 were measured by ELISA, according to manufacturers' instructions kits (TNF- α , IL-4, and IFN- γ Ready-SET-Go!TM Kits from eBioscience; IL-10, IL-1 β , and IL-6 ELISA MAXTM Deluxe Kits from Biolegend). The detection limit was 3 pg/ml for TNF- α ; 8 pg/ml for IL-10 and IL-6; 6.25 pg/ml for IFN- γ and IL-4; and 15.6 pg/ml for IL-1 β . Murine TNF- α and IL-10 were measured by ELISA, according to manufacturer's instructions (OptEIATM Set kits from BD Bioscience) with a detection limit at 30 pg/ml.

Cytokine Depletions of PE

Tuberculosis-PE were incubated with 10 μ g/ml of the following neutralizing antibodies for 1 h at 4°C for the specific depletion of IL-10 (α IL-10, clone 19F1; Biolegend), IL-6 (α IL-6, clone MQ2-13A5; BD Bioscience), IL-1 β (α IL-1 β , clone 8516.311; SIGMA), or TNF- α (α TNF- α , clone MAb1; Biolegend). Then, 100 μ l/ml of Protein G Sepharose beads (Amersham) were added and incubated for 1 h at 4°C. Finally, TB-PE were centrifuged at 12,000 g to remove antibody-bead complexes and then filtered (0.22- μ m pores) before use. IFN- γ depletion was performed by incubating TB-PE for 2 h in sterile 96-well plates that had been coated with the capture antibody provided by the Human IFN- γ ELISA Kit (BD Bioscience). In all cases, depletions were controlled by ELISA.

Electron Microscopy

Macrophages exposed (or not) to TB-PE, and depleted (or not) for IL-10, were prepared for transmission electron microscopy study. For this purpose, cells were centrifuged at 6,000 rpm for 1 min, fixed in 1% glutaraldehyde dissolved in 0.1 M cacodylate buffer (pH 7); post-fixed in 2% osmium tetroxide; dehydrated with increasing concentrations of ethanol and gradually infiltrated with Epon resin (Pelco). Thin sections were contrasted with uranyl acetate and lead citrate (Electron Microscopy Sciences, Fort Washington, PA, USA) and examined with a FEI Tecnai transmission electron microscope (Hillsboro, OR, USA). For morphometry, 30 cells from each condition were randomly selected and digitalized at 40,000 \times magnification. Then the area of lipid electron dense vacuoles per cell were measured and compared in each experimental group by automated morphometry.

Proliferation of Antimycobacterial CD4 T Cells Induced by Macrophages

We purified and maintained CD4 T cells from blood derived from healthy PPD⁺ donors as previously demonstrated (23). In parallel, we cultured autologous monocytes to generate macrophages and exposed them or not to TB-PE 20% v/v for 24 h. The next day, the medium was replaced, and macrophages were loaded with mycobacterial antigens by adding γ -irradiated Mtb at 2 bacteria to 1 macrophage ratio for further 24 h. Thereafter, the medium was replaced and autologous carboxyfluorescein succinimidyl ester (CFSE)-labeled CD4 T cells (Invitrogen) were added at a ratio of 10 lymphocytes to 1 macrophage for 5 days, as detailed previously (24). To determine IFN- γ production among proliferating CD4 T cells (CFSE^{low}), brefeldin A (5 μ g/ml; Sigma Chemical Co.) was added 4 h prior the end of the coculture to block cytokine secretion. Thereafter, CFSE-labeled lymphocytes were first stained with anti-CD4-PerCP-Cy5.5 mAbs (eBioscience), then fixed with 0.5% PFA for 15 min. Second, cells were permeabilized with 500 μ l Perm2 (Becton Dickinson, Cockysville, MD, USA) for 10 min and incubated with anti-IFN- γ -PE mAb (Invitrogen, CA, USA). Cells were gated according to its FSC and side scatter (SSC) properties analyzed on FACScan (Becton Dickinson). In order to gate out dead lymphocytes, the gate of CD4 T cells with increased SSC and low FSC was excluded (25). Isotype matched controls were used to determine auto-fluorescence and non-specific staining. Analysis was performed using the FCS Express (*De Novo* Software) and results were expressed as percentages of IFN- γ ^{pos}/CFSE^{low}/CD4^{pos} T cells induced by the different macrophage populations. To complement these results, the amounts of IFN- γ released in the supernatant throughout the coculture were determined by ELISA according to the manufacturer's kit indications (BD Bioscience).

Measurement of Bacterial Intracellular Growth in Macrophages by Colony Forming Unit (CFU) Assay

Macrophages exposed (or not) to TB-PE, were infected with H37Rv Mtb strain at a MOI of 1 bacteria/cell in triplicates. After 2 h, extracellular bacteria were removed by gently washing four times with pre-warmed PBS. At 4 h and days 3, 6, and 10, cells were lysed in 0.1% SDS and neutralized with 20% Bovine Serum Albumine in Middlebrook 7H9 broth. Serial dilutions of the lysates were plated in triplicate, onto 7H11-Oleic Albumin Dextrose Catalase (OADC, Difco) agar medium for CFU scoring at 21 days later.

Western Blots

Macrophages were treated (or not) with TB-PE. Following the different experimental treatments, cells were lysed in ice-cold buffer consisting of 150 mM NaCl, 10 mM Tris, 5 mM EDTA, 1% SDS, 1% Triton X-100, 1% sodium deoxycholate, gentamicin/streptomycin, 0.2% azide plus a cocktail of protease inhibitors (Sigma-Aldrich). Lysates were incubated on ice for 3 h and cleared by centrifugation for 15 min at 14,000 rpm at 4°C. Protein concentrations were determined using the

BCA protein assay (Pierce). Equal amounts of protein (40 μ g) were then resolved on a 10% SDS-PAGE. Proteins were then transferred to Hybond-ECL nitrocellulose membranes (Amersham) for 2 h at 100 V and blocked with 1% BSA-0.05% Tween-20 for 1 h at room temperature. Membranes were then probed with primary anti-human ACAT (1:200 dilution, SOAT; Santa Cruz) or anti-human pY705-STAT3 (1:1,000 dilution, Cell Signaling Technology, clone D3A7) overnight at 4°C. After extensive washing, blots were incubated with a HRP-conjugated goat anti-rabbit IgG Ab (1:5,000 dilution; Santa Cruz Biotechnology) or HRP-conjugated goat anti-mouse IgG Ab (1:2,000 dilution; Santa Cruz Biotechnology) for 1 h at room temperature. Immunoreactivity was detected using ECL Western Blotting Substrate (Pierce). Protein bands were visualized using Kodak Medical X-Ray General Purpose Film. For internal loading controls, membranes were stripped by incubating in buffer consisting of 1.5% Glycine, 0.1% SDS, 1% Tween-20, pH 2.2 for 10 min twice, extensively washed and then reprobed with anti- β -actin (1:2,000 dilution; ThermoFisher, clone AC-15) or anti-STAT3 Ab (1:1,000 dilution; Cell Signaling Technology, clone D1A5). Results from Western blot were analyzed by densitometric analysis (Image J software).

Immunostaining

Macrophages were plated on glass coverslips and were treated with or without 20% v/v of TB-PE for 24 h. Cells were fixed with PFA 4% for 20 min at room temperature and then PFA was quenched with 50 mM NH_4Cl for 2 min. Cells were rinsed in PBS once and then were labeled with 1 μ g/ml of BODIPY 493/503 (Life technologies) for 15 min before permeabilization with PBS-Triton X-100 0.1% for 10 min. Cells were then incubated with PBS-BSA 3% w/v for 30 min prior to overnight incubation at 4°C with primary anti-human pY705-STAT3 (dilution 1/100, Cell Signaling Technology, Clone D3A7). Cells were then washed and incubated with Goat anti-Mouse IgG, AlexaFluor 555 (dilution 1/1,000, Cell Signaling Technology) for 1 h at room temperature. Cells were extensively washed and then incubated for 10 min with DAPI in PBS-BSA 1% (500 ng/ml, Sigma-Aldrich). Finally, slides were mounted and visualized with a Leica DM-RB fluorescence microscope.

Mice

Wild-type (WT) BALB/c and IL-10 knockout (IL-10 KO) (C.129P2(B6)-IL-10 tm1Cgn/J) BALB/c male mice (8–12 weeks old), were obtained from the Leloir Institute Foundation. Animals were bred and housed in accordance with the guidelines established by the Institutional Animal Care and Use Committee of Institute of Experimental Medicine (IMEX)-CONICET-ANM. All animal procedures were shaped to the principles set forth in the Guide for the Care and Use of Laboratory Animals (26).

Generation of BMDMs

Femurs and tibia from WT and IL-10 KO mice were removed after euthanasia and the bones were flushed with RPMI-1640 medium by using syringes and 25-Gauge needles. The cellular suspension

was centrifuged and the red blood cells were removed. The BMDMs were obtained by culturing the cells with RPMI-1640 medium containing L-glutamine, pyruvate, β -mercaptoethanol (all from Sigma-Aldrich), 10% FCS and 20 ng/ml of murine recombinant M-CSF (Biolegend) at 37°C in a humidified incubator for 7–8 days. Differentiated BMDMs were re-plated into 24-well tissue culture plates in complete medium prior to cell stimulation with Mtb lipids for 24 h. Alternatively, recombinant murine IL-10 (Peprotech) at 10 ng/ml was added to the cultures for 24 h.

Statistical Analysis

All values are presented as mean and SEM of a number of independent experiments. Independent experiments are defined as those performed with macrophages derived from monocytes isolated independently from different donors. As most of our datasets did not pass the normality tests, non-parametric tests were applied. Comparisons between more than two paired data sets were made using the Friedman test followed by Dunn's Multiple Comparison Test. Comparisons between two paired experimental conditions were made using the two-tailed Wilcoxon Signed Rank. Correlation analyses were determined using the Spearman's rank test. For all statistical comparisons, a *p* value < 0.05 was considered significant.

RESULTS

Tuberculous PE Fluids Induce Lipid Bodies Accumulation in Macrophages

It has been demonstrated that Mtb induces a lipid-rich foam cell phenotype in host macrophages (6–8, 27), possibly *via* TLR2 and TLR6 activation (28). Moreover, merely isolated lipids from Mtb were able to induce the foamy phenotype (7, 27). Based on this knowledge, we aimed to determine whether soluble factors found in physiological samples derived from active TB patients could promote the generation of FM. To this end, we treated human M-CSF-driven macrophages with cell-free preparations of PE derived from patients with tuberculosis (TB-PE) in order to mimic a genuine microenvironment derived during Mtb infection. According to the pattern of staining of neutral lipids with ORO, we observed that TB-PE treatment induced lipid bodies accumulation in macrophages to the same extent as Mtb infection or exposure to Mtb-derived lipids (**Figure 1A**). We also demonstrated that the formation of lipid bodies was specific for TB-PE treatment in comparison to PE from patients with heart failure (HF-PE) (**Figure 1B**). Moreover, biochemical analysis of the lipids recovered from macrophages identified higher abundance of cholesteryl esters and triacylglycerols in TB-PE-treated macrophages in comparison to control or HF-PE-treated macrophages (**Figure 1C**). Additionally, unlike HF-PE, the treatment with TB-PE resulted in an increase of the total intracellular cholesterol content (**Figure 1D**) and a twofold increase of CD36 expression (**Figure 1E**). Therefore, soluble factors released during pleural Mtb infection induced lipid body accumulation in human macrophages that typically confirm the FM phenotype.

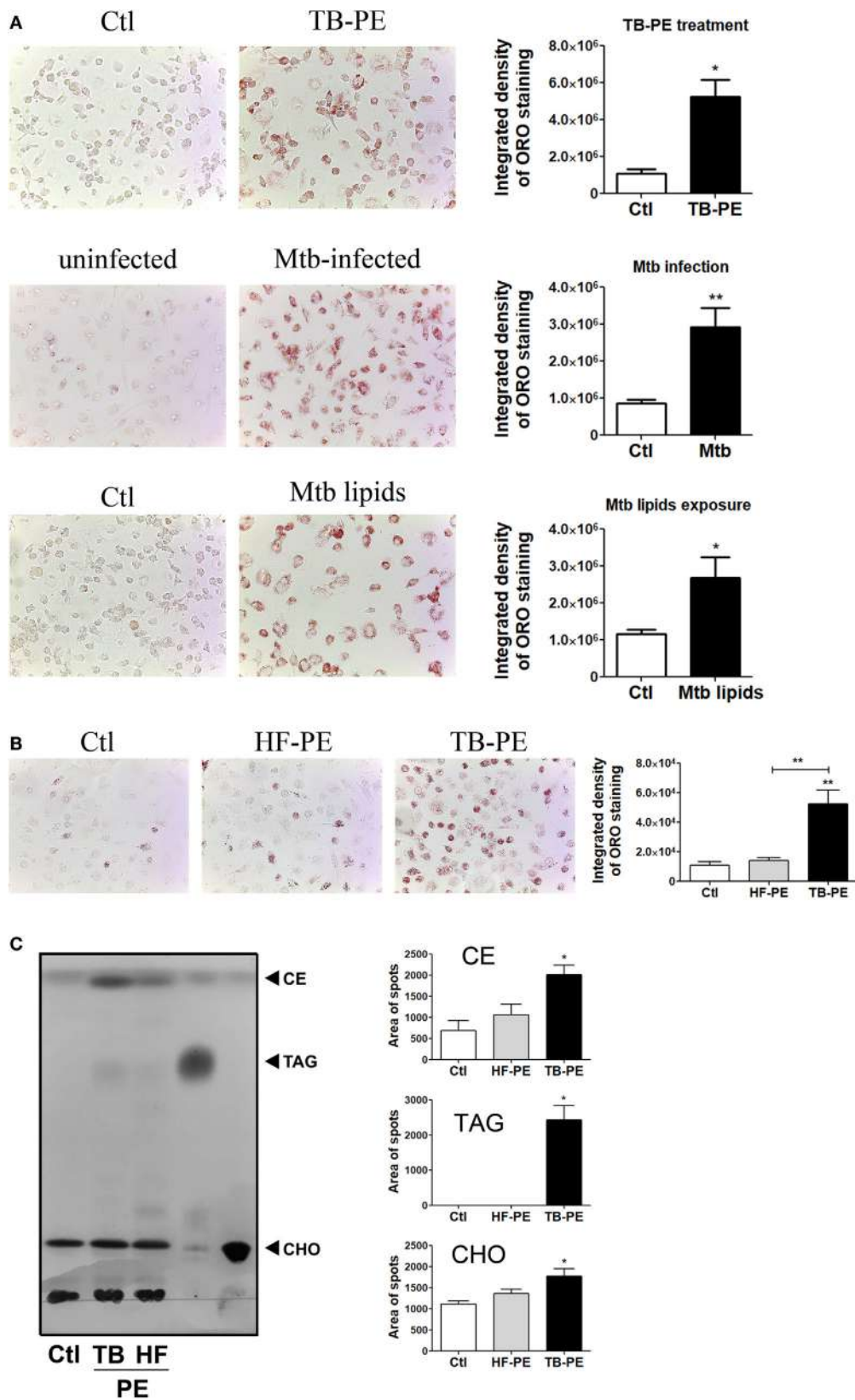


FIGURE 1 | Continued

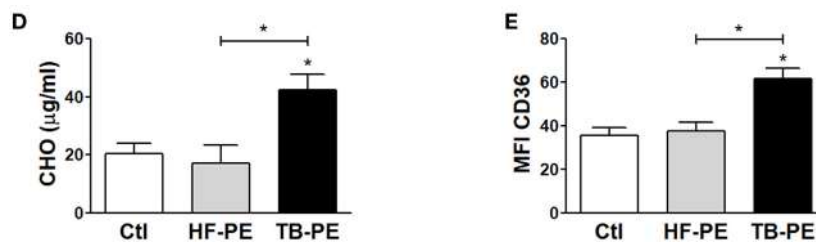


FIGURE 1 | Tuberculous pleural effusions (TB-PE) induce lipid bodies accumulation in macrophages. **(A)** Human monocyte-derived macrophages (MDM) were treated either with TB-PE or with *Mycobacterium tuberculosis* (Mtb) lipids, or infected with Mtb H37Rv for 24 h and then stained with Oil Red O (ORO). Representative images are shown in left panels (40x magnification) and the integrated density of ORO staining is shown in right panels. Values are expressed as means \pm SEM of six independent experiments, considering five microphotographs per experiment. Wilcoxon signed rank test: * $p < 0.05$. **(B)** MDM were treated with TB-PE or PE from heart failure patients (HF-PE) and stained with ORO ($n = 5$). **(C)** Left panel shows a representative thin layer chromatographic analysis of lipids from MDM treated or not with either TB-PE or HF-PE. Total lipids were extracted from untreated MDM (lane 1), TB-PE-treated MDM (lane 2), HF-PE-treated MDM (lane 3), and the standard lipids triacylglycerol (TAG, lane 4) and free cholesterol (CHO, lane 5). Cholesterol esters (CE) are also indicated. Right panels depict the area of spots for CE, TAG, and CHO in control and TB-PE or HF-PE treated MDM ($n = 4$). **(D)** Intracellular total cholesterol (CHO) content in MDM exposed or not to TB-PE or HF-PE measured by an enzymatic method ($n = 5$). **(E)** Mean fluorescence intensity (MFI) of CD36 cell-surface expression in MDM exposed or not to TB-PE or HF-PE measured by flow cytometry ($n = 5$). **(B–E)** Friedman test followed by Dunn's Multiple Comparison Test: * $p < 0.05$; ** $p < 0.01$ for TB-PE vs Ctl or as depicted by lines.

FM Induced by Tuberculous PE Display Immunosuppressive Properties

In order to assess whether the differentiation into FM induced by TB-PE may have a negative impact on the development of the antimycobacterial response, we determined phenotype and functions of TB-PE-induced FM. As observed in **Figure 2A**, macrophages treated with TB-PE displayed a higher expression of anti-inflammatory markers such as CD163, mannose receptor or CD206 (MRC1), and PD-L1, and a lower expression of the MHC class II cell-surface receptor, HLA-DR. In accordance with the acquisition of this anti-inflammatory profile, TB-PE-induced FM secreted higher levels of IL-10 and lower levels of TNF- α upon stimulation with irradiated *Mycobacterium tuberculosis* (iMtb) than untreated cells (**Figure 2B**). In order to assess the effect of TB-PE treatment on the presentation of mycobacterial antigens, macrophages were treated with or without TB-PE for 24 h, washed and stimulated with iMtb for further 24 h. Thereafter, cells were washed and cocultured with autologous CFSE-labeled CD4 T cells derived from healthy PPD positive subjects for 5 days. Based on the CFSE labeling of CD4 T cells, while TB-PE-treated macrophages did not induce differential levels of proliferation of antimycobacterial CD4 T cells (**Figure 2C**), they promoted differential distribution of the IFN- γ producing clones (**Figure 2D**). In particular, those macrophages treated with TB-PE induced lower percentages of IFN- γ producing clones (**Figure 2D**) and a lower release of IFN- γ (**Figure 2E**), as compared to untreated macrophages in response to iMtb stimulation. Of note, IL-4 and IL-17 contents were undetectable in these assays (data not shown). Therefore, the activation of Ag-specific IFN- γ -producing CD4 T cells was impaired when macrophages were exposed to TB-PE, suggesting that the accumulation of lipid bodies is accompanied by a reduced capacity to activate antimycobacterial Th1 cells.

Next, we assessed whether the treatment with TB-PE had an impact on the control of the bacillary load. To accomplish this, macrophages were treated with TB-PE for 24 h, washed and

infected with Mtb. Although no differences were observed in the uptake of the mycobacteria as judged by the scoring of the CFU at 4 h post-infection (**Figure 2F**), a significant increase in the bacillary load was observed in TB-PE-treated macrophages at later time points (**Figure 2G**). Therefore, FM induced by TB-PE are more susceptible to Mtb intracellular growth.

IL-10 Promotes Accumulation of Lipid Bodies in Macrophages under TB-PE Treatment

In order to evaluate the host factors involved in promoting the accumulation of lipid bodies by TB-PE, we depleted different cytokines known to be highly present in this fluids (29, 30), including IL-10, TNF- α , IL-1 β , IL-6, and IFN- γ . We then evaluated the ability of these depleted-PE to induce the foamy phenotype in macrophages. The depletion of each individual cytokine was confirmed by ELISA (Figure S1A in Supplementary Material). Interestingly, only the depletion of IL-10 from TB-PE was capable of preventing lipid bodies accumulation (**Figure 3A**). This result was also confirmed by labeling the cells with Bodipy staining (Figure S1B in Supplementary Material). In addition, macrophages exposed to IL-10-depleted TB-PE showed a reduction of intracellular cholesterol content and CD36 cell-surface expression in comparison to those cells treated with non-depleted or depleted of any other cytokines (**Figures 3B,C**). In line with these results, the addition of recombinant IL-10 to the IL-10-depleted TB-PE restored the acquisition of the foamy phenotype in a dose-dependent manner (**Figure 3D**). Of note, the addition of IL-10 in the absence of TB-PE did not induce the foamy phenotype (**Figure 3D**). Thereafter, we determined the presence of the lipidic vacuoles by electron microscopy in macrophages treated with TB-PE depleted (or not) of IL-10. As it is shown in **Figure 3E**, while untreated macrophages showed numerous pseudopodia and empty cytoplasmic vacuoles, TB-PE-treated macrophages displayed electron dense lipid osmiophilic vacuoles,

which correspond to lipid bodies. Interestingly, macrophages treated with IL-10-depleted TB-PE showed smaller-sized lipidic vacuoles than those exposed to non-depleted TB-PE. These results indicate that the IL-10 present in TB-PE is a key host factor promoting the lipid-laden phenotype in the presence of exogenous lipids.

IL-10 Levels Correlate with FM Abundance in PE

In order to evaluate whether IL-10 level is associated to the acquisition of the foamy phenotype in the course of a Mtb natural infection, we assessed the levels of IL-10 and total cholesterol in individual preparations of TB-PE, and the numbers of FM found

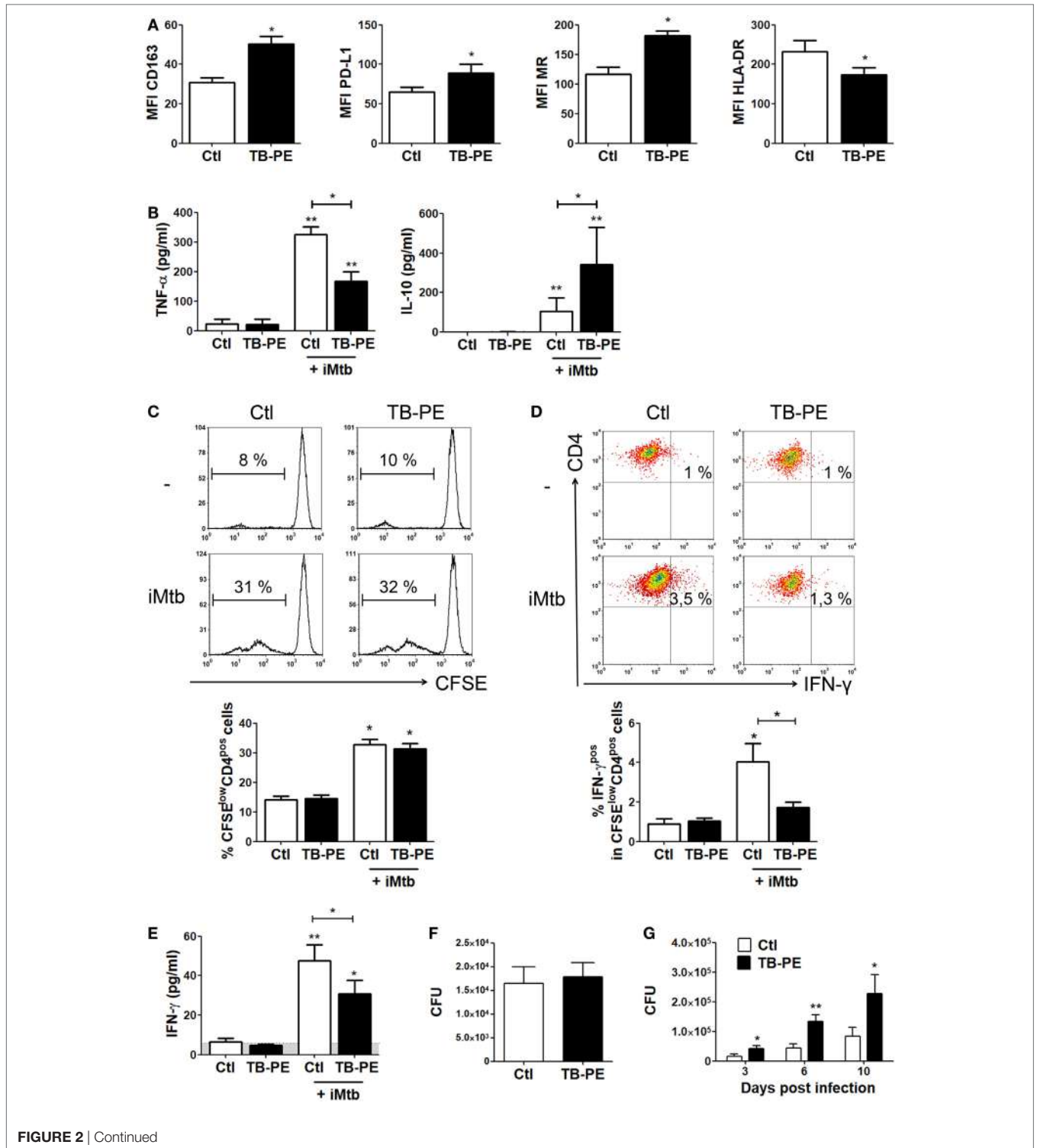


FIGURE 2 | Continued

FIGURE 2 | Macrophages treated with tuberculous pleural effusion (TB-PE) display immunosuppressive properties. **(A)** Mean fluorescence intensity (MFI) of CD163, PDL-1, MR, and HLA-DR measured by flow cytometry in human monocyte-derived macrophages (MDM) exposed or not to TB-PE ($n = 5$). Wilcoxon signed rank test: $*p < 0.05$. **(B)** Levels of secreted IL-10 and TNF- α by MDM exposed or not to TB-PE in response to irradiated *Mycobacterium tuberculosis* (iMtb) measured by ELISA ($n = 5$). Friedman test followed by Dunn's Multiple Comparison Test: $*p < 0.05$; $**p < 0.01$, for iMtb-stimulated vs unstimulated, or as indicated in the graph. **(C–E)** MDM from healthy PPD⁺ donors exposed or not to TB-PE for 24 h, were stimulated or not with iMtb for 24 h and then used as antigen presenting cells (APC) in autologous proliferation assays. Cocultures were performed with autologous carboxyfluorescein succinimidyl ester (CFSE)-labeled CD4 T cells at a ratio of 10 T cells: 1MDM. **(C)** Representative histograms showing CFSE labeling in CD4^{pos} T cells activated by macrophages exposed (or not) to TB-PE, loaded (or not) with iMtb. Right panel shows the quantification of the percentages of proliferating CD4^{pos} T cells (CFSE^{low}/CD4^{pos} cells) in each condition. Loaded vs unloaded with iMtb: $*p \leq 0.05$ ($n = 4$). **(D)** Representative dot plots showing CD4 and IFN- γ expression among CFSE^{low}/CD4^{pos} T cells activated by MDM exposed (or not) to TB-PE, loaded (or not) with iMtb. Right panel shows the quantification of the percentages of proliferating IFN- γ -producing CD4^{pos} T cells (IFN- γ ^{pos}/CFSE^{low}/CD4^{pos} T cells) in each condition ($n = 4$). Friedman test followed by Dunn's Multiple Comparison Test: $*p < 0.05$, for iMtb-stimulated vs unstimulated, or as indicated in the graph. **(E)** The amounts of IFN- γ released throughout the coculture were determined by ELISA. Friedman test followed by Dunn's Multiple Comparison Test: $*p < 0.05$; $**p < 0.01$, for iMtb-stimulated vs unstimulated, or as indicated in the graph. **(F)** Bacillary loads in MDM treated (or not) with TB-PE, washed, and infected with *Mycobacterium tuberculosis* (Mtb) strain H37Rv for 4 h ($n = 6$). Wilcoxon signed rank test. **(G)** Intracellular colony forming units were determined at different time points in MDM treated with TB-PE for 24 h, washed and infected with Mtb ($n = 10$). Wilcoxon signed rank test: $*p < 0.05$; $**p < 0.01$; $***p < 0.001$ for TB-PE treated vs Ctl.

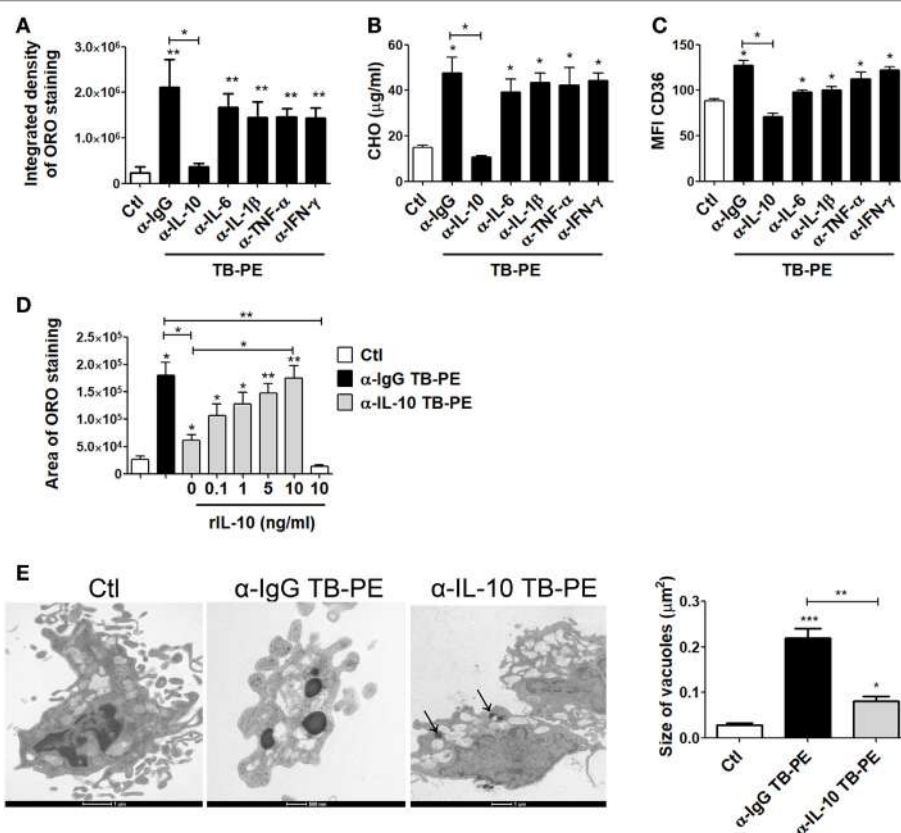
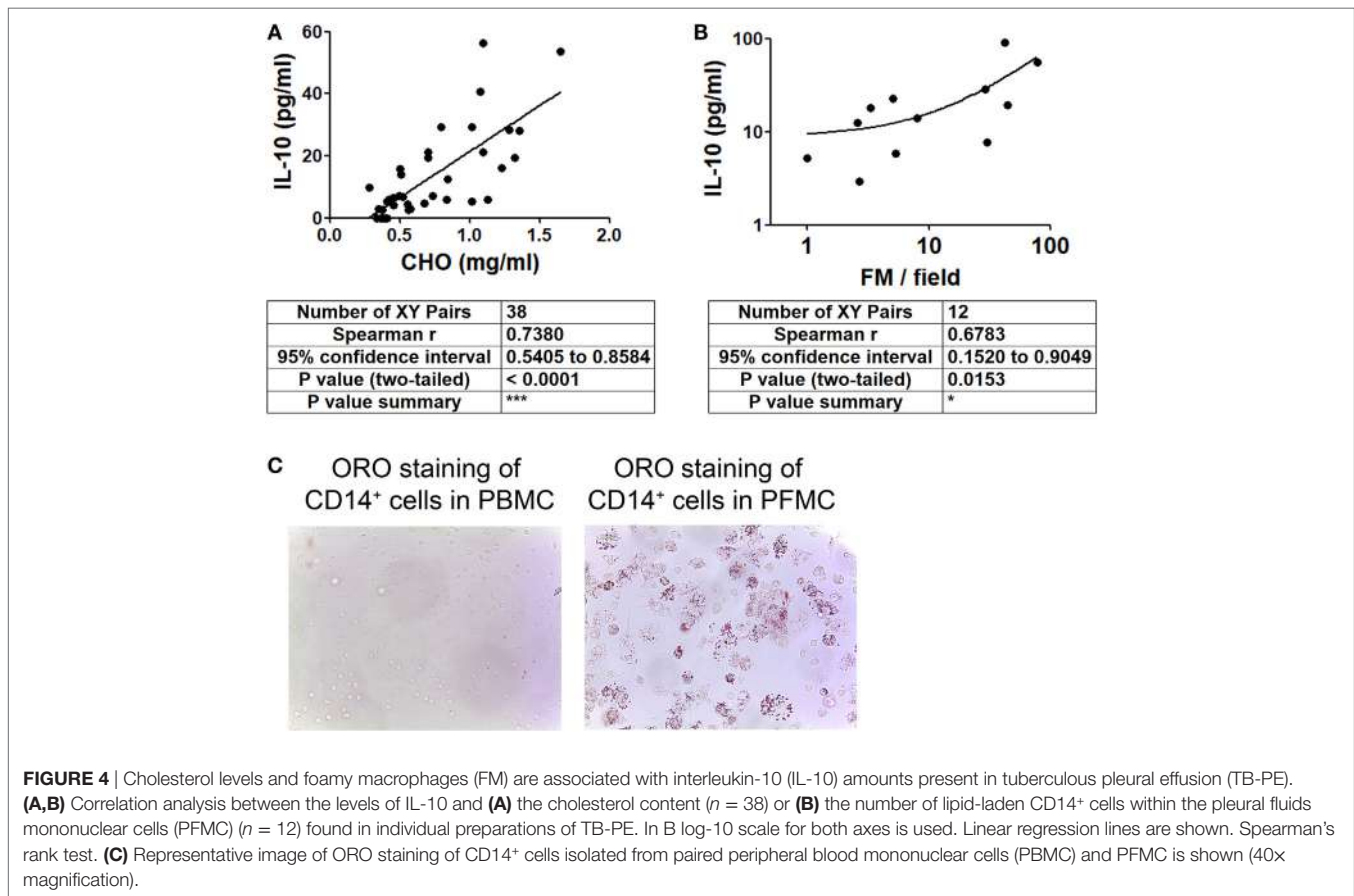


FIGURE 3 | Interleukin-10 (IL-10) promotes lipid bodies accumulation in macrophages treated with tuberculous pleural effusion (TB-PE). **(A–C)** Human monocyte-derived macrophages (MDM) were treated with TB-PE depleted or not for different cytokines for 24 h and **(A)** lipid bodies' content was measured by Oil Red O (ORO) staining ($n = 4$). **(B)** Intracellular cholesterol (CHO) content measured by an enzymatic method ($n = 4$) was determined. **(C)** Mean fluorescence intensity (MFI) of CD36 cell-surface expression was measured by flow cytometry ($n = 4$). **(D)** MDM were treated (or not) with TB-PE depleted or not of IL-10 in the presence of different amounts of recombinant human IL-10 (rIL-10) for 24 h and lipid bodies content was measured by ORO staining ($n = 6$). **(E)** Representative electron microscopy micrographs of MDM treated with TB-PE depleted or not of IL-10. White asterisks indicate large electron dense osmiophilic vacuoles and arrows point small sized ones. Morphometric study of the area per vacuole in each condition is shown ($n = 14$). **(A–E)** Friedman test followed by Dunn's Multiple Comparison Test: $*p < 0.05$; $**p < 0.01$; $***p < 0.001$ for experimental condition vs Ctl or as depicted by lines.

within the pleural fluids mononuclear cells (PFMC). We found that levels of IL-10 and total cholesterol were positively correlated (**Figure 4A**), unlike other cytokines such as IFN- γ , IL-6, TNF- α , and IL-1 β (Figure S2 in Supplementary Material). Noticeably,

there was also a positive correlation between the level of IL-10 and the number of FM among the PFMC (**Figure 4B**). Moreover, lipid-laden CD14⁺ cells were found in the pleural compartment but not in paired peripheral blood (**Figure 4C**). These results



support the idea that IL-10 potentiates the acquisition of the foamy program in human macrophages in the context of a natural infection.

IL-10 Deficiency Prevents the Foamy Phenotype in BMDM

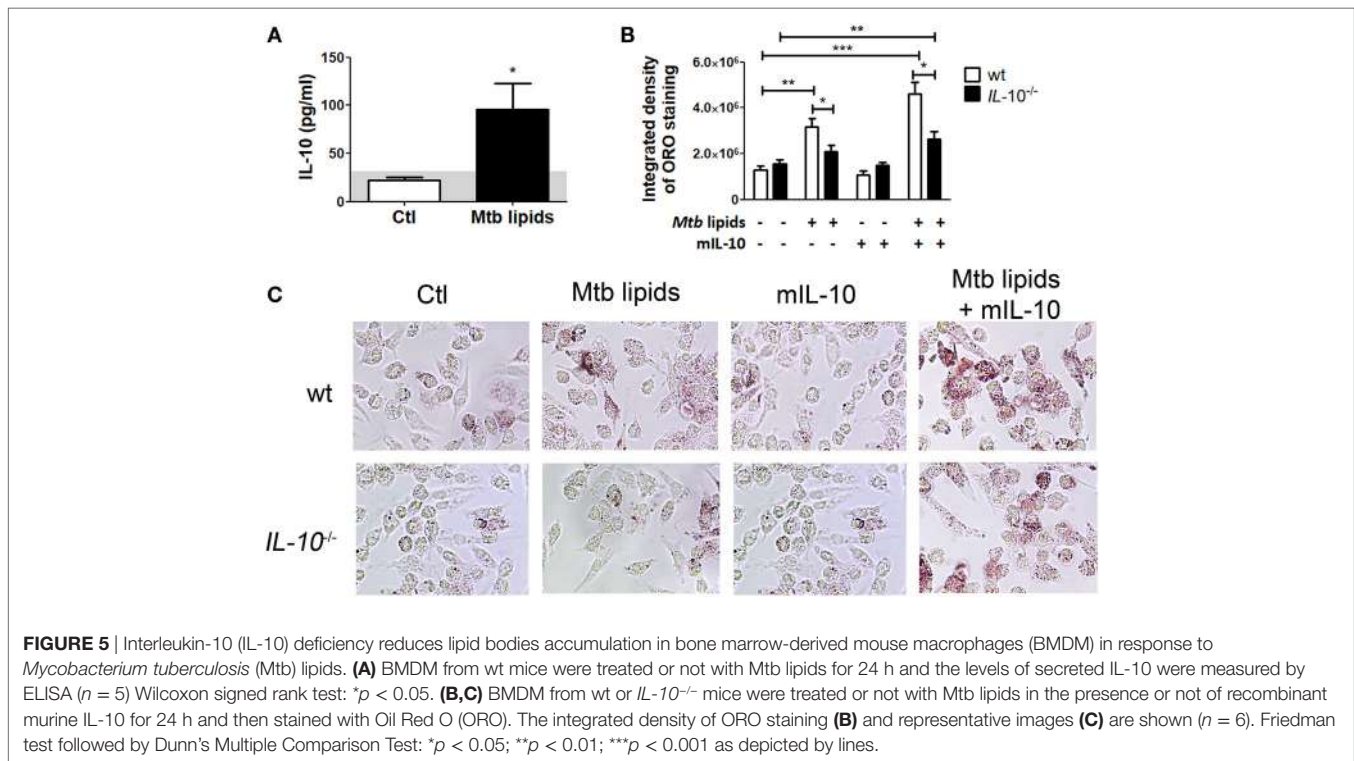
To confirm the role of IL-10 in the differentiation of FM, we evaluated whether BMDM derived from IL-10-knock out (KO) mice could indeed become FM after the treatment with lipids from Mtb. First, we determined IL-10 production in M-CSF-derived BMDM from WT mice stimulated with mycobacterial lipids for 24 h. As shown in **Figure 5A**, unlike the undetectable level of TNF- α (data not shown), BMDM secreted IL-10 in response to mycobacterial lipid-stimulation. Second, we compared whether BMDM derived from WT or IL-10-KO mice differed in their propensity to accumulate lipid bodies in response to Mtb-derived lipids. As illustrated in **Figures 5B,C**, IL-10-deficiency prevented the foamy phenotype induced by Mtb lipids, which in turn could be partially reverted by the addition of exogenous IL-10. In agreement with our previous results, exogenous IL-10 did not induce the foamy phenotype in the absence of the source of lipids in BMDM. These results obtained in murine macrophages confirm those obtained in human TB-PE-treated macrophages, demonstrating the key role of IL-10 in favor of the differentiation program toward foamy cells.

The IL-10/STAT3 Axis Is Involved in the FM Differentiation Induced by TB-PE

Considering the role of IL-10 in promoting the differentiation of macrophages into FM, and that STAT3 is a pivotal transcriptional factor induced by IL-10 (31, 32), we studied the contribution of STAT3 activation in the induction of the foamy phenotype by measuring its phosphorylated form (pSTAT3). First, we determined that STAT3 was activated in TB-PE-treated macrophages detecting its phosphorylated form by western blot and immunofluorescence microscopy (**Figures 6A,B**). As depicted in **Figure 6B** FM induced by TB-PE showed nuclear localization of STAT3 phosphorylated on tyrosine 705, reflecting STAT3 activation. Importantly, pharmacological inhibition of STAT3 with Stattic (or with cucurbitacin I) prevented the accumulation of lipid bodies in macrophages in a dose-dependent manner (**Figure 6C**; **Figures S3A,B** in Supplementary Material). Therefore, the enhancement of FM differentiation driven by IL-10 is mediated by STAT3.

IL-10 Enhances ACAT Expression in TB-PE-Treated Macrophages Leading to FM Differentiation

In order to elucidate the mechanism by which IL-10 promotes FM differentiation, we assessed the expression of ACAT, which is central for the biogenesis of lipid bodies by converting free- into



esterified-cholesterol that are eventually packed inside the lipid droplets (33). We first showed that the foamy phenotype induced by TB-PE was dependent on ACAT activity, as judged both by the increase of ACAT expression after TB-PE treatment (Figure 7A), and by the blocking of the accumulation of lipid bodies in the presence of Sandoz, a specific inhibitor of ACAT (Figure 7B). Noticeably, the inhibition of ACAT lead to reduced amounts of both cholesteryl esters and triacylglycerols in TB-PE-treated macrophages (Figure 7C), confirming the involvement of ACAT in FM formation upon TB-PE treatment. We then assessed ACAT expression in IL-10-depleted TB-PE and we found that its expression was reduced in the absence of IL-10 (Figure 7A). In agreement with this result, ACAT induction by TB-PE was abolished when STAT3 activity was inhibited (Figure 7D). Therefore, the IL-10/STAT3 axis activated by TB-PE enhances FM differentiation through the upregulation of ACAT expression, leading to an increased biogenesis and accumulation of lipid bodies.

Based on our findings, we propose a model for the modulation of FM in the context of a physiologically relevant microenvironment promoted by Mtb infection for which the axis IL-10/STAT3 induces the accumulation of lipid bodies *via* ACAT upregulation. This in turn is accompanied by an increase of CD36 and the acquisition of immunosuppressive properties, such as a reduced induction of antimycobacterial Th1 clones, an enhanced production of IL-10 and a more permissive phenotype for bacillary growth (Figure 8).

DISCUSSION

Tuberculosis, as a chronic condition, entails the establishment of extensive metabolic remodeling in both host and pathogen.

One of the consequences of this adaptation is the formation of FM. Since FM have been associated with the bacilli persistence and tissue pathology (6, 8, 12, 27, 34), we aimed to determine which host factors may contribute to enlarge the pool of FM in TB. In this sense, we used the acellular fraction of TB-PE to mimic those soluble factors released locally during Mtb infection. Although pleural disease due to *Mtb* is generally categorized as extra-pulmonary, there is an intimate anatomic relationship between the pleura and the pulmonary parenchyma (35, 36). Current literature supports the notion that TB-PE is the consequence of a direct local infection with a cascade of events, including an immunological response, instead of the result of a pure delayed hypersensitivity reaction, as previously thought (37). Even though we cannot state that macrophages infiltrating the pleural cavity will reproduce with fidelity those macrophages in the infected alveolar space or lung interstitial tissue, we can affirm that TB-PE represents microenvironment from a human respiratory cavity that is impacted by the infection. To our knowledge, this is the first time that such a complex but physiologically relevant human sample has been used in order to study the biology of FM. Using this *in vitro* model, we demonstrated that the acellular fraction of TB-PE induces the accumulation of lipid bodies in human macrophages. Moreover, our finding was validated by the detection of lipid-laden CD14⁺ cells isolated directly from the mononuclear cells of the PE, providing physiological relevance to our *in vitro* model. Taking into account that tuberculous PE has, if any, very few bacilli content (38), and that it displays high cholesterol content, we infer that in our model the source of lipids feeding the lipid bodies in the macrophages are likely host-derived components instead of mycobacterial ones.

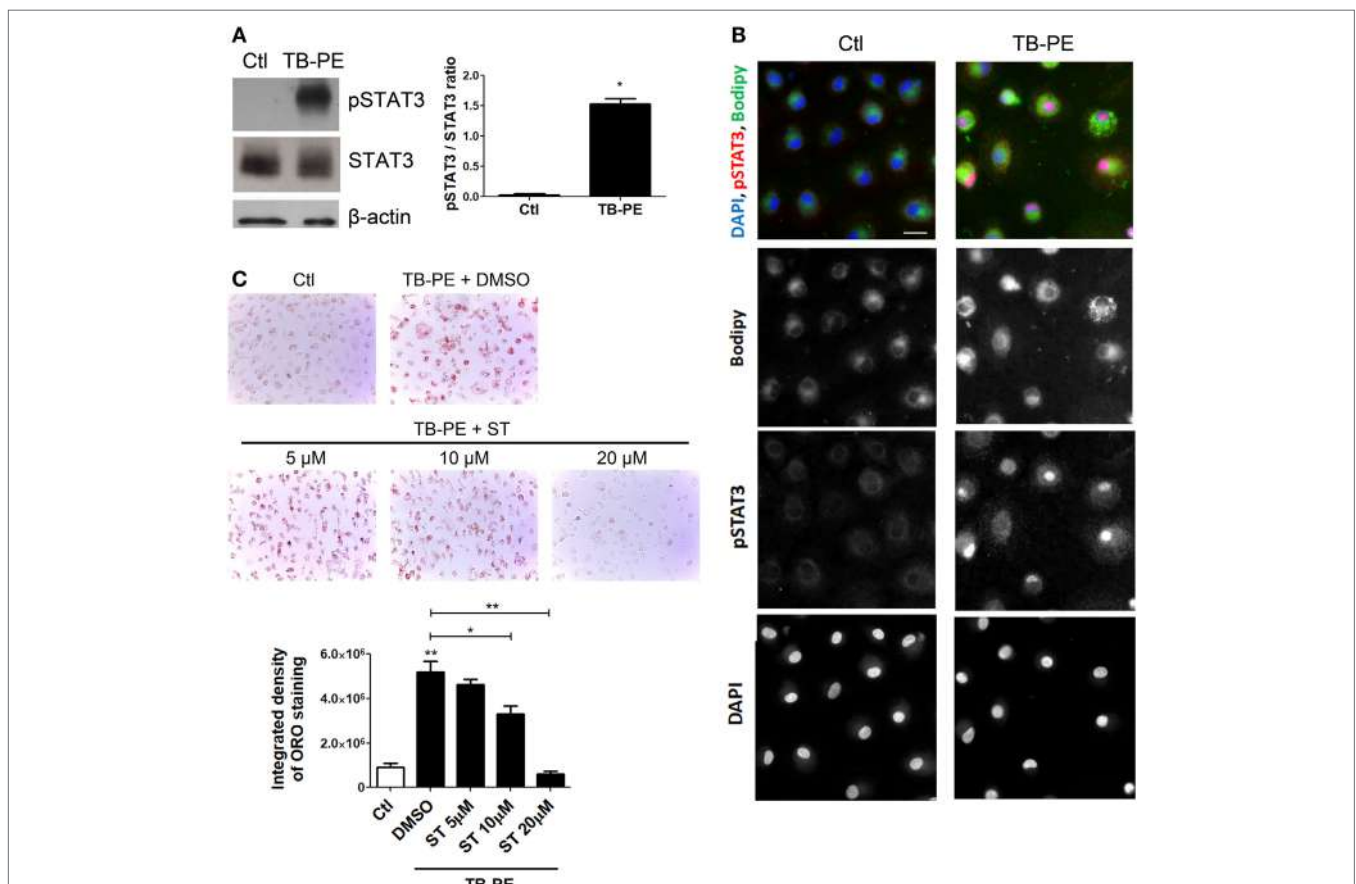


FIGURE 6 | Signal transducer and activator of transcription 3 (STAT3) activation enhances lipid bodies accumulation induced by treatment of macrophages with tuberculous pleural effusion (TB-PE). **(A)** Analysis of p705-STAT3, STAT3, and β-actin protein expression level by western Blot (left panel) and quantification (right panel; $n = 4$) in human monocyte-derived macrophages (MDM) treated with TB-PE for 24 h. Wilcoxon signed rank test: * $p < 0.05$ **(B)** MDM were treated or not with TB-PE for 24 h and then were fixed, labeled with Bodipy 493/503 (green), permeabilized, and stained for p705-STAT3 (Red) and DAPI (blue). Representative images are shown. Scale bar, 10 μm. **(C)** MDM were treated or not with different concentrations of Stattic (STAT3 inhibitor, ST) for 2 h and then exposed or not to TB-PE for 24 h. Lipid bodies' content was determined by Oil red O (ORO) staining ($n = 6$). Representative images are shown and the integrated density of ORO staining is shown. Friedman test followed by Dunn's Multiple Comparison Test: * $p < 0.05$; ** $p < 0.01$ for TB-PE treated vs Ctl, or as depicted by lines.

Although lipid bodies were qualified as passive organelles involved in lipid storage, it became clear that these organelles play a central role in several inflammatory (e.g., atherosclerosis) or chronic infectious diseases (e.g., TB) (8, 13). In this work, we provide evidence that FM differentiation induced by TB-PE is potentiated by IL-10 in association with the acquisition immunosuppressive properties, impairing the activation of antimicrobial Th1 clones, producing the anti-inflammatory cytokine IL-10 and bearing higher bacillary loads. This is in line with previous reports characterizing the immunosuppressive profile in macrophages activated by the IL-10/STAT3 signaling pathway (39, 40). In this study, we show that FM formation depends (albeit partially) on the IL-10/STAT3 axis, and thus establishing an association between both processes (accumulation of lipid bodies and immunosuppression). Within this context, we observed that both processes are enhanced by the IL-10/STAT3 signaling pathway, arguing for likelihood of two independent outcomes emanating from the same signaling axis (Figure 8).

Of note, it has been reported that the synthetic glucocorticoid dexamethasone can upregulate ACAT expression promoting formation of FM (41). Although there are extensive reports demonstrating transcriptional interactions between STAT3 and glucocorticoids leading to repression or synergism of target genes (42), it is interesting to notice that both IL-10 and glucocorticoids can polarize macrophages into an immunoregulatory profile (43). Based on that, we propose that the establishment of a foamy phenotype is accompanied by the acquisition of immunosuppressive properties.

It should be mentioned that Stattic is not an inhibitor completely specific for STAT3 (44). In this regard, a desirable goal is the discrimination between STAT3 and STAT1 involvement because both transcription factors can be activated by IL-10 (albeit at different levels), and because of their high degree of homology, particularly in their SH2 domains (44). Under our experimental conditions, unlike the strong activation of STAT3, we did not observe the phosphorylation of STAT1

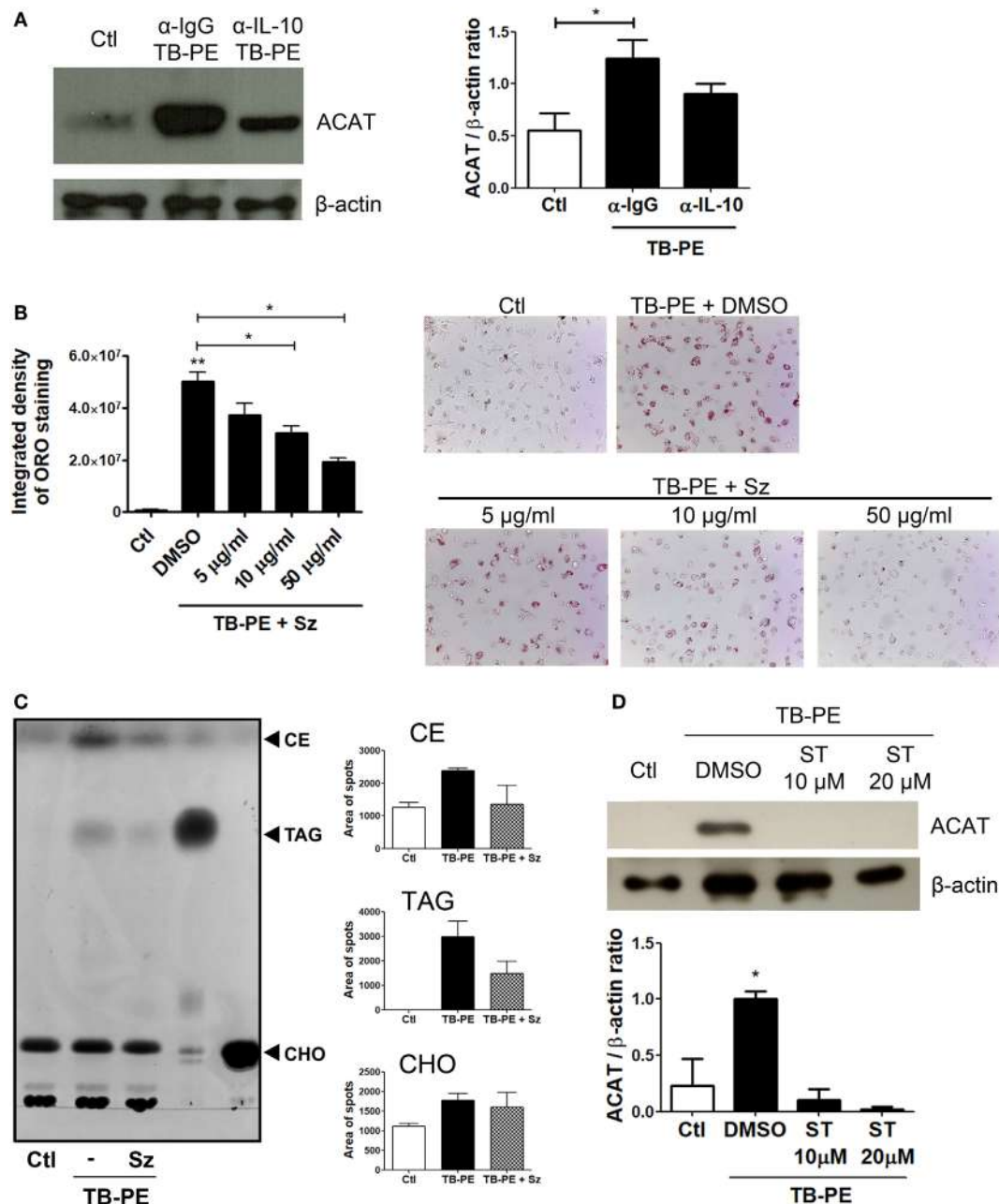
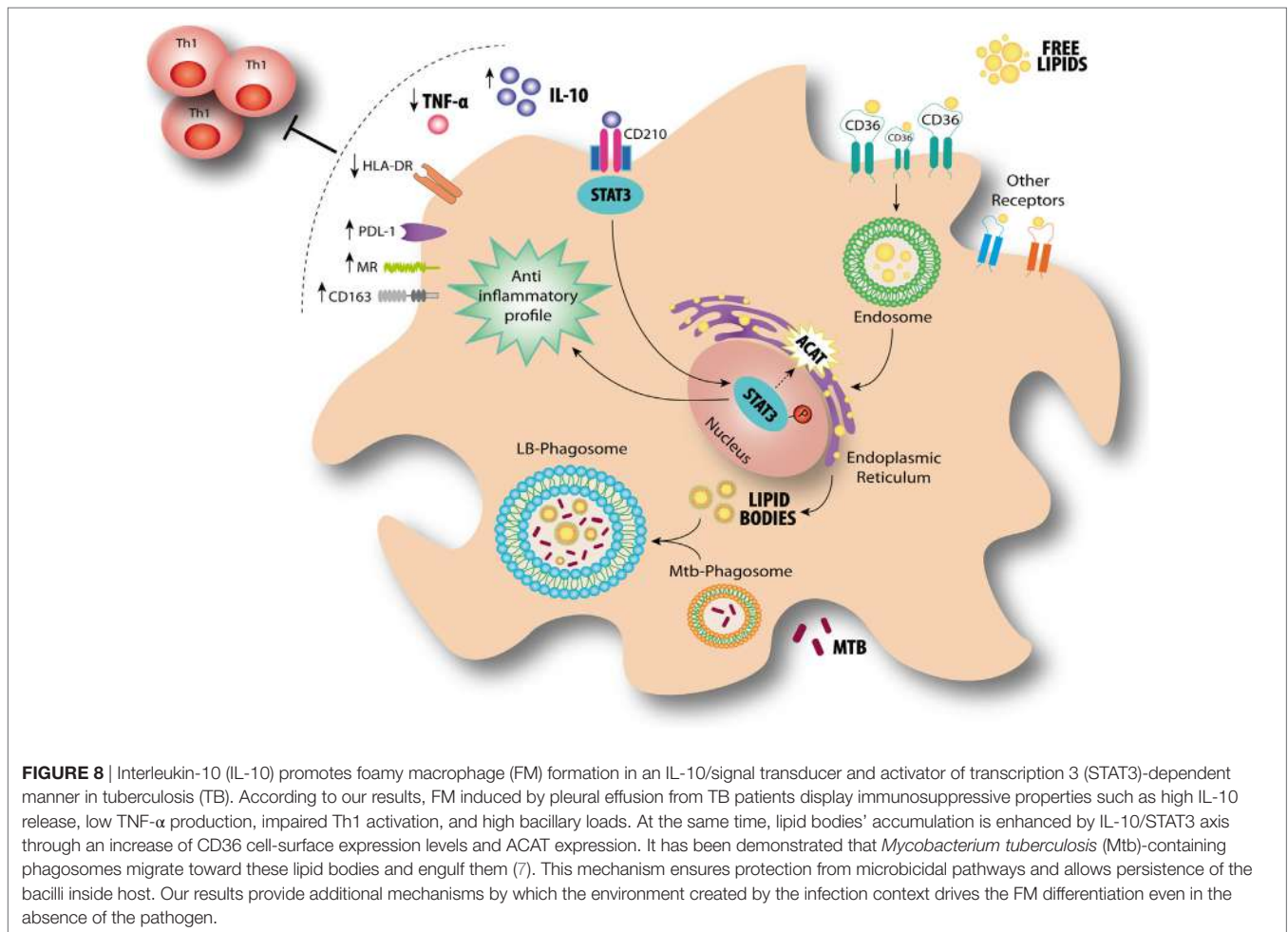


FIGURE 7 | The interleukin-10 (IL-10)/signal transducer and activator of transcription 3 (STAT3) axis promotes foamy macrophage formation through ACAT upregulation. **(A)** Analysis of ACAT and β -actin protein expression level by western Blot (left panel) and quantification (right panel; $n = 5$) in human monocyte-derived macrophages (MDM) treated with tuberculous pleural effusion (TB-PE) for 24 h depleted or not for IL-10. **(B)** MDM were treated or not with different concentrations of Sandoz (Sz, ACAT inhibitor) for 1 h, exposed or not to TB-PE for 24 h, and then stained with Oil Red O (ORO). The Integrated density and representative images are shown ($n = 6$). **(A,B)** Friedman test followed by Dunn's Multiple Comparison Test: * $p < 0.05$; ** $p < 0.01$ for TB-PE treated vs Ctl, or as depicted by lines. **(C)** Thin layer chromatographic analysis of lipids from MDM treated or not with TB-PE in the presence or not of Sz. Total lipids were extracted from untreated MDM (lane 1), TB-PE-treated MDM (lane 2), TB-PE-treated MDM in the presence of Sz (lane 3), and the standard lipids triacylglycerol (TAG, lane 4) and cholesterol (CHO, lane 5). Cholesterol esters (CE) are also indicated. Right panels depict the area of spots for CE, TAG, and CHO in control and TB-PE in the presence or not of Sz treated MDM ($n = 2$). **(D)** Analysis of ACAT and β -actin protein expression level by Western Blot (left panel) and quantification (right panel; $n = 3$) in MDM treated or not with different concentrations of Stattic (ST) for 2 h and then exposed or not to TB-PE for 24 h. Friedman test followed by Dunn's Multiple Comparison Test: * $p < 0.05$ for TB-PE treated vs Ctl.

in macrophages treated with TB-PE (data not shown and **Figure 6**). Likewise, the depletion of IFN- γ (a STAT1 activating cytokine) from TB-PE did not prevent the accumulation

lipid bodies in macrophages (**Figures 3A–C**). Therefore, we consider that our experimental model is dependent of STAT3 instead of STAT1.



Our findings are in agreement with previous reports that demonstrated that macrophages exposed to lipids displayed impaired immune functions. Particularly, FM generated *in vitro* by the incubation with acetylated LDL displayed a reduced expression of pro-inflammatory genes (45). In addition, the ligation of the pregnane X receptor in human macrophages, which was associated to foamy formation, resulted in the impairment of the secretion of pro-inflammatory cytokines, phagolysosomal fusion and apoptosis (46). Moreover, a recent study showed that the treatment of human macrophages with surfactant lipids resulted in the reduction of TNF- α release and the enhancement of Mtb growth (14). Likewise, cholesterol-exposed THP1 macrophages failed both to produce TNF- α in response to Mtb and to clear the infection (15). To the best of our knowledge, we provide the first evidence that FM display a reduced ability to activate a recall Th1 response of specific antimycobacterial T cell clones. Therefore, we propose that FM significantly subvert the host immune response by impairing both the innate and the adaptive immune branches, and we predict a close relationship between lipid exposure, foamy phenotype acquisition and immunosuppressive properties.

Our study also provides additional mechanisms by which the environment created during infection can drive the foamy

differentiation even in the absence of a direct contact with the pathogen. On the one hand, Mtb-infected macrophages can acquire a foamy phenotype as demonstrated in this study and several others (6–9, 27). Indeed, the accumulation of lipid bodies within infected cells has undesirable effects for the host, such as the protection of the pathogen against microbicidal mechanisms (10) and the acquisition of a dormancy phenotype, which confers tolerance to several front-line antibiotics (9). On the other hand, uninfected macrophages can also be driven into foamy cells by IL-10 and a source of lipids. These uninfected lipid-rich cells abrogate the host innate and adaptive cellular defense mechanisms, and when infected, they become a niche favoring pathogen persistence. In the latter case, we infer that uninfected individuals suffering from a lipid dysbalance may bear an enlarged pool of lipid-rich cells that potentially increase the susceptibility, persistence and/or progression of TB. In fact, diabetes and obesity have been associated with TB disease progression (47, 48), and even asymptomatic dyslipidemia was correlated to a reduced antimycobacterial activity (15).

In the past, most reports focused on assessing the impact of certain cytokines in the accumulation of lipid bodies in macrophages within the context of atherosclerosis; FM were proposed to cause the formation of atheroma (49). In fact, IL-1 β

and TNF- α are known to impede neutral lipid turnover in THP-1 cells loaded with lipoproteins (50), and these pro-inflammatory cytokines can decrease the efflux of lipids in J774 murine macrophages (51). In addition, IL-10 was shown to regulate lipid metabolism in human macrophages loaded with acetylated and oxidized LDL by increasing both cholesterol uptake and efflux resulting in a net increase in cholesterol content (52, 53). Considering that both pro- and anti-inflammatory cytokines were associated to the accumulation of lipid bodies, we evaluated in this study the effect of depleting several cytokines from TB-PE on the FM formation. In our hands, unlike the depletion of IL-10, the foamy phenotype induced by TB-PE was not altered by depletion of IL-1 β , TNF- α , IL-6 or IFN- γ , pointing toward a specific role of IL-10 in promoting FM formation in the context of the pleural infection. Moreover, anti-inflammatory cytokines such as IL-4 and IL-13 were shown to alter lipid metabolism in macrophages through the activation of the lipid-activated nuclear receptors PPAR γ (54), which mediates accumulation of lipid bodies (55, 56). Yet, we dismiss a potential role for IL-4 in our model given that its level was undetectable in TB-PE samples (data not shown).

In summary, our present study provides insights into the mechanisms by which host factors can enhance FM formation in macrophages. This knowledge may contribute to the identification of host molecular pathways that could be modulated to the benefit of the patient. Besides, the complementation of the conventional anti-TB therapy with host-directed therapies is desirable in order to achieve shorter treatment times, reduction in lung damage caused by the disease, and lower risk of relapse or reinfection. In this regard, a better understanding of the molecular mechanisms underlying host-pathogen interactions could provide a rational basis for the development of effective anti-TB therapeutics.

ETHICS STATEMENT

Human samples: The research was carried out in accordance with the Declaration of Helsinki (2013) of the World Medical Association, and was approved by the Ethics Committees of the Hospital F. J. Muñiz and the Academia Nacional de Medicina de Buenos Aires (protocol number: NIN-1671-12). Written informed consent was obtained before sample collection. **Mice samples:** Animals were bred and housed in accordance with the guidelines established by the Institutional Animal Care and Use Committee of Institute of Experimental Medicine (IMEX)-CONICET-ANM. All animal procedures were shaped to the principles set forth in the Guide for the Care and Use of Laboratory Animals (NIH, 1996).

AUTHOR CONTRIBUTIONS

MG designed experiments; MG, JF, MD, DK, AM, DM-E, EG-D, and CC performed experiments and analyzed data; BR, AF, and MM performed experiments with mice; EM, SP, and DP collected and provided TB samples; AA and GG performed TLC

determinations; JC and RH-P performed ME determinations; PS, PB, ON, IM-P, CS-T, CC, and RH-P supervised experiments and wrote sections of the manuscript; CV, GL-V, MS, and LB contributed to conception and design of the study, supervised experiments, and wrote the manuscript. All authors contributed to manuscript revision, read, and approved the submitted version.

ACKNOWLEDGMENTS

The authors thank Federico Fuentes for his technical assistance. This work was supported by the Argentinean National Agency of Promotion of Science and Technology (PICT-2015-0055), the Argentinean National Council of Scientific and Technical Investigations (CONICET, PIP 112-2013-0100202), the Alberto J. Roemmers Foundation (2016), the bilateral cooperation programs ECOS-Sud (A14S01) and CONACYT/CONICET, the National Council for Science and Technology Mexico (CONACyT FC 2015-1/115), the Centre National de la Recherche Scientifique, the Agence Nationale de la Recherche (ANR 2010-01301, ANR14-CE11-0020-02, ANR16-CE13-0005-01, ANR-11-EQUIPEX-0003), the University of Toulouse, and the Fondation pour la Recherche Médicale (www.frm.org, grants DEQ20160334902 to ON and DEQ20160334894 to IM-P). The funders had no role in study design, data collection, and analysis, decision to publish, or preparation of the manuscript.

SUPPLEMENTARY MATERIAL

The Supplementary Material for this article can be found online at <http://www.frontiersin.org/articles/10.3389/fimmu.2018.00459/full#supplementary-material>.

FIGURE S1 | Interleukin-10 (IL-10) promotes lipid bodies' accumulation in TB-PE-treated macrophages. **(A)** TB-PE were incubated with neutralizing antibodies for 1 h (4°C) for the depletion of IL-10, IL-6, IL-1 β , or TNF- α , and then, Protein G Sepharose beads were added and incubated for 1 h (4°C). Finally, TB-PE was centrifuged at 12,000 $\times g$ to remove antibody-bead complexes. In the case of IFN- γ depletion, it was performed by incubating TB-PE for 2 h in sterile 96-well plates that had been coated with the capture antibody provided by the human IFN- γ ELISA Kit. In all cases, depletions were controlled by ELISA. **(B)** Human monocyte-derived macrophages were treated with TB-PE depleted or not of IL-10 for 24 h and then, cells were labeled with BODIPY 493/503 to visualize the lipid bodies by green fluorescence emission. The left panels are DIC images of the same field.

FIGURE S2 | Correlation between cholesterol levels and different cytokines present in TB-PE. Correlation analysis between the levels of IL-6, IL-1 β , TNF- α , or IFN- γ and the cholesterol content found in individual preparations of TB-PE ($n = 23-24$).

FIGURE S3 | Signal transducer and activator of transcription 3 (STAT3) activation enhances lipid bodies accumulation by TB-PE. **(A)** Immunoblot images of p705-STAT3, STAT3, and β -actin (left panel); quantification of p705-STAT3 vs STAT3 on macrophages treated or not with Static (20 μ M) or curcubitacin (100 nM) for 2 h and then exposed or not to TB-PE for 24 h (right panel; $n = 3$). **(B)** Macrophages were treated or not with different concentrations of curcubitacin for 2 h and then were exposed or not to TB-PE for 24 h. Lipid bodies' content was assessed by Oil Red O (ORO) staining. The results are shown like the integrated density of ORO staining ($n = 6$) ($*p \leq 0.05$).

REFERENCES

- World Health Organization. *Global Tuberculosis Report 2017*. Geneva: World Health Organization (2017). 76 p.
- Russell DG, VanderVen BC, Lee W, Abramovitch RB, Kim MJ, Homolka S, et al. *Mycobacterium tuberculosis* wears what it eats. *Cell Host Microbe* (2010) 8(1):68–76. doi:10.1016/j.chom.2010.06.002
- Getz GS, Reardon CA. The mutual interplay of lipid metabolism and the cells of the immune system in relation to atherosclerosis. *Clin Lipidol* (2014) 9(6):657–71. doi:10.2217/clp.14.50
- D'Avila H, Melo RC, Parreira GG, Werneck-Barroso E, Castro-Faria-Neto HC, Bozza PT. *Mycobacterium bovis* bacillus Calmette-Guerin induces TLR2-mediated formation of lipid bodies: intracellular domains for eicosanoid synthesis in vivo. *J Immunol* (2006) 176(5):3087–97. doi:10.4049/jimmunol.176.5.3087
- Cardona PJ, Llatjos R, Gordillo S, Diaz J, Ojanguren I, Ariza A, et al. Evolution of granulomas in lungs of mice infected aerogenically with *Mycobacterium tuberculosis*. *Scand J Immunol* (2000) 52(2):156–63. doi:10.1046/j.1365-3083.2000.00763.x
- Kim MJ, Wainwright HC, Locketz M, Bekker LG, Walther GB, Dittrich C, et al. Caseation of human tuberculosis granulomas correlates with elevated host lipid metabolism. *EMBO Mol Med* (2010) 2(7):258–74. doi:10.1002/emmm.201000079
- Peyron P, Vaubourgeix J, Poquet Y, Levillain F, Botanch C, Bardou F, et al. Foamy macrophages from tuberculosis patients' granulomas constitute a nutrient-rich reservoir for *M. tuberculosis* persistence. *PLoS Pathog* (2008) 4(11):e1000204. doi:10.1371/journal.ppat.1000204
- Russell DG, Cardona PJ, Kim MJ, Allain S, Altare F. Foamy macrophages and the progression of the human tuberculosis granuloma. *Nat Immunol* (2009) 10(9):943–8. doi:10.1038/ni.1781
- Daniel J, Maamar H, Deb C, Sirakova TD, Kolattukudy PE. *Mycobacterium tuberculosis* uses host triacylglycerol to accumulate lipid droplets and acquires a dormancy-like phenotype in lipid-loaded macrophages. *PLoS Pathog* (2011) 7(6):e1002093. doi:10.1371/journal.ppat.1002093
- Singh V, Jamwal S, Jain R, Verma P, Gokhale R, Rao KV. *Mycobacterium tuberculosis*-driven targeted recalibration of macrophage lipid homeostasis promotes the foamy phenotype. *Cell Host Microbe* (2012) 12(5):669–81. doi:10.1016/j.chom.2012.09.012
- Ridley DS, Ridley MJ. Rationale for the histological spectrum of tuberculosis. A basis for classification. *Pathology* (1987) 19(2):186–92. doi:10.3109/00313028709077132
- Hunter RL, Jagannath C, Actor JK. Pathology of postprimary tuberculosis in humans and mice: contradiction of long-held beliefs. *Tuberculosis* (2007) 87(4):267–78. doi:10.1016/j.tube.2006.11.003
- Santucci P, Bouzid F, Smichi N, Poncin I, Kremer L, De Chastellier C, et al. Experimental models of foamy macrophages and approaches for dissecting the mechanisms of lipid accumulation and consumption during dormancy and reactivation of tuberculosis. *Front Cell Infect Microbiol* (2016) 6:122. doi:10.3389/fcimb.2016.00122
- Dodd CE, Pyle CJ, Glowinski R, Rajaram MV, Schlesinger LS. CD36-mediated uptake of surfactant lipids by human macrophages promotes intracellular growth of *Mycobacterium tuberculosis*. *J Immunol* (2016) 197(12):4727–35. doi:10.4049/jimmunol.1600856
- Asalla S, Mohareer K, Banerjee S. Small molecule mediated restoration of mitochondrial function augments anti-mycobacterial activity of human macrophages subjected to cholesterol induced asymptomatic dyslipidemia. *Front Cell Infect Microbiol* (2017) 7:439. doi:10.3389/fcimb.2017.00439
- Martinez FO, Gordon S, Locati M, Mantovani A. Transcriptional profiling of the human monocyte-to-macrophage differentiation and polarization: new molecules and patterns of gene expression. *J Immunol* (2006) 177(10):7303–11. doi:10.4049/jimmunol.177.10.7303
- Ferrer J. Pleural tuberculosis. *Eur Respir J* (1997) 10(4):942–7.
- Pascutti MF, Rodriguez AM, Falivene J, Giavedoni L, Drexler I, Gherardi MM. Interplay between modified vaccinia virus Ankara and dendritic cells: phenotypic and functional maturation of bystander dendritic cells. *J Virol* (2011) 85(11):5532–45. doi:10.1128/JVI.02267-10
- Light RW. Update on tuberculous pleural effusion. *Respirology* (2010) 15(3):451–8. doi:10.1111/j.1440-1843.2010.01723.x
- Xu S, Huang Y, Xie Y, Lan T, Le K, Chen J, et al. Evaluation of foam cell formation in cultured macrophages: an improved method with Oil Red O staining and DiI-oxLDL uptake. *Cytotechnology* (2010) 62(5):473–81. doi:10.1007/s10616-010-9290-0
- Trinder P. Determination of glucose in blood using glucose oxidase with an alternative oxygen acceptor. *Ann Clin Biochem* (1969) 6(1):24–7. doi:10.1177/000456326900600108
- Bligh EG, Dyer WJ. A rapid method of total lipid extraction and purification. *Can J Biochem Physiol* (1959) 37(8):911–7. doi:10.1139/o59-099
- Balboa L, Kviatkovsky D, Schierloh P, Garcia M, de la Barrera S, Sasiain MDC. Monocyte-derived dendritic cells early exposed to *Mycobacterium tuberculosis* induce an enhanced T helper 17 response and transfer mycobacterial antigens. *Int J Med Microbiol* (2016) 306(7):541–53. doi:10.1016/j.ijmm.2016.06.004
- Balboa L, Romero MM, Laborde E, Sabio YGCA, Basile JI, Schierloh P, et al. Impaired dendritic cell differentiation of CD16-positive monocytes in tuberculosis: role of p38 MAPK. *Eur J Immunol* (2013) 43(2):335–47. doi:10.1002/eji.201242557
- Swat W, Ignatowicz L, Kisielow P. Detection of apoptosis of immature CD4+8+ thymocytes by flow cytometry. *J Immunol Methods* (1991) 137(1):79–87. doi:10.1016/0022-1759(91)90396-W
- National Institutes of Health. *Guide for the Care and Use of Laboratory Animals*. Bethesda, MD: National Institutes of Health Publication (1996).
- Podinovskaia M, Lee W, Caldwell S, Russell DG. Infection of macrophages with *Mycobacterium tuberculosis* induces global modifications to phagosomal function. *Cell Microbiol* (2013) 15(6):843–59. doi:10.1111/cmi.12092
- Mattos KA, D'Avila H, Rodrigues LS, Oliveira VG, Sarno EN, Atella GC, et al. Lipid droplet formation in leprosy: toll-like receptor-regulated organelles involved in eicosanoid formation and *Mycobacterium leprae* pathogenesis. *J Leukoc Biol* (2010) 87(3):371–84. doi:10.1189/jlb.0609433
- Schierloh P, Landoni V, Balboa L, Musella RM, Castagnino J, Morana E, et al. Human pleural B-cells regulate IFN-gamma production by local T-cells and NK cells in a *Mycobacterium tuberculosis*-induced delayed hypersensitivity reaction. *Clin Sci* (2014) 127(6):391–403. doi:10.1042/CS20130769
- Yang L, Hu YJ, Li FG, Chang XJ, Zhang TH, Wang ZT. Analysis of cytokine levers in pleural effusions of tuberculous pleurisy and tuberculous empyema. *Mediators Inflamm* (2016) 2016:3068103. doi:10.1155/2016/3068103
- Lang R. Tuning of macrophage responses by Stat3-inducing cytokines: molecular mechanisms and consequences in infection. *Immunobiology* (2005) 210(2–4):63–76. doi:10.1016/j.imbio.2005.05.001
- Murray PJ. Understanding and exploiting the endogenous interleukin-10/STAT3-mediated anti-inflammatory response. *Curr Opin Pharmacol* (2006) 6(4):379–86. doi:10.1016/j.coph.2006.01.010
- Pol A, Gross SP, Parton RG. Review: biogenesis of the multifunctional lipid droplet: lipids, proteins, and sites. *J Cell Biol* (2014) 204(5):635–46. doi:10.1083/jcb.201311051
- Russell DG. *Mycobacterium tuberculosis* and the intimate discourse of a chronic infection. *Immunol Rev* (2011) 240(1):252–68. doi:10.1111/j.1600-065X.2010.00984.x
- Dutt AK, Stead WW. Treatment of extrapulmonary tuberculosis. *Semin Respir Infect* (1989) 4(3):225–31.
- Seibert AF, Haynes J Jr, Middleton R, Bass JB Jr. Tuberculous pleural effusion. Twenty-year experience. *Chest* (1991) 99(4):883–6. doi:10.1378/chest.99.4.883
- Vorster MJ, Allwood BW, Diacon AH, Koegelenberg CF. Tuberculous pleural effusions: advances and controversies. *J Thorac Dis* (2015) 7(6):981–91. doi:10.3978/j.issn.2072-1439.2015.02.18
- Klimiuk J, Krenke R, Safianowska A, Korczynski P, Chazan R. Diagnostic performance of different pleural fluid biomarkers in tuberculous pleurisy. *Adv Exp Med Biol* (2015) 852:21–30. doi:10.1007/5584_2014_105
- Hutchins AP, Diez D, Miranda-Saavedra D. Genomic and computational approaches to dissect the mechanisms of STAT3's universal and cell type-specific functions. *JAKSTAT* (2013) 2(4):e25097. doi:10.4161/jkst.25097
- Lastrucci C, Benard A, Balboa L, Pingris K, Souriant S, Poincloux R, et al. Tuberculosis is associated with expansion of a motile, permissive and immunomodulatory CD16(+) monocyte population via the IL-10/STAT3 axis. *Cell Res* (2015) 25(12):1333–51. doi:10.1038/cr.2015.123
- Yang L, Yang JB, Chen J, Yu GY, Zhou P, Lei L, et al. Enhancement of human ACAT1 gene expression to promote the macrophage-derived foam cell

- formation by dexamethasone. *Cell Res* (2004) 14(4):315–23. doi:10.1038/sj.cr.7290231
42. Langlais D, Couture C, Balsalobre A, Drouin J. The Stat3/GR interaction code: predictive value of direct/indirect DNA recruitment for transcription outcome. *Mol Cell* (2012) 47(1):38–49. doi:10.1016/j.molcel.2012.04.021
 43. Murray PJ, Allen JE, Biswas SK, Fisher EA, Gilroy DW, Goerdt S, et al. Macrophage activation and polarization: nomenclature and experimental guidelines. *Immunity* (2014) 41(1):14–20. doi:10.1016/j.immuni.2014.06.008
 44. Schust J, Sperl B, Hollis A, Mayer TU, Berg T. Stattic: a small-molecule inhibitor of STAT3 activation and dimerization. *Chem Biol* (2006) 13(11):1235–42. doi:10.1016/j.chembiol.2006.09.018
 45. da Silva RF, Lappalainen J, Lee-Rueckert M, Kovanen PT. Conversion of human M-CSF macrophages into foam cells reduces their proinflammatory responses to classical M1-polarizing activation. *Atherosclerosis* (2016) 248:170–8. doi:10.1016/j.atherosclerosis.2016.03.012
 46. Bhagyaraj E, Nanduri R, Saini A, Dkhar HK, Ahuja N, Chandra V, et al. Human xenobiotic nuclear receptor PXR augments *Mycobacterium tuberculosis* survival. *J Immunol* (2016) 197(1):244–55. doi:10.4049/jimmunol.1600203
 47. Hanrahan CF, Golub JE, Mohapi L, Tshabangu N, Modisenyane T, Chaisson RE, et al. Body mass index and risk of tuberculosis and death. *AIDS* (2010) 24(10):1501–8. doi:10.1097/QAD.0b013e32833a2a4a
 48. Kumar NP, Moideen K, Sivakumar S, Menon PA, Viswanathan V, Kornfeld H, et al. Tuberculosis-diabetes co-morbidity is characterized by heightened systemic levels of circulating angiogenic factors. *J Infect* (2017) 74(1):10–21. doi:10.1016/j.jinf.2016.08.021
 49. Randolph GJ. Mechanisms that regulate macrophage burden in atherosclerosis. *Circ Res* (2014) 114(11):1757–71. doi:10.1161/CIRCRESAHA.114.301174
 50. Persson J, Nilsson J, Lindholm MW. Interleukin-1beta and tumour necrosis factor-alpha impede neutral lipid turnover in macrophage-derived foam cells. *BMC Immunol* (2008) 9:70. doi:10.1186/1471-2172-9-70
 51. Khovidhunkit W, Moser AH, Shigenaga JK, Grunfeld C, Feingold KR. Endotoxin down-regulates ABCG5 and ABCG8 in mouse liver and ABCA1 and ABCG1 in J774 murine macrophages: differential role of LXR. *J Lipid Res* (2003) 44(9):1728–36. doi:10.1194/jlr.M300100-JLR200
 52. Halvorsen B, Waehre T, Scholz H, Clausen OP, von der Thusen JH, Muller F, et al. Interleukin-10 enhances the oxidized LDL-induced foam cell formation of macrophages by antiapoptotic mechanisms. *J Lipid Res* (2005) 46(2):211–9. doi:10.1194/jlr.M400324-JLR200
 53. Han X, Kitamoto S, Lian Q, Boisvert WA. Interleukin-10 facilitates both cholesterol uptake and efflux in macrophages. *J Biol Chem* (2009) 284(47):32950–8. doi:10.1074/jbc.M109.040899
 54. Almeida PE, Carneiro AB, Silva AR, Bozza PT. PPARgamma expression and function in mycobacterial infection: roles in lipid metabolism, immunity, and bacterial killing. *PPAR Res* (2012) 2012:383829. doi:10.1155/2012/383829
 55. Ahluwalia PK, Pandey RK, Sehajpal PK, Prajapati VK. Perturbed microRNA expression by *Mycobacterium tuberculosis* promotes macrophage polarization leading to pro-survival foam cell. *Front Immunol* (2017) 8:107. doi:10.3389/fimmu.2017.00107
 56. Vosper H, Patel L, Graham TL, Khoudoli GA, Hill A, Macphee CH, et al. The peroxisome proliferator-activated receptor delta promotes lipid accumulation in human macrophages. *J Biol Chem* (2001) 276(47):44258–65. doi:10.1074/jbc.M108482200

Conflict of Interest Statement: Authors declare that the submitted work was carried out in the absence of personal, professional, or financial relationships that could potentially be construed as a conflict of interest.

Copyright © 2018 Genoula, Marín Franco, Dupont, Kviatcovsky, Milillo, Schierloh, Moraña, Poggi, Palmero, Mata-Espinosa, González-Domínguez, León Contreras, Barrionuevo, Rearte, Córdoba Moreno, Fontanals, Crotta Asis, Gago, Cougoule, Neyrolles, Maridonneau-Parini, Sánchez-Torres, Hernández-Pando, Vérolet, Lugo-Villarino, Sasiain and Balboa. This is an open-access article distributed under the terms of the Creative Commons Attribution License (CC BY). The use, distribution or reproduction in other forums is permitted, provided the original author(s) and the copyright owner are credited and that the original publication in this journal is cited, in accordance with accepted academic practice. No use, distribution or reproduction is permitted which does not comply with these terms.

Tuberculosis is associated with expansion of a motile, permissive and immunomodulatory CD16⁺ monocyte population via the IL-10/STAT3 axis

Claire Lastrucci^{1,2}, Alan Bénard^{1,2,*}, Luciana Balboa^{3,*}, Karine Pingris^{1,2}, Shanti Souriant^{1,2}, Renaud Poincloux^{1,2}, Talal Al Saati⁴, Voahangy Rasolofo⁵, Pablo González-Montaner⁶, Sandra Inwentarz⁶, Eduardo Jose Moraña⁶, Ivanela Kondova⁷, Frank AW Verreck⁷, Maria del Carmen Sasiain³, Olivier Neyrolles^{1,2}, Isabelle Maridonneau-Parini^{1,2}, Geanncarlo Lugo-Villarino^{1,2,#}, Céline Cougoule^{1,2,#}

¹CNRS, Institut de Pharmacologie et de Biologie Structurale (IPBS), Département of Tuberculosis and Infection Biology, Toulouse, France; ²Université de Toulouse; Université Paul Sabatier, UPS, IPBS, Toulouse, France; ³Inmunologia de Enfermedades Respiratorias, Instituto de Medicina Experimental (IMEX)-CONICET, Academia Nacional de Medicina, Pacheco de Melo 3081, 1425, Buenos Aires, Argentina; ⁴INSERM/UPS-US006/CREFRE, Service d'Histopathologie, CHU Purpan, 31024, Toulouse, France; ⁵Mycobacteria Unit, Pasteur Institute in Antananarivo, Antananarivo, Madagascar; ⁶Instituto Prof. Dr. Raúl Vaccarezza, Hospital de Infecciosas Dr. F.J. Muñiz, Buenos Aires, Argentina; ⁷Department of Parasitology, Biomedical Primate Research Centre, Rijswijk, the Netherlands

The human CD14⁺ monocyte compartment is composed by two subsets based on CD16 expression. We previously reported that this compartment is perturbed in tuberculosis (TB) patients, as reflected by the expansion of CD16⁺ monocytes along with disease severity. Whether this unbalance is beneficial or detrimental to host defense remains to be elucidated. Here in the context of active TB, we demonstrate that human monocytes are predisposed to differentiate towards an anti-inflammatory (M2-like) macrophage activation program characterized by the CD16⁺CD163⁺MerTK⁺pSTAT3⁺ phenotype and functional properties such as enhanced protease-dependent motility, pathogen permissivity and immunomodulation. This process is dependent on STAT3 activation, and loss-of-function experiments point towards a detrimental role in host defense against TB. Importantly, we provide a critical correlation between the abundance of the CD16⁺CD163⁺MerTK⁺pSTAT3⁺ cells and the progression of the disease either at the local level in a non-human primate tuberculous granuloma context, or at the systemic level through the detection of the soluble form of CD163 in human sera. Collectively, this study argues for the pathogenic role of the CD16⁺CD163⁺MerTK⁺pSTAT3⁺ monocyte-to-macrophage differentiation program and its potential as a target for TB therapy, and promotes the detection of circulating CD163 as a potential biomarker for disease progression and monitoring of treatment efficacy.

Keywords: tuberculosis; STAT3; macrophage activation; monocyte; biomarker; immunomodulation; migration

Cell Research (2015) 25:1333-1351. doi:10.1038/cr.2015.123; published online 20 October 2015

Introduction

Tuberculosis (TB) is a severe chronic bacterial infection caused by *Mycobacterium tuberculosis* (Mtb). In 2013, TB claimed the life of nearly 1.5 million people, ranking this disease as the second leading cause of death from a single infectious agent (*Global TB report*, WHO, 2014). While TB mortality is slowly declining each year, it is still unacceptably high given that most cases would be curable if better diagnostic tools and correct treatment

*These two authors contributed equally to this work.

#These two authors are co-senior authors.

Correspondence: Isabelle Maridonneau-Parini^a, Olivier Neyrolles^b

Tel: +33-0-5 61 17 54 58; Fax: + 33-0-5 61 17 59 94

^aE-mail: Isabelle.Maridonneau-Parini@ipbs.fr

^bE-mail: Olivier.Neyrolles@ipbs.fr

Received 5 March 2015; revised 31 July 2015; accepted 6 September 2015; published online 20 October 2015

were available to complement existing technologies. A major obstacle is the lack of TB-specific and non-specific immune activation biomarker and bio-signature tools to estimate disease severity, follow drug treatment efficacy, allow prognosis of disease outcome (recovery or relapse) and estimate vaccine protection [1, 2]. As the basis for maintaining the flow of novel biomarker candidates in the product pipeline, fundamental science is necessary to better characterize Mtb interaction with the human host.

Innate immunity plays a key role in host defense against Mtb. Among the immune innate cells involved in this resistance, macrophages are primordial regulators of the balance of pro- and anti-inflammatory immune response in order to ensure the control of bacterial replication and limit the extent of tissue damage following pathogenic insult [3-5]. They perform these roles according to their high degree of phenotypic and functional plasticity in response to environmental clues within tissues, and are classified within a spectrum ranging from pro-inflammatory (M1) to anti-inflammatory (M2) activation programs [6]. Remarkably, Mtb displays a great capacity to influence the differentiation, maturation and activation of macrophages, resulting in an effective evasion of the immune response and increased persistence in the host (for review, see [7-9]). Despite the significant progress in understanding macrophage subversion by Mtb, one aspect that remains poorly studied is how monocytes contribute to the dynamic alteration of the macrophage compartment during ongoing Mtb infection. As monocytes are the precursors of macrophages during inflammation, substantial insights into host defenses are likely to be gained by determining the role of these leukocytes within the TB context. In particular, while there are important clues coming from the zebrafish and mouse models, the human context remains poorly explored [7, 9, 10].

Human blood monocytes are broadly segregated into two major subsets: CD14⁺CD16⁻ (classical) and CD14⁺CD16⁺ (non-classical) monocytes, hereafter designated as CD16⁻ and CD16⁺, respectively [11, 12]. Notably, the CD16⁺ subset accounts for only 10% of the total monocyte population in healthy donors, displaying a unique cell-surface marker expression and cytokine secretion pattern in comparison with its CD16⁻ counterpart [13, 14]. Indeed, upon stimulation with lipopolysaccharide, CD16⁺ monocytes isolated from healthy donors secrete higher amounts of pro-inflammatory factors such as tumor necrosis factor-alpha (TNF α), interleukin-1-beta (IL-1) and IL-6, but low amount of the anti-inflammatory mediator IL-10 [13, 15-17]. Other features distinguishing the CD16⁺ subset are higher antigen processing and presentation, pro-angiogenic behavior and motility [10]. The

expansion of CD16⁺ monocytes is well documented in different types of diseases, mainly deriving from infection or inflammatory conditions [10]. For these reasons, CD16⁺ monocytes are usually referred to as pro-inflammatory monocytes.

Interestingly, the human monocyte compartment is perturbed in TB patients, as illustrated by the expansion of CD16⁺ monocytes, which can account for up to 50% of the total monocyte population, and its correlation with the disease severity [18]. This unbalance in the monocyte population is also associated with a higher cell-surface expression for CD14, CD11b, toll-like receptor-2 (TLR2), TLR5, chemokine C-C motif receptor-1 (CCR1), CCR2 and CCR5, as compared with that of healthy individuals [18]. Functional characterization *in vitro* shows that monocytes isolated from TB patients are refractory to efficient dendritic cell (DC) differentiation and deficient in the activation of T lymphocytes, as compared with monocytes from healthy donors [19, 20]. The cause and consequence of this unbalance are still relatively unknown. In addition, it remains to be elucidated whether there is an effect on the ability of monocytes from TB patients to differentiate into macrophages that are capable of controlling the bacillus' intracellular growth and mount an effective immune response. Indeed, this is a critical functional aspect to assess, along with its prognostic value, in order to determine whether the unbalanced monocyte population is beneficial or detrimental to host defense against TB, and whether this represents a potential bio-signature and target for treatment.

Here we describe that, in the context of TB, human monocytes differentiating towards a macrophage program (referred here to as monocyte-macrophages) are tilted towards an M2-like activation program characterized by the CD16⁺CD163⁺MerTK⁺pSTAT3⁺ marker phenotype and functional properties such as high protease-dependent motility, pathogen permissivity and immunomodulatory activity. The establishment of this program is mainly dependent on the signal transducer and activator of transcription 3 (STAT3)-dependent signaling pathway, and points towards a detrimental role in host defense against TB. Importantly, our study provides direct correlation of the abundance of CD16⁺CD163⁺MerTK⁺pSTAT3⁺ cells with TB disease severity in humans and non-human primates (NHPs), and proposes the presence of the soluble form of CD163 (sCD163) in sera as a potential biomarker to monitor disease progression and treatment efficacy.

Results

The secretome of Mtb-infected macrophages favors the

differentiation of human monocytes towards an M2-like activation program

Mtb infection is known to significantly alter monocyte differentiation upon recruitment to pulmonary tissue in mice, alluding to a bystander effect derived from infected resident cells [21]. As the secretome of Mtb-infected macrophages inhibits human monocyte differentiation towards DC program [22], we investigated whether it also alters monocyte-to-macrophage differentiation. To this aim, we devised an *in vitro* model whereby freshly isolated CD14⁺ monocytes from healthy donors were dif-

ferentiated towards a macrophage program (M-CSF driven) in the presence of conditioned media from Mtb-infected human macrophages (cmMTB). As a control, we differentiated monocytes using a conditioned media from non-infected macrophages (cmCTR). Unlike treatment with cmCTR, we observed an expansion of the CD16⁺ population in the cmMTB-treated monocytes (Figure 1A). In addition, we assessed their activation program by flow cytometry in terms of M1 and M2 cell-surface marker expression. Monocytes conditioned with cmMTB differentiated into cells displaying an equivalent or low-

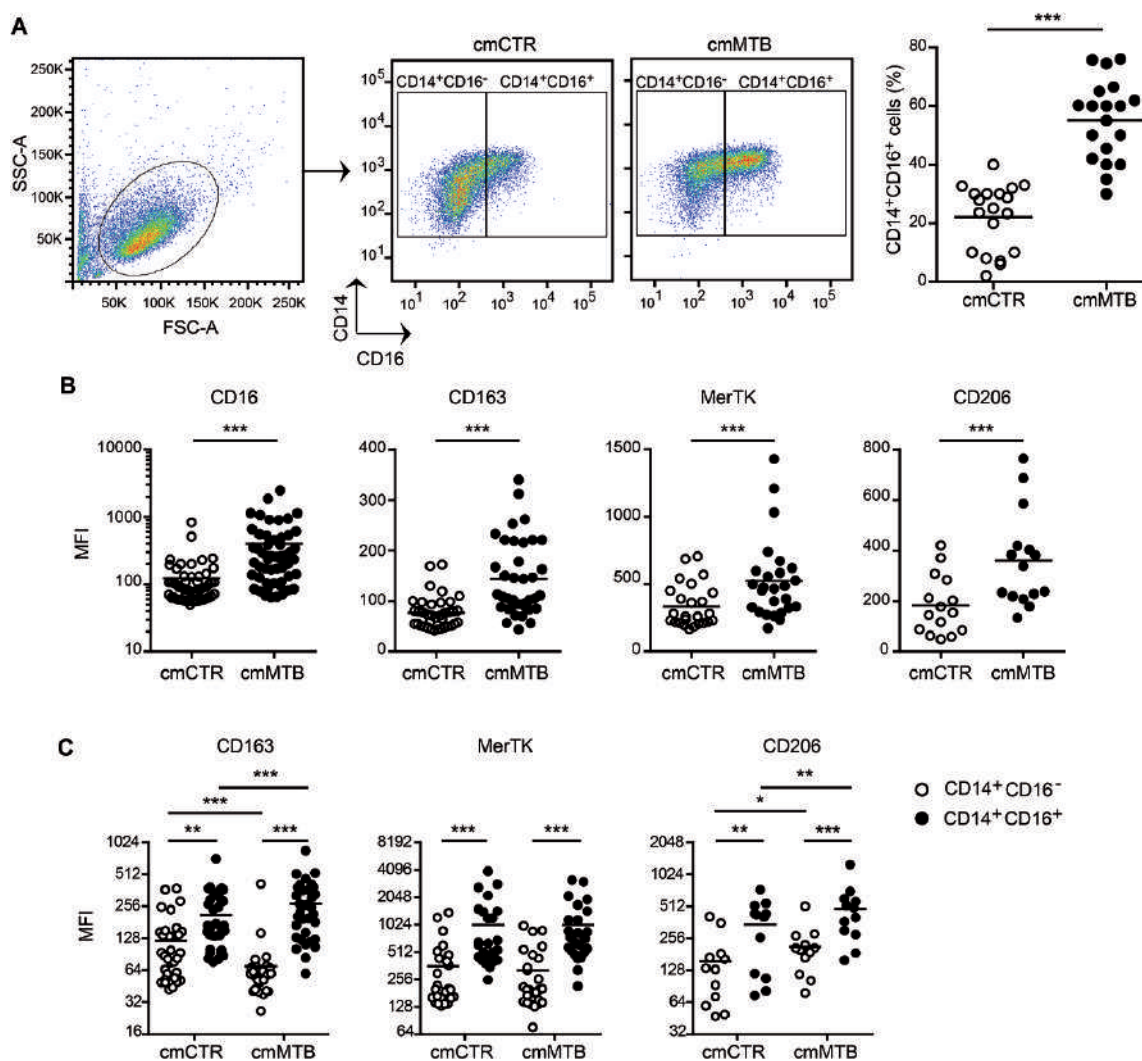


Figure 1 The secretome of Mtb-infected macrophages induces the differentiation of CD16⁺ monocytes towards an M2-like phenotype. Monocytes were cultured with conditioned media from Mtb-infected (cmMTB, black) or non-infected (cmCTR, white) macrophages. **(A)** Flow cytometry gating strategy of a representative donor and the percentage of CD14⁺CD16⁺ cells. **(B)** Vertical scatter plots showing the median fluorescent intensity (MFI) of cell-surface markers during cmCTR or cmMTB treatment. **(C)** Vertical scatter plots showing the MFI of CD163, MerTK or CD206 in the CD14⁺CD16⁻ (white circles) and CD14⁺CD16⁺ (black circles) cell populations during cmCTR or cmMTB treatment. **P* < 0.05, ***P* < 0.01, ****P* < 0.001. Each circle within vertical scatter plots represents a single donor.

er expression of M1 polarization markers (i.e., CD86, HLA-DR, FCAR and Serpine1) compared with cells differentiated in the presence of cmCTR (Supplementary information, Figure S1A-S1B). By contrast, the expression of markers related to M2 macrophage activation, such as CD16, CD163, MerTK, CD206, AMAC1 and CD200R1 [23-27], was upregulated in cmMTB-conditioned cells (Figure 1B, Supplementary information, Figure S1B). Similarly, the expression of CCR2 and CCR5 chemokine receptors was higher in the presence of cmMTB, supporting the acquisition of the M2 program (Supplementary information, Figure S1C) [28, 29]. More precisely, the expression of M2 markers was specifically augmented within CD16⁺ population compared with the CD16⁻ counterpart, with a higher increase of CD163 and CD206 upon cmMTB treatment monocytes (Figure 1C).

These results indicate that soluble factors secreted by Mtb-infected macrophages exert bystander effect affecting monocyte differentiation towards an M2-like activation program.

The monocyte activation towards CD16⁺CD163⁺MerTK⁺ phenotype is dependent on the IL-10/STAT3 signaling pathway in the TB context

In the presence of M-CSF, IL-10 triggers macrophage M2 activation that promotes tolerance mechanisms, including the resolution of inflammation and tissue repair [28, 30]. Moreover, this cytokine is not only increased in serum and pleural effusion from TB patients compared with healthy donors [31, 32], but also in the lungs of Mtb-infected NHPs [33]. As IL-10 is secreted by Mtb-infected human macrophages [34], we investigated whether it is responsible for the Mtb-derived bystander effect observed in our *in vitro* model. We first examined whether human recombinant IL-10 (recIL-10), in combination with M-CSF, recapitulated the effect of the cmMTB. As expected, the expression of CD206 was not influenced by recIL-10, rather confirming the regulation of this receptor by IL-4/STAT6 axis [35]. By contrast, recIL-10 treatment on monocytes stimulated the expression of M2 markers (i.e., CD16, CD163 and MerTK) compared with control cells, whereas M1 markers were significantly decreased (Supplementary information, Figure S2A). Moreover, when IL-10 was depleted from cmMTB using blocking antibodies (Supplementary information, Figure S2B), we observed impairment in the establishment of the M2 marker signature (except for CD206) (Figure 2A), accompanied by a slight increasing tendency of M1 markers (Supplementary information, Figure S2C), indicating that this cytokine is one of the main soluble factors present in the secretome of Mtb-infected macrophages responsible for the induction of M2-like mono-

cyte-macrophages.

The binding of IL-10 to its receptor leads to the subsequent activation of STAT3, whose role is essential for all known functions of IL-10 [36]. As shown in Figure 2B, short-term exposure of freshly isolated monocytes to cmMTB resulted in STAT3 phosphorylation on tyrosine 705, reflecting its activation. This activation was dependent on the presence of IL-10 since incubation of monocytes with IL-10-depleted cmMTB failed to trigger significant phosphorylation of STAT3 (Figure 2B). Next, we assessed whether STAT3 was crucial for the establishment of M2-like monocyte-macrophages, using a siRNA-mediated gene silencing method [37], or pharmacological inhibition of STAT3 activation with either cucurbitacin I (CCB), which inhibits JAK2 (Janus kinase 2)-dependent phosphorylation of STAT3, or STATTIC, which targets the STAT3-SH2 domain thereby preventing its association with upstream kinases. Both approaches enabled a nearly complete inhibition of STAT3 expression or phosphorylation in human monocyte-macrophages (Supplementary information, Figure S3A-S3C). As expected, inhibition of STAT3 in cmMTB-treated cells reversed the acquisition of the CD16⁺CD163⁺MerTK⁺ phenotype, while CD206 or M1 marker expression remained unaffected (Figure 2C and Supplementary information, Figure S3D-S3F).

Altogether, the secretome of Mtb-infected macrophages favors the human monocyte differentiation towards an M2-like activation program, which is mainly but not absolutely dependent (as best indicated by CD206 expression) on the IL-10/STAT3 axis.

The CD16⁺ monocyte expansion is predisposed towards an M2-like phenotype in patients with active TB

Results obtained through our *in vitro* approach inferred that the reported imbalance in circulating monocyte subsets in TB patients might be associated with a predisposition towards a STAT3-driven M2-like program. To address the physiological relevance of this issue, we analyzed in more detail the activation program of the circulating monocytes in TB patients. We collected peripheral blood from healthy subjects (PB-HS), patients with active (PB-TB) or confirmed latent (PB-LTB) TB (Supplementary information, Table S1), to evaluate the status of the CD14⁺ monocyte compartment. As previously described [18], we confirmed the higher proportion of CD16⁺ cells in PB-TB compared with PB-HS, accounting for about 40% of the CD14⁺ monocytes (Figure 3A, Supplementary information, Figure S4A). Strikingly, the expansion of CD16⁺ monocytes is non-existent in PB-LTB, indicating that the abundance of these cells is associated with active TB (Figure 3A, Supple-

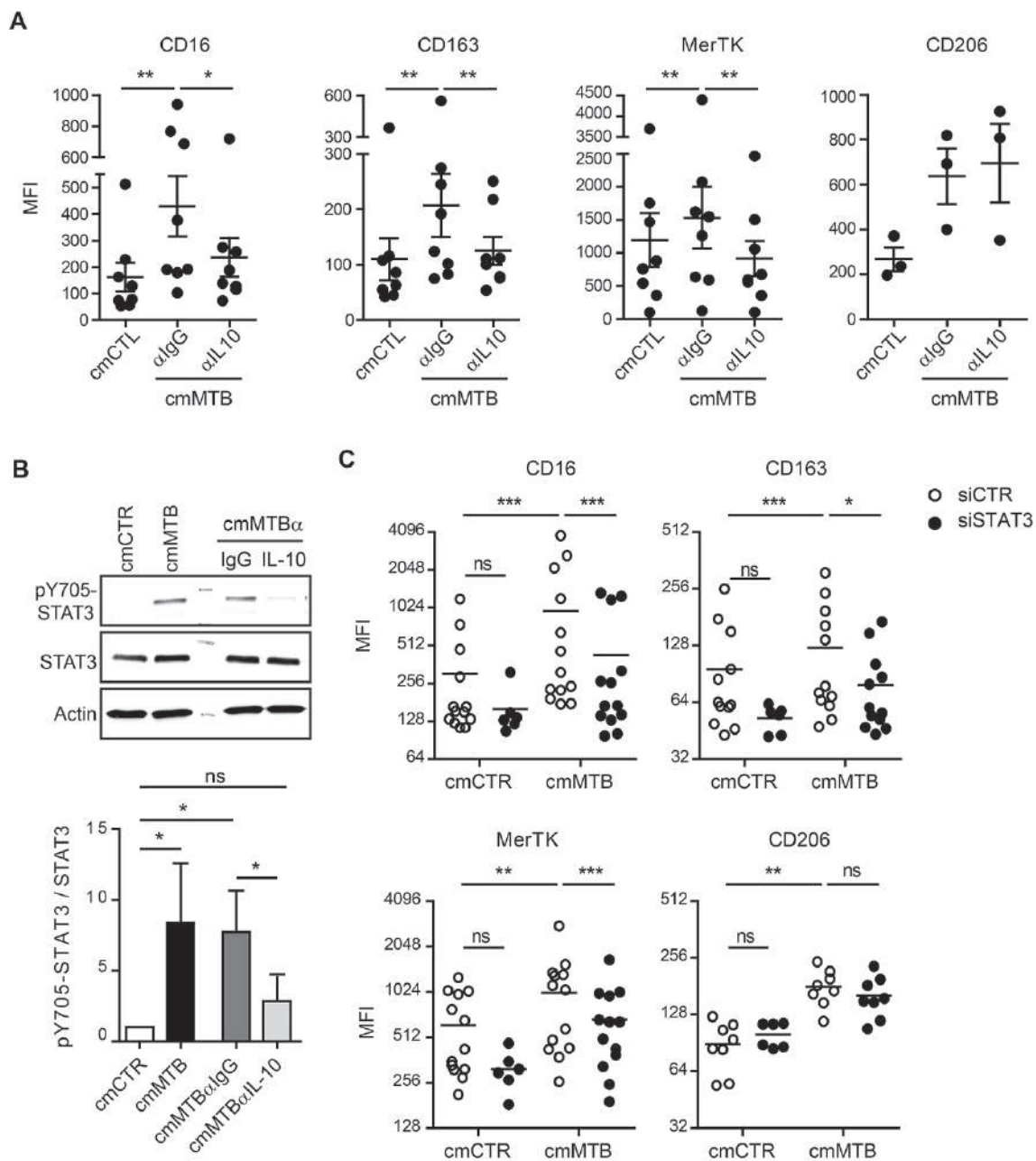


Figure 2 The IL-10/STAT3 pathway drives the predisposition of CD16⁺ monocytes towards an M2-like phenotype. **(A)** Vertical scatter plots showing the MFI of cell-surface markers in monocytes cultured with IL-10-depleted cmMTB (cmMTB α IL-10) or the mock depletion control (cmMTB α IgG). **(B)** Immunoblot images of pY705-STAT3, STAT3 and actin (upper panel); quantification of pY705-STAT3 versus STAT3 on monocytes after 1 h treatment with cmCTR, cmMTB, cmMTB α IL-10 or cmMTB α IgG ($n = 6$ donors; lower panel). **(C)** Vertical scatter plots showing the MFI of cell-surface markers in monocytes transfected with STAT3 (siSTAT3-black) or non-targeting control (siCTR-white) siRNAs, and conditioned with cmCTR or cmMTB. * $P < 0.05$, ** $P < 0.01$, *** $P < 0.001$. Each circle within vertical scatter plots represents a single donor.

mentary information, Figure S4B). While we failed to correlate the enhanced level of CD16 expression with the M2-like phenotype characterized in our *in vitro* model (Supplementary information, Figure S4B), freshly isolat-

ed monocytes from TB patients displayed higher level of phosphorylated STAT3 compared with their counterparts from healthy subjects (HS), as measured by western blot analysis (Figure 3B). Using a flow cytometry-based

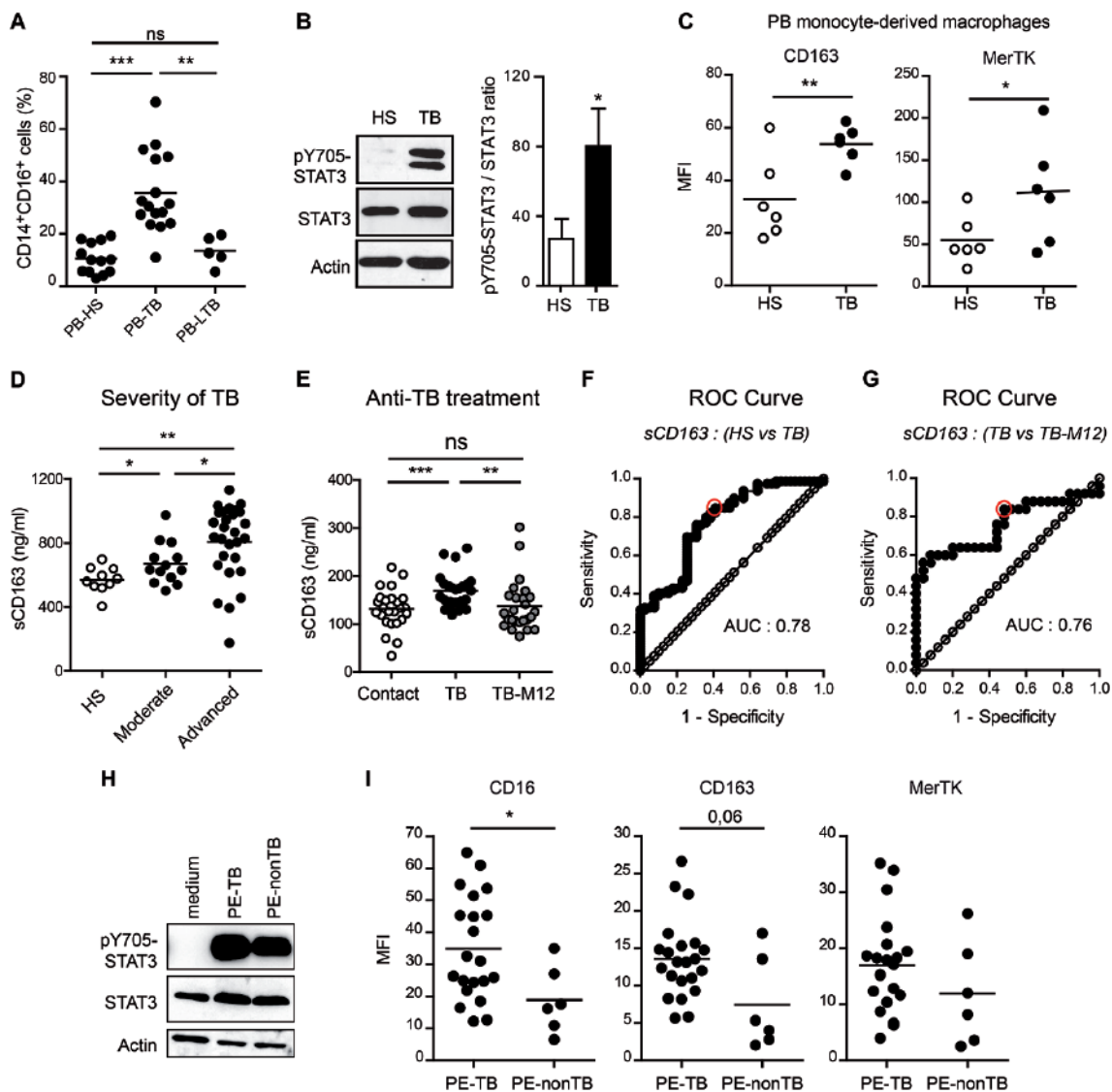


Figure 3 The CD16⁺ monocyte expansion is predisposed towards an M2-like phenotype in patients with active TB. **(A)** Vertical scatter plots showing the percentage of CD14⁺CD16⁺ cells in the peripheral blood of healthy subjects (PB-HS), TB patients (PB-TB) or subjects with latent TB (PB-LTB). **(B)** Immunoblot images of pY705-STAT3, STAT3 and actin (left), and quantification of pY705-STAT3 versus STAT3 (right) on monocytes from healthy subjects (HS) or TB patients (TB) (*n* = 5 donors). **(C)** Vertical scatter plots showing the MFI of cell-surface markers in HS or TB monocyte-derived macrophages differentiated *in vitro* for 7 days. **(D)** Analysis of soluble form of CD163 (sCD163) level in sera of TB patients according to disease severity, as compared with HS. **(E)** Vertical scatter plots showing the serum level of sCD163 in TB patients before and 12 months after start of treatment (TB-M12), as compared with contact donors. **(F)** ROC (receiver operating characteristic) curve of sCD163 concentration in TB patients compared with HS. **(G)** ROC curve of sCD163 concentration in TB patients before versus after treatment (TB versus TB-M12). The red circle represents the optimal cut point. **(H)** Monocytes from HS were treated with pleural effusion (PE) from TB (PE-TB) or non-TB (PE-nonTB) patients, or culture medium. Representative images of western blot illustrating the expression of pY⁷⁰⁵-STAT3, STAT3 and actin (*n* = 3). **(I)** Vertical scatter plots showing the MFI of CD16, CD163 or MerTK on CD14⁺ monocytes present in PE-TB or PE-nonTB from patients. **P* < 0.05; ***P* < 0.01; ****P* < 0.001. Each circle within vertical scatter plots represents a single donor. AUC, area under the curve.

approach, we found that CD14⁺CD16⁺ can be differentiated into two sub-populations according to the phosphorylation status of STAT3 (CD14⁺CD16⁺pSTAT3⁻ and

CD14⁺CD16⁺pSTAT3⁺). In TB patients, the percentage of CD14⁺CD16⁺pSTAT3⁺ is significantly increased (37.5% ± 11.2%) compared with control donors (13.2% ± 6.1%,

$P < 0.01$, $n = 6$). Moreover, when differentiated *in vitro* with M-CSF, blood monocytes from TB patients exhibited a CD163^{hi}MerTK^{hi}HLA-DR^{lo}CD86^{lo} macrophage phenotype (Figure 3C, Supplementary information, Figure S4C). Together, these results point out a predisposition of the human monocyte compartment towards an M2-like program in the TB context.

We previously reported that the expansion of peripheral CD16⁺ monocytes correlates with disease severity of TB patients [18]. To further characterize the activation program of this expanded cell population, we then assessed the M2-like phenotype of circulating monocytes isolated from patients with different clinical parameters to distinguish TB severity (Supplementary information, Table S2). Unlike CD163, we observed that the cell-surface expression of MerTK is significantly augmented in the case of patients with an advanced degree of the disease and accentuated within the CD16⁺ monocyte subset (Supplementary information, Figure S4D-S4E). Given that membrane-bound CD163 and MerTK receptors are subjected to inflammation-driven shedding [38, 39], we hypothesized that chronic infection with Mtb may also lead to the shedding of these receptors from the surface of circulating monocytes, and thus increase the expression of soluble CD163 (sCD163) and MerTK (MerTK ectodomain: sMer) in the serum of TB patients. Aside from a single report describing the circulating sCD163 as a predictive value for patient survival [40], there is virtually no information about this scavenger receptor and MerTK in the TB context. We thus evaluated the sera from pulmonary TB patients and revealed a progressively increasing trend in the levels of sCD163, particularly striking in cases with an advanced degree of the disease (Figure 3D). Next, to examine whether the soluble expression of this receptor is related to the presence of bacilli, we measured sCD163 serum concentration in TB patients before and after treatment (Supplementary information, Table S3). Noticeably, the TB-induced expression of sCD163 is decreased significantly after treatment (Figure 3E). This was further supported by receiver operating characteristic (ROC) curve analysis showing the relationship between the sensitivity and specificity at any cutoff values for sCD163 (Figure 3F and 3G). For TB patients in relation to HS, the area under the ROC curve (AUC) value for sCD163 was 0.78 (± 0.04) with a 95% confidence interval (CI) of 0.69 to 0.86 ($P < 0.0001$), with an optimal cut point yielding a sensitivity of 84.8% and specificity of 58.9% (Figure 3F). For TB patients, before treatment in relation to the same cases after 12-month treatment (TB-M12), the AUC value for sCD163 was 0.76 (± 0.07) with a CI of 0.61 to 0.90 ($P < 0.001$), with an optimal cut point providing a sensitivity

of 84% and specificity of 52% (Figure 3G). In the case for sMer, however, we found no evidence supporting its shedding in TB (Supplementary information, Figure S4F-S4I). These results indicate that altered serum levels of sCD163 might be of potential use as a non-invasive biomarker for pulmonary TB disease progression and monitoring of treatment efficacy.

To further explore the association between Mtb infection and the alteration of the human monocyte compartment, we obtained pleural effusion fluids from TB patients (PE-TB) and other non-TB-related infectious diseases (PE-nonTB; Supplementary information, Table S1). As PE-TB is the most common form of extrapulmonary TB, we tested its capacity to influence the activation program of freshly isolated monocytes from HS, and noticed that both PE-TB and PE-nonTB were able to induce a rapid phosphorylation of STAT3 (Figure 3H). Importantly, when assessing the CD14⁺ population isolated directly from PE-TB, we observed that these cells tend to display a higher acquisition of the CD16⁺CD163⁺MerTK⁺ phenotype in comparison with their counterparts from PE-nonTB (Figure 3I), suggesting that an Mtb-derived microenvironment influences the human monocyte compartment via STAT3.

The abundance of the CD16⁺CD163⁺MerTK⁺pSTAT3⁺ cell population correlates with pathology severity in non-human primate pulmonary TB

Pulmonary granuloma formation is a hallmark of TB, and the activation program of monocyte-macrophages is thought to play an important role in this process [41]. Therefore, we further investigated whether the M2-like CD16⁺CD163⁺MerTK⁺ cell population is present in pulmonary granulomas of Mtb-infected NHPs. The NHP tissue samples were derived from BCG (Bacillus Calmette-Guérin) vaccinated and unvaccinated Mtb-infected rhesus macaques, exhibiting different degrees of lung pathology that was in general inversely correlated with time to end point (survival; Supplementary information, Figure S5A). Immunohistochemical analyses revealed that macrophage infiltration (CD68⁺) increased according to lung pathology severity (Figure 4A, Supplementary information, Figure S5B); this pattern was also accompanied by increased CD163 expression in tuberculous granulomas in NHPs (Figure 4A, Supplementary information, Figure S5B) [42]. Concomitantly, we observed an elevated expression of CD16 and MerTK in NHP tuberculous granulomas (Figure 4A, Supplementary information, Figure S5B). Notably, the expression of CD163, CD16 and MerTK positively correlated with the severity of lung pathology (Figure 4B). Co-localization analysis within CD163⁺ macrophages revealed that CD16 and

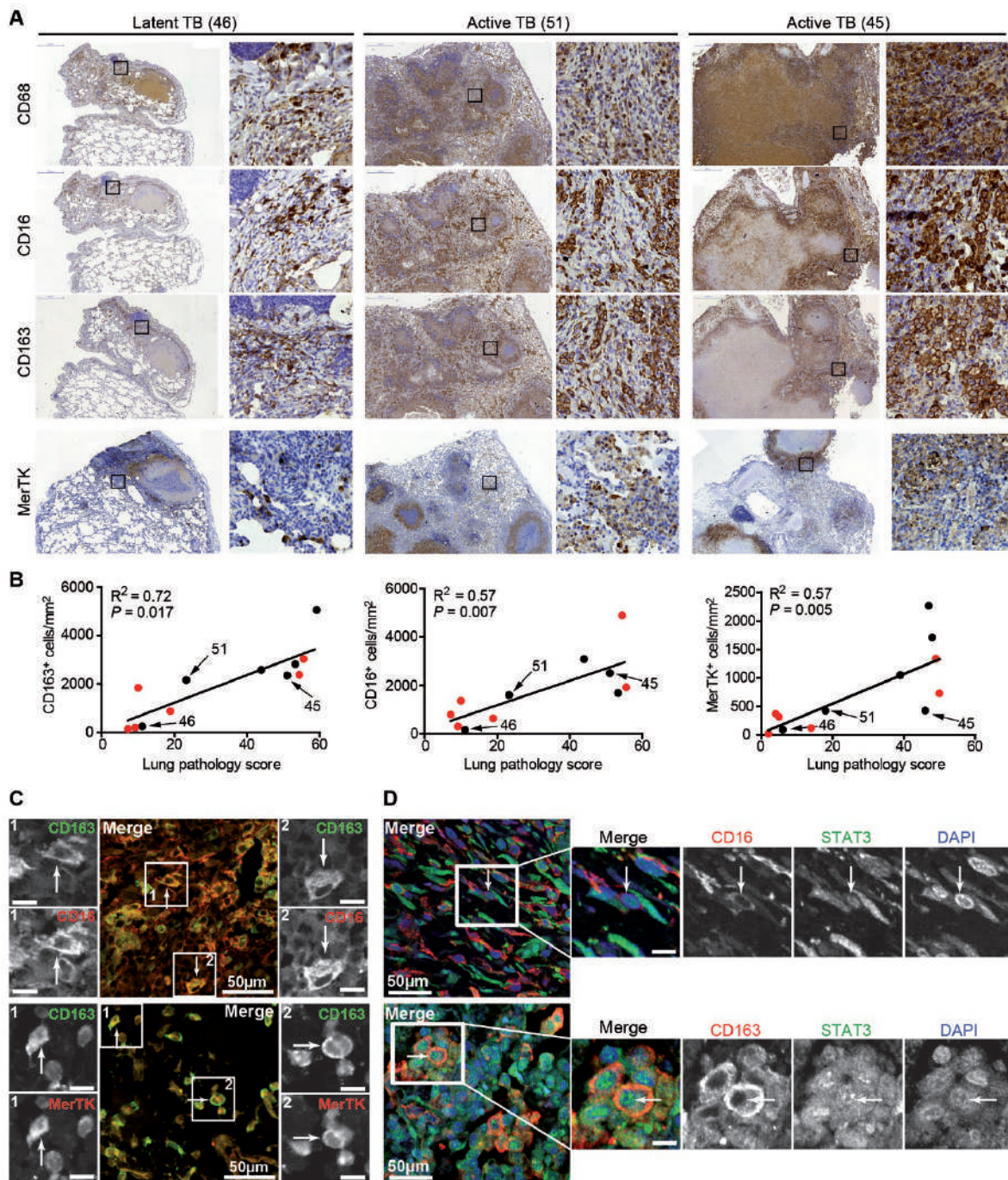


Figure 4 The abundance of the CD16⁺CD163⁺MerTK⁺pSTAT3⁺ cell population correlates with pathology severity in non-human primate (NHP) pulmonary TB. **(A)** Representative immunohistochemical images demonstrate expression and distribution of CD68, CD16, CD163 and MerTK in lung granulomas from non-vaccinated Mtb-infected NHPs exhibiting different severity of pulmonary TB. NHP numbers refer to Supplementary information, Table S6. **(B)** Correlation analysis between the number of CD16⁺, CD163⁺ or MerTK⁺ cells in lung tissue and lung pathology score in BCG-vaccinated (red circles) or -non-vaccinated (black circles) Mtb-infected NHPs. **(C, D)** Immunohistochemistry stainings of lung biopsies from NHP n°51 (intermediate). **(C)** Upper panel: co-localization of CD163 (green; Alexa-488) and CD16 (red; Alexa-555) in lung tissue; lower panel: co-localization of CD163 (green; Alexa-488) and MerTK (red; Alexa-555) in lung tissue. White arrows indicate double-positive cells that are magnified in 1 and 2 (inset scale bar = 10 μ m). **(D)** Upper panel: nuclear localization of STAT3 (green; Alexa-488) in CD16 (red; Alexa-555)-positive cells in lung tissue; lower panel: nuclear localization of STAT3 (green; Alexa-488) in CD163 (red; Alexa-555)-positive cells in lung tissue. White arrows indicate CD16- or CD163-positive cells with STAT3 translocated in the nucleus stained with DAPI (blue; inset scale bar = 10 μ m).

MerTK were co-expressed in this population (Figure 4C). Even though phosphorylated STAT3 could not be assessed in the NHP samples due to technical reasons, we did observe accumulation of STAT3 in the nuclear area of CD163⁺ and CD16⁺ cell populations, indicating that this transcription factor is activated in these leukocytes (Figure 4D).

Collectively, these results suggest that the environment created during pulmonary TB is capable to modulating macrophage activation into an M2-like program, which becomes accentuated according to disease severity.

The CD16⁺CD163⁺MerTK⁺pSTAT3⁺ monocyte-macrophages display an efficient ability to migrate in dense matrices

To determine whether the expansion of the M2-like monocyte-macrophages is beneficial or detrimental to host defense against TB, we investigated functional con-

sequences of this activation program. Studies performed in zebrafish model showed that the environment induced by mycobacterial infection stimulates the recruitment of highly motile macrophages in a matrix metalloproteases (MMP)-dependent manner, which is known to enhance the pathogenesis [43, 44]. On the basis of these observations, we investigated whether cmMTB influences human monocyte-macrophages migration in different 3D environments that mimic tissues [45]. Cell migration was first analyzed in dense Matrigel in which protease-mediated matrix digestion is mandatory for macrophage infiltration, in contrast to protease-independent migration in porous fibrillar collagen I matrices [45]. In Matrigel, when cmMTB was used as chemoattractant, the migration of human monocyte-macrophages into this matrix was enhanced and the distance covered by the cells was increased (Figure 5A, Supplementary information, Figure S6A). Similar results were obtained using another

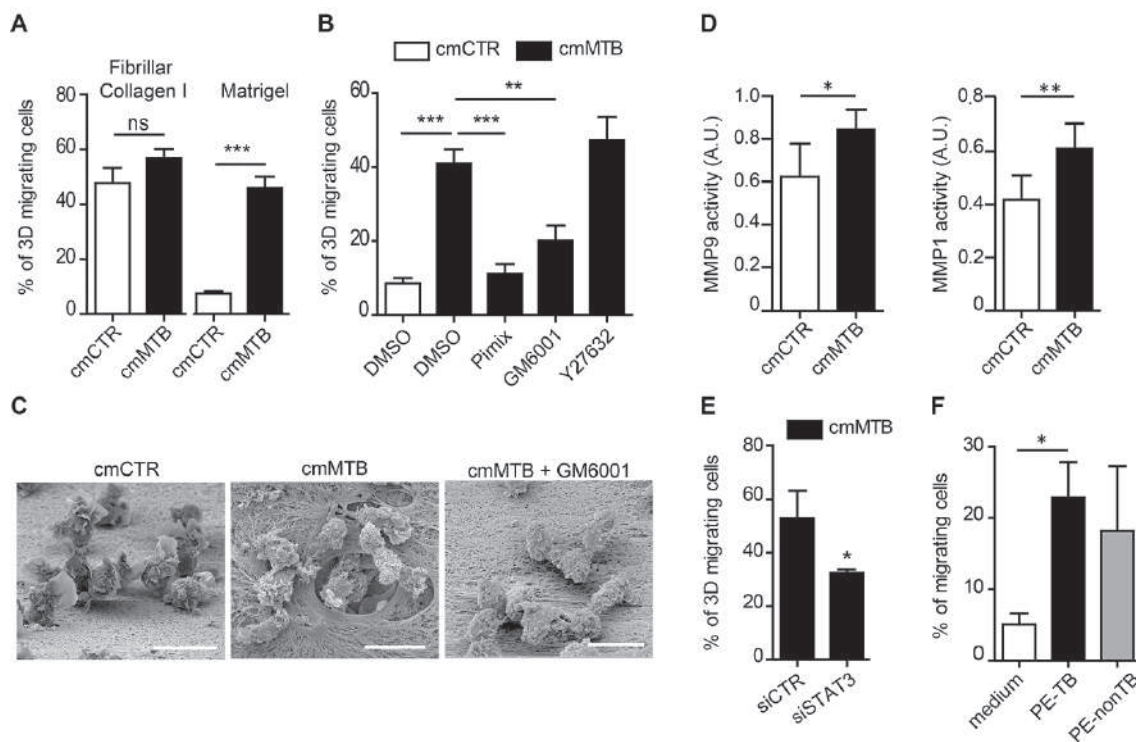


Figure 5 The CD16⁺CD163⁺MerTK⁺pSTAT3⁺ monocyte-macrophages display a strong ability to migrate in dense matrices. **(A)** Human monocytes were seeded on the top of fibrillar collagen I or Matrigel matrices, and allowed to migrate in response to cmCTR (white) or cmMTB (black). Quantification of the percentage of migrating cells (*n* = 7 donors). **(B)** Effect of protease (Pimix), matrix metalloprotease (GM6001), Rho-associated kinase (Y27632) inhibitors or DMSO on cell migration in Matrigel (*n* = 9 donors). **(C)** Representative scanning electron microscopy images showing the matrix remodeling activity of cells on Matrigel (*n* = 3 donors, scale bar = 10 μm). **(D)** Quantification of gelatin zymogram gels for MMP9 (left) and MMP1 (right) activities (*n* > 4 donors). **(E)** Monocytes transfected with SMARTpool targeting STAT3 (siSTAT3) or non-targeting control siRNAs (siCTR) were seeded on Matrigel and allowed to migrate in response to cmMTB (*n* = 3 donors). **(F)** Monocytes from HS were seeded on Matrigel and allowed to migrate in response to PE-TB, PE-nonTB or culture medium (*n* = 3 donors). Results are expressed as mean ± SEM. **P* < 0.05, ***P* < 0.01, ****P* < 0.001.

dense matrix such as gelled collagen I, strengthening the use of protease activity during cmMTB-induced migration (Supplementary information, Figure S6B). In contrast, cells infiltrated the porous fibrillar collagen I matrix efficiently regardless of the provided chemoattractant, cmMTB or cmCTR (Figure 5A). We showed in the past that macrophage 3D migration in dense matrices depends on both protease activity and the tyrosine kinase Hck, but not the ROCK kinase pathway [37, 45-47]. In line with these previous findings, both a cocktail of protease inhibitors (Pimix) and the broad-spectrum MMP inhibitor GM6001 abrogated the cmMTB-enhanced migration into Matrigel (Figure 5B). Moreover, this process was also partially inhibited by siRNA-mediated silencing of Hck in these cells (Supplementary information, Figure S6C). As expected, the use of a ROCK kinase inhibitor (Y27632) had no effect on the cmMTB-enhanced motility in Matrigel (Figure 5B). To further support the role of MMP in the monocyte-macrophage migration, we performed scanning electron microscopy. Our observations revealed that in response to cmMTB, cells profoundly remodeled the matrix compared with those treated with the cmCTR or the MMP inhibitor (Figure 5C). Interestingly, while MMP1 and MMP9 activities were increased in the culture medium of cmMTB-treated cells (Figure 5D), the MMP2 activity was unchanged (Supplementary information, Figure S6D), alluding to the selectivity of MMPs in cmMTB-enhanced motility.

Next, we investigated which soluble factor in cmMTB induces monocyte 3D migration in Matrigel. In zebrafish and mouse models, the chemokine C-C motif ligand-2 (CCL2)-dependent recruitment of CCR2⁺ macrophages plays a critical role in the mycobacterial pathogenesis [44, 48]. Here we found that migration in Matrigel is mainly based on chemoattraction mediated by recombinant CCL5 but not CCL2 or CCL4 (Supplementary information, Figure S6E). Despite the fact that the expression of CCR2 and CCR5 was enhanced by cmMTB (Supplementary information, Figure S1C), and that their different chemokine ligands are strongly secreted by Mtb-infected macrophages [29, 34], the depletion of CCL2, CCL4 and CCL5 from cmMTB did not significantly alter their migration properties (Supplementary information, Figure S6F). Since the activation program of macrophages modulates their 3D migration capacities [49], we hypothesized that the enhanced cell motility in response to cmMTB might result from the acquisition of the M2-like phenotype. To explore this possibility, we first conditioned freshly isolated monocytes with cmCTR or cmMTB, and then tested their migration capacity in Matrigel without a specific chemoattractant. Compared with cmCTR-treated cells, those treated with cmMTB

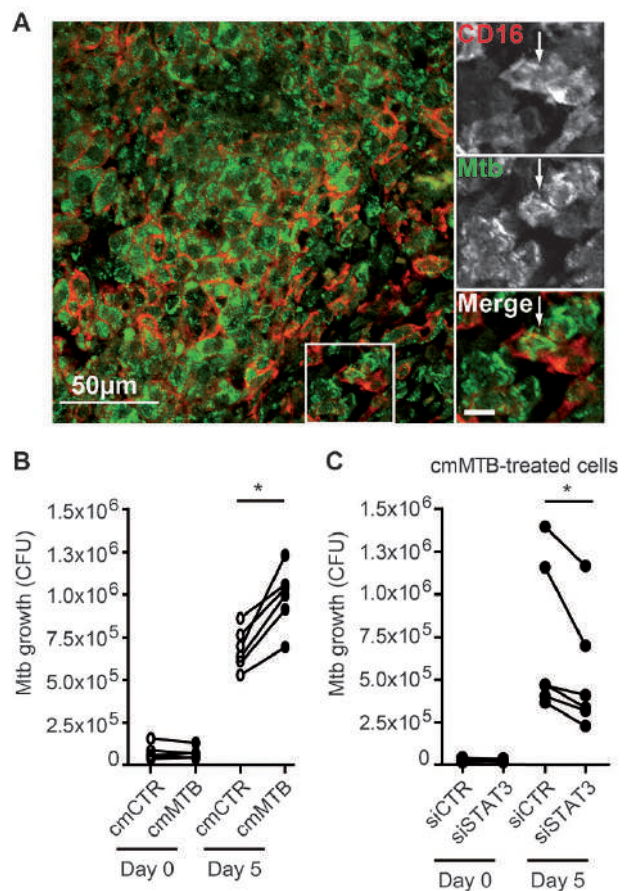


Figure 6 The CD16⁺CD163⁺MerTK⁺pSTAT3⁺ monocyte-macrophages are associated with a permissive phenotype to Mtb infection. **(A)** Representative confocal microscopy images of CD16⁺ cells (red, Alexa-555) in lung granulomas from NHP N°51 infected by Mtb (green, Alexa-488). White arrow indicates CD16⁺ cells containing Mtb bacilli (inset, scale bar = 10 μm). **(B)** Monocytes conditioned with cmCTR (white circles) or cmMTB (black circles) were infected with Mtb. On day 0 and day 5 after infection, the intracellular growth of Mtb was scored by colony-forming unit (CFU) assay. **(C)** Monocytes transfected with SMARTpool targeting STAT3 (siSTAT3) or non-targeting control siRNAs (siCTR) were conditioned with cmMTB, and then infected with Mtb. The CFU scoring was measured on day 0 and day 5 after infection. Results are expressed as before-and-after plot; **P* < 0.05.

efficiently infiltrated and remodeled Matrigel (Supplementary information, Figure S6G), indicating that acquisition of the M2-like phenotype is sufficient to enhance 3D migration regardless of a chemoattractant gradient. Furthermore, the Mtb-derived bystander effect can be mimicked when monocytes were conditioned with reIL-10 (Supplementary information, Figure S6H-S6I). Consistently, when STAT3 expression was inhibited in

these cells, or IL-10 was depleted from cmMTB, the protease-dependent migratory capacity of conditioned cells was impaired (Figure 5E, Supplementary information, Figure S6I).

Since the monocyte-macrophages characterized by the CD16⁺CD163⁺MerTK⁺ signature are abundant in the TB pleural cavity, we assessed whether PE-TB fluid activates the motility of these cells. For these experiments, we used non-TB pleural fluid (PE-nonTB) as a positive control since it is known to activate STAT3 and serve as a chemoattractant [50]. As illustrated in Figure 5F, freshly isolated monocytes from healthy donors displayed a greater capacity to infiltrate Matrigel when PE-TB and PE-nonTB were used as chemoattractants.

Taken together, our analysis shows that the acquisition of CD16⁺CD163⁺MerTK⁺pSTAT3⁺ activation program via the IL-10/STAT3 axis triggers MMP-dependent motility and allows human monocytes to penetrate and remodel dense tissue environments.

The CD16⁺CD163⁺MerTK⁺pSTAT3⁺ monocyte-macrophages are associated with a permissive phenotype to Mtb infection

The migration of mononuclear phagocytes towards infectious sites is essential for effective control and clearance of bacteria [51]. First, we observed that, among other cell types, CD16⁺ cells in NHP tuberculous granulomas contained bacilli, implying that these leukocytes can be infected *in vivo* (Figure 6A). Since M2 macrophages are associated with pathogen permissivity [3], we evaluated the ability of monocytes conditioned with cmMTB or cmCTR, and then infected with Mtb, to control bacilli growth. CFU scoring at four hours post infection (p.i.) revealed that there was no difference in the bacterial loads present in cmCTR- and cmMTB-treated cells, suggesting that soluble factors present in cmMTB do not affect the recognition and uptake of the bacilli (Figure 6B). However, cmMTB-treated cells were significantly more permissive to Mtb growth than cmCTR-treated cells, as illustrated at day 5 p.i. (Figure 6B). Inhibition of STAT3 by siRNA-mediated gene silencing in cmMTB-treated cells reversed their pathogen-permissive phenotype (Figure 6C, Supplementary information, Figure S7A). Similar results were obtained by an alternative approach using the pharmacological inhibition of STAT3 activation with STAT3IC (Supplementary information, Figure S7B).

Collectively, these results show that the CD16⁺CD163⁺MerTK⁺pSTAT3⁺ activation program acquisition renders human monocyte-macrophages more susceptible to intracellular bacterial growth.

The CD16⁺CD163⁺MerTK⁺pSTAT3⁺ monocyte-macro-

phages display immuno-modulatory properties

M2 macrophages programmed with IL-10, TGFβ or glucocorticoids are known as “deactivators” of the immune response [28]. Among the features that distinguish these cells is the low production of pro-inflammatory cytokines (e.g., TNFα and IL-12), contrasting with high expression of anti-inflammatory mediators (e.g., IL-10, TGFβ and Gas6) [28, 39]. We first assessed the ability of cmMTB-conditioned cells to engage production of inflammatory signals in response to killed Mtb, in order to discriminate the well-described suppressive effects using live Mtb [4]. Our results indicate that, compared with cells treated with cmCTR, those conditioned with cmMTB expressed less pro-inflammatory genes, such as *TNF*, *IL12A* and *CCL1* (Supplementary information, Figure S8A). The reduced secretion of TNFα was confirmed in the supernatant of cmMTB-treated cells (Supplementary information, Figure S8B). Strikingly, a weaker expression of *IL-10* was observed in contrast to the elevated level of *GAS6* and *PROS1*, in cells pretreated with cmMTB (Supplementary information, Figure S8A). Another feature that distinguishes deactivator macrophages is the poor ability to activate T cells [28]. To evaluate this, we first examined the programmed death ligand 1 (PD-L1) expression relative to that of CD86, since an increased PD-L1/CD86 ratio in mononuclear phagocytes is reported to inhibit T cell proliferation and interferon-gamma (IFNγ) production [52]. Noticeably, we found that the PD-L1/CD86 ratio was highly elevated in cmMTB-conditioned cells compared with cmCTR treatment (Figure 7A, Supplementary information, Figure S8C). Stimulation with killed Mtb did not change this unbalanced ratio in cmMTB-conditioned cells (Figure 7A, Supplementary information, Figure S8C). Next, we measured the capacity of cmMTB-conditioned monocyte-macrophages to activate allogeneic human T cells, using peripheral blood lymphocytes labeled with CFSE. Importantly, the cmMTB-conditioned cells displayed a significantly lower capacity to stimulate T cell proliferation and IFNγ production in comparison with cmCTR-treated cells (Figure 7A). While we only observed a tendency towards the reversion of the unbalanced PD-L1/CD86 ratio (Figure 7B), the inhibition of STAT3 phosphorylation with curcubitacin significantly reverted the cell surface expression of PD-L1 in cmMTB-treated cells and their poor capacity to activate T cells (Figure 7B and Supplementary information, Figure S8D). To validate these observations *in vivo*, we examined whether monocyte-macrophages in TB patients display immunomodulatory properties. As shown in Figure 7C, upon stimulation with killed Mtb, monocytes from PB-TB displayed an elevated PD-L1/CD86 ratio compared with those from PB-HS. In

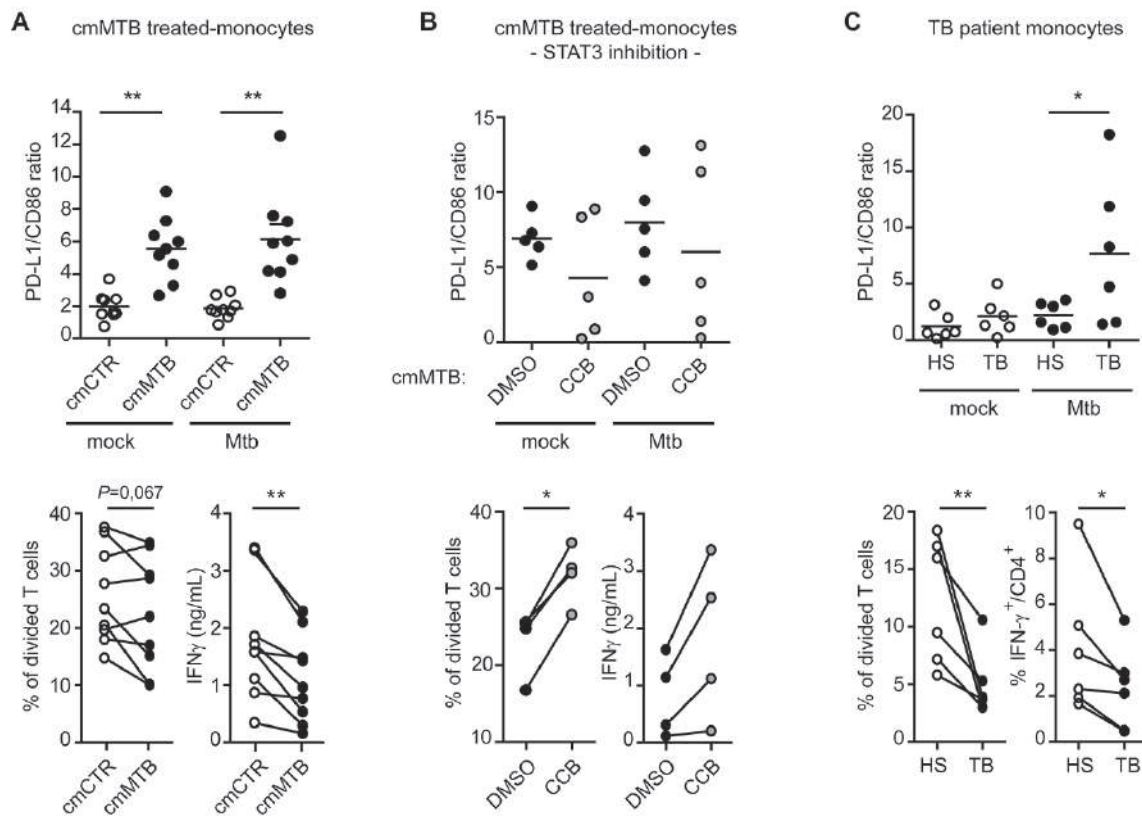


Figure 7 The CD16⁺CD163⁺MerTK⁺pSTAT3⁺ monocyte-macrophages display immunomodulatory properties. **(A-C)** Monocytes were stimulated with killed Mtb or PBS (mock). Top panels: vertical scatter plots showing the ratio of MFI obtained for PD-L1 and CD86. Results are expressed as mean \pm SEM. Bottom panels: allogeneic human T lymphocytes labeled with CFSE were co-cultured with monocytes. Before-and-after plots showing T cell proliferation illustrated as the percentage of CFSE-dividing cells (left) and the production of IFN γ by proliferating T cells quantified by **(A-B)** ELISA in co-culture supernatants or **(C)** flow cytometry (right). **(A)** cmCTR- or cmMTB-conditioned monocytes were stimulated with PFA-killed Mtb or PBS (mock). **(B)** cmMTB conditioning of monocytes was performed in the presence of the STAT3 inhibitor, cucurbitacin I (CCB) or DMSO as control. Cells were then stimulated with PFA-killed Mtb or mock. **(C)** Monocytes from HS or TB patients were stimulated with irradiated Mtb or mock. * $P < 0.05$; ** $P < 0.01$. Each circle within vertical scatter plots represents a single donor.

addition, PB-TB monocytes exhibited a lower ability to induce T cell proliferation and the production of IFN γ in allogeneic T cells compared with PB-HS monocytes (Figure 7C).

Taken together, these data demonstrate that the acquisition of the CD16⁺CD163⁺MerTK⁺pSTAT3⁺ activation program is characterized by a (i) low ratio of pro-/anti-inflammatory factor production, (ii) high ratio of PD-L1/CD86 co-stimulatory molecule expression and (iii) poor capacity to activate T cells, which indicates a negative contribution to a dedicated host response against TB.

Discussion

TB mortality is unacceptably high given that most deaths are preventable. The identification of new bio-

markers that could reduce the size and duration of clinical trials of new drug candidates and define treatment efficacy, disease activity, cure and relapse, is highly desirable to reduce the impact of TB. Considering that the monocyte compartment is perturbed in TB, we asked whether this shift is beneficial or detrimental to host defense against TB, and whether this could represent a target for treatment. We believe that this study makes four major contributions to the interface between hypothesis-driven basic research and the identification of potential bio-signatures and molecular markers for human disease (Figure 8).

First, we present evidence for how human monocytes are predisposed in the context of TB towards an anti-inflammatory M2-like (CD16⁺CD163⁺MerTK⁺pSTAT3⁺) macrophage activation program, a process that is mainly

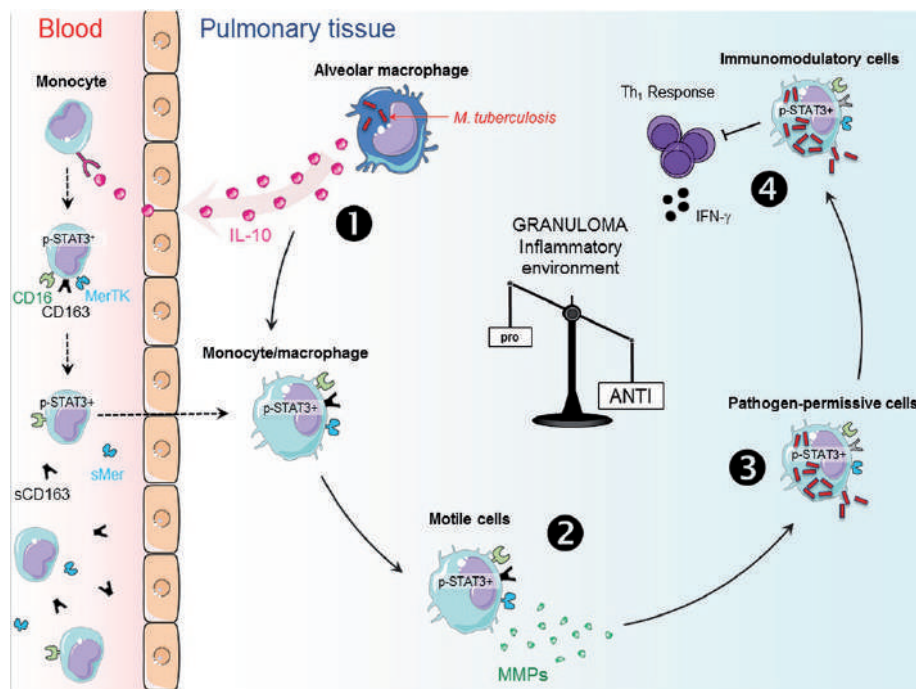


Figure 8 Model illustrating how the environment induced by Mtb infection predisposes human monocyte differentiation towards an M2-like macrophage, altering host defense during infection. Alveolar macrophages are one of the first leukocytes able to recognize and phagocytose Mtb upon entry in the respiratory system. At this site, infected macrophages reshape their microenvironment by secreting many soluble factors including cytokines and chemokines, which for the most part are responsible for the leukocyte infiltration during the earliest stages of infection. However, (1) Mtb has the capacity to modulate the macrophage response and to induce the secretion of anti-inflammatory cytokines, such as IL-10. IL-10, tilts, through a bystander effect, monocytes towards an M2-like macrophage program (CD16⁺CD163⁺MerTK⁺pSTAT3⁺) in a STAT3-dependent manner. In the blood, CD163 and MerTK receptors are cleaved off, and concentration of their soluble form correlates positively with disease severity. The CD16⁺CD163⁺MerTK⁺pSTAT3⁺ phenotype acquisition is accompanied by (2) an enhanced protease-dependent motility through matrix metalloprotease activity (e.g., MMP-1), which allows extracellular matrix remodeling, and hypothetically, trans-tissue migration. This phenotype acquisition also renders (3) monocyte-macrophages permissive to Mtb intracellular growth, and (4) immunomodulatory in terms of their reduced ability to secrete pro-inflammatory cytokines (e.g., low TNF α) and activate the T-helper 1 (Th1) response via co-stimulatory signaling (e.g., high ratio PD-L1/CD86). Collectively, the Mtb-derived bystander activation of STAT3 in monocytes predisposes their differentiation program towards a macrophage population that ultimately shifts the microenvironment (e.g., tuberculous granulomas) in favor of microbial resilience in the host.

dependent on the IL-10/STAT3 signaling pathway. This phenotype can also be obtained *in vitro* using the secretome of Mtb-infected macrophages. We provide a new set of markers to characterize this M2-like activation program in terms of hallmark cell-surface markers (i.e., CD16⁺, CD163⁺ and MerTK⁺), the transcription factor STAT3, cytokine content (e.g., TNF α ^{low}), chemokines receptors (i.e., CCR2^{high} and CCR5^{high}), co-stimulatory molecules (i.e., PD-L1^{high} and CD86^{low}) and MMP (i.e., MMP1^{high} and MMP9^{high}). Interestingly, we also detected CD206 expression as part of the described M2-like phenotype, which was independent of the IL-10/STAT3 axis. Since CD206 is known to be dependent of STAT6 signaling [53], it is probable that alternative signals (e.g., IL-

2, IL-15 and IFN α), which are part of the secretome of Mtb-infected macrophages, are partially responsible for the establishment of this M2-like phenotype. Nevertheless, in our *in vitro* model, the blocking of IL-10 in the Mtb-derived conditioned media seems to be sufficient to impair STAT3 activation and the establishment of M2-like phenotype. This is in line with the fact that IL-10 is considered to be an important clinical biomarker of disease progression [54], increased levels for this cytokine are reported in both the blood [31, 55] and in the bronchoalveolar lavage of active TB patients [56], and in the tuberculous granuloma context in NHP model [57]. The fact that we observed elevated levels of activated STAT3 in monocyte-macrophages in both TB patients and in the

NHP tuberculous granuloma context, suggests that over-active production of IL-10 may be responsible. It remains to be seen whether activation of STAT3 by other signals, such as IL-6 or IL-27, generates a similar activation program with critical consequences for TB pathogenesis and other chronic inflammatory diseases.

Second, mainly based on our *in vitro* approach, we characterized key functional properties for the human CD16⁺CD163⁺MerTK⁺pSTAT3⁺ monocyte-macrophages. To begin, we provided evidence that these cells display an enhanced capacity to migrate through dense matrices in an MMP-dependent manner contrasting with our previous observations that 3D migration in dense matrices rather involves cathepsins [45, 47, 58, 59]. While we cannot exclude that chemokines present in cmMTB could be involved in the migration capacity of CD16⁺CD163⁺MerTK⁺pSTAT3⁺ monocyte-macrophages, we showed that STAT3-dependent acquisition of the M2-like phenotype is essential for the enhanced motility and extracellular matrix remodeling activity in these cells. This process is accompanied by MMP1 and MMP9 activity that may contribute to lung tissue damage and TB pathogenesis, as suggested by the formation of protease-mediated tunnels in 3D matrices [47, 60, 61], by a study demonstrating that MMP1 is increased during Mtb infection and is responsible for lung immunopathology [62], and by other reports evidencing the role of MMP9 in the recruitment of macrophages, granuloma maturation and bacterial dissemination [44]. This is an exciting finding given that, in the zebrafish and mouse models, mycobacteria infection recruits highly motile macrophages as a tool for bacterial dissemination [44, 48]. Another functional characteristic described in this study is the permissive nature of CD16⁺CD163⁺MerTK⁺pSTAT3⁺ cells to handle Mtb intracellular growth. To our knowledge, our study is the first to demonstrate that abrogation of STAT3 in monocyte-macrophages restores the control of Mtb intracellular growth. Actually, STAT3 has been shown to block phagolysosome fusion, induction of autophagy, and optimal release of nitric oxide and reactive oxygen species [63]. However, the regulation of these microbicidal activities by STAT3 has yet to be explored for TB [63]. This is in line with the antagonistic effect of IL-10 on microbicidal activities of Mtb-infected macrophages, such as phagosome-lysosome fusion [63, 64], and IFN γ -induced production of oxygen and nitrogen species [65]. Likewise, mice overexpressing IL-10 specifically in the macrophage compartment present susceptibility to Mtb infection due to macrophages displaying an exaggerated M2-like activation program associated with a high pulmonary bacterial load [66]. In parallel, we also demonstrate that CD16⁺CD163⁺MerTK⁺pSTAT3⁺

monocyte-macrophages display an immunomodulatory functional capacity. Besides the diminished pro-inflammatory cytokine response, CD16⁺CD163⁺MerTK⁺pSTAT3⁺ cells also display a high PD-L1 to CD86 ratio and tolerant capacity to control T cell activation. This is in accordance with different reports showing that STAT3 is a key anti-inflammatory mediator that inhibits important pro-inflammatory processes [36, 63]. For instance, mice deficient for the IL-27 receptor (a STAT3 activator) exhibited an uncontrolled production of pro-inflammatory cytokines, elevated levels of IFN γ -producing T cells, enhanced macrophage effector functions and reduced bacterial loads, in response to Mtb infection. Yet, these animals eventually succumb to uncontrolled immunopathology [67]. In a reciprocal case, a mouse with targeted deletion in the myeloid compartment for the suppressor of cytokine signaling-3 (SOCS3), which is known to inhibit STAT3, showed increased susceptibility to Mtb infection [68]. On the basis of these functional observations, our study provides an original biological context to further understand at the molecular level how STAT3 activity grants protease-dependent migration capacity and inhibits antimycobacterial effector mechanisms, consequently opening up new venues to investigate how it might contribute to tissue remodeling, pathogen dissemination and immunomodulation. Beyond the immunomodulatory capacity (Figure 7C), it remains to be shown whether this IL-10/STAT3-dependent functional program is truly established during the expansion of CD16⁺CD163⁺MerTK⁺pSTAT3⁺ monocyte-macrophages in patients with active TB.

The third major contribution from this study concerns the critical correlation of the abundance of CD16⁺CD163⁺MerTK⁺pSTAT3⁺ monocyte-macrophages with the severity of TB disease in the human and NHP contexts. Recent studies by Zizzo *et al.* [25, 69] suggested a strict correlation between systemic lupus erythematosus (SLE) disease severity and the activation of an M2-like macrophage characterized by CD163 and MerTK expression during the monocyte-to-macrophage differentiation. Expanding upon our previous observation that the monocyte compartment becomes perturbed in TB patients [18], we now report that the CD163⁺MerTK⁺pSTAT3⁺ signature accompanies the expansion of the CD16⁺ monocytes. As these results contrast with the pro-inflammatory phenotype of CD16⁺ monocytes in healthy donors [13, 15-17], we infer that all CD16⁺ monocytes are not created in a similar manner, and thus the CD16 expression in monocyte-macrophages cannot be extrapolated to indicate a pro- or anti-inflammatory nature. Their final differentiation program might result as a consequence of the microenvironment shaped in health and disease pro-

gression contexts. In agreement with a recent description of CD163⁺ macrophages during the onset of tuberculous pleurisy [70], we show that this M2-like macrophage is particularly enriched within the CD14⁺CD16⁺ cell population isolated from the pleural cavity of TB patients. Considering that the CD16⁺ population expansion displays an M2-like phenotype in the pleural cavity from TB patients, and that TB pleural effusion activates STAT3 phosphorylation in monocytes from healthy donors and stimulates their protease-dependent migration, we infer that the environmental signals within Mtb infection sites perpetuate the CD16⁺CD163⁺MerTK⁺pSTAT3⁺ activation program and possibly also serve as chemoattractant. At the tissue level, although there are key reports integrating the concept of macrophage activation within tuberculous granulomas [41, 42], to our knowledge this is the first study to identify the CD16⁺CD163⁺MerTK⁺ macrophage activation program along with the co-localization of activated STAT3. Beyond the detection of CD163, we now provide a novel marker signature composed of CD16, MerTK and activated STAT3, which could be helpful to identify the anti-inflammatory and immunomodulatory macrophage program in the progression of TB disease. Based on the known inhibitory role for IL-10 in the formation of protective mature granulomas during Mtb infection [63, 71], the presence of these cells may represent a cellular indicator of granulomas that foment the expansion and dissemination of disease [41, 44]. Indeed, human CD16⁺CD163⁺MerTK⁺pSTAT3⁺ macrophages meet the criteria for the formation of pathogenic granulomas mainly described in the zebrafish model: secretion of MMPs involved in granuloma formation (i.e., MMP1 and MMP9), high protease-dependent motility, pathogen permissiveness and immunomodulatory capacity to regulate a pro-inflammatory environment [44]. For example, the monocyte predisposition towards M2-like macrophage program alters protective granuloma formation during *Schistosoma mansoni* infection, which indicates a general process contributing to granulomatous diseases [72]. On the basis of these observations, we propose that the unbalanced monocyte compartment in TB is predisposed to differentiate towards the anti-inflammatory M2-like macrophages as a continuously failed attempt by the host to limit immunopathology, whose abundance is directly related to the severity of TB disease, ultimately contributing to the establishment of chronic infection.

The last major contribution of this study is the identification of soluble form of CD163 as a potential biomarker to monitor, in combination with actual and next to be discovered biomarkers, TB disease progression and anti-TB treatment efficacy. Unlike the CD14⁺CD16⁺ cell population found in the pleural cavity, we failed to detect

CD163 as part of the cell-surface marker signature in circulating monocytes in TB patients. This was an intriguing observation as circulating monocytes from TB patients still displayed high level of phosphorylated STAT3 and immunomodulatory potential in terms of high PD-L1 to CD86 expression ratio along with a poor capacity to activate allogeneic T cells. The detection of sCD163 in TB patients reconciled these observations, as monocytes are the only circulating cell population known to express CD163 and MerTK [38, 73]. Indeed, the plasma level of these soluble receptors correlated with TB disease severity in patients, and upon anti-TB treatment, it significantly decreased to the plasma concentration level obtained from contact individuals. As sCD163 shows optimal sensitivity and specificity according to the ROC analysis provided in the TB context, we thus propose this soluble receptor, in combination with actual diagnosis tools and next to be discovered molecules, as a potential biomarker to evaluate disease progression and predict drug treatment outcome. In a second step, these results need to be confirmed in a larger cohort of individuals from different genetic background. Indeed, there is only one study that correlated the plasma concentration of sCD163 to the survival of verified TB patients [40]. However, there has been no confirmation of these results ever since, and more importantly, there is no actual evaluation available on the effect of anti-TB drugs on sCD163 levels until now. Interestingly, sCD163 is considered as a valuable marker of the activation of an M2-like monocyte-macrophage program and biomarkers of disease activity in SLE [25, 40], alluding to a critical biological significance for the presence of this soluble receptor as immune response biomarkers in TB disease.

In conclusion, our study provides a novel cellular context, along with identification of molecules and pathways, which may fuel new research venues concerning monocyte-macrophages in the TB context. Newly recommended guidelines for the nomenclature of the macrophage activation process are based on three principles: source of macrophages, definition of activators and a consensus collection of markers to describe macrophage activation [23]. On the basis of these guidelines, the human CD16⁺CD163⁺MerTK⁺pSTAT3⁺ activation program described in this study within the TB context is reasonably related to the proposed “M(IL-10)” nomenclature. However, in a pathological context, multiple signals can activate STAT3-dependent signaling pathways (e.g., IL-6, IL-23 and IL-27) [36, 63]. Consequently, it remains to be determined whether they activate STAT3 in a similar fashion as IL-10 to specifically establish the TB-associated CD16⁺CD163⁺MerTK⁺pSTAT3⁺ phenotype and functional profile reported in this study; if so, the no-

menclature “M(STAT3)” would be a way to subsume the phenotype and functions of cells belonging to STAT3-dependent activation program(s). Interestingly, global biomarker studies are sometimes criticized as being non-hypothesis driven [2]. We believe that the functional characterization of this M(IL-10)-like program, and its critical *in vivo* assessment in TB patients and NHP tuberculous granulomas, adds a significant pathological context to the biomarker potential of sCD163. Finally, since immune impairment is usually observed in patients with chronic infections, and given that the STAT3 activity grants a tolerance capacity to the myeloid compartment [36], we estimate that short-term blockade of STAT3 within the monocyte-to-macrophage differentiation program has the potential to modulate mechanisms of disease tolerance and restore the antimicrobial immunity. STAT3 inhibitors, currently assessed in phase I clinical trials for their antitumor effects [74, 75], might be particularly useful in patients with TB meningitis, for example, who fail to control mycobacterial proliferation because of intrinsic exacerbation of immune suppression, and in which dexamethasone treatment has deleterious effects [76].

Materials and Methods

Human and NHP samples

Studies involving human samples from healthy donors and TB patients, and samples from NHPs were performed in accordance to guidelines approved by all indicated Ethical committees; see Supplementary information, Data S1.

Preparation of human monocytes and monocyte-derived macrophages

Monocytes from healthy donors and from TB patients were isolated by CD14 positive magnetic labeling and differentiated into macrophages as previously described [18, 37, 45]; see Supplementary information, Data S1.

Preparation of conditioned media and monocyte treatment

The cmMTB medium was prepared from *Mtb*-infected monocyte-derived macrophages at a multiplicity of infection (MOI) of three bacteria per cell, in RPMI 1640 (Gibco) containing 10% FBS (Sigma-Aldrich). The cmCTR medium was obtained from uninfected macrophages. After overnight incubation at 37 °C, culture media were collected, sterilized by filtration and aliquots were stored at -80 °C. For conditioning, human CD14⁺ sorted monocytes were allowed to adhere for 1 h on glass coverslips in the absence of serum and then cultured for 3 days with 50% dilution of cmMTB or cmCTR containing M-CSF (Peprotech, 10 ng/ml) and 10% FBS. Cell surface expression of macrophage activation markers (Supplementary information, Table S4), and bacterial intracellular growth, were measured using standard procedures detailed in Supplementary information, Data S1.

3D migration assays

3D migration assays were performed as previously described [45]. Briefly, fibrillar collagen I, gelled collagen I or Matrigel was polymerized in transwell inserts and used immediately. Cells were seeded on top of matrices, the lower chamber of each insert was filled with a 50% dilution of cmMTB or cmCTR in complete medium or with complete medium supplemented with recIL-10. Cell migration into fibrillar collagen I was quantified after 24 h, whereas the migration in dense matrices (Matrigel or gelled collagen I) was quantified after 72 h. The percentage of cell migration was obtained as the ratio of cells within the matrix to the total number of counted cells as described [45].

Assessment of the inflammatory cytokine response and activation of T cells

Total RNAs were reverse transcribed and amplified as detailed in Supplementary information, Data S1. Primers for qPCR are listed in Supplementary information, Table S5. The mRNA content was normalized to the metastatic lymph node protein 51 (MLN51) mRNA and quantified using the $\Delta\Delta C_t$ method. Secreted TNF α and IL-10 were measured by ELISA. Activation of allogeneic T cells was evaluated in mixed lymphocyte reactions including cell proliferation by flow cytometry and secreted IFN γ analysis by ELISA or flow cytometry.

Plasma biomarker measurements

Concentrations of soluble sCD163 and sMer (R&D system DuoSet) were assessed in cryopreserved human serum samples maintained at -80 °C, according to the manufacturer’s instruction. For sCD163 analysis, the serum was diluted at 1/10, and for sMer at 1/2, in PBS.

Statistical analyses

One-tailed paired or unpaired *t*-test was applied on data sets with a normal distribution, whereas one-tailed Mann-Whitney (unpaired test) or Wilcoxon (matched-paired test) tests were used otherwise. *P* < 0.05 was considered statistically significant. Correlations were evaluated using the Pearson’s test. For biomarker measurements, a ROC curve was generated. The AUC value and 95% CI were calculated to determine the specificity and sensitivity of TB infection. All statistical analyses were performed using GraphPad Prism 6.0 (GraphPad Software Inc., USA).

Acknowledgments

This work was supported by the CNRS, the European Union (ERA-NET/ERASysBio grant TB-HOST-NET, and FP7 grants HEALTH-F4-2011-282095-TARKINAID and 241745 NEWTB-VAC), the French National Research Agency (ANR grants 2010-01301 MigreFlame and ANR-12-BSV3-0002 B-TB) and by Fondation pour la Recherche Médicale (FRM, DEQ 20110421312). CL (FDT 20130928326) and GL-V (SPF20110421334) acknowledge support from FRM; AB acknowledges support from ANR-12-BSV3-0002. FAWV acknowledges support from Aeras (Rockville, MD, USA) for the NHP study. This work was also partially supported by the PICT 2012-0221 and PICT 2011-0572 grants given by the Agencia Nacional de Promoción Científica y Tecnológica, Argentina.

References

- 1 Wallis RS, Kim P, Cole S, *et al.* Tuberculosis biomarkers discovery: developments, needs, and challenges. *Lancet Infect Dis* 2013; **13**:362-372.
- 2 Kaufmann SH, Parida SK. Tuberculosis in Africa: learning from pathogenesis for biomarker identification. *Cell Host Microbe* 2008; **4**:219-228.
- 3 Benoit M, Desnues B, Mege JL. Macrophage polarization in bacterial infections. *J Immunol* 2008; **181**:3733-3739.
- 4 Lugo-Villarino G, Verollet C, Maridonneau-Parini I, Neyrolles O. Macrophage polarization: convergence point targeted by *Mycobacterium tuberculosis* and HIV. *Front Immunol* 2011; **2**:43.
- 5 Flynn JL, Chan J, Lin PL. Macrophages and control of granulomatous inflammation in tuberculosis. *Mucosal Immunol* 2011; **4**:271-278.
- 6 Martinez FO, Gordon S. The M1 and M2 paradigm of macrophage activation: time for reassessment. *F1000prime Rep* 2014; **6**:13.
- 7 Lugo-Villarino G, Neyrolles O. Manipulation of the mononuclear phagocyte system by *Mycobacterium tuberculosis*. *Cold Spring Harb Perspect Med* 2014; **4**:a018549.
- 8 O'Garra A, Redford PS, McNab FW, *et al.* The immune response in tuberculosis. *Annu Rev Immunol* 2013; **31**:475-527.
- 9 Cambier CJ, Falkow S, Ramakrishnan L. Host evasion and exploitation schemes of *Mycobacterium tuberculosis*. *Cell* 2014; **159**:1497-1509.
- 10 Wong KL, Yeap WH, Tai JJ, *et al.* The three human monocyte subsets: implications for health and disease. *Immunol Res* 2012; **53**:41-57.
- 11 Robbins CS, Swirski FK. The multiple roles of monocyte subsets in steady state and inflammation. *Cell Mol Life Sci* 2010; **67**:2685-2693.
- 12 Ziegler-Heitbrock L. The CD14⁺ CD16⁺ blood monocytes: their role in infection and inflammation. *J Leukoc Biol* 2007; **81**:584-592.
- 13 Frankenberger M, Sternsdorf T, Pechumer H, Pforte A, Ziegler-Heitbrock HW. Differential cytokine expression in human blood monocyte subpopulations: a polymerase chain reaction analysis. *Blood* 1996; **87**:373-377.
- 14 Frankenberger M, Hofer TP, Marei A, *et al.* Transcript profiling of CD16-positive monocytes reveals a unique molecular fingerprint. *Eur J Immunol* 2012; **42**:957-974.
- 15 Szaflarska A, Baj-Krzyworzeka M, Siedlar M, *et al.* Antitumor response of CD14⁺/CD16⁺ monocyte subpopulation. *Exp Hematol* 2004; **32**:748-755.
- 16 Belge KU, Dayyani F, Horelt A, *et al.* The proinflammatory CD14⁺CD16⁺DR⁺⁺ monocytes are a major source of TNF. *J Immunol* 2002; **168**:3536-3542.
- 17 Aguilar-Ruiz SR, Torres-Aguilar H, Gonzalez-Dominguez E, *et al.* Human CD16⁺ and CD16⁻ monocyte subsets display unique effector properties in inflammatory conditions *in vivo*. *J Leukoc Biol* 2011; **90**:1119-1131.
- 18 Balboa L, Romero MM, Basile JI, *et al.* Paradoxical role of CD16⁺CCR2⁺CCR5⁺ monocytes in tuberculosis: efficient APC in pleural effusion but also mark disease severity in blood. *J Leukoc Biol* 2011; **90**:69-75.
- 19 Balboa L, Romero MM, Laborde E, *et al.* Impaired dendritic cell differentiation of CD16-positive monocytes in tuberculosis: role of p38 MAPK. *Eur J Immunol* 2013; **43**:335-347.
- 20 Tung YC, Ou TT, Tsai WC. Defective *Mycobacterium tuberculosis* antigen presentation by monocytes from tuberculosis patients. *Int J Tuberc Lung Dis* 2013; **17**:1229-1234.
- 21 Skold M, Behar SM. Tuberculosis triggers a tissue-dependent program of differentiation and acquisition of effector functions by circulating monocytes. *J Immunol* 2008; **181**:6349-6360.
- 22 Remoli ME, Giacomini E, Petruccioli E, *et al.* Bystander inhibition of dendritic cell differentiation by *Mycobacterium tuberculosis*-induced IL-10. *Immunol Cell Biol* 2011; **89**:437-446.
- 23 Murray PJ, Allen JE, Biswas SK, *et al.* Macrophage activation and polarization: nomenclature and experimental guidelines. *Immunity* 2014; **41**:14-20.
- 24 Calzada-Wack JC, Frankenberger M, Ziegler-Heitbrock HW. Interleukin-10 drives human monocytes to CD16 positive macrophages. *J Inflamm* 1996; **46**:78-85.
- 25 Zizzo G, Hilliard BA, Monestier M, Cohen PL. Efficient clearance of early apoptotic cells by human macrophages requires M2c polarization and MerTK induction. *J Immunol* 2012; **189**:3508-3520.
- 26 Sironi M, Martinez FO, D'Ambrosio D, *et al.* Differential regulation of chemokine production by Fcγ receptor engagement in human monocytes: association of CCL1 with a distinct form of M2 monocyte activation (M2b, Type 2). *J Leukoc Biol* 2006; **80**:342-349.
- 27 Jaguin M, Houlbert N, Fardel O, Lecreur V. Polarization profiles of human M-CSF-generated macrophages and comparison of M1-markers in classically activated macrophages from GM-CSF and M-CSF origin. *Cell Immunol* 2013; **281**:51-61.
- 28 Mantovani A, Sica A, Sozzani S, *et al.* The chemokine system in diverse forms of macrophage activation and polarization. *Trends Immunol* 2004; **25**:677-686.
- 29 Verreck FA, de Boer T, Langenberg DM, van der Zanden L, Ottenhoff TH. Phenotypic and functional profiling of human proinflammatory type-1 and anti-inflammatory type-2 macrophages in response to microbial antigens and IFN-γ and CD40L-mediated costimulation. *J Leukoc Biol* 2006; **79**:285-293.
- 30 Verreck FA, de Boer T, Langenberg DM, *et al.* Human IL-23-producing type 1 macrophages promote but IL-10-producing type 2 macrophages subvert immunity to (myco)bacteria. *Proc Natl Acad Sci USA* 2004; **101**:4560-4565.
- 31 Olobo JO, Geletu M, Demissie A, *et al.* Circulating TNF-α, TGF-β, and IL-10 in tuberculosis patients and healthy contacts. *Scand J Immunol* 2001; **53**:85-91.
- 32 Liang L, Zhao YL, Yue J, *et al.* Interleukin-10 gene promoter polymorphisms and their protein production in pleural fluid in patients with tuberculosis. *FEMS Immunol Med Microbiol* 2011; **62**:84-90.
- 33 Roodgar M, Lackner A, Kaushal D, *et al.* Expression levels of 10 candidate genes in lung tissue of vaccinated and TB-infected cynomolgus macaques. *J Med Primatol* 2013; **42**:161-164.
- 34 Wang C, Peyron P, Mestre O, *et al.* Innate immune response to *Mycobacterium tuberculosis* Beijing and other genotypes. *PLoS One* 2010; **5**:e13594.
- 35 Szanto A, Balint BL, Nagy ZS, *et al.* STAT6 transcription factor is a facilitator of the nuclear receptor PPARγ-reg-

- ulated gene expression in macrophages and dendritic cells. *Immunity* 2010; **33**:699-712.
- 36 Lang R. Tuning of macrophage responses by Stat3-inducing cytokines: molecular mechanisms and consequences in infection. *Immunobiology* 2005; **210**:63-76.
 - 37 Troegeler A, Lastrucci C, Duval C, *et al.* An efficient siRNA-mediated gene silencing in primary human monocytes, dendritic cells and macrophages. *Immunol Cell Biol* 2014; **92**:699-708.
 - 38 Fabrick BO, Dijkstra CD, van den Berg TK. The macrophage scavenger receptor CD163. *Immunobiology* 2005; **210**:153-160.
 - 39 Zagorska A, Traves PG, Lew ED, Dransfield I, Lemke G. Diversification of TAM receptor tyrosine kinase function. *Nat Immunol* 2014; **15**:920-928.
 - 40 Knudsen TB, Gustafson P, Kronborg G, *et al.* Predictive value of soluble haemoglobin scavenger receptor CD163 serum levels for survival in verified tuberculosis patients. *Clin Microbiol Infect* 2005; **11**:730-735.
 - 41 Lugo-Villarino G, Hudrisier D, Benard A, Neyrolles O. Emerging trends in the formation and function of tuberculosis granulomas. *Front Immunol* 2012; **3**:405.
 - 42 Mattila JT, Ojo OO, Kepka-Lenhart D, *et al.* Microenvironments in tuberculous granulomas are delineated by distinct populations of macrophage subsets and expression of nitric oxide synthase and arginase isoforms. *J Immunol* 2013; **191**:773-784.
 - 43 Cambier CJ, Takaki KK, Larson RP, *et al.* Mycobacteria manipulate macrophage recruitment through coordinated use of membrane lipids. *Nature* 2014; **505**:218-222.
 - 44 Ramakrishnan L. Revisiting the role of the granuloma in tuberculosis. *Nat Rev Immunol* 2012; **12**:352-366.
 - 45 Van Goethem E, Poincloux R, Gauffre F, Maridonneau-Parini I, Le Cabec V. Matrix architecture dictates three-dimensional migration modes of human macrophages: differential involvement of proteases and podosome-like structures. *J Immunol* 2010; **184**:1049-1061.
 - 46 Cougoule C, Le Cabec V, Poincloux R, *et al.* Three-dimensional migration of macrophages requires Hck for podosome organization and extracellular matrix proteolysis. *Blood* 2010; **115**:1444-1452.
 - 47 Maridonneau-Parini I. Control of macrophage 3D migration: a therapeutic challenge to limit tissue infiltration. *Immunol Rev* 2014; **262**:216-231.
 - 48 Antonelli LR, Gigliotti Rothfuchs A, Goncalves R, *et al.* Intranasal Poly-IC treatment exacerbates tuberculosis in mice through the pulmonary recruitment of a pathogen-permissive monocyte/macrophage population. *J Clin Invest* 2010; **120**:1674-1682.
 - 49 Cougoule C, Van Goethem E, Le Cabec V, *et al.* Blood leukocytes and macrophages of various phenotypes have distinct abilities to form podosomes and to migrate in 3D environments. *Eur J Cell Biol* 2012; **91**:938-949.
 - 50 Yeh HH, Lai WW, Chen HH, Liu HS, Su WC. Autocrine IL-6-induced Stat3 activation contributes to the pathogenesis of lung adenocarcinoma and malignant pleural effusion. *Oncogene* 2006; **25**:4300-4309.
 - 51 Shi C, Pamer EG. Monocyte recruitment during infection and inflammation. *Nat Rev Immunol* 2011; **11**:762-774.
 - 52 Freeman GJ, Long AJ, Iwai Y, *et al.* Engagement of the PD-1 immunoinhibitory receptor by a novel B7 family member leads to negative regulation of lymphocyte activation. *J Exp Med* 2000; **192**:1027-1034.
 - 53 Lawrence T, Natoli G. Transcriptional regulation of macrophage polarization: enabling diversity with identity. *Nat Rev Immunol* 2011; **11**:750-761.
 - 54 Jamil B, Shahid F, Hasan Z, *et al.* Interferon gamma/IL10 ratio defines the disease severity in pulmonary and extra pulmonary tuberculosis. *Tuberculosis (Edinb)* 2007; **87**:279-287.
 - 55 Verbon A, Juffermans N, Van Deventer SJ, *et al.* Serum concentrations of cytokines in patients with active tuberculosis (TB) and after treatment. *Clin Exp Immunol* 1999; **115**:110-113.
 - 56 Bonecini-Almeida MG, Ho JL, Boechat N, *et al.* Down-modulation of lung immune responses by interleukin-10 and transforming growth factor beta (TGF-beta) and analysis of TGF-beta receptors I and II in active tuberculosis. *Infect Immun* 2004; **72**:2628-2634.
 - 57 Souza-Lemos C, de-Campos SN, Teva A, Porrozzini R, Grimaldi G Jr. *In situ* characterization of the granulomatous immune response with time in nonhealing lesional skin of *Leishmania braziliensis*-infected rhesus macaques (*Macaca mulatta*). *Vet Immunol Immunopathol* 2011; **142**:147-155.
 - 58 Wiesner C, Le-Cabec V, El Azzouzi K, Maridonneau-Parini I, Linder S. Podosomes in space: macrophage migration and matrix degradation in 2D and 3D settings. *Cell Adh Migr* 2014; **8**:179-191.
 - 59 Jevnikar Z, Mirkovic B, Fonovic UP, *et al.* Three-dimensional invasion of macrophages is mediated by cysteine cathepsins in protrusive podosomes. *Eur J Immunol* 2012; **42**:3429-3441.
 - 60 Van Goethem E, Guet R, Balor S, *et al.* Macrophage podosomes go 3D. *Eur J Cell Biol* 2011; **90**:224-236.
 - 61 Guet R, Van Goethem E, Cougoule C, *et al.* The process of macrophage migration promotes matrix metalloproteinase-independent invasion by tumor cells. *J Immunol* 2011; **187**:3806-3814.
 - 62 Elkington P, Shiomi T, Breen R, *et al.* MMP-1 drives immunopathology in human tuberculosis and transgenic mice. *J Clin Invest* 2011; **121**:1827-1833.
 - 63 Rottenberg ME, Carow B. SOCS3 and STAT3, major controllers of the outcome of infection with *Mycobacterium tuberculosis*. *Semin Immunol* 2014; **26**:518-532.
 - 64 O'Leary S, O'Sullivan MP, Keane J. IL-10 blocks phagosome maturation in *mycobacterium tuberculosis*-infected human macrophages. *Am J Respir Cell Mol Biol* 2011; **45**:172-180.
 - 65 Moore KW, de Waal Malefyt R, Coffman RL, O'Garra A. Interleukin-10 and the interleukin-10 receptor. *Annu Rev Immunol* 2001; **19**:683-765.
 - 66 Schreiber T, Ehlers S, Heitmann L, *et al.* Autocrine IL-10 induces hallmarks of alternative activation in macrophages and suppresses antituberculosis effector mechanisms without compromising T cell immunity. *J Immunol* 2009; **183**:1301-1312.
 - 67 Holscher C, Holscher A, Ruckerl D, *et al.* The IL-27 receptor chain WSX-1 differentially regulates antibacterial immunity and survival during experimental tuberculosis. *J Immunol* 2005; **174**:3534-3544.
 - 68 Carow B, Reuschl AK, Gavier-Widen D, *et al.* Critical and

- independent role for SOCS3 in either myeloid or T cells in resistance to *Mycobacterium tuberculosis*. *PLoS Pathog* 2013; **9**:e1003442.
- 69 Zizzo G, Guerrieri J, Dittman LM, Merri JT, Cohen PL. Circulating levels of soluble MER in lupus reflect M2c activation of monocytes/macrophages, autoantibody specificities and disease activity. *Arthritis Res Ther* 2013; **15**:R212.
- 70 Tang Y, Hua SC, Qin GX, Xu LJ, Jiang YF. Different subsets of macrophages in patients with new onset tuberculous pleural effusion. *PLoS One* 2014; **9**:e88343.
- 71 Cyktor JC, Carruthers B, Kominsky RA, *et al.* IL-10 inhibits mature fibrotic granuloma formation during *Mycobacterium tuberculosis* infection. *J Immunol* 2013; **190**:2778-2790.
- 72 Girgis NM, Gundra UM, Ward LN, *et al.* Ly6Chigh monocytes become alternatively activated macrophages in schistosome granulomas with help from CD4+ cells. *PLoS Pathog* 2014; **10**:e1004080.
- 73 Graham DK, Dawson TL, Mullaney DL, Snodgrass HR, Earp HS. Cloning and mRNA expression analysis of a novel human protooncogene, c-mer. *Cell Growth Differ* 1994; **5**:647-657.
- 74 Hayakawa F, Sugimoto K, Harada Y, *et al.* A novel STAT inhibitor, OPB-31121, has a significant antitumor effect on leukemia with STAT-addictive oncokinasases. *Blood Cancer J* 2013; **3**:e166.
- 75 Iwamaru A, Szymanski S, Iwado E, *et al.* A novel inhibitor of the STAT3 pathway induces apoptosis in malignant glioma cells both *in vitro* and *in vivo*. *Oncogene* 2007; **26**:2435-2444.
- 76 Tobin DM, Roca FJ, Oh SF, *et al.* Host genotype-specific therapies can optimize the inflammatory response to mycobacterial infections. *Cell* 2012; **148**:434-446.

(**Supplementary information** is linked to the online version of the paper on the *Cell Research* website.)



Bone degradation machinery of osteoclasts: An HIV-1 target that contributes to bone loss

Brigitte Raynaud-Messina^{a,b,c,1}, Lucie Bracq^{d,e,f,2}, Maeva Dupont^{a,b,c,g,2}, Shanti Souriant^{a,b,c,2}, Shariq M. Usmani^{h,i}, Amsha Proag^a, Karine Pingris^{a,b,c}, Vanessa Soldan^j, Christophe Thibault^{k,l}, Florence Capilla^m, Talal Al Saati^m, Isabelle Gennero^{n,o}, Pierre Jurdic^p, Paul Jolicoeur^{q,r,s}, Jean-Luc Davignon^{m,n}, Thorsten R. Mempel^{h,i}, Serge Benichou^{d,e,f}, Isabelle Maridonneau-Parini^{a,b,c,1,3}, and Christel Vérolet^{a,b,c,1,3}

^aInstitut de Pharmacologie et de Biologie Structurale, Université de Toulouse, CNRS, Université Paul Sabatier, 31400 Toulouse Cedex 4, France; ^bInternational Associated Laboratory, CNRS "Immuno-Metabolism-Macrophages-Tuberculosis/HIV" (1167), 31000 Toulouse, France; ^cInternational Associated Laboratory, CNRS "Immuno-Metabolism-Macrophages-Tuberculosis/HIV" (1167), 1425 Buenos Aires, Argentina; ^dINSERM U1016, Institut Cochin, 75014 Paris, France; ^eCNRS UMR8104, Université Paris Descartes, 75006 Paris, France; ^fInstitut Pasteur Shanghai, Chinese Academy of Sciences, 200000 Shanghai, China; ^gInstitute of Experimental Medicine-Consejo Nacional de Investigaciones Científicas y Técnicas de Argentina, National Academy of Medicine, 1425 Buenos Aires, Argentina; ^hCenter for Immunology and Inflammatory Diseases, Massachusetts General Hospital, Charlestown, MA 02129; ⁱHarvard Medical School, Boston, MA 02115; ^jMultiscale Electron Imaging Platform, 31062 Toulouse, France; ^kLaboratory for Analysis and Architecture of Systems, CNRS, 31400 Toulouse, France; ^lInstitut National des Sciences Appliquées de Toulouse, Université de Toulouse, 31400 Toulouse, France; ^mINSERM, Université Paul Sabatier, École Nationale Vétérinaire de Toulouse, Centre Régional d'Exploration Fonctionnelle et de Ressources Expérimentales, Service d'Histopathologie, 31000 Toulouse Cedex 3, France; ⁿCentre de Physiopathologie de Toulouse-Purpan, INSERM-CNRS UMR 1043, Université Paul Sabatier, 31062 Toulouse, France; ^oInstitut Fédératif de Biologie, Centre Hospitalier Universitaire Toulouse, 31059 Toulouse, France; ^pInstitut de Génétique Fonctionnelle de Lyon, CNRS UMR3444, Université de Lyon, École Normale Supérieure de Lyon, 69007 Lyon, France; ^qDivision of Experimental Medicine, McGill University, Montreal, QC H3G 1A4, Canada; ^rDepartment of Microbiology and Immunology, University of Montreal, Montreal, QC H3T 1J4, Canada; and ^sLaboratory of Molecular Biology, Clinical Research Institute of Montreal, Montreal, QC H2W 1R7, Canada

Edited by Stephen P. Goff, Columbia University Medical Center, New York, NY, and approved January 19, 2018 (received for review July 28, 2017)

Bone deficits are frequent in HIV-1-infected patients. We report here that osteoclasts, the cells specialized in bone resorption, are infected by HIV-1 in vivo in humanized mice and ex vivo in human joint biopsies. In vitro, infection of human osteoclasts occurs at different stages of osteoclastogenesis via cell-free viruses and, more efficiently, by transfer from infected T cells. HIV-1 infection markedly enhances adhesion and osteolytic activity of human osteoclasts by modifying the structure and function of the sealing zone, the osteoclast-specific bone degradation machinery. Indeed, the sealing zone is broader due to F-actin enrichment of its basal units (i.e., the podosomes). The viral protein Nef is involved in all HIV-1-induced effects partly through the activation of Src, a regulator of podosomes and of their assembly as a sealing zone. Supporting these results, Nef-transgenic mice exhibit an increased osteoclast density and bone defects, and osteoclasts derived from these animals display high osteolytic activity. Altogether, our study evidences osteoclasts as host cells for HIV-1 and their pathological contribution to bone disorders induced by this virus, in part via Nef.

osteoclast | HIV-1 infection | bone loss | Nef | podosome

Reduced bone mineral density is a frequent complication of HIV-1-infected patients and often progresses to osteoporosis and high prevalence of fractures. A sixfold increased risk of low bone mineral density is observed in HIV-1⁺ individuals compared with the general population (1). The use of highly active antiretroviral therapy (HAART) has significantly improved the lifespan of patients, revealing these long-term effects of the infection and the persistence of latent proviruses in reservoir cells (2). Multiple factors can contribute to bone loss in infected patients. HAART is one of these factors, especially during the first years of therapy. In addition, there is evidence of bone deficit in nontreated patients, showing that the virus alone alters bone homeostasis (3–6).

Bones undergo continual remodeling, which mainly relies on the sequential actions of bone-resorbing osteoclasts (OC) and bone-forming osteoblasts, under the control of osteocytes (7, 8). In the case of aging or HIV-1 infection, this balance can be disrupted in favor of bone loss. HIV-1-induced bone disorders are associated with an increase of blood biomarkers for bone resorption and minor changes in bone formation-specific markers, suggesting a major contribution of OC in this process (6, 9). OC are multinucleated cells derived from the monocytic lineage,

which have the unique ability to resorb bone matrix. They terminally differentiate by fusion from mononucleated precursors, including blood-circulating monocytes and bone-resident precursors (10). This process is regulated by macrophage colony-stimulating factor (M-CSF) and the key osteoclastogenic cytokine, receptor activator of NF- κ B ligand (RANKL), mainly secreted by osteocytes but also by osteoblasts and activated B and T cells (10, 11). Terminally differentiated OC express high levels of the α v β 3 integrin adhesion receptor and enzymes involved in resorption including cathepsin K, matrix metalloproteinase 9 (MMP9), and tartrate-resistant acidic phosphatase (TRAP). Bone attachment and resorption are mediated

Significance

Bone deficits are frequent complications observed in HIV-1-infected patients. Our study demonstrates that HIV-1 infects osteoclasts, the cells specialized in bone degradation, using different models including HIV-1-infected humanized mice. We decipher the cellular mechanisms by which HIV-1 contributes to enhanced bone degradation in human osteoclasts, showing that the virus modifies the structure and function of the sealing zone, the bone resorption machinery of osteoclasts. We identify the viral protein Nef as the key factor responsible for such effects. As a proof-of-concept, we correlate bone deficit in transgenic Nef-expressing mice with enhanced osteoclast activity. Therefore, our findings provide formal evidence that osteoclasts constitute HIV-1 host target cells, contributing to bone deficits in vivo.

Author contributions: B.R.-M., T.A.S., P. Jurdic, I.M.-P., and C.V. designed research; B.R.-M., L.B., M.D., S.S., S.M.U., A.P., K.P., V.S., C.T., F.C., T.A.S., I.G., J.-L.D., and C.V. performed research; P. Jolicoeur, T.R.M., and S.B. contributed new reagents/analytic tools; B.R.-M., L.B., M.D., S.S., T.A.S., J.-L.D., I.M.-P., and C.V. analyzed data; and B.R.-M., I.M.-P., and C.V. wrote the paper.

The authors declare no conflict of interest.

This article is a PNAS Direct Submission.

Published under the PNAS license.

See Commentary on page 2551.

¹To whom correspondence may be addressed. Email: raynaud@ipbs.fr, maridono@ipbs.fr, or verollet@ipbs.fr.

²L.B., M.D., and S.S. contributed equally to this work.

³I.M.-P. and C.V. contributed equally to this work.

This article contains supporting information online at www.pnas.org/lookup/suppl/doi:10.1073/pnas.1713370115/-DCSupplemental.

Published online February 20, 2018.

by an OC-specific structure called the sealing zone (SZ). It is composed of a dense array of interconnected F-actin structures, the podosomes. The SZ anchors the cells to the bone surface and creates a confined resorption environment where protons and osteolytic enzymes are secreted (11–14). Alteration in SZ formation and dynamics are linked to defective bone resorption, and ultimately to bone disorders, as demonstrated by knocking out regulators or constituents of the SZ (14–17).

To explain the increase in osteolytic activity associated to HIV-1-induced bone loss, only a few mechanisms have been proposed: disruption of the immune system (6, 18), increased production of proinflammatory cytokines (19), and direct infection of OC (20). Regarding the immune system, studies from the HIV-1-transgenic rat model revealed that bone damage results, in part, from an altered production of regulatory factors of osteoclastogenesis secreted by B cells (18). This modified cytokine profile correlates with some bone mineral defects in non-treated HIV-1-infected patients (6). Along with CD4⁺ T lymphocytes, macrophages serve as primary target cells for HIV-1 *in vivo* (21–23). Because OC share a common myeloid origin with macrophages, the last proposed hypothesis is that OC are targets for HIV-1, and their infection would then contribute to bone loss. Indeed, it has recently been shown that HIV-1 may replicate *in vitro* in human monocyte-derived OC and enhance their bone resorption activity (20). However, the relevance of this observation has yet to be provided *in vivo*, along with the corresponding cellular and viral mechanisms involved in the bone resorption process.

Here, we report the occurrence of infected OC in bones of HIV-1-infected humanized mice and in human synovial explants exposed to HIV-1. We further demonstrate that the exacerbated osteolytic activity of infected OC results from modified structure and function of the SZ, correlates with Src activation, and is dependent on the viral protein Nef.

Results

Infected OC Are Found in the Bones of HIV-1-Infected Humanized Mice and in Human Synovial Explants Exposed to HIV-1. We first investigated whether OC are infected *in vivo*. Because bone marrow/liver/thymus (BLT) humanized mice infected with HIV-1 reproduce most hallmarks of infection in humans (22, 24, 25), we used these mice infected for 14–21 d (2×10^4 – 8×10^4 RNA copies/mL in blood, $n = 4$) to examine the growth plate of femurs and tibias, the OC-enriched zone. For each bone section (head of femur or tibia from four mice), we quantified 85 ± 22 cells that exhibit OC characteristics (multiple nuclei, TRAP activity, and localization at the bone surface). Importantly, for each infected animal, we identified by immunohistochemistry (IHC) one or two OC positive for the viral protein p24, which is used as an indicator of productive viral infection (Fig. 1A and Fig. S1). Negative controls were included for each sample by omitting the primary antibody.

We then assessed whether OC can be infected in human tissue using synovial membrane explants, which contain fibroblasts, macrophages, lymphocytes, dendritic cells, and OC, in an abundant extracellular matrix (26). Fresh human synovial tissues were incubated *ex vivo* with the HIV-1 macrophage R5-tropic ADA strain and maintained in culture with osteoclastogenic cytokines to keep resident OC and OC precursors alive throughout the experiment. Fifteen days postinfection, OC were characterized by multiple nuclei, TRAP-, and cathepsin K-positivity by IHC. Remarkably, we observed that about 10% of these cells were positive for the viral p24 ($n = 5$ synovial explants examined) (Fig. 1B).

Altogether, these data show that infection of OC occurs both *in vivo* in humanized mice and *ex vivo* in human tissues.

Human OC Are Permissive to HIV-1 Infection by Cell-Free Viruses at Different Stages of Differentiation. To examine the stage of differentiation at which the cells become capable to be infected, we

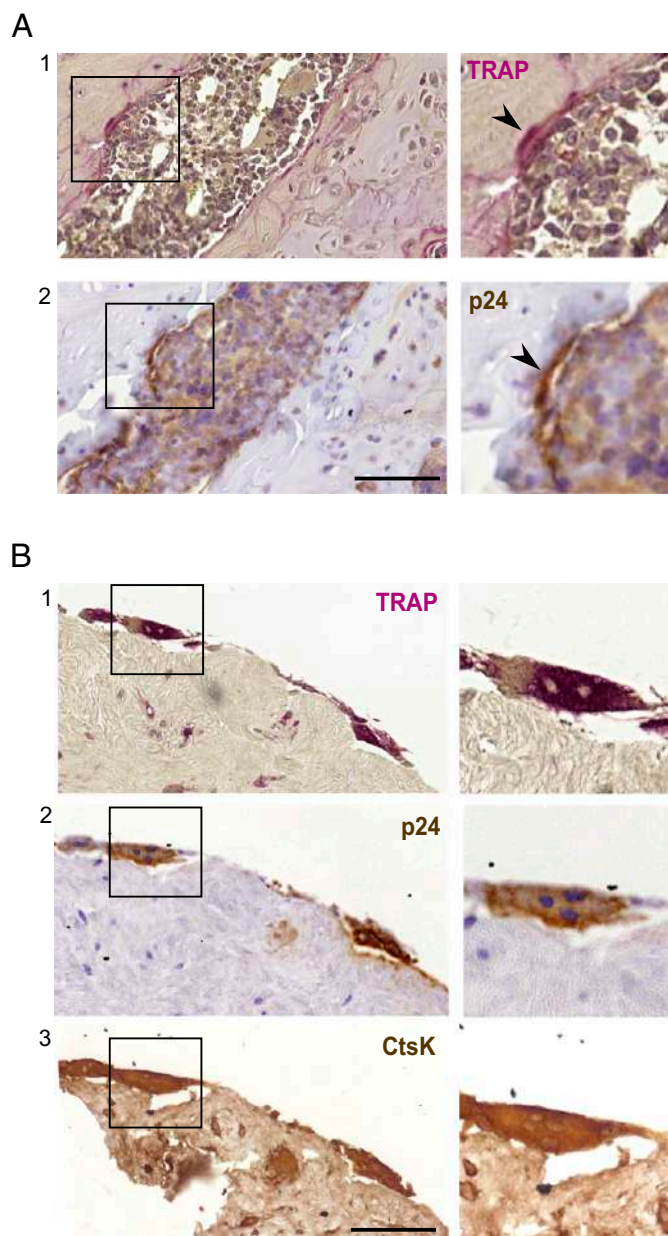


Fig. 1. Tissue OC are infected with HIV-1 *in vivo* and *ex vivo*. (A) HIV-1 infects OC *in vivo* in HIV-1-infected BLT-humanized mice. Two serial sections (3- μ m thick, 1 and 2) of the head of a tibia of HIV-1-BLT mice were stained for TRAP activity (in purple, 1) and with a monoclonal antibody directed toward human viral protein p24 (in brown, 2). Representative sections ($n = 4$ mice, two sections per mouse of tibia and femur heads). Arrowheads show an infected OC. (Scale bar, 50 μ m.) Enlarged frames, 2 \times zoom. (B) Human OC are infected with HIV-1 in synovial explants. Pieces of a noninflammatory human synovial tissue were cultured with M-CSF and RANKL and infected with HIV-1 (ADA strain). Two weeks postinfection, histological analyses [TRAP activity in purple (1), p24 (2) and cathepsin K (CtsK) (3) IHC in brown, nuclei in blue] were performed on three serial sections (3- μ m thick, 1–3). Representative histological sections ($n = 3$ synovial tissues, four pieces per tissue). (Scale bar, 100 μ m.) Enlarged frames, 2.3 \times zoom.

turned to human OC derived from primary monocytes differentiated *in vitro* in the presence of M-CSF and RANKL. The OC differentiation process was assessed by measuring OC protein level at different stages. While we observed a rapid increase of TRAP and $\beta 3$ integrin as soon as day 1, we noticed the acquisition of cathepsin K (a late-stage differentiation marker) at day 6; the expression level for all these proteins increased until day

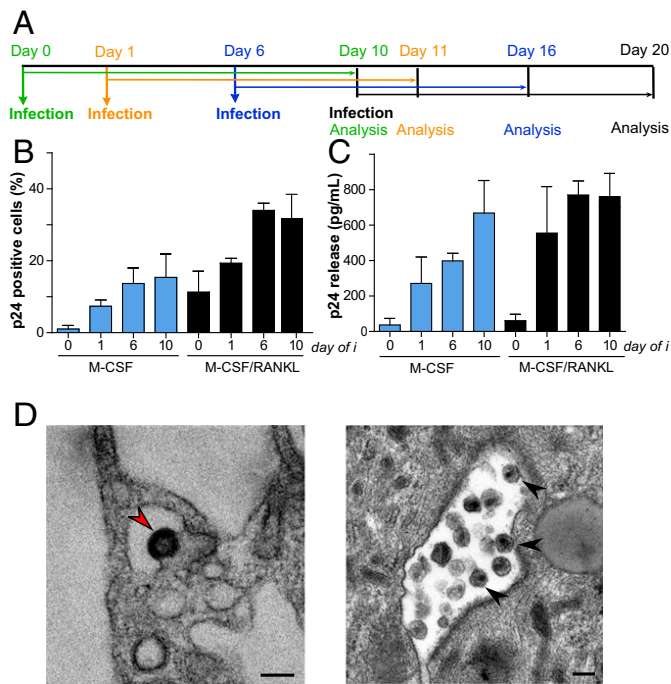


Fig. 2. HIV-1 infects human OC and their precursors in vitro. (A–C) OC are infected by cell-free viruses at different stages of differentiation. (A) Experimental design of infection (ADA strain). (B and C) Kinetics of the percentage of p24⁺ cells (B, determined by IF) and of p24 release in the supernatants (C, determined by ELISA) in cells maintained in M-CSF plus RANKL (OC, black bars) or M-CSF alone (MDM, blue bars) from the same donors are shown. Results are expressed as mean \pm SEM ($n = 3$ donors and 5 donors for day 10). Day of i, day of infection. (D) Transmission electron microscopy images of infected OC. Mature OC were infected with HIV-1 and examined 10 d postinfection. Images of a budding virus (Left, red arrowhead) and viruses contained in a cytoplasmic membrane compartment (Right, black arrowheads show mature viruses). (Scale bar, 100 nm.)

10, when cells presented characteristics of mature OC, including high fusion index, high TRAP and MMP9 activities, and bone degradation activity (Fig. S2A–E). Of note, monocyte-derived macrophages (MDM) from the same donors differentiated with M-CSF (at day 10) only exhibited undetectable or low levels of OC markers, low fusion index, and lacked osteolytic activity (Fig. S2B–E). Cells were infected in vitro with the HIV-1 R5 ADA strain at day 0, 1, 6, or 10 of differentiation (Fig. 2A). The extent of HIV-1 infection and replication was evaluated at day 10 postinfection by immunofluorescence (IF) analysis of p24 and quantified by measuring the concentration of p24 released in the supernatant. While monocytes (day 0) were poorly able to sustain infection, cells became increasingly permissive to infection along the differentiation process (Fig. 2B and C, black bars); this correlated with the increased expression of the CCR5 entry coreceptor from day 1 (Fig. S2F). Moreover, we observed that virus production was inhibited by pretreatment of OC with the CCR5 antagonist Maraviroc, the reverse-transcriptase inhibitor AZT, the integrase inhibitor Raltegravir, or the protease inhibitor Ritonavir (Fig. S2G), indicating that the p24 signal corresponds to productively infected cells. We noticed that MDM and OC equally sustained infection (Fig. 2B and C) ($\geq 95\%$ donors supported infection, $n = 29$), which is consistent with similar levels of CD4 and CCR5 receptors expressed during differentiation (Fig. S2F) and at day 10 (20). Moreover, the viral particles produced by infected OC or MDM had comparable infectivity, as assessed using the TZM-bl reporter cell line ($27 \pm 5\%$ of p24⁺ TZM-bl for OC-produced particles vs. $26 \pm 7\%$ for MDM, $n = 5$), indicating that both cell types released infectious

virions. Importantly, HIV-1 did not affect OC viability, as cell density was not altered even at day 20 postinfection ($1,580 \pm 276$ nuclei/mm² for noninfected OC vs. $1,560 \pm 352$ for infected OC, $n = 6$ donors, $\geq 3,000$ cells per condition). Finally, we observed virus budding in OC and both mature and immature virus particles accumulating in membrane-delineated intracellular compartments by electron microscopy (Fig. 2D).

Collectively, these results show that HIV-1 infects and replicates in OC and their precursors, without significant cytotoxic effect.

Human OC Are Preferentially Infected by Transmission from Infected T Cells. HIV-1 spreads by infecting target cells either as cell-free particles or more efficiently via cell-to-cell transmission, both in vitro and in vivo (27–30). We thus examined whether mature OC could be infected by contact with infected CD4⁺ T lymphocytes, first using Jurkat T cells infected with the HIV-1 R5-tropic NLAD8-VSVG strain ($>50\%$ of infected T cells, $n = 8$). Briefly, after 6 h of contact with OC, Jurkat cells were washed out (more than 99% of the T cells were eliminated) (Fig. S3A) and OC were harvested either immediately (day 0) or 5 d later (day 5) and stained for intracellular viral p24 by IF (Fig. 3A and B). We observed that 6-h contact (day 0) was sufficient for T cell-to-OC virus transfer with about 15% of p24⁺ OC, while no detectable infection was observed at this time point when OC were cultured with cell-free virions produced by T cells. The difference was maintained at day 5. At this time point, the high rate of infected OC could result from the initial infection by T cell-to-OC transmission and from enhanced OC cell fusion. Noticeably, virus transfer via infected T cells led to a productive infection of OC as shown by the amount of p24 detected in the supernatant at day 5 (Fig. 3C), which is higher than in the case of infection with cell-free virions. Finally, we confirmed the efficient virus transfer from infected T cells leading to productive infection of

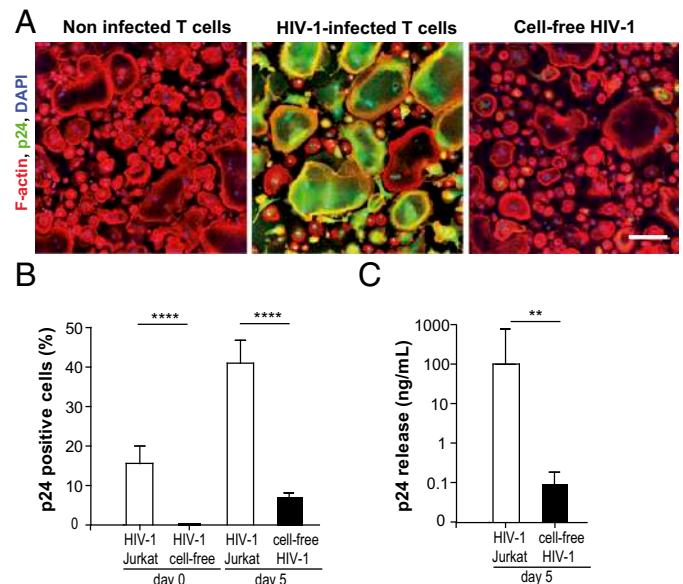


Fig. 3. HIV-1 is transmitted from infected T lymphocytes to OC. (A–C) OC have been in contact for 6 h with noninfected Jurkat T lymphocytes (Left), with HIV-1-infected T lymphocytes (Center), or with cell-free viral particles produced by T cells during 6 h (Right); they were washed, then harvested immediately (day 0) or 5 d later (day 5). (A) Representative mosaic of 3×3 confocal fields of original magnification 20 \times , after staining for p24 (green), F-actin (phalloidin-Texas red, red), and nuclei (DAPI, blue) at day 5. (Scale bar, 50 μ m.) (B and C) Quantifications (mean \pm SD, $n = 8$ donors) of the percentage of p24⁺ cells evaluated by IF (B) immediately (day 0) or 5 d (day 5) postinfection and of p24 release in the supernatants determined by ELISA after 5 d (day 5) (C). ** $P \leq 0.01$; **** $P \leq 0.0001$.

OC by using autologous infected T lymphocytes as virus donor cells (Fig. S3 B and C).

These results show that OC are not only infected by cell-to-cell transfer via infected T cells, but it is also more efficient than infection by cell-free virions.

HIV-1 Infection Enhances OC Precursor Migration and OC Bone Resorption Activity. In HIV-1 transgenic rats, severe bone loss has been correlated to an increase in the number and size of OC (18). This increase could reflect an enhanced recruitment of OC precursors or a stimulated OC differentiation. We tested both hypotheses. It is known that migration of OC precursors from blood to bones requires proteases in vivo (31), and that defects in the 3D protease-dependent mesenchymal migration of these cells in vitro correlates with lower recruitment of OC to bones (16). For these reasons, we assessed whether HIV-1 infection alters OC precursor mesenchymal migration (32, 33). Human OC precursors were infected at day 1 of differentiation, seeded at day 2 on Matrigel, and migration was measured 48 h later (Fig. 4). Of note, OC precursors inside Matrigel exhibited the characteristic elongated shape of the mesenchymal migration (32). The percentage of migrating cells and the distance covered by the cells were both significantly increased upon HIV-1 infection.

Next, to test whether HIV-1 infection affects OC differentiation, we examined the consequences of infection on the extent of OC fusion and bone resorption activity. HIV-1 infection significantly enhanced cell fusion, as measured by the fusion index and the area covered by infected versus noninfected OC (Fig. 5A), the percentage of TRAP⁺ multinucleated cells, and the number of nuclei per multinucleated cell (Fig. S4 A and B). When cells were treated with Maraviroc before infection, the fusion index was reduced to a similar level to controls (Fig. S4C). Moreover, to explore the effects of OC infection on bone resorption activity, we characterized the morphology of the resorption lacunae. The total bone resorption area increased upon HIV-1 infection (Fig. 5 B–D) and resorption pits displayed profound morphological modifications (Fig. 5 B–F). Infected OC generated resorption pits that appeared deeper ($28 \pm 1.2 \mu\text{m}$ vs. $17 \pm 0.7 \mu\text{m}$ for controls, $***P < 0.0001$) (Fig. 5C) and less elongated (Fig. 5E) than those of noninfected OC, which form resorption trails reminiscent of “inchworm-like migration” (34). These modifications correlated with a significant up-regulation of the bone

volume resorbed per pit in the HIV-1 infection context (Fig. 5F). Furthermore, we also found a significant increase in the concentration of the C-terminal telopeptide of type 1 collagen (CTX) released in the supernatants and used as an additional marker of bone resorption (Fig. 5G).

Osteolytic activity is mediated by acidic dissolution of the minerals and enzymatic digestion of the organic components (35). HIV-1 infection enhanced these two activities, as evidenced by the increase in the capacity of OC to dissolve minerals (Fig. 5H) and release TRAP (Fig. 5I). No variation in protein expression and activity was noticed regarding secreted cathepsin K and MMP9 (Fig. 5J and K).

Finally, we examined OC attachment/detachment, a critical factor for bone degradation (12), given that OC resorption partly proceeds through a succession of migratory phases alternating with bone resorption stationary phases (12, 36). When infected, OC were more resistant to detachment induced by Accutase treatment than noninfected counterparts (Fig. 5L). This increased adhesion likely slows down OC motility on bone, which should contribute to the modified morphology of resorption lacunae and to the higher bone degradation activity.

All in all, these results indicate that HIV-1 infection enhances the 3D migration of OC precursors, which may favor recruitment of OC to bones, as well as the adhesion and bone resorption activity of mature OC.

HIV-1 Infection Alters the Architecture of the SZ and Activates Src Kinase. Because the SZ has been related to adhesion and bone degradation capacities of OC (11, 37), we characterized the architecture of this structure in infected OC. We observed that in OC seeded on bones, the number of cells harboring SZ was increased (Fig. 6 A and B). This effect was not duplicated by infection with *Mycobacterium tuberculosis*, *Francisella novicida*, or *Salmonella typhimurium* (infection rates $\geq 50\%$ for each bacteria, percentage of cells harboring SZ: 18 ± 9 for *M. tuberculosis*, 22 ± 6 for *F. novicida*, 25 ± 4 for *S. typhimurium* vs. 25 ± 10 in noninfected OC, mean \pm SD, $n = 4$), suggesting that this parameter was not generally influenced by OC infection. In addition, the size of the SZ was increased (Fig. 6 A and C), delineating an area corresponding to $25 \pm 1\%$ of the cell surface of infected OC vs. $18 \pm 2\%$ in control cells (Fig. 6D). We also noticed that the fluorescence intensity of F-actin was higher in the SZ of infected cells (Fig. 6 A and E) and the F-actin core of podosomes, the basal element of the SZ, was larger (Fig. 6 F and G). The tyrosine kinase Src plays a key role in bone homeostasis by controlling the formation and stability of the SZ and the rate of actin turnover within OC podosomes (14, 16, 38). Consequently, OC from Src^{-/-} mice do not assemble functional SZ and the mice exhibit a strong osteopetrotic phenotype (15). Interestingly, we showed that in the context of HIV-1-infected OC, the activity of Src kinase family was enhanced as measured by phosphorylation of the regulatory tyrosine (Fig. 6H).

These results show that the increase in bone adhesion and resorption observed in infected OC is associated with larger and more numerous SZ as well as higher Src kinase activity.

The Viral Factor Nef Is Involved in HIV-1-Induced Effects on OC Both in Vitro and in Vivo. To better understand the viral mechanisms involved in HIV-1-induced effects in OC, we focused on the viral accessory factor Nef because it is known, among other functions, to modulate F-actin organization and to stimulate both the kinase activity of Src (39–44) and cell fusion (45). To this end, we used wt HIV-1 and nef-deleted HIV-1 (δnef HIV-1) ADA strains that present the same level of infectivity in macrophages (33, 45–47) and in OC (Fig. S5A). Importantly, the viral particles produced by OC infected with the wt or mutant strains showed the same level of infectivity ($26 \pm 7\%$ of p24⁺ TZM-bl cells for the wt strain vs. $22 \pm 5\%$ for δnef HIV-1, $n = 4$). As shown in Fig. 7A,

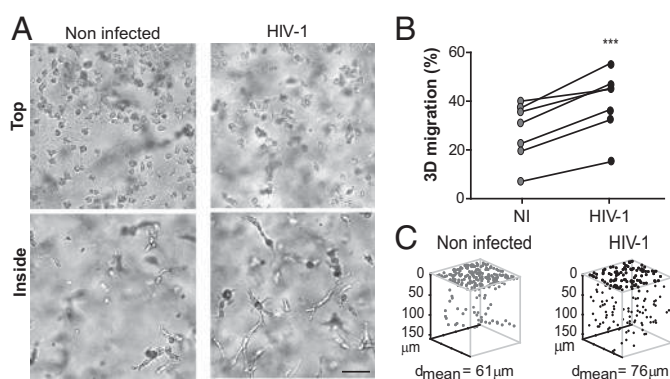


Fig. 4. HIV-1 enhances 3D migration of OC precursors in Matrigel. OC precursors were infected or not at day 1, seeded at day 2 on thick layers of Matrigel polymerized in transwell chambers, and migration was measured 48 h later. (A) Representative brightfield images of live cells either at the surface (top) or within the matrix (inside), taken after 48 h of migration using an inverted video microscope. (Scale bar, 50 μm .) (B) The percentage of migrating cells was measured (mean \pm SEM, $n = 7$ donors) (NI, noninfected). $***P \leq 0.001$. (C) Three-dimensional positions of OC precursors in the matrix and mean distance of migration (d_{mean}) from a representative experiment of seven are shown using the TopCat software.

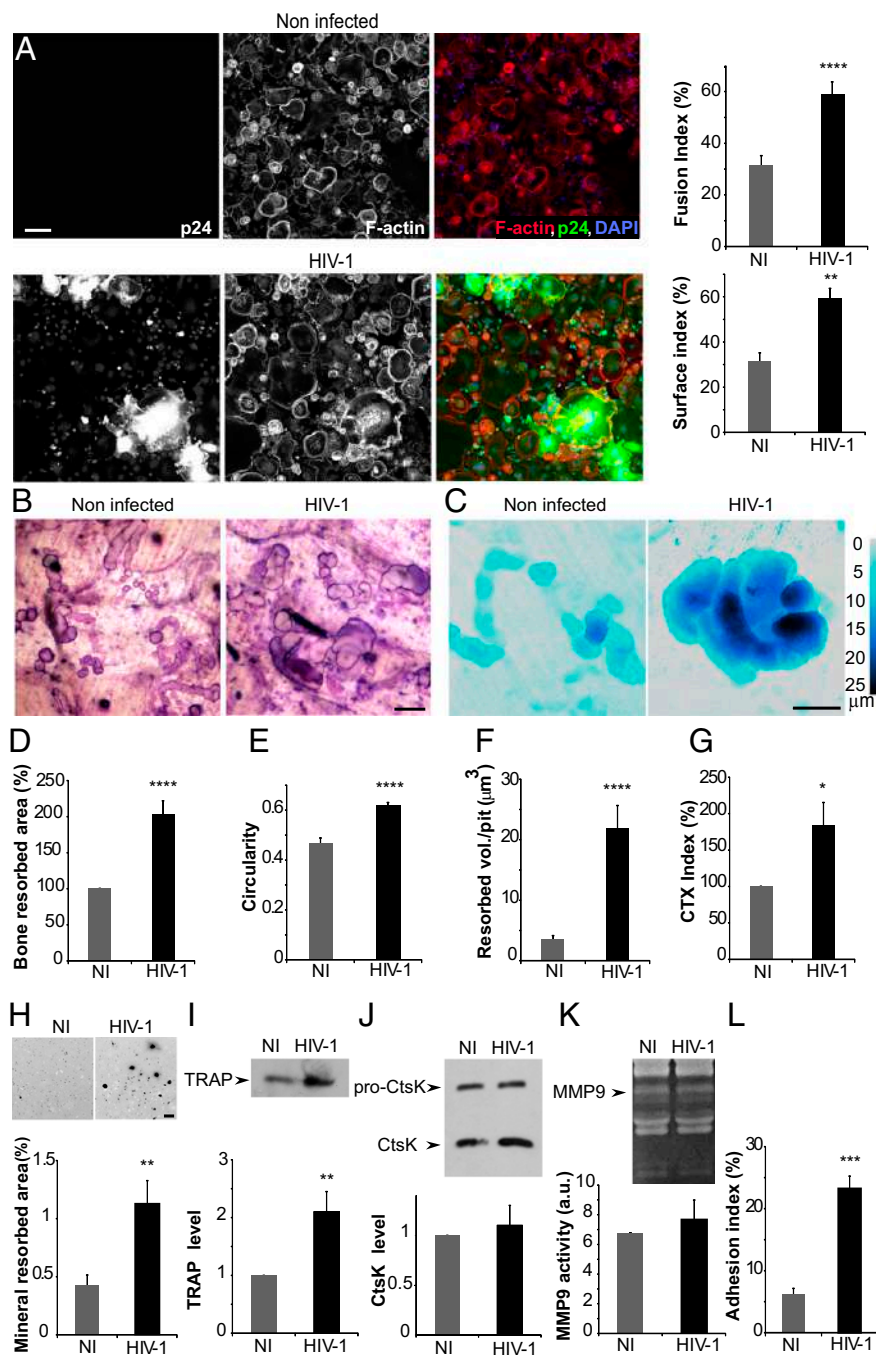


Fig. 5. HIV-1 enhances OC fusion, osteolytic activity, and adhesion of OC. (A) HIV-1 triggers OC fusion. Ten days postinfection, cells were stained for p24 (green), F-actin (red), and nuclei (blue). Images from a mosaic of 4 × 4 confocal fields of original magnification 20×. (Scale bar, 150 μm.) The cell fusion index (nuclei number in multinucleated cells/total nuclei number) and the surface percentage covered by multinucleated cells (surface index) were measured for >3,000 cells in each condition, *n* = 6 donors. Results are expressed as mean ± SEM. (B–G) HIV-1 infection increases the bone resorption activity of OC. Day 10-noninfected and HIV-1-infected OC were seeded on cortical bone slides for 48 h. Then, OC were removed, the supernatants collected, and the bone slices stained with Toluidine blue to visualize resorption pits in purple. Data were obtained from six donors. (B) Representative brightfield images of bone-resorption pits (purple). (Scale bar, 20 μm.) (C) Representative confocal images of pits. Color codes for the depth of resorption pits (color scale bar). (Scale bar, 20 μm.) Quantification of the percentage of degradation area (D) and circularity (E) from brightfield images and resorbed volume (F) from confocal images are shown. In D, the degradation area of noninfected OC, normalized to 100%, corresponded to 9% of the total area. (G) The concentration of CTX in the supernatant was measured by ELISA and normalized to 100% for noninfected cells (mean CTX concentration = 1,790 pg/mL), *n* = 6 donors. (H–K) Effects of infection on mineral dissolution and extracellular osteolytic enzymes. (H) Day 10-noninfected and HIV-1-infected OC were seeded on crystalline inorganic phosphate-coated multiwells. The cells were removed and the wells stained to reveal demineralized area (black). (Scale bar, 50 μm.) Graph shows the area covered by mineral dissolution pits from 10 fields per condition and per donor, *n* = 3 donors. (I–K) The supernatants of noninfected and HIV-1-infected OC seeded on glass were collected at day 10. TRAP and CtsK expression levels (Western blot, I and J) and MMP9 activity (zymography analysis, K) were quantified. Protein loading has been controlled by Coomassie blue staining, *n* = 4 donors. (L) HIV-1 infection increases OC adhesive properties. Noninfected and HIV-1-infected OC were removed at day 10 with Accutase for 10 min and the percentage of remaining adherent cells quantified by counting nuclei (adhesion index). Graph represents average of five fields per condition from *n* = 3 donors (NI, noninfected). **P* ≤ 0.05; ***P* ≤ 0.01; ****P* ≤ 0.001; *****P* ≤ 0.0001.

the 3D mesenchymal migration of OC precursors infected with *Δnef*HIV-1 was similar to noninfected cells. In mature OC, Src kinase phosphorylation, bone resorption activity, percentage of cells with SZ, fusion index, and SZ area were reduced in *Δnef*HIV-1-infected OC in comparison with cells infected with the *wt* virus (Fig. 7 B–F).

Next, we considered performing ectopic expression of Nef-GFP in OC, but we encountered a technical limitation; only 5% of Nef-expressing cells were obtained, precluding a rigorous quantification of SZ size and bone resorption activity. Nonetheless, when the transfected cells were plated on glass, we observed a fraction of Nef-GFP localized at the SZ on bones and that podosomes occupied a larger area than those of control cells (Fig. 7 G and H), thus mimicking the results obtained with OC infected with the *wt* virus (Fig. 6 F and G).

Next, we took advantage of transgenic (Tg) mice expressing Nef under the regulatory sequence of the human CD4C gene to overcome the transfection difficulty of human OC. The CD4C regulatory element drives Nef expression in CD4⁺ T cells, macrophages, and dendritic cells (48, 49), and also in OC (Fig. S5B). In fact, in the absence of any available Nef antibody for IHC, we used CD4C/HIV-1^{GFP} Tg mice. We verified that the GFP was expressed in all OC, indicating that CD4C drives the expression of ectopic genes in OC (Fig. S5B). To characterize the effects of Nef expression in OC, OC precursors were isolated from bone marrow of Nef-Tg and non-Tg mice and differentiated ex vivo. While the fusion of OC from Nef-Tg mice was not modified compared with OC derived from control mice (Fig. 8A), the bone resorption (Fig. 8B) and the width of F-actin staining in the SZ were enhanced (Fig. 8 C and D), indicating that Nef expression is sufficient to increase the osteolytic activity of OC.

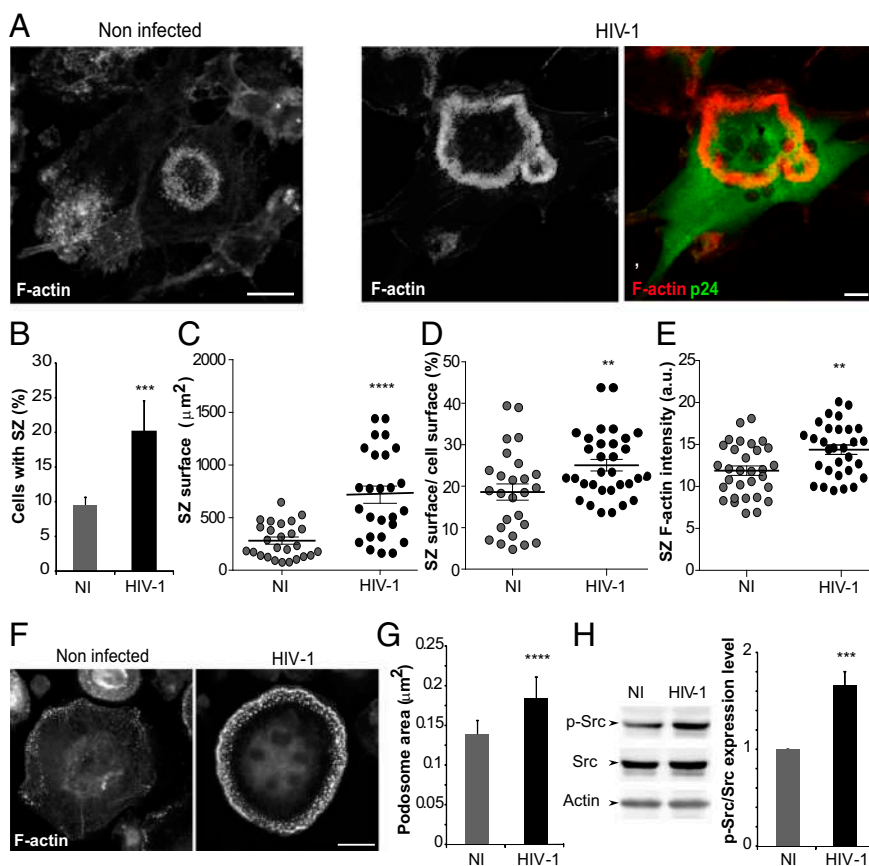


Fig. 6. HIV-1 modifies the organization of the SZ and induces Src-kinase activation in human OC. (A–E) HIV-1 infection increases the size and F-actin intensity of the SZ. (A) Confocal images of noninfected or HIV-1–infected OC seeded on bone slides. Cells were stained for p24 (green) and F-actin (red). (Scale bar, 10 μm.) (B) Quantification of the percentage of cells forming SZ ($n = 4$ donors, 300 cells per donor). (C–E) Vertical scatter plots showing for each SZ, the surface (C), the percentage of the cell surface occupied by SZ (D), and the F-actin intensity (E) ($n = 3$ donors, >25 SZ). Graphs show individual SZ values and the mean \pm SEM. (F and G) HIV-1 infection increases the size of individual podosomes. OC seeded on glass were infected with HIV-1 and stained for F-actin. (F) IF images. (Scale bar, 10 μm.) (G) Automated quantification of the F-actin fluorescence area of individual podosomes. Mean \pm SEM, $n = 3$ donors (>2,000 podosomes, 10 cells per donor). (H) HIV-1 infection induces Src-kinase activation. Whole-cell lysates were subjected to Western blotting using antibodies against the phospho-Tyr416 of Src kinases, Src and Actin. A representative blot and quantification of the phospho-Tyr416 kinase ratio over total Src are shown. Results are expressed as mean \pm SEM, $n = 6$ donors (NI, noninfected). ** $P \leq 0.01$; *** $P \leq 0.001$, **** $P \leq 0.0001$.

Finally, we addressed the role of Nef on bone remodeling in vivo. Nef-Tg mice exhibited bone defects as evidenced by abnormal bone fragility during dissection and by an overall decrease in bone density (Fig. S5C). In tibia growth plates of 7-wk-old female mice, we observed a decrease of the bone area (trabecular surface) in Nef-Tg mice compared with non-Tg mice (Fig. 8E and F, gray), and a disorganized hypertrophic chondrocyte zone (Fig. 8E, delineated by the red line), which appeared thinner and irregular. Moreover, a marked increase in TRAP⁺ signal was noticed (Fig. 8E and F, purple), indicating that OC were larger and more numerous in Nef-Tg mice compared with control littermates.

Altogether, these results support that the viral protein Nef is sufficient to increase the osteolytic activity of OC and, thereby, potentially contribute to bone loss in vivo.

Discussion

Bone defects resulting from HIV-1 infection have long been described, but the causes remain poorly investigated (1). We report that HIV-1 infects OC in vivo, ex vivo, and in vitro. In infected OC, the structure and function of the SZ are modified, affecting bone attachment and resorption. The viral protein Nef is instrumental in these processes. Hence, OC are cell targets for HIV-1, which is, to our knowledge, the only pathogen able to manipulate the SZ.

Using HIV-1–infected BLT-humanized mice, we obtained evidence of the presence of infected OC in bones. Infected OC appear as a rare event, either due to the moderated viremia (we worked shortly after infection) and low sensitivity of the IHC detection, or to the fact that infected OC are poorly detected in tissues similarly to infected macrophages (22, 50–54). OC can also be infected ex vivo in fresh human synovial explants. Importantly, OC infection in vivo and ex vivo was detected by IHC of the viral p24, which is suggestive of viral replication. In vitro, electron microscopy images of infected OC revealed that the virus particles bud and accumulate in intracellular compartments, suggestive of the virus-containing compartments described in macrophages (55–57). The virus production by OC was quantitatively similar to that of macrophages, a well-known HIV-1 host cell (21, 22, 58). Infection of OC occurred at different time points along the differentiation process, starting at day 1 in OC precursors and correlating with CCR5 expression. This suggests that circulating OC precursors, which encounter the virus in blood, could become infected and migrate to bones, where they terminally differentiate (59, 60) (Fig. 9). Whether mature OC can be infected directly in bones is difficult to explore. Up to now, the presence of HIV-1 in bones has not been documented. As recently shown for macrophages (61), direct contact of OC with infected Jurkat or primary CD4⁺ T lymphocytes leads to virus transfer and productive infection of OC,

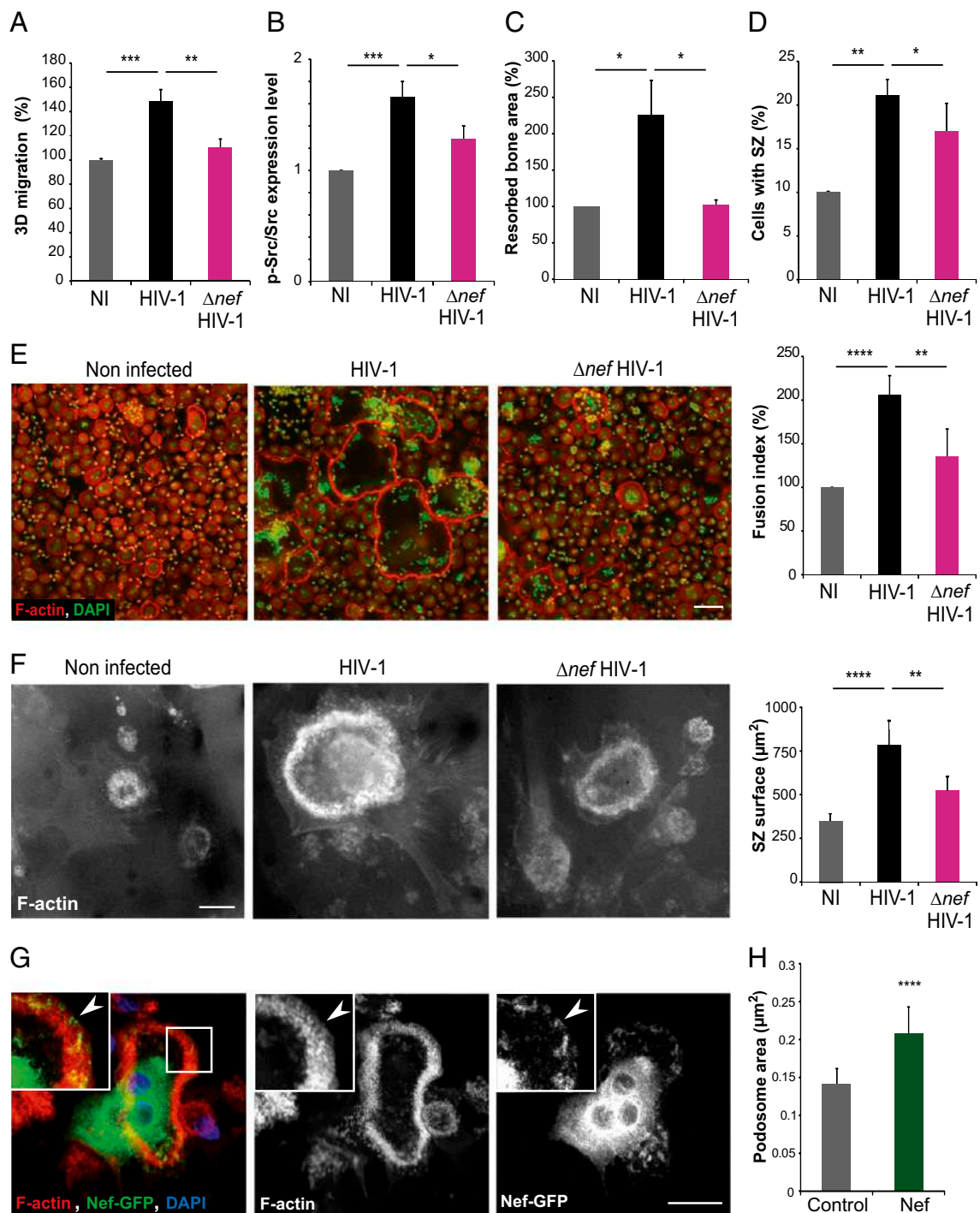


Fig. 7. HIV-1 effects on differentiation and function of OC involve the viral protein Nef. (A–F) Nef is necessary for HIV-1–induced effects in OC. Human OC precursors (A) or mature OC (B–F) were infected with wt HIV-1 or with delta *nef*HIV-1 (NI, noninfected). (A) Percentage of migrating OC precursors after 48 h measured as in Fig. 4, $n = 4$ donors. (B) Quantification of Western blot analyses on whole-cell lysates using antibodies against the phospho-Tyr416 of Src kinases, Src and Actin as in Fig. 6H. Results are expressed as mean \pm SEM, $n = 6$ donors. Quantification of (C) resorbed bone area ($n = 4$), (D) the percentage of cells forming SZ ($n = 4$ donors, 300 cells per donor), (E) the fusion index ($>3,000$ cells per condition, $n = 6$ donors) illustrated by mosaics of 4×4 confocal fields (F-actin in red and nuclei in green), (F) the SZ surface in OC seeded on bones and stained for F-actin (phalloidin), ($n = 3$ donors, >25 SZ). (Scale bars, $150 \mu m$ in E, $10 \mu m$ in F.) Results are expressed as mean \pm SEM. (G and H) Expression of Nef-GFP in OC. OC were transfected with Nef_{5F2}-GFP or GFP (control) and stained for F-actin (phalloidin, red) and nuclei (blue). (G) A fraction of Nef localizes at the SZ. Confocal images of OC expressing Nef_{5F2}-GFP. Arrowheads show colocalization of Nef-GFP with F-actin at the SZ. (Scale bar, $10 \mu m$, Insets, $2 \times$ zoom.) (H) Nef expression increases the size of individual podosomes. Automated quantification of the F-actin fluorescence area of individual podosomes. Mean \pm SEM, $n = 4$ donors ($>2,000$ podosomes from over five cells per donor). * $P \leq 0.05$; ** $P \leq 0.01$; *** $P \leq 0.001$, **** $P \leq 0.0001$.

which is clearly more efficient than infection by cell-free viruses. This is likely to be the physio-pathological route to infect OC in situ, which would be consistent with data showing that cell-to-cell

infection is critical for efficient viral spread in vitro and in vivo (25, 29, 61–69). Altogether, these results show that OC are host cells for HIV-1.

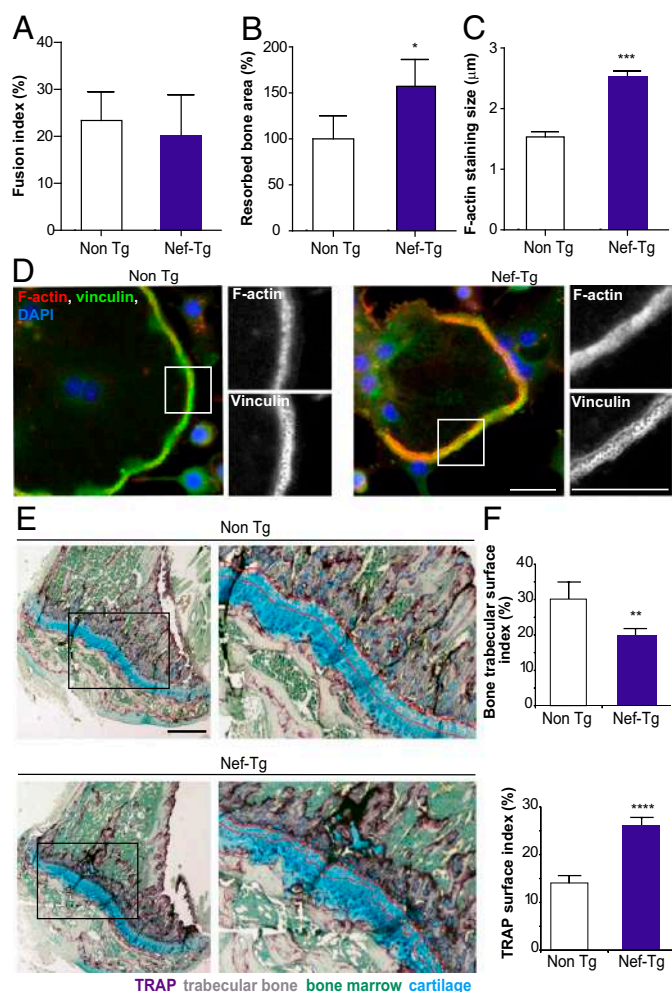


Fig. 8. In Nef-Tg mice, the osteolytic activity of OC and bone defects are enhanced. (A–D) OC differentiated ex vivo from Tg-mice are more osteolytic. OC were differentiated from bone marrow precursors isolated from Nef-Tg and non Tg mice and the fusion index (A), the bone resorption area (B), and the F-actin belt thickness (C) were quantified (50 SZ per condition, $n = 3$ mice per genotype). (D) Representative images of belt structures of OC from non Tg and Nef-Tg mice stained for F-actin (red), vinculin (green) and DAPI (blue). Enlarged frames, 2 \times zoom. (Scale bars, 10 μ m.) (E and F) Nef-Tg mice exhibit bone defects. (E) Representative histological sections of tibia from 7-wk-old mice stained for TRAP to visualize OC (purple), and counterstained with Methyl green and Alcian blue: the bone tissue appears in gray, nuclei in green (corresponding to the nuclei of bone marrow cells), and cartilage in blue. (Scale bar, 200 μ m.) Enlarged frames: $\times 4$ zoom. (F) Quantification of the surface occupied by trabecular bone and surface occupied by TRAP-positive signal in three separate histological sections per mouse ($n = 3$ mice per genotype) are shown. * $P \leq 0.05$; ** $P \leq 0.01$; *** $P \leq 0.001$, **** $P \leq 0.0001$.

Regarding the consequence of HIV-1 infection on OC function, along with this study, there is another report describing that the bone resorption activity of infected OC is exacerbated (20). Herein, we revealed potential mechanisms involved in enhanced bone resorption that concern the structure and function of the SZ, the cell structure instrumental for bone resorption. SZ are larger in HIV-1-infected OC and, consequently, they can degrade larger bone areas. This is in line with the formation of giant OC, which contain twice as more nuclei when they are infected. This exacerbated bone degradation by HIV-1-infected OC also resulted from an increased demineralization process combined with an enhanced secretion of TRAP. The SZ is made of densely connected podosomes, F-actin-rich cell structures involved in cell adhesion, mechanosensing, and cell migration

(70). SZ assembly and patterning are under the control of Src (14, 38). Interestingly, we report that the Src kinase activity was activated in infected OC and that podosomes were enlarged, as visualized by an increase of F-actin staining. In human macrophages, modifications of the F-actin content in individual podosomes have been correlated with fluctuations of protrusion forces exerted onto the extracellular matrix by these cell structures (71). In OC, these modified podosomes may promote more efficient sealing to bone surface. Indeed, we observed stronger adhesion for HIV-1-infected OC compared with noninfected OC. Because the SZ is a barrier that limits the diffusion of acidic and proteolytic molecules released in the resorption lacunae (11–14), increased adhesion would likely enhance the efficiency of containment and favor bone resorption (72). From these results, we propose that modification of several parameters of the SZ (i.e., increased size, adhesion, and degradative activity) contribute to the enhanced osteolytic activity and to the modifications of the topography of resorption pits on infection (12, 36, 73). Pharmacological destabilization of the SZ would reduce the impact of HIV-1 on bone degradation. Several ongoing therapeutic strategies, including the inhibition of the SZ component DOCK5 or cathepsin K activity, are being developed to reduce osteoporotic syndromes while preserving OC viability and differentiation, and thus bone homeostasis (17, 74, 75). We also noticed that OC precursors displayed an enhanced ability to migrate when infected with HIV-1. Interestingly, the efficiency of OC precursor migration has been correlated to OC density in bones (10, 16). Therefore, in addition to enhanced bone resorption activity of infected OC, increased migration of OC precursors should favor OC recruitment to bones, as depicted in Fig. 9, contributing to bone disorders in infected patients.

Nef is a crucial determinant of viral pathogenesis and disease progression. It is known to physically interact with several host proteins to control their activity at the benefit of the virus. Namely, it regulates intracellular protein trafficking (76), actin cytoskeleton (41), cell–cell fusion (45), cell migration (33, 42, 77, 78), and the kinase activity of several members of the Src family (40). In infected OC, all these effects could contribute to the enhanced bone resorption activity that is observed in the present study. In vitro experiments show that Nef, in part located at the SZ, was necessary for all of the HIV-induced effects. The role of Nef was also revealed in vivo in CD4C-Nef-Tg mice that exhibit reduced bone density and an increase of the surface occupied by OC-TRAP staining, suggesting an increase in recruitment and differentiation of OC. Similarly, in HIV-1-Tg rats, a model involving the global transgenic expression of a nonreplicative HIV-1, reduced bone mass was reported, which correlated with a high OC-TRAP staining (18). OC derived from the bone marrow of CD4C-Nef-Tg mice resorbed more and exhibited wider SZ, mimicking the results obtained with human OC infected with HIV-1. Therefore, it is likely that OC participate in the bone remodeling defects evidenced in Nef-Tg mice. Because these mice express Nef in CD4⁺ cells, including T cells, macrophages, OC, and dendritic cells, we propose that the observed bone defects are due, at least in part, to OC expressing Nef in addition to disrupted immune responses, which are known to participate in bone homeostasis (6, 18, 48, 79). Although we do not exclude potential contribution by other viral proteins (80, 81), our results reveal Nef as an essential mediator of the HIV-1 effect on bones (Fig. 9).

It remains to be shown how the virus benefits from manipulating OC. Although OC are giant cells, they do not produce more viral particles than macrophages and these virions exhibit the same infectivity. In contrast with T cells, the cell viability of infected OC is not affected and we can suspect that these infected cells may survive for a long time in bones. Moreover, drug delivery to bones is limited by the unique anatomical features of

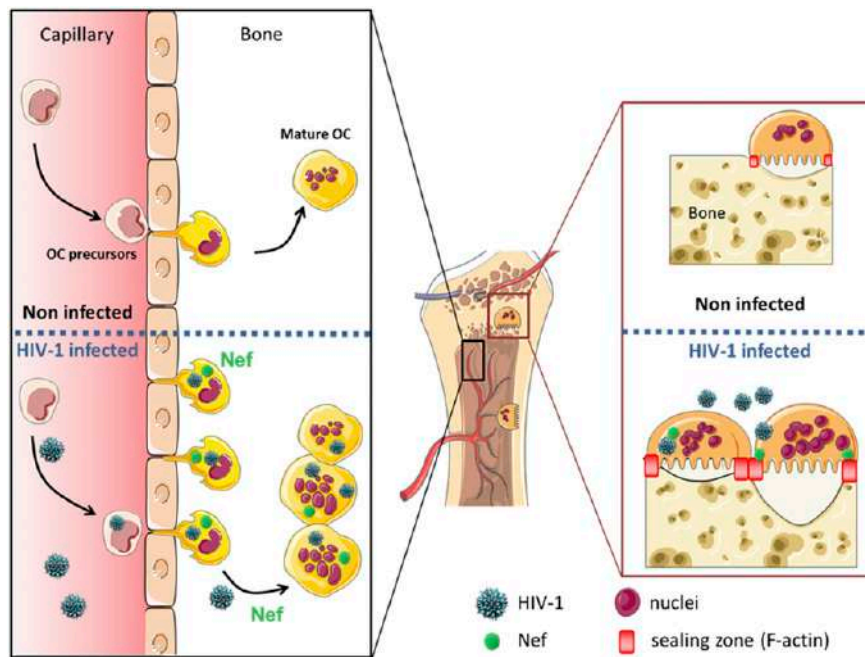


Fig. 9. Graphical abstract proposed to explain HIV-1-induced bone defects in patients. HIV-1 infection affects OC precursor recruitment to bones and the OC differentiation process. These effects, dependent on the viral protein Nef, result in more numerous and more osteolytic OC exhibiting larger and denser SZ.

this tissue (82). Therefore, a putative advantage for the virus may consist in the use of OC as viral reservoirs to hide and survive.

In conclusion, OC are host target cells for HIV-1 that become more osteolytic as a consequence of larger and more degradative SZ. We propose that infected OC participate in bone disorders encountered in HIV-1-infected patients and may constitute a reservoir for the virus. The viral protein Nef appears as a key regulator of the bone resorption activity of OC infected by HIV-1. In summary, this study provides a better understanding of the underlying causes of bone loss following HIV-1 infection.

Materials and Methods

Materials and methods, cell culture and transfection, HIV-1 infection of BLT-humanized mice, viral transfer from infected T cells to primary human OC, cell-free infection of OC and macrophages, and histological analyses of mice bones and of human synovial tissues, are described in *SI Materials and Methods*. Additional materials and methods included flow cytometry analysis, immunoblotting, gel zymography, TRAP staining, IF and transmission electron microscopy analyses, 3D migration, adhesion and resorption assays, chemicals and antibodies, and statistical analysis are also available in *SI Materials and Methods*. Human monocytes were provided by Etablissement Français du Sang, Toulouse, France, under contract 21/PLER/TOU/IPBS01/2013-0042. Experiments with CD4/C HIV Nef mice were approved by the Institutional Animal Ethics committee (Laboratory of Molecular Biology, Clinical Research Institute of Montreal, Montreal, QC, Canada), and experiments with female BLT mice were per-

formed in accordance with guidelines and regulations implemented by the Massachusetts General Hospital Institutional Animal Care and Use Committee.

ACKNOWLEDGMENTS. We thank G. Lugo-Villarino and R. Poincloux for critical reading of the manuscript; C. Salon from US006/Centre Régional d'Exploration Fonctionnelle et de Ressources Expérimentales; M. Dubois, M. Cazabat, M. Requena, and J. Izopet from the BSL3 laboratory of the BiVic facility; F. Moreau and C. Berrone from the animal BSL3 facilities at Institut de Pharmacologie et de Biologie Structurale; C. Bordier for help with cytometry experiments; N. Ortega and A. Métais for help in histology; A. Labrousse for help with RT-PCR; E. Cavaignac for providing synovium samples; E. Meunier for infections with intracellular bacteria; Marie-Chantal Simard and Julio Roberto Caceres-Corte for taking X-rays of Nef-Tg mice, the TRI imaging facility and ANEXPLO functional exploration facility; Stephanie Balor from the Multiscale Electron Imaging platform of the Centre de Biologie Intégrative for his assistance; and the AIDS Research and Reference Reagent Program, Division of AIDS, National Institute of Allergy and Infectious Diseases. This work was supported by the Centre National de la Recherche Scientifique, the Agence Nationale de la Recherche (ANR 2010-01301, ANR14-CE11-0020-02, ANR16-CE13-0005-01, ANR-11-EQUIPEX-0003); the Agence Nationale de Recherche sur le Sida et les hépatites virales (ANRS2014-CI-2, ANRS2014-049); the Fondation pour la Recherche Médicale (DEQ2016 0334894); INSERM Plan Cancer, the Human Frontier Science Program (RGP0035/2016); German Science Foundation research Fellowship US116-2-1 (to S.M.U.); and National Institutes of Health Grants R01 AI097052 and DA036298 (to T.R.M.). L.B. and S.B. are supported by grants from the Institut Pasteur International Network, Institut Pasteur Shanghai, and the Chinese Academy of Sciences. Work in the P. Jolicœur laboratory was supported by the Canadian Institute of Health Research.

- Cotter AG, Mallon PW (2014) The effects of untreated and treated HIV infection on bone disease. *Curr Opin HIV AIDS* 9:17–26.
- Descours B, et al. (2017) CD32a is a marker of a CD4 T-cell HIV reservoir harbouring replication-competent proviruses. *Nature* 543:564–567, and erratum (2017) 546:686.
- Bruera D, Luna N, David DO, Bergoglio LM, Zamudio J (2003) Decreased bone mineral density in HIV-infected patients is independent of antiretroviral therapy. *AIDS* 17: 1917–1923.
- Gibellini D, et al. (2007) RANKL/OPG/TRAIL plasma levels and bone mass loss evaluation in antiretroviral naive HIV-1-positive men. *J Med Virol* 79:1446–1454.
- Grijzen ML, et al. (2010) High prevalence of reduced bone mineral density in primary HIV-1-infected men. *AIDS* 24:2233–2238.
- Titanji K, et al. (2014) Dysregulated B cell expression of RANKL and OPG correlates with loss of bone mineral density in HIV infection. *PLoS Pathog* 10:e1004497.
- Boyle WJ, Simonet WS, Lacey DL (2003) Osteoclast differentiation and activation. *Nature* 423:337–342.
- Prideaux M, et al. (2016) Isolation of osteocytes from human trabecular bone. *Bone* 88:64–72.
- Aziz N, Butch AW, Quint JJ, Detels R (2014) Association of blood biomarkers of bone turnover in HIV-1 infected individuals receiving anti-retroviral therapy (ART). *J AIDS Clin Res* 5:1000360.
- Kotani M, et al. (2013) Systemic circulation and bone recruitment of osteoclast precursors tracked by using fluorescent imaging techniques. *J Immunol* 190: 605–612.
- Teitelbaum SL (2011) The osteoclast and its unique cytoskeleton. *Ann N Y Acad Sci* 1240:14–17.
- Georgess D, Machuca-Gayet I, Blangy A, Jurdic P (2014) Podosome organization drives osteoclast-mediated bone resorption. *Cell Adh Migr* 8:191–204.
- Jurdic P, Saltel F, Chabadel A, Destaing O (2006) Podosome and sealing zone: Specificity of the osteoclast model. *Eur J Cell Biol* 85:195–202.
- Luxenburg C, Parsons JT, Addadi L, Geiger B (2006) Involvement of the Src-cortactin pathway in podosome formation and turnover during polarization of cultured osteoclasts. *J Cell Sci* 119:4878–4888.
- Soriano P, Montgomery C, Geske R, Bradley A (1991) Targeted disruption of the c-src proto-oncogene leads to osteopetrosis in mice. *Cell* 64:693–702.

16. Vérollet C, et al. (2013) Hck contributes to bone homeostasis by controlling the recruitment of osteoclast precursors. *FASEB J* 27:3608–3618.
17. Vives V, et al. (2011) The Rac1 exchange factor Dock5 is essential for bone resorption by osteoclasts. *J Bone Miner Res* 26:1099–1110.
18. Vikulina T, et al. (2010) Alterations in the immuno-skeletal interface drive bone destruction in HIV-1 transgenic rats. *Proc Natl Acad Sci USA* 107:13848–13853.
19. de Menezes EG, Machado AA, Barbosa F, Jr, de Paula FJ, Navarro AM (2017) Bone metabolism dysfunction mediated by the increase of proinflammatory cytokines in chronic HIV infection. *J Bone Miner Metab* 35:234–242.
20. Gohda J, et al. (2015) HIV-1 replicates in human osteoclasts and enhances their differentiation in vitro. *Retrovirology* 12:12.
21. Honeycutt JB, et al. (2017) HIV persistence in tissue macrophages of humanized myeloid-only mice during antiretroviral therapy. *Nat Med* 23:638–643.
22. Honeycutt JB, et al. (2016) Macrophages sustain HIV replication in vivo independently of T cells. *J Clin Invest* 126:1353–1366.
23. Sattentau QJ (1988) The role of the CD4 antigen in HIV infection and immune pathogenesis. *AIDS* 2(Suppl 1):S11–S16.
24. Brainard DM, et al. (2009) Induction of robust cellular and humoral virus-specific adaptive immune responses in human immunodeficiency virus-infected humanized BLT mice. *J Virol* 83:7305–7321.
25. Murooka TT, et al. (2012) HIV-infected T cells are migratory vehicles for viral dissemination. *Nature* 490:283–287.
26. Hayder M, et al. (2011) A phosphorus-based dendrimer targets inflammation and osteoclastogenesis in experimental arthritis. *Sci Transl Med* 3:81ra35.
27. Casartelli N, et al. (2010) Tetherin restricts productive HIV-1 cell-to-cell transmission. *PLoS Pathog* 6:e1000955.
28. Iwami S, et al. (2015) Cell-to-cell infection by HIV contributes over half of virus infection. *eLife* 4:e08150.
29. Sewald X, et al. (2015) Retroviruses use CD169-mediated trans-infection of permissive lymphocytes to establish infection. *Science* 350:563–567.
30. Casartelli N (2016) HIV-1 cell-to-cell transmission and antiviral strategies: An overview. *Curr Drug Targets* 17:65–75.
31. Blavier L, Delaissé JM (1995) Matrix metalloproteinases are obligatory for the migration of preosteoclasts to the developing marrow cavity of primitive long bones. *J Cell Sci* 108:3649–3659.
32. Van Goethem E, Poincloux R, Gauffre F, Maridonneau-Parini I, Le Cabec V (2010) Matrix architecture dictates three-dimensional migration modes of human macrophages: Differential involvement of proteases and podosome-like structures. *J Immunol* 184:1049–1061.
33. Vérollet C, et al. (2015) HIV-1 reprograms the migration of macrophages. *Blood* 125:1611–1622.
34. Saltel F, Destaing O, Bard F, Eichert D, Jurdic P (2004) Apatite-mediated actin dynamics in resorbing osteoclasts. *Mol Biol Cell* 15:5231–5241.
35. Väänänen HK, Zhao H, Mulari M, Halleen JM (2000) The cell biology of osteoclast function. *J Cell Sci* 113:377–381.
36. Soe K, Delaissé JM (2017) Time-lapse reveals that osteoclasts can move across the bone surface while resorbing. *J Cell Sci* 130:2026–2035.
37. Geblinger D, Addadi L, Geiger B (2010) Nano-topography sensing by osteoclasts. *J Cell Sci* 123:1503–1510.
38. Destaing O, et al. (2008) The tyrosine kinase activity of c-Src regulates actin dynamics and organization of podosomes in osteoclasts. *Mol Biol Cell* 19:394–404.
39. Moarefi I, et al. (1997) Activation of the Src-family tyrosine kinase Hck by SH3 domain displacement. *Nature* 385:650–653.
40. Saksela K (2011) Interactions of the HIV/SIV pathogenicity factor Nef with SH3 domain-containing host cell proteins. *Curr HIV Res* 9:531–542.
41. Stolp B, Fackler OT (2011) How HIV takes advantage of the cytoskeleton in entry and replication. *Viruses* 3:293–311.
42. Stolp B, et al. (2009) HIV-1 Nef interferes with host cell motility by deregulation of Cofilin. *Cell Host Microbe* 6:174–186.
43. Tribble RP, Emert-Sedlak L, Smithgall TE (2006) HIV-1 Nef selectively activates Src family kinases Hck, Lyn, and c-Src through direct SH3 domain interaction. *J Biol Chem* 281:27029–27038.
44. Nobile C, et al. (2010) HIV-1 Nef inhibits ruffles, induces filopodia, and modulates migration of infected lymphocytes. *J Virol* 84:2282–2293.
45. Vérollet C, et al. (2010) HIV-1 Nef triggers macrophage fusion in a p61Hck- and protease-dependent manner. *J Immunol* 184:7030–7039.
46. Mazzolini J, et al. (2010) Inhibition of phagocytosis in HIV-1-infected macrophages relies on Nef-dependent alteration of focal delivery of recycling compartments. *Blood* 115:4226–4236.
47. Swingler S, et al. (2008) Evidence for a pathogenic determinant in HIV-1 Nef involved in B cell dysfunction in HIV/AIDS. *Cell Host Microbe* 4:63–76.
48. Hanna Z, et al. (1998) Nef harbors a major determinant of pathogenicity for an AIDS-like disease induced by HIV-1 in transgenic mice. *Cell* 95:163–175.
49. Hanna Z, et al. (2009) Selective expression of human immunodeficiency virus Nef in specific immune cell populations of transgenic mice is associated with distinct AIDS-like phenotypes. *J Virol* 83:9743–9758.
50. Avalos CR, et al. (2016) Quantitation of productively infected monocytes and macrophages of simian immunodeficiency virus-infected macaques. *J Virol* 90:5643–5656.
51. Cribbs SK, Lennox J, Caliendo AM, Brown LA, Guidot DM (2015) Healthy HIV-1-infected individuals on highly active antiretroviral therapy harbor HIV-1 in their alveolar macrophages. *AIDS Res Hum Retroviruses* 31:64–70.
52. Jambo KC, et al. (2014) Small alveolar macrophages are infected preferentially by HIV and exhibit impaired phagocytic function. *Mucosal Immunol* 7:1116–1126.
53. Smith PD, Meng G, Salazar-Gonzalez JF, Shaw GM (2003) Macrophage HIV-1 infection and the gastrointestinal tract reservoir. *J Leukoc Biol* 74:642–649.
54. Williams KC, et al. (2001) Perivascular macrophages are the primary cell type productively infected by simian immunodeficiency virus in the brains of macaques: Implications for the neuropathogenesis of AIDS. *J Exp Med* 193:905–915.
55. Benaroch P, Billard E, Gaudin R, Schindler M, Jouve M (2010) HIV-1 assembly in macrophages. *Retrovirology* 7:29.
56. Tan J, Sattentau QJ (2013) The HIV-1-containing macrophage compartment: A perfect cellular niche? *Trends Microbiol* 21:405–412.
57. Welsch S, et al. (2007) HIV-1 buds predominantly at the plasma membrane of primary human macrophages. *PLoS Pathog* 3:e36.
58. Sattentau QJ, Stevenson M (2016) Macrophages and HIV-1: An unhealthy constellation. *Cell Host Microbe* 19:304–310.
59. Delobel P, et al. (2005) Persistence of distinct HIV-1 populations in blood monocytes and naive and memory CD4 T cells during prolonged suppressive HAART. *AIDS* 19:1739–1750.
60. Zhu T, et al. (2002) Evidence for human immunodeficiency virus type 1 replication in vivo in CD14(+) monocytes and its potential role as a source of virus in patients on highly active antiretroviral therapy. *J Virol* 76:707–716.
61. Bracq L, et al. (2017) T cell-macrophage fusion triggers multinucleated giant cell formation for HIV-1 spreading. *J Virol* 91:e01237-17.
62. Law KM, et al. (2016) In vivo HIV-1 cell-to-cell transmission promotes multicopy micro-compartmentalized infection. *Cell Rep* 15:2771–2783.
63. Russell RA, Martin N, Mitar I, Jones E, Sattentau QJ (2013) Multiple proviral integration events after virological synapse-mediated HIV-1 spread. *Virology* 443:143–149.
64. Sigal A, et al. (2011) Cell-to-cell spread of HIV permits ongoing replication despite antiretroviral therapy. *Nature* 477:95–98.
65. Baxter AE, et al. (2014) Macrophage infection via selective capture of HIV-1-infected CD4+ T cells. *Cell Host Microbe* 16:711–721.
66. Dale BM, Alvarez RA, Chen BK (2013) Mechanisms of enhanced HIV spread through T-cell virological synapses. *Immunol Rev* 251:113–124.
67. Eugenin EA, Gaskill PJ, Berman JW (2009) Tunneling nanotubes (TNT) are induced by HIV-infection of macrophages: A potential mechanism for intercellular HIV trafficking. *Cell Immunol* 254:142–148.
68. Sattentau Q (2008) Avoiding the void: Cell-to-cell spread of human viruses. *Nat Rev Microbiol* 6:815–826.
69. Sowinski S, et al. (2008) Membrane nanotubes physically connect T cells over long distances presenting a novel route for HIV-1 transmission. *Nat Cell Biol* 10:211–219.
70. Wiesner C, Le-Cabec V, El Azzouzi K, Maridonneau-Parini I, Linder S (2014) Podosomes in space: Macrophage migration and matrix degradation in 2D and 3D settings. *Cell Adh Migr* 8:179–191.
71. Proag A, et al. (2015) Working together: Spatial synchrony in the force and actin dynamics of podosome first neighbors. *ACS Nano* 9:3800–3813.
72. Stenbeck G, Horton MA (2000) A new specialized cell-matrix interaction in actively resorbing osteoclasts. *J Cell Sci* 113:1577–1587.
73. Merrill DM, et al. (2015) Pit- and trench-forming osteoclasts: A distinction that matters. *Bone Res* 3:15032.
74. Panwar P, et al. (2016) A novel approach to inhibit bone resorption: Exosite inhibitors against cathepsin K. *Br J Pharmacol* 173:396–410.
75. Vives V, et al. (2015) Pharmacological inhibition of Dock5 prevents osteolysis by affecting osteoclast podosome organization while preserving bone formation. *Nat Commun* 6:6218.
76. Foster JL, Garcia JV (2006) HIV pathogenesis: Nef loses control. *Cell* 125:1034–1035.
77. Stolp B, et al. (2012) HIV-1 Nef interferes with T-lymphocyte circulation through confined environments in vivo. *Proc Natl Acad Sci USA* 109:18541–18546.
78. Vérollet C, Le Cabec V, Maridonneau-Parini I (2015) HIV-1 infection of T lymphocytes and macrophages affects their migration via Nef. *Front Immunol* 6:514.
79. Hanna Z, et al. (2001) The pathogenicity of human immunodeficiency virus (HIV) type 1 Nef in CD4C/HIV transgenic mice is abolished by mutation of its SH3-binding domain, and disease development is delayed in the absence of Hck. *J Virol* 75:9378–9392.
80. Chew N, Tan E, Li L, Lim R (2014) HIV-1 tat and rev upregulates osteoclast bone resorption. *J Int AIDS Soc* 17(Suppl 3):19724.
81. Gibellini D, et al. (2010) HIV-1 Tat protein enhances RANKL/M-CSF-mediated osteoclast differentiation. *Biochem Biophys Res Commun* 401:429–434.
82. Hirabayashi H, Fujisaki J (2003) Bone-specific drug delivery systems: Approaches via chemical modification of bone-seeking agents. *Clin Pharmacokinet* 42:1319–1330.

Supporting Information

Raynaud-Messina et al. 10.1073/pnas.1713370115

SI Materials and Methods

Chemicals and Antibodies. Human and mouse recombinant M-CSF were purchased from Peprotech and human and mouse RANKL from Miltenyi Biotec. Leukocyte acid phosphatase kit for TRAP staining and DAPI were purchased from Sigma-Aldrich. Matrigel (10–12 mg/mL) was from BD Biosciences. The following antibodies were used: Rabbit anti-Phospho-Src (Tyr416) (Cell Signaling Technology, Ozyme), rabbit antiintegrin $\beta 3$ (Cell Signaling), mouse monoclonal anticalthepsin K (clone 3F9, ab37259; Abcam) and anti-TRAP antibodies (sc-28204) (Santa Cruz Biotechnologies, TEBU-Bio), monoclonal antiactin (clone 20–33), anti- β -tubulin (clone B-5-1-2), mouse antivinculin (clone hVin-1) (Sigma-Aldrich), and mouse monoclonal anti-human p24 (clone Kal-1) (Dako) or anti-Gag/p24-FITC monoclonal antibody clone KC57-FITC (Beckman Coulter). Secondary biotin-conjugated antibodies and avidin-biotin-peroxydase complex were from Dako and Vector laboratories (LTP) and fluorescent secondary antibodies and Texas Red/Alexa Fluor 488-conjugated phalloidins were obtained from Molecular probes (Invitrogen). Maraviroc (Sigma-Aldrich) was used at 10 μ M, 30 min before infection. Ritonavir, Raltegravir, and AZT were obtained from the AIDS Research and Reference Reagent Program, Division of AIDS, National Institute of Allergy and Infectious Diseases, and were also used at 10 μ M, 30 min before infection.

Mice. The CD4C/HIV Nef (previously named CD4C/HIV^{MutG}) (1) and CD4C/HIV^{GFP} Tg mice (2) have been described previously. Experiments were approved by the Institutional Animal Ethics committee (Laboratory of Molecular Biology, Clinical Research Institute of Montreal, Montreal, QC, Canada).

Female BLT mice were generated as previously described (3). Briefly, NOD/SCID/ $\gamma c^{-/-}$ (NSG) mice 6–8 wk of age were conditioned with sublethal (2 Gy) whole-body irradiation, and 1-mm³ fragments of human fetal thymus and liver (17–19 wk of gestational age) (Advanced Bioscience Resources) were implanted under the recipient kidney capsules bilaterally. Remaining fetal liver tissue was used to isolate CD34 cells with anti-CD34 microbeads (Miltenyi Biotec), which were then injected intravenously (1×10^5 to 5×10^5 cells per mouse) within 6 h.

Intravaginal HIV-1 infection. NSG-BLT humanized mice were subcutaneously injected with 200 μ g progesterone (Depo-Provera; Pfizer) 5–7 days before intravaginal infection to synchronize their estrus cycle. Before intravaginal inoculation, mice were anesthetized with a mixture Ketamine and Xylazine and infected with 10- μ L viral inoculum containing 2×10^4 infectious units of NL4-3 virus that was engineered to express V3 loop from a Bal strain, thus conferring CCR5 tropism (4). The control group received 10 μ L of PBS intravaginally. Plasma viremia was monitored weekly by collecting few drops of blood from facial vein and basis by quantitating plasma viral loads by qPCR. All animal experiments were performed in accordance with guidelines and regulations implemented by the Massachusetts General Hospital Institutional Animal Care and Use Committee.

Plasma viral loads. Viral RNA was isolated from ~50 μ L of plasma using the QIAamp viral RNA kit (Qiagen). Quantitative reverse transcription and PCR was performed using HIV-1 gag specific primers 5'-AGTGGGGGACATCAAGCAGCCATGCAAAT-3' and 5'-TGCTATGTCACTTCCCCTTGGTTCTCT-3' by using single step QuantiFast SYBR Green RT-PCR Kit (Qiagen) on Lightcycler 480-II (Roche). Plasma from uninfected BLT mice was used to determine the background signal, as described previously (4).

Cell Culture and Transfection. Human monocytes were isolated from the blood of healthy donors and differentiated as hMDM, as described previously (5). For differentiation to human OC, monocytes were seeded on slides in 24-well plates at a density of 5×10^5 cells per well in Roswell Park Memorial Institute medium (RPMI) supplemented with 10% FBS, M-CSF (50 ng/mL), and RANKL (30 ng/mL). The medium was replaced every 3 days with medium containing M-CSF (25 ng/mL) and RANKL (100 ng/mL). hMDM and OC from the same donor were used from days 1–6 of differentiation (OC precursors) or at day 10 of differentiation (mature OC). For transient expression of Nef, we used a Neon MP 5000 electroporation system (Invitrogen) in human OC (parameters: 1,000 V, 40 ms, two pulses, and 1 μ g of DNA for 2×10^5 cells), as in ref. 6. The constructs encoding the GFP-tagged Nef for expression of HIV-1_{NL4-3} Nef fused to GFP have been described previously (6). Cells were used within 24 h (5% transfection efficiency).

HEK293T, TZM-bl and Jurkat T cells were from S.B.'s laboratory and were cultured as described previously (7).

Autologous human primary CD4⁺ T cells (from the same donors as the one used for monocyte preparation) were purified by negative selection (CD4⁺ T cell isolation kit, Miltenyi). CD4⁺ T cells were kept for 10–12 days in RPMI supplemented with 20% FBS and interleukin-2 at 10 U/mL (IL-2; Miltenyi). The day of infection, phytohemagglutinin-P at 5 μ g/mL (PHA-P; Sigma) was added to the medium.

Mouse OC were differentiated from bone marrow cells isolated from long bones, as previously described (8). Briefly, nonadherent cells were cultured in α -MEM supplemented with 30 ng/mL mouse M-CSF (Miltenyi Biotec) for 48 h. Then, OC differentiation was initiated in medium containing 100 ng/mL mouse RANKL (Miltenyi Biotec) and 30 ng/mL M-CSF, at the density 1.5×10^5 cells per well (six-well plate) or of 4×10^4 cells per well (96-well plate). Media was changed and cytokines were replenished every 2 d. Cells were maintained in culture for 4–6 d before analyses.

Cell-Free HIV-1 Infection of Macrophages and OC. *Wt*- and Δ *nef*-HIV ADA strains were produced in HEK293T cells as in ref. 6, and the NLAD8-VSVG strain was produced by cotransfection with the proviral plasmid in combination with pVSVG (from S.B.'s laboratory). Amount of HIV-1 p24 in viral stocks was assessed by an home-made ELISA (with NIH reagents, NIH AIDS Reagent Program, Division of AIDS, National Institute of Allergy and Infectious Diseases). HIV-1 infectious units were quantified by reverse transcriptase assay (9, 10) and using TZM-bl cells, as reported previously (6). Macrophages and OC were infected at multiplicity of infection (MOI) 0.1 (corresponding to 0.7 ng of p24 for 2×10^6 OC) with the macrophage-tropic HIV-1 isolate ADA or Δ *nef*-ADA, as described previously (11). Infectivity and replication was assessed by measuring p24⁺ cells by immunostaining, p24 level in cell supernatants by our home-made ELISA, and using TZM-bl indicator cells, as previously described (6, 12).

Viral Transfer to OC via Infected T Cells. To study the transfer of HIV-1 from T cells to OC, Jurkat cells (J77 provided by S.B.), or human primary CD4⁺ T cells were infected with the CCR5-tropic virus (NLAD8) coexpressing VSV-G envelope glycoprotein, to allow efficient infection independently of entry receptors. The cells were infected for 24 h at a MOI of 0.5 (MOI 10 for primary T cells), then washed and cultured for another 24 h. At this stage, T cell infection rate was evaluated to at least 50% by flow cytometry. After three PBS-washes to remove free-cell viral particles, infected

T cells were cocultured 6 h with OC (ratio 2:1), as in ref. 7. Then, T cells were eliminated by washing extensively (once with PBS, once with PBS-10 mM EDTA and twice with PBS) and OC were maintained in culture in presence of M-CSF (25 ng/mL) and RANKL (100 ng/mL) for additional 5 days.

Bacterial Infection of OC. Human mature OC (day 10) seeded on bones were infected with *Salmonella typhimurium* MOI 15 (as described in ref. 13), *Francisella novicida* MOI 7 (as described in ref. 14), or *Mycobacterium tuberculosis* MOI 6 (as described in ref. 15). Twenty-four hours after infection, cells were fixed and stained for F-actin and DAPI, as previously described (6, 16). The percentage of cells forming SZ was quantified for four independent experiments ($n = 4$ donors); at least 200 cells were analyzed per condition.

Flow Cytometry Analysis. Cells detached by Accutase (Gibco Technology) were incubated for 30 min on ice with the following antibodies and fixed in 4% paraformaldehyde before analysis: Alexa Fluor 488 anti-human CD16, APC anti-human CD4, PE anti-human CCR5, APC anti-human CD61 ($\beta 3$ integrin) from Biolegend (Ozyme). Data were acquired on BD LSR II (BD Biosciences) and analyzed with Flow Jo software (TreeStar).

Immunoblotting. Cells were lysed and total proteins were separated through SDS/PAGE, transferred and immunoblotted. Quantification of immunoblot intensity for several donors was performed using Image Lab (Bio-Rad). The quantification was reported to tubulin or actin (used as a loading control). Systematic Coomassie blue staining was performed to control the charges of extracellular lysates.

Gelatin Zymography. OC cell-conditioned medium was analyzed for MMP9 activity by gelatin substrate gel electrophoresis, as in ref. 17.

TRAP Staining and IF Microscopy. Cells were fixed with PFA 3.7% and stained for TRAP (Sigma-Aldrich), according to the manufacturer's protocol. IF experiments in 2D (on glass coverslips or on bone slices) were performed as described previously (6, 16). Quantification of OC fusion index (total number of nuclei in multinucleated cells divided by total number of nuclei \times 100), number of nuclei per multinucleated cells and surface index (surface covered by multinucleated cells/total surface \times 100) were assessed by using a semiautomatic quantification with a homemade ImageJ macro, allowing the study of more than 3,000 cells per condition in at least five independent donors. All images were prepared with Adobe Photoshop software. The number of cells with podosomes and SZ was quantified after phalloidin staining. F-actin fluorescence intensity inside podosomes and inside SZ (three zones per SZ) was assessed using ImageJ software. Slides were visualized with a Leica DM-RB fluorescence microscope or on a FV1000 confocal microscope (Olympus), and the associated software. Images were processed with ImageJ and Adobe Photoshop software.

Resorption Assays. To assess bone resorption activity, mature OC were detached using Accutase treatment (Gibco Technology, ThermoFischer Scientific) 10 min, at 37 °C, and cultured on bovine cortical bone slices (IDS Nordic Biosciences) for 48 h in medium supplemented with M-CSF (25 ng/mL) and RANKL (100 ng/mL). Following complete cell removal by immersion in water and scraping, bone slices were stained with Toluidine blue to detect resorption pits under a light microscope (Leica DMIRB; Leica Microsystems). Circularity and the surface of bone degradation areas were quantified manually with ImageJ software. For quantification of the volume of bone degradation, we imaged the resorption pits with a confocal microscope (Olympus LEXT OLS 3100, 50 \times , $z = 50$ nm). Cross-linked CTX

concentrations were measured using betaCrosslaps assay (Immunodiagnostic System laboratory) in the culture medium of OC grown on bone slices. To assess demineralization activity, OC were differentiated in multiwell Osteologic Biocoat (Corning, VWR), fixed, stained with the Von Kossa method, as described previously (18), and quantified using ImageJ software.

Adhesion Assays. OC were differentiated on glass coverslips in 24-well plates, incubated for 10 min at 37 °C in Accutase (Gibco Technology) or in a nonenzymatic cell dissociation buffer (Gibco Technology). Cells were washed with PBS, adherent cells were fixed and nuclei were quantified after DAPI staining.

Three-Dimensional Migration Assays. For 3D migration assays with OC precursors, experiments were performed as described previously (16) and quantified at 48 h. Briefly, pictures of cells were taken automatically with a 10 \times objective at constant intervals using the motorized stage of an inverted microscope (Leica DMIRB; Leica Microsystems); cells were counted using ImageJ software as described previously (19). The number of cells inside the matrix (percent of migration measured after 48 h of migration) and the distance of migration were quantified using ImageJ.

Histological Analysis of GFP-Tg, Nef-Tg, and HIV-1-Infected BLT Mice. Femurs and tibia from adult mice were fixed in 10% buffered formalin solution (Sigma-Aldrich), decalcified in EDTA, and embedded in paraffin. Longitudinal serial sections of the median portion of whole bone were stained for TRAP (Sigma-Aldrich) according to the manufacturer's protocols and counterstained with Fast green or Hematoxylin Gill 3. Stained slides were digitized using Panoramic 250 Flash digital microscope (P250 Flash; 3DHisTech). Whole-slides were scanned in brightfield scan mode with a 40 \times /NA 0.8 Zeiss Plan-Apochromat dry objective, and images were acquired with a two megapixels 3CCD color camera (CIS Cam Ref#VCC-F52U25CL; CIS Americas). This objective and camera combination yield a 0.22 μ m per pixel resolution in fluorescence scan mode, which corresponds, in conventional microscopy, to 56 \times magnification at the highest optical resolution. Panoramic Viewer software (RTM 1.15.0.53) was used for viewing, analyzing, and quantification of the digital slides. Cortical bone surface and TRAP⁺ cells were quantified. Animal groups were composed of three mice. Mononucleated and multinucleated TRAP⁺ cells were counted on a minimum of four serial sections chosen among the most median part of four different tibias for each genotype. For histological analysis of GFP-Tg, sections (3 μ m) were stained for TRAP activity (Sigma-Aldrich), Hemalum/Eosin, or with a rabbit antibody directed toward GFP (ab6556; Abcam, dilution 1/400, epitope retrieval: citrate buffer pH 6, boiling micro-oven, 2 \times 10 min).

For histological analysis of HIV-1-infected BLT mice, serial sections were stained for TRAP activity (Sigma-Aldrich), Hemalum/Eosin, or with a monoclonal antibody directed toward human p24 (clone Kal-1, dilution 1/10, usual epitope retrieval: Tris-EDTA buffer pH 9, 95 °C, 40 min). In addition to the commonly critical technical issues associated with performing IHC on calcified bone tissue, we needed to overcome first, the high background due to the presence of some endogenous mouse Ig (to this end we used a blocking step, mouse-on-mouse kit; Vector Laboratory, LTP) and second, the detachment of samples from the slides due to the high temperature required for p24 antigen retrieval (adapted epitope retrieval: Tris-EDTA buffer pH 9, 70 °C, 5 h) (20, 21). Animal groups were composed of four viremic mice and three noninfected mice. The total number of OC (TRAP⁺ cell along the bone) was quantified for each section (heads of tibia and femur) and the number of double-positive p24⁺/TRAP⁺ was quantified in the corresponding section ($n = 4$ infected mice).

Histological Analysis of Human Synovial Tissues. Synovial tissues obtained from arthroplastic surgery of nonarthritic patients were cut into blocks of around 1–2 mm³ and incubated on gel-foam sponges (Pfizer) with M-CSF (50 ng/mL) alone or with M-CSF (50 ng/mL) and RANKL (33 ng/mL). Explants were infected with the macrophage-tropic HIV-1 isolate ADA for 24 h, washed free of virus particles and maintained in culture for 21 d at 37 °C, 5% CO₂ in α -MEM supplemented with 10% FBS. Medium was replaced every 3 d with M-CSF (50 ng/mL) and RANKL (100 ng/mL) as described previously (22). Tissues were then fixed in 10% phosphate-buffered formalin and embedded in paraffin. Sections (3 μ m) were stained for TRAP activity (Sigma-Aldrich), Hemalum/Eosin, or with mouse monoclonal antibodies directed toward p24 (clone Kal-1; Dako) and cathepsin K (clone 3F9, ab37259; Abcam, dilution 1/600, epitope retrieval: EDTA buffer 1 mM pH8, boiling 8 min).

Transmission Electron Microscopy. Mature OC (day 10 of differentiation) were infected at a MOI 1 (corresponding to 7 ng of p24 for 2 \times 10⁶ OC) with the HIV-1 ADA strain. Ten days

postinfection, cells were fixed 2 h at room temperature with 2.5% glutaraldehyde and 2% paraformaldehyde (EMS, Delta-Microscopies) in 0.1 M phosphate buffer, pH 7.2 and postfixed at 4 °C with 1% OsO₄ in cacodylate buffer 0.1 M. Adherent cells were treated for 1 h with 1% aqueous uranyl acetate then dehydrated in a graded ethanol series and embedded in Epon. Sections were cut on a Leica Ultracut microtome and ultrathin sections were mounted on 200 mesh onto Formvar carbon-coated copper grids. Finally, thin sections were stained with 1% uranyl acetate and lead citrate and examined with a transmission electron microscope (Jeol JEM-1400) at 80 kV. Images were acquired using a digital camera (Gatan Orius) at 10,000 \times and 15,000 \times magnification, respectively.

Statistical Analysis. One-tailed paired or unpaired *t* test was applied on data sets with a normal distribution, whereas one-tailed Mann-Whitney (unpaired test) or Wilcoxon (matched-pair test) tests were used otherwise (Prism). **P* \leq 0.05; ***P* \leq 0.01; ****P* \leq 0.001, *****P* \leq 0.0001.

- Hanna Z, et al. (1998) Nef harbors a major determinant of pathogenicity for an AIDS-like disease induced by HIV-1 in transgenic mice. *Cell* 95:163–175.
- Chrobak P, et al. (2014) HIV Nef expression favors the relative preservation of CD4+ T regulatory cells that retain some important suppressive functions. *J Immunol* 192:1681–1692.
- Brainard DM, et al. (2009) Induction of robust cellular and humoral virus-specific adaptive immune responses in human immunodeficiency virus-infected humanized BLT mice. *J Virol* 83:7305–7321.
- Murooka TT, et al. (2012) HIV-infected T cells are migratory vehicles for viral dissemination. *Nature* 490:283–287.
- Le Cabec V, Maridonneau-Parini I (1995) Complete and reversible inhibition of NADPH oxidase in human neutrophils by phenylarsine oxide at a step distal to membrane translocation of the enzyme subunits. *J Biol Chem* 270:2067–2073.
- Vérollet C, et al. (2015) HIV-1 reprograms the migration of macrophages. *Blood* 125:1611–1622.
- Bracq L, et al. (2017) T cell-macrophage fusion triggers multinucleated giant cell formation for HIV-1 spreading. *J Virol* 91:e01237–17.
- Vives V, et al. (2015) Pharmacological inhibition of Dock5 prevents osteolysis by affecting osteoclast podosome organization while preserving bone formation. *Nat Commun* 6:6218.
- Chapuy-Regaud S, et al. (2013) Progesterone and a phospholipase inhibitor increase the endosomal bis(monoacylglycero)phosphate content and block HIV viral particle intercellular transmission. *Biochimie* 95:1677–1688.
- Laguet N, et al. (2009) Nef-induced CD4 endocytosis in human immunodeficiency virus type 1 host cells: Role of p56lck kinase. *J Virol* 83:7117–7128.
- Vérollet C, et al. (2010) HIV-1 Nef triggers macrophage fusion in a p61Hck- and protease-dependent manner. *J Immunol* 184:7030–7039.
- Bertin J, Jalaguier P, Barat C, Roy MA, Tremblay MJ (2014) Exposure of human astrocytes to leukotriene C4 promotes a CX3CL1/fractalkine-mediated transmigration of HIV-1-infected CD4+ T cells across an in vitro blood-brain barrier model. *Virology* 454–455:128–138.
- Meunier E, Broz P (2015) Quantification of cytosolic vs. vacuolar *Salmonella* in primary macrophages by differential permeabilization. *J Vis Exp*, e52960.
- Meunier E, et al. (2015) Guanylate-binding proteins promote activation of the AIM2 inflammasome during infection with *Francisella novicida*. *Nat Immunol* 16:476–484.
- Lastrucci C, et al. (2015) Tuberculosis is associated with expansion of a motile, permissive and immunomodulatory CD16(+) monocyte population via the IL-10/STAT3 axis. *Cell Res* 25:1333–1351.
- Vérollet C, et al. (2013) Hck contributes to bone homeostasis by controlling the recruitment of osteoclast precursors. *FASEB J* 27:3608–3618.
- Cougoule C, et al. (2010) Three-dimensional migration of macrophages requires Hck for podosome organization and extracellular matrix proteolysis. *Blood* 115:1444–1452.
- Brazier H, Pawlak G, Vives V, Blangy A (2009) The Rho GTPase Wrch1 regulates osteoclast precursor adhesion and migration. *Int J Biochem Cell Biol* 41:1391–1401.
- Van Goethem E, Poincloux R, Gauffre F, Maridonneau-Parini I, Le Cabec V (2010) Matrix architecture dictates three-dimensional migration modes of human macrophages: Differential involvement of proteases and podosome-like structures. *J Immunol* 184:1049–1061.
- Li S, et al. (2015) An effective and practical immunohistochemical protocol for bone specimens characterized by hyaluronidase and pepsin predigestion combined with alkaline phosphatase-mediated chromogenic detection. *Histol Histopathol* 30:331–343.
- Shi SR, Cote RJ, Taylor CR (1998) Antigen retrieval immunohistochemistry used for routinely processed celloidin-embedded human temporal bone sections: Standardization and development. *Auris Nasus Larynx* 25:425–443.
- Hayder M, et al. (2011) A phosphorus-based dendrimer targets inflammation and osteoclastogenesis in experimental arthritis. *Sci Transl Med* 3:81ra35.

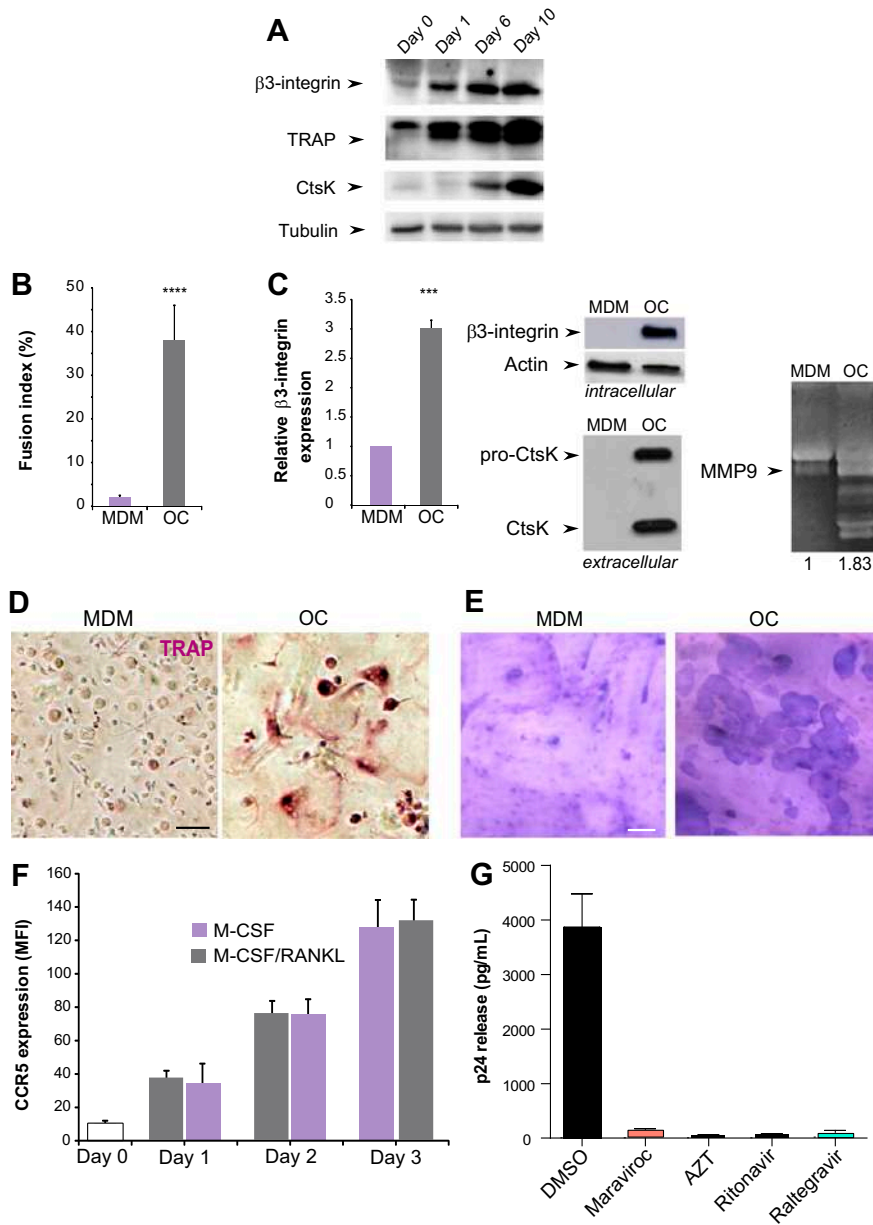


Fig. S2. (A) Kinetics of OC differentiation. Whole-cell extracts of cells maintained in culture with the osteoclastogenic cytokines during 0, 1, 6, or 10 d were blotted using antibodies against β 3 integrin, TRAP, cathepsin K (CtsK), and tubulin (loading control). A representative blot out of three independent experiments is shown. (B–E) Characteristics of OC compared with human MDM at day 10 of differentiation. MDM (purple) and OC (gray) from the same donors ($n = 6$) were examined for fusion index by IF (B), cell-surface expression of β 3-integrin by flow cytometry (expression in MDM was used as reference), β 3-integrin (intracellular), and CtsK (extracellular) expression level by Western blot and MMP9 activity by zymography (C). (D) Representative brightfield images of TRAP staining of MDM and OC seeded on glass at day 10. (Scale bar, 30 μ m.) (E) Brightfield images of bone-resorption pits. MDM and OC were seeded on bovine cortical bone slides for 48 h and bone resorption pits revealed with Toluidine blue. (Scale bar, 20 μ m.) (F) CCR5 cell-surface expression in OC precursors at day 0, 1, 2, and 3 of differentiation. The kinetics of cell-surface CCR5 expression in monocytes maintained in M-CSF (purple) and M-CSF/RANKL (gray) from same donors were determined by the median fluorescent intensity (MFI) ($n = 5$ donors). (G) Treatment with several drugs abolishes HIV-1 production by mature OC. Mature (10 d-differentiated) OC were treated with 10 μ M Maraviroc, AZT, Ritonavir, or Raltegravir 30 min before infection, and p24 release was measured by ELISA 10 d postinfection ($n = 4$ donors). *** $P \leq 0.001$, **** $P \leq 0.0001$.

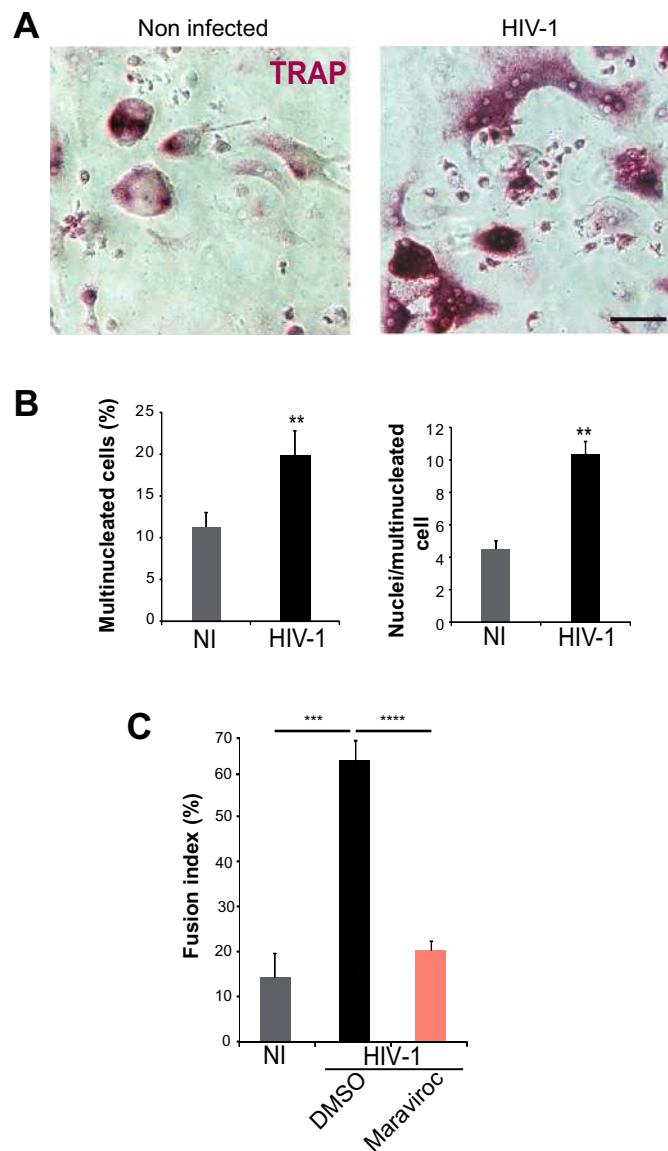


Fig. 54. (A and B) HIV-1 enhances OC differentiation. (A) Representative brightfield images of TRAP staining of noninfected OC (Left) or HIV-1-infected OC (Right) at day 10 postinfection. (Scale bar, 30 μ m.) (B) Quantification of the percentage of multinucleated cells (\geq two nuclei) and of the number of nuclei per multinucleated cells after confocal analysis as in Fig. 5A. (C) Maraviroc inhibits the increase of the fusion index induced by infection. Mature (10 d-differentiated) OC were treated with Maraviroc 30 min before infection and the fusion index was determined 10 d postinfection (n = 5 donors). NI, noninfected. ** $P \leq 0.01$; *** $P \leq 0.001$, **** $P \leq 0.0001$.

